UNIVERSITÉ DU QUÉBEC

RAPPORT PRÉSENTÉ À
L'UNIVERSITÉ DU QUÉBEC À TROIS-RIVIÈRES

COMME EXIGENCE PARTIELLE
DU DOCTORAT EN SCIENCES ET GÉNIE
DES MATÉRIAUX LIGNOCELLULOSIQUES

PAR
VINAY KHATRI

# FLUORESCENT PROTEIN-TAGGED CARBOHYDRATE-BINDING MODULES METHOD (FTCM) AND APPLICATIONS

APRIL 2018

*Dedicated to my mom, dad, grandparents*
*and my lovely sister*

## Acknowledgements

First and foremost, I want to thank my advisor Dr. Marc Beauregard. It has been an honor to be his Ph.D. student. I appreciate all his contributions of time, ideas, and funding to make my Ph.D. experience productive and stimulating. The joy and enthusiasm he has for his research was contagious and motivational for me, even during tough times in the Ph.D. pursuit. I would like to thank him for encouraging my research and for allowing me to grow as a research scientist. His advice on both research as well as on my career have been invaluable. I am also thankful for the excellent example he has provided as a successful biochemist and professor.

I would like to thank Dr. Fatma Meddeb-Mouelhi (adjunct professor, former Buckman North America employee), who has been an inspiring figure for me. She provided me with every bit of guidance, assistance, and expertise that I needed during this journey. I appreciate her contribution of valuable feedback and insightful advice. I am grateful to her for always believing in me and for encouraging me to reach new heights. I acknowledge her for keeping me organized and forging me as a better researcher. I am also thankful to Dr. Yannick Hébert-Ouellet (former post-doc), who has been an excellent supervisor. I very much appreciated his immense contribution to this study. His friendly guidance and expert advice have been invaluable throughout all stages of this work.

I gratefully acknowledge the members of my Ph.D. committee for their time and valuable feedback on a preliminary version of this thesis. I also acknowledge the funding sources that made my Ph.D. work possible. This work was supported by Buckman Laboratories of Canada and funded by grants from Fonds de Recherche du Quebec – Nature et Technologies (FRQNT). This work was also partially funded by PROTEO, Centre de Recherche sur les Matériaux Renouvelables (CRMR), Consortium de Recherche et Innovations en Bioprocedes Industriels au Quebec (CRIBIQ) and Natural Sciences and Engineering Research Council (NSERC) of Canada (CRDPJ445143-12).

Profound gratitude goes to Dr. Normand Voyer (Université Laval, QC), Dr. Alisdair Boraston (University of Victoria, BC) and Dr. Simon Barnabé for their suggestions, insightful discussions and valuable editorial contributions. I would like to acknowledge my program director Dr. Eric Loranger for his availability and suggestions while drafting this thesis. I am also hugely appreciative to Dr. Roberto Chica (University of Ottawa, Ottawa, ON) for the donation of fluorescent protein and Dr. Nicolas Doucet (INRS-Institut Armand-Frappier, Laval, QC) for his expert assistance while performing isothermal titration calorimetry (ITC) measurements. I am grateful to Dr. Simon Barnabé and Dr. Kokou Adjalle for their donation of lignocellulosic biomass and their contribution to the analysis of biomass samples.

I would like to express my gratitude to Pierre-Louis Bombeck (Ph.D. student, University of Liège, Belgium) for his valuable contribution to this study. I owe a great debt of gratitude to Nikolas Beauchesne (undergraduate student) for his skillful technical assistance throughout this study. I am also thankful to Samy, Vincent Bolduc, and Guillaume L. Lemieux for their lab assistantship.

Special mention goes to Akshay Rawal and Sumit Kaila for their moral and social support throughout my studies. My time at Trois-Rivières, QC, Canada was made enjoyable in large part due to the many friends that became a part of my life. I have very fond memories of my time there and I would also like to mention my friends Manel Ghribi and Jessica Moisan for their accompanying personality.

Lastly, but by no means least, I am deeply thankful to my family for all their love, encouragement and sacrifices. For my mom and dad who raised me with a love of science and supported me in all my pursuits. And most of all for my loving, supportive, encouraging, and patient sister Lavi whose faithful support during this Ph.D. is so appreciated. Without them, this thesis would never have been written. Thank you.

February 26, 2018

## Abstract

Lignocellulosic biomass (LCB) is the most abundant, renewable and sustainable feedstock, allowing for our ever-increasing energy demand to be satiated as fossil fuels progressively disappear. The development of a viable bio-based economy, however promising, is ridden with challenges related to the cost-effective utilization of LCB, namely our imperfect understanding of biomass structure and suboptimal industrial processes. To achieve economic viability requires direct and rapid monitoring of lignocellulosic polymers as they are physically, chemically, and/or enzymatically treated. Unfortunately, such monitoring is difficult as current methods are non-specific, cumbersome, time-consuming, incompatible with on-site use and require the availability of specialized equipment and expertise. In this Ph.D. work, we have developed a novel, rapid, convenient, unambiguous and affordable monitoring approach named Fluorescent protein-Tagged Carbohydrate-binding modules Method (FTCM). This approach is based on the use of four highly specific probes composed of fluorescent-tagged carbohydrate-binding modules. The carbohydrate-binding module (CBM) component of these genetically modified probes recognizes and binds to biopolymers (*i.e.* mannan, xylan, crystalline and non-crystalline cellulose) while its specific fluorescent protein component makes it possible to quickly detect and measure the binding of each probe to their intended target. Throughout this Ph.D. study, FTCM was used to specifically track mechanical, chemical and enzymatically-induced variations of lignocellulosic polysaccharides at the surface of diverse wood fibers (*i.e.* wood pulps and agricultural crop residues). This monitoring approach was used to study 5 different objectives: 1) tracking xylan, a physical barrier which limits cellulose accessibility; 2) tracking enzymatic hydrolysis of lignocellulosic polymers; 3) tracking impact of wood fibers processing and correlating such impact with their strength properties; 4) predicting the most appropriate wood biomass for industrial applications; and 5) determining optimal biomass pretreatment strategies for biofuel production.

The FTCM approach allowed for rapid, unambiguous and high-throughput analysis of the enzymatic hydrolysis of lignocellulosic polymers, enzyme inactivation and the apparent

complementarity (additive and/or synergistic effect) between cellulase and other enzymes (xylanase and mannanase). Subsequent addition of cellulase, xylanase and mannanase enzymes provided cogent evidence regarding cell wall ultrastructure and its organization. Furthermore, FTCM efficiently monitored and predicted the impact of various treatments on the strength properties of wood pulps produced from such processed fibers. Monitoring fiber surface using FTCM also revealed that treatments with enzymes from *Trichoderma* were most appropriate for generating the crystalline cellulose from wood fibers for nanocellulose and composites applications (nanofibrillated cellulose). Moreover, a xylan specific FTCM probe enabled the highly sensitive detection of xylan variations at the surface of kraft wood fibers which can be applied where partial or complete xylan removal is required. Finally, clear and robust correlations were observed between cellulose accessibility by FTCM probes and enzymatic hydrolysis rates which can be evolved into a powerful prediction tool for the determination of optimal biomass pretreatment strategies for biofuel production.

This study proposes that the implementation of this simple, rapid and environmentally-friendly approach can revolutionize wood fiber processing and deconstruction within biomass industries, thereby substantially improving the cost-effectiveness of the production of bioenergy and other LCB-based products.

Keywords: Carbohydrate-binding module, Fluorescent protein, FTCM, Lignocellulosic biomass

# Résumé

La biomasse lignocellulosique est la matière première renouvelable qui est la plus abondante et qui pourrait combler les besoins énergétiques de l'humanité à mesure que les carburants fossiles disparaissent. Bien que prometteur, le développement de cette filière énergétique est pour l'instant mitigé à cause de notre compréhension limitée de la structure de la biomasse forestière et aussi à cause d'un manque d'efficacité des processus industriels associés à la production de bioénergie. En fait, l'impossibilité de suivre l'état des fibres lignocellulosiques en temps réel, pendant ou après divers traitements (physique, chimique et/ou enzymatique) mine notre capacité à atteindre des conditions qui soient économiquement positives. Bien sur il existe des méthodes pour étudier l'impact de ces traitements, mais ces méthodes manquent de spécificité, sont compliquées, demandent du temps et de l'expertise pointue, et sont incompatibles avec une utilisation en temps réel, sur un site industriel. Dans ce cadre nous avons développé une nouvelle méthode qui soit rapide, facile d'utilisation et spécifique qu'on a baptisé Fluorescent protein-tagged Carbohydrate-binding Method (FTCM). Cette méthode repose sur l'utilisation de quatre sondes faites d'une portion «carbohydrate-binding module» (CBM) et d'une protéine fluorescente (obtenues par fusion des gènes correspondants). Le module CBM se lie avec discrimination avec un type de polymère (parmi différentes versions de celluloses et d'hémicelluloses) tandis que la protéine fluorescente (de couleur variée) permet de suivre la liaison d'une sonde à la surface des fibres et ce, indépendamment des autres sondes. Dans cette étude, nous avons utilisé la FTCM pour étudier l'impact de traitements mécaniques, chimiques et enzymatiques sur les polymères de différentes fibres (pâte, papiers, résidus agricoles). Ceci nous a permis de nous attaquer à cinq objectifs: 1) détection du xylan, une barrière importante qui empêche d'accéder à la cellulose; 2) détection de l'hydrolyse des polymères lignocellulosiques; 3) étude de l'impact du traitement des fibres du bois et la corrélation de cet impact avec les propriétés papetières; 4) prédiction des meilleures applications possibles pour différentes biomasses forestières et 5) détermination de la meilleure stratégie de prétraitement pour la production de biocarburant à partir de différentes biomasses agricoles.

Tout au long de ce projet, nous avons démontré que la FTCM est rapide, spécifique, et utilisable en mode «haut débit» pour la détection de l'hydrolyse enzymatique des fibres, pour la détection de l'inhibition des enzymes pendant ce procédé et pour l'étude des synergies entre la cellulase et d'autres enzymes (xylanases, mannanases). L'ajout subséquent de ces différentes enzymes ont permis de révéler des détails de l'ultrastructure de la paroi cellulaire végétale et de son organisation. L'application de FTCM a non seulement permis de détecter l'impact de divers procédés industriels sur les propriétés physiques du papier, mais aussi permis de prédire cet impact avant de mesurer les propriétés. Pour des applications importantes comme la production de cellulose cristalline menant à des composites innovants, nous avons montré que le traitement des fibres avec les enzymes de *Trichoderma* était très approprié. D'autre part, la grande sensibilité des sondes pour la détection du xylan a permis de détecter les variations du xylan à la surface des fibres de bois traitées chimiquement (pâtes kraft) fort utile pour des applications où l'enlèvement partiel ou total du xylan est déterminant. Finalement, nous avons démontré une corrélation claire et solide entre l'accessibilité de la cellulose et l'efficacité des enzymes hydrolytiques. Cette corrélation pourrait être développée en un outil de prédiction et de suivi des procédés de prétraitement dans une usine de production de bioéthanol.

Cette étude permet de démontrer le potentiel de la méthode FTCM pour révolutionner l'industrie de la modification et de la déconstruction de la biomasse. En effet, l'adaptation de la FTCM en milieu industriel pourra augmenter de façon substantielle l'efficacité économique de la production de bioénergie à partir de biomasse lignocellulosique.

Mots-clé: Module de liaison aux hydrates de carbone («Carbohydrate-binding module»), Protéines fluorescentes, FTCM, Biomasse lignocellulosique

# Table of Content

# List of Figures

# List of Tables

## List of Additional Files

## List of Abbreviations

| | |
|---|---|
| ABX | Arabino-xylan |
| AC | Amorphous (non-crystalline) cellulose |
| AE | Alfalfa stover pretreated by alkali-extrusion |
| AFM | Atomic force microscopy |
| AGE | Affinity gel electrophoresis |
| AN | Alfalfa stover pretreated by alkali |
| AR | Raw alfalfa stover |
| AW | Alfalfa stover pretreated by liquid hot water |
| BSA | Bovine serum albumin |
| BKP | Bleached kraft pulp |
| BMP | Bleached mechanical pulp |
| CaE | Cattail stems pretreated by alkali-extrusion |
| CaN | Cattail stems pretreated by alkali |
| CaR | Raw cattail stems |
| CaW | Cattail stems pretreated by liquid hot water |
| CAZy | Carbohydrate active enzymes |
| CBM | Carbohydrate-binding module |
| CBM3a | Family 3a carbohydrate-binding module |
| CBM17 | Family 17 carbohydrate-binding module |
| CBM15 | Family 15 carbohydrate-binding module |
| CBM27 | Family 27 carbohydrate-binding module |
| CC | Crystalline cellulose |
| CC17 | mCherry fluorescent protein linked to a family 17 carbohydrate-binding module |
| CC27 | Cyan fluorescent protein linked to a family 27 carbohydrate-binding module |
| CFP | Cyan fluorescent protein |
| CMC | Carboxymethyl cellulose |
| CMCase | Carboxymethyl cellulase |

| | |
|---|---|
| CoE | Corn crop residues pretreated by alkali-extrusion |
| CoN | Corn crop residues pretreated by alkali |
| CoR | Raw corn crop residues |
| CoW | Corn crop residues pretreated by liquid hot water |
| CTM | Chemical-thermo-mechanical |
| DNS | 3,5-dinitrosalicylic acid |
| E | Alkali-extrusion pretreatment |
| eGFP | Enhanced green fluorescent protein |
| FE | Flax shives pretreated by alkali-extrusion |
| FN | Flax shives pretreated by alkali |
| FQA | Fiber quality analyzer |
| FR | Raw flax shives |
| FTCM | Fluorescent protein-tagged carbohydrate-binding module method |
| ft-CBM | Fluorescent-tagged recombinant carbohydrate-binding module |
| FTIR | Fourier transform infrared spectroscopy |
| FW | Flax shives pretreated by liquid hot water |
| GC | Gas chromatography |
| GC3a | Green fluorescent protein linked to a family 3a carbohydrate-binding module |
| GH | Glycoside hydrolase |
| HK | Hardwood kraft pulp |
| HM | Hardwood chemical-thermo-mechanical pulp |
| HPLC | High-performance liquid chromatography |
| IPTG | Isopropyl-β-D-thiogalactopyranoside |
| ITC | Isothermal titration calorimetry |
| LB | Luria-Bertani |
| LCB | Lignocellulosic biomass |
| mAbs | monoclonal antibodies |
| mCherry | Monomeric cherry |
| mOrange2 | Monomeric orange2 |

| | |
|---|---|
| N | Alkali pretreatment |
| NMR | Nuclear magnetic resonance |
| NREL | National renewable energy laboratory |
| OC15 | mono-orange2 fluorescent protein linked to a family 15 carbohydrate-binding module |
| PCR | Polymerase chain reaction |
| *p*NPG | 4-nitrophenyl-β-D-glucopyranoside |
| R | Raw lignocellulosic biomass |
| RAC | Regenerated amorphous cellulose |
| SDS-PAGE | Sodium dodecyl sulfate - polyacrylamide gel electrophoresis; |
| SEM | Scanning electron microscopy |
| SK | Softwood kraft pulp |
| SM | Softwood chemical-thermo-mechanical pulp |
| SSDA | Solid state depletion assay |
| TAPPI | Technical association of the pulp and paper industry |
| TEM | Transmission electron microscopy |
| UBKP | Unbleached kraft pulp |
| UBMP | Unbleached mechanical pulp |
| W | Liquid hot water pretreatment |
| XPS | X-ray photoelectron spectrometry |
| XRD | X-ray diffraction |

# Chapter 1 - Introduction

Global production of biofuels and bioproducts is increasing steadily, allowing our ever-increasing energy demand to be satiated while fossil fuels progressively disappear [1,2]. In addition, the greenhouse gas mitigation and near carbon neutrality afforded by the conversion of biomass to bioenergy (biofuel) and chemicals are important advantages over conventional fossil fuels [2]. Concomitantly, numerous new products and technologies based on the conversion of biomass have been developed over the last decade [3-5]. Securing sufficient biomass as raw materials is a prerequisite to moving from a petrochemical to a bio-based economy. Using food-based feedstocks, namely corn and sugar, to support first-generation biofuel and bioproducts has shown its limits and produces certain undesirable socio-economic and environmental outcomes [6,7]. The use of lignocellulosic biomass (LCB, including dedicated lignocellulosic crops, agricultural and forestry residues and municipal and industrial wastes), to produce second-generation biofuel and bioproducts would avoid the negative impacts associated with first-generation feedstocks use [8].

## 1.1 Lignocellulosic sources

LCB is the most abundant, renewable and sustainable feedstock. There are vast groups of lignocellulosic materials that are differentiated according to their origin, composition and structure. Forestland materials comprises woody biomass (hardwood and softwood) while grassland martials include agricultural residues (food or non-food crops) and grasses (switch grass, alfalfa, etc.). Municipal and industrial wastes, such as food waste and paper mill sludge, are also potential recyclable cellulosic materials [9-11]. The availability of biomass for bioenergy production is summarized in Table 1.1.

**Table 1.1** **Annual total tonnages of biomass for biofuel in the U.S. (U.S. Department of Energy Biomass Program)** (adapted from [9])

| Lignocellulosic biomass | Million dry tons/year |
|---|---|
| Forestry resources | 370 |
| Agricultural residues | 428 |
| Energy crops | 377 |
| Grains and corn | 87 |
| Municipal and industrial wastes | 58 |
| Algae Biomass | 46 |
| Total | 1320 |

### 1.1.1 Forest woody feedstocks

There are mainly two different types of woody feedstocks, namely softwood and hardwood. Softwood are conifers and gymnosperm trees which possess lower densities and grow faster [12]. Softwood trees include mostly evergreen species such as spruce, pine, cedar and redwood. In contrast, hardwood originate from mostly deciduous and angiosperm trees which comprise trees such as poplar, oak, cottonwood and aspen [13]. Unlike agricultural biomass, forest woody feedstocks offer high density, minimal ash content, flexible harvesting times and avoid long latency periods of storage [14].

### 1.1.2 Agricultural residues, herbaceous and municipal solid wastes

Agricultural crop residues mostly comprised of agricultural waste such as corn stover, corn stalks, sugarcane bagasse, rice and wheat straws. The use of agricultural residues is environmental friendly which minimize our dependence over forest woody biomass and thus reduce excessive deforestation. In addition, short-harvest rotation makes crop residues more consistently available than forest woody biomass for the production of bioenergy and various value-added by-products [15]. Aside from crop residues, switch

grass is the primary herbaceous grass and energy crop of interest due to their abundance, low-cost investment, diseases resistance and high yield of sugar per acre. Moreover, switch grass is fast-growing grass with little or no fertilization required. In addition, the utilization of municipal and industrial solid wastes limits various environmental problems associated with the disposal of municipal garbage and wood, textile and food industries waste and processing by-products. These biomasses contain relatively less lignin than woody feedstocks and thus they are less recalcitrant [9] (Table 1.1).

### 1.1.3 Algae biomass

Algae biomass is the most interesting third generation biofuel feedstock due to the rapid expansion of biorefineries which are leading to the shortage of current energy crops (switch grass and *Miscanthus giganteus*) designated for bioethanol industries [9]. Algae feedstock has a very high carbohydrate composition and is capable of yielding 10-60 times more alcohol than corn and soybeans per acre of land [16,17]. Unlike woody biomass and agricultural crop residues, algae biomass does not compete directly with food and does not require fresh water and agricultural land to be cultivated. In addition, algae also consume very high level of $CO_2$ and act as an environmentally friendly $CO_2$ sink [18]. On the other hand, one of the major disadvantage of algae biomass for biofuel production is the higher capital cost and the rather intensive care required by algal farming compared to conventional agricultural farming [18].

## 1.2 Lignocellulosic biomass composition

LCB is a complex structure consisting of cellulose (β-1,4-linked glucose polymer), hemicellulose (polysaccharide of varying composition) and lignin. Cellulose and hemicelluloses, which make up approximately 70% of the entire biomass, are tightly linked to the lignin via covalent and hydrogen bonds that makes LCB structure highly recalcitrant (Figure 1.1 and 1.2 [19]. Figure 1.2 illustrates a typical lignocellulosic wood fiber with its complex organization. Potential LCBes and their composition are summarized in Table 1.2 [9].

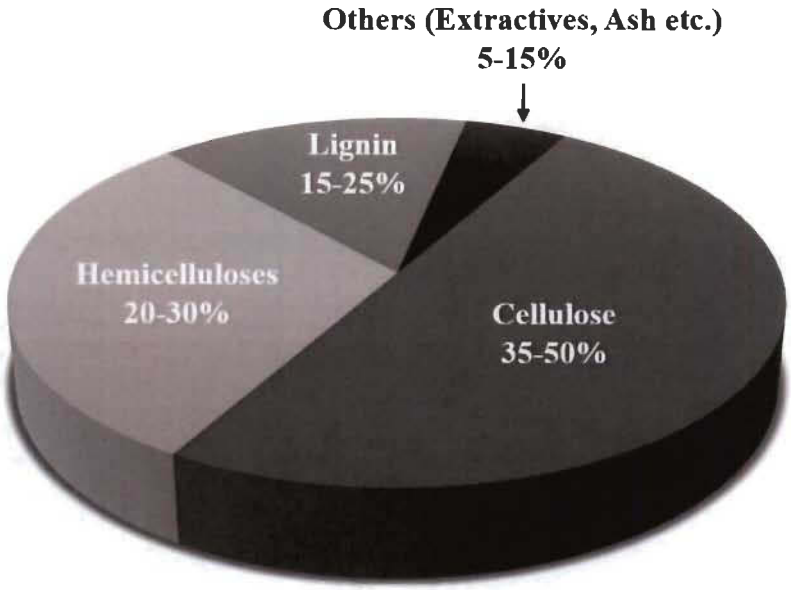


**Figure 1.1 General composition of lignocellulosic biomass feedstock**

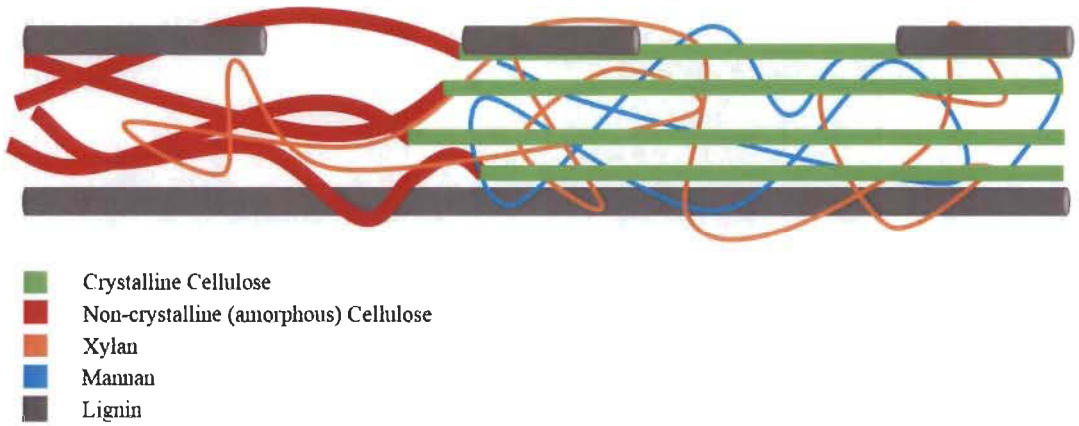


**Figure 1.2 Schematic representation of lignocellulosic wood fiber**

**Table 1.2** **Potential lignocellulosic biomass source and their composition (% dry weight)** (adapted from [9])

| Lignocellulosic biomass | Cellulose | Hemicelluloses | Lignin | Others (*i.e.*, ash) |
|---|---|---|---|---|
| Hardwood | 45-47 | 25-40 | 20-25 | 0.80 |
| Softwood | 40-45 | 25-29 | 30-60 | 0.50 |
| Agricultural residues | 37-50 | 25-50 | 5-15 | 12-16 |
| Grasses | 25-40 | 35-50 | - | - |
| Waste papers from chemical pulps | 50-70 | 12-20 | 6-10 | - |
| Newspaper | 40-55 | 25-40 | 18-30 | - |
| Switch grass | 40-45 | 30-35 | 12 | - |

### 1.2.1 Cellulose

Cellulose is the most abundant polysaccharide in nature and constitutes about 35-50% of the total LCB [20]. Cellulose is a linear polymer that consists of a long-chain of D-glucose subunits linked to each other by β-(1,4)-glycosidic bonds (Figure 1.3). The hydrogen bonds and van der Waals interactions packed long-chain cellulose polymers into microfibrils which give the cellulose more strength and compactness [21]. Cellulose in LCB is present in two different forms: highly ordered crystalline form (major proportion of cellulose) and a small percentage of unorganized non-crystalline (also known as amorphous) form. Cellulose has been shown to be more susceptible towards enzymatic degradation in its non-crystalline form [22]. In general, softwood and hardwood comprise approximately 45% of cellulose while cotton, flax and chemical pulp represent the purest sources of cellulose (80-95% and 60-80%, respectively) [9,23].

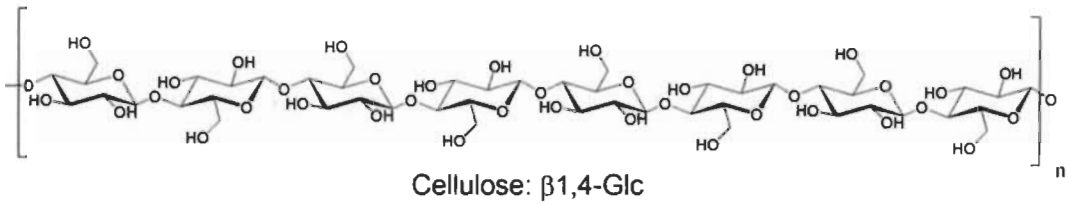


**Figure 1.3 Schematic representative structure of cellulose** [27]

### 1.2.2 Hemicellulose

Hemicelluloses, which represent about 20-30% of the total biomass, are the second most common polysaccharides [20,24]. Unlike cellulose, hemicelluloses are heterogeneous polymers of pentoses (xylose, arabinose), hexoses (mannose, glucose, galactose) and/or uronic acids (glucuronic acid, galacturonic acid) [19,25]. Hemicellulose in softwood (from gymnosperms) contains mostly glucomannans whereas in hardwood (from angiosperms) it mostly consists of xylan [26]. Xylan backbone is made up of β-(1,4)-linked D-xylose subunits that may include arabinan and glucuronic acid side chains (Figure 1.4A). In contrast, mannan comprises of β-(1,4)-linked D-mannose backbone with almost no branching (Figure 1.4B). Galactomannans have α-(1,6)-galactose branches linked to the β-(1,4)-mannose backbones. Glucomannans and galactoglucomannans contain both β-(1,4)-mannose and β-(1,4)-glucose backbones. In addition, galactoglucomannans have α-(1,6)-galactose branches linked to the mannose backbone [27]. The hemicelluloses distribution on the surface of wood fibers/cellulose fibrils is of utmost importance for the complex structure of LCB, since hemicelluloses have been proposed to act as a physical barrier which increases the stiffness of the cellulose fiber network by coating the rigid cellulose crystallites and forming links between the fibrils [28,29].

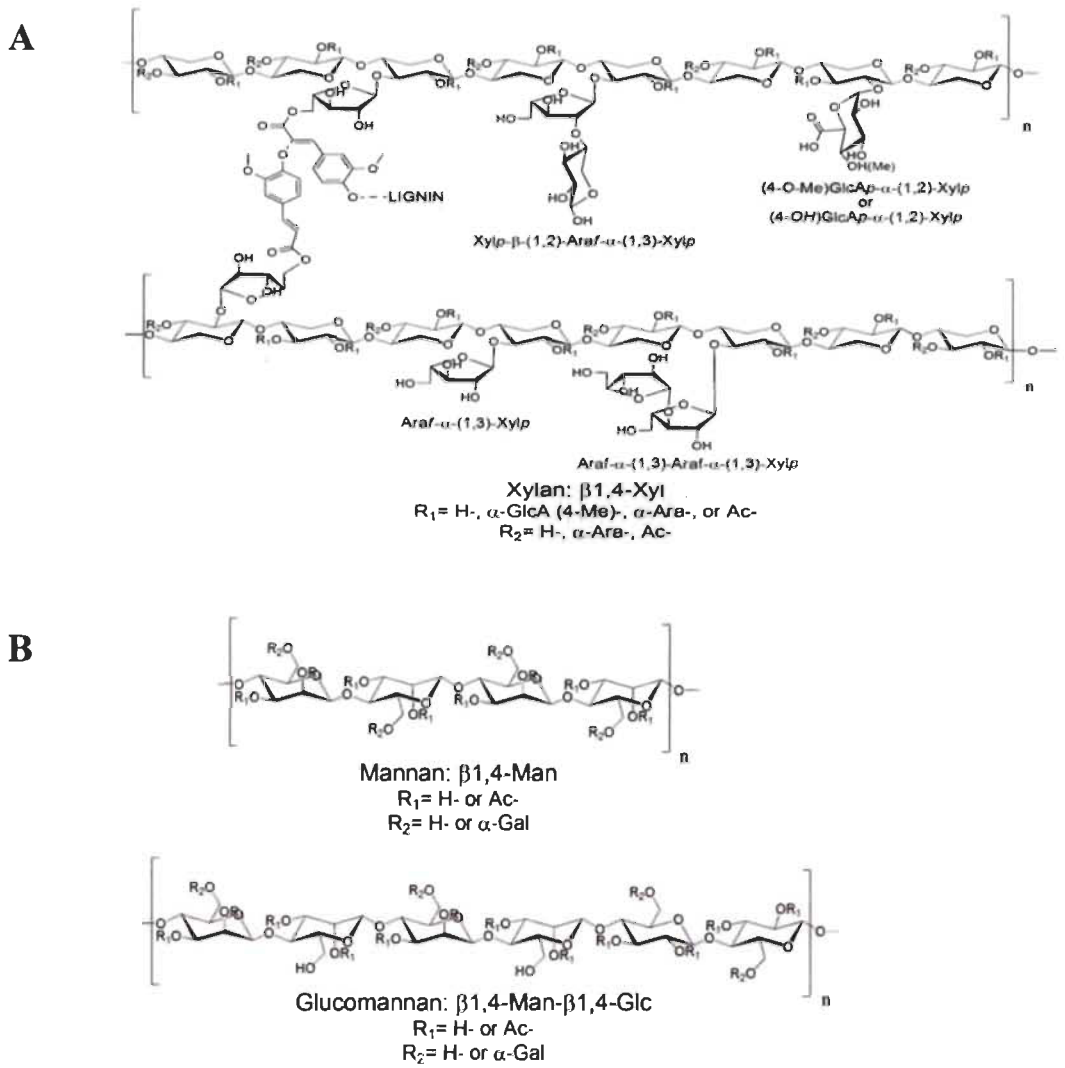


**Figure 1.4 Schematic representative structures of hemicelluloses. A) xylan and B) mannan** [27]

### 1.2.3 Lignin

Lignin is an aromatic biopolymer with an average molecular weight of 10,000 Da synthesized from phenylpropanoid precursors [30]. Lignin is covalently bond to the xylan and gives rigidity, impermeability, resistance against microbial attack and high level of compactness to the plant cell wall [31]. Lignin is composed of three different phenyl pro-

pionic alcohol: coniferyl alcohol (guaiacyl propanol), coumaryl alcohol (para-hydroxyphenyl propanol), and sinapyl alcohol (syringyl alcohol) (Figure 1.5). In general, herbaceous and agricultural residues contain the lowest amount of lignin (10-30% and 3-15%, respectively), whereas softwood contain highest level of lignin (30-60%) followed by hardwood (30-35%) [9,32]. Ladish *et al.* (2010) have demonstrated that lignin components, recovered from the biofuel process, can be used as a potential energy self-sustaining source to make current biorefineries more economical viable [33].

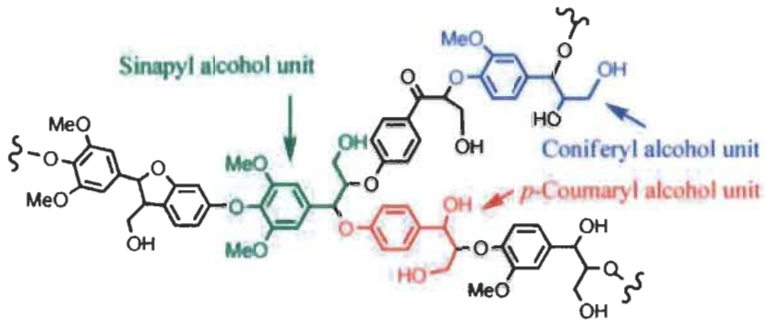


**Figure 1.5 Schematic representative structure of lignin** [32]

## 1.3 Lignocellulosic biomass recalcitrance

LCB is a promising, abundant and renewable resource of sugars for the production of biofuel [34,35]; however, its production has always been hindered by several economical and technical obstacles [28,36]. The main obstacle for biofuel and chemicals production is associated with the inherent recalcitrant nature of LCB [1,28,37-39]. The recalcitrance nature of cellulosic biomass translates into strong resistance against pathogens, enzyme/microbes, and/or chemicals, and is perceived to be mainly contributed by lignin (including its amount, location, and type (coniferyl vs. coumaryl vs. sinapyl)) [37,40-42]. Both macroscopic and microscopic barriers contribute to the plant cell wall recalcitrance (Figure 1.6 ). The macroscopic barriers involve species, tissue and cell wall heterogeneity while microscopic factors comprise lignin-carbohydrate cross linking and cellulose crystallinity. Due to this structural complexity of LCB (cellulose fibrils wrapped in a network

of lignin and hemicelluloses), the complete hydrolysis of its polysaccharides remains difficult. The network of lignin and hemicelluloses, collectively referred as the lignin-carbohydrate complexes, is highly recalcitrant and limit the access of cellulase to cellulose [34,37]. Consequently, several steps including pretreatments and enzymatic hydrolysis are needed to improve access to polysaccharides, mainly cellulose, before it can be used in value-added applications [43].

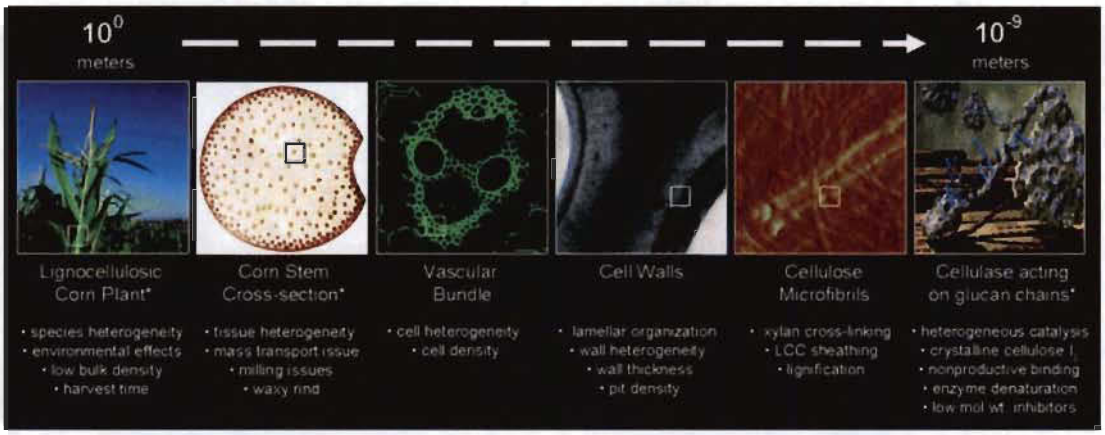


**Figure 1.6** **Plant cell wall recalcitrance, a multi scale phenomenon spanning several orders of magnitude encompassing both macroscopic and microscopic barriers** (adapted from [60])

### 1.3.1 Pretreatments

The main objective of pretreatments for subsequent biochemical conversion is to increase cellulose accessibility, which can later be hydrolyzed by enzymatic hydrolysis processes (Figure 1.7 ) [43]. However, pretreatments vary greatly in the way they help to expose cellulose. Physical pretreatments help reduce particles size and fiber crystallinity [44,45]; alkali (and acid) pretreatments remove lignin and hemicelluloses but can lead to loss of cellulose [46-48]; solvent fractionation leads to disruption of biomass components with lesser impact on lignin [49-51], while liquid hot water mainly removes hemicelluloses [29,52]. Because of the variety of lignocellulosic composition found among feedstocks, not all feedstocks require the same pretreatment [39,53].

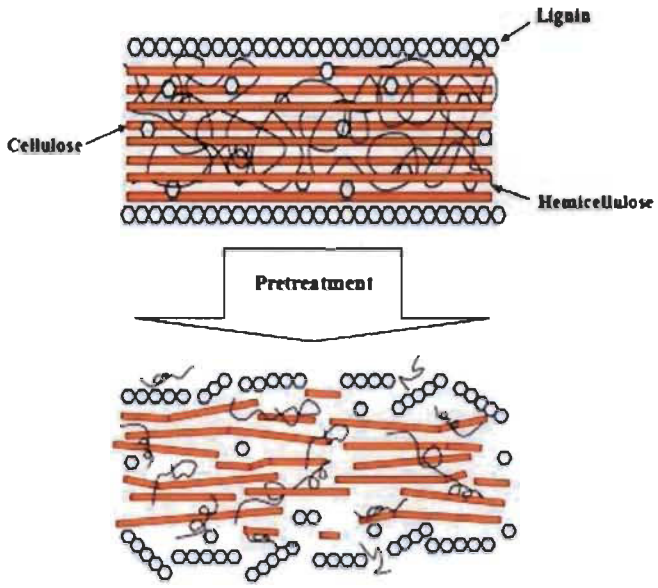


**Figure 1.7 Schematic representation of pretreatment of lignocellulosic biomass**

An in-depth understanding of the impact of a given pretreatment on a particular biomass is believed to be a key issue for reducing costs associated with biofuel production [54,55]. Pretreatment is the most important and costly step in biofuel production [56]. Accordingly, optimizing pretreatment is part of on-going development efforts that will help the competitiveness of LCB-derived ethanol. Furthermore, ideally, any variation in such impact (due to variation in feedstock properties, chemicals efficiency, mechanical wearing, changes in temperature and humidity) should be monitored on a continuous basis, or "on line" when feasible, in order to maintain optimal process operations. Currently no methodology allows for such on line monitoring.

### 1.3.2 Enzymatic hydrolysis

Due to the structural complexity of LCB, the bioconversion of biomass to biofuel is a multiple stage process [36,42]. The enzymatic hydrolysis of the lignocellulosic component to fermentable sugars is a crucial step in this bioconversion. It is considered as one of the major rate limiting and costly step [22,57-61]. Apart from lignin, the complex recalcitrance nature of biomass is partly attributed to hemicelluloses. As described earlier, hemicelluloses constitute about 20-30% of the total biomass, and are the second most

common polysaccharides [19,20,24] in nature, after cellulose. The hemicelluloses have frequently been recognized to act as a physical barrier that cover the outer surface of cellulose fibers and interfibrillar space, limiting the accessibility of cellulase enzymes to cellulose [62-70]. The hemicellulose-degrading activities in most commercially available cellulase enzymes are too low to achieve sufficient hydrolysis of the hemicelluloses [71,72]. Therefore, addition of enzyme extracts or additives with higher level of hemicellulases are important for eliminating the significant hindering effect of residual hemicelluloses (mostly xylan and mannan) on the enzymatic hydrolysis of cellulose [62,64,70,73-78]. Moreover, the inherent recalcitrance nature of plants directly or indirectly impacts enzyme accessibility [70,73], inactivation [79], inhibition [75,76,80-89] and, as a consequence, cost of use [62,90,91]. The recent improvement in enzymes stabilization, activity, cost-effectiveness [76,91,92-97] and development of new promising pretreatment conditions [50,98,99] improved enzyme-limited production yields. However, the high dose requirements of these enzymes often jeopardize commercial viability [62,77,79,100-103]. One way to better understand and control hydrolysis of LCB is to monitor the complex polymers composition of fibers at every stage of processing. Therefore, investigating biomass recalcitrance of typical wood biomass substrates, and correlating process parameters such as enzyme dosage, temperature, incubation time, inactivation and inhibition, with polymers hydrolysis efficiency is important.

Pulp and paper production is another LCB based industry which has to deal with the complexities described above. In addition, this industry faces immense pressure from the society and/or governments to move toward green chemistry. Biocatalysts (enzymes) are recognized as a key element of green chemistry and are being progressively introduced in a number of processes with extremely positive consequences for the environment [104,105]. An increasing number of enzymatic strategies are used by paper makers, including the application of hemicellulases enzymes in the pre-bleaching or bio-bleaching of kraft pulp. The presence of hemicelluloses, and their re-deposition on the surface of cellulose fiber during the kraft pulping of hardwood, inhibits the bleaching process. Hemicellulases enzymes have been found to be most effective for limiting this problem and

are now in use at several mills worldwide for biobleaching [26,62,104-106]. The use of enzymatic strategies has shown to improve the quality of end products thus minimize the capital investment related to the conventional bleaching processes [104]. Further, hemicelluloses are also known to contribute to fiber strength and their removal is known to influence pulp fiber properties [62,107,108]. Xylan and mannan are believed to contribute to physical properties of the paper by enhancing the inter-fiber bonding [107]. Here again, the close monitoring of hemicelluloses would help optimizing the enzymatic treatment, better control paper properties, and minimizing its cost.

## 1.4 Analytical methods for investigating biomass recalcitrance

The development of a bio-based economy, however promising, is faced with challenges related to the cost-effective utilization of the LCB. Improving biomass processes would increase cost effectiveness and competitiveness for large scale applications [1,90,91]. Therefore, in addition to pretreatments and enzymatic hydrolysis of hemicelluloses, it is considered to be highly important to utilize all wood fiber constituents (including hemicelluloses and lignin) in an economically feasible way (providing other valuable wood-derived materials beside biofuel) in order to increase the efficiency of wood fiber utilization. However, this requires a better understanding of the ultrastructure of the cell wall and its organization, which are not yet fully understood [60].

To date, different chromatographic, spectroscopic and microscopic analytical techniques such as compositional analysis (e.g., by NREL/TP-510-42618), X-ray photoelectron spectroscopy (XPS or ESCA) [109,110], atomic force microscopy (AFM) [111], scanning electron microscopy (SEM) [110], time-of-flight secondary ion mass spectrometry (ToF-SIMS) [110], gas chromatography (GC) [112], Fourier transform infrared spectroscopy (FTIR) [113], nuclear magnetic resonance (NMR) and compositional analysis methods [114,115] have been used to study pretreatments [60], lignin-carbohydrate complexes [73], polymers interactions [78] and plant cell wall deconstruction [60]. For instance, a compositional analysis method [115], provided by the National Renewable Energy Laboratory (NREL), is extensively used in the literature for the determination of

carbohydrates, lignin and ash contents for application in the second-generation biofuels production. In addition, microscopy (*i.e.* AFM, SEM, TEM), XPS and NMR were used to visualize and characterize the lignocellulosic plant cell wall deconstruction during pretreatments. These studies greatly enhance our understanding about the ultrastructure of plant cell wall and enzyme accessibility to cellulose [60]. Furthermore, an FT-IR study of softwood fiber (kraft pulp) dedicated to investigating the interactions between wood polymers revealed that glucomannan was closely associated to cellulose while there existed no mechanical interactions between xylan and cellulose [78]. Current models suggest that hemicelluloses play a major role in biomass recalcitrance and are closely associated with both lignin and cellulose, forming lignin-hemicellulose complexes and cellulose-hemicellulose complexes [73,78]. These techniques revealed important information on location and types of hemicelluloses and their influence on the recalcitrance nature of fibers, and improved our understanding of the structural arrangement of fibers. However, use of these methods for LCB analysis is laborious, requires specialized equipment, tedious sample preparation and long analysis time (typically hours for each sample) [116,117]. One of the major difficulties in studying biomass recalcitrance and process parameters is the lack of rapid, high throughput and reliable tools for monitoring and/or tracking lignocellulosic composition at the surface of wood fibers. In addition, current methods for tracking surface exposure of biomass are vague and are not compatible with industrial constraints. As a result, it is highly challenging to select a most efficient pretreatment for a given biomass and to tightly modulate processing variables such as the amount of enzymes used for removal (complete or selective) of a particular lignocellulosic component for process optimization.

Over the past decade, other techniques have been developed for the direct and rapid detection of LCB polymers. The use of chemical dyes to stain lignocellulosic biopolymers was one of the initial approaches for the detection of cellulose within various materials. Unfortunately, these dyes are rarely specific to cellulose [118]. In recent years, several *in situ* detection techniques have been developed, not only for cellulose but also

for other cell wall components, including hemicellulose and pectic polysaccharides detection [119]. Among these techniques, monoclonal antibodies (mAbs) have been used successfully for developmental studies of vegetal materials. However, antibodies targeting complex polysaccharides, made of crystalline and insoluble structures, are difficult to generate [118,120]. Somewhat like antibodies, carbohydrate-binding modules (CBMs) are nature's detection molecules that are highly specific towards their substrate polysaccharides. In addition, they have been shown to discriminate crystalline cellulose from non-crystalline cellulose [118,120]. The high specificity of CBMs toward lignocellulosic polymers and their cost of production make them more interesting as probes compared to mAbs [118-121].

## 1.5 Carbohydrate-binding modules

The molecular recognition of carbohydrates by proteins, such as carbohydrate-active enzymes (CAZymes), is vital for several biological processes, including cell-cell recognition, cellular adhesion and host-pathogen interactions. Many CAZymes are modular proteins with at least two distinct modules: the catalytic module and the CBM [122,123]. CBMs are the non-catalytic polysaccharide-recognizing module of CAZymes [121,124,125]. The CBM were originally defined as cellulose binding domains (CBDs), because the first example of these protein domains bound crystalline cellulose as their primary target [121,123]. Subsequently, the broader term CBM evolved to depict the diverse ligand specificity of these modules [124]. The CAZymes, such as glycoside hydrolases, glycosyltransferases, polysaccharide lyases, carbohydrate esterases, and auxiliary activities (redox enzymes that act in conjunction with CAZymes), with their polysaccharide-recognizing module (CBMs) are classified in the Carbohydrate Active enZymes (CAZy) database (http://www.cazy.org/). Briefly, the CAZy database describes the families of structurally related catalytic module and the CBMs (or functional domains) of CAZymes that degrade, modify, or create glycosidic bonds [121,124]. Most of the CBMs are an integral part of either bacterial or fungal glycoside hydrolases.

### 1.5.1 CBMs classification

Currently, CBMs are grouped into 83 different families, based on amino acid sequence homology, binding specificity and structure, in the CAZy (http://www.cazy.org/Carbohydrate-Binding-Modules.html) database [121,124]. These characterized CBMs display substantial variation in ligand specificity. Some CBMs recognize and bind to crystalline cellulose, non-crystalline cellulose, xylan, mannan, chitin and starch, while some CBMs display 'lectin like' specificity and bind to a variety of cell surface glycans. Thus, CBMs are excellent model systems for studying the mechanism of protein-carbohydrate recognition and have been used for numerous biotechnological applications [124].

#### 1.5.1.1 Protein fold classification

The catalytic modules of glycoside hydrolases are classified into 149 different families and 17 different clans or 'superfamilies' based on the criteria of conservation of protein fold and others, but there are currently no formal 'super' groupings of the 83 CBM families. According to the Boraston *et al.* (2004) besides amino acid similarity classification, CBMs can also be classified into 7 'fold families' (Table 1.3 and Figure 1.8) conferring to their protein fold and tridimensional structure [124]. The dominant fold among the CBMs, in terms of total number of families and entries in CAZy database, is the β-sandwich fold (fold family 1). This fold comprises two β-sheets, each consisting of three to six antiparallel β-strands. Almost all the CBMs with β-sandwich fold have at least one bound metal atom, except for CBM2a from *Cellulomonas fimi* xylanase 10A. The second most frequent fold among the CBMs is β-trefoil fold (fold family 2). This fold is characterized by twelve strands of β-sheet, forming six hairpin turns [121,124].

**Table 1.3** **CBM fold families** (Adapted from [121,124])

| Fold Family | Fold | CBM families |
|---|---|---|
| 1 | β-Sandwich | 2, 3, 4, 6, 9, 11, 15, 16, 17, 20, 21, 22, 25, 26, 27, 28, 29, 30, 31, 32, 33, 34, 35, 36, 40, 41, 42, 44, 47, 48, 51, 70 |
| 2 | β-Trefoil | 13,42 |
| 3 | Cysteine knot | 1 |
| 4 | Unique | 5,12 |
| 5 | OB fold | 10 |
| 6 | Hevein fold | 18 |
| 7 | Unique; contains hevein-like fold | 14 |

Among these twelve strands, the six strands form a β-barrel structure associated with three hairpin turns. The remaining three hairpin turns form a triangular cap on one end of the β-barrel called the 'hairpin triplet'. Each trefoil domain, as defined by Boraston *et al.* (2004), contributes one hairpin (two β-strands) to the β-barrel and one hairpin to the hairpin triplet [124]. The members of cysteine knot (fold family 3), unique (fold family 4), OB (oligonucleotide/oligosaccharide binding) fold (fold family 5), hevein fold (fold family 6) and hevein-like fold (fold family 7) are small 30-60 amino acids polypeptides. The members of families 3-5 comprises only β-sheet and coil. Further, the members of families 6 and 7 contains mainly coil, but also have two small β-sheets and a small region of helix (121,124).

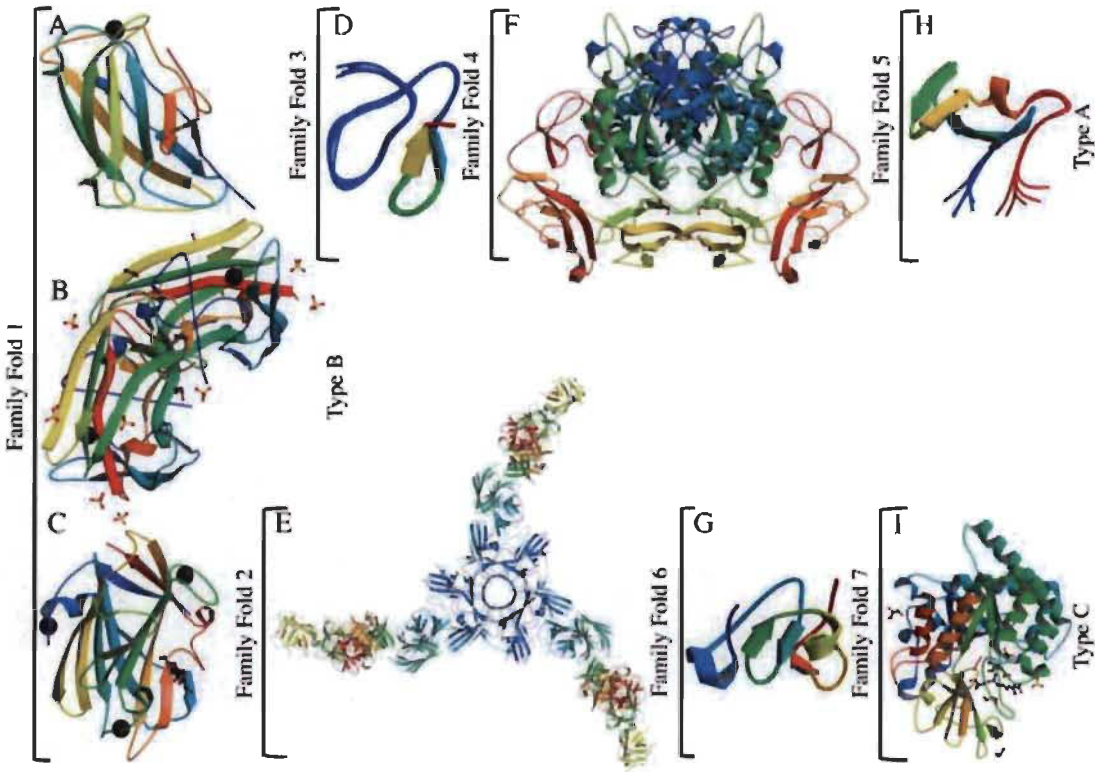


**Figure 1.8 CBM fold families and functional types (CBMs represented as ribbon structures, assumed biological molecule)**

CBMs shown are as follows: (A) family 3 CBM from *Clostridium thermocellum* (*Ct*CBM3), PDB code 4B9C; (B) family 4 from *Clostridium thermocellum* (*Ct*CBM4), PDB code 3P6B; (C) family 9 from *Thermotoga maritima* (*Tm*CBM9), PDB code 1I82; (D) family 1 CBM from *Trichoderma reesei* (*Tr*CBM1), PDB code 4BMF; (E) family 13 from *Clostridium botulinum* (*Cb*CBM13), PDB code 3WIN; (F) family 5 from *Moritella marina* (*Mm*CBM5), PDB code 4HMC; (G) family 18 CBM from *Triticum kiharae* (*Tk*CBM18) PDB code 2LB7; (H) family 10 CBM from *Cellvibrio japonicus* Ueda107 (*Cj*CBM10), PDB code 1E8R; (I) family 14 CBM from *Homo sapiens* (*Hs*CBM14) PDB code 1WAW (adapted from [121]).

### 1.5.1.2 Structural and functional classification

The protein fold classification of CBMs is based on the conservation of the protein fold and are not predictive of their function. Thus, CBMs are further classified into three

types A, B and C, based on three-dimensional structure and functional similarity. Type A or 'surface-binding' CBMs recognize and bind to the surface of insoluble, highly crystalline cellulose and/or chitin with little or no affinity for soluble polysaccharides [126]. Type A CBMs binding sites exhibits a planer architecture, which compliments the flat surfaces of cellulose or chitin crystals [127,128]. Type B or 'glycan-chain-binding' CBMs recognize and displays high affinity towards the hexasaccharides and show no interaction with oligosaccharides with a degree of polymerization of three or less. The binding site architecture of Type B CBMs displays grooves or clefts, and comprise several subsites able to accommodate the individual sugar units of the oligosaccharides (Figure 1.9 and 1.10). Type C 'small-sugar-binding' CBMs are identified as binding modules that recognize terminal (*exo*-type) glycans such as mono-, di- or tri-saccharides. The binding site architecture of Type C CBMs lacks the extended binding site grooves of Type B CBMs [125,129].

### 1.5.2 Structural determinants of CBMs binding specificity

The binding-site topography is a key determinant of binding specificity of CBMs. One of the major factor for varying binding-site topography is the aromatic amino acid side chains of tryptophan, tyrosine and phenylalanine. The aromatic amino acid side chains interaction with ligand is ubiquitous to CBM polysaccharide recognition. The side chain form hydrophobic platforms in CBM-binding sites, which can be planar, twisted, or sandwich (Figure 1.11). The 'planar' platforms of aromatic amino acid side chains are a hallmark of Type A CBMs (Figure 1.11A) while 'twisted' and 'sandwich' binding-site platforms are common in Type B CBMs and accommodate the conformations of soluble oligosaccharide ligands (Figure 1.11B and C) [124].

### 1.5.3 CBMs functions

CBMs play a central role in the optimization of the catalytic activity of plant cell wall hydrolases by their specific binding to plant polysaccharides. The CBMs present in most CAZymes are believed to have one or more of the following functions with respect to the function of their associated catalytic modules: proximity effect, substrate targeting and disruptive function.

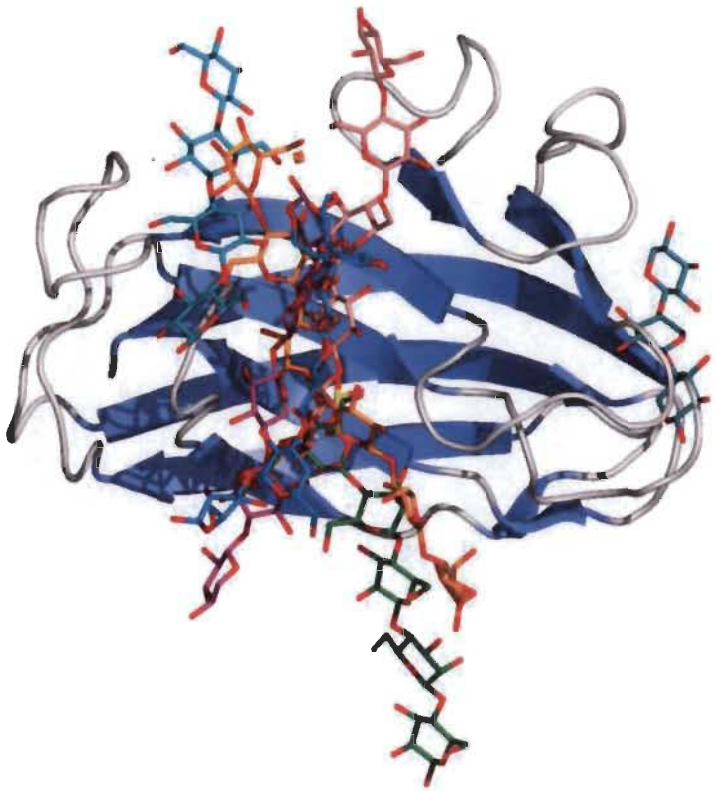

**Figure 1.9 Schematic diagram showing the location of binding sites in the β-sandwich Type B CBMs**

This figure was produced by overlapping the C-$\alpha$ carbons for all the β-sandwich Type B CBMs for which ligand bound complexes were available. Only the ribbon structure of the family 4 CBM from the N-terminus of Cel9B from *Cellulomonas fimi* is shown as a representative β-sandwich Type B CBM. Oligosaccharide ligands are shown in 'liquorice' representation and colored as follows: cyan, cellotetraose from *Cc*CBM17 (PDB code 1J84); blue, laminariohexaose from *Tm*CBM4-2 (PDB code 1GUI); pink, cellopentaose from *Cf*CBM4-2 (PDB code 1GU3); marine/aqua, xylotriose from *Cs*CBM6-3 (PDB code 1NAE); orange, cellohexaose from *Pe*CBM29-2 (PDB code 1GWM); green, mannopentaose from *Tm*CBM27 (PDB code 1OF4); purple, xylopentaose from *Cj*CBM15 (PDB code 1GNY) (adapted from [124]).

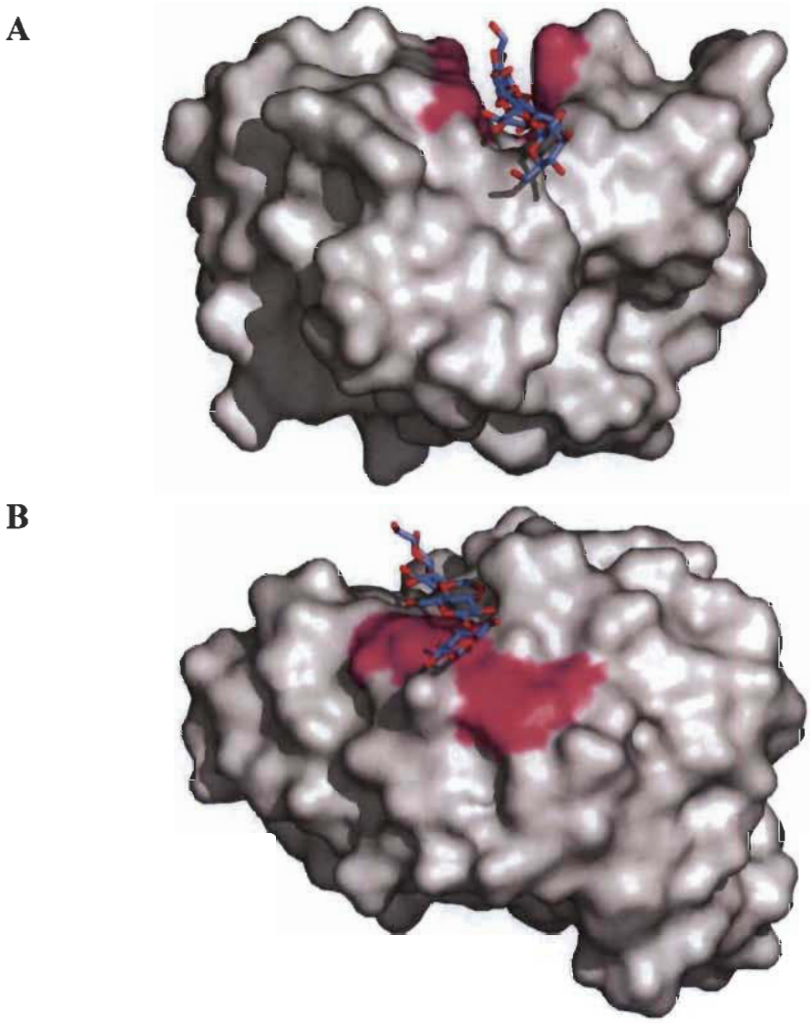


**Figure 1.10 Solvent-accessible surface representation of two CBMs showing the depth of binding grooves in Type B CBMs**

(A) Example of a cellopentaose molecule occupying a deep binding groove in *Cf*CBM4-2 (PDB code 1GU3). (B) Example of a cellotetraose molecule occupying a shallow binding groove in *Cc*CBM17 (PDB code 1J84). The surfaces created by the aromatic amino acid side chains involved in binding are shown in magenta (adapted from [124]).

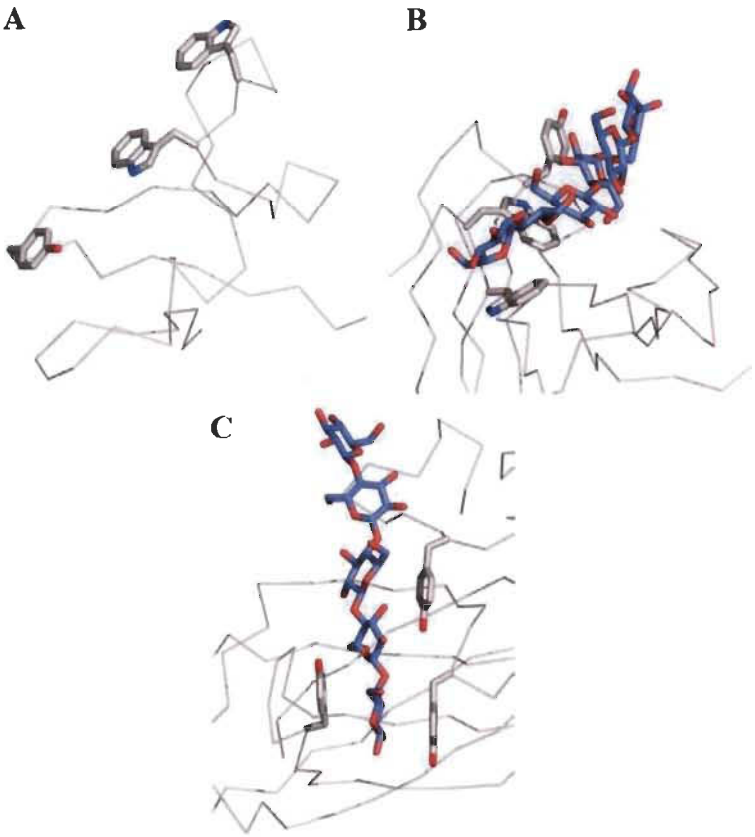


**Figure 1.11 The three types of binding-site 'platforms' formed by aromatic amino acid residues** (adapted from [124])

(A) The 'planar' platform in the family 10 Type A CBM, *Cj*CBM10. (B) The 'twisted' platform of the Type B family 29 CBM, *Pe*CBM29-2. (C) The 'sandwich' platform of the Type B family 4 CBM, *Cf*CBM4-2. The C-α backbone is shown as grey cylinders, the aromatic amino acid side chains forming the binding sites are shown in grey 'liquorice' representations, and the bound oligosaccharide are shown in blue 'liquorice' representation.

The CBMs recognize and bind to the accessible sites on a polysaccharides substrate to form a complex via specific, non-covalent, thermodynamically favorable bonds [122,130]. Consequently, the CBMs promote the association of the enzyme with the substrate to secure a prolonged contact and effectively increase the enzyme concentration on the surface of the substrate thus enhancing enzymatic activity (the so-called proximity

function) [121,122,124]. Numerous studies have shown that removal of CBM decreases the hydrolytic activity of the catalytic domain on insoluble, crystalline substrate, whereas their activity on soluble, non-crystalline cellulose remains mostly unaffected [59,131,132].

CBMs are highly specific towards their substrate and able to recognize different polysaccharides such as crystalline cellulose, non-crystalline cellulose and cello-oligosaccharides (the so-called substrate targeting function). The substrate targeting effect of the CBMs has been studied extensively and used in various biotechnological applications, namely protein-carbohydrate interaction mechanism and as molecular probes for various polysaccharides localization, tracking and quantification [121].

In addition, some CBMs isolated from both bacteria and fungi have been proposed to facilitate cellulose hydrolysis by disrupting the fibrous cellulosic network thus increasing the substrate accessibility (the so-called disruptive function). In recent studies, the CBMs have been shown to promote non-hydrolytic disruption of crystalline cellulose by weakening and splitting the hydrogen bond in the cotton fibers [133,134] and reducing the interfiber interaction in Whatman CF11 cellulosic fibers [135].

The proposed mechanism of amorphogenesis of cellulose fibers starts with the adsorption of the CBM at cellulose micro-cracks or defects (disturbance in the crystalline structure of cellulose) (Figure 1.12A), followed by the penetration of CBM into the interfibrillar space. This induce a mechanical pressure on the cellulose micro-cracks, swelling the cellulose structure and accommodating water molecules within the micro-cracks (Figure 1.12B). The mechanical pressure aids water molecules to penetrate further into the interfibrillar space, breaking the hydrogen bonds, resulting in the disassociation of the individual microfibrils (Figure 1.12C). This consequently helps catalytic domain of the glycoside hydrolase for cellulose hydrolysis. The adsorbed enzyme also prevents the realigning and re-adhering of the cellulose chains [122,136-140].

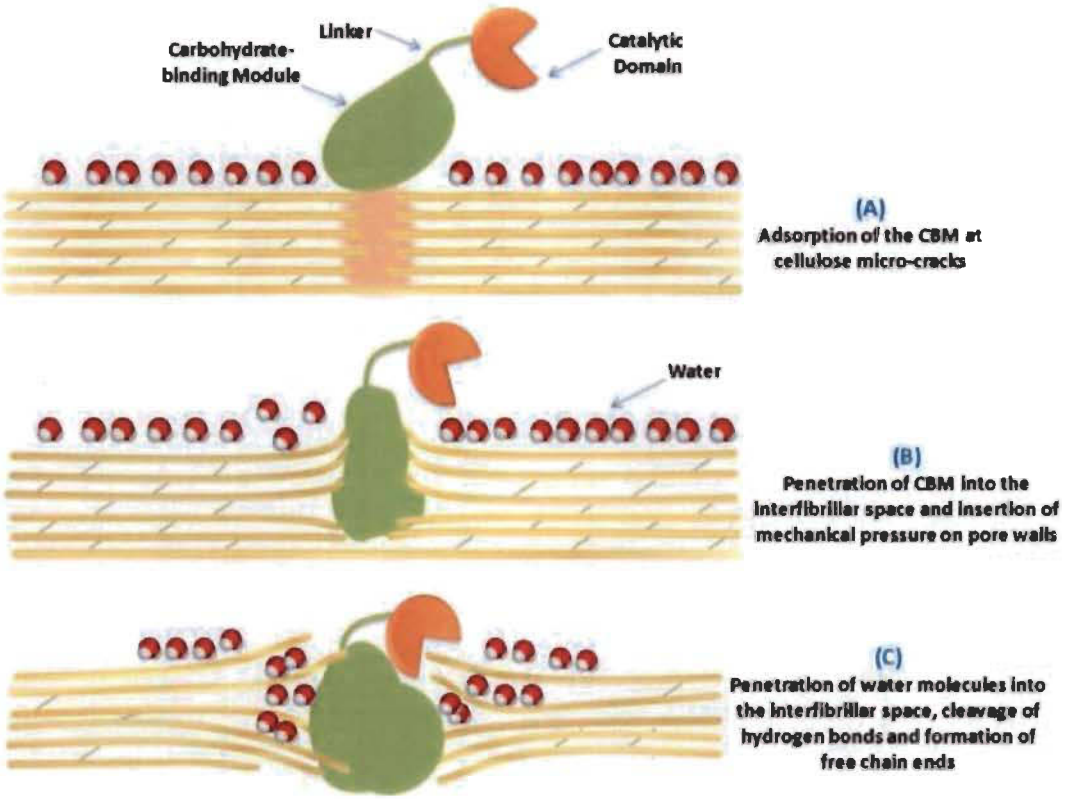


**Figure 1.12 Schematic representation of amorphogenesis of cellulose fibers mediated by the carbohydrate-binding module (CBM) of cellobiohydrolase I (CBHI)**

For clarity, the carbohydrate-binding module is oversized compared with the catalytic domain (adapted from [122]).

Although the functions of CBMs during the enzymatic hydrolysis of polysaccharides are still partly unclear and that consequently more research is needed, it is well understood that the primary role of a CBM is to anchor the catalytic module of the glycoside hydrolase to polysaccharide [141].

### 1.5.4 Applications of CBMs

In recent years, CBMs have been used for several applications related to biomedicine, environment, molecular biology, microarrays, paper, textile, food and biofuel industries [142] (Figure 1.13). There are three basic properties of CBMs which contributes

to their compatibility for the applications mentioned above: (1) CBMs are independent folding modules and can function autonomously in a chimeric protein; (2) CBMs are diverse, abundant, highly substrate specific and inexpensive (in terms of their production and purification as both wild type and recombinant proteins) with excellent chemical and physical properties; and (3) the binding specificities and affinities of CBMs can be, in principle, controlled according to an existing problem (using directed evolution for instance) [121,124,142].

#### 1.5.4.1 Bioprocessing

One of the major applications of CBMs is in bioprocessing of biologically active molecules for various biotechnological applications. CBMs have been studied and used as high-capacity purification tags for the isolation, production and purification of biologically active target peptides and proteins at relatively low cost. Numerous other reports have also shown CBM as an affinity tag for enzyme immobilization and processing. Another area of CBMs bioprocessing application includes enhanced bioethanol production from cellulosic materials. A study by Berdichevsky *et al.* showed that a CBM could be used for matrix-assisted refolding of a single-chain antibody in order to prevent the aggregation of protein during the course of renaturation [143]. In another study, a CBM fused to single chain antibody increased the efficiency of the phage display screening process for recombinant antibodies [144].

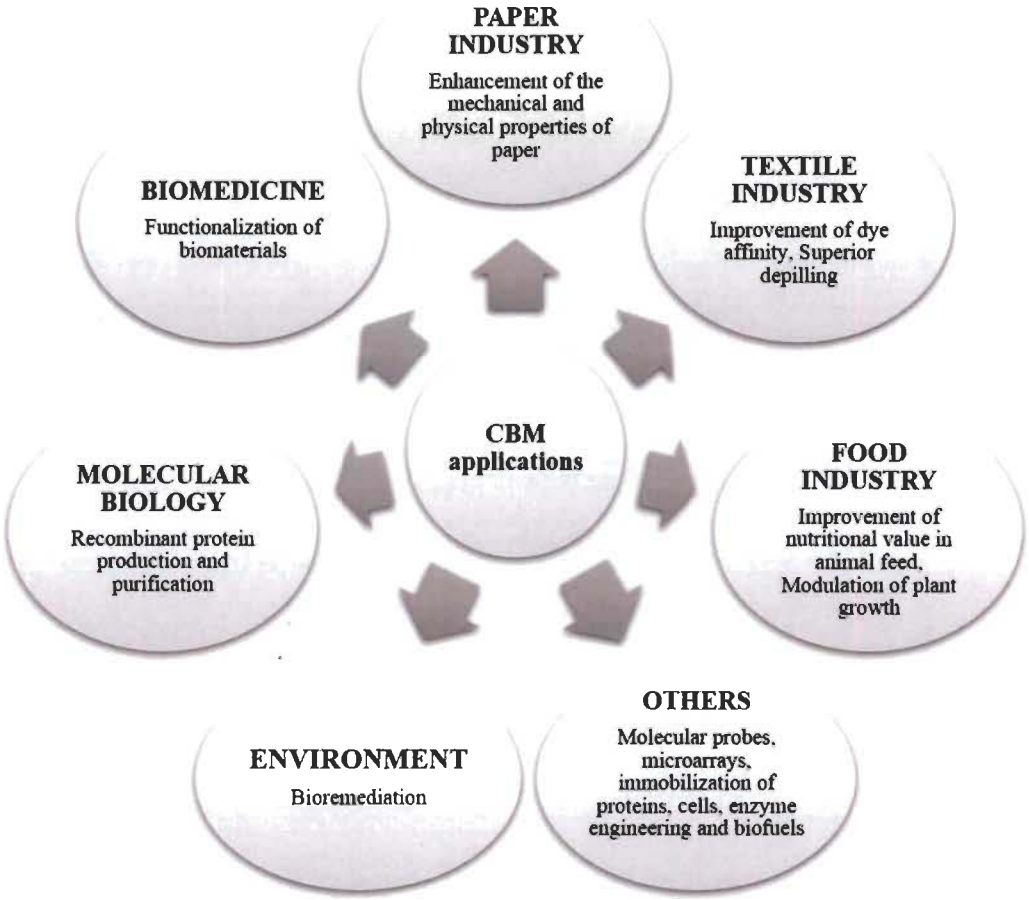


**Figure 1.13 CBMs applications** (adapted from [121])

### 1.5.4.2 Targeting

Cellulose is the most abundant and renewable substrate with various commercial applications. Therefore, CBMs can be used for targeting desired functional molecules to the substrate containing cellulosic fibers, such as cotton fibers in the textile industries. CBMs have been used extensively for the denim washing, an alternative to the original abrasive stonewashing and laundry powders for targeting recombinant enzymes (amylases, proteases and lipases) and fragrance particles to the cellulosic fibers [145,146].

### 1.5.4.3 Cell immobilization

CBMs have been used efficiently for the cell immobilization technology for various applications including ethanol production and phenol degradation. CBMs were also used for immobilization of mammalian cells to a cellulosic surface for improving the performance of vascular graft [147] and cartilage regeneration [148].

### 1.5.4.4 Bioremediation

CBMs have been studied and shown to be an excellent mediator for the bioremediation of the pollutants. They have been used as recombinant proteins for the removal of toxic heavy metals such as cadmium [149] and a commonly used pesticide atrazine [150] from water. These findings have shown strong potential for the improvement of sustainable wastewater treatment technologies [151].

### 1.5.4.5 Analytical tool

Many studies have been using CBMs as analytical tools for research and diagnostics of cellulosic fiber surface. McCartney *et al.* [152] and Jamal-Talabani *et al.* [153] developed novel molecular CBM probes for the detection, characterization and mapping of plant cell wall polysaccharides. The CBMs were also used in the optimization of the bioprocesses such as fermentation [154], rapid detection of the pathogenic microbes in food samples [155] and production of CBM based non-DNA microarrays for various medical applications [156].

### 1.5.4.6 Modification of fibers

The CBMs have also been used for the modification of cellulosic fibers in the paper and textile industries [157-159]. A recombinant CBM3 conjugated with polyethylene glycol (PEG) has shown to improve the drainability of the wood pulps without affecting the physical properties of the paper sheets [160]. The recombinant CBMs were also applied to Whatman filter paper and it was found to enhance its mechanical properties, such

as tensile strength, brittleness, Young's modules and paper dry strength. Moreover, a recent study by Shi *et al.* (2014) demonstrated that the use of recombinant double CBMs, such as CBM1-NL-CBM1, significantly enhanced the mechanical properties of pulp and papers [161]. Additionally, CBMs were also successfully used for the scouring process, one of the most important process determining the fabric quality, to remove the cutical layer of cotton fibers and increasing the efficiency of the process [162].

### 1.6 Fluorescent protein-tagged CBMs

Fluorescence is a very sensitive and specific spectroscopy where absorption and emission wavelengths determine what molecules contribute to the detected signals [125,163]. Further, plate readers allow increasing measurement throughput, a valuable criterion in the development of any novel assay. Hence, detection of CBM probes that would emit fluorescence would be advantageous. Fluorescence detection can be achieved directly or indirectly depending on the methods used [118]. The indirect methods involve the use of a secondary or tertiary reagent such as anti-His-IgG coupled to a fluorophore to detect the His-tag of a CBM, which may also allow amplification of signal intensities. This method provides great flexibility in CBM use but has a potential disadvantage related to multi-step incubations, which decrease analysis speed and are less compatible with a high throughput strategy [118]. On the other hand, in direct methods, coupled CBMs would require a straightforward, single-step incubation, affording the possibility of rapid, high throughput protocols. In the first direct method reported, a CBM was chemically coupled with a fluorophore (such as FITC/Alexa Fluor) [118]. Unfortunately, these molecules react non-specifically with various moieties at the surface of CBMs, deleteriously affecting specificity, affinity and detection reproducibility. Another direct detection method uses CBMs genetically fused to a fluorescence protein such as the green fluorescent protein (or any of its variants) [118]. This method allows maintenance of the original CBM behavior, avoiding the limitations described for the first direct method discussed. Hence, CBMs coupled with fluorescence protein have been used for mapping the chemistry and structure of various carbohydrate-containing substrates (*i.e.* LCB) [164,165]. The production and purification of these fluorescent protein-tagged carbohydrate-binding

modules is part of a broader 'recombinant CBM-fusion technology', which has been used to obtain CBMs fused with other proteins for specific applications. Recombinant CBMs can either be produced in heterologous organisms (*Escherichia coli* and *Pichia pastoris*) or in the CBM's original host. Figure 1.14 illustrate the recombinant CBM-fusion technology from cloning to applications [121].

### 1.6.1 Fluorescent protein

#### 1.6.1.1 Green fluorescent protein (GFP)

GFP, the famous chemiluminescent protein, was discovered by Shimomura *et al.* [166] from *Aequorea* jellyfish. GFP is an 11-stranded β-barrel structure threaded by an α-helix running up the axis of the cylinder, which is also known as β-can (Figure 1.15). The ability of fluorescent proteins to emit visible light derives from the post-translational modification of three amino acids at positions 65-67 (Ser-Tyr-Gly in the native protein), which result in chromophore formation. The chromophore, a *p*-hydroxybenzylideneimidazolinone, is attached to the α-helix and is buried in the center of the cylinder. Figure 1.16 shows the mechanism for chromophore formation. First, GFP folds into a nearly native conformation, then the imidazolinone is formed by nucleophilic attack of the amide of Gly67 on the carbonyl of residue 65, followed by dehydration. Finally, molecular oxygen dehydrogenates the α-β bond of residue 66 to put its aromatic group into conjugation with the imidazolinone. Only at this stage the chromophore acquires visible absorbance and fluorescence. The β-can structure protects the chromophore and is presumably responsible for GFP's stability [167]. Figure 1.17 and Table 1.4 describes the different classes of green fluorescent proteins and their properties [168].

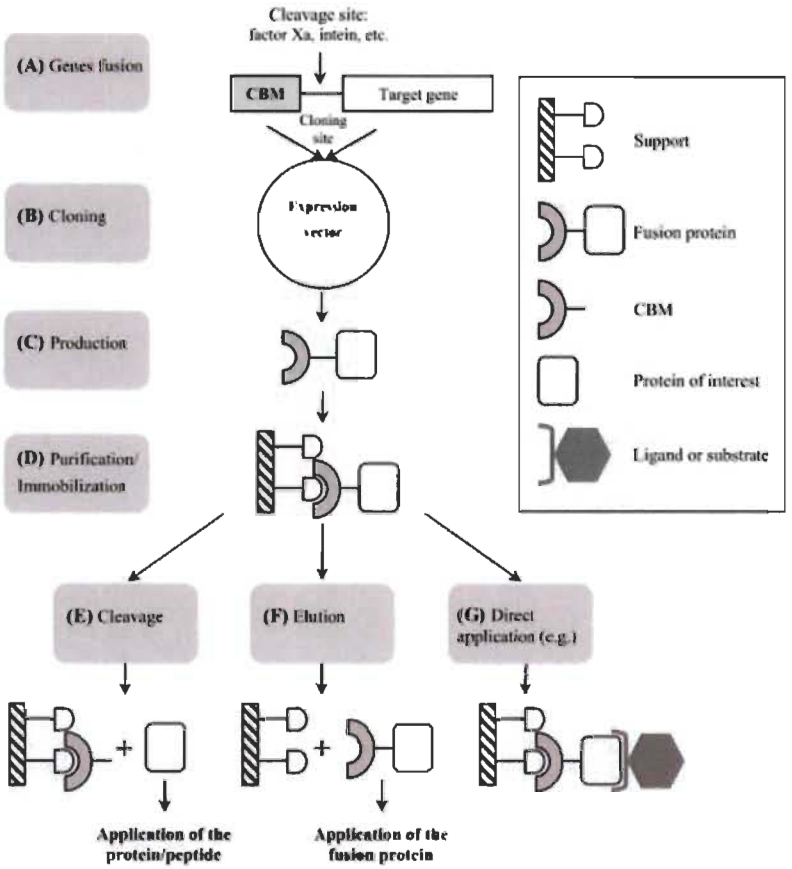


**Figure 1.14 Schematic representation of the recombinant CBM-fusion technology, from cloning to application**

(A) Gene fusion between CBM and a gene of interest. CBM can either be cloned at the C-terminal or N-terminal of the target gene (the N-terminal fusion is represented). (B) Transformation of ligated plasmid vector into a prokaryotic or eukaryotic expression system. (C) Overexpression of the recombinant protein. (D) Purification/immobilization of the fusion protein. (E) The immobilized protein is released from CBM and support by proteolytic cleavage of the engineered sequence located between the CBM and the protein (application of CBM-free protein or peptide). (F) The fusion protein is eluted from support for further application. (G) The immobilized fusion protein is directly used by the addition of a ligand or a substrate (adapted from [121]).

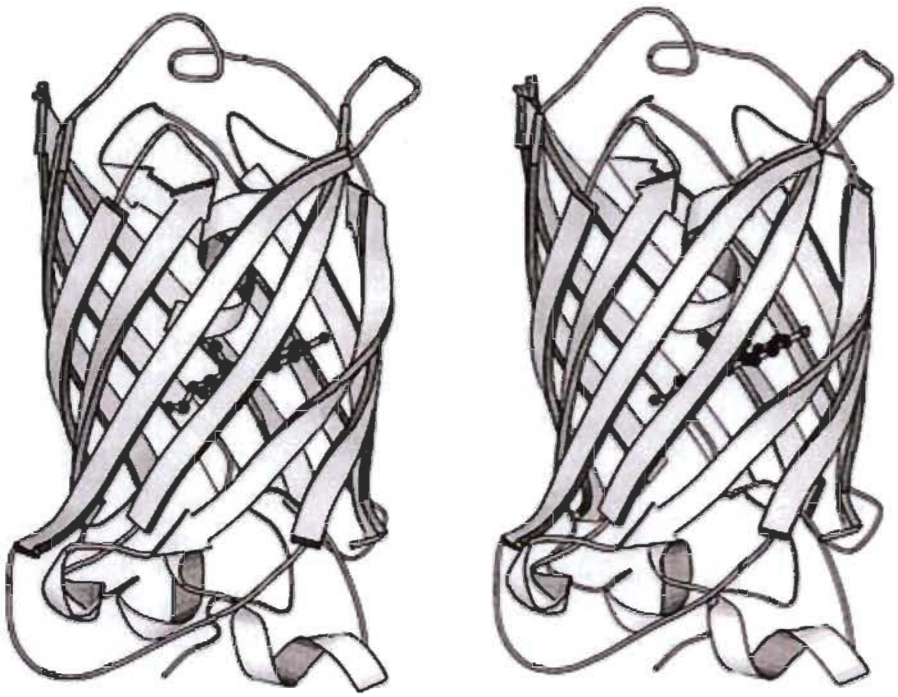

**Figure 1.15 The three-dimensional structure of GFP**

Showing 11 β-strands forming a hollow cylinder through which is threaded a helix bearing the chromophore, shown in ball-and-stick representation (adapted from [167]).

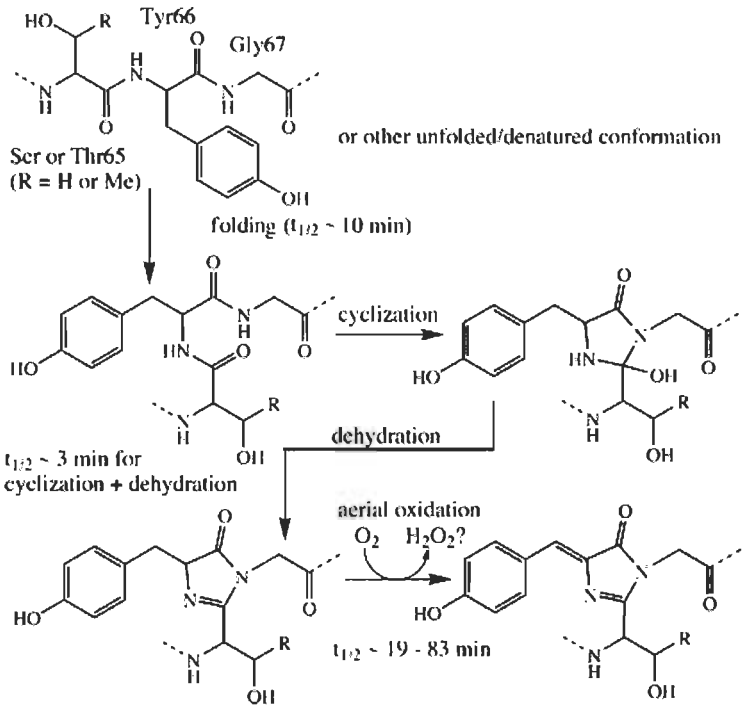


**Figure 1.16 Mechanism for the intramolecular biosynthesis of the GFP chromophore** (adapted from [167])

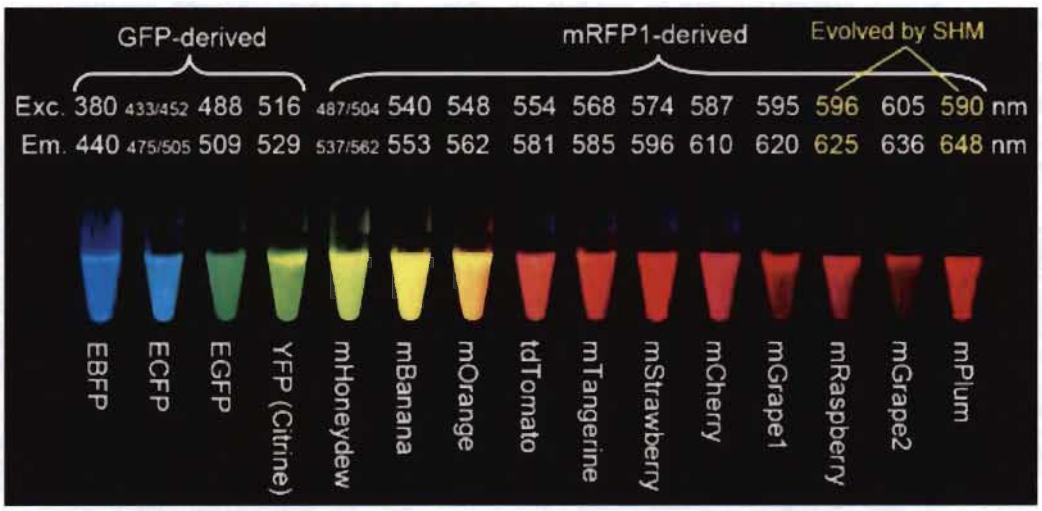


**Figure 1.17 Fluorescent proteins**

"SHM" stands for 'somatic hypermutation', "E" stands for enhanced versions of GFP and "m" identify monomeric proteins (adapted from [169]).

**Table 1.4 Spectral characteristics of the major classes of green fluorescent proteins (GFPs)**

| Class | Protein | Excitation (nm) | Emission (nm) | Brightness | Photostability | Oligomerization |
|---|---|---|---|---|---|---|
| Red | mCherry | 587 | 610 | 16 | 96 | Monomer |
| | mStrawberry | 574 | 596 | 26 | 15 | Monomer |
| Orange | mOrange | 548 | 562 | 49 | 9 | Monomer |
| | mKO | 548 | 559 | 31 | 122 | Monomer |
| Yellow-green | mCitrine | 516 | 529 | 59 | 49 | Monomer |
| | EYFP | 514 | 527 | 53 | 15 | Weak dimer |
| Green | Emerald | 487 | 509 | 39 | 0.69 | Weak dimer |
| | EGFP | 488 | 507 | 34 | 174 | Weak dimer |
| Cyan | CyPet | 435 | 477 | 18 | 59 | Weak dimer |
| | mCFPm | 433 | 475 | 13 | 64 | Monomer |

(adapted from [168])

Nowadays, GFP is a commonly used protein as a biological marker tool in molecular biology, medicine, and cell biology. The major advantage of using GFP as a molecular marker is its stability and the fact that its chromophore is formed in an autocatalytic cyclization that does not require a cofactor. Furthermore, the fusion of GFP to a protein does not alter the function or location of the protein. These advantages enabled GFP's widespread use in cell dynamics and development studies [170].

CBMs coupled with fluorescence protein have been used for mapping the chemistry and structure of various carbohydrate-containing substrates (LCB) [55,125,171]. Using fluorescent-tagged CBMs, Gao *et al.* (2014) and Hong *et al.* (2007) successfully quantified the change in crystalline and non-crystalline (amorphous) celluloses accessibilities during enzymatic hydrolysis [125,171].

## 1.7 Fluorescent protein-Tagged Carbohydrate-binding module Method (FTCM)

Considering the importance of LCB tracking, in this Ph.D. work we have established a novel, rapid, high-throughput, easy-to-use, unambiguous and affordable approach to track lignocellulosic polymers at the surface of diverse pulps (mechanically, chemically and enzymatically treated) and LCB fibers (raw (untreated) and pretreated). Named "Fluorescent protein-Tagged Carbohydrate-binding module Method", or FTCM, this method relies on the use of four specific ready-to-use probes made of recombinant CBMs genetically linked to a designated fluorescent protein of the GFP family. The CBM part of these genetically modified probes recognizes and binds to biopolymers (*i.e.* mannan, xylan, crystalline and non-crystalline cellulose) while the fluorescence emitted by the GFP (or a selected derivative of GFP with different spectroscopic properties) permits rapid and specific quantification of the probes bound to the surface. The fluorescence can be measured by using an ordinary fluorescence plate reader. We developed four fluorescent-tagged fusion proteins for FTCM: Probe eGFP-CBM3a (GC3a), specific to crystalline cellulose (made of the fluorescent protein eGFP and CBM3a); Probe mCherry-CBM17 (CC17), specific to non-crystalline cellulose (fluorescent protein mC linked to CBM17); Probe

mOrange2-CBM15 (OC15), specific to xylan (composed of mOrange2 and CBM15); and Probe eCFP-CBM27 (CC27), specific to mannan (a chimera made of eCFP and CBM27). Figure 1.18 illustrate the construction schemes and 3D structure of the FTCM probes.

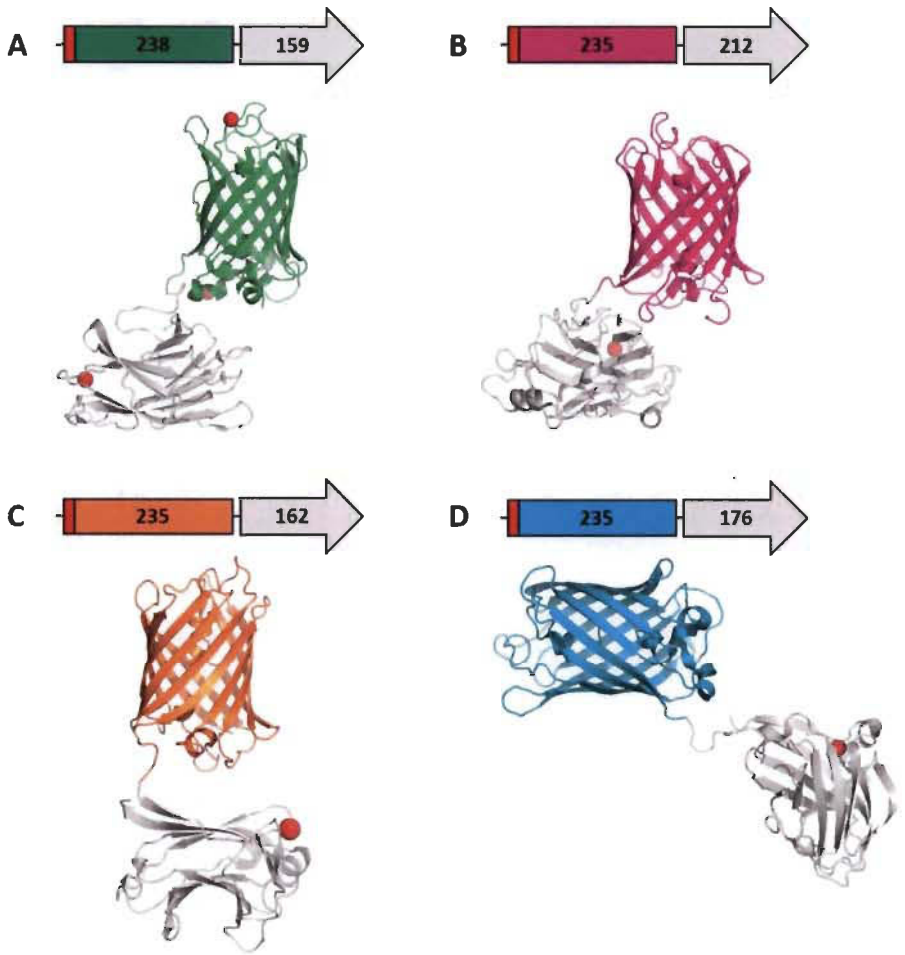


**Figure 1.18 Construction schemes and tridimensional structures of the probes**

Unless otherwise noted, the sequence linking the fluorescent protein to the CBM is composed of a glycine. **A**) The crystalline cellulose probe (GC3a) was formed by linking eGFP via a thrombin cleavage site to CBM3a (46.26 kDa). **B**) The non-crystalline cellulose probe (CC17) is composed of mCherry linked to CBM17 (50.56 kDa). **C**) The xylan probe (OC15) was formed by mOrange2 and CBM15 (44.68 kDa). **D**) The mannan probe (CC27) was constructed using eCFP and CBM27 (48.06 kDa). All fluorescent proteins C-terminal ends are linked to the N-terminal ends of the CBMs. The red portions in the ORFs represent N-terminal six histidine tags. The red spheres represent metal ions.

Mixing the probes with wood fiber and measuring fluorescence (after removing CBMs that are not specifically bound) allows for quick monitoring of the distribution of the targeted polymers on the fiber, as depicted in Figure 1.19.

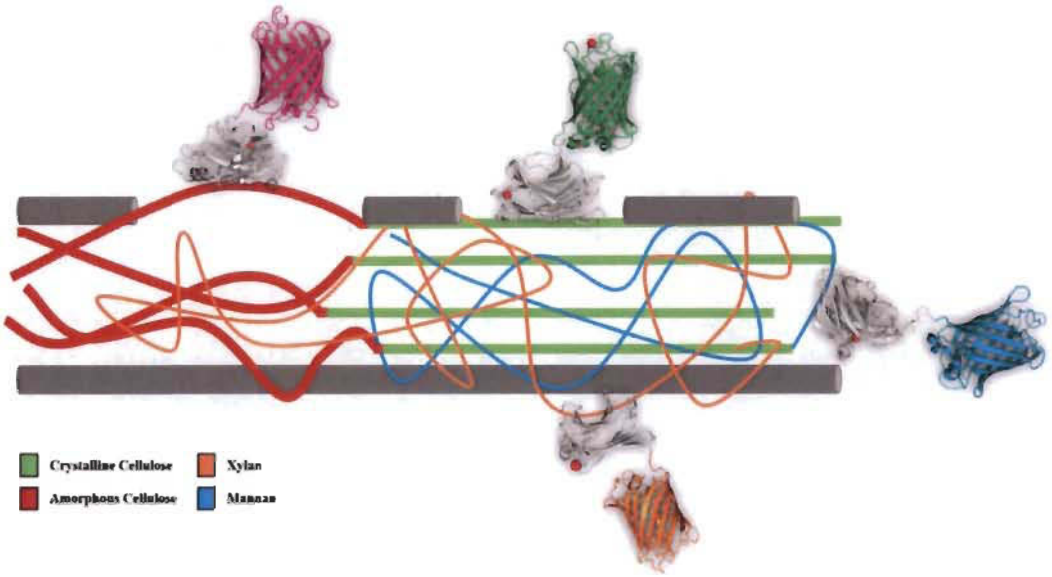


**Figure 1.19 Schematic representation of probe binding to wood fiber**

The left side of the fiber depicts a partially lignin-free fiber where non-crystalline cellulose dominates (red strings). On the right side, the straight green bars represent crystalline cellulose. Hemicelluloses such as xylan (orange) and mannan (cyan) are shown as polymers that help keep the fiber together. The grey cylinders represent the lignin coating. The probes designed in this study were shown to attach specifically to their respective target polymer, as indicated in this figure by the matching color of their fluorescent module.

### 1.7.1 Family 3 CBM

The family 3a CBM (CBM3a) comprises the non-catalytic crystalline cellulose-recognizing module of the scaffolding subunit Cip (Cip-CBD) of the cellulosome from *Clostridium thermocellum* [127]. The crystal structure of CBM3a represents a nine-stranded β-sandwich fold with a jellyroll topology with a calcium ion (Figure 1.20). The

nine β strands align in a way to form two defined surfaces located on opposite sides of the molecule. The bottom sheet is comprised of strands 1, 2, 7, and 4; whereas the top sheet contains strands 9, 8, 3, 6, 5. The two sheets show different curvatures. The bottom sheet surface is dominated by a planar linear strip of aromatic and polar residues that are proposed to interact with crystalline cellulose [127].

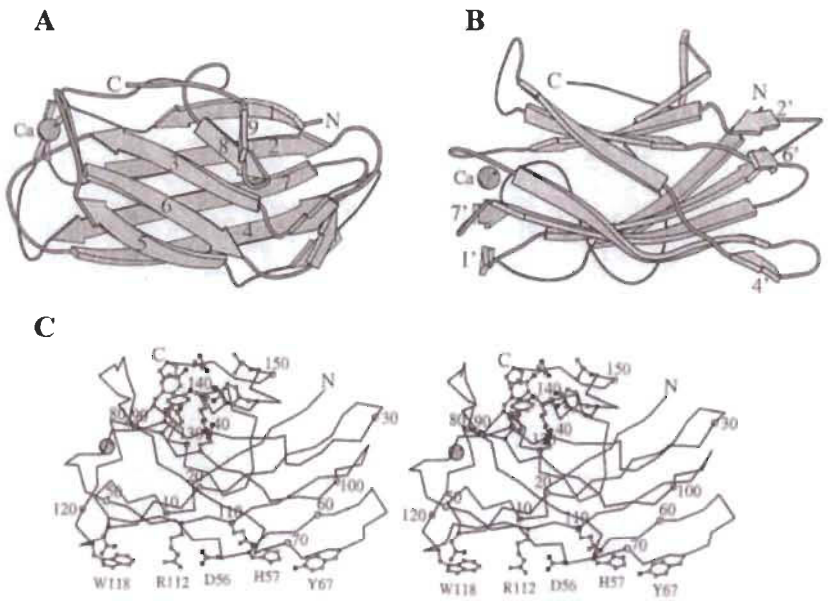


**Figure 1.20 Overall structural organization of the CBD**

(A) Ribbon diagram of Cip-CBD. The C- and N-termini are labeled C and N, respectively, and the position of the calcium ion (Ca) is shown. β Strands are depicted as arrows and unstructured loops as tubes. Strands that form the two β sheets are labeled 1-9. (B) 90° rotation around the horizontal axis of the CBD molecule in (A). (C) Stereo diagram of the $C_\alpha$ trace of Cip-CBD with every tenth $C_\alpha$ position labeled. The molecule has been rotated 40° around the horizontal axis with respect to the view in (B). Side chains of conserved surface-exposed residues are shown, and those forming the aromatic strip proposed to interact with a single glucose chain of crystalline cellulose are labeled (adapted from [127]).

### 1.7.2 Family 17 CBM

The family 17 CBM (CBM17) contains the non-catalytic cellulose-recognizing module of a cellulase 5A (Cel5A from *Clostridium cellulovorans*). Biochemical studies

on the CBM17 showed that it binds to non-crystalline cellulose and soluble β-(1,4)-glucans, with a minimal binding requirement of cellotriose and optimal affinity for cellohexaose [172]. CBM17 does not show any affinity towards crystalline cellulose or xylan, including substituted xylan and xylooligosaccharides or carbogalactomannan and mannooligosaccharides. The crystal structure of CBM17 complexed with cellotetraose revealed a four by five-stranded β-sandwich fold with a single α-helix at the base of both sheets. Cellotetraose binds to the wide but shallow groove on the surface of CBM17, where two Trp residues (W88 and W135) stack the reducing ends of the oligomer, while the polar residues (N52, D54, R92, Q129, N137, and N185) makes contacts with the non-reducing end of the sugar (Figure 1.21 and 1.22) [172].

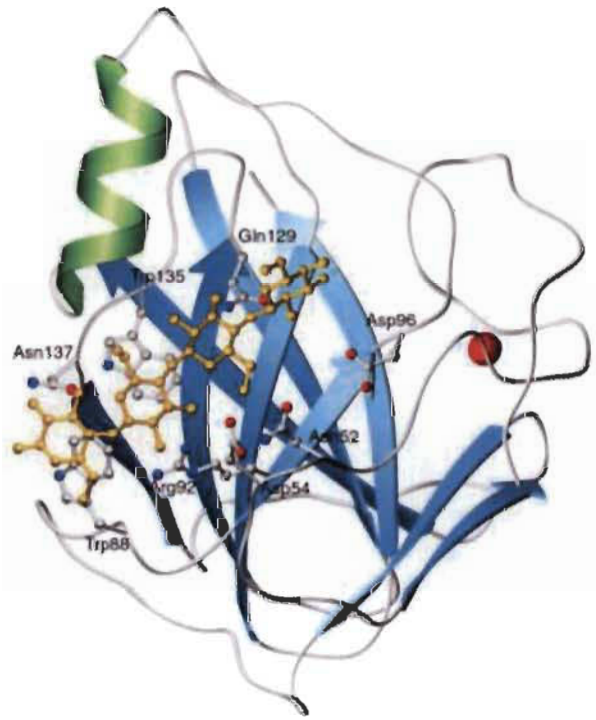


**Figure 1.21 Ribbon representation of the 3D structure of CBM17**

Depicted in gold is the cellotetraose moiety as observed in the crystal structure. Residues that were predicted to form interactions with the ligand by alanine scanning mutagenesis are shown as ball and stick (adapted from [172]).

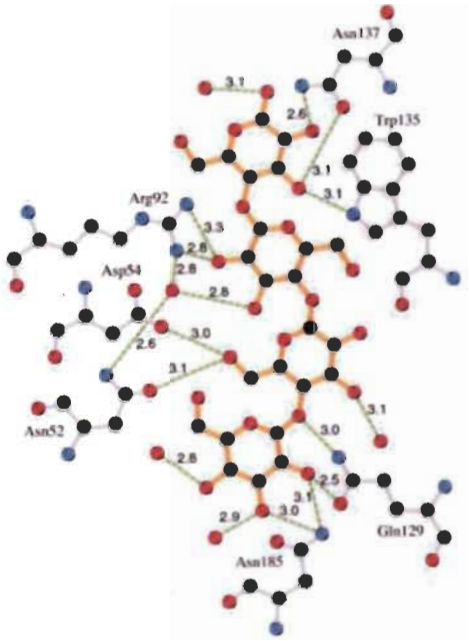


**Figure 1.22 Cartoon representation of ligand interactions in the binding cleft of CBM17**

Green broken lines depict hydrogen bonds (lengths in Å). Orange flares around atoms represent hydrophobic contacts between ligand and protein (adapted from [172]).

### 1.7.3 Family 15 CBM

Among type B CBMs, the family 15 CBM (CBM15) includes the non-catalytic xylan-recognizing module of a xylanase (Xyn10C from *Cellvibrio japonicus*) which has been demonstrated to bind xylan, including substituted xylan and xylooligosaccharides. The CBM15 was also shown to bind to cellooligosaccharide (cellohexaose) but with 10 times less affinity than xylohexaose [173]. The 3D structure of the CBM15 reveals a β-jelly roll structure of two β-sheets displaying an extended groove that runs along the face of the protein (Figure 1.23). Within this groove two tryptophan residues form hydrophobic stacking interactions with two xylopyranose units at *n* and *n*+2 (Figure 1.24) [173].

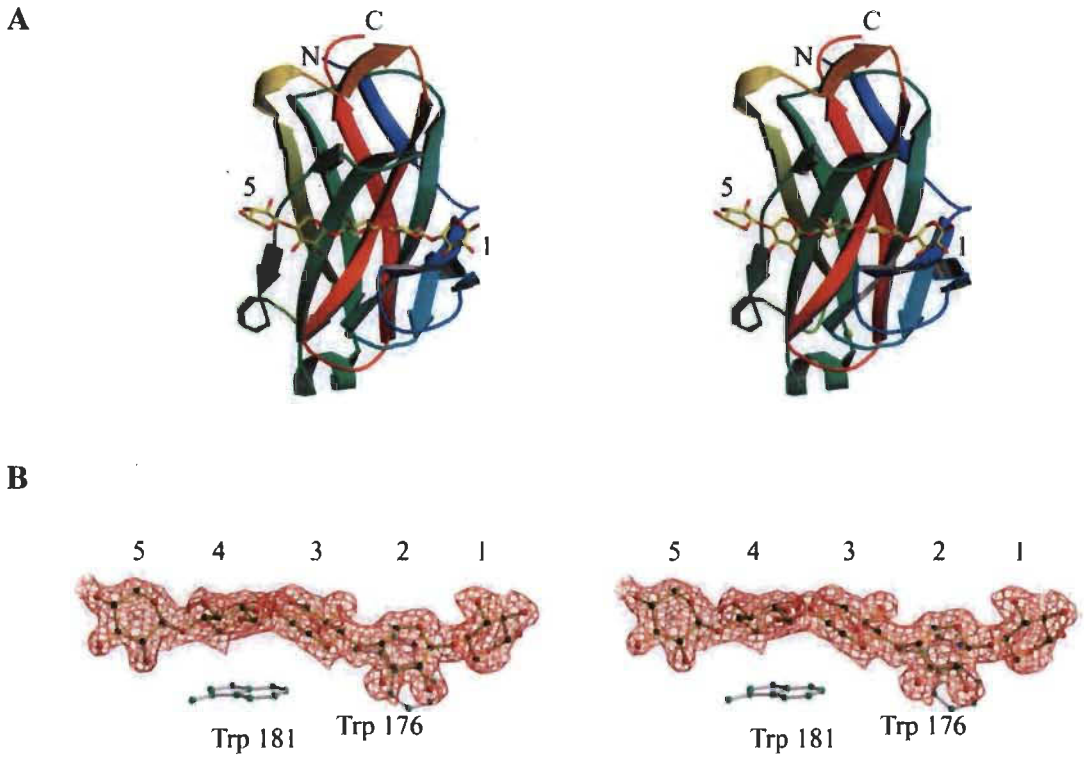


**Figure 1.23 The three-dimensional structure of the Cellvibrio japonicus CBM15 in complex with xylopentaose**

(A) The secondary structures of the protein with the location of bound xylopentaose. (B) The electron density of xylopentaose bound to CBM15 (adapted from [173]).

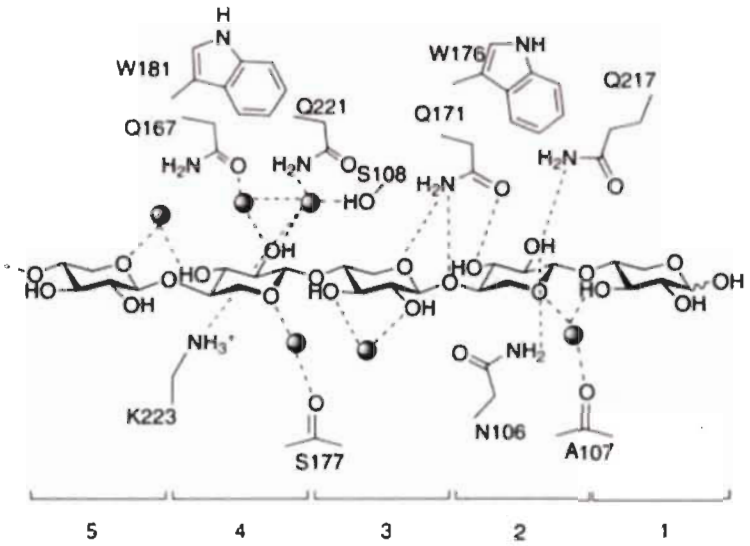


**Figure 1.24 Schematic diagram of the interactions of CBM15 with xylopentaose** (adapted from [173])

### 1.7.4 Family 27 CBM

The Family 27 CBM (CBM27) comprises the non-catalytic mannan-recognizing module of a mannanase (Man5 from *Thermotoga maritima*). The CBM27 binds tightly to β-(1,4)-mannooligosaccharides, carbogalactomannan, and konjac glucomannan, but not to cellulose (insoluble and soluble) or xylan, including substituted xylan and xylooligo-saccharides [174]. The 3D structure of the CBM27 reveals a β-sandwich comprising 13 β starnds with a single, small α-helix and a single metal atom (modeled as a calcium atom) (Figure 1.25). The structure is heptahedrally coordinated by the side chain of D165; the backbone carbonyls of D12, G46 and D93; and two water molecules. Relative to the interaction of CBM27 with mannohexaose ($M_6$), a hydrogen bond is made with galactose side chain and a bond is lost between D59 and the mannose residue in subsite 2 of $6^3$,$6^4$-α-D-galactosyl-mannopentose ($G_2M_5$) (Figure 1.26) [174].

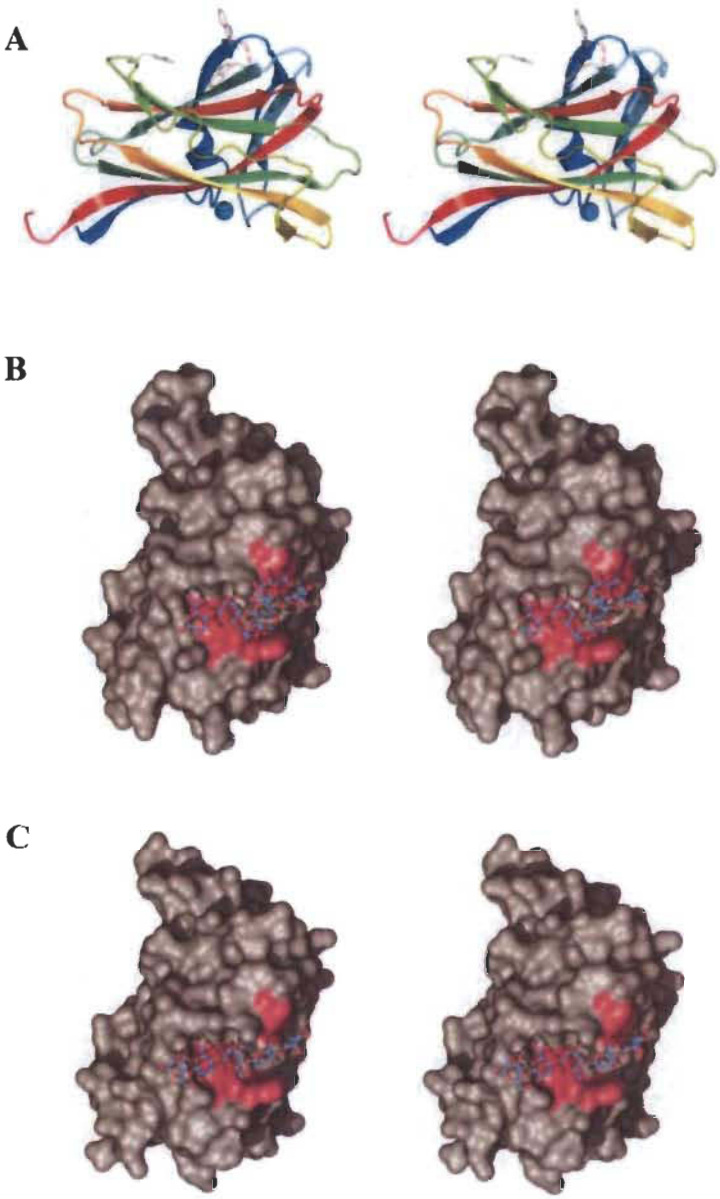


**Figure 1.25 Three-dimensional structure of uncomplexed TmCBM27**

(A) The secondary structures of the protein are shown with the aromatic amino acids in the binding site shown in "licorice". The bound metal ion is shown as a blue sphere. Solvent-accessible surfaces of *Tm*CBM27 complexed with (B) $G_2M_5$ and (C) mannohexaose. Purple regions indicate the surface contributed by the binding site aromatic residues. The sugar molecules are shown in blue and red licorice (adapted from [174]).

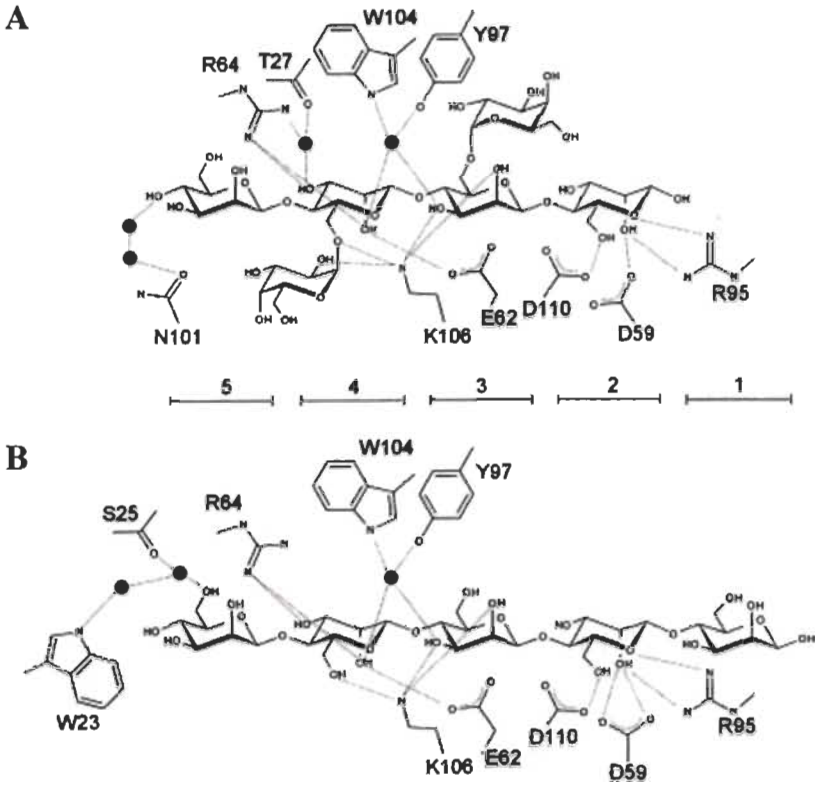


**Figure 1.26 A schematic showing the interaction of TmCBM27 with G2M5 (A) and mannohexaose (B)**

Hydrogen bonds are shown as dashed lines; water molecules as filled circles. Binding subsites referred to in the text are shown underneath the schematics with brackets (adapted from [174]).

## 1.8 Objectives

The main goal of this PhD work was to develop and optimize the FTCM and exploit its potential for five different objectives.

### 1.8.1 Objective I (scientific article I)

- To demonstrate the development, working procedure and the sensitivity of FTCM method;
- To study the potential of a fluorescent-tagged fusion protein OC15 for monitoring xylan at the surface of paper samples.

### 1.8.2 Objective II (scientific article II)

- To investigate and track variations in hemicelluloses after various mechanical, chemical and enzymatic treatments;
- To investigate the inherent recalcitrance nature of plants and its impact on enzyme accessibility, inactivation, inhibition and, as a consequence, cost of use;
- To study the location of hemicelluloses with respect to lignin and cellulose.

### 1.8.3 Objective III (scientific article III)

- To demonstrate rapid, high-throughput monitoring of wood fibers and predicting the impact of various treatments on the strength properties of paper produced from such processed fibers.

### 1.8.4 Objective IV (scientific article IV)

- To investigate that which combination of enzyme treatment and biomass substrate is best suited for industrial applications in which various levels of fiber deconstruction and precise control of fiber surface composition are desirable, such as the production of nanocellulose, fiber-reinforce composites, or paper.

### 1.8.5 Objective V (scientific article V)

- To explore the applicability and adaptability of FCTM to FTCM-depletion assay in order to study the LCB pretreatments in a biofuel production perspective.
- To characterize suspensions of biomass fibers (untreated and after various pretreatments) and investigate the correlations between FTCM probes binding and enzymatic production of reducing sugars.

# Chapter 2 - Scientific Article I

**Specific tracking of xylan using fluorescent-tagged carbohydrate-binding module 15 as molecular probe**

Vinay Khatri[1, 2], Yannick Hébert-Ouellet[1, 2], Fatma Meddeb-Mouelhi[1, 2, 3], and Marc Beauregard[1, 2*]

[1] Centre de recherche sur les matériaux lignocellulosiques, Université du Québec à Trois-Rivières, Trois-Rivières (Québec) G9A 5H7, Canada.
[2] PROTEO, Université Laval, Québec (Québec) G1V 4G2, Canada.
[3] Buckman North America, Vaudreuil-Dorion (Québec) J7V 5V5, Canada.

*Corresponding author: Centre de recherche sur les matériaux lignocellulosiques, Université du Québec à Trois-Rivières, C.P. 500, Trois-Rivières (Québec), G9A 5H7 Canada, Tel: (819) 376-5011 # 3354, Fax: (819) 376-5084, E-mail: marc.beauregard@uqtr.ca

## Authors' contributions

VK carried out all the experiments and drafted the manuscript. YHO contributed to experiments related to the construction of plasmid for OC15 expression, design of high throughput assay and drafted the manuscript. FMM and MB participated in its design and coordination, and helped to draft and revise the manuscript. All authors read and approved the final manuscript.

## Acknowledgments

This research was supported in part by Buckman Laboratories of Canada and funded by grants from CRIBIQ and NSERC (CRDPJ445143-12). We would like to thank Dr. Roberto Chica (University of Ottawa) for the donation of fluorescent protein and Dr. Nicolas Doucet (INRS-Institut Armand-Frappier) for his expert assistance while performing isothermal titration calorimetry (ITC) measurements. The skillful technical assistance of Nikolas Beauchesne, Vincent Bolduc, Daniel Agudelo, Rene Diene and Guillaume L. Lemieux is acknowledged. We would like to thank Mary A. Hefford for her valuable editorial contributions.

## Competing interests

VK, YHO and MB declare that they have no competing interests. FMM was an employee of Buckman North America, which financially supported parts of this work. The project results are included in a provisional patent (assignee: Buckman International, Memphis, TN, USA).

## 2.1 Abstract

**Background:** Xylan has been identified as a physical barrier which limits cellulose accessibility by covering the outer surface of fibers and interfibrillar space. Therefore, tracking xylan is a prerequisite for understanding and optimizing LCB processes.

**Results:** In this study, we developed a novel xylan tracking approach using a two-domain probe called OC15 which consists of a fusion of *Cellvibrio japonicus* carbohydrate-binding domain 15 with the fluorescent protein mOrange2. The new probe specifically binds to xylan with an affinity similar to that of CBM15. The sensitivity of the OC15-xylan detection approach was compared to that of standard methods such as x-ray photoelectron spectroscopy (XPS) and chemical composition analysis (NREL/TP-510-42618). All three approaches were used to analyze the variations of xylan content of kraft pulp fibers. XPS, which allows for surface analysis of fibers, did not clearly indicate changes in xylan content. Chemical composition analysis responded to the changes in xylan content, but did not give any specific information related to the fibers surface. Interestingly, only the OC15 probe enabled the highly sensitive detection of xylan variations at the surface of kraft pulp fibers. At variance with the other methods, the OC15 probe can be used in a high throughput format.

**Conclusions:** We developed a rapid and high throughput approach for the detection of changes in xylan exposure at the surface of paper fibers. The introduction of this method into the LCB based industries should revolutionize the understanding and optimization of most wood biomass processes.

**Keywords:** Carbohydrate-binding module, Fluorescent protein, kraft pulp, X-ray photoelectron spectroscopy, Xylan, Xylanase

## 2.2 Introduction

LCB is a major source of sugars for the production of biofuel [1,2]; however, its production has always been hindered by several economical and technical obstacles [3,4]. One of these obstacles is the complex structure of the lignocellulosic substrate. As a consequence, the enzymatic hydrolysis of lignocellulosic components to fermentable sugars is considered as one of the major rate-limiting and costly step [3,5-8]. One way to better understand and control hydrolysis of LCB is to monitor the complex polymers composition of fibers at every stage of processing.

LCB is a complex structure consisting of cellulose (β-1,4-linked glucose polymer), hemicellulose (polysaccharide of varying composition) and lignin [9]. Cellulose is the most abundant polysaccharide in nature and constitutes about 35-50% of the total LCB [10]. Hemicelluloses, which represent about 20-30% of the total biomass, are the second most common polysaccharides [10,11]. Unlike cellulose, hemicelluloses are heterogeneous polymers of pentoses (xylose, arabinose), hexoses (mannose, glucose, galactose) and/or uronic acids (glucuronic acid, galacturonic acid) [9,12]. Hemicellulose in softwood (from gymnosperms) contains mostly glucomannans whereas in hardwood (from angiosperms) mostly consists of xylan [13]. The hemicelluloses distribution on the surface of wood fibers/cellulose fibrils is of utmost importance for the complex structure of LCB, since hemicelluloses have been proposed to act as a physical barrier which increases the stiffness of the cellulose fiber network by coating the rigid cellulose crystallites and forming links between the fibrils [3,14].

Among hemicelluloses, xylans are the most abundant and complex hemicelluloses comprising a backbone of β-1,4-linked xylopyranosyl residues [10,11,13]. Xylan has been shown to limit the accessibility of cellulase enzymes to cellulose [15-20]. As a consequence, biomass bioconversion requires the presence of accessory enzymes such as xylanase, which allows for controlling the significant effect of residual xylan on cellulose accessibility during bioconversion [4]. The cost associated to enzyme utilization is an important aspect of bioenergy production. [15,21,22,23]. Enzymes cost can be minimized by

tighter control of process parameters (such as dosage and incubation time). To this end, one needs to track lignocellulosic polymers, including xylan, at various stages of processing.

Pulp and paper production is another LCB based industry which has to deal with the complexities described above. In addition, this industry faces immense pressure from the society and/or governments to move towards green chemistry. Biocatalysts are recognized as a key element of green chemistry and are being progressively introduced in a number of processes with extremely positive consequences for the environment [24,25]. An increasing number of enzymatic strategies are used by paper makers, including the application of xylanase enzymes in the pre-bleaching or bio-bleaching of kraft pulp. The presence of xylan, and its redeposition on the surface of cellulose fiber during the kraft pulping of hardwood, inhibits the bleaching process. Xylanase enzymes have been found to be most effective for limiting this problem and are now in use at several mills worldwide for biobleaching [13,15,24-26]. Further, xylan is also known to contribute to fiber strength and its removal is known to influence pulp fiber properties [15,27,28]. Xylan is believed to contribute to physical properties of the paper by enhancing the inter-fiber bonding [27]. Here again, the close monitoring of xylan would help optimizing the enzymatic treatment, better control paper properties, and minimizing its cost.

In order to make these LCB based processes highly productive and cost effective while improving quality of end-products, one should correlate the process parameters (such as enzyme loading, temperature or treatment time) to the substrate availability in a given biomass sample, or to a given percent removal target (*i.e.* x % decrease in xylan at the surface of cellulose fibers). Unfortunately, current methods for tracking xylan are not compatible with industrial constraints. To date, tools such as X-ray photoelectron spectroscopy (XPS or ESCA) [29,30], atomic force microscopy (AFM) [31], scanning electron microscopy (SEM) [30], time-of-flight secondary ion mass spectrometry (ToF-SIMS) [30], gas chromatography (GC) [32], Fourier transform infrared spectroscopy (FTIR) [33] and chemical methods [34,35] have been used to study the surface and bulk chemistry of

wood fibers. However, use of these methods for LCB analysis is laborious, requires specialized equipment, tedious sample preparation and long analysis time (typically hours for each sample) [36,37]. As a result, it is highly challenging to tightly modulate the amount of xylanase used for complete or selective xylan removal for process optimization.

Over the past decade, other techniques have been developed for the direct and rapid detection of LCB polymers. The use of chemical dyes to stain lignocellulosic biopolymers was one of the initial approaches for the detection of cellulose within various materials. Unfortunately, these dyes are rarely specific to cellulose [38]. In recent years, several *in situ* detection techniques have been developed, not only for cellulose but also for other cell wall components, including hemicellulose and pectic polysaccharides detection [39]. Among these techniques, monoclonal antibodies (mAbs) have been used successfully for developmental studies of vegetal materials. However, antibodies targeting complex polysaccharides, made of crystalline and insoluble structures, are difficult to generate [38,40]. Like antibodies, carbohydrate-binding modules (CBMs) are highly specific towards their substrate polysaccharides. They have been shown to discriminate crystalline cellulose from non-crystalline cellulose [38,40].

CBMs are the non-catalytic polysaccharide-recognizing module of enzymes such as glycoside hydrolases [41-43]. CBMs play a central role in the optimization of the catalytic activity of plant cell wall hydrolases by their specific binding to plant polysaccharides. These CBMs are grouped into 71 different families, based on amino acid sequence homology, in the Carbohydrate Active enZymes (CAZy) database (http://www.cazy.org/) [41]. CBMs are further classified into three types A, B and C, on the basis of three-dimensional structure and functional similarity. Type A CBMs recognize the surface of crystalline cellulose, type B and type C CBMs are identified as CBMs that recognize internal glycan chain (*endo*-type) and terminal (*exo*-type) glycans, respectively [43,44]. Among type B CBMs, the family 15 CBM (CBM15) includes the non-catalytic xylan-recognizing module of a xylanase (Xyn10C from *Cellvibrio japonicus)* which has been demonstrated to bind xylan, including substituted xylan and xylooligosaccharides [45]. The high specificity of CBMs toward lignocellulosic polymers makes them more interesting as probes

compared to mAbs [38,40,41]. CBMs have been used for several applications related to biomedicine, environment, molecular biology, microarrays, paper, textile, food and biofuel industries [41]. Considering the importance of xylan detection for industrial processing of LCB, we propose to use nature's own recognition molecules (CBMs) as the spearhead of an efficient xylan detection method.

Fluorescence is a very sensitive and specific spectroscopy where absorption and emission wavelengths determine what molecules contribute to the detected signals [43,46]. Further, plate readers allow increasing measurement throughput, a valuable criterion in the development of any novel assay. Hence, detection of CBM probes that would emit fluorescence would be advantageous. Fluorescence detection can be achieved directly or indirectly depending on the methods used [38]. The indirect methods involve the use of a secondary or tertiary reagent such as anti-His-IgG coupled to a fluorophore to detect the His-tag of a CBM, which may also allow amplification of signal intensities. This method provides great flexibility in CBM use but has a potential disadvantage related to multi-step incubations which decrease analysis speed and are less compatible with a high throughput strategy [38]. On the other hand, in direct methods, coupled CBMs would require a straightforward, single-step incubation, affording the possibility of rapid, high throughput protocols. In the first direct method reported, a CBM was chemically coupled with a fluorophore (such as FITC/Alexa Fluor) [38]. Unfortunately, these molecules react non-specifically with various moieties at the surface of CBMs, deleteriously impacting specificity, affinity and detection reproducibility. Another direct detection method uses CBMs as fusion with a fluorescence protein such as the green fluorescent protein (or any of its variants) [38]. This method allows maintenance of the original CBM behavior, avoiding the limitations described for the first direct method discussed. Hence, CBMs coupled with fluorescence protein have been used for mapping the chemistry and structure of various carbohydrate-containing substrates (LCB) [47,48]. More recently, two different recombinant fluorescent CBM probes have been used for quantitative study of the change of accessibilities of amorphous cellulose and crystalline cellulose regions during the enzymatic hydrolysis of Avicel [43].

In this study, we demonstrate the potential of a fluorescent-tagged fusion protein mOrange2-CBM15 probe (hereafter named OC15) for monitoring xylan at the surface of paper samples. To evaluate the potential of our novel method, we decided to use two different grades of kraft pulps (unbleached and bleached), and we analyzed xylanase treated pulp in order to study the sensitivity of the developed method. Our results suggest that such probes can form the basis of a rapid, easy to use, unambiguous and affordable diagnostic approach, helping optimizing treatment strategy and reducing the cost of processes which rely on controlled xylan removal.

## 2.3 Materials and methods

### 2.3.1 Chemicals and strains

Unless otherwise noted, all chemicals were reagent grade and purchased from Sigma-Aldrich or Fisher Scientific. *Escherichia coli* XL10 cells (Agilent Technologies) were used for all DNA manipulations while *E. coli* BL21-Gold(DE3)pLysS competent cells (Agilent Technologies) were used for recombinant protein expression. *Trichoderma viride* xylanase from glycoside hydrolase (GH) family 11 (cat no. 95595; *Sigma*-Aldrich) was used for the digestion of LCBes. Xylanase activity was 16.57 U/g.

### 2.3.2 Construction of pET11a-mOrange2-CBM15 expression vector

The CBM15 gene (xylan binding domain) was cloned into the C-terminal end of the mOrange2 gene (detection domain) in a pET11a vector. Briefly, *Cellvibrio japonicus* CBM15 (GenBank Accession Z48928) was synthetized by Genscript and provided as part of the pUC57-CBM15 vector. In order to insert the *Bsr*GI and *Bam*HI restriction sites (underlined) at each end of CBM15, we amplified the gene using forward (5'-TGTACAAGGGTGTCGCTGCCAGC-3') and reverse primers (5'- GGATCCTTAATT-GGCTGAATAGGCTTCC-3'). The resulting PCR product was then purified using Qiagen Minelute PCR purification kit. In addition, the mOrange2 gene was excised from the pmOrange2 vector (Clontech) using a *Dra*III and *Bam*HI double digestion and inserted

into the corresponding sites of pET11a vector. Finally, the double *Bsr*GI and *Bam*HI digestion of CBM15 was purified and inserted into the corresponding site of the pET11a-mOrange2 vector, resulting into the pET11a-mOrange2-CBM15 expression vector. At each step, the constructs were sequenced to ascertain the integrity and fidelity of the products DNA sequence.

### 2.3.3 Expression and purification of OC15 probe

*E. coli* BL21-Gold(DE3)pLysS cells (Agilent Technologies) bearing the OC15 expression plasmid were grown at 37°C and 200 rpm in Luria-Bertani broth containing 100 µg/mL of ampicillin. Induction of recombinant protein expression was performed by the addition of 500 µM IPTG (ThermoFisher Scientific) to mid-log-phase cells ($O.D._{600nm}$ of 0.6-0.8) and subsequent incubation for 18 hours at 25°C. Cells were then harvested and kept at -80°C. Thawed cell pellets were resuspended in 50 mM sodium phosphate pH 8 containing 300 mM NaCl, 2 mM imidazole, 1 mM PMSF and then lysed by sonication using six cycles of 60 sec (Branson Ultrasonics Corporation) at 200 W. Clarification of lysate was achieved by centrifugation at 10,000 *g* for 30 minutes at 4°C. The protein of interest was purified by affinity chromatography over a HisPrep FF 16/10 column (GE Healthcare Life Sciences) equilibrated in 50 mM sodium phosphate buffer pH 8.0 containing 300 mM NaCl and 10 mM imidazole. After washing with ten column volumes of buffer, the desired protein was eluted using a gradient of imidazole (10 to 250 mM) in 50 mM sodium phosphate pH 8.0 buffer containing 300 mM NaCl. A final purification step was performed using a Superdex 200 HR 16/50 column (GE Healthcare Life Sciences) in 50 mM Tris-HCl pH 7.5 buffer containing 300 mM NaCl to insure its homogenous purity. The purified probe was then dialyzed in a 20 Tris-HCl pH 7.5 buffer containing 20 mM NaCl and 5 mM $CaCl_2$ at 4°C and concentrated using a 10k Macrosep Advance centrifugal device (Pall Corporation). Concentrated protein solutions were stored at -80°C using flash freezing. Protein purity (expected mass 44.68 kDa) was verified by SDS-PAGE. The amount of protein was quantified by the Bradford method [64].

### 2.3.4 Affinity gel electrophoresis (AGE)

AGE was used for qualitative assessment of OC15 (10 μg) specificity toward selected ligands. The experiment was performed as described elsewhere [49,65], by adding 0.5 % (w/v) of beechwood xylan (Sigma-Aldrich), carboxymethyl cellulose (CMC) (Sigma-Aldrich) and galactomannan (Megazyme) to a native, 12% polyacrylamide gel. Bovine serum albumin (BSA) (10 μg/well) was used as negative control since it has no affinity towards carbohydrates [49].

### 2.3.5 Isothermal titration calorimetry (ITC)

ITC was employed to measure the affinity of the OC15 probe towards selected hexaoses (Megazyme). Cellohexaose, xylohexaose and mannohexaose were reconstituted in a 20 mM Tris-HCl pH 7.5 buffer which contained 20 mM NaCl and 5 mM $CaCl_2$. The purified OC15 probe was also dialyzed into that same buffer. All experiments were performed with a Nano ITC microcalorimeter (TA Instruments) operated at 25°C with a stirring rate set of 250 rpm. Pre-equilibrated solutions of probe (200 μM) and hexaoses (5 mM) were used for each assay. The control experiments were based on titrations of hexaoses into the buffer and buffer into the OC15 probe. Each experiment consisted of 25 injections of 2 μL hexaose into the probe solution, with an interval of 130 seconds between injections. All experiments were performed in triplicates. Data were analyzed and fitted using the NanoAnalyze software v2.3.6 (TA Instruments).

### 2.3.6 Pulp characterization

The kraft pulps used for this study were provided by an Eastern Canadian pulp and paper company. The kraft pulping was performed using a mixture of softwood and hardwood. Two different grades of pulps, unbleached kraft pulp (UBKP) and bleached kraft pulp (BKP), were used. The cellulose, hemicellulose, and lignin contents of these pulps were analyzed according to NREL/TP-510-42618 protocol [35]. The hydrolyzed monosaccharides contents of the pulps (10 μl injection) were determined by ion chromatog-

raphy (ICS-5000, Dionex) and detection was performed using an electrochemical detection cell (combined pH-Ag/AgCl reference electrode). Each experiment was conducted at 40°C with 1 mL/min isocratic elution of NaOH (1 mM) on a Dionex CarboPac SA10 (250 mm × 4 mm) column coupled with a Dionex CarboPac PA100 (50 mm × 4 mm) guard column. Data analysis was performed using Dionex Chromeleon 7 software.

### 2.3.7 Handsheets preparation

UBKP and BKP were used as lignocellulosic substrates for the preparation of handsheets and paper discs. Handsheets (basis weight of 60 ± 2 g/m$^2$) were prepared from pulp according to Tappi standard method T 205 sp-02. Prior to testing, the handsheets were conditioned for 24 h at room temperature and 50% of relative humidity according to Tappi method T 402 sp-03 [66]. These handsheets were then used for the preparation of the paper punches. The paper punches are define as paper discs having diameter of 3 mm.

### 2.3.8 Xylanase digestion of unbleached kraft pulp

Xylanase digestion of UBKP was done according to Li *et al.* [66]. Briefly, the presoaked, disintegrated pulp at 2 % consistency was incubated 1h at pH 6 and room temperature under continuous agitation (150 rpm), with or without xylanase (500 U/g of pulp). The reactions were stopped by a 15 minutes incubation on ice. The pulp was then used for chemical composition analysis (NREL/TP-510-42618) and handsheets formation.

### 2.3.9 X-ray photoelectron spectroscopy (XPS)

The 300 Watts, monochromatic Al K-α radiation source originating from an AXIS-ULTRA apparatus (KRATOS ANALYTICAL) was used to study xylan. The analyser was set in the constant pass energy mode, the lens set to the hybrid configuration (both magnetic and electrostatic lenses), and the electrostatic lens aperture in the slot position. This configuration provided the highest sensitivity for scanning 700 μm × 300 μm area. Three different spots were analysed to obtain an average. The pressure of the system was set at $10^{-8}$ Torr. Elemental analysis of the surface area was performed by recording

survey spectra at 160 eV with energy increment of 1 eV per channel. High resolution spectra were recorded at 20 eV with energy increment of 0.05 eV. This setup gave an overall instrumental resolution of 0.6 eV as measured on $Ag3d_{5/2}$. Analyses of the peak decompositions were performed using the CasaXPS software.

### 2.3.10 Xylan tracking on the surface of papers using the OC15 probe

All fluorescence readings were acquired at room temperature with a Synergy Mx microplate reader (BioTek) using the area scanning feature (3 x 3) with the top detection height set at 4.5 mm and the filters bandwidth at 9 mm. The excitation and emission wavelengths were set at 549 and 568 nm for the OC15 probe. Each experiment was done in triplicates. Two different grades of kraft pulps, unbleached (UBKP) and bleached (BKP), were investigated regarding their xylan content. The following method is a modified, high throughput version of the methodology described by Knox [38]. Hence, it was performed into 96-well black microtiter plates (Corning), where each well contained a 3-mm diameter paper disc obtained from 60 $g/m^2$ handsheet. The discs were glued to the bottom of each well and first incubated for 1 hour at room temperature with agitation in 3% (w/v) milk (20 mM Tris-HCl, pH 7.5 with 20 mM NaCl and 5 mM $CaCl_2$) to minimize paper auto-fluorescence and the non-specific binding of the OC15 probe. Milk excess was then removed with 3 x 5 washing steps using the assay buffer. At this stage, the fluorescence intensity of the paper discs was measured and referred as to blank fluorescence. The specific binding of the OC15 probe to the surface of the paper discs was initiated by adding 0.5 µg/µl of the OC15 probe in assay buffer to each well. After a 1h incubation at room temperature under agitation, the excess and/or non-specifically bound probe were removed by 3 x 5 minutes washes with buffer that also contained 0.05% (v/v) of Tween 20. The residual fluorescence intensity associated with the specific detection of xylan was then recorded. Quantification of the bound OC15 probe was achieved by subtracting the value of the mean blank fluorescence from the mean residual fluorescence obtained for each well. These fluorescence values were then converted into $\mu g/mm^2$ using the appropriate standard curves and the surface area of paper discs.

## 2.4 Results and Discussion

### 2.4.1 OC15 expression and purification

A two-domain recombinant probe named OC15 was designed for specific tracking of variations of xylan on the surface of lignocellulosic material (Figure 2.1). *Cellvibrio japonicus* CBM15 composed the xylan recognition domain (C-terminal) while monomeric fluorescent protein Orange2 constituted the probe detection domain (N-terminal). OC15 was expressed in *E. coli* BL21-Gold(DE3)pLysS cells which contained the pET11a-mOrange2-CBM15 plasmid (Figure 2.1A and B). The expected molecular weight of OC15 is 44.68 kDa. Following affinity and size exclusion chromatography steps, the probe purity was verified using SDS-PAGE (Additional file 2.1). Interestingly, the gel analysis of OC15 revealed two bands: one intense band, corresponding to OC15 expected size (44.68 kDa), and another, less intense band (less than 1% on the basis of staining intensity) of a smaller size. A similar result has been observed for the purified mCherry-CBM17 probe designed by Gao *et al.* [43]. These authors showed that the smaller band was the result of an incomplete denaturation of the probe under standard SDS-PAGE conditions. We investigated this possibility and found that increasing the SDS concentration in the gel, sample and running buffers decreased the intensity of the smaller band (data not shown). Therefore, we concluded that, like the probes of Gao *et al.* the OC15 probe is incompletely denatured under standard SDS-PAGE conditions.

### 2.4.2 Determination of OC15 ligand specificity using affinity gel electrophoresis (AGE)

Affinity gel electrophoresis (AGE) was used to qualitatively evaluate the specificity of the OC15 probe towards soluble polysaccharides [49]. Interaction between the studied protein and the gel-embedded polysaccharide is revealed by a reduced mobility compared to the mobility of the protein in absence of saccharide.

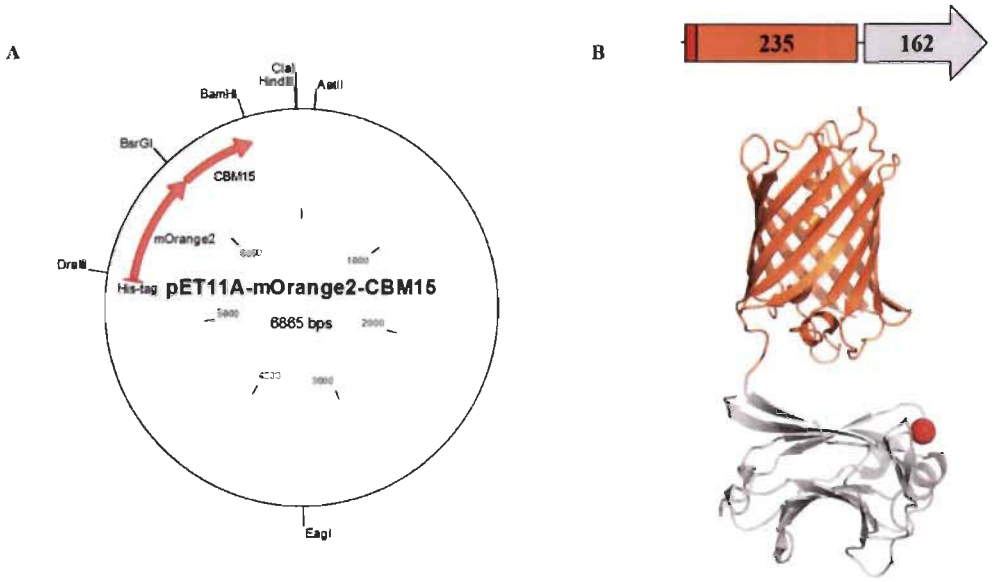


**Figure 2.1 Plasmid map (A), construction scheme and pictorial representation (B) of the OC15 probe**

mOrange2 C-terminal end is linked to the N-terminal end of CBM15 (*Cellvibrio japonicus*). The red rectangle represents N-terminal six histidines tag. The red sphere represents the metal ion in CBM15. The structural model shown was constructed using PDB files 1GNY and 2H5O (obtained for the closely related mOrange fluorescent protein). The sequence linking the fluorescent protein to the CBM is composed of a glycine residue.

BSA, which has no affinity towards carbohydrates, was used as negative control [49]. Figure 2.2 shows that OC15 interacts only with beechwood xylan (Figure 2.2B). Similarly to BSA, no binding was detected between OC15 and carboxymethyl cellulose (Figure 2.2C) or galactomannan (Figure 2.2D). These results confirm that the well-known specific binding to xylan of CBM15 is unaltered by its fusion with mOrange2 in the OC15 probe. However, the affinity of the recognition module of the OC15 must still be determined in order to ascertain its ability to sensitively detect xylan on the surface of paper.

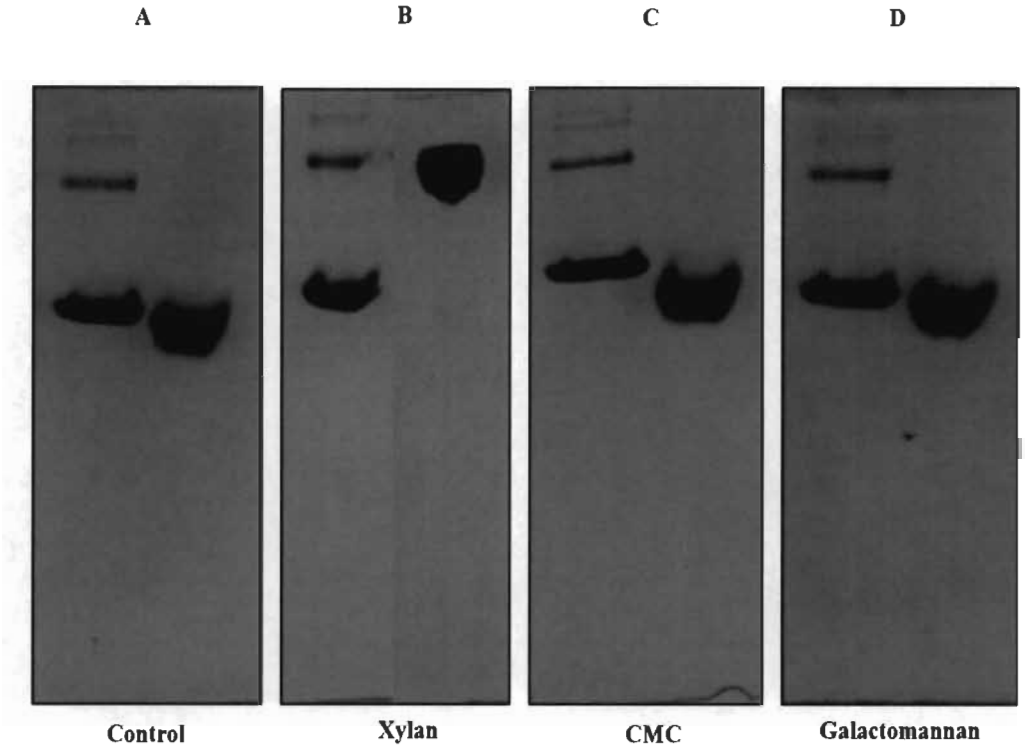


**Figure 2.2 Affinity gel electrophoresis (AGE) of OC15 probe**

Panel **A**) Control (no polysaccharide), Panel **B**) xylan, Panel **C**) CMC, Panel **D**) galactomannan. In each panel the first well contained BSA (10 μg) and the second well was loaded with OC15 probe (10 μg). All soluble polysaccharides were used at final concentration of 0.5% (w/v) and a 12% polyacrylamide gel was used for affinity analysis.

### 2.4.3 Determination of OC15 ligand affinity using isothermal titration calorimetry (ITC)

The affinity of OC15 toward hexaoses was also investigated by ITC (Table 2.1 and Additional file 2.2). Analysis of the binding isotherms showed that the recognition module of the OC15 probe bound to both cellohexaose and xylohexaose, albeit with different affinity, but not to mannohexaose (Table 2.1). As expected, OC15 interacted 16 times more strongly with xylohexaose (34 x $10^3$ $M^{-1}$) than with cellohexaose (2.1 x $10^3$

$M^{-1}$). These affinity values are similar to those previously reported for CBM15 and confirm that the binding site of the recognition module of the OC15 probe is unaltered by the fusion with mOrange2 [45]. However, a small 1.7-fold increase is observed in the affinity constant of OC15 toward xylohexaose compared to CBM15 [45]. We attributed this increase to difference in experimental conditions in our study compared to those used previously. For instance, the sodium and calcium salt added to the binding buffer in our study may account for the observed difference. Such ions have also been observed in the crystallographic structure of CBM15 [45], although no biological relevance to their presence was given. We hypothesize that such a metallic ion may be important for the affinity and specificity of OC15 towards xylohexaose. We also found that OC15 bound weakly to cellohexaose but not to CMC (Figure 2.2C). This result was unexpected, since the concentration of gel-embedded cellulose was 2.9 times higher than the $K_d$ for cellohexaose (Table 2.1). This suggests that the bulkier carboxymethyl substitutions found in CMC may interfere with the affinity of the binding module of OC15 for cellulose. On the other hand, the presence of xylose moieties and/or xylan in a cellohexaose sample of high but imperfect purity (90%) would also explain such an apparent contradiction.

**Table 2.1 Affinity of the OC15 probe for various hexaoses as determined by ITC**

| Ligand | $K_a \times 10^3$ ($M^{-1}$) | $K_d$ (M) | n[a] |
|---|---|---|---|
| Xylohexaose | 34 ± 0.2 | $2.938 \times 10^{-5} \pm 0.8$ | 0.922 ± 0.1 |
| Mannohexaose | NB[b] | - | - |
| Cellohexaose | 2.1 ± 0.3 | $4.795 \times 10^{-4} \pm 0.1$ | 1 ± 0.7 |

[a] Number of ligand binding sites.

[b] No binding detected.

### 2.4.4 Comparing XPS, NREL/TP-510-42618 and OC15 methodologies for the detection of xylan

Pulps composed of a mixture of softwood and hardwood from an Eastern Canadian paper mill were used as LCB for the formation of handsheets utilized in this study. Handsheets prepared form two grades of kraft pulp, UBKP and BKP, were investigated to determine differences in biopolymers content and their exposure at fiber surfaces. Kraft pulping, and bleaching processes degrade and/or dissolve lignin. The removal of lignin through pulping increased access to xylan. In addition, removed xylan may redeposit onto the surface of cellulose fibers during pulping [26,50-53]. The standard methods usually used for the detection of xylan are NREL/TP-510-42618 and XPS [35,54-56]. These two approaches will be used and compared to our OC15 probe method.

The chemical composition of UBKP and BKP was determined by NREL/TP-510-42618 (Additional file 2.3) [35]. As expected, the pulp bleaching process decreased lignin by 2.3-fold without affecting the other biopolymers. Unfortunately, due to the nature of this technique, NREL/TP-510-42618 can only provide an overall bulk estimation of biopolymers content. It cannot detect small biopolymers changes nor than measure variations of biopolymers exposition on the surface of fibers.

In contrast XPS has been extensively used for surface analysis of simple LCBes to detect changes in surface coverage by cellulose, lignin and extractives [54-56]. Elementary identification and bonding state discrimination are advantages associated to XPS analysis [37]. The C 1s band associated with LCB which is monitored by XPS carries the most relevant information on surface polymers. C 1s spectrum has been suggested to result from the contribution of four different carbon functionalities: C1 (C–C, C–H, C=C), C2 (C–O or C–O–C), C3 (C=O or O–C–O) and C4 (O–C=O), which account for the chemical heterogeneity of paper fibers [54]. In cellulose, each glucose monomer harbors five C2 carbon atoms and one C3 carbon. Hemicelluloses are heterogeneous in their composition. Its monomers typically comprise fewer than five C2 carbon atoms, less than one C4 carbon atom and one C3 carbon atom. In contrast, lignin is more complex, having all four

types of carbons with a greater contribution from C1 and C2 atoms [57-59]. In a typical fiber XPS analysis, C1 component mainly arises from lignin and extractives, while C2 signal is primarily associated to cellulose and hemicelluloses. C3 component is not easily assigned to a given polymer, as it is related to either carbonyl groups of lignin and extractives, or to carbon atoms bonded to two oxygen atoms in cellulose and hemicellulose [57-60]. C1 to C4 peaks were inferred from the deconvolution of the C 1s band for UBKP and BKP (Additional file 2.4). These deconvolutions were calculated using spectra as shown in Additional file 2.5 and 2.6. The bleaching process led to a 2.2-fold decrease in C1 functionality at the surface of the paper. This difference may be attributed to the removal of lignin from the surface as a normal consequence of bleaching. The decrease in lignin associated to C1 functionality is in line with the corresponding decrease in lignin measured by NREL/TP-510-42618 (Additional file 2.3). Interestingly, the bleaching process increased the C2 functionality by 1.1-fold, suggesting that cellulose and/or hemicellulose are slightly more exposed on the surface of BKP. The exposure of cellulose and hemicelluloses also increased C3 carbon detection by 1.2-fold. Due to the low concentration of carboxylic groups on the surface of kraft pulp the C4 carbon functionality was minor and rather similar for either pulps. Like NREL/TP-510-42618, XPS analysis revealed the impact of the bleaching process on lignin. Moreover, XPS analyses suggested that lignin loss resulted in the increased exposure of cellulose and hemicellulose on the surface of BKP. Unfortunately, the C 1s spectra cannot distinguish cellulose from hemicellulose since both biopolymers possess similar carbon types. Moreover, XPS is not always reproducible due to problems resulting from X-ray contamination and samples degradation [54,61].

Using OC15 we attempted to monitor the difference in xylan on the surface of UBKP and BKP papers resulting from the bleaching process. Complex LCB fluoresces naturally when excited at the same wavelength as that for fluorescent protein mOrange2 *i.e.* 549 nm (data not shown). This auto-fluorescence is mainly attributed to the lignin biopolymer found in kraft paper [62]. Thus, in order to minimize paper auto-fluorescence, we added a milk blocking step that also acted as a non-specific binding deterrent. Figure 2.3 describes the quantification of OC15 bound to the surface of UBKP and BKP papers.

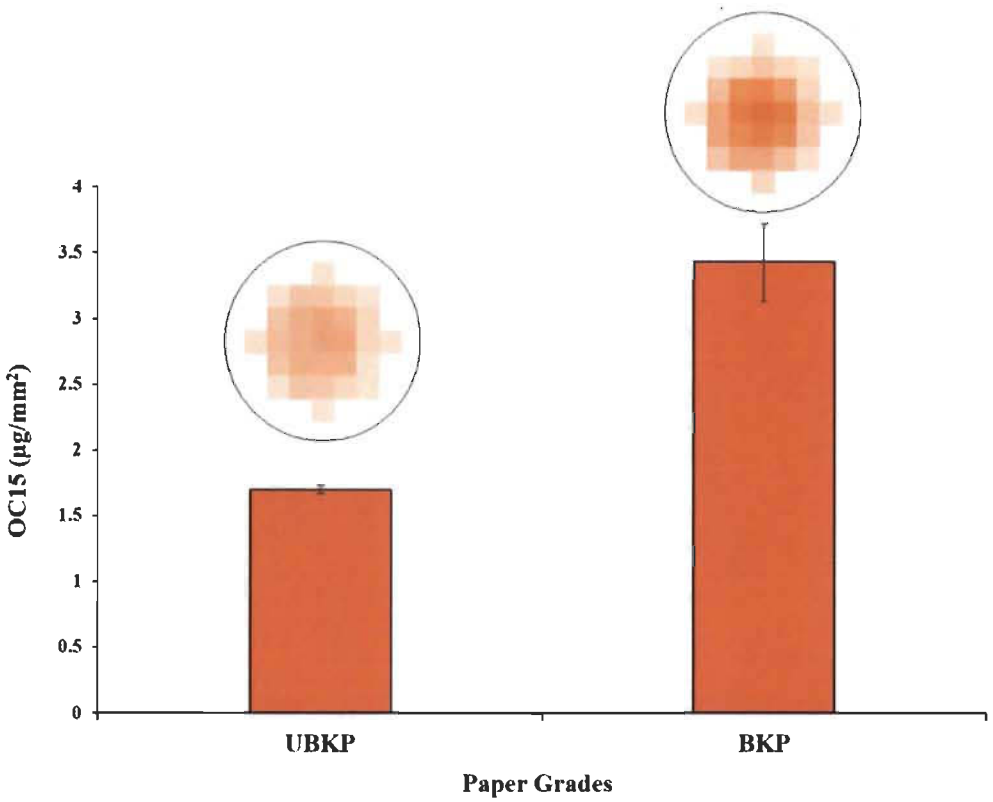


**Figure 2.3 Quantification of OC15 binding to the surface of UBKP and BKP papers**

UBKP and BKP paper punches were incubated with OC15 probe (0.5 µg/µL) for 1h at room temperature under agitation. Three percent (w/v) milk (20 mM Tris-HCl, pH 7.5 with 20 mM NaCl and 5 mM $CaCl_2$) was used to minimize paper auto-fluorescence and the non-specific binding of the OC15 probe. The fluorescence values were converted to OC15 (µg/mm$^2$) by using a standard curve (additional file 2.9). The inset above each histogram columns represents the fluorescence intensity acquired by area scanning of the surface of each paper disc.

The bleached paper bound twice the amount of OC15 compared to the unbleached one, indicating that xylan exposure on the surface of kraft paper has increased after bleaching. This increase is fully compatible with the 2.3-fold decrease in lignin observed by chemical analysis, which was shielding xylan from surface detection before bleaching. This result confirms the loss of lignin that we measured using NREL/TP-510-42618 and

XPS, demonstrating that our approach can efficiently detect the impact of the bleaching process on xylan. Therefore, introducing this xylan tracking approach as a quality control measurement would assuredly bolster the effectiveness of the LCB process for selective as well as complete xylan removal.

### 2.4.5 Monitoring xylan hydrolysis using NREL/TP-510-42618, XPS and the OC15 probe

The effectiveness of xylan removal by xylanase hydrolysis of UBKP was investigated using NREL/TP-510-42618, XPS and the OC15 probe. Chemical composition of untreated and xylanase-treated UBKP was analyzed (Additional file 2.7). As expected, xylanase treatment of pulp decreased xylose content by 1.7-fold without affecting lignin. The extractive content increased from 0.1 to 3.2 after xylanase treatment. This unexpected result is a consequence of the NREL lipids extraction methodology which consists into weighting the pulp before and after acetone solubilization of lipids [63]. Since the added xylanase accounts for 24.3% of the pulp initial weight, its acetone removal from the pulp induces an apparent but false increase in lipids extractives.

We then studied the surface of untreated and xylanase-treated UBKP papers using XPS (deconvolution results described in Additional file 2.8). Overall, xylanase treatment of UBKP induced rather small variations in the carbon functionalities (C1 to C4). As such, the curve fitting component ascribed to C1 atoms slightly decreased (1.1-fold), indicating that the lignin biopolymer was marginally affected by xylose removal. Surprisingly, the C2 functionality associated to cellulose and hemicellulose was not altered by xylan hydrolysis. This result may be attributed to the exposure of cellulose on the fibers surface as a consequence of xylan removal by hydrolysis. The exposure of cellulose also increased C3 carbon functionality by 1.2-fold. The C4 carbon signal was minor and rather similar for either pulps. This study reveals that the impact of xylan digestion (which was clearly detected by NREL/TP-510-42618 (Additional file 2.7)) cannot be monitored unambiguously or directly by XPS.

The impact of xylanase on xylan at the surface of UBKP paper discs was investigated using OC15 probe. A decrease in xylan was clearly indicated by the 7.7-fold decrease in OC15 binding after xylanase treatment (Figure 2.4). The use of OC15 probe confirmed the loss of xylan suggested by chemical analysis (NREL/TP-510-42618) with the distinction that OC15 specifically probes fiber surface. We also studied the binding of OC15 to xylanase-treated UBKP paper discs as a function of time and enzyme dosages (0.4 U vs 0.1 U). The xylanase digestions were performed on paper discs glued in 96-wells microtiter plates over an 18 hours incubation period at room temperature. Figure 2.5 reveals that after one hour a significant removal of surface xylan was detected. Xylan was reduced 8.2-fold by 0.1 xylanase units and 17-fold when 0.4 units were used. The complete removal of xylan was detected after 18 hours of incubation (0.4 unit dosage). OC15 binding responded proportionally to enzyme load and allowed monitoring xylanase treatment kinetics. This high throughput method enables the screening for optimal xylanase hydrolysis conditions, necessary for removal of xylan from kraft paper. We predict that OC15 usefulness is not limited to kraft paper analysis, but should include optimization of any biomass process for which surface xylan is determinant.

## 2.5 Conclusion

Monitoring the impact of mechanical, chemical and enzymatic modifications of biopolymers found in LCBes is a complex endeavor. The currently available methods for chemical composition analysis of biopolymers in pulp, such as NREL/TP-510-42618, are able to only quantify bulk xylan but give no information on biopolymers surface exposition. On the other hand, XPS, while being highly sensitive, cannot unambiguously monitor changes in surface xylan since cellulose and hemicellulose share similar C 1s carbon functionalities.

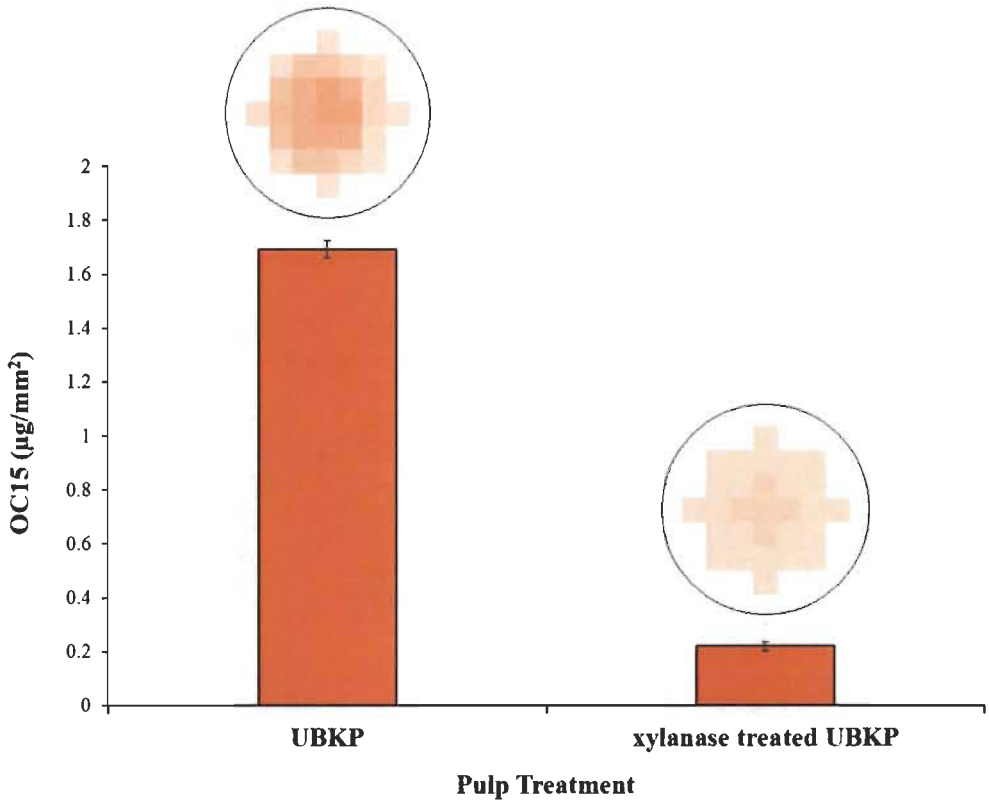


**Figure 2.4 Quantification of OC15 binding to the surface of untreated and xylanase treated UBKP papers**

Pulps were incubated with or without the xylanase (500 U/g of pulp) for 1 hour (pH 6) at room temperature under continuous agitation (150 rpm). Untreated UBKP and xylanase-treated UBKP paper discs were incubated with OC15 probe (0.5 µg/µL) for 1h at room temperature under agitation. Three percent (w/v) milk (20 mM Tris-HCl, pH 7.5with 20 mM NaCl and 5 mM $CaCl_2$) was used to minimize paper auto-fluorescence and the non-specific binding of the OC15 probe. The fluorescence values were converted to OC15 (µg/mm$^2$) by using a standard curve (additional file 2.9). The inset above each histogram columns represents the fluorescence intensity acquired by area scanning of the surface of each paper disc.

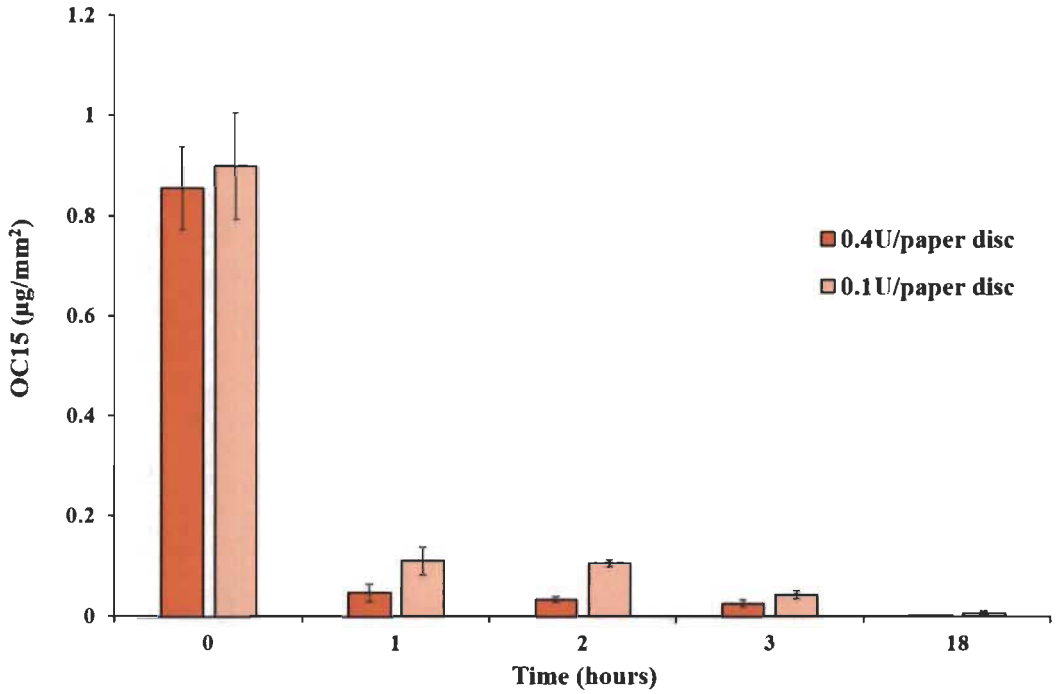


**Figure 2.5 Tracking xylanase hydrolysis of UBKP using OC15 probe**

Paper discs were incubated with xylanase (0.4U/paper disc and 0.1U/paper disc) for up to 18 hours (pH 6) at room temperature under continuous agitation (150 rpm). Untreated UBKP and xylanase treated UBKP paper discs were incubated with OC15 probe (0.06 µg/µL) for 1h at room temperature under agitation. Three percent (w/v) milk (20 mM Tris-HCl, pH 7.5 with 20 mM NaCl and 5 mM $CaCl_2$) was used to minimize paper auto-fluorescence and non-specific binding of the OC15 probe. The fluorescence values were converted to OC15 (µg/mm$^2$) by using a standard curve (additional file 2.9).

These standard methods are poorly adapted to important problematics associated with biofuels and pulp and paper industries. To address those issues, we developed a novel xylan detection approach that is sensitive, specific, reproducible, rapid (hundreds of samples analyzed in less than 4 hours), high throughput, cost-effective and that requires minimal specialized equipment. This approach involves solely the utilization of a two-domain probe, OC15, which harnesses the specific xylan recognition power of CBM15 and the high sensitivity of mOrange2 fluorescence emission.

Our results demonstrate that OC15 enables the specific tracking of chemical and enzymatic-induced variations of xylan on the surface of kraft pulps. In addition, we demonstrated here that our approach can be readily adapted to a high throughput format (tests were performed in multiwell plates and analysed with a plate reader). We believe that this tracking approach could perform various functions, such as 1) fine-tuning the conditions surrounding the mechanical and enzymatic removal of xylan; 2) decreasing costs associated with LCB processes; 3) expanding our understanding of biofuels and papermaking productions; 4) correlating surface xylan with performances of the relevant lignocellulosic products; and 5) improving the productivity of large-scale operations. This study testifies to the incredible versatility of CBMs as spearheads of innovations which can successfully tackle biotechnological challenges.

**List of abbreviations**

AGE: affinity gel electrophoresis; BSA: bovine serum albumin; BKP: bleached kraft pulp; CAZy: carbohydrate active enzymes; CBMs: carbohydrate-binding modules; CBM15: family 15 carbohydrate-binding module; CMC: carboxymethyl cellulose; GH: glycoside hydrolase; IPTG: isopropyl-β-D-thiogalactopyranoside; ITC: isothermal titration calorimetry; LB: Luria-Bertani; mAbs: monoclonal antibodies; mOrange2: mono-orange2; NREL: national renewable energy laboratory; OC15: mono-orange2 fluorescent protein linked to a family 15 carbohydrate-binding module; PCR: polymerase chain reaction; SDS-PAGE: sodium dodecyl sulfate - polyacrylamide gel electrophoresis; UBKP: unbleached kraft pulp; XPS: x-ray photoelectron spectroscopy.

## 2.6 References


1. Himmel ME, Ding SY, Johnson DK, Adney WS, Nimlos MR, Brady JW, Foust TD. Biomass recalcitrance: engineering plants and enzymes for biofuels production. Science. 2007;315:804-807.
2. Jørgensen H, Kristensen JB, Felby C. Enzymatic conversion of lignocellulose into fermentable sugars: challenges and opportunities. Biofuels Bioprod Biorefin. 2007;1:119-134.
3. Penttilä PA, Várnai A, Pere J, Tammelin T, Salmén L, Siika-aho M, Viikari L, Serimaa, R. Xylan as limiting factor in enzymatic hydrolysis of nanocellulose. Bioresour Technol. 2013;129:135-141.
4. Li M, Tu M, Cao D, Bass P, Adhikari S. Distinct roles of residual xylan and lignin in limiting enzymatic hydrolysis of organosolv pretreated loblolly pine and sweetgum. J Agric Food Chem. 2013;61(3):646-654.
5. Igarashi K, Uchihashi T, Koivula A, Wada M, Kimura S, Okamoto T, Penttilä M, Ando T, Samejima M. Traffic jams reduce hydrolytic efficiency of cellulase on cellulose surface. Science. 2011;333:1279-1282.
6. Zhu L, O'Dwyer JP, Chang VS, Granda CB, Holtzapple MT. Structural features affecting biomass enzymatic digestibility. Bioresour Technol. 2008;99:3817-3828.
7. Mansfield SD, Mooney C, Saddler JN. Substrate and enzyme characteristics that limit cellulose hydrolysis. Biotechnol Prog. 1999;15:804-816.
8. Hall M, Bansal P, Lee JH, Realff MJ, Bommarius AS. Cellulose crystallinity-a key predictor of the enzymatic hydrolysis rate. FEBS J. 2010;277(6):1571-1582.
9. Hendriks ATWM, Zeeman G. Pretreatments to enhance the digestibility of lignocellulosic biomass. Bioresour Technol. 2009;100(1):10-18.
10. Subramaniyan S, Prema P. Biotechnology of microbial xylanases: enzymology, molecular biology, and application. Crit Rev Biotechnol. 2002;22(1):33-64.
11. Saha BC. Hemicellulose bioconversion. J Ind Microbiol Biotechnol. 2003;30(5):279-291.

12. Gírio FM, Fonseca C, Carvalheiro F, Duarte LC, Marques S, Bogel-Łukasik R. Hemicelluloses for fuel ethanol: a review. Bioresour Technol. 2010;101(13):4775-4800.
13. Timell TE. Recent progress in the chemistry of wood hemicelluloses. Wood Sci Technol. 1967;1(1):45-70.
14. Kumar P, Barrett DM, Delwiche MJ, Stroeve P. Methods for pretreatment of lignocellulosic biomass for efficient hydrolysis and biofuel production. Ind Eng Chem Res. 2009;48(8):3713-3729.
15. Hu J, Arantes V, Saddler JN. The enhancement of enzymatic hydrolysis of lignocellulosic substrates by the addition of accessory enzymes such as xylanase: is it an additive or synergistic effect? Biotechnol Biofuels. 2011;4(1):1-14.
16. Selig MJ, Vinzant TB, Himmel ME, Decker SR. The effect of lignin removal by alkaline peroxide pretreatment on the susceptibility of corn stover to purified cellulolytic and xylanolytic enzymes. Appl Biochem Biotechnol. 2009;155(1-3):397-406.
17. Bura R, Chandra R, Saddler J. Influence of xylan on the enzymatic hydrolysis of steam-pretreated corn stover and hybrid poplar. Biotechnol Prog. 2009;25(2):315-322.
18. Frommhagen M, Sforza S, Westphal AH, Visser J, Hinz SW, Koetsier MJ, van Berkel WJ, Gruppen H, Kabel MA. Discovery of the combined oxidative cleavage of plant xylan and cellulose by a new fungal polysaccharide monooxygenase. Biotechnol Biofuels. 2015;8(1):1-12.
19. Suurnakki A, Li TQ, Buchert J, Tenkanen M, Viikari L, Vuorinen T, Odberg L. Effects of enzymatic removal of xylan and glucomannan on the pore size distribution of kraft fibres. Holzforschung. 1997;51(1):27-33.
20. Zhang J, Siika-aho M, Tenkanen M, Viikari L. The role of acetyl xylan esterase in the solubilization of xylan and enzymatic hydrolysis of wheat straw and giant reed. Biotechnol Biofuels. 2011;4(1):1-10.
21. Merino ST, Cherry J. Progress and challenges in enzyme development for Biomass utilization. Biofuels. 2007;108:95-120.

22. Ogeda TL, Petri DFS. Biomass Enzymatic Hydrolysis. Quimica Nova. 2010;33(7):1549-1558.
23. Pribowo AY, Hu J, Arantes V, Saddler JN. The development and use of an ELISA-based method to follow the distribution of cellulase monocomponents during the hydrolysis of pretreated corn stover. Biotechnol Biofuels. 2013;6(1):1-15.
24. Bajpai P. Application of enzymes in the pulp and paper industry. Biotechnol Prog. 1999;15(2):147-157.
25. Roncero MB, Torres AL, Colom JF, Vidal T. The effect of xylanase on lignocellulosic components during the bleaching of wood pulps. Bioresour Technol. 2005;96(1):21-30.
26. Viikari L, Kantelinen A, Sundquist J, Linko M. Xylanases in bleaching: from an idea to the industry. FEMS Microbiol Rev. 1994;13(2-3):335-350.
27. Roberts JC, McCarthy AJ, Flynn NJ, Broda P. Modification of paper properties by the pretreatment of pulp with *Saccharomonospora viridis* xylanase. Enzyme Microb Technol. 1990;12(3):210-213.
28. Savitha S, Sadhasivam S, Swaminathan K. Modification of paper properties by the pretreatment of wastepaper pulp with *Graphium putredinis*, *Trichoderma harzianum* and fusant xylanases. Bioresour Technol. 2009;100(2):883-889.
29. Johansson LS. Monitoring fibre surfaces with XPS in papermaking processes. Microchim Acta. 2002;138(3-4):217-223.
30. Fardim P, Durán N. Modification of fibre surfaces during pulping and refining as analysed by SEM, XPS and ToF-SIMS. Colloids Surf A. 2003;223(1):263-276.
31. Fardim P, Gustafsson J, von Schoultz S, Peltonen J, Holmbom B. Extractives on fiber surfaces investigated by XPS, ToF-SIMS and AFM. Colloids Surf A. 2005;255(1):91-103.
32. Belgacem MN, Czeremuszkin G, Sapieha S, Gandini A. Surface characterization of cellulose fibres by XPS and inverse gas chromatography. Cellulose. 1995;2(3):145-157.

33. Matuana LM, Balatinecz JJ, Sodhi RNS, Park CB. Surface characterization of esterified cellulosic fibers by XPS and FTIR spectroscopy. Wood Sci Technol. 2001;35(3):191-201.
34. Li J, Kisara K, Danielsson S, Lindström ME, Gellerstedt G. An improved methodology for the quantification of uronic acid units in xylans and other polysaccharides. Carbohydr Res. 2007;342(11):1442-1449.
35. Sluiter A, Crocker D, Hames B, Ruiz R, Scarlata C, Sluiter J, Templeton D. Determination of Structural Carbohydrates and Lignin in Biomass. Laboratory Analytical Procedure (LAP). 2008;NREL/TP-510-42618.
36. Lupoi JS, Singh S, Simmons BA, Henry RJ. Assessment of lignocellulosic biomass using analytical spectroscopy: an evolution to high-throughput techniques. BioEnergy Res. 2014;7(1):1-23.
37. Andrade JD. X-ray photoelectron spectroscopy (XPS). In: Surface and interfacial aspects of biomedical polymers. Springer US; 1985. p. 105-195.
38. Knox JP. In Situ Detection of Cellulose with Carbohydrate-Binding Modules. Cellulases. 2012;510:233-245.
39. Knox JP. Revealing the structural and functional diversity of plant cell walls. Curr Opin Plant Biol. 2008;11(3):308-313.
40. Hervé C, Marcus SE, Knox JP. Monoclonal antibodies, carbohydrate-binding modules, and the detection of polysaccharides in plant cell walls. The Plant Cell Wall. 2011;715:103-113.
41. Oliveira C, Carvalho V, Domingues L, Gama FM. Recombinant CBM-fusion technology-Applications overview. Biotechnol Adv. 2015;33(3):358-369.
42. Boraston AB, Bolam D, Gilbert H, Davies GJ. Carbohydrate-binding modules: fine-tuning polysaccharide recognition. Biochem J. 2004;382:769-781.
43. Gao S, You C, Renneckar S, Bao J, Zhang YHP. New insights into enzymatic hydrolysis of heterogeneous cellulose by using carbohydrate-binding module 3 containing GFP and carbohydrate-binding module 17 containing CFP. Biotechnol Biofuels. 2014;7(1):1-11.

44. Gilbert HJ, Knox JP, Boraston AB. Advances in understanding the molecular basis of plant cell wall polysaccharide recognition by carbohydrate-binding modules. Curr Opin Struct Biol. 2013;23(5):669-677.
45. Szabó L, Jamal S, Xie H, Charnock SJ, Bolam DN, Gilbert HJ, Davies GJ. Structure of a family 15 carbohydrate-binding module in complex with xylopentaose evidence that xylan binds in an approximate 3-fold helical conformation. J Biol Chem. 2001;276(52):49061-49065.
46. Lakowicz JR. Principles of fluorescence spectroscopy. Springer Science & Business Media; 2013.
47. Ding S, Xu Q, Ali MK, Baker JO, Bayer EA, Barak Y, Lamed R, Sugiyama J, Rumbles G, Himmel ME. Versatile derivatives of carbohydrate-binding modules for imaging of complex carbohydrates approaching the molecular level of resolution. BioTechniques. 2006;41(4):435.
48. Kawakubo T, Karita S, Araki Y, Watanabe S, Oyadomari M, Takada R, Tanaka F, Abe K, Watanabe T, Honda Y, Watanabe T. Analysis of exposed cellulose surfaces in pretreated wood biomass using carbohydrate-binding module (CBM)-cyan fluorescent protein (CFP). Biotechnol Bioeng. 2010;105(3):499-508.
49. Abbott DW, Boraston AB. Quantitative approaches to the analysis of carbohydrate-binding module function. Methods Enzymol. 2012;510:211-231.
50. Tavast D, Mansoor ZA, Brännvall E. Xylan from Agro Waste As a Strength Enhancing Chemical in kraft Pulping of Softwood. Ind Eng Chem Res. 2014;53(23):9738-9742.
51. Linder Å, Bergman R, Bodin A, Gatenholm P. Mechanism of assembly of xylan onto cellulose surfaces. Langmuir. 2003;19(12):5072-5077.
52. Gierer J. Chemical aspects of kraft pulping. Wood Sci and Technol. 1980;14(4):241-266.
53. Bajpai P. Pulp Bleaching and Bleaching Effluents. In: Bleach Plant Effluents from the Pulp and Paper Industry. Springer International Publishing; 2013. p. 13-19.

54. Fardim P, Hultén AH, Boisvert JP, Johansson LS, Ernstsson M, Campbell JM, Lejeune A, Holmbom B, Laine J, Gray D. Critical comparison of methods for surface coverage by extractives and lignin in pulps by X-ray photoelectron spectroscopy (XPS). Holzforschung. 2006;60(2):149-155.
55. Inari GN, Pétrissans M, Dumarcay S, Lambert J, Ehrhardt JJ, Šernek M, Gérardin P. Limitation of XPS for analysis of wood species containing high amounts of lipophilic extractives. Wood Sci Technol. 2011;45(2):369-382.
56. Istone WK. X-Ray photoelectron spectroscopy (XPS). CRC Press; 1995. p. 235-268.
57. Inari GN, Petrissans M, Lambert J, Ehrhardt JJ, Gérardin P. XPS characterization of wood chemical composition after heat-treatment. Surf Interface Anal. 2006;38(10):1336-1342.
58. Nzokou P, Kamdem DP. X-ray photoelectron spectroscopy study of red oak-(*Quercus rubra*), black cherry-(*Prunus serotina*) and red pine-(*Pinus resinosa*) extracted wood surfaces. Surf Interface Anal. 2005;37(8):689-694.
59. Sernek M. Comparative analysis of inactivated wood surfaces. Doctoral dissertation: Virginia Polytechnic Institute and State University, 2002.
60. Awada H, Elchinger PH, Faugeras PA, Zerrouki C, Montplaisir D, Brouillette F, Zerrouki R. Chemical modification of kraft cellulose fibres: influence of pretreatment on paper properties. BioResources. 2015;10(2):2044-2056.
61. Johansson LS, Campbell JM, Fardim P, Hultén AH, Boisvert JP, Ernstsson M. An XPS round robin investigation on analysis of wood pulp fibres and filter paper. Surf sci. 2005;584(1):126-132.
62. Radotić K, Kalauzi A, Djikanović D, Jeremić M, Leblanc RM, Cerović ZG. Component analysis of the fluorescence spectra of a lignin model compound. J Photoch Photobio B. 2006;83(1):1-10.
63. Sluiter A, Ruiz R, Scarlata C, Sluiter J, Templeton D. Determination of extractives in biomass. Laboratory Analytical Procedure (LAP) 2005, 1617.

64. Bradford MM. A rapid and sensitive method for the quantitation of microgram quantities of protein utilizing the principle of protein-dye binding. Anal biochem. 1976;72(1):248-254.
65. Tomme P, Boraston A, Kormos JM, Warren RAJ, Kilburn DG. Affinity electrophoresis for the identification and characterization of soluble sugar binding by carbohydrate-binding modules. Enzyme Microb Technol. 2000;27(7):453-458.
66. Cui L, Meddeb-Mouelhi F, Laframboise F, Beauregard M. Effect of commercial cellulases and refining on kraft pulp properties: Correlations between treatment impacts and enzymatic activity components. Carbohyd polym. 2015;115, 193-199.

## 2.7 Additional Files

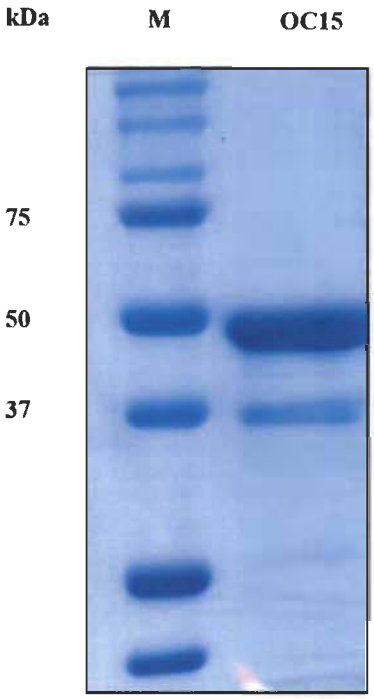


**Additional file 2.1** **SDS-PAGE analysis of the OC15 probe purified by affinity chromatography**

The expected molecular weight of the OC15 fusion protein is 44.68 kDa. A 12% polyacrylamide gel was used for SDS-PAGE analysis. Well M: Precision plus protein standards (5 μg). Well OC15: Purified OC15 probe (10 μg).

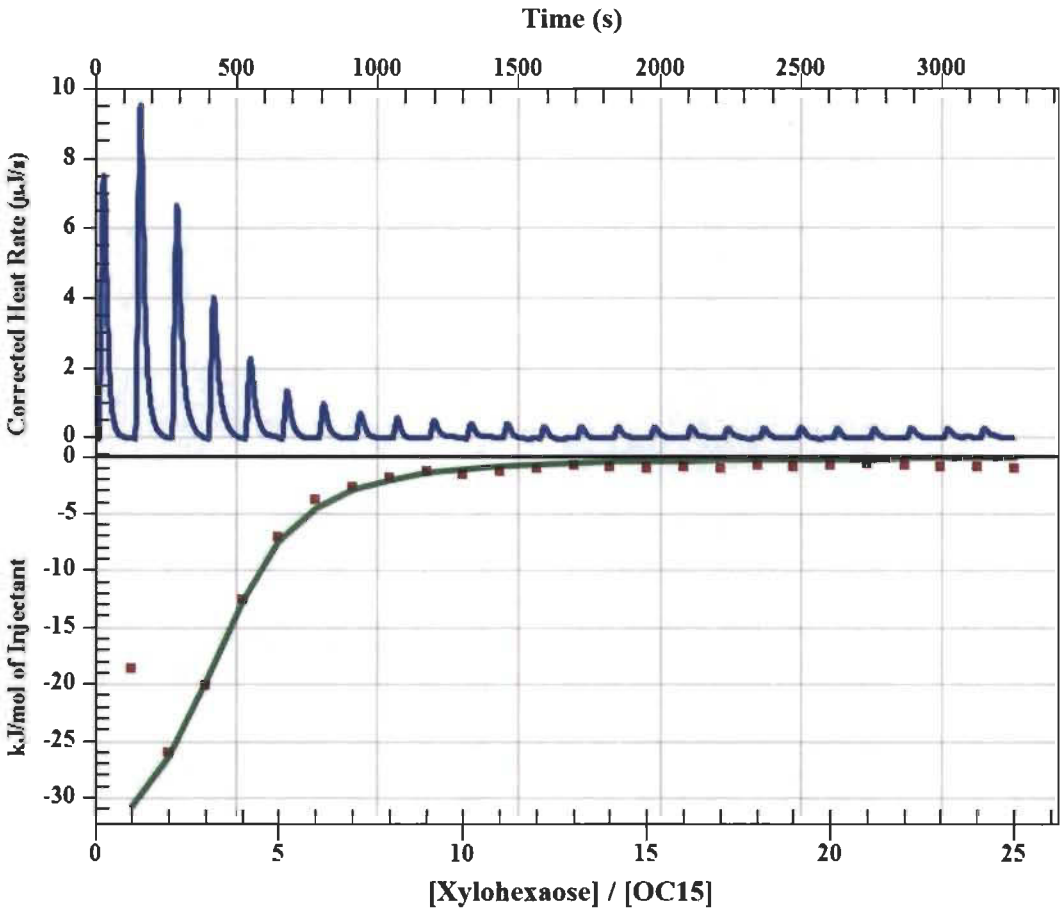


**Additional file 2.2** **Isothermal calorimetric titration of the OC15 probe with xylohexaose**

Top panel: Typical ITC experiment carried out by adding 25 injections of 2 µL xylohexaose (5 µM) into the OC15 probe (200 mM) solution, with an interval of 130 seconds between each injection. Bottom panel: Heat release per mole of xylohexaose as a function of xylohexaose/OC15 molar ratio. The titration was performed at 25°C in a 20 mM Tris-HCl pH 7.5 buffer which contained 20 mM NaCl and 5 mM $CaCl_2$. Injectant: xylohexaose.

**Additional file 2.3 Chemical composition of UBKP and BKP determined by NREL/TP-510-42618**

| Compound | UBKP (%) | BKP (%) |
|---|---|---|
| Extractives | 0.3 ± 0.01 | 0.3 ± 0.01 |
| Lignin | 4.4 ± 0.10 | 1.9 ± 0.05 |
| Glucose | 80.8 ± 0.92 | 83.6 ± 1.97 |
| Xylose | 7.9 ± 0.63 | 8.5 ± 0.76 |
| Mannose | 6.7 ± 0.67 | 7.0 ± 0.65 |
| Galactose | 0.0 ± 0.00 | 0.0 ± 0.00 |
| Arabinose | 0.0 ± 0.00 | 0.0 ± 0.00 |

UBKP: Unbleached kraft pulp; BKP: Bleached kraft pulp

**Additional file 2.4 XPS analysis of UBKP and BKP**

Results include O/C ratios and contributions (%) from each carbon type (C1-C4) to curve fitting of the C 1s peak measured by low- and high-resolution XPS. UBKP: Unbleached kraft pulp. BKP: Bleached kraft pulp.

| Functionality | UBKP (%) | BKP (%) |
|---|---|---|
| O/C* | 0.61 ±0.04 | 0.64 ±0.01 |
| C1 | 20.1 ±0.1 | 9.1 ±0.5 |
| C2 | 63.0 ±1.6 | 71.6 ±1.9 |
| C3 | 15.8 ±0.1 | 18.3 ±0.4 |
| C4 | 1.1 ±0.3 | 1.0 ± 0.7 |

Spectra were taken from unextracted pulp samples.
*Low-resolution XPS spectra was used to obtain the oxygen and carbon percentage in order to ascertain that the O/C ratio does not vary as a function of chemical treatment. The bleaching process did not change the overall percentage of oxygen and carbon.

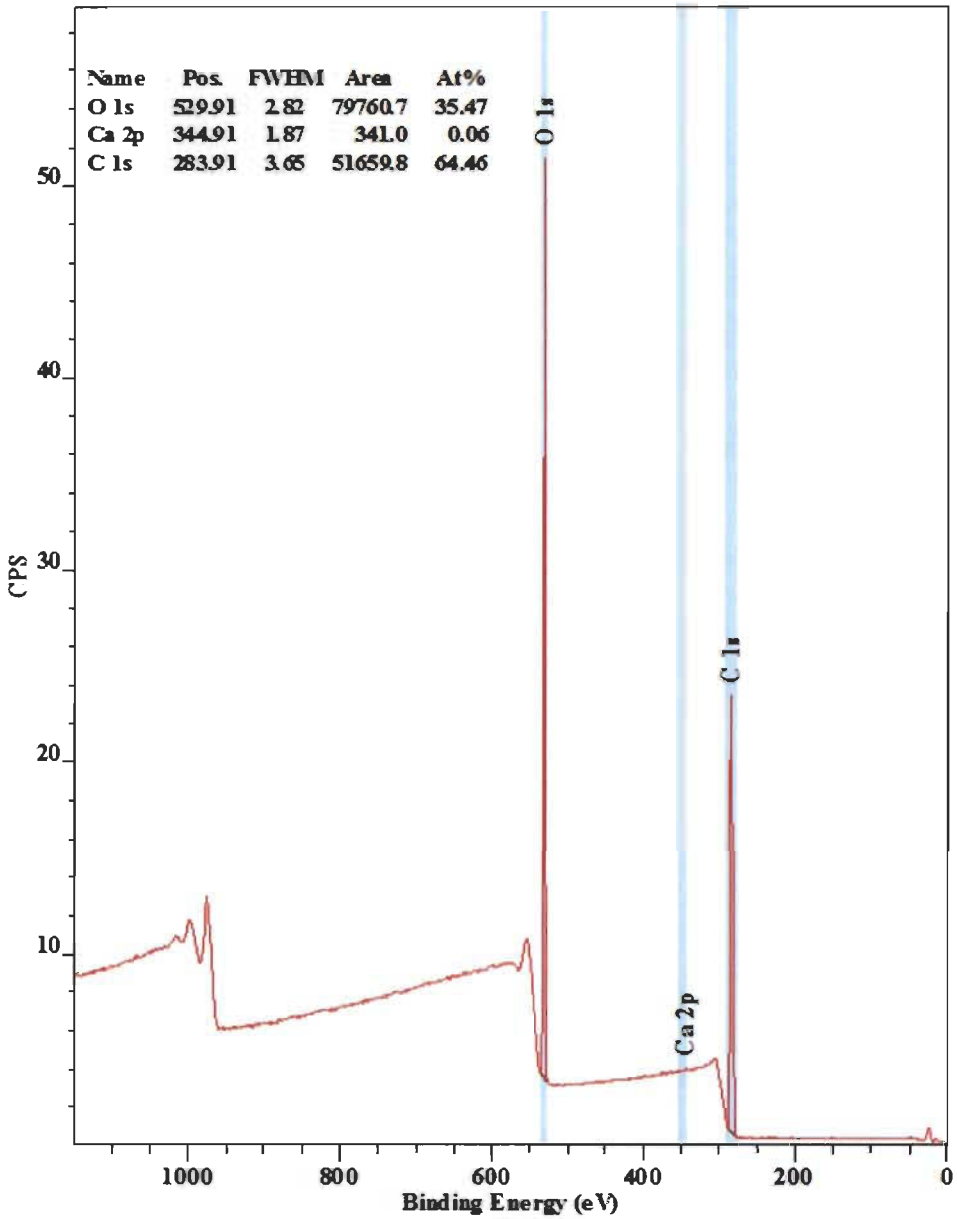


**Additional file 2.5 Low-resolution XPS spectrum of UBKP surface**

UBKP: unbleached kraft pulp. Unextracted pulp samples were analyzed.

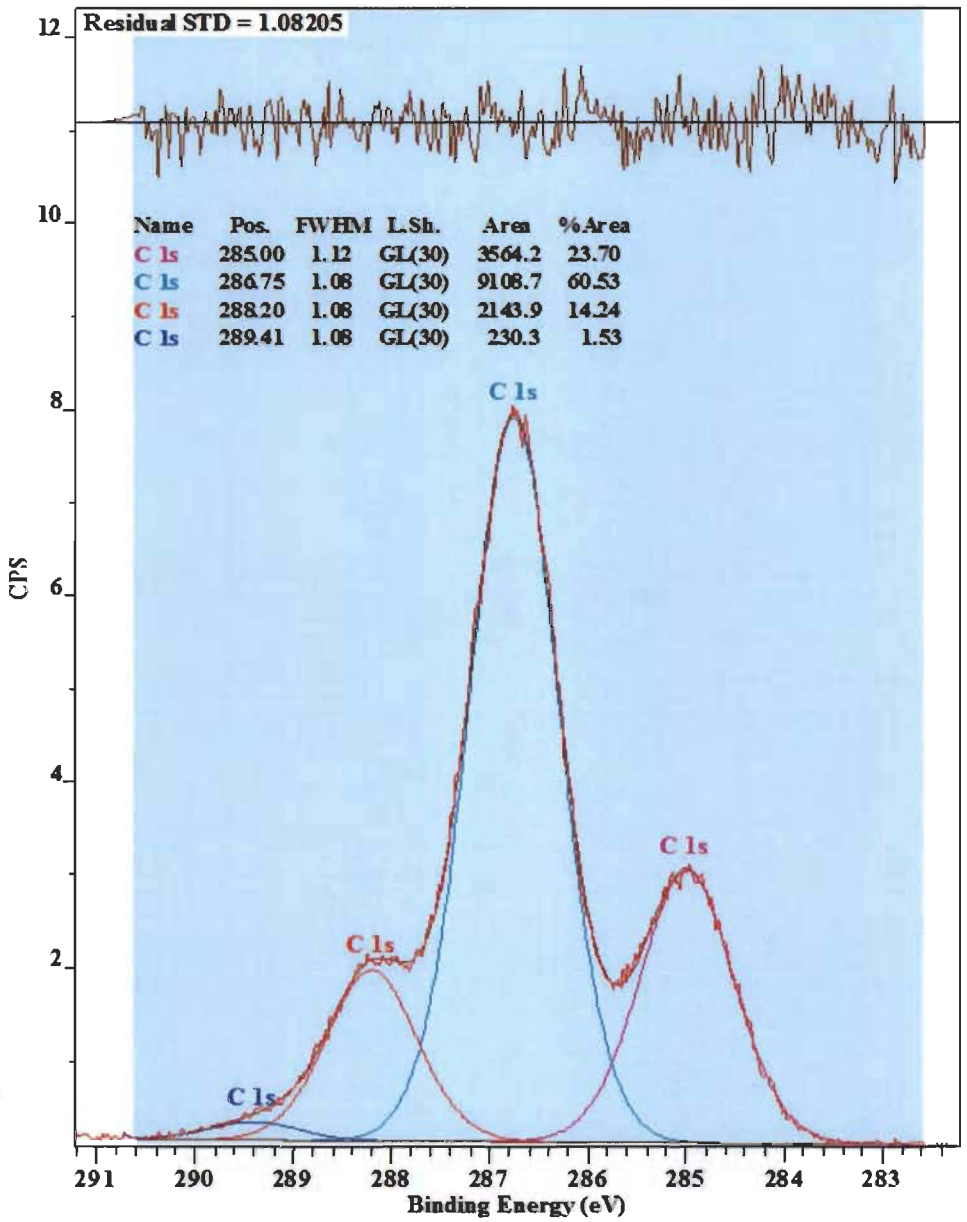


**Additional file 2.6 Deconvolution of high-resolution XPS spectrum of UBKP**

UBKP: unbleached kraft pulp. Unextracted pulp samples were analyzed.

**Additional file 2.7 Chemical composition of untreated and xylanase-treated UBKP determined by NREL/TP-510-42618**

| Compound | UBKP (%) | Xylanase-treated UBKP (%) |
|---|---|---|
| Extractives | 0.1 ± 0.04 | 3.2 ± 0.02 |
| Lignin | 4.6 ± 0.07 | 4.6 ± 0.10 |
| Glucose | 81.0 ± 0.54 | 81.8 ± 0.73 |
| Xylose | 8.1 ± 0.28 | 4.8 ± 0.25 |
| Mannose | 2.9 ± 0.37 | 4.0 ± 0.19 |
| Galactose | 0.4 ± 0.04 | 0.4 ± 0.04 |
| Arabinose | 0.7 ± 0.01 | 0.5 ± 0.08 |

UBKP: Unbleached kraft pulp

**Additional file 2.8 XPS analysis of UBKP and xylanase-treated UBKP**

Results include O/C ratios and contributions (%) from each carbon type (C1-C4) to curve fitting of the C 1s peak measured by low- and high-resolution XPS. UBKP: Unbleached kraft pulp.

| Functionality | UBKP (%) | Xylanase-treated UBKP (%) |
|---|---|---|
| O/C* | 0.52 ± 0.01 | 0.55 ± 0.04 |
| C1 | 24.1 ± 0.5 | 21.6 ± 0.4 |
| C2 | 61 ± 2.3 | 61 ± 1.4 |
| C3 | 13.8 ± 0.1 | 16.0 ± 0.9 |
| C4 | 1.5 ± 0.4 | 1.7 ± 0.2 |

Spectra were taken from unextracted pulp samples.
*Low-resolution XPS spectra was used to obtain the oxygen and carbon percentage in order to ascertain that the O/C ratio does not vary as a function of chemical treatment. The xylanase treatment did not change the overall percentage of oxygen and carbon.

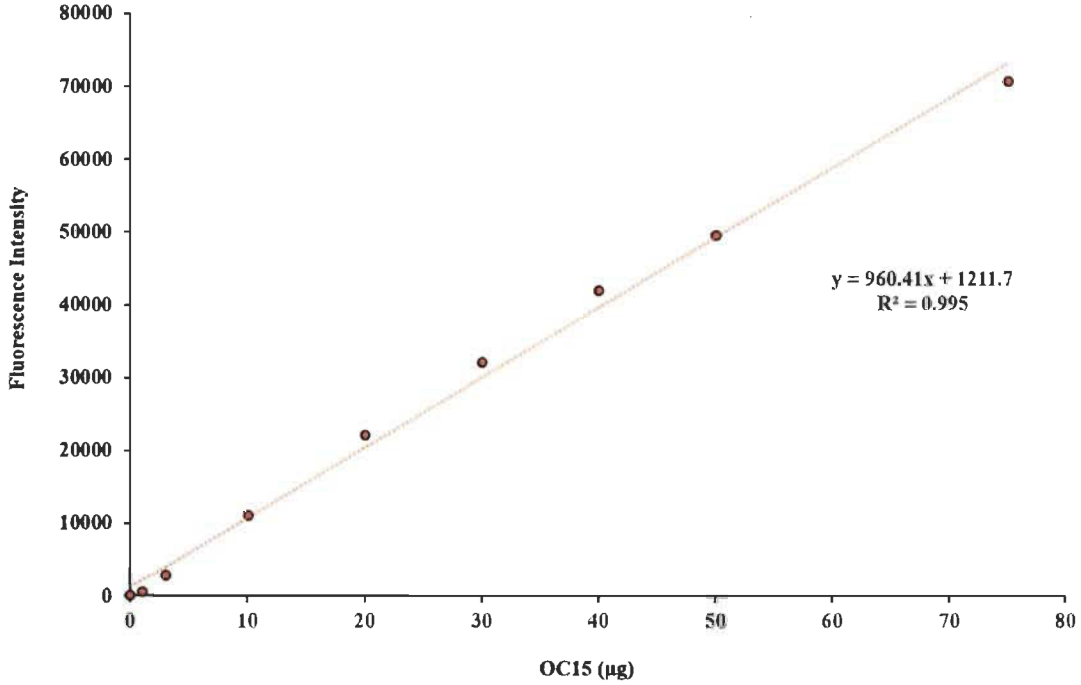


**Additional file 2.9 Standard curve for the conversion of fluorescence intensity into µg of OC15 probes**

The excitation and emission wavelengths were set at 549 and 568 nm, respectively.

# Chapter 3 - Scientific Article II

**New insights into enzymatic hydrolysis of lignocellulosic polymers by using fluorescent-tagged carbohydrate-binding modules**

Vinay Khatri[1, 2] Fatma Meddeb-Mouelhi[1, 2] and Marc Beauregard[1, 2*]

[1] Centre de recherche sur les matériaux lignocellulosiques, Université du Québec à Trois-Rivières, Trois-Rivières (Québec) G9A 5H7, Canada.

[2] PROTEO, Université Laval, Québec (Québec) G1V 4G2, Canada.

*Corresponding author: Centre de recherche sur les matériaux lignocellulosiques, Université du Québec à Trois-Rivières, C.P. 500, Trois-Rivières (Québec), G9A 5H7 Canada, Tel: (819) 376-5011 # 3354, Fax: (819) 376-5084, E-mail: marc.beauregard@uqtr.ca

## Authors' contributions

VK carried out all the experiments and drafted the manuscript. FMM and MB helped to draft and revise the manuscript. All authors read and approved the final manuscript.

## Acknowledgments

This research was supported in part by Buckman Laboratories of Canada and funded by grants from CRIBIQ and NSERC (CRDPJ445143-12). We would like to thank Dr. Roberto Chica (University of Ottawa) for the donation of fluorescent protein and Dr. Nicolas Doucet (INRS-Institut Armand-Frappier) for his expert assistance while performing isothermal titration calorimetry (ITC) measurements. The skillful technical assistance of Nikolas Beauchesne, Vincent Bolduc, and Guillaume L. Lemieux is acknowledged. We would like to thank Ojas Bhatia for his valuable editorial contributions.

## Competing interests

VK and MB declare that they have no competing interests. FMM was an employee of Buckman North America which financially supported parts of this work.

## 3.1 Abstract

The development of a bio-based economy requires the utilization of LCB in a cost-effective way. The economic viability of LCB-based industries is hindered by our imperfect understanding of biomass structure and suboptimal industrial processes. To achieve such goals requires direct and rapid monitoring of lignocellulosic polymers as they are physically, chemically, and/or enzymatically treated. In this study, the recently reported fluorescent protein-tagged carbohydrate-binding modules method (FTCM) was used to specifically track mechanical, chemical and enzymatic-induced variations of hemicelluloses at the surface of different wood fibers. Our results showed that susceptibility to hydrolysis in kraft pulp was higher for xylan, while mannan was more vulnerable in mechanical pulps. Furthermore, FTCM rapidly and efficiently detected enzymatic inactivation and the apparent complementarity (additive and/or synergistic effect) between cellulase and other enzymes (xylanase and mannanase), significantly bolstering cellulose and hemicelluloses hydrolysis. Subsequent addition of xylanase and mannanase enzymes directly proved that xylan was acting as a physical shield which was covering mannan in bleached kraft pulp. This study suggests that mannan was closely associated with cellulose or was deeply embedded in the cell wall organization of such fibers. FTCM provided direct support for previous models on fiber structure that were based on time-consuming and complicated approaches (*i.e.* chromatography, spectroscopy and microscopy). FTCM allowed for the monitoring of layers of polymers as they were exposed after treatments, providing key information regarding hydrolysis optimization and the specific susceptibility of xylan and mannan to biomass treatments. We believe that by applying this simple and rapid method on site, biomass industries could substantially improve cost-effectiveness of production of biofuels and other LCB-based products.

**Keywords:** Lignocellulosic polymers, Hydrolysis, Carbohydrate-binding module, Fluorescent protein, Cellulase, Xylanase, Mannanase

## 3.2 Introduction

LCB is the most abundant, renewable and sustainable feedstock allowing our ever-increasing energy demand to be satiated while fossil fuels progressively disapear.[1-5] In addition, the greenhouse gas mitigation and near carbon neutrality afforded by the conversion of biomass to bio energy (biofuel) and chemicals are important advantages over conventional fossil fuels.[2,6-8] The development of a bio-based economy, however promising, is faced with challenges related to the cost-effective utilization of the LCB. Improving biomass processes would increase cost effectiveness and competitiveness for large scale applications.[3,9,10] The main obstacle for biofuel and chemicals production is associated with the inherent recalcitrant nature of LCB.[3,11-14] Due to the structural complexity of LCB, the bioconversion of biomass to biofuel is a multiple stage process.[8,15] The enzymatic hydrolysis of the lignocellulosic component to fermentable sugars is a crucial step in this bioconversion. It is considered as one of the major rate limiting and costly step.[16-21]

The complex recalcitrance nature of biomass is partly attributed to hemicelluloses. They constitute about 20-30% of the total biomass, and are the second most common polysaccharides[22-24] in nature, after cellulose. Unlike cellulose, hemicelluloses are heterogeneous polymers of pentoses (xylose, arabinose), hexoses (mannose, glucose, galactose) and/or uronic acids (glucuronic acid, galacturonic acid).[22,25] Hemicelluloses in hardwood (from angiosperms) mostly consist of xylan, whereas softwood (from gymnosperms) typically contains glucomannans.[26] The hemicelluloses have frequently been recognized to act as a physical barrier, that cover the outer surface of cellulose fibers and interfibrillar space, limiting the accessibility of cellulase enzymes to cellulose.[27-35] The hemicellulose-degrading activities in most commercially available cellulase enzymes are too low to achieve sufficient hydrolysis of the hemicelluloses.[36,37] Therefore, addition of enzyme extracts or additives with higher level of hemicellulases are important for eliminating the significant hindering effect of residual hemicelluloses (mostly xylan and mannan) on the enzymatic hydrolysis of cellulose.[27,29,35,38-43] In order to increase the efficiency of wood

fiber utilization, it is important to utilize all wood fiber constituents (including hemicelluloses and lignin) in an economically feasible way (providing other valuable wood-derived materials beside biofuel). However, this requires a better understanding of the ultrastructure of the cell wall and its organization, which are not yet fully understood.[20] Different chromatography, spectroscopy and microscopy techniques have been used to study lignin-carbohydrate complexes,[38] polymers interactions[44] and plant cell wall deconstruction.[20] For instance, an FT-IR study of softwood fiber (kraft pulp) dedicated to investigate the interactions between wood polymers revealed that glucomannan was closely associated to cellulose while there existed no mechanical interactions between xylan and cellulose.[44] Current models suggest that hemicelluloses play a major role in biomass recalcitrance and are closely associated with both lignin and cellulose, forming lignin-hemicellulose complexes and cellulose-hemicellulose complexes.[38] These techniques revealed important information on hemicellulose's location and their influence on the recalcitrance nature of fibers, and enhanced our understanding of the structural arrangement of fibers. They are however invasive, time-consuming, complex and are dependent on specialized equipment and expertise.

The inherent recalcitrance nature of plants directly or indirectly impacts enzyme accessibility,[12,35,38,43] inactivation,[45] inhibition[40.41.46-55] and, as a consequence, cost of use.[9,10,27] The recent improvement in enzymes stabilization, activity, cost-effectiveness[41,43,56-61] and development of new promising pretreatment conditions[62-64] improved production yields. However, the high dose requirements of these enzymes often jeopardize commercial viability.[27,42,45,65-68] Therefore, investigating biomass recalcitrance of typical wood biomass substrates, and correlating process parameters such as enzyme dosage, temperature, incubation time, inactivation and inhibition, with polymers hydrolysis efficiency is important. We anticipate that such advances would support engineers for increasing yields and mitigate production costs associated with LCB based industries.

One of the major difficulties in studying biomass recalcitrance and process parameters is the lack of rapid, high throughput and reliable tools[21] for monitoring and/or tracking hemicelluloses at the surface of wood fibers. Over the past decade, several techniques

have been developed for direct and rapid detection of biomass polymers.[69-71] Among these techniques, carbohydrate-binding modules (CBMs) are more powerful and advantageous as detection probes compared to others (such as chemical dyes, monoclonal antibodies etc.) due to their high specificity towards lignocellulosic polymers.[70-72] CBMs are the non-catalytic polysaccharide-recognizing modules of glycoside hydrolases enzymes.[70,71,72-76] Until now, CBMs have been implemented for various fundamental research on plant cell chemistry and their structure,[77,78] cellulose accessibility and surface morphology,[74,79,80] as well as for several industrial applications.[72;81-83]

Considering the importance of LCB tracking, we have recently established a novel, rapid, high-throughput, easy-to-use, unambiguous and affordable approach to track lignocellulosic polymers at the surface of mechanically, chemically and enzymatically treated pulps.[82,83] This approach is based on the use of four highly specific probes made of fluorescent-tagged carbohydrate-binding modules. The CBM part of these genetically modified probes recognizes and binds to biopolymers (*i.e.* mannan, xylan, crystalline and non-crystalline cellulose) while the fluorescent protein part makes it possible to quickly detect and measure binding of probes to their intended targets. This approach, called fluorescent-protein-tagged CBM method (FTCM), proved to be instrumental for our understanding of LCB processing, and exhibited both process optimizing and outcome predicting potential.[82,83]

Here we investigated the potential of FTCM for bolstering our understanding of hemicelluloses hydrolysis and factors that have an impact on such hydrolysis. To this end, we used two fluorescent protein-tagged fusion proteins of FTCM: mOrange2-CBM15 (OC15) and eCFP-CBM27 (CC27). The family 15 CBM (CBM15) is a xylan recognizing module of a xylanase (Xyn10C) from *Cellvibrio japonicus*[84] and family 27 CBM (CBM27) consists of the mannan recognizing module of mannanase (Man5) from *Thermotoga maritima*.[85] Both CBM15 and CBM27 are classified as type B CBMs and have been demonstrated to bind specifically to xylooligosaccharides and mannooligosaccharides, respectively.[84,85] Mono-orange2 (mOrange2) and cyan fluorescent protein (CFP) were used as fluorescent proteins (detector molecules), and can be quantitatively measured

with very high sensitivity and specificity, due to their independent fluorescent signals (each probe has its specific pair of emission and absorption maxima). For this study, we used four different pulp samples (unbleached mechanical pulp, bleached mechanical pulp, unbleached kraft pulp and bleached kraft pulp) to investigate and track variations in hemicelluloses after various treatments. Our results showed that FTCM can monitor the impact of mechanical and chemical treatment on the surface distribution of hemicelluloses, and helped understand and optimize enzymatic-induced hydrolysis of lignocellulosic polymers. We anticipate that FTCM can be developed into a monitoring tool for optimization of treatments and process strategies leading to a cost-effective hydrolysis of hemicelluloses.

## 3.3 Materials and methods

### 3.3.1 Chemicals and microbial strains

Unless otherwise noted, all chemicals were reagent grade and purchased from Sigma-Aldrich and/or Fisher Scientific. *Escherichia coli* XL10 cells (Agilent Technologies) were used for all DNA manipulations while *E. coli* BL21-Gold(DE3)pLysS competent cells (Agilent Technologies) were used for recombinant proteins expression. *Trichoderma viride* xylanase (endo-1,4-β-xylanase) from glycoside hydrolase (GH) family 11 (E-XYTRI; Megazyme), *Cellvibrio japonicus* mannanase (endo-1,4-β-mannanase) from glycoside hydrolase (GH) family 26 (E-BMACJ; Megazyme) and *Trichoderma reesei* Celluclast 1.5L (C2730; Sigma-Aldrich) were used for the hydrolysis of LCB. Carboxymethyl cellulose sodium salt (C5678; Sigma), xylan from beechwood (X4252; Sigma) and galactomannan (P-GALML; Megazyme) were used for affinity gel electrophoresis (AGE) and for enzymatic assays using the 3,5-dinitrosalicylic acid (DNS) method.

### 3.3.2 Construction, production and purification of CBM recombinant probes

Probes were produced and purified from recombinant *E. coli* BL21-Gold(DE3)pLysS cells as described by Khatri *et al.* (2016)[82] and Hébert-Ouellet *et al.* (2017)[83] (note that in this study, probe eGFP-CBM3a was named GC3a; probe mOrange2-

CBM15 was named OC15 and probe eCFP-CBM27 was named CC27, for the sake of simplicity). Following affinity and size exclusion chromatography steps, the probes purities were verified using SDS-PAGE (Additional files 3.1 and 3.8 ). The amount of protein was quantified using the Bradford method.[86] Concentrated protein solutions were stored at -80°C following flash freezing.

### 3.3.3 Affinity gel electrophoresis (AGE)

AGE was used as described by Khatri *et al.* (2016)[82] for qualitative assessment of the CC27 (10 μg) specificity toward selected ligands.

### 3.3.4 Isothermal titration calorimetry (ITC)

ITC was employed as described by Khatri *et al.* (2016)[82] to measure the affinity of the CC27 probe towards selected hexaoses (xylohexaose (O-XHE; Megazyme), mannohexaose (O-MHE; Megazyme), cellohexaose (O-CHE; Megazyme)). All experiments were performed in triplicates. Data were analyzed and fitted using the NanoAnalyze software v2.3.6 (TA Instruments).

### 3.3.5 Pulp characterization

The mechanical and kraft pulps used for this study were provided by an Eastern Canadian pulp and paper company. Both mechanical and kraft pulping were performed using a mixture of softwood (80-85%) and hardwood (20-15%). Four different grades of pulps: unbleached mechanical pulp (UBMP), bleached mechanical pulp (BMP), unbleached kraft pulp (UBKP) and bleached kraft pulp (BKP), were used. The cellulose, hemicellulose, and lignin contents of these pulps were analyzed in triplicates using NREL/TP-510-42618 protocol[87] as described in Khatri *et al.* (2016).[82]

### 3.3.6 Handsheets preparation

UBMP, BMP, UBKP and BKP were used as lignocellulosic substrates for the preparation of handsheets and paper discs. Handsheets (basis weight of 60 ± 2 g/m$^2$) were

prepared from pulps according to the Tappi standard method T 205 sp-02 as described in Khatri *et al.* (2016).[82] These handsheets were then used for the preparation of the paper punches. These punches were defined as paper discs having a diameter of 3 mm.

### 3.3.7 Enzymatic digestion of paper discs

The enzymatic digestions of paper discs were performed in triplicates using *Trichoderma viride* xylanase, *Cellvibrio japonicus* mannanase and *Trichoderma reesei* Celluclast 1.5L enzyme(s). Celluclast 1.5L is a mixture of fungal hydrolytic enzymes containing mostly two cellobiohydrolases, two endoglucanases and various accessory enzymes such as hemicellulases.[27,88] We used the 3,5-dinitrosalicylic acid (DNS) method[97] to monitor the accessory enzymes activities (such as xylanase and mannanase) in the Celluclast 1.5L (Additional file 3.12). Xylanase and mannanase treatment concentrations ranged from 0.1 to 0.4 U/paper discs. Celluclast 1.5L enzyme was used at 0.1 U/paper discs. Cocktail CX was prepared by mixing Celluclast 1.5L (0.1 U/paper disc) with *Trichoderma viride* xylanase (0.1 U/paper disc). Cocktail CM was prepared by mixing Celluclast 1.5L (0.1 U/paper disc) with *Cellvibrio japonicus* mannanase (0.1 U/paper disc)) and cocktail CXM was prepared by mixing Celluclast 1.5L (0.1 U/paper disc) with *Trichoderma viride* xylanase (0.1 U/paper disc) and *Cellvibrio japonicus* mannanase (0.1 U/paper disc). Units used here were as specified by respective enzyme suppliers. All experiments were performed with paper discs placed/glued at the bottom of 96-well black microtiter plate (Corning). All reactions were performed at room temperature or 50°C, in sodium phosphate buffer (100 mM), pH 7.0 supplemented with 0.5 mg/mL BSA under continuous agitation (150 rpm) in order to reduce enzyme adsorption. Unless otherwise noted, after each enzymatic digestion, the reactions were removed, and paper discs were washed (3 x 5 minutes) with buffer (20 mM Tris-HCl, pH 7.5 with 20 mM NaCl and 5 mM $CaCl_2$) and later washed (3 x 5 minutes) with 0.05% (v/v) Tween 20. This buffer was shown to remove most proteins from paper discs in a previous report.[83] Following Tween 20 washing, paper discs were washed again with buffer (without Tween) before analyzing the variations in biopolymers levels, or digested again with refreshing enzymes solution every hour to reach maximum possible hydrolysis when specified.

### 3.3.8 Lignocellulosic polymers tracking on the surface of paper discs using the OC15, CC27 and GC3a probes

The FTCM tracking assay was performed as described by Khatri *et al.* (2016).[82] All fluorescence readings were acquired at room temperature with a Synergy Mx micro-plate reader (BioTek). These fluorescence values were then converted into $\mu g/mm^2$ using the appropriate standard curves (Additional files 3.6 , 3.7 and 3.9) and the surface area of the paper discs.

## 3.4 Results and Discussion

### 3.4.1 Determination of the CC27 probe specificity using affinity gel electrophoresis (AGE)

In this study, we have used three FTCM probes (GC3a, OC15 and CC27). GC3a and OC15 were previously characterized and shown to be specific to their intended target.[82, 83] Affinity gel electrophoresis (AGE) was used to qualitatively evaluate the specificity of the CC27 probe (mannan specific) towards soluble polysaccharides.[89] In AGE, interactions between the studied protein and the gel-embedded polysaccharide are typically revealed by a reduced mobility compared to the mobility of the protein in absence of saccharide. Figure 3.1 shows that CC27 interacts only with galactomannan (Figure 3.1B). Similar to BSA, no binding was detected between CC27 and beechwood xylan (Figure 3.1C) or carboxymethyl cellulose (CMC) (Figure 3.1D). These results confirm that the well-known specific binding of CBM27 to mannan is unaltered by its fusion with CFP in the CC27 probe. BSA, which has no affinity towards carbohydrates, was used as negative control.[89]

### 3.4.2 Determination of CC27 probe affinity using isothermal titration calorimetry (ITC)

The affinity of the recognition module of CC27 was investigated to quantify its sensitivity for a representative derivative of mannan. To this end, the affinity of CC27 toward various hexaoses was investigated by ITC (Table 3.1 and Additional file 3.2).

Analysis of the binding isotherms showed that the recognition module of CC27 probe bound tightly to mannohexaose ($K_a$ = 692.6 × $10^3$ $M^{-1}$), but not to cellohexaose or xylohexaose (Table 3.1). The affinity value is similar to those previously reported for CBM27 ($K_a$ (×$10^4$ $M^{-1}$) =136.5 ± 17.68) confirming that the binding site of the recognition module of the CC27 probe is unaltered by its fusion with CFP.[85]

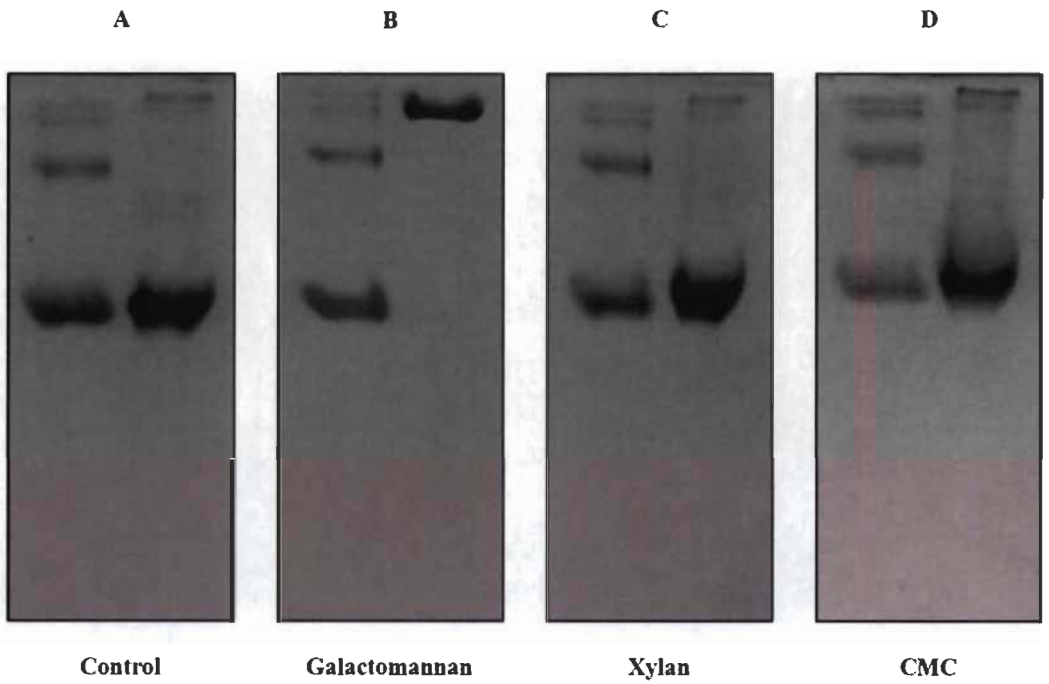


**Figure 3.1 Affinity gel electrophoresis (AGE) of the CC27 probe**

Panel **A**) control (no polysaccharide), Panel **B**) galactomannan, Panel **C**) xylan, Panel **D**) CMC. In each panel the first well contained BSA (10 μg) and the second well was loaded with the CC27 probe (10 μg). All soluble polysaccharides were used at final concentration of 0.5% (w/v) and a 12% polyacrylamide gel was used for affinity analysis.

**Table 3.1 Affinity of the CC27 probe for various hexaoses as determined by ITC**

| Ligand | $K_a \times 10^3$ ($M^{-1}$) | $K_d$ (M) | n |
|---|---|---|---|
| Xylohexaose | NB | - | - |
| Mannohexaose | 692.6 ± 0.5 | $4.413 \times 10^{-6} \pm 0.2$ | 1.1 ± 0.3 |
| Cellohexaose | NB | - | - |

n: Number of ligand binding sites.
NB: No binding detected.
-: binding not detected

### 3.4.3 Tracking hemicelluloses at the surface of wood biomass

Pulps composed of a mixture of softwood (80-85%) and hardwood (20-15%) from an Eastern Canadian paper mill were used as LCB samples. Four different types of pulps were used in this study, allowing for the comparison of mechanically and chemically treated wood biomass: unbleached mechanical pulp (UBMP), bleached mechanical pulp (BMP), unbleached kraft pulp (UBKP) and bleached kraft pulp (BKP). These pulps were first investigated to determine differences in the hemicelluloses polymer content and their exposure at fiber surface.

Comparison of CC27 with OC15 binding to pulps (Figure 3.2) revealed that mannan exposure is 2.3-fold higher than xylan exposure in both mechanical pulps (UBMP and BMP). Only minute differences were observed between exposures of both hemicelluloses studied here in kraft pulps: mannan exposure was 1.13-fold higher than xylan exposure in UBKP and only 1.08-fold higher in BKP (Figure 3.2). The dominance of mannan for all pulps is compatible with the high softwood content of the four different pulps studied here.[26] Our results also indicate that mannan was the dominant hemicellulose at the surface of mechanical pulps in agreement with an earlier study on lignin-hemicellulose complexes.[38] Even though the pulp was primarily composed of softwood fibers, kraft processing led to the exposure of similar amounts of xylan and mannan on the surface of both kraft pulps (Figure 3.2, UBKP and BKP). Note that the trends observed in FTCM signals, which responds to surface polymers, were in accordance with the bulk measurements of

simple sugars by chemical composition analysis (NREL/TP-510-42618) of these pulps (Additional file 3.3 ).

Bleaching of mechanical pulp resulted in no significant difference between the exposure of xylan and mannan (Figure 3.2). These results can be attributed to the pulping methodology involved. Mechanical pulping is a high yield process which tends to retain most wood constituents when producing UBMP and during the transformation of UBMP to BMP.[90] FTCM indicates that the distribution of hemicelluloses at the surface of mechanically treated fibers were comparable to fiber bulk composition (revealed by NREL/TP-510-42618) (Additional file 3.3 ).

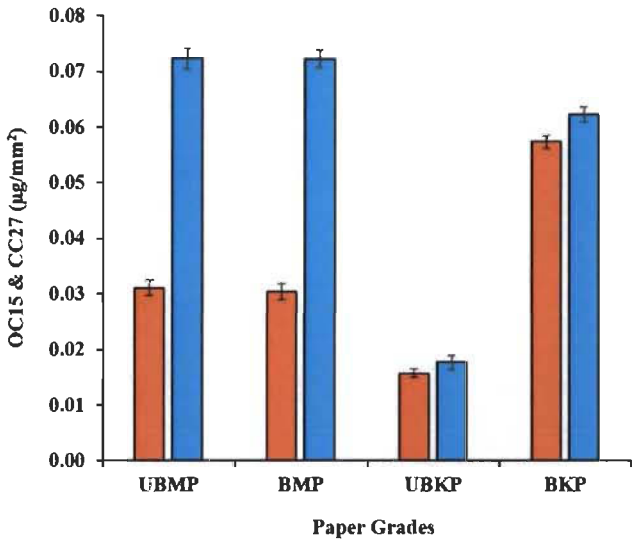


**Figure 3.2 Tracking hemicelluloses on the surface of UBMP, BMP, UBKP and BKP papers using OC15 and CC27 probes**

UBMP, BMP, UBKP and BKP paper discs were incubated with the OC15 probe (0.5 µg/µL) (for xylan detection) and the CC27 probe (0.5 µg/µL) (for mannan detection) for 1h at room temperature under agitation. Three percent (w/v) milk (20 mM Tris-HCl, pH 7.5 with 20 mM NaCl and 5 mM $CaCl_2$) was used to minimize the auto-fluorescence of paper discs and the non-specific binding of the OC15 and CC27 probes. The fluorescence values were converted to OC15 (µg/mm$^2$) and CC27 (µg/mm$^2$) by using the standard curves (Additional file 3.6 and 3.7 ). Orange color represents the OC15 probe detection and cyan color represents the CC27 probe detection. Error bars represent the standard deviation.

The goal of kraft pulping process is to degrade and/or dissolve lignin with minimum dissolution or degradation of hemicelluloses.[90] UBKP was characterized by the smallest exposure of hemicelluloses, a possible consequence of the dissolution or degradation of lignin-hemicelluloses complexes[38] during kraft pulping. Bleaching of kraft pulp completely changed hemicelluloses exposure. As shown in Figure 3.2, BKP binds 3.6-fold the amount of OC15 and 3.5-fold the amount of CC27 in comparison to UBKP, indicating that the surface exposure of xylan and mannan has increased after the bleaching process. Kraft pulping did not remove all lignin (lignin still represents 4.3% according to chemical composition analysis, Additional file 3.3 ) in UBKP. Bleaching revealed additional hemicelluloses at the surface of BKP, resulting from the removal of this residual lignin. These "deep" hemicelluloses would become accessible after the full removal of lignin. Another explanation for this higher exposure or detection of hemicelluloses would involve mannan and xylan redeposition onto the surface of cellulose fibers during kraft processes.[91-93]

The strength of FTCM lies in its ability to detect changes in hemicelluloses exposure at the surface of fibers. While the trends observed were in general compatible with overall composition analysis (Additional file 3.3 ), the amplitude of changes at the surface could not be predicted by chemical analysis. For instance, mannan dropped by 71% when comparing both mechanical pulps (UBMP and BMP) with UBKP (Figure 3.2). Chemical analysis detected a mere decrease of 30-34% in mannan for the same comparison. In kraft pulps, the impact of bleaching on hemicelluloses exposure (an increase of 67%) (Figure 3.2) could not be predicted by chemical composition analysis (showing an increase of only 13-15%, Additional file 3.3 ). We also confirmed that the fluorescent proteins (alone, without CBM) did not bind to the biomass surface (data not shown), and we found no difference in binding signals, regardless of using the OC15 and CC27 probes together or separately (Additional file 3.4 and 3.5 ). This indicates that the probes did not interfere with one another, as expected from the different targets to which they are specific. We also confirmed that there were no unspecific interactions between lignin and probes (data not shown).

We also investigated physical parameters such as roughness and porosity of paper discs made from pulps and their impact on probe binding. For the four pulps and all probes used in this study, we found that porosity had no obvious impact on probe binding (even when porosity was varied over a 40-fold range, see additional files 3.10 and 3.11). Probes are much smaller than pores or crevices that may be of various sizes or numbers in pulps with different porosities. Roughness was found to vary by about 10% when we compared papers made from pulp in our experiments. Increased roughness did result into moderate increase of probe binding, but we did not observe any change in comparative binding of probes due to roughness (*i.e.* relative binding of a probe *vs.* binding of other probes is unchanged by roughness, see additional files 3.10 and 3.11).

### 3.4.4 Investigation of reaction parameters by FTCM

Figures 3.3 and 3.4 show probe binding to various pulps using increasing concentrations of enzymes. Our results revealed that the maximal impact of xylanase and mannanase enzymes on pulps were detected at the minimal loading used here (0.1 U of enzyme/paper disc). All the pulps (UBMP, BMP, UBKP and BKP) showed no significant loss in the exposure of xylan and mannan as we increased the concentration from 0.1 U to 0.4 U/paper disc. This suggests that a 0.1 U/paper disc concentration of both xylanase and mannanase was sufficient for the maximal digestion of available/exposed xylan and mannan. The impact of temperature was also studied. All the pulps showed maximal hydrolysis or decrease in the exposure of xylan and mannan at 50°C. This suggests that both xylanase and mannanase enzymes were comparatively more active at 50°C than at room temperature. At room temperature, an overnight treatment showed relatively higher decrement in the exposure of hemicelluloses than a treatment duration of one hour. In contrast, at 50°C, both 1h and overnight treatments led to a maximal and similar decrement for both xylanase and mannanase enzymes treatments. FTCM unambiguously reveals that using 0.1 U of enzyme/paper disc for 1h at 50°C was sufficient for maximal reduction in available/exposed xylan and mannan. Production of reducing sugars by enzyme hydrolysis was also monitored using the DNS method. Conditions chosen for this control experi-

ment were the ones that led to maximal removal of xylan (Figure 3.3D). Using same biomass and same treatments, we found that reducing sugar production correlated with the decrease in xylan as detected by the probes (see additional file 3.13).

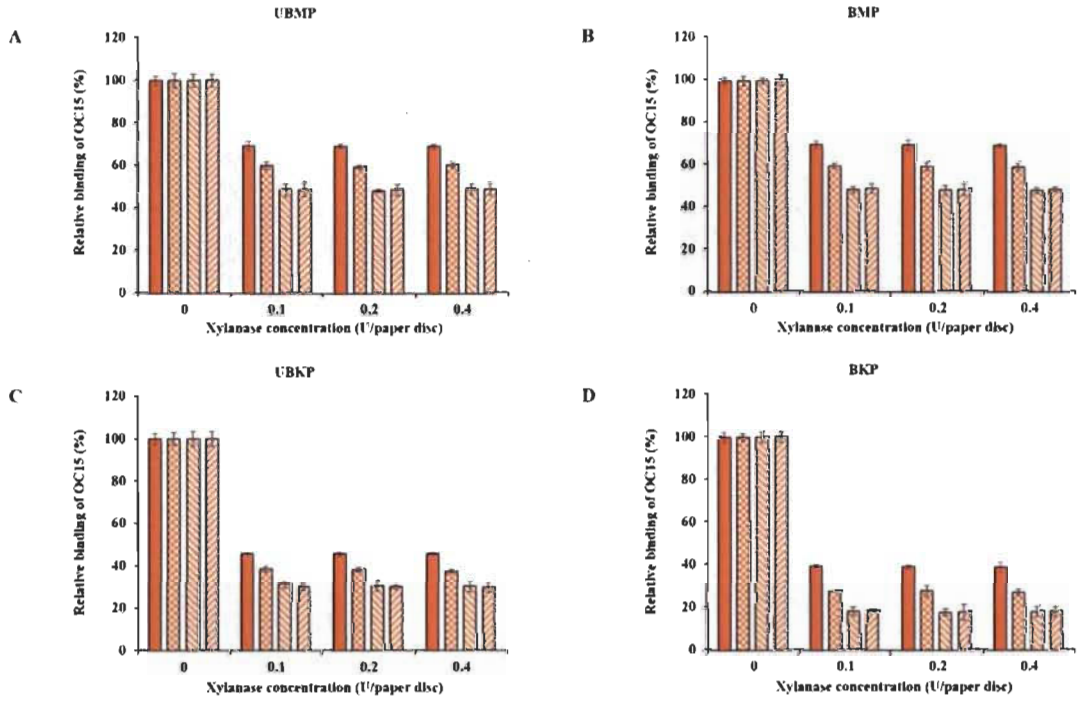


**Figure 3.3 Tracking xylan for optimizing hydrolysis conditions for xylanase treatments using the OC15 probe**

**A)** UBMP, **B)** BMP, **C)** UBKP and **D)** BKP paper discs were incubated with xylanase (0.1, 0.2 and 0.4 U/paper disc) at four different opted conditions (1h; RT (■), overnight; RT (▨), 1h; 50°C (▧) and overnight; 50°C (▨)) under continuous agitation (150 rpm). Following this, untreated and treated paper discs were incubated with the OC15 probe (0.5 µg/µL) for 1h at room temperature under agitation to detect xylan exposure. Three percent (w/v) milk (20 mM Tris-HCl, pH 7.5 with 20 mM NaCl and 5 mM $CaCl_2$) was used to minimize the auto-fluorescence of paper discs and the non-specific binding of the OC15 probe. Orange color represents the OC15 probe detection. Error bars represent the standard deviation.

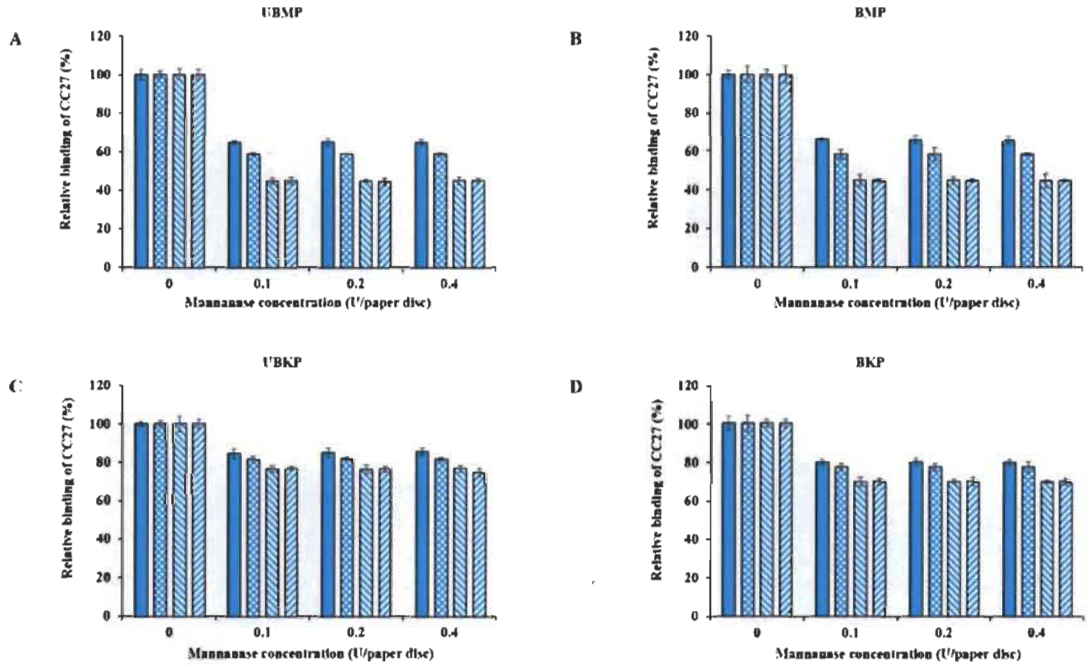


**Figure 3.4 Tracking mannan for optimizing hydrolysis conditions for mannanase treatments using the CC27 probe**

**A)** UBMP, **B)** BMP, **C)** UBKP and **D)** BKP paper discs were incubated with mannanase (0.1, 0.2 and 0.4 U/paper disc) at four different opted conditions (1h; RT (■), overnight; RT (▩), 1h; 50°C (▧) and overnight; 50°C (▨)) under continuous agitation (150 rpm). Following this, untreated and treated paper discs were incubated with the CC27 probe (0.5 µg/µL) for 1h at room temperature under agitation to detect mannan exposure. Three percent (w/v) milk (20 mM Tris-HCl, pH 7.5 with 20 mM NaCl and 5 mM $CaCl_2$) was used to minimize the auto-fluorescence of paper discs and the non-specific binding of the CC27 probe. Cyan color represents the CC27 probe detection. Error bars represent the standard deviation.

The xylanase enzyme appeared to hydrolyze xylan more efficiently in BKP than all the other pulps (Figure 3.3). Xylanase treated BKP paper discs showed a maximum decrement of 82% in the exposure of xylan. This may be ascribed to the most efficient removal of lignin in BKP compared to all other pulps studied here, as described earlier (Figure 3.2 and Additional file 3.3 ). In contrast, the mannanase enzyme was more effi-

cient on both mechanical pulps (UBMP and BMP) (Figure 3.4) due to the very high exposure of mannan in mechanical pulps as described earlier (Figure 3.2 and Additional file 3.3 ). Both UBMP and BMP paper discs showed a maximum decrement of at least 55% in the exposure of mannan after mannanase hydrolysis under our assay conditions. Although hemicelluloses were detectable by our probes, these were not completely hydrolyzed or reachable by the enzyme used. This suggests a possible hindrance or inactivation of enzymes during our assay.

Mannanase hydrolysis showed that the relative amounts of mannan removed from mechanical pulps are higher than the percentage removed from the kraft pulps (Figure 3.4). This suggests a higher digestibility of lignin-associated mannan (lignin-hemicelluloses complexes) in mechanical pulp. The hydrolysis of mannan polymers in kraft pulps might be hindered by significant exposure of xylan (mostly associated to cellulose-hemicelluloses complexes), in agreement with an earlier study on lignin-hemicellulose complexes.[38]

In contrast, xylanase hydrolysis showed that xylan was more susceptible to hydrolysis in kraft pulps compared to mannan. In kraft pulps, bleaching increased the exposure of xylan and eventually increased hydrolysis of xylan by a few percentage points. This suggests that after removal of lignin and the so-called lignin-hemicelluloses complexes via kraft pulping, xylan is more vulnerable or exposed at the surface of kraft pulps fibers than mannan. The xylanase hydrolysis in mechanical pulps seems to be hindered by the abundance of mannan, which is the main hemicellulose associated with lignin and/or lignin-hemicelluloses complexes, as shown by the lower binding of OC15 to xylan in both mechanical pulps (Figure 3.2). This study revealed that FTCM, a rapid and high throughput approach, can improve our knowledge and understanding of biomass hydrolysis as well as the economic feasibility of LCB based industries.

### 3.4.5 Addressing possible impact of enzyme inactivation

Above results suggested that neither of these enzymes were able to completely eliminate all the available hemicelluloses at the surface of fibers under our conditions.

This might be explained, in part, by the inactivation of enzymes by reaction products, plant derived inhibitors, adsorption to fibers or denaturation of the enzymes over time.[41] Recent studies have suggested that enzyme inhibition by their own end products and other components, generated during the bioconversion process, can be a key factor which impedes the hydrolysis processes.[40,41,46-55] To further investigate a potential inactivation scenario, we chose BKP paper discs and treated them using optimum hydrolysis conditions (0.1 U of enzyme/paper disc, 50°C). After a one-hour treatment, the enzymatic reactions were removed, and the surfaces of the paper discs were tracked with the OC15 and CC27 probes, individually, for residual hemicelluloses. The tracking of xylan and mannan showed an 80% and 30% decrement, respectively (Figure 3.5) (similar to the results described in Figure 3.3D and 3.4D). Prolonging enzymatic reactions longer than one hour (and/or overnight) at 50°C did not promote any further drop in the exposure of hemicelluloses. Therefore, we washed paper discs to remove the inactivated enzyme which might be inhibiting hydrolysis. To this end, the BKP paper discs, which were already incubated with enzymes for an hour, were washed with buffer and Tween (0.05%) before adding another load of freshly prepared enzymes. After refreshing enzymes (xylanase or mannanase) solution, the reactions were kept again under optimum hydrolysis conditions (0.1 U of enzyme/paper disc, 50°C) for another hour. Later, the tracking of xylan and mannan showed an additional decrement of 2.3% and 5.3%, respectively, in the exposure of hemicelluloses (Figure 3.5). Likewise, the enzymatic reactions were washed again before adding fresh enzymes for an additional one-hour reaction period and then measured by probes, for up to 24 hours. The results exhibited a gradual decrement in the binding of OC15 and CC27 probes. After 24 hours, the maximum decrement in the exposure of xylan was 92% and 50% in the exposure of mannan. The maximal impact was reached after 12 hours (in the case of xylanase hydrolysis) and 5 hours (in the case of mannanase hydrolysis), regardless of washing paper discs and adding freshly prepared enzymes (Figure 3.5 ).

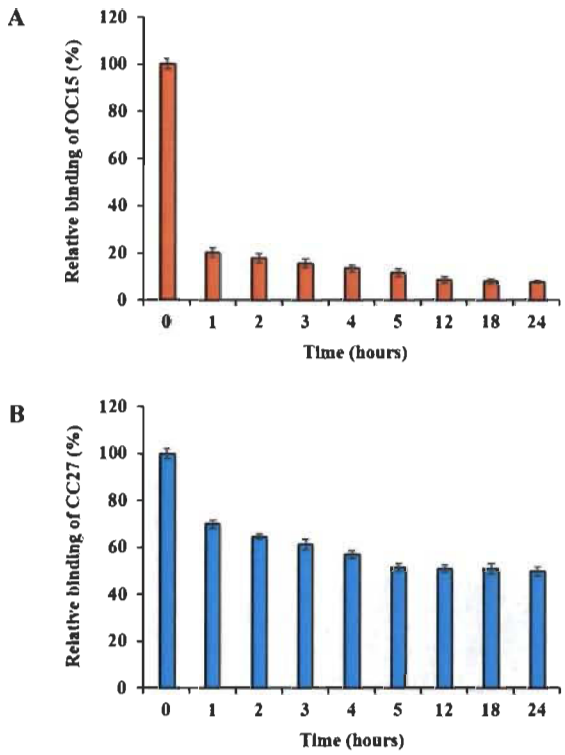


**Figure 3.5 Tracking A) xylan and B) mannan to address the impact of xylanase and mannanase inactivation on BKP paper discs using the OC15 and CC27 probes**

**A)** Paper discs were incubated with xylanase (0.1U/paper disc) at 50°C under continuous agitation (150 rpm) with refreshing enzyme solution every hour up to 24 hours. Following this, untreated and xylanase treated BKP paper discs were incubated with the OC15 probe (0.5 μg/μL) for 1h at room temperature under agitation. **B)** Paper discs were incubated with mannanase (0.1U/paper disc) at 50°C under continuous agitation (150 rpm) with refreshing enzyme solution every hour up to 24 hours. Following this, untreated and mannanase treated BKP paper discs were incubated with the CC27 probe (0.5 μg/μL) for 1h at room temperature under agitation. Orange color (■) and cyan color (■) represent the OC15 and CC27 probes detection, respectively. Error bars represent the standard deviation.

This suggests that the xylanase and mannanase enzymes might have reached their maximum possible hydrolysis activity, or that such activity had no more detectable impact on the hemicelluloses. Nevertheless, FTCM indicates that there was an inactivation

(and/or inhibition) which was somewhat overcome by washing followed by a fresh load of enzyme (xylanase or mannanase). FTCM reveals that despite an apparent interruption of net hydrolysis, there remains a large amount of mannan at the surface of BKP fibers. Such information cannot be provided by chromatographic analysis of hydrolysis products. Chemical analysis, which depends on total hemicellulose content would not be as sensitive as FTCM for detecting changes in hemicellulose hydrolysis at surface and for optimizing enzymatic processes. Note that measurements of reducing sugars production by enzymes were also performed, allowing to confirm that smaller quantities of sugars were released upon renewing enzymes, but that maximal production of sugars was generated in the first hour with the first exposure to enzyme (additional files 3.14 and 3.15).

### 3.4.6 Investigating the impact of cellulose on the hydrolysis of hemicelluloses

Despite finding out the optimum hydrolysis conditions and achieving additional removal of hemicelluloses by spiking enzymes, both xylanase and mannanase enzymes were unable to completely eliminate/hydrolyze all the available hemicelluloses that could be detected by FTCM. To achieve additional hydrolysis of hemicelluloses and simultaneously improve our understanding of fiber deconstruction, we explored the potential impact of cellulase treatments on hemicelluloses availability. The use of enzyme cocktails comprised of cellulase and so-called accessory enzymes (xylanase and/or mannanase) has been previously studied and found to enhance the cellulose hydrolysis.[27,29,35,37-40,42,43] Here we reexamined the apparent complementarity between enzymes using FTCM. To this end, BKP paper discs were hydrolyzed with commercial cellulase enzyme (Celluclast 1.5L) under conditions which were optimal for hemicelluloses hydrolysis (0.1 U/paper disc, 50°C) for an hour. Celluclast 1.5L possesses some contaminant activity of both xylanase and mannanase (Additional file 3.12). After hydrolysis, an eGFP-CBM3a (named GC3a here) probe was used to track the exposure of crystalline cellulose (as described by Hébert Ouellet *et al.*, 2017).[83] Results in Figure 3.6A suggest that Celluclast 1.5L treatment reduced exposure of crystalline cellulose by 63%.

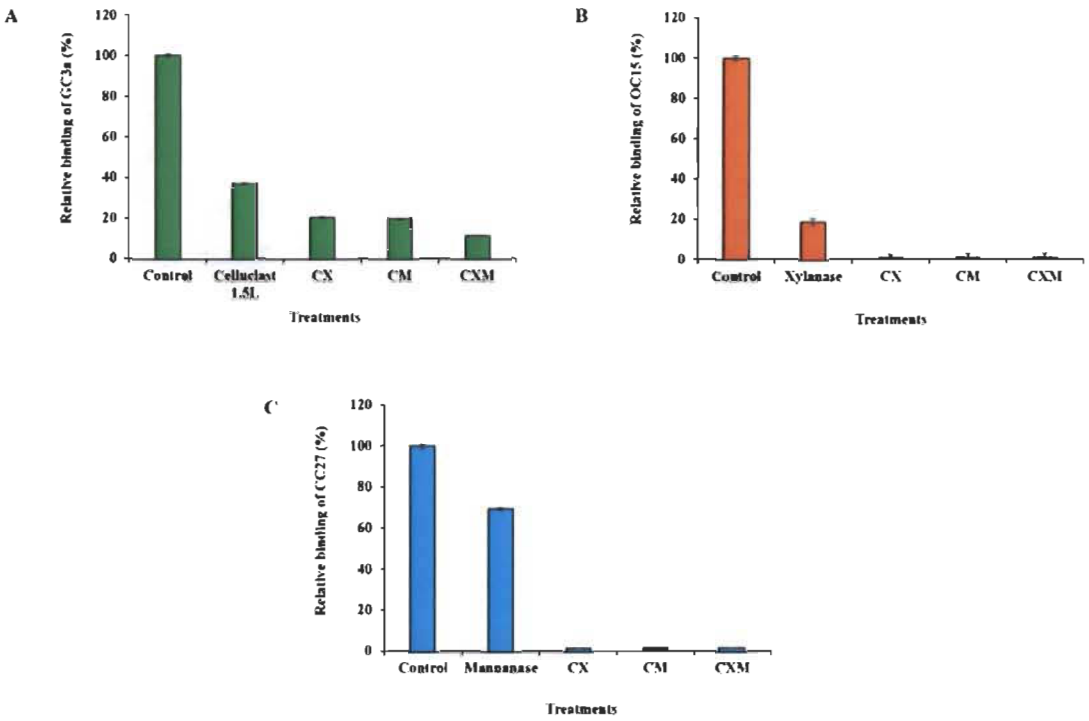


**Figure 3.6** **Impact of Celluclast 1.5L, xylanase, mannanase and their cocktails hydrolysis of BKP on the exposure of (A) crystalline cellulose, (B) xylan and (C) mannan polymers**

**A)** Paper discs were incubated with Celluclast 1.5L (0.1 U/paper disc), cocktail CX, cocktail CM and cocktail CXM at 50°C for 1h under continuous agitation (150 rpm). Following this, untreated and treated BKP paper discs were incubated with the GC3a probe (0.5 µg/µL) for 1h at room temperature under agitation. **B)** Paper discs were incubated with xylanase (0.1 U/paper disc), cocktail CX, cocktail CM and cocktail CXM at 50°C for 1h under continuous agitation (150 rpm). Following this, untreated and treated BKP paper discs were incubated with the OC15 probe (0.5 µg/µL) for 1h at room temperature under agitation. **C)** Paper discs were incubated with mannanase (0.1 U/paper disc), cocktail CX, cocktail CM and cocktail CXM at 50°C for 1h under continuous agitation (150 rpm). Following this, untreated and treated BKP paper discs were incubated with the CC27 probe (0.5 µg/µL) for 1h at room temperature under agitation. Green (■), orange (■) and cyan (■) color represent the GC3a, OC15 and CC27 probes detection, respectively. Error bars represent the standard deviation.

Then, supplementation of Celluclast 1.5L with a xylanase accessory enzyme (cocktail CX) and a mannanase accessory enzyme (cocktail CM) was investigated. Addition of hemicellulases led to an additional reduction of exposed cellulose, suggesting that they helped the hydrolysis of cellulose by the Celluclast 1.5L enzyme (Figure 3.6A). Finally, the supplementation of Celluclast 1.5L with both xylanase and mannanase enzymes (cocktail CXM) drastically decreased the cellulose exposure (down by 88%, see Figure 3.6A). These results confirm that to achieve highest cellulose hydrolysis at surface of BKP fibers, it is vital to supplement cellulase with accessory enzymes such as xylanase and mannanase. These results also suggest that not only one type but both types of hemicelluloses (xylan and mannan) restrict cellulose accessibility or cellulase action.

We then investigated a potential reciprocal additive and/or synergistic action by supplementing xylanase and mannanase enzymes with Celluclast 1.5L and monitoring hemicelluloses removal after treatment. Using the same BKP paper discs treated as explained above, we found that the xylanase enzyme led to 81% decrement in the exposure of xylan (Figure 3.6B), which is compatible with the result shown in Figure 3.3D. BKP paper discs were also treated with cocktail CX, cocktail CM and cocktail CXM and all led to the nearly complete elimination of xylan at the surface of BKP fibers. Likewise, BKP paper discs hydrolyzed with the mannanase enzyme showed 30% decrement in mannan exposure (Figure 3.6C). Subsequently, cocktail CX, cocktail CM and cocktail CXM promoted further hydrolysis of BKP paper, leading to the near complete elimination of mannan from the surface of BKP fibers. These results suggest that cellulose is an important barrier limiting access to hemicelluloses in BKP.

The presence of both hemicellulases (xylanase and mannanase) were required with Celluclast 1.5L for maximal hydrolysis of crystalline cellulose. In contrast, either one of the hemicellulases or both were required with Celluclast 1.5L for maximal hydrolysis of xylan and mannan. This suggests that xylan and mannan were providing protection to cellulose, but that a portion of cellulose remains protected by other fiber components, or that a portion of exposed cellulose remains stable despite enzymatic attack. Such results

are compatible with the existence of deeply embedded hemicelluloses, part of a carbohydrate-hemicellulose complexes, shielding the cellulose fibers. Note that in BKP, the hemicelluloses associated with lignin are expected to be mostly absent. These results suggest that FTCM can also be used to design enzyme cocktails preparations for specific applications. Exposure of fibers to enzymes had a drastic impact on all polysaccharides at surface. The question of "what is left" at surface after such important decrease in probe binding is legitimate but not necessarily relevant. Note that when preparing paper discs prior to FTCM reading, the discs were washed, and any loosen material was removed. Hydrolysis of high surface fragments such as microfibrils and their removal prior to FTCM may explain the important decrease in probe binding observed here.

### 3.4.7 Exploring the impact of xylan polymers on the hydrolysis of mannan

The previous section has revealed the proximity of cellulose and "deep" hemicelluloses. Here we focused on the impact of xylan on the hydrolysis of mannan in order to address structural relationships and their potential impact on hydrolysis yield. To this end, BKP paper discs were hydrolyzed with mannanase enzyme as a control reaction. Results showed a decrement of at least 30% in the exposure of mannan for all the enzyme concentrations used (Figure 3.7A, solid cyan color bars). The results were as expected and fully compatible with Figure 3.4D.

In another reaction, BKP paper discs were digested with the xylanase enzyme. In order to reach the maximum xylan hydrolysis, the reaction was performed as described above (section Addressing possible impact of enzyme inactivation) with refreshing enzyme solution every hour up to 12 hours. By refreshing enzyme solution, this treatment led to a stronger reduction in xylan exposure (an additional 10-13%) as detected with the OC15 probe (Figure 3.7B, solid orange color bars). The results were as expected and fully compatible with Figure 3.5A. The same xylanase hydrolyzed paper discs were then inspected using the CC27 probe to track mannan exposure.

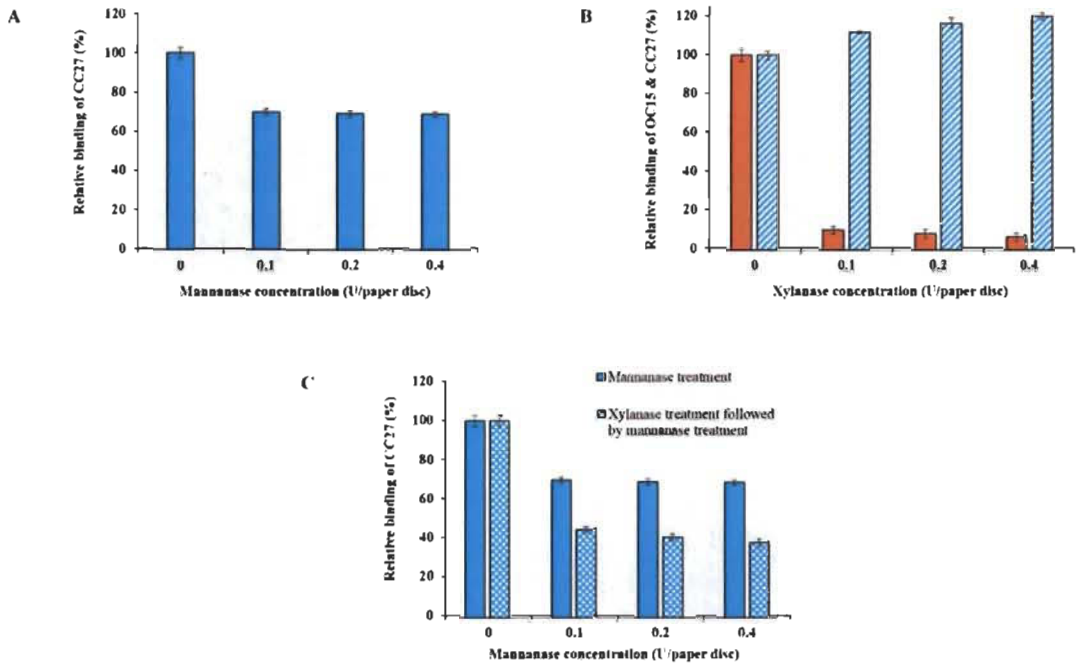


**Figure 3.7 Impact of mannanase and xylanase hydrolysis of BKP on the exposure of mannan polymers**

**A)** Untreated and mannanase treated (0.1, 0.2 and 0.4 U/paper disc, at 50°C for 1h) BKP paper discs were incubated with the CC27 probe (0.5 µg/µL) for 1h at room temperature under agitation to detect mannan exposure (■). **B)** Untreated and xylanase treated BKP paper discs (0.1, 0.2 and 0.4 U/paper disc, at 50°C with refreshing enzyme solution every hour up to 12 hours) were incubated with the OC15 probe (0.5 µg/µL) for 1h at room temperature under agitation (■) for xylan detection. The same xylanase hydrolyzed BKP paper discs were also incubated with the CC27 probe (0.5 µg/µL) to detect mannan exposure (■). **C)** Previously xylanase treated BKP paper discs (as described in panel B) were later treated with mannanase enzyme (0.1, 0.2 and 0.4 U/paper disc, at 50°C for 1h). Following this, untreated and mannanase treated BKP paper discs were incubated with the CC27 probe (0.5 µg/µL) (■). Data of panel A (■) has also shown in panel C for comparison. Orange color (■) represents the OC15 probe detection and cyan color (■) represents the CC27 probe detection. Error bars represent the standard deviation.

The results revealed that mannan exposure at the surface of xylanase hydrolyzed BKP paper discs increased by 20% when pulp was treated with a 0.4 xylanase U/paper

disc (Figure 3.7B, cyan color bars with upward diagonal stripes). Xylanase hydrolysis for 1h or overnight, without refreshing enzyme solution (as described above in section Investigation of reaction parameters by FTCM), lead to no significant mannan exposure at the surface of xylanase hydrolyzed BKP paper discs (data not shown).

In another reaction, the xylanase hydrolyzed BKP paper discs were later washed and exposed to the hydrolysis with mannanase enzyme. In this case, mannan exposure decreased by 55% (in case of 0.1 mannanase U/paper disc) which is an additional decrement of 25% compared to when xylanase was not used as a pretreatment (Figure 3.7C, cyan color bars with checker board). This study showed that xylan hydrolysis exposed more detectable mannan on the surface of BKP wood fibers, leading to higher enzymatic hydrolysis of mannan. This suggests that xylan was wrapping or covering mannan in the so-called cellulose-hemicellulose complexes. The mannan detected here seems to be deeply embedded in the BKP wood fibers.

Plant cell wall organization directly affects the nature of biomass recalcitrance.[20,21] Therefore, it is important to understand the organization of hemicelluloses and FTCM offers a unique means of addressing this issue. So far, various studies looking for the arrangement of the different wood polymers in delignified samples have revealed that mannan is closely associated with cellulose and xylan is more associated with condensed lignin in the secondary cell wall of the softwood fibers.[44,94] This FTCM study provides direct evidence in support of this suggested model. Using FTCM probes, we detected two different mannan populations in the wood fibers. The first mannan population was associated with lignin-hemicellulose complexes as seen in mechanical pulps. This population was dominant at the outer surface of wood fibers. In contrast, during kraft pulping, lignin and lignin-hemicellulose complexes get dissolved and/or degraded, which exposes deeper hemicelluloses. The second mannan population was found deeper in fiber, probably associated to the earlier proposed cellulose-hemicellulose complexes in kraft pulps. Overall the results suggest that xylan was acting as a physical shield which was covering or wrapping the mannan polymers in BKP fibers. This also indicates that the second population of mannan is hidden beneath the surface of xylan polymers,

closely associated to cellulose or deeply embedded in the cell wall organization in BKP fibers. FTCM analysis fully supports the concept of a complex network of hemicelluloses around the cellulose fibers as reported by Varnai *et al.* (2011)[43] but in addition, FTCM highlighted the presence of deeply embedded hemicelluloses. Working with bleached softwood dissolving pulp, Gübitz *et al.* (1998)[38] proposed that hemicelluloses hydrolysis is stronger when cellulase enzymes are used with hemicellulases and proposed two different fractions of hemicelluloses: one associated with lignin and another one with cellulose. The FTCM results are compatible with the findings of Gübitz *et al.* (1998)[38] which suggested two different mannan populations. This study also provides a rationale for the findings of Kansoh *et al.* (2004)[95] and Clarke *et al.* (2000)[96] which indicated that the use of the mannanase enzyme is not very efficient if xylan is still present in kraft pulps.

Overall, FTCM has been shown to help understanding cell wall ultrastructure and its organization by studying the presence of hemicelluloses in various parts of fibers, as lignin is progressively removed by kraft pulping and bleaching processes. Although most FTCM investigations reported here were compatible with chemical analysis (dependent on overall/bulk composition analysis; NREL/TP-510-42618), they revealed that changes in surface hemicelluloses after various treatments are much more important than indicated by chemical analysis. Monitoring surface modifications is much more informative on biomass recalcitrance than performing analysis of fiber bulk composition.

## 3.5 Conclusion

FTCM showed that it can specifically track mechanical, chemical and enzymatic-induced variations of hemicelluloses on the surface of different wood fibers in a rapid and high throughput format. Optimum hydrolysis parameters for both xylanase and mannanase enzymes, for all the studied pulps, were 0.1 U of enzyme/paper disc at 50°C for a treatment duration of 1h. FTCM identified the major factor limiting hydrolysis efficiency as enzyme inactivation (by any mechanism). By directly detecting polymers remaining after various enzymatic treatments, using CBM probes revealed additive and/or synergistic interactions between Celluclast 1.5L, xylanase and mannanase enzymes. The ability of

FTCM to directly map layers of cellulose and hemicelluloses fractions as they were attacked by enzymes provided support for an embedded population of mannan, protected by xylan, probably associated to cellulose-hemicellulose complexes.[38] We believe that this method can enhance our understanding of lignocellulosic polymers response to various treatments, therefore bolstering development of cost-effective processes for production of biofuels and other LCB-based products.

**List of abbreviations**

AGE: affinity gel electrophoresis; BSA: bovine serum albumin; BKP: bleached kraft pulp; BMP: bleached mechanical pulp; CAZy: carbohydrate active enzymes; CBMs: carbohydrate-binding modules; CBM15: family 15 carbohydrate-binding module; CMC: carboxymethyl cellulose; CFP: cyan fluorescent protein; DNS: 3,5-dinitrosalicylic acid; GFP: green fluorescent protein; GH: glycoside hydrolase; IPTG: isopropyl-β-D-thiogalactopyranoside; ITC: isothermal titration calorimetry; LB: Luria-Bertani; mOrange2: mono-orange2; NREL: national renewable energy laboratory; CC27: cyan fluorescent protein linked to a family 27 carbohydrate-binding module; GC3a: green fluorescent protein linked to a family 3a carbohydrate-binding module; OC15: mono-orange2 fluorescent protein linked to a family 15 carbohydrate-binding module; SDS-PAGE: sodium dodecyl sulfate - polyacrylamide gel electrophoresis; UBKP: unbleached kraft pulp; UBMP: unbleached mechanical pulp.

## 3.6 References


1. M. E. Himmel, S. Y. Ding, D. K. Johnson, W. S. Adney, M. R. Nimlos, J. W. Brady, T. D. Foust, *Science,* 2007, **315**, 804-807.
2. C. E. Wyman, *Trends. Biotechnol.,* 2007, **25**(4), 153-157.
3. L. R. Lynd, M. S. Laser, D. Bransby, B. E. Dale, B. Davison, R. Hamilton, M. Himmel, M. Keller, J. D. McMillan, J. Sheehan, C. E. Wyman, *Nat. Biotechnol.,* 2008, **26**(2), 169-172.
4. L. R. Lynd, J. H. Cushman, R. J. Nichols, C. E. Wyman, *Science,* 1991, **251**(4999), 1318-1323.
5. H. Jørgensen, J. B. Kristensen, C. Felby, *Biofuels Bioprod. Biorefin.,* 2007, **1**, 119-134.
6. C. E. Wyman, *Bioresour. Technol.,* 1994, **50**(1), 3-16.
7. A. E. Farrell, R. J. Plevin, B. T. Turner, A. D. Jones, M. O'hare, D. M. Kammen, *Science*, 2006, **311**(5760), 506-508.
8. R. Kumar, M. Tabatabaei, K. Karimi, I. Sárvári Horváth, *Biofuel Res. J.,* 2016, **3**(1), 347-356.
9. A. Culbertson, M. Jin, L. da Costa Sousa, B. E. Dale, V. Balan, *RSC Adv.,* 2013, **3**(48), 25960-25969.
10. Y. Hong, A. S. Nizami, M. Pour bafrani, B. A. Saville, H. L. MacLean, *Biofuels Bioprod. Biorefin.,* 2013, **7**(3), 303-313.
11. L. R. Lynd, C. E. Wyman, T. U. Gerngross, *Biotechnol. Prog.,* 1999, **15**(5), 777-793.
12. R. Kumar and C. E. Wyman, Bioalcohol production: Biochemical conversion of lignocellulosic biomass, ed. K. Waldon, Woodhead Publishing Limited, Oxford, 2010, pp. 73–121.
13. R. Kumar and C. E. Wyman, Aqueous Pretreatment of Plant Biomass for Biological and Chemical Conversion to Fuels and Chemicals, ed. C. E. Wyman, John Wiley and Sons Ltd, 2013, pp. 281–310.

14. P. A. Penttilä, A. Várnai, J. Pere, T. Tammelin, L. Salmén, M. Siika-aho, L. Viikari, R. Serimaa, *Bioresour. Technol.*, 2013, **129**, 135-141.
15. M. Li, M. Tu, D. Cao, P. Bass, S. Adhikari, *J. Agric. Food Chem.*, 2013, **61**(3), 646-654.
16. K. Igarashi, T. Uchihashi, A. Koivula, M. Wada, S. Kimura, T. Okamoto, M. Penttilä, T. Ando, M. Samejima, *Science,* 2011, **333**, 1279-1282.
17. L. Zhu, J. P. O'Dwyer, V. S. Chang, C. B. Granda, M. T. Holtzapple, *Bioresour. Technol.*, 2008, **99**, 3817-3828.
18. S. D. Mansfield, C. Mooney, J. N. Saddler, *Biotechnol. Prog.*, 1999, **15**, 804-816.
19. M. Hall, P. Bansal, J. H. Lee, M. J. Realff, A. S. Bommarius, *FEBS J.*, 2010, **277**(6), 1571-1582.
20. S. P. Chundawat, B. S. Donohoe, L. da Costa Sousa, T. Elder, U. P. Agarwal, F. Lu, J. Ralph, M. E. Himmel, V. Balan, B. E. Dale, *Energy Environ. Sci.*, 2011, **4**(3), 973-984.
21. J. D. DeMartini, S. Pattathil, J. S. Miller, H. Li, M. G. Hahn, C. E. Wyman, *Energy Environ. Sci.*, 2013, **6**(3), 898-909.
22. A. T. W. M. Hendriks, G. Zeeman, *Bioresour. Technol.*, 2009, **100**(1), 10-18.
23. S. Subramaniyan, P. Prema, *Crit. Rev. Biotechnol.*, 2002, **22**(1), 33-64.
24. B. C. Saha, *J. Ind. Microbiol. Biotechnol.*, 2003, **30**(5), 279-291.
25. F. M. Gírio, C. Fonseca, F. Carvalheiro, L. C. Duarte, S. Marques, R. Bogel-Łukasik, *Bioresour. Technol.*, 2010, **101**(13), 4775-4800.
26. T. E. Timell. *Wood Sci. Technol.*, 1967, **1**(1), 45-70.
27. J. Hu, V. Arantes, J. N. Saddler, *Biotechnol. Biofuels.*, 2011, **4**(1), 1-14.
28. M. J. Selig, T. B. Vinzant, M. E. Himmel, S. R. Decker, *Appl. Biochem. Biotechnol.*, 2009, **155**(1-3), 397-406.
29. R. Bura, R. Chandra, J. Saddler, *Biotechnol. Prog.*, 2009, **25**(2), 315-322.
30. M. Frommhagen, S. Sforza, A. H. Westphal, J. Visser, S. W. Hinz, M. J. Koetsier, W. J. van Berkel, H. Gruppen, M. A. Kabel, *Biotechnol. Biofuels,* 2015, **8**(1), 1-12.

31. A. Suurnakki, T. Q. Li, J. Buchert, M. Tenkanen, L. Viikari, T. Vuorinen, L. Odberg, *Holzforschung*, 1997, **51**(1), 27-33.
32. J. P. Vincken, A. de Keizer, G. Beldman, A. G. J. Voragen, *Plant Physiol.*, 1995, **108**(4), 1579-1585.
33. T. Oksanen, J. Buchert, L. Viikari, *Holzforschung*, 1997, **51**(4), 355-360.
34. T. Kohnke, K. Lund, H. Brelid, G. Westman, *Carbohydr Polym.*, 2010, **81**(2), 226-233.
35. J. Zhang, M. Siika-aho, M. Tenkanen, L. Viikari, *Biotechnol. Biofuels.*, 2011, **4**(1), 1-10.
36. A. Berlin, V. Maximenko, N. Gilkes, J. Saddler, *Biotechnol. Bioeng.*, 2007, **97**(2), 287-296.
37. K. Ohgren, R. Bura, J. Saddler, G. Zacchi, *Bioresour. Technol.*, 2007, **98**(13), 2503-2510.
38. G. M. Gübitz, D. W. Stebbing, C. I. Johansson, J. N. Saddler, *Appl. Microbiol. Biotechnol.*, 1998, **50**(3), 390-395.
39. M. P. Garcia-Aparicio, M. Ballesteros, P. Manzanares, I. Ballesteros, A. Gonzalez, M. J. Negro, *Appl. Biochem. Biotechnol.*, 2007, **137**, 353-365.
40. R. Kumar, C. E. Wyman, *Biotechnol. Prog.*, 2009a, **25**(2), 302-314.
41. R. Kumar, C. E. Wyman, *Biotechnol. Bioeng.*, 2014, **111**(7), 1341-1353.
42. Q. Qing, C. E. Wyman, *Biotechnol. Biofuels*, 2011, **4**(1), 18.
43. A. Varnai, L. Huikko, J. Père, M. Siika-aho, L. Viikari, *Bioresour. Technol.*, 2011, **102**(19), 9096-9104.
44. M. Åkerholm, L. Salmén, *Polymer*, 2001, **42**(3), 963-969.
45. D. Klein-Marcuschamer, P. Oleskowicz-Popiel, B. A. Simmons, H. W. Blanch, *Biotechnol. Bioeng.*, 2012, **109**(4), 1083-1087.
46. E. Ximenes, Y. Kim, N. Mosier, B. Dien, M. Ladisch, *Enzyme Microb. Technol.*, 2010, **46**, 170-176.
47. Y. Kim, E. Ximenes, N. S. Mosier, M. R. Ladisch, *Enzyme Microb. Technol.*, 2011, **48**(4-5), 408-415.
48. M. Mandels, E. T. Reese, *Annu. Rev. Phytopathol.*, 1965, **3**, 85-102.

49. E. T. Reese, M. Mandels, *Biotechnol. Bioeng.*, 1980, **22**(2), 323-335.
50. G. Halliwell, M. Griffin, *Biochem.*, 1973, **135**(4), 587-594.
51. R. Kumar, C. E. Wyman, *Enzyme Microb. Technol.*, 2008, **42**(5), 426-433.
52. R. Kumar, C. E. Wyman, *Biotechnol. Bioeng.*, 2009b, **102**(2), 457-467.
53. Q. Qing, B. Yang, C. E. Wyman, *Bioresour. Technol.*, 2010, **101**(24), 9624-9630.
54. M. Holtzapple, M. Cognata, Y. Shu, C. Hendrickson, *Biotechnol. Bioeng.*, 1990, **36**(3), 275-287.
55. P. Andric, A. S. Meyer, P. A. Jensen, K. Dam-Johansen, *Biotechnol. Adv.*, 2010, **28**(3), 308-324.
56. J. D. Stephen, W. E. Mabee, J. N. Saddler, *Biofuels Bioprod. Biorefin.*, 2012, **6**(2), 159-176.
57. Y. H. P. Zhang, M. E. Himmel, J. R. Mielenz, *Biotechnol. Adv.*, 2006, **24**(5), 452-481.
58. Z. Zhang, A. A. Donaldson, X. Ma, *Biotechnol. Adv.*, 2012, **30**(4), 913-919.
59. R. Kumar, C. E. Wyman, *Biotechnol. Bioeng.*, 2009c, **102**(6), 1544-1557.
60. R. Kumar, C. E. Wyman, *Biotechnol. Prog.*, 2009d, **25**(2), 302-314.
61. B. Yang, C. E. Wyman, *Biotechnol. Bioeng.*, 2006, **94**(4), 611-617.
62. T. Y. Nguyen, C. M. Cai, O. Osman, R. Kumar, C. E. Wyman. *Green Chem.*, 2015a, **18**(6), 1581-1589.
63. T. Y. Nguyen, C. M. Cai, R. Kumar, C. E. Wyman. *ChemSusChem,* 2015b, **8**(10), 1716-1725.
64. H. P. Zhang, S. Y. Ding, J. R. Mielenz, J. B. Cui, R. T. Elander, M. Laser, M. E. Himmel, J. R. Mcmillan, L. R. Lynd, *Biotechnol. Bioeng.*, 2007, **97**(2), 214-223.
65. S. T. Merino, J. Cherry, *Biofuels,* 2007, **108**, 95-120.
66. T. L. Ogeda, D. F. S. Petri, *Quimica. Nova.*, 2010, **33**(7), 1549-1558.
67. A. Y. Pribowo, J. Hu, V. Arantes, J. N. Saddler, *Biotechnol. Biofuels,* 2013, **6**(1), 1-15.
68. S. D. Risio, C. S. Hu, B. A. Saville, D. Liao, J. Lortie, *Biofuels, Bioprod. Biore-fin.*, 2011, **5**(6), 609–620.

69. J. D. DeMartini, S. Pattathil, U. Avci, K. Szekalski, K. Mazumder, M. G. Hahn, C. E. Wyman, *Energy Environ. Sci.*, 2011, **4**(10), 4332-4339.

70. J. P. Knox, *Cellulases,* 2012, **510**, 233-245.

71. J. P. Knox, *Curr. Opin. Plant Biol.*, 2008, **11**(3), 308-313.

72. C. Oliveira, V. Carvalho, L. Domingues, F. M. Gama, *Biotechnol. Adv.,* 2015, **33**(3), 358-369.

73. A. B. Boraston, D. Bolam, H. Gilbert, G. J. Davies, *Biochem. J.,* 2004, **382**, 769-781.

74. S. Gao, C. You, S. Renneckar, J. Bao, Y. H. P. Zhang, *Biotechnol. Biofuels,* 2014, **7**(1), 1-11.

75. H. J. Gilbert, J. P. Knox, A. B. Boraston, *Curr. Opin. Struct. Biol.,* 2013, **23**(5), 669-677.

76. C. Hervé, S. E. Marcus, J. P. Knox, *The Plant Cell Wall,* 2011, **715**, 103-113.

77. S. Ding, Q. Xu, M. K. Ali, J. O. Baker, E. A. Bayer, Y. Barak, R. Lamed, J. Sugiyama, G. Rumbles, M. E. Himmel, *Biotechniques*, 2006, **41**(4), 435.

78. T. Kawakubo, S. Karita, Y. Araki, S. Watanabe, M. Oyadomari, R. Takada, F. Tanaka, K. Abe, T. Watanabe, Y. Honda, T. Watanabe, *Biotechnol. Bioeng.*, 2010, **105**(3), 499-508.

79. K. Gourlay, V. Arantes, J. N. Saddler, *Biotechnol. Biofuels*, 2012, **5**(1), 51.

80. J. Hong, X. Ye, Y. H. P. Zhang, *Langmuir*, 2007, **23**(25), 12535-12540.

81. J. M. Fox, P. Jess, R. B. Jambusaria, G. M. Moo, J. Liphardt, D. S. Clark, H. W. Blanch, *Nat. Chem. Biol*, 2013, **9**(6), 356-361.

82. V. Khatri, Y. Hebert-Ouellet, F. Meddeb-Mouelhi and M. Beauregard, *Biotechnol. Biofuels,* 2016, **9**, 74.

83. Y. Hébert-Ouellet, F. Meddeb-Mouelhi, V. Khatri, L. Cui, B. Janse, K. MacDonald, M. Beauregard, *Green Chem.*, 2017, **19**, 2603-2611.

84. L. Szabó, S. Jamal, H. Xie, S. J. Charnock, D. N. Bolam, H. J. Gilbert, G. J. Davies, *J. Biol. Chem.,* 2001, **276**(52), 49061-49065.

85. A. B. Boraston, T. J. Revett, C. M. Boraston, D. Nurizzo, G. J. Davies, *Structure*, 2003, **11**(6), 665-675.

86. M. M. Bradford, *Anal. Biochem.,* 1976, **72**(1), 248-254.

87. A. Sluiter, D. Crocker, B. Hames, R. Ruiz, C. Scarlata, J. Sluiter, D. Templeton, *Laboratory Analytical Procedure (LAP)*, 2008, NREL/TP-510-42618.

88. K. Gourlay, J. Hu, V. Arantes, M. Penttilä, J. N. Saddler, *J. Biol. Chem.,* 2015, **290**, 2938–2945.

89. D. W. Abbott, A. B. Boraston, *Methods Enzymol.,* 2012, **510**, 211-231.

90. G. A. Smook, *Handbook for pulp & paper technologists*, 1992, Tappi.

91. L. Viikari, A. Kantelinen, J. Sundquist, M. Linko, *FEMS Microbiol. Rev.*, 1994, **13**(2-3), 335-350.

92. D. Tavast, Z. A. Mansoor, E. Brännvall, *Ind. Eng. Chem Res.*, 2014, **53**(23), 9738-9742.

93. Å. Linder, R. Bergman, A. Bodin, P. Gatenholm, *Langmuir*, 2003, **19**(12), 5072-5077.

94. M. Åkerholm, B. Hinterstoisser, L. Salmén, *Carbohydr. Res*, 2004, **339**(3), 569-578.

95. A. L. Kansoh, Z. A. Nagieb, *Antonie Van Leeuwenhoek*, 2004, **85**(2), 103-114.

96. J. H. Clarke, K. Davidson, J. E. Rixon, J. R. Halstead, M. P. Fransen, H. J. Gilbert, G. P. Hazlewood, *Appl. Microbiol. Biotechnol.*, 2000, **53**(6), 661-667.

97. G. L. Miller, *Anal. Chem.,* 1959, **31**, 426-428.

## 3.7 Additional Files

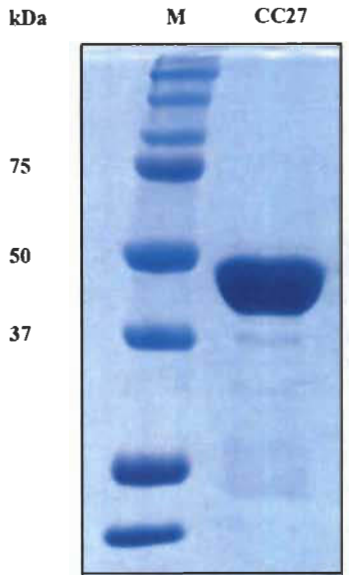


**Additional file 3.1** **SDS-PAGE analysis of the CC27 probe purified by affinity chromatography**

The expected molecular weight of the CC27 fusion protein is 48.06 kDa. A 12% polyacrylamide gel was used for SDS-PAGE analysis. Well M: Precision plus protein standards (5 μg). Well CC27: Purified CC27 probe (10 μg).

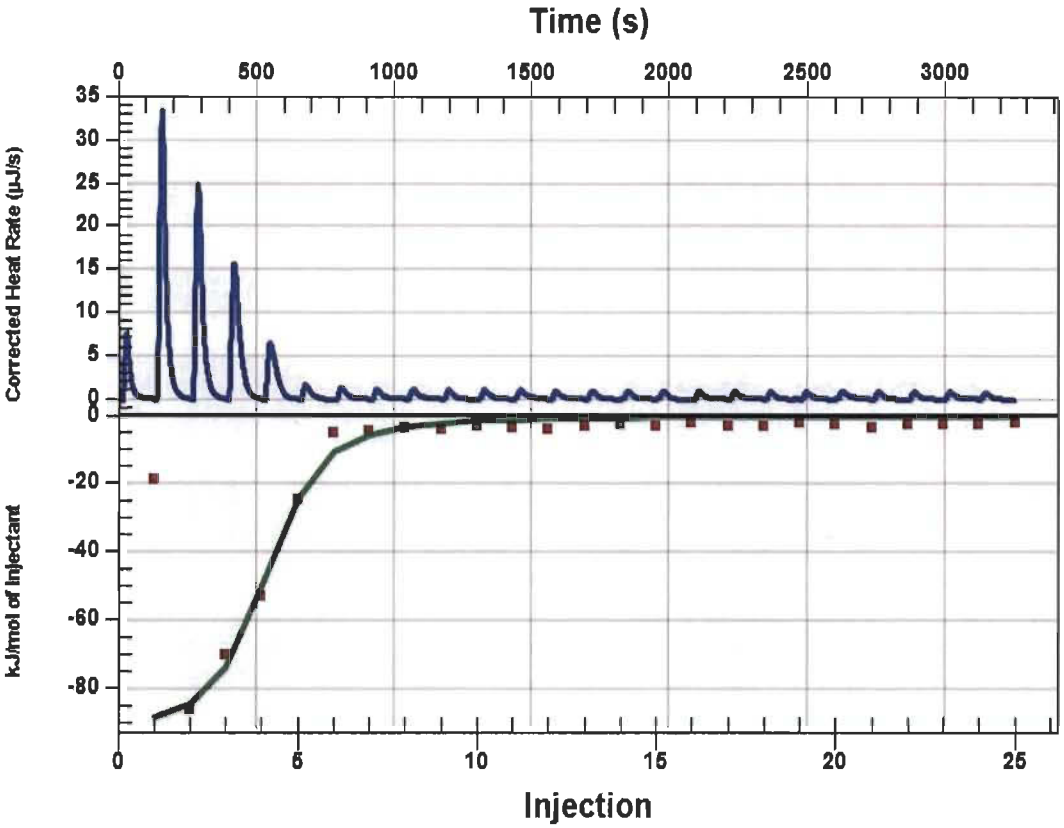


**Additional file 3.2** **Isothermal calorimetric titration of the CC27 probe with mannohexaose**

Top panel: Typical ITC experiment carried out by adding 25 injections of 2 µL mannohexaose (5000 µM) into the CC27 probe (200 µM) solution, with an interval of 130 seconds between each injection. Bottom panel: Heat release per mole of mannohexaose as a function of mannohexaose/OC15 molar ratio. The titration was performed at 25°C in a 20 mM Tris-HCl pH 7.5 buffer which contained 20 mM NaCl and 5 mM $CaCl_2$. Injectant: mannohexaose.

**Additional file 3.3 Chemical composition analysis of UBMP, BMP, UBKP and BKP determined by NREL/TP-510-42618**

| Compound | UBMP (%) | BMP (%) | UBKP (%) | BKP (%) |
|---|---|---|---|---|
| Extractives | 2.79 ± 0.01 | 2.54 ± 0.01 | 0.23 ± 0.01 | 0.27 ± 0.01 |
| Lignin | 29.03 ± 0.12 | 28.90 ± 0.20 | 4.30 ± 0.08 | 0.96 ± 0.05 |
| Glucose | 42.18 ± 1.01 | 43.53 ± 1.97 | 76.78 ± 1.15 | 79.47 ± 1.28 |
| Xylose | 5.25 ± 0.63 | 5.50 ± 0.76 | 5.57 ± 0.51 | 6.43 ± 0.59 |
| Mannose | 9.37 ± 0.57 | 9.95 ± 0.65 | 6.54 ± 0.47 | 7.74 ± 0.55 |
| Galactose | 1.57 ± 0.01 | 1.68 ± 0.01 | 0.24 ± 0.01 | 0.26 ± 0.01 |
| Arabinose | 0.97 ± 0.01 | 1.03 ± 0.01 | 0.46 ± 0.01 | 0.50 ± 0.01 |

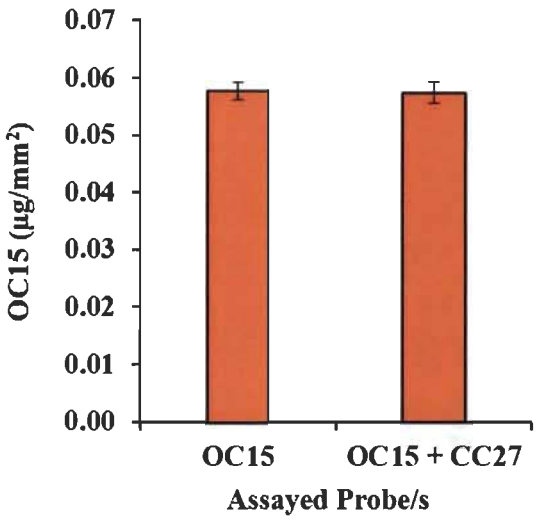


**Additional file 3.4** **Tracking xylan on the surface of BKP paper discs using OC15 and cocktail of OC15 + CC27 probes**

BKP paper discs were incubated with the OC15 (0.5 µg/µL) and the cocktail of OC15 (0.5 µg/µL) + CC27 (0.5 µg/µL) probes for 1h at room temperature under agitation. The fluorescence readings were acquired for the OC15 probe and converted to OC15 (µg/mm$^2$) by using standard curve (Additional file 3.6 ). Orange color represents the OC15 probe detection.

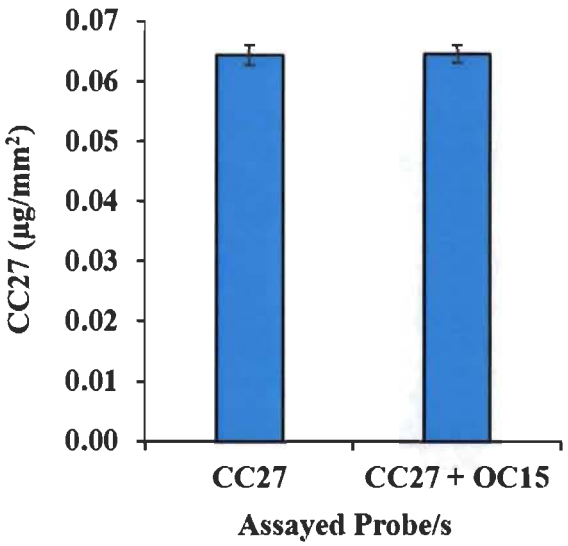


**Additional file 3.5** **Tracking mannan on the surface of BKP paper discs using CC27 and cocktail of CC27 + OC15 probes**

BKP paper discs were incubated with the CC27 (0.5 µg/µL) and the cocktail of CC27 (0.5 µg/µL) + OC15 (0.5 µg/µL) probes for 1h at room temperature under agitation. The fluorescence readings were acquired for the CC27 probe and converted to CC27 (µg/mm$^2$) by using standard curve (Additional file 3.7 ). Cyan color represents the CC27 probe detection.

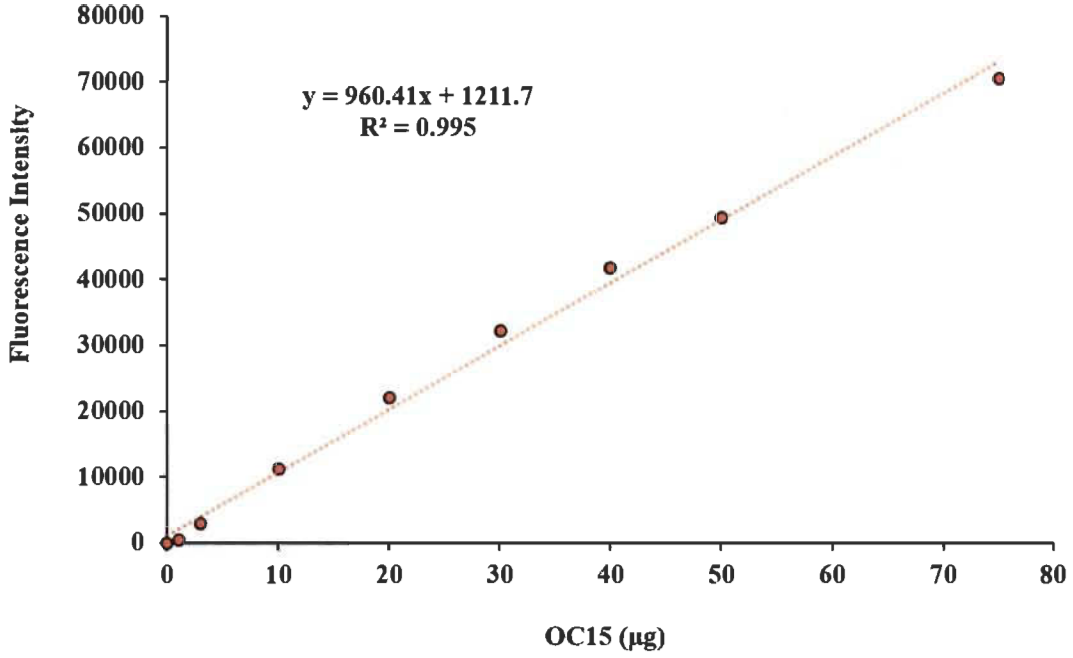


**Additional file 3.6** **Standard curve for the conversion of fluorescence intensity into µg of OC15 probe**

The excitation and emission wavelengths were set at 549 and 568 nm, respectively.

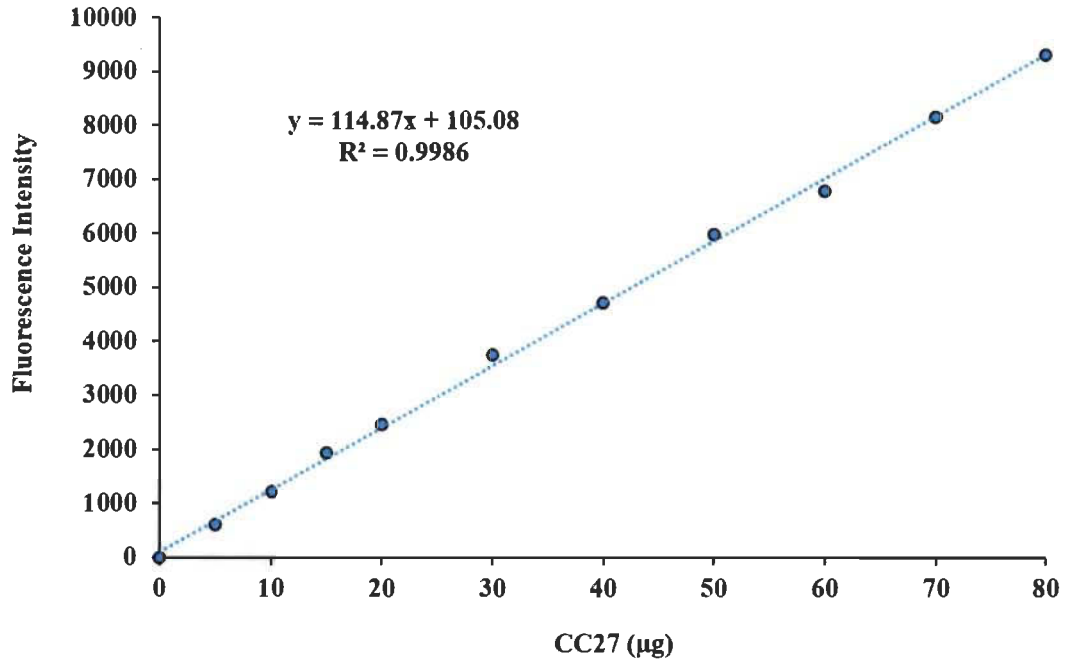


**Additional file 3.7** **Standard curve for the conversion of fluorescence intensity into µg of CC27 probe**

The excitation and emission wavelengths were set at 434 and 477 nm, respectively.

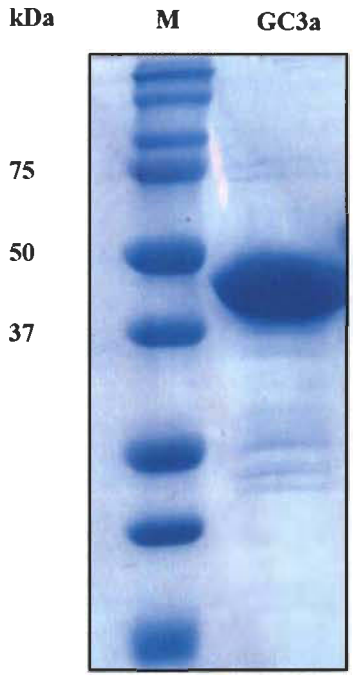


**Additional file 3.8** **SDS-PAGE analysis of the GC3a probe purified by affinity chromatography**

The expected molecular weight of the GC3a fusion protein is 46.26 kDa. A 12% polyacrylamide gel was used for SDS-PAGE analysis. Well M: Precision plus protein standards (5 μg). Well GC3a: Purified GC3a probe (10 μg).

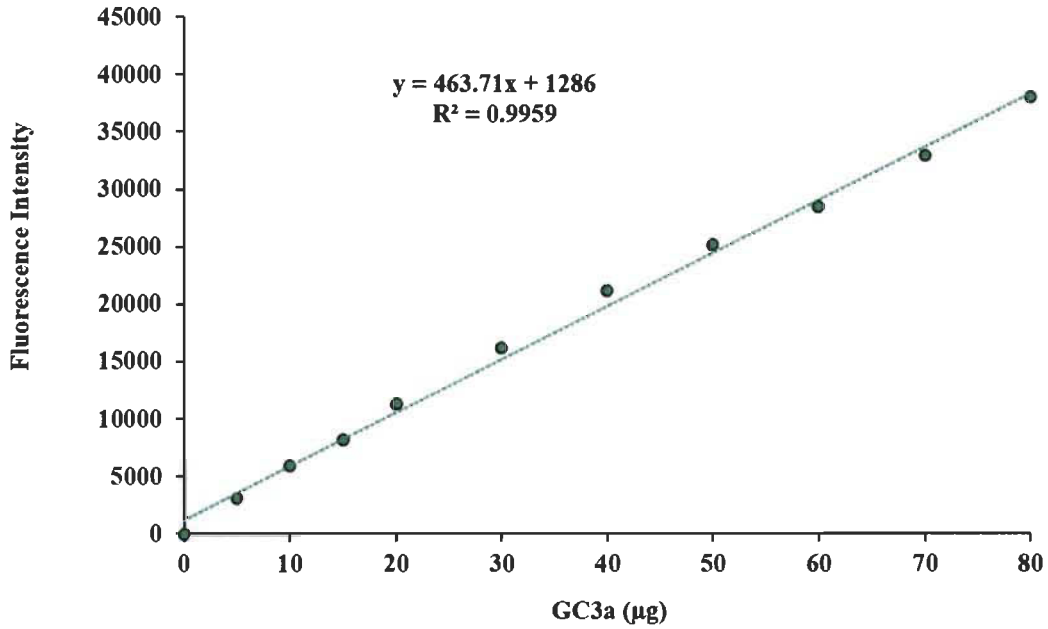


**Additional file 3.9** **Standard curve for the conversion of fluorescence intensity into µg of GC3a probe**

The excitation and emission wavelengths were set at 488 and 510 nm, respectively.

**Additional file 3.10 Porosity and roughness analysis of UBMP, BMP, UBKP and BKP handsheets**

(both smooth and rough-side) determined by Tappi standard methods T 460 om-02 (for porosity measurements) and T 538 om-16 (for roughness measurements)

| Pulp Grade | Porosity (mL/minute) | | Roughness (μm) | |
|---|---|---|---|---|
| | Smooth-Side | Rough-Side | Smooth-Side | Rough-Side |
| UBMP | 211.03 ± 1.7 | 217.07 ± 1.3 | 6.29 ± 0.1 | 8.80 ± 0.07 |
| BMP | 208.03 ± 1.2 | 210.63 ± 1.1 | 6.19 ± 0.09 | 9.24 ± 0.6 |
| UBKP | 8544.67 ± 5.7 | 8133.00 ± 4.1 | 6.47 ± 0.3 | 9.09 ± 0.1 |
| BKP | 6250.33 ± 3.2 | 6192.33 ± 4.5 | 5.53 ± 0.3 | 8.39 ± 0.4 |

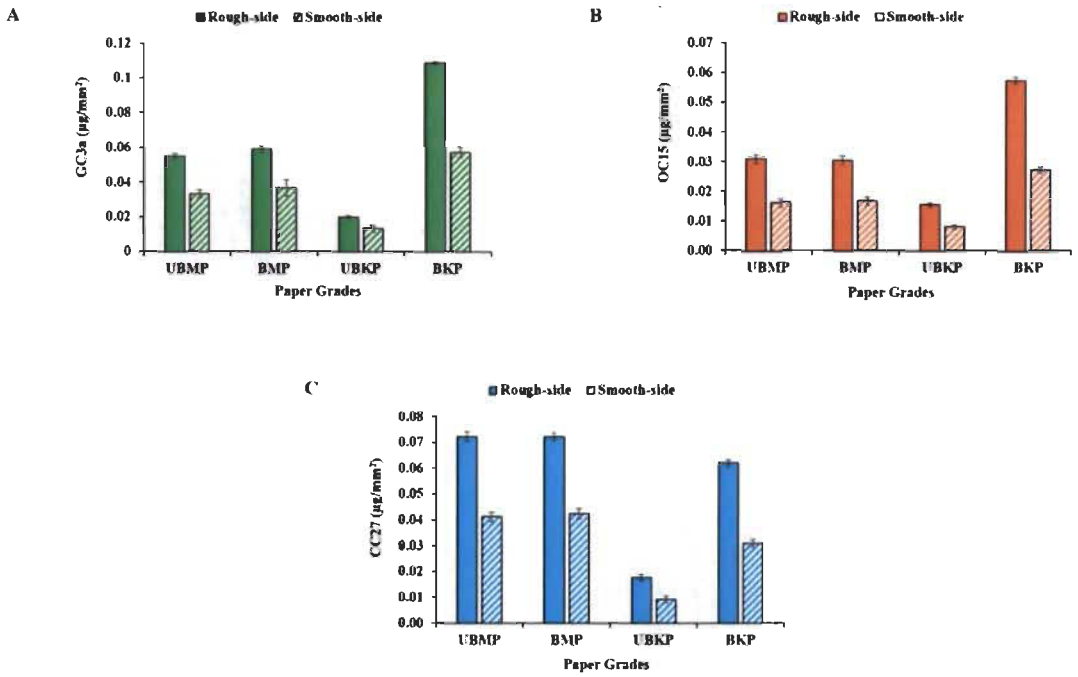


**Additional file 3.11 Tracking hemicelluloses on the rough and smooth surface of UBMP, BMP, UBKP and BKP papers using GC3a, OC15 and CC27 probes**

UBMP, BMP, UBKP and BKP paper discs were incubated with the GC3a probe (0.5 µg/µL) (for crystalline cellulose detection) **(A)**, OC15 probe (0.5 µg/µL) (for xylan detection) **(B)** and the CC27 probe (0.5 µg/µL) (for mannan detection) for 1h at room temperature under agitation **(C)**. Three percent (w/v) milk (20 mM Tris-HCl, pH 7.5 with 20 mM NaCl and 5 mM $CaCl_2$) was used to minimize the auto-fluorescence of paper discs and the non-specific binding of the GC3a, OC15 and CC27 probes. The fluorescence values were converted to GC3a (µg/mm$^2$), OC15 (µg/mm$^2$) and CC27 (µg/mm$^2$) by using the standard curves (Additional files 3.6 , 3.7 and 3.9). Green color represents the GC3a probe detection, orange color represents the OC15 probe detection and cyan color represents the CC27 probe detection. Error bars represent the standard deviation.

**Additional file 3.12 Specific activities of Celluclast 1.5L on model substrates**

| Specific activities (IU/mg) | Celluclast 1.5L |
|---|---|
| CMCase | 24.70 |
| Xylanase | 18.95 |
| Mannanase | 3.94 |

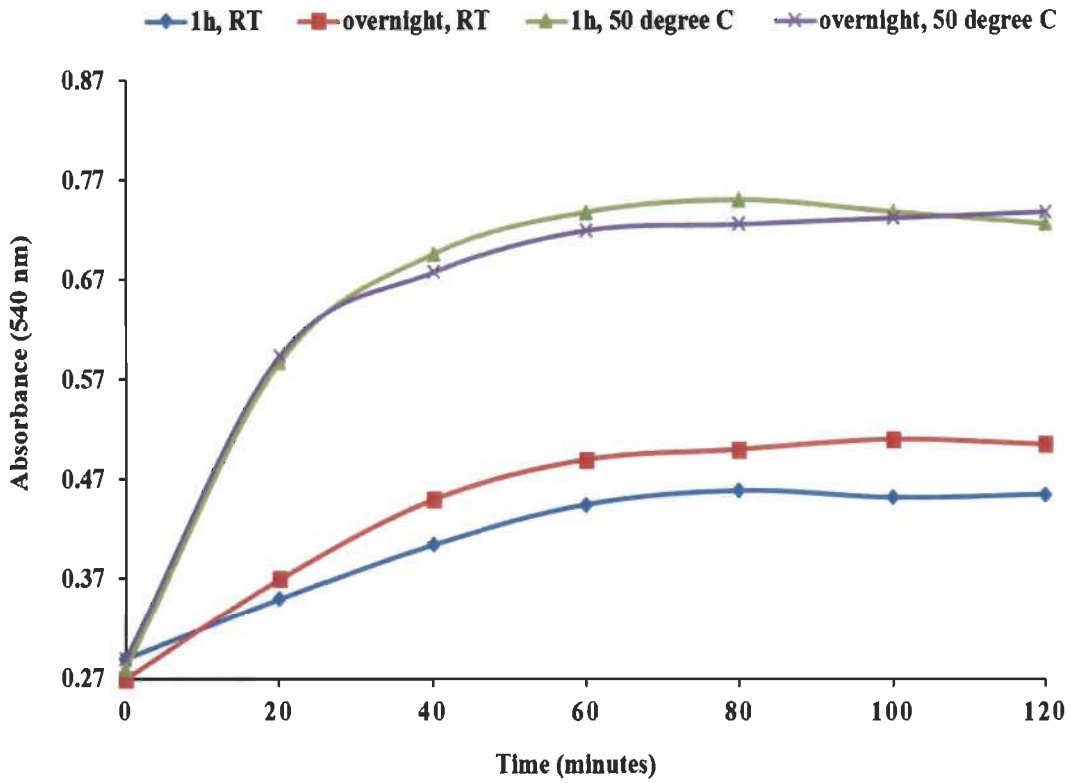


**Additional file 3.13 Sugar release analysis of BKP paper discs hydrolyzed with xylanase (0.1 U/paper disc) at four different opted conditions (1h; RT, overnight; RT, 1h; 50°C and over-night; 50°C)**

*This figure supports the FTCM analysis of BKP paper discs hydrolyzed with xylanase (0.1 U/paper disc) in Figure 3.3D of manuscript.

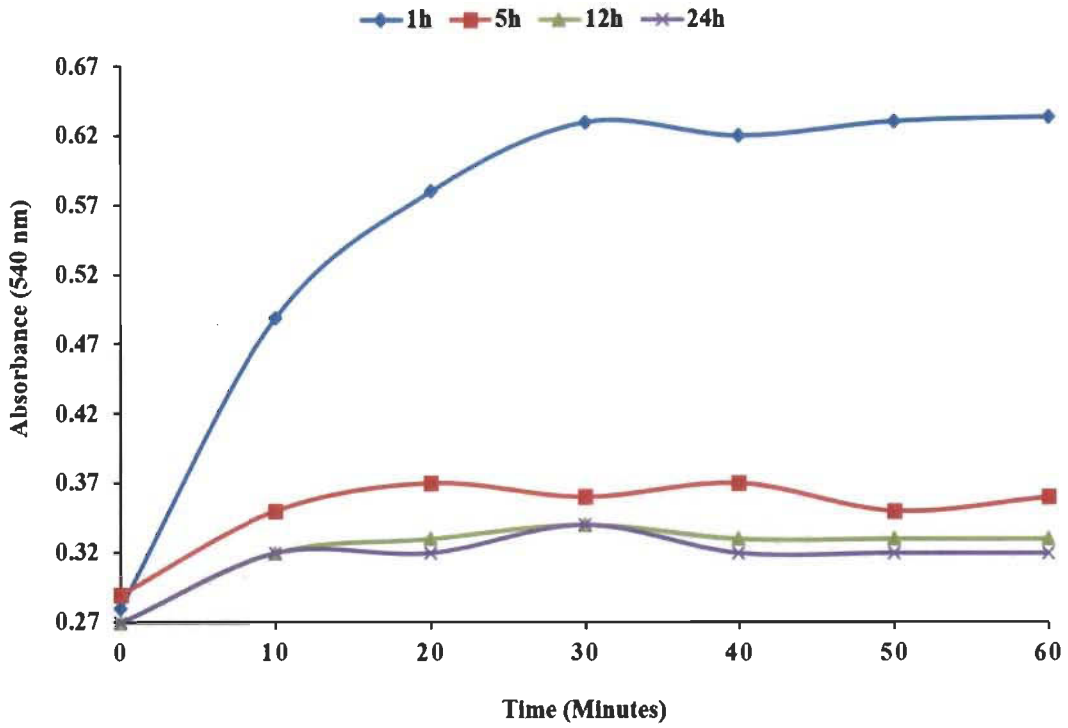


**Additional file 3.14** **Sugar release analysis of BKP paper discs hydrolyzed with xylanase (0.1 U/paper disc) at 50°C with refreshing enzyme solution every hour up to 24 hours. The results are reported for 1$^{st}$h, 5$^{th}$h, 12$^{th}$h and 24$^{th}$h sugar release**

*This figure supports the FTCM analysis of BKP paper discs hydrolyzed with xylanase (0.1 U/paper disc) in Figure 3.5A of manuscript.

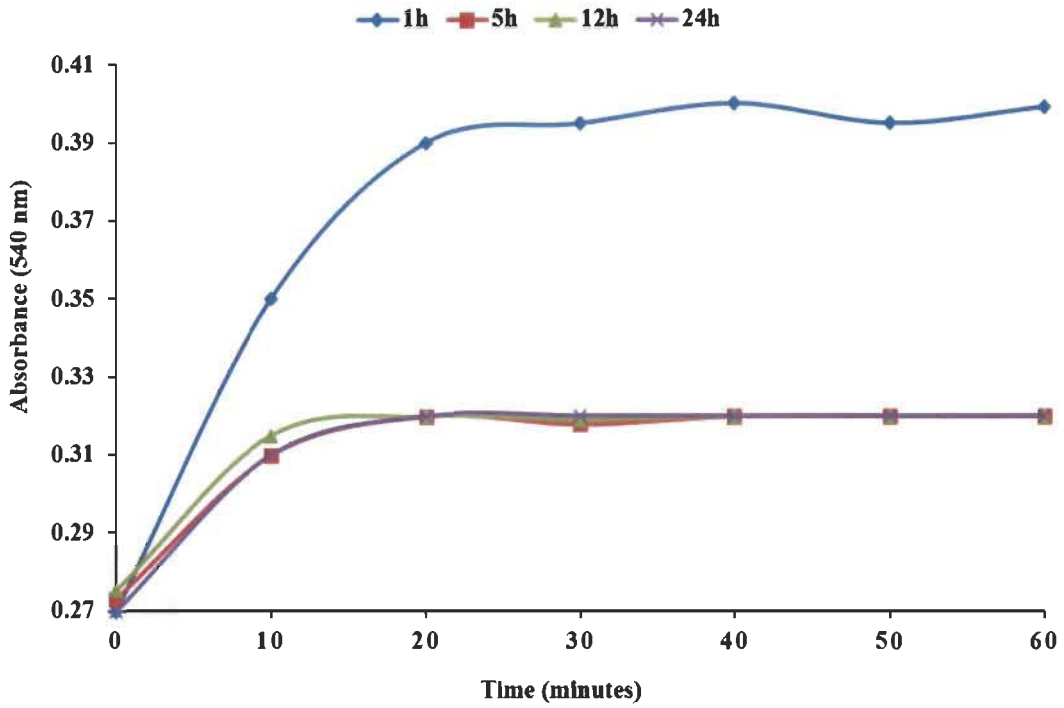


**Additional file 3.15 Sugar release analysis of BKP paper discs hydrolyzed with mannanase (0.1 U/paper disc) at 50°C with refreshing enzyme solution every hour up to 24 hours. The results are reported for 1$^{st}$h, 5$^{th}$h, 12$^{th}$h and 24$^{th}$h sugar release**

*This figure supports the FTCM analysis of BKP paper discs hydrolyzed with mannanase (0.1 U/paper disc) in Figure 3.5B of manuscript.

# Chapter 4 - Scientific Article III

**Tracking and predicting wood fibers processing with fluorescent carbohydrate-binding modules**

Yannick Hébert-Ouellet[a-c], Fatma Meddeb-Mouelhi[a-b,d], Vinay Khatri[a-c], Li Cui[a-c], Bernard Janse[d], Kevin MacDonald[d] and Marc Beauregard[a-c*]

[a] Département de Chimie-Biochimie et Physique, Université du Québec à Trois-Rivières, Trois-Rivières, Québec, G9A 5H7, Canada.

[b] Centre de recherche sur les matériaux lignocellulosiques, Université du Québec à Trois-Rivières, Trois-Rivières, Québec, G9A 5H7, Canada.

[c] Proteo, Université Laval, Québec, Québec, G1V 4G2, Canada.

[d] Buckman, Tennessee, 38108-1241, U.S.A.

*Corresponding author: Centre de recherche sur les matériaux lignocellulosiques, Université du Québec à Trois-Rivières, C.P. 500, Trois-Rivières (Québec), G9A 5H7 Canada, Tel: (819) 376-5011 # 3354, Fax: (819) 376-5084, E-mail: marc.beauregard@uqtr.ca

## Authors' contributions

YHO carried out all the experiments and drafted the manuscript. VK contributed to experiments related to the construction of CBM probes, their expression and purification, and drafted the manuscript. FMM and MB participated in its design and coordination, and helped to draft and revise the manuscript. The original concept leading to FTCM was proposed by FMM, BJ and MB. All authors read and approved the final manuscript.

## Acknowledgements

This work was supported by Buckman International, the Natural Sciences and Engineering Council of Canada (NSERC grant CRDPJ 445143 - 2012), the Consortium de recherche et innovations en bioprocédés industriels au Québec (CRIBIQ) and by MITACS via partial stipends to YHO, LC, and VK (Accelerate program). We would like to thank Dr. Roberto Chica (University of Ottawa) for the donation of mCherry plasmid. The skillful technical assistance of Daniel Steven Agudelo, Rene Diene and Nikolas Beauchesne is acknowledged. We would like to thank Mary A. Hefford for her valuable editorial contributions as well as Dr. N. Voyer and Dr J. Bowie for insightful discussions.

## Competing interests

VK, YHO and MB declare that they have no competing interests. FMM was an employee of Buckman North America which financially supported parts of this work. The project results are included in a provisional patent (assignee: Buckman International, Memphis, TN, USA).

## 4.1 Abstract

Wood fiber is a source of raw materials for established wood-based industries and for the nascent biofuel sector. Efficient processing of wood fiber polymers such as cellulose and hemicellulose requires close monitoring with methods such as FTIR, XPS or chemical analysis. Such methods are time-consuming and require the availability of specialized equipment and expertise. Recently, the carbohydrate recognition domains of glycohydrolases, known as carbohydrate-binding modules, were used for studying the development and the biochemistry of plant cell walls. In this study, we engineered a series of color-coded fluorescent carbohydrate-binding modules with specificities for four major carbohydrate fiber polymers. This approach allowed for quick, high-throughput analysis of fiber surface carbohydrates signatures and is herein used for monitoring and predicting the impact of various treatments on the strength properties of paper produced from such processed fibers. We believe that the simplicity of this environmental-friendly approach could change the way industry optimizes wood fibers processing and deconstruction.

## 4.2 Introduction

Wood fiber is a major source of raw, renewable material for both the paper and biofuel industries. However, its complex organization involves a network of tightly ordered cellulose chains intertwined with other biopolymers, making it recalcitrant to modifications.[1] Accordingly, LCB conversion into paper and/or its deconstruction for biofuel production are costly, energy avid processes.[2-4] Key advances in biochemistry have the potential to change this situation. One promising way of dealing with plant biomass recalcitrance involves the manipulation of plant genes that are associated with cell wall architecture, leading to easier access to cellulose.[5] In wood-degrading fungi, such recalcitrance is dealt with by an array of enzymes, which are sometimes associated in cellulosomes.[6] Such organised enzymatic machinery is highly informative when considering how we can make biofuel from wood materials more efficiently.[7]

Currently, our ability to track the effect of any industrial processing, including enzymatic processing, is limited as most methods are not suitable for quantifying changes in individual lignocellulosic biopolymers. Such methods include the following: compositional analysis (FTIR, XPS and NREL), surface imaging (SEM, TEM and AFM), index of crystallinity (XRD and NMR) and measurements of the degree of polymerization. They are low-throughput, time-consuming and require access to specialized equipment and expertise.[8-10] Among these methods, XPS can be used to monitor lignin and the combination celluloses (crystalline and non-crystalline) and hemicellulose at the surface of fibers but without any distinction between these polymers. Also, it is sensitive to X-ray contamination and sample degradation which may prevent XPS analysis reproductibility.[11,12] Currently, there is no available method which rapidly provide specific information on each major class of polymers at the surface of fibers. Unfortunately, this greatly impairs monitoring fiber surface composition, which essentially limits technological developments and governs the economic viability of several LCBes processes (biofuels production) and/or of its end products (papers manufacturing). The development of a diagnostic approach, which would afford rapid, easy and, if possible, on-site monitoring of fiber structure and composition, would change the way biomass industries achieve optimization of their processes. To this end, carbohydrate-binding modules (CBMs) have tremendous potential. CBMs are defined as small, non-catalytic proteins (which are often attached to glycoside hydrolases via a linker) whose function is to act as substrate-recognition devices thereby enhancing the catalytic efficiency of these enzymes.[13-14] They have been successfully employed for the characterization of fiber surfaces composed of simple and complex carbohydrates.[15-17] Specific advances were achieved using CBMs as fusion with a fluorescence protein such as the green fluorescent protein (or any of its variants).[18] CBMs coupled with fluorescence protein have been used for mapping the chemistry and structure of various carbohydrate-containing substrates (LCB).[15,19] Gao *et al.* using fluorescent CBM3 and CBM17, successfully quantified the change of accessibilities to crystalline and amorphous celluloses during enzymatic hydrolysis.[20] Recently, using fluorescent CBM15, we developed a rapid assay that specifically track surface variations of xylan which enable a better understanding and facilitate the optimization of the LCBes processes.[21]

In this study, we exploited the specificity of CBMs CBM3, CBM15, CBM17 and CBM27 and constructed four fluorescent CBM probes (Figure 1.18), each of which tracks a particular lignocellulosic carbohydrate polymer, *i.e.* mannan, xylan, non-crystalline and crystalline cellulose. Mixing the probes with wood fiber and measuring fluorescence (after removing CBMs that are not specifically bound) allows for quick monitoring of the distribution of the targeted polymers on the fiber, as depicted in Figure 1.19. Here we demonstrate that these probes can monitor processing impact, and help fine-tune wood fiber refining and deconstruction. Applying this approach in an industrial setting will lead to improving the cost efficiency and energy efficiency of fiber treatments.

## 4.3 Materials and methods

### 4.3.1 Reagents and pulps

Unless otherwise noted, all reagents were supplied by Sigma-Aldrich. Softwood (resinous) paper sheets were used here to quantify the variations of the carbohydrates-recognition probes on their surface. These paper sheets were derived from two different kraft pulps, albeit HYKP (Jack pine) and KP (Black spruce). *Cellvibrio japonicus* mannanase (Endo-1, 4-β-Mannanase) purchased from Megazyme was utilized to digest pulp and paper discs.

### 4.3.2 Pulps Characterization

Quantification of the pulps cellulose, hemicellulose, lignin as well as monosaccharides contents were determined using NREL/TP-510-42618 methodologies.[21,25] Determination of the surface exposed polymers of the papers was achieved using X-ray photoelectron spectroscopy.[11,21,29-30]

### 4.3.3 Pulps refining and paper sheets formation

A PFI laboratory refiner was used to reproduce the industrial refining process.[34] Refining of pulps (from 0 to 3000 revolutions) was performed according to the standard

Tappi method T248 sp-00. Afterward, paper sheets of 60 ± 2 g $m^{-2}$ in density were prepared as per the Tappi T205 sp-02 methodology.

### 4.3.4 Enzymatic digestions of pulps and paper discs

The enzymatic digestions of pulp and paper discs were performed in duplicates using *Cellvibrio japonicus* mannanase enzyme. All reactions were performed over a 1h period at room temperature with agitation in 0.1 M phosphate buffer pH 7 supplemented with 0.5 mg/ml BSA. Mannanase concentrations ranged from 250 to 50 000 U/g substrate for paper discs (3 mm) digestions while pulp trials were done at 250 U /g substrate.

### 4.3.5 Fiber quality analysis and paper physical properties determination

The impact of the mechanical and mannanase treatments of pulps on fiber properties was determined using a HiRes LDA02-090 Fibre Quality Analyzer (Optest Equipment Inc.). Paper sheets physical strength properties such as tear, burst, tensile and internal bond strength were determined according to Tappi standard methods T414 om-98, T403 om-02, T494 om-01 and T569 pm-00, respectively.

### 4.3.6 Construction of the recombinant probe expression systems

All carbohydrate-recognition probes genes were inserted into pET11a expression vectors. CBM 3a (*Clostridium thermocellum* CipA, NZYTech), CBM15 (*Cellvibrio japonicas,* Z48928), CBM17 (*Clostridium cellulovorans*, U37056) and CBM27 (*Thermotoga maritima*, NC 000853) genes were synthetized by GenScript. The fluorescent protein genes (eGFP, mOrange2, mCherry and eCFP) were cloned into the *Dra*III and *Bam*HI sites while the CBM genes were introduced into the *Bsr*GI and *Bam*HI sites. All encoding genes were sequenced to ascertain the integrity and fidelity of the probes. The resulting probes eGFP-CBM3a, mOrange2-CBM15, mCherry-CBM17 and eCFP-CBM27 (Figure 1.18) were used to detect crystalline cellulose, xylan, non-crystalline cellulose and mannan, respectively.

### 4.3.7 Expression and purification of recombinant probes

*E. coli* BL21(DE3) Gold pLysS cells (AgilentTechnologies) bearing the selected pET11a expression plasmids were grown at 37 °C in Luria-Bertani broth. Induction of recombinant protein expression was performed by the addition of 0.5 M IPTG (ThermoFisher Scientific) to mid-log-phase cells ($O.D._{600nm}$ of 0.6-0.8) and their subsequent incubation for 18 hours at 25 °C. Cells were afterward harvested and kept at -80 °C. Thawed cell pellets were resuspended in 50 mM sodium phosphate pH 8 containing 300 mM NaCl, 2 mM imidazole, 1 mM PMSF and then lysed using six cycles (60 sec) of sonication (Branson Ultrasonics Corporation) at 200 W. Clarification of the lysate was achieved by centrifugation at 10 000 *g* for 30 minutes at 4 °C. The protein of interest was then purified by affinity chromatography over a HisPrep FF 16/10 column (GE Healthcare Life Sciences) equilibrated in 50 mM sodium phosphate pH 8.0 buffer containing 300 mM NaCl and 10 mM imidazole. Following washes with ten column volumes of buffer, the desired protein was eluted using a gradient (ten column volumes) of imidazole (10 to 100 mM) in 50 mM sodium phosphate pH 8.0 buffer containing 300 mM NaCl. A final purification step was performed using a Superdex 200 HR 16/50 column (GE Healthcare Life Sciences) and 50 mM Tris-HCl pH 7.5 buffer containing 300 mM NaCl to insure purity. The purified probes were then dialyzed against a 20 Tris-HCl pH 7.5 buffer containing 20 mM NaCl and 5 mM $CaCl_2$ at 4 °C and concentrated using a 10k Macrosep Advance centrifugal device (Pall Corporation). Concentrated protein solutions were stored at -80 °C after flash freezing. Protein purity was verified by SDS-PAGE. The amount of protein was quantified by the Bradford method.

### 4.3.8 Quantification of the variations of the carbohydrates signatures on the surface of fiber discs

All fluorescence readings were acquired at room temperature on a Synergy Mx microplate reader using the 3 x 3 area scanning feature with the top detection height set at 4.5 mm and the filter bandwidth at 9 nm. The excitation and emission wavelengths were set at 488 and 510 nm for eGFP-CBM3a, 587 and 610 nm for mCherry-CBM17, 549 and

568 nm for mOrange2-CBM15 and 434 and 477 nm for eCFP-CBM27. Fluorescence measurements were recorded after each step of the assay. Each experiment was done in triplicates. Preparation of the microplate was carried out by gluing 3 mm diameter paper discs on the bottom of 96-wells, black microplate (Costar, Corning Life Sciences) using a transparent nail polish. The carbohydrates quantification assay started by incubating the paper discs 1h, at room temperature with agitation in a 20 Tris-HCl pH 7.5 buffer containing 20 mM NaCl, 5 mM $CaCl_2$ and 3% milk (binding buffer). Unbound milk constituents were removed by washing three times with the 20 Tris-HCl pH 7.5 buffer containing 20 mM NaCl, 5 mM $CaCl_2$ (washing buffer). Afterward, the blocked paper discs were incubated with agitation for 1h, at room temperature into the binding buffer containing 0.5 µg/µl of the appropriate probe. Non-specifically bound probe was removed with three buffer washes (washing buffer) followed by three 0.05 % Tween 20 washes. Treatment of the resulting data involved subtraction of the mean blocked fluorescence values from the mean residual ones. Then these corrected mean residual fluorescence values were converted into µg and $\mu g/mm^2$ using the appropriate standard curves and weight of cellulose in each fiber discs.

### 4.3.9 Determination of the probes affinity for Avicel and fiber discs

Solid state depletion assays[43] were used to measure the affinity of all probes using heterogeneous substrates such as Whatman, HYKP and KP fiber discs, and substrate Avicel PH105 (crystalline cellulose) for eGFP-CBM3a probe. Determination of the affinity of eGFP-CBM3a regarding Avicel was performed under the following procedure. The assay started with a 1h incubation at room temperature of 10 mg of the presoaked Avicel with increasing concentrations of eGFP-CBM3a in a 20 Tris-HCl pH 7.5 buffer containing 20 mM NaCl, 5 mM $CaCl_2$ and 3 % milk. Following equilibration, the solid phase was separated from the liquid phase by centrifugation at 20 000 g for 5 min. Fluorescence measurements of the supernatant (containing free protein (Pfree)) were acquired using a Synergy Mx microplate reader (BioTek) with the end point feature active and the filters bandwidth set at 9 mm. The excitation and emission wavelengths for eGFP-CBM3a were set at 488 and 510 nm, respectively. Protein concentrations were determined using the

appropriate standard curves. All binding isotherms were calculated using the OriginLab software and fitted to a one binding site equation follows:

$$[P_{bound}] = N_o K_a [P_{free}] / (1 + K_a [P_{free}])$$

where ($K_a$) represent binding affinity and ($N_o$) represent the capacity of CBM probe (Additional files 4.1 and 4.3).

The determination of the probes affinity for fibers discs was achieved using the acquisition settings as described in the previous paragraph for the quantification. Fluorescence measurements were again recorded after each step of the assay. Briefly, the glued fiber discs were incubated for 1h at room temperature with agitation in the binding buffer. Unbound milk constituents were removed by washing three times with the washing buffer. Afterward, the blocked paper discs were incubated 1h at room temperature with binding buffer which contained increasing concentrations of the appropriate probe. Non-specifically bound probe was then removed with three washing steps. Treatment of the resulting data involved subtraction of the mean blocked fluorescence values from the mean residual ones. These corrected mean residual fluorescence values were converted into µg and µg/g of substrate using the appropriate standard curves and weight of cellulose in each paper disc. All binding isotherms fitted to a one binding site equation.

## 4.4 Results and Discussion

Wood pulping is a well-known treatment that promotes exposure of carbohydrate polymers such as cellulose and hemicellulose.[22-24] Depending on the treatment, changes in polymers are expected. For example, the lignin covering kraft pulp fibers is substantially lower than for high yield kraft pulp (HYK) fiber. Typically, total chemical analyses (NREL/TP-510-42618) are used to determine the chemical composition of pulps.[25] As expected, these analyses revealed that HYK has a higher lignin content (1.4-fold) than kraft pulp (Additional file 4.4). Unfortunately, this approach can only provide an overall bulk estimation of polymers content. It cannot detect nor than measure variations of pol-

ymers specifically located at the surface of fibers. Another classical method for fiber analysis is X-ray photoelectron spectroscopy (XPS). XPS analysis consists in acquiring and deconvoluting the C 1s band of high-resolution spectra in order to expose the C1 to C4 peaks (Additional files 4.2 and 4.5). The C1 component of the C 1s band mainly arises from lignin and extractives, while C2 is primarily associated to cellulose and hemicelluloses. The C3 component is not easily assigned to a given polymer, as it is related to either carbonyl groups of lignin and extractives, or to carbon atoms bonded to two oxygen atoms in cellulose and hemicellulose.[26-28] Consequently, XPS has been used extensively for surface analysis of simple LCBes for detection of changes in surface coverage by cellulose, lignin, and extractives.[11,29-30] When comparing HYK paper to kraft paper, we found a 1.4-fold increase in C1 spectral component intensity at HYK surface (Additional file 4.5). Again, this result suggests that HYK has a higher lignin content. The C2 functionality in HYK paper is 1.1-fold lower than for kraft paper, suggesting that cellulose and/or hemicellulose are slightly less present on its surface. The values of the C3 and C4 functionalities were relatively low and similar for either paper. XPS analysis did reveal the impact of the different pulping processes on the exposure of major polymer classes. Unfortunately, the C 1s spectra cannot distinguish cellulose (be it non-crystalline or crystalline) from hemicellulose since these polymers (or polymer forms) possess similar carbon types.

Using CBM-probes, we endeavored to avoid such limitations associated with chemical and XPS analyses. We attempted to monitor the difference in the exposure of carbohydrate polymers on the surface of fibers from the same pulps as described above (HYK and kraft). The binding of CBM probes to fiber discs made of two pulp grades is shown in Figure 4.1. The calibrated fluorescence signals indicate that the most abundant carbohydrate polymer at the surface of the fiber discs was crystalline cellulose, followed by non-crystalline cellulose, and then by hemicelluloses. This distribution of individual fiber polymers is compatible with the measured chemical compositions of these pulps (Additional file 4.4).

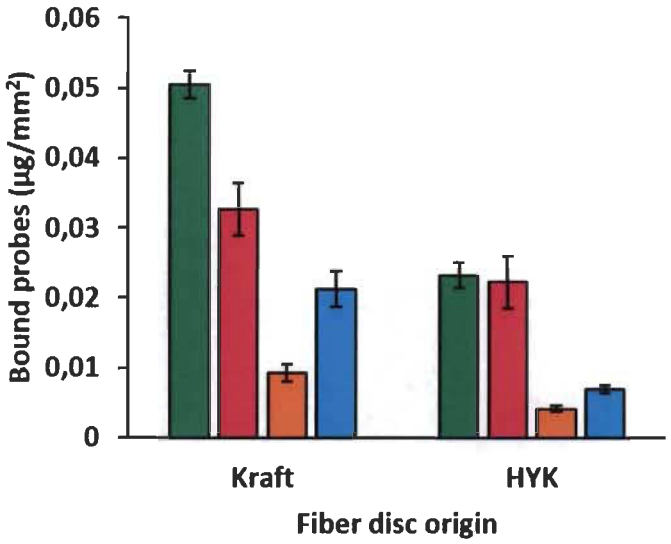


**Figure 4.1 CBM binding to the surface of unrefined kraft and high yield kraft (HYK) fiber discs**

The probes attached to crystalline and non-crystalline celluloses are shown in green and cherry, while hemicelluloses xylan and mannan probes are shown in orange and cyan, respectively.

The access of CBM-probes to surface carbohydrates appears to be hindered in high-yield kraft pulp (HYK). This pulp contains 1.4 fold the amount of fiber-coating lignin found in the other kraft pulp (Additional file 4.4). Clearly, the probes allow to quickly distinguish between two pulping grades. In addition, the analysis of fiber surface with CBM probes indicates that mannan, and not xylan, is the primary hemicellulose carbohydrates detected in kraft pulp, confirming that both fiber discs were manufactured principally from softwood. These results suggest that introducing this tracking approach as a quality control measurement would bolster the effectiveness of the LCB processes.

Mechanical refining is essential for modifying the characteristics of wood fibers.[21,31] One important consequence of refining is the external fibrillation of the wood fiber S2 layer which promotes the formation of hydrogen bonds between fibers. On the molecular

level, refining translates into the partial conversion of crystalline into non-crystalline cellulose (made of hydrated cellulose fibrils), a phenomenon known as amorphogenesis.[32,33] In addition to being the primary source of hydrogen bonds strengthening the fiber matrices in paper, non-crystalline cellulose is also more sensitive to enzymatic hydrolysis into fermentable sugars.[2,17,32,33] Monitoring non-crystalline cellulose formation during refining would help detect the minimal amount of mechanical energy required to promote efficient amorphogenesis which is critical for both wood based biofuel and papermaking industries. Optimizing energy input would also reduce possible mechanical sheer and help maintain fiber integrity.

Figure 4.2 shows the evolution of the carbohydrates surface signatures as a function of increasing refining intensities as revealed by the CBM probes. This experiment revealed that the non-crystalline cellulose to crystalline cellulose ratio (AC/CC) is maximal at 2000 PFI revolutions, suggesting that amorphogenesis would be optimal using the corresponding mechanical energy (Figure 4.2A). Interestingly, the mannan to crystalline cellulose ratio (Man/CC) also peaked at 2000 (Figure 4.2B) meaning that exposure of the cellulose-sheathing mannan layer is maximal at such refining intensity. In contrast, the xylan to crystalline cellulose ratio (Xyl/CC) initially increased but then remained constant after reaching 1500 revolutions. Overall, the application of mechanical energy to wood fibers lowered the surface detection of all carbohydrates. This result is consistent with the lowering of probe accessibility that results from the production of a tighter fiber network in the paper discs after refining.[19,31,34]

A critical issue in the wood biomass industry is the cost of process optimization. The ability to not only rapidly monitor, but also predict the impact of a treatment on a small scale would be of great benefit to the industry. In this context, we measured the physical properties of paper hand sheets after various refining intensities in order to establish correlations between the carbohydrate to crystalline cellulose ratios (revealed by the probes) and the paper strength properties.

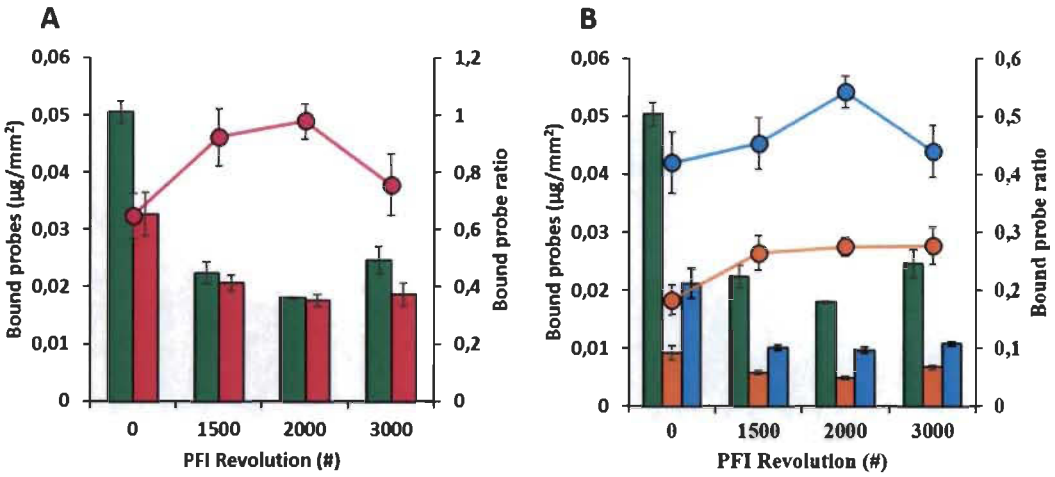


**Figure 4.2** **Impact of refining intensity on the binding of CBM-probes to kraft fiber discs**

**A)** Variations of crystalline (green bars) and non-crystalline (cherry bars) cellulose as a function of refining intensity. The cherry open circles correspond to the evolution of the non-crystalline cellulose to crystalline cellulose ratio (AC/CC). **B)** Variations of xylan (orange bars), mannan (cyan bars) and crystalline cellulose as a function of refining intensity. The orange and cyan circles correspond to the variations of the xylan to crystalline cellulose ratio (Xyl/CC) and mannan to crystalline cellulose (Man/CC), respectively.

Figure 4.3 reveals that the optimal values of a number of important paper strength properties (such as internal bond strength and tear and tensile indices) were effectively correlated with optimal AC/CC ratio at 2000 revolutions. Note that all these parameters are a function of fiber mean length, since shorter and deformed fibers lower the paper's strength properties.[35,36] However, taking only fiber length into account would have been misleading since this parameter peaked at 1500 revolutions. We show here that the carbohydrate surface signatures closely correlated with the paper strength properties. Consequently, we believe that the correlations between the developed probe surface signatures and paper strength properties can be evolved into a powerful prediction tool for the quick and efficient determination of optimal refining conditions.

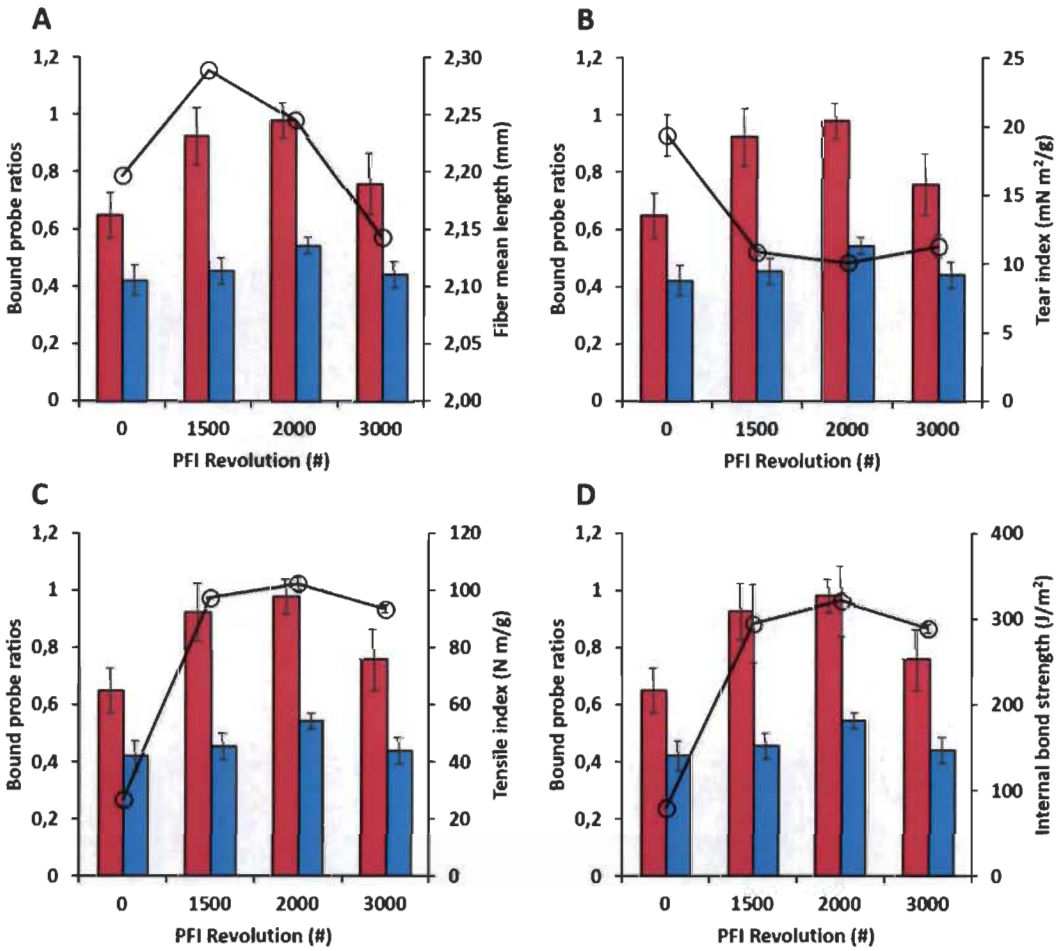


**Figure 4.3 Impact of refining intensity on the relationship between the bound probe AC/CC, Man/CC ratios and paper physical properties**

**A**) Fiber mean length (mm). **B**) Tear index (mN $m^2$/g). **C**) Tensile index (N m/g). **D**) Internal bound strength (J/$m^2$). The variations in physical properties values are shown by black lines and circles, while the AC/CC and Man/CC ratios are shown with bars in cherry and in cyan, respectively.

Enzymes have been used for many years to improve papermaking as well as for the deconstruction processes of LCBes in order to reduce energy consumption and increase productivity.[37-39] One such enzyme, mannanase, was found to be particularly effec-

tive when used on kraft pulp and in relieving mannan inhibition of cellulases.[40-42] Unfortunately, mannanase usage is frequently restricted to certain biomasses and conditions, and this mixed success has limited its usage on the industrial scale. As a result, efficient prediction of the impacts of mannanase activity on biomass properties is imperative. Therefore, we developed a small-scale paper discs digestion assay and applied our CBM technology to detect the optimal condition required for mannanase to promote the efficient uncovering of crystalline cellulose and thereby improve the reactiveness of fibers towards mechanical refining without negatively affecting paper properties. Figure 4.4 shows the impact of mannanase hydrolysis on the removal of mannan and on the exposure of crystalline cellulose at the surface of unrefined kraft fiber discs.

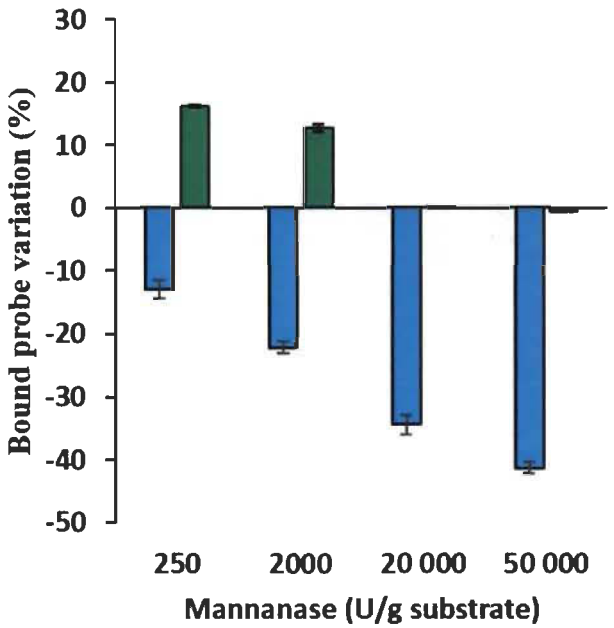


**Figure 4.4** **Impact of mannanase hydrolysis (250-50 000 U/g substrate) on the binding of mannan (cyan) and crystalline cellulose (green) probes on the surface of unrefined kraft fiber discs**

The negative percentage values indicate that mannan removal was commensurate with enzyme concentration (12.9 % for 250 U/g substrate up to 41.3% for 50 000 U/g substrate). This result shows that our experimental conditions were adequate for hydrolyzing mannan in a complex LCB. Optimal crystalline cellulose exposure was detected using 250 U/g substrate of mannanase. The probes signals indicated that increasing mannanase concentrations beyond 250 U/g did not lead to additional detection of cellulose on the fiber surface.

Subsequently we investigated the impact of mannanase pre-treatment on the fibers response to mechanical refining and the consequent paper properties. To identify possible correlations between probe binding to surface polymers and paper properties, larger pulp samples were treated with mannanase, then by mechanical refinining and then converted into handsheets for further analysis. Figure 4.5A shows the changes in polymer detection measured on unrefined fiber discs (0 revolution) and on refined fibers. All samples were pre-treated with mannanase. Without refining, mannan and crystalline cellulose detection was similar to results previously recorded on smaller samples (Figure 4.4). Before any mechanical energy was applied (0 revolution) cellulose (both crystalline and non-crystalline) and xylan detection was increased by mannanase treatment. Applying mechanical refining on enzyme treated pulp samples resulted in increased binding of probes, suggesting that refining generated increased fibrillation, as observed earlier for a similar treatment sequence (refining applied onto enzyme-treated pulp, see reference 34). The impact of refining on mannanase treated pulp lead to a complete reversal in mannan exposure (-15% without refining, +3.5% after 1500 revolutions, +10% after 3000 revolutions). It appears that refining exposed new mannan polymers compensating for surface mannan that was hydrolyzed before refining. Crystalline cellulose detection was not stimulated by moderate refining intensity (1500 revolutions) but after 3000 revolutions on a PFI refiner, exposure of crystalline cellulose was increased by 26%. Non-crystalline cellulose steadily increased with refining intensity, in agreement with the well-known impact of refining on amorphogenesis, while xylan detection did not correlate with refining intensity. Xylan

was severely reduced at moderate refining (from 27% down to 3% variation vs control), and then made available again for detection after 3000 revolutions.

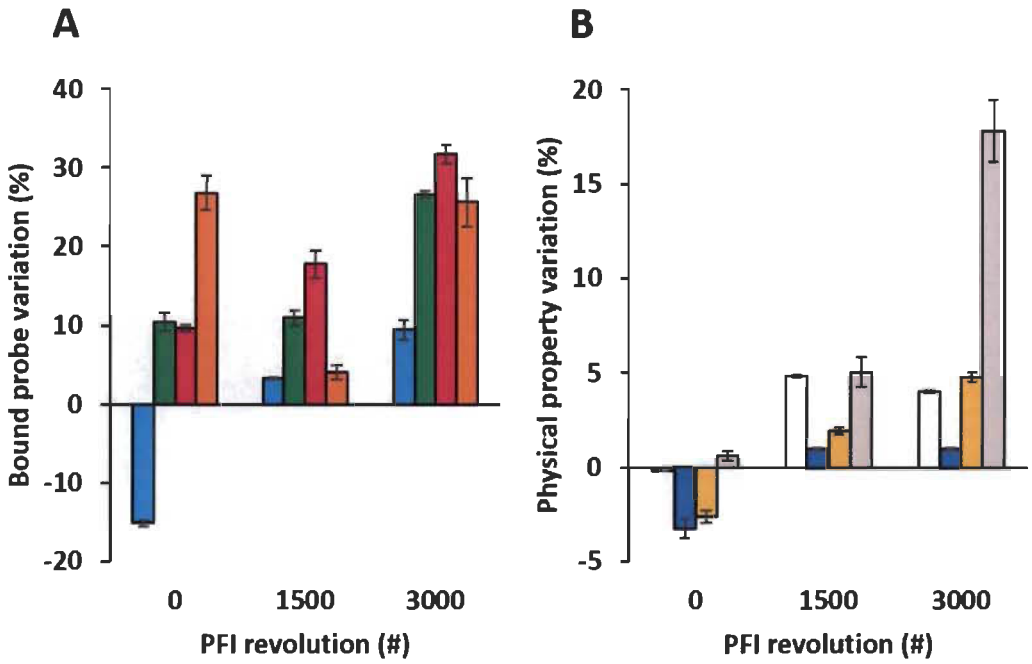


**Figure 4.5** **Impact (%) of mannanase hydrolysis (250 U/g substrate) and mechanical refining of kraft pulp on A) the variations of the carbohydrate signatures on the surface of paper discs and on B) the variations of the strength properties of the resulting paper sheets**

Variations of mannan, xylan, crystalline and non-crystalline celluloses are colored blue, orange, green and cherry while those for fiber mean length, tear index, tensile index and internal bound strength are colored white, dark blue, yellow and grey, respectively.

Figure 4.5B reveals the impact of mannanase hydrolysis and mechanical refining of kraft pulp on the strength properties of the paper sheets (from which paper discs were sampled and exposed to probes (Figure 4.5A). Overall these results indicate that exposure

of hemicelluloses and cellulose (crystalline or non-crystalline) correlated with important paper strength properties (maximal exposure and best properties were observed after treatment with 3000 revolutions on the PFI). Specific correlations were observed for each probe. Mannan detection was correlated with tear index and internal bond, showing negative variations after mannan hydrolysis but positive values after refining of mannanase treated fibers. Non-crystalline cellulose variations were correlated with tensile and internal bond in its response to refining. For xylan and crystalline cellulose, detection was maximal after 3000 revolutions where optimal paper properties were observed too. But it did not correlate with paper properties trends observed at 0 or 1500 revolutions. The fiber length peaked at 1500 revolutions where sub-optimal paper properties were observed. These results attest to the close relationship that exists between the carbohydrates signatures (especially mannan and non-crystalline cellulose) on the surface of wood fibers on the one hand, and the properties of paper derived from such fibers on the other hand. We suggest that these correlations form the basis of a novel approach for predicting the impact of mechanical and enzymatic processes in wood biomass industries.

## 4.5 Conclusions

We developed a simple yet powerful approach that allows for the surface characterization of fiber surfaces. The CBM probes were successfully employed to characterize the impacts of pulping, mechanical and enzymatic modifications on the carbohydrates distribution on LCB surfaces. Correlations with paper strength properties would enable the rapid determination of these properties and allow one to predict in a high throughput yet low volume the optimal conditions with which to treat a given biomass. Such probes provide a new and novel approach for monitoring process development and scale-up of processes that affect fiber properties – in either the manufacture of paper or the deconstruction of cellulose into sugars for biofuel production.

## 4.6 References


1. M. E. Himmel, S. Y. Ding, D. K. Johnson, W. S. Adney, M. R. Nimlos, J. W. Brady and T. D. Foust, *Science*, 2007, **315**, 804-807.
2. V. Arantes and J. N. Saddler, *Biotechnol Biofuels*, 2010, **3**, 4.
3. M. Sabourin, paper presented at the 2003 Fall Technical Conference, Chicago, IL, 2003.
4. L. P. Walker and D. B. Wilson, *Bioresource Technology*, 1991, **36**, 3-14.
5. B. Vanholme, T. Desmet, F. Ronsse, K. Rabaey, F. Van Breusegem, M. De Mey, W. Soetaert and W. Boerjan, *Front Plant Sci*, 2013, **4**, 174.
6. Q. Xu, M. G. Resch, K. Podkaminer, S. Yang, J. O. Baker, B. S. Donohoe, C. Wilson, D. M. Klingeman, D. G. Olson, S. R. Decker, R. J. Giannone, R. L. Hettich, S. D. Brown, L. R. Lynd, E. A. Bayer, M. E. Himmel and Y. J. Bomble, *Sci Adv*, 2016, **2**, e1501254.
7. R. A. Dixon, *Nature*, 2013, **493**, 36-37.
8. T. P. Schultz, M. C. Templeton and G. D. McGinnis, *Anal. Chem.*, 1985, **57**, 2867-2869.
9. S. Burkhardt, L. Kumar, R. Chandra and J. Saddler, *Biotechnol Biofuels*,2013, **6**, 90.
10. K. Karimi and M. J. Taherzadeh, *Bioresour Technol*, 2016, **200**, 1008-1018.
11. P. Fardim, H. Hultén Anette, J.-P. Boisvert, L.-S. Johansson, M. Ernstsson, M. Campbell Joseph, A. Lejeune, B. Holmbom, J. Laine and D. Gray, *Holzforschung*, 2006, **60**, 149.
12. L.-S. Johansson, J. M. Campbell, P. Fardim, A. H. Hultén, J.-P. Boisvert and M. Ernstsson, *Surface Science*, 2005, **584**, 126-132.
13. A. B. Boraston, V. Notenboom, R. A. J. Warren, D. G. Kilburn, D. R. Rose and G. Davies, *J. Molec. Biol.*, 2003, **327**, 659-669.
14. O. Shoseyov, Z. Shani and I. Levy, *Microbiol. Molec. Biol. Rev.*, 2006, **70**, 283-295.
15. S. Y. Ding, Q. Xu, M. K. Ali, J. O. Baker, E. A. Bayer, Y. Barak, R. Lamed, J. Sugiyama, G. Rumbles and M. E. Himmel, *Biotechniques*, 2006, **41**, 435.

16. M. C. Hernandez-Gomez, M. G. Rydahl, A. Rogowski, C. Morland, A. Cartmell, L. Crouch, A. Labourel, C. M. G. A. Fontes, W. G. T. Willats, H. J. Gilbert and J. P. Knox, *FEBS Letters*, 2015, **589**, 2297-2303.
17. K. Gourlay, J. Hu, V. Arantes, M. Penttilä and J. N. Saddler, *J. Biol. Chem.*, 2015, **290**, 2938.
18. J. P. Knox, *Cellulases,* 2012, **510**:233–45.
19. T. Kawakubo, S. Karita, Y. Araki, S. Watanabe, M. Oyadomari, R. Takada, F. Tanaka, K. Abe, T. Watanabe, Y. Honda, and T. Watanabe, *Biotechnol Bioeng.* 2010, **105**, 499.
20. S. Gao, C. You, S. Renneckar, J. Bao and Y. H. P. Zhang, *Biotechnol Biofuels*, 2014, **7**, 1.
21. V. Khatri, Y. Hebert-Ouellet, F. Meddeb-Mouelhi and M. Beauregard, *Biotechnol Biofuels*, **9**, 74.
22. G. Smook, *Handbook for pulp and paper technologists*, Angus Wilde Publications Inc., Vancouver, 2003.
23. C. J. Biermann, *Handbook of pulping and papermaking*, Academic Press, San Diego, 1996.
24. P. Bajpai, in *Biotechnology for pulp and paper processing*, ed. P. Bajpai, Springer, New York, edition 1, 2012, chapter 2, 7-14.
25. A. Sluiter, B. Hames, R. Ruiz, C. Scarlata, J. Sluiter, D. Templeton and D. Crocker, *Laboratory Analytical Procedure*, 2008, NREL/TP-510-42618.
26. G. N. Inari, M. Pétrissans, J. Lambert, J. J. Ehrhardt and P. Gérardin, *Surface and Interface Analysis*, 2006, **38**, 1336-1342.
27. P. Nzokou and D. Pascal Kamdem, *Surface and Interface Analysis*, 2005, **37**, 689-694.
28. H. Awada, P. H. Elchinger, P.A. Faugeras, C. Zerrouki, D. Montplaisir, F. Brouillette and R. Zerrouki, *BioResources*, 2015, **10**(2), 2044-2056.
29. G. N. Inari, M. Pétrissans, S. Dumarcay, J. Lambert, J. J. Ehrhardt, M. Sernek and P. Gérardin, *Wood Sci Technol*, 2011, **45**(2), 369.

30. W.K. Istone, *X-ray photoelectron spectroscopy (XPS)*, CRC Press, Boca Raton, 1995.
31. S. Gharehkhani, E. Sadeghinezhad, S. N. Kazi, H. Yarmand, A. Badarudin, M. R. Safaei and M. N. M. Zubir, *Carbohydrate Polymers*, 2015, **115**, 785.
32. J. O. Baker, M. R. King, W. S. Adney, S. R. Decker, T. B. Vinzant, S. E. Lantz, R. E. Nieves, S. R. Thomas, L.-C. Li, D. J. Cosgrove and M. E Himmel, *Appl. Biochem. Biotech.*, 2000, **84**, 217.
33. M. P. Coughlan, *Biotechnology and Genetic Engineering Reviews*, 1985, **3**, 39.
34. L. Cui, F. Meddeb-Mouelhi and M. Beauregard, *Nordic Pulp and Paper Research Journal*, 2015, **31**, 315.
35. R. E. Mark, in *Handbook of Physical Testing of Paper*, eds. R. E. Mark, C. C. Habeger Jr, J. Borch and M. B. Lyne, Marcel Dekker Inc., New York, edition 2, 2002, chapter 14, 727-872.
36. M. A. Hubbe, R. A. Venditti and O. J. Rojas, *BioResources*, 2007, **2**, 739.
37. T. Oksanen, J. Pere, L. Paavilainen, J. Buchert and L. Viikari, *J. Biotechnol.*, 2000, **78**, 39.
38. S. D. Mansfield, K. K. Y. Wong, E. D. De Jong and J. N. Saddler, *Tappi Journal*, 1996, **79**, 125-132.
39. A. Suurnäkki, M. Tenkanen, J. Buchert and L. Viikari, in *Biotechnology in the Pulp and Paper Industry*, eds. K. E. L. Eriksson, W. Babel, H. W. Blanch, C. L. Cooney, S. O. Enfors, K. E. L. Eriksson, A. Fiechter, A. M. Klibanov, B. Mattiasson, S. B. Primrose, H. J. Rehm, P. L. Rogers, H. Sahm, K. Schügerl, G. T. Tsao, K. Venkat, J. Villadsen, U. von Stockar and C. Wandrey, Springer Berlin Heidelberg, Berlin, Heidelberg, 1997, pp. 261-287.
40. R. Kumar and C. E. Wyman, *Biotechnol Bioeng*, 2014, **111**, 1341-1353.
41. G. Strey, J. Wesley-Smith and F. Wolfaardt, *Holzforschung*, 2009, **63**, 521-527.
42. E. J. Taylor, A. Goyal, C. I. P. D. Guerreiro, J. A. M. Prates, V. A. Money, N. Ferry, C. Morland, A. Planas, J. A. Macdonald, R. V. Stick, H. J. Gilbert, C. M. G. A. Fontes and G. J. Davies, *Journal of Biological Chemistry*, 2005, **280**, 32761.
43. D. W. Abbott and A. B. Boraston, *Methods Enzymol*, 2012, **510**, 211.

## 4.7 Additional Files

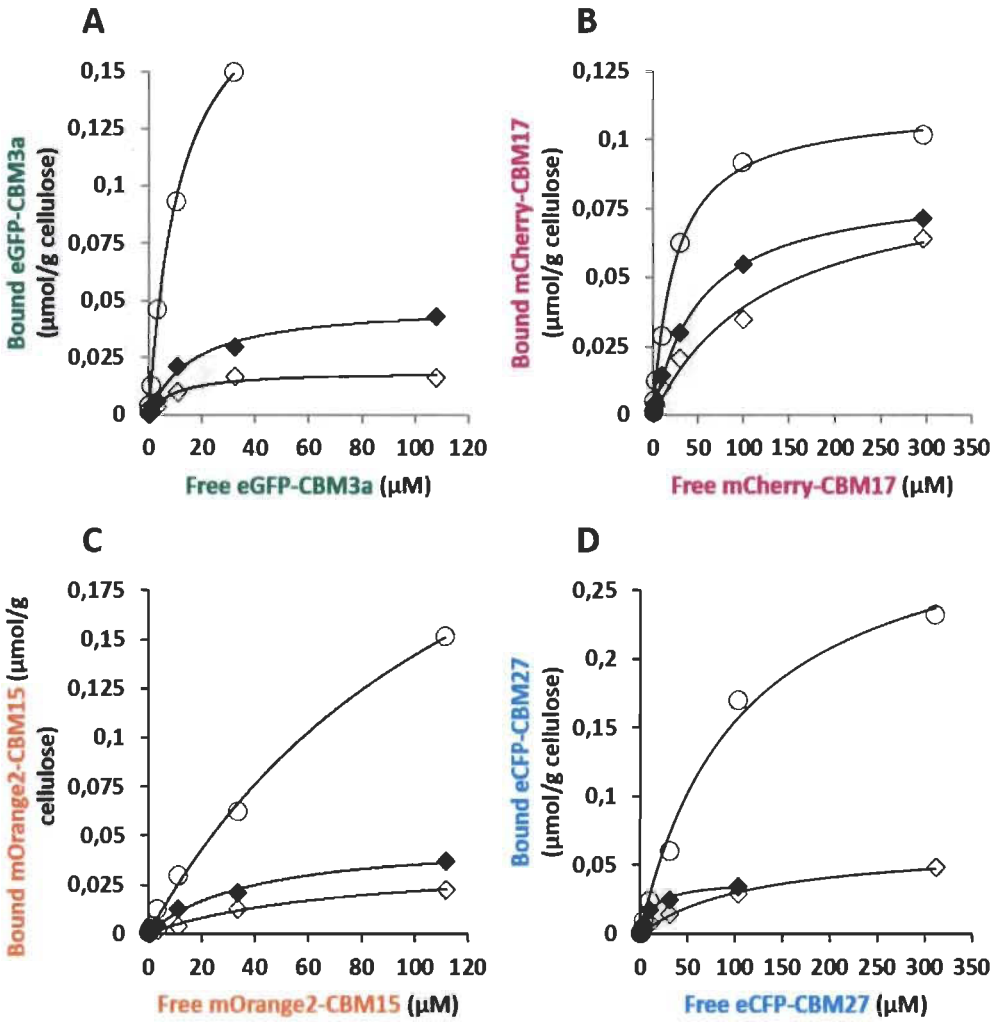


**Additional file 4.1** **Affinity of the probes for various paper support**

Binding curves of eGFP-CBM3a **(A)**, mCherry-CBM17 **(B)**, mOrange2-CBM15 **(C)** and eCFP-CBM27 **(D)** as calculated from solid state depletion assays. Cellulose substrates were: Whatman paper (*open circle*), kraft paper (*filled diamond*) and HYK (*open diamond*) unrefined papers. Binding was recorded after a 1h incubation at 23 °C of the various cellulose supports with the probes (100 µg/well) in a 20 mM Tris-HCl pH 7.5 buffer containing 20 mM NaCl and 5 mM $CaCl_2$.

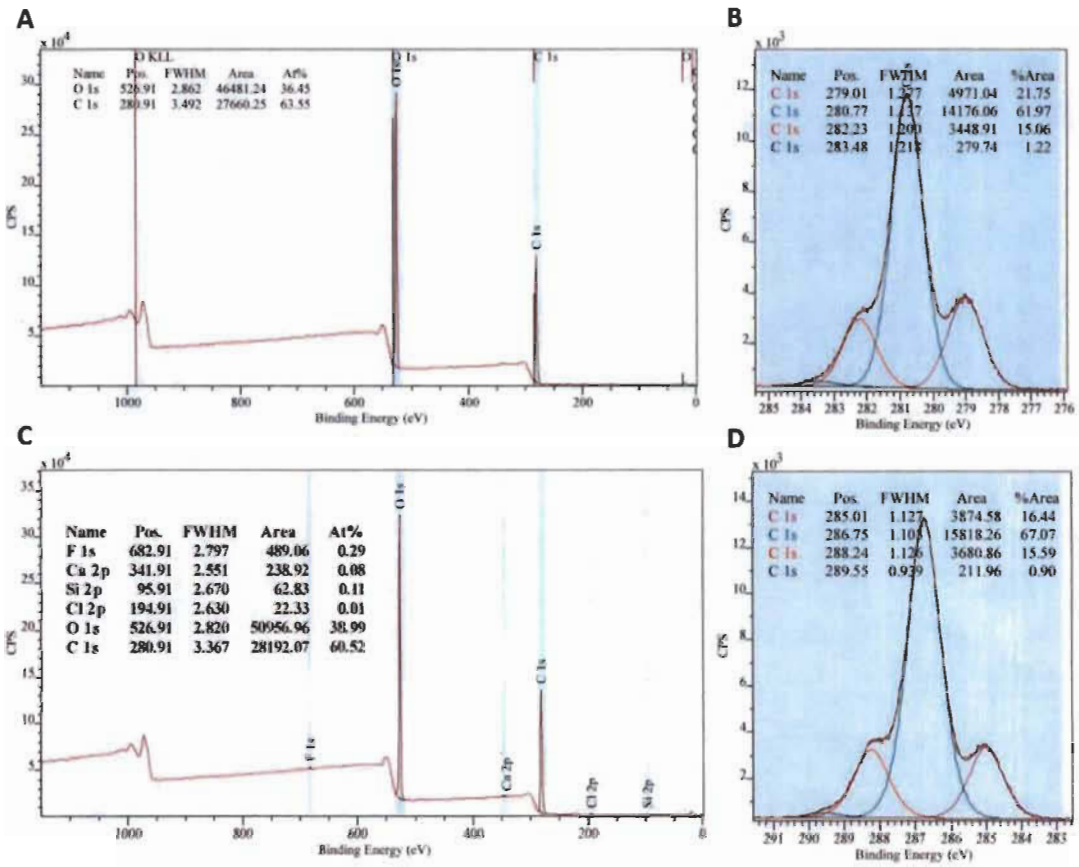


**Additional file 4.2 XPS analysis of the HYK (A-B) and kraft (C-D) pulps**

Low-resolution spectra of the surface of the pulps **(A-C)**. Deconvolution of the C 1s band of the high-resolution spectra **(B-D)**. The 300 W monochromatic Al K-α radiation source was used to study the surface composition of the pulps. The instrument resolution was 0.6 eV. The average of three different spots were recorded and analyzed using the CasaXPS software.

**Additional file 4.3** **Binding affinities (Ka) and capacities (No) of CBM probes for various carbohydrates polymers after 1h incubation at 23 °C in 20 mM Tris-HCl pH 7.5 containing 20 mM NaCl and 5 mM $CaCl_2$**

| Probe | Binding support | $K_a$ ($\mu M^{-1}$) | $N_o$ (µmol/g cellulose) |
|---|---|---|---|
| eGFP-CBM3a | Avicel | 7.999 | 0.277 |
| | Whatman | 0.083 | 0.205 |
| | KP | 0.059 | 0.049 |
| | HYKP | 0.101 | 0.019 |
| mCherry-CBM17 | Whatman | 0.041 | 0,112 |
| | KP | 0.019 | 0,084 |
| | HYKP | 0.008 | 0.089 |
| mOrange2-CBM15 | Xylohexaose | 0.034 [a] | 0.920 [a] |
| | Whatman | 0.007 | 0.335 |
| | KP | 0.026 | 0.049 |
| | HYKP | 0.013 | 0.038 |
| eCFP-CBM27 | Mannohexaose | 0.227 [b] | 1.100 [b] |
| | Whatman | 0.070 | 0.039 |
| | KP | 0.008 | 0.066 |
| | HYKP | 0.009 | 0.317 |

These values ([a-b]) were determined by ITC.
[a] Reference 21.

**Additional file 4.4 Chemical composition of kraft pulps measured using NREL/TP-510-42618 method-ologies[21,25]**

| Pulp polymer | kraft (%) | HYK (%) |
|---|---|---|
| Extractives | 0.28 ± 0.01 | 0.43 ± 0.01 |
| Lignin | 4.8 ± 0.07 | 6.7 ± 0.15 |
| Glucose | 86.9 ± 1.22 | 81.93 ± 1.38 |
| Xylose | 7.1 ± 0.67 | 7.4 ± 0.87 |
| Mannose | 8.4 ± 0.58 | 8.7 ± 0.55 |

**Additional file 4.5** **XPS analysis of kraft pulps. Results include O/C ratios and contributions (%) from each carbon type (C1-C4) to curve fitting of the C 1s peak measured by low- and high-resolution XPS[11,21,29-30]**

| Functionality | kraft (%) | HYK (%) |
|---|---|---|
| O/C* | 0.63 ± 0.02 | 0.56 ± 0.01 |
| C1 | 16.06 ± 0.36 | 23.10 ±1.92 |
| C2 | 67.63 ± 0.57 | 61.25 ±1.35 |
| C3 | 15.33 ± 0.27 | 14.59 ± 0.68 |
| C4 | 0.98 ± 0.07 | 1.07 ± 0.25 |

Spectra were taken from unextracted pulp samples.
*Low-resolution XPS spectra was used to obtain the oxygen and carbon percentage in order to ascertain that the O/C ratio does not vary as a function of chemical treatment.

# Chapter 5 - Scientific Article IV

**Predicting the most appropriate wood biomass for selected industrial applications: comparison of wood, of pulping and of enzymatic treatments using fluorescent-tagged carbohydrate-binding modules**

Pierre-Louis Bombeck[a], Vinay Khatri[b†], Fatma Meddeb-Mouelhi[b†], Daniel Montplaisir[c], Aurore Richel[a] and Marc Beauregard[b*]

[a]University of Liège, Gembloux Agro-Bio tech, AgroBioChem Department, Laboratory of Biomass and Green Technologies, 5030 Gembloux, Belgium
Pierre-Louis Bombeck
[b]Université du Québec à Trois-Rivières, Centre de Recherche sur les Matériaux Lignocellulosiques, C.P. 500, Trois-Rivières, QC G9A 5H7, Canada and PROTEO, Université Laval, Québec, QC G1V 0A6, Canada
[c]Université du Québec à Trois-Rivières, Département de Chimie, Biochimie et Physique, C.P. 500, Trois-Rivières, QC G9A 5H7, Canada
†These authors have contributed equally to this work.

*Corresponding author: Centre de recherche sur les matériaux lignocellulosiques, Université du Québec à Trois-Rivières, C.P. 500, Trois-Rivières (Québec), G9A 5H7 Canada, Tel: (819) 376-5011 # 3354, Fax: (819) 376-5084, E-mail: marc.beauregard@uqtr.ca

## Authors' contributions

PLB carried out all the experiments and drafted the manuscript. VK contributed to experiments related to the construction of ft-CBM probes, and their production and purification, and drafted the manuscript. FMM drafted the manuscript. VK and FMM have contributed equally to this work. DM, AR, FMM and MB participated in its design and coordination, and helped to draft and revise the manuscript. All authors read and approved the final manuscript.

## Acknowledgements

This work was supported by Wallonie-Bruxelles International through the WBI World program and by grants awarded by the Consortium de recherche et innovations en bioprocédés industriels au Québec (CRIBIQ) and Kruger inc. The skillful technical assistance of Nikolas Beauchesne and Virginie Byttebier is acknowledged. The authors would like to thank Glenn Bousfield (University of Liège) for his valuable support and editorial contributions.

## Competing interests

The authors declare that they have no competing interests.

## 5.1 Abstract

**Background:** LCB will progressively become the main source of carbon for a number of products as the Earth's oil reservoirs disappear. Technology for conversion of wood fiber into bioproducts (wood biorefining) continues to flourish, and access to reliable methods for monitoring modification of such fibers is becoming an important issue. Recently, we developed a simple, rapid approach for detecting four different types of polymer on the surface of wood fibers. Named FTCM (Fluorescent protein-Tagged Carbohydrate-binding module Method), this method is based on the fluorescence signal from carbohydrate-binding modules (CBM)-based probes designed to recognize specific polymers such as crystalline cellulose, non-crystalline cellulose, xylan and mannan.

**Results:** Here we used FTCM to characterize pulps made from softwood and hardwood that were prepared using kraft or chemical-thermo-mechanical pulping. Comparison of chemical analysis (NREL protocol) and FTCM revealed that FTCM results were consistent with chemical analysis of the hemicellulose composition of both hardwood and softwood samples. kraft pulping increased the difference between softwood and hardwood surface mannans, and increased xylan exposure. This suggests that kraft pulping leads to exposure of xylan after removal of both lignin and mannan. Impact of enzyme cocktails from *Trichoderma reesei* (Celluclast 1.5L) and from *Aspergillus sp.* (Carezyme 1000L) was investigated by analysis of hydrolyzed sugars and by FTCM. Both enzymes preparations released cellobiose and glucose from pulps, with the cocktail from *Trichoderma* being the most efficient. Enzymatic treatments were not as effective at converting chemical-thermomechanical pulps to simple sugars, regardless of wood type. FTCM revealed that non-crystalline cellulose was the primary target of either enzyme preparation, which resulted in a higher proportion of crystalline cellulose on the surface after enzymatic treatment. FTCM confirmed that enzymes from *Aspergillus* had little impact on exposed hemicelluloses, but that enzymes from the more aggressive *Trichoderma* cocktail reduced hemicelluloses at the surface.

**Conclusions:** Overall this study indicates that treatment with enzymes from *Trichoderma* is appropriate for generating crystalline cellulose at fiber surface. Applications such as nanocellulose or composites requiring chemical resistance would benefit from this enzymatic treatment. The milder enzyme mixture from *Aspergillus* allowed for removal of non-crystalline cellulose while preserving hemicelluloses at fiber surface, which makes this treatment appropriate for new paper products where surface chemical responsiveness is required.

**Keywords:** FTCM, Carbohydrate-binding module, Fluorescent protein, LCB (lignocellulosic biomass), Cellulose, Hemicellulose, Enzymes

## 5.2 Introduction

Global production of biofuels and bioproducts is increasing steadily because such products are greener alternatives to fossil fuels and their derivatives [1–3]. Concomitantly, numerous new products and technologies based on the conversion of biomass have been developed over the last decade [4–9]. Securing sufficient biomass as raw materials is a prerequisite to moving from a petro-chemical to a bio-chemical economy. Using feedstocks to support first-generation biofuel and bioproducts has shown its limits and produces certain undesirable socio-economic and environmental outcomes [10, 11]. The use of LCB, (including dedicated lignocellulosic crops, agricultural and forestry residues and municipal and industrial wastes), to produce second-generation biofuel and bioproducts would avoid the negative impacts associated with first-generation feedstocks use [12, 13].

Although LCB is a promising, abundant and renewable resource, it is difficult to treat due to its complex structure consisting of cellulose fibrils wrapped in a network of lignin and hemicelluloses. This network, collectively referred to as the lignin-carbohydrate complex, is highly recalcitrant and difficult to modify [8, 14–18]. Consequently, several steps of pretreatments are needed to isolate each of the components before they can be used in value-added applications.

For the production of biofuels based on carbohydrates from LCB, such as bioethanol, the principal goal is the complete hydrolysis of polysaccharide components (mainly cellulose) of the raw material into monomers for subsequent fermentation [18–22]. Utilization of all other lignocellulosic components is not as well developed but is the focus of intensive research efforts [8, 9, 23, 24]. This "integrated biorefinery" concept involves a succession of steps for transforming the entire LCB into biofuels and bioproducts. This concept has been demonstrated using a variety of physical, chemical and biological treatments [25–27] in a range of configurations [28–31]. Total utilization of LCB, will permit commercial exploitation of the entire LCB in a wide spectrum of bioproducts and bioenergy [5, 32, 33]. In this context, new bioproducts (*e.g.* biomaterials, biocomposites, biomembranes and biofilms) from previously unused components of LCB are receiving growing interest because they are also biodegradable, produced from a renewable carbon source, and can have a wide variety of applications[5, 7, 34–36]. Unlike bioethanol, specific bioproducts based on lignocellulosic fibers do not require complete separation or deconstruction of the raw lignocellulosic polymers. Removal of some specific components or alteration of structural features of fibers leading to modulation of their physical and chemical properties is often sufficient [5, 7, 32, 37–39].

A largely used green process for the removal or alteration of specific structural features of the biomass is the enzymatic hydrolysis or biocatalysis. Enzymes have been used for improving papermaking processes (for fiber cutting action, peeling, delamination, weakening effect, bleaching, refining) [40–42] and also for the deconstruction of lignocellulosic biopolymers [7, 43–51]. Actually, cellulases from *Trichoderma reesei* are subject to many studies and have been used to efficiently hydrolyze cellulose for decades [40, 52]. Enzymes have high selectivity and turnover frequency, permitting processes with high selectivity and increased productivity on a variety of substrates [53]. For example, enzymatic hydrolysis avoids or drastically decreases the production of degradation products that are generated by classical acid hydrolysis (*e.g.* 5-hydroxymethylfurfural, 2-furfural) [54, 55]. Many types of enzyme can catalyze LCB hydrolysis: endo- and exo-glu-

canase, cellobiase, xylanase, mannanase, and many others. Synergy between several enzymes in a mixture and with their lignocellulosic substrates has also been demonstrated but are not yet completely known [52, 56–58]. In addition to this, enzymes are costly, and accordingly, real-time dosage control is an important parameter in most industrial processes [57, 59–63].

The effectiveness and impact of enzymatic processes on a substrate can be quantified using physical and chemical methods. Among them, the most commonly used are: compositional analysis of the substrate after treatment (using FTIR, XPS) or of the hydrolysates (hydrolysis products content, using GC or HPLC), surface imaging (using SEM, TEM and AFM), index of crystallinity (using XRD and NMR) and mass balance calculations [64–66]. However, current methods of analysis cannot directly monitor enzymatic action. It is not possible to determine the precise order in which components of the substrate were hydrolyzed as the enzymes penetrate the materials and what components are left exposed on fibers after treatment. While direct chemical characterization of the surface, a critical parameter for determination of enzymatic effectiveness, is possible with XPS, this method is expensive and does not distinguish well between different polysaccharides because they harbor similar functional groups [67].

The ability to directly monitor changes to the surface of LCB fibers during enzymatic treatment is essential for controlling and optimizing processes according to the final bioproducts targeted. To this end, a rapid and low-cost method to directly monitor the deconstruction of heterogeneous LCB during enzymatic hydrolysis has been developed [67, 68]. Called Fluorescent protein-Tagged Carbohydrate-binding module Method, or FTCM, this method is based on the use of four specific ready-to-use probes made of fluorescent-tagged recombinant carbohydrate-binding modules (named ft-CBM or probes throughout the text). In these probes, the recombinant CBM part binds to a specific component of the substrate surface. The fluorescence of the probe permits rapid quantification of the probes bound to the surface. The fluorescence can be measured by using an ordinary fluorescence plate reader. This new approach allows for specific surface changes to be tracked and for changes to biopolymers, in this case mannan, xylan, crystalline and non-

crystalline cellulose, to be monitored. FTCM can detect these polymers at the surface of the substrate before and after any given treatment, be it mechanical, chemical or enzymatic [67, 68].

In this study, we use FTCM to characterize how the surfaces of a variety of LCB are modified by two different commercial enzyme cocktails. The substrates include two chemical-thermo-mechanical pulps, referred to as CTM pulps, and two kraft wood pulps. This investigation provides information on which combination of enzyme treatment and biomass substrate is best suited for industrial applications in which various levels of fiber deconstruction and precise control of fiber surface composition are desirable, such as the production of nanocellulose, fiber-reinforce composites, or paper.

## 5.3 Materials and methods

### 5.3.1 Lignocellulosic biomass

Four wood pulps were selected to evaluate the effect of woody biomass composition and pretreatment on the experiment. Hardwood mix kraft pulp (here referenced as HK) was kindly provided by Burgo Ardennes S.A. (Virton, Belgium). Softwood from spruce chemical-thermo-mechanical pulp (referenced as SM) and hardwood from poplar chemical-thermo-mechanical pulp (referenced as HM) were kindly provided by SAPPI Lanaken N.V. (Lanaken, Belgium). Softwood mix kraft pulp (referenced as SK) was kindly provided by Kruger Wayagamac Inc. (Trois-Rivières, Canada). All pulps used in this study were unbleached. The chemical composition of the of the pulps was determined according to the NREL-TP-510-42618 standard method [69]. The length, width, fine percentage and zero span breaking length of wood pulp fibers were analyzed with a fiber quality analyzer (FQA) (LDA02-090 HiRes, OpTest Equipment Inc, Hawkesbury Canada) following the TAPPI T271 om-12 and T231 standard methods.

### 5.3.2 Enzyme solutions

Two different commercial enzyme mixtures were used in this study, CelluClast 1.5L (cat no # C2730) and Carezyme 1000L (cat no # C2605), which were purchased from Sigma-Aldrich. CelluClast 1.5L (named "T" in this study) is a mixture of fungal hydrolytic enzymes from *Trichoderma reesei* and principally consists of two cellobiohydrolases and two endoglucanases, as well as small amounts of other cellulases and also various accessory enzymes which function as hemicellulases [40, 57, 70]. Carezyme 1000L (named "A" in this study) consists of a mixture of several hydrolytic enzymes mixture from *Aspergillus sp.* Both enzyme mixtures are widely employed for hydrolysis and deconstruction of LCB. Both enzymes mixtures contain cellulase (CMCase), xylanase, and mannanase enzymes, whose activities were tested using carboxymethyl cellulose, xylan from birch wood, and galactomannan as substrates, respectively. The activities of cellulase, mannanase and xylanase were assayed quantitatively using the 3,5-dinitrosalicylic acid (DNS) method which measures the reducing sugars generated by enzymatic hydrolysis from their absorption at 540 nm) as described by Miller [64]. Protein content was quantified using the assay developed by Bradford [71].

### 5.3.3 Enzymatic treatments of pulp

Three samples of each pulp were prepared in suspension for three different treatments: one without enzyme addition (control sample, called "Std"), a second to which CelluClast 1.5L was added (called "T"), and third to which Carezyme 1000L was added (called "A"). Prior to enzyme addition, each sample was disintegrated in citrate buffer (having a concentration of 0,05 M and pH 4,8) at 1,2 % consistency (24 grams of pulp on an oven dry matter basis in 2 liter of buffer) with a standard pulp disintegrator and transferred into a 4-liter Erlenmeyer flask. Suspensions were pre-heated until 50 °C using a controlled-environment incubator-shaker (New Brunswick Scientific Inc.). Enzyme solutions were then added to a final loading of 1,275 milligrams of enzyme per gram of oven dry pulp. Hydrolysis was carried out in the incubator at 50 °C for 4 h under continuous orbital agitation (150 rpm). Enzymatic hydrolysis was stopped by incubating the pulp on

ice for 15 minutes. Each sample was filtered, and filtrate was boiled in a 95 °C water bath for 10 minutes and kept frozen at -20 °C until sugars analysis. Filtration of untreated and enzymes treated pulps produced paper sheets, of 60 ± 2 $g.m^{-2}$ in basis weight, as per the TAPPI T205 sp-02 standard methodology. The pH was measured before and after enzymatic treatment. Optimization of hydrolysis conditions, such as duration and enzymes loading, was done on a small scale at high throughput using 96-wells microtiter plates with 3 mm diameter paper discs. After enzymatic digestion of the discs, FTCM test was applied to detect the optimal condition required for enzymes to promote the efficient degradation in cellulose and hemicellulose.

### 5.3.4 Handsheet and paper disc preparation

Four different pulps were used for the preparation of handsheets and paper discs. Handsheets of 60 ± 2 $g.m^{-2}$ basis weight were prepared as per the TAPPI T205 sp-02 standard. 3-mm paper discs were punched from handsheet [67].

### 5.3.5 Construction of recombinant probe expression systems

All carbohydrate-recognition probe genes were inserted into pET11a expression vectors. CBM3a (*Clostridium thermocellum* CipA, NZYTech), CBM15 (*Cellvibrio japonicas*, Z48928), CBM17 (*Clostridium cellulovorans*, U37056) and CBM27 (*Thermotoga maritima*, NC 000853) genes were synthetized by GenScript. The fluorescent protein genes (eGFP, mOrange2, mCherry and eCFP) were cloned into the *Dra*III and *Bam*HI sites while the CBM genes were introduced into the *Bsr*GI and *Bam*HI sites. All encoding genes were sequenced to ascertain the integrity and fidelity of the probes. The resulting probes GC3a, OC15, CC17 and CC27 [67, 68] were used to detect crystalline cellulose, xylan, non-crystalline cellulose and mannan, respectively.

### 5.3.6 Expression and purification of probes

All probes were produced in *E. coli* BL21(DE3) Gold pLysS cells and purified as described by Hébert-Ouellet *et al.* [68].

### 5.3.7 Quantification of the carbohydrates on the surface of fiber paper discs using FTCM

Tracking of the variation of carbohydrate on the surface of paper discs using the four different probes was done as described by Khatri *et al.* and Hébert-Ouellet *et al.* [67, 68]. Note that lignin fluorescence was subtracted from total fluorescence, and that affinity of all probes used here for their respective substrates was previously characterized, as detailed in [67, 68].

### 5.3.8 Sugar analysis

After enzymatic hydrolysis, a filtered hydrolysate was analyzed for cellobiose, glucose, xylose and mannose concentrations using a HPAEC-PAD (Dionex ICS-5000+) and a GC-FID (Agilent Technologies 7890B) following methods from the work of Vanderghem *et al.* [72, 73]. Results were processed using Chromeleon 7® and OpenLAB CDS ChemStation software.

### 5.3.9 Scanning electron microscope (SEM) images

Scanning electron microscope (SEM) images were used to analyze surface morphology and to characterize the effect of the pulping process on paper fibers. Samples of dried handsheets having a basis weight of 60 g ± 2 $g.m^{-2}$ were coated with gold in a Quorum SC-7620 sputter-coater. Images were produced of several different locations on the surface of SM and SK pulp samples with a scanning electron microscope (JEOL, JSM-5500).

### 5.3.10 Statistical analysis

Minitab17© and Microsoft Excel 2010© software were used for statistical analysis of data.

## 5.4 Results and discussion

### 5.4.1 Enzyme characterization

Two commercial enzyme mixtures produced by *Trichoderma reesei* and by *Aspergillus sp.* were used for this study. Under our specific assay conditions, both commercial preparations contained cellulase (CMCase), xylanase and moderate mannanase activities. Enzyme mixture T was characterized by higher cellulase and xylanase activities, although its low mannanase activity was roughly equal to mixture A (Additional file 5.1).

### 5.4.2 Pulp fiber characterization

Pulp fiber characteristics prior to treatments are presented in Table 5.1, which show how the pulp grades used in this experiment differed from one another.

**Table 5.1. Pulp fibers properties before enzymatic treatments. (HM) hardwood CTM pulp, (SM) softwood CTM pulp, (HK) hardwood kraft pulp and (SK) softwood kraft pulp**

| Fibers characteristics (average values) | HM | SM | HK | SK |
|---|---|---|---|---|
| Length (mm) | 0.71 | 1.31 | 0.76 | 2.35 |
| Fines (0 to 0.2 mm) (%) | 15.31 | 13.25 | 13.64 | 3.01 |
| Width (μm) | 22.6 | 27.4 | 17.7 | 26.0 |

As expected, softwood fibers were longer and wider than hardwood fibers [17]. All of the grades contained similar quantities of fine fibers except for the softwood kraft pulp. These fine fibers could impair hydrolysis yield on full fibers because finer fibers have a greater susceptibility for hydrolysis, so hydrolysis yield is altered by the quantity of fine fiber in a sample during our four-hour hydrolysis [74]. Hardwood pulp was only slightly affected by kraft pulping, while for softwood pulp, the kraft treatment had an

obvious impact on length and fines, but none on width. SEM images showed that softwood kraft pulp has lower fibrillation and greater homogeneity than softwood CTM (Figure 5.1) as observed earlier [75, 76] and which is fully compatible with a decreased content in fines.

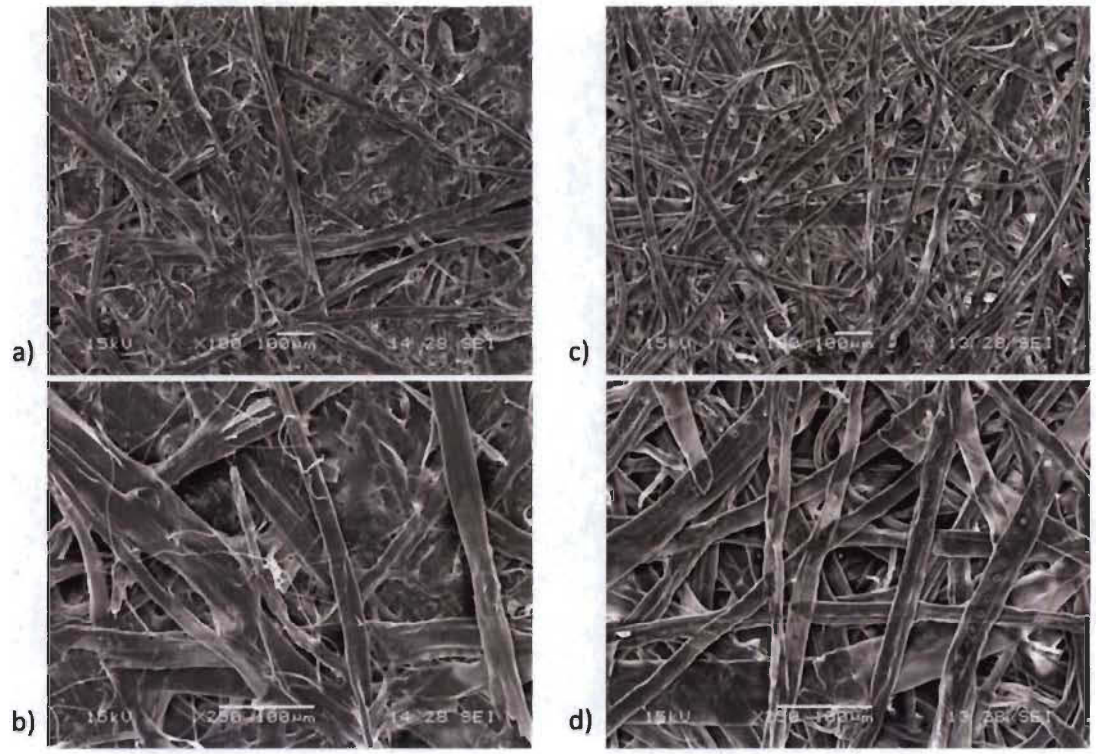


**Figure 5.1. SEM micrographs obtained from (SM) untreated softwood CTM pulp (a, b) and from (SK) untreated softwood kraft pulp (c, d) at two levels of resolution**

Mechanically treated pulps contained more lignin than the kraft pulps (Figure 5.2). The kraft process dissolves lignin from wood raw material to liberate fibers, while by contrast mechanical separation of wood fibers does not involve the extraction of lignin [76]. Lignin protects the other components of the biomass against degradation, so the absence of lignin in kraft pulp permits enzymatic hydrolysis to occur more effectively [77].

As expected, softwood hemicelluloses were glucomannan-rich, while hardwood hemicelluloses were xylose-rich [17, 78, 79]. HK and SK pulps yield the greatest quantity of glucose, making them the most promising of the samples as a potential biofuel substrate.

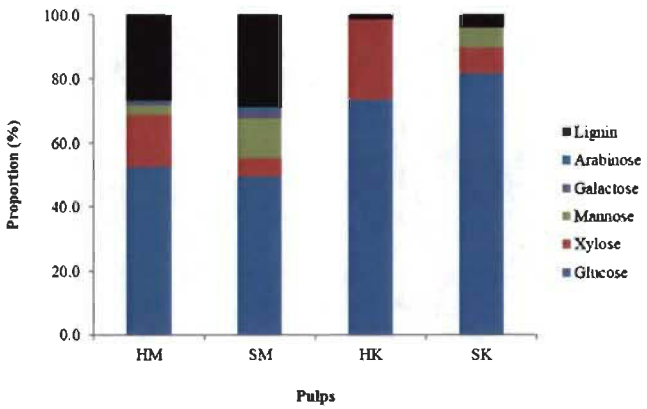


**Figure 5.2. Lignin and carbohydrate monomer content of pulps. (HM) hardwood CTM pulp, (SM) softwood CTM pulp, (HK) hardwood kraft pulp and (SK) softwood kraft pulp**

### 5.4.3 Hydrolysate analysis

Hydrolysate sugar content of the control samples (*i.e.* without enzyme addition) was negligible (data not shown). This demonstrates that hydrolysis did not occur in the absence of enzymes. Figure 5.3 shows cellobiose, glucose, xylose and mannose concentration of hydrolysates solutions recovered after treating pulps with T and A enzyme cocktails.

Figure 5.3 presents the amounts of selected mono- and disaccharides which were liberated by enzymatic hydrolysis of pulp fibers. The quantity of sugar detected in the hydrolysate was better related to pulp grade than to the enzyme cocktail used. Kraft pulps released more of each sugar, indicating they are more susceptible to enzymatic hydrolysis in the relevant conditions. This can be explained by the difference in lignin content, since the presence of lignin protects polysaccharides from enzymatic hydrolysis [60, 80–84].

As discussed earlier and in the literature, pretreatments which remove lignin and hemicellulose expose a greater proportion of the cellulose in the substrate and increase pore volume and surface area, which results in increased hydrolysis rate [85]. The high glucose content of the kraft pulps presented in Figure 5.2 suggests that these pulps are composed primarily of cellulose, an inference that is consistent with the composition of the hydrolysate produced from their enzymatic hydrolysis.

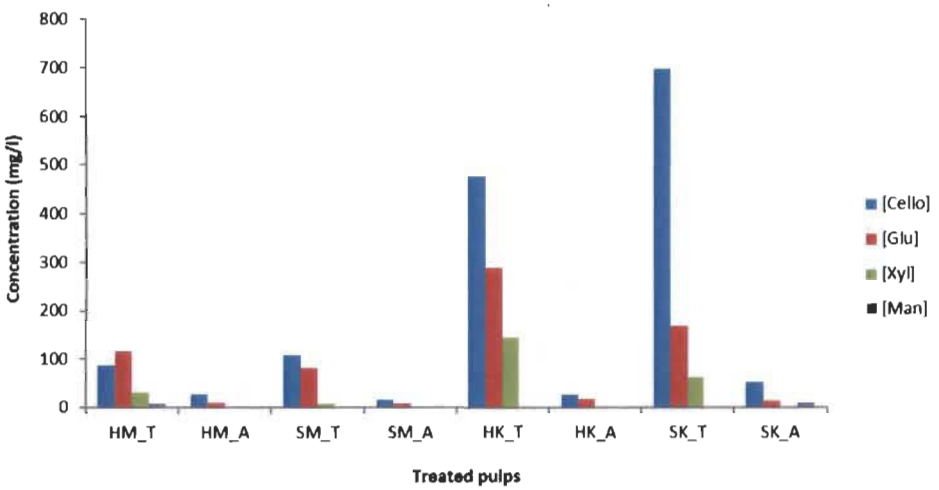


**Figure 5.3. Concentrations of selected carbohydrates in hydrolysate recovered after hydrolysis of pulp. T and A refer to mixtures of enzymes used for hydrolysis**

Hydrolysate sugar content also demonstrated that enzyme "A" was less effective than "T" under same hydrolysis conditions. More xylose was released from hardwood pulp in the presence of T enzyme cocktail, which again corresponds with the abundance of xylose monomers in the substrate, as shown in Figure 5.2. The cellobiose yield from hydrolysis of SK was greater than that from hydrolysis of HK, although HK hydrolysis produced more glucose when catalyzed by T treatment. Finally, hydrolysate composition suggests that the mannanase activity of both enzyme cocktails is low. Such results may indicate that mannans are not as accessible as other polymers, or that mannanase activity is too low (consistent with activity measurements for both enzyme preparations; see Additional file 5.1). The sugar content of the hydrolysates is a good indicator of enzyme

activity with respect to specific carbohydrates, but does not provide any information on the surface chemistry of the treated fiber.

### 5.4.4 Effect of enzymatic treatment on pulp fibers

Biofuel production from LCB depends on polymer accessibility during enzymatic treatment, but many other applications require specific surface functionality linked to distribution of polymers left *after* treatment at the surface of fibers. One way to obtain information about the outcome of an enzymatic treatment on LCB is by investigating properties of its fibers and of paper formed using these fibers. Enzyme hydrolysis used here only affected the length of kraft pulp grade. Treatment of hardwood kraft pulp with T enzymes decreased length by 20 %. Enzymes, A and T, decreased softwood kraft fiber length by 15 % and 25 % respectively (Additional file 5.2). These results suggest a fiber cutting action, ascribed to endoglucanase activity in enzyme cocktails [57, 70]. While kraft pulp fiber length decreased as a consequence of treatment, fines increased (Additional file 5.3). This phenomenon has been suggested as a consequence of the combination of cutting, peeling, delaminating and weakening effects on the surface of the fibers by enzymatic hydrolysis [40–42]. Although the enzymatic hydrolysis reduced the length of some fibers, it did not affect the average width of any samples, regardless of pulping or enzymes used (Additional file 5.4). Concerning zero span breaking length, a measure of the average strength of individual fibers (Additional file 5.5), treatment had no effect on mechanical CTM pulps but both enzymes degraded chemical kraft pulp strength. The higher lignin content of the mechanical pulps may explain why their mechanical strength was not affected by the treatment. Analysis of these paper properties corroborates previous studies of simple sugars release by hydrolysis of paper pulp, and confirms that kraft pulps are more susceptible to enzymatic treatments [47, 50, 86]. For applications where strength properties are very important, such combination pulp-enzymatic treatments (kraft pulps treated with cellulase mixtures) would be deleterious.

### 5.4.5 Detection of pulp fiber polymers using FTCM analysis before and after enzymatic treatments

FTCM probes provide a rapid and cost-effective method to map the surface of LCB samples in terms of composition. Running 96 experiments requires a simple plate reader, is currently performed in less than 3 hours and would cost a few dollars when scaled up. Here this analysis was performed using the four probes in order to characterize pulp fibers prior to enzymatic treatments (Figures 5.4 and 5.5). A probe (GC3a) which indicates the presence of crystalline cellulose regions (referred to here as CC) indicated greater CC exposure on hardwood surfaces than on softwood. CC made up a greater proportion of CTM pulps surface than of kraft pulps surface, despite the higher lignin content of CTM pulps. This result is counterintuitive, since lignin is thought to act as protective barrier around cellulose, but the higher proportion of fibrils and fines in CTM pulps may explain the result since fine fibers tend to have greater specific area and therefore offer the most accessible polymers for the probes [68]. Fibrils and fines are partially removed by kraft pulping, which may explain such results.

Figure 5.4 also shows the FTCM performed using the amorphous (non-crystalline) cellulose (referred to as AC) specific probe (named CC17). Mechanical pulps had the strongest AC binding signal, also in accordance with the explanation of its higher content in high specific surface areas such as fibrils. Although three of the four pulps exposed much less AC than CC, the opposite was observed for SK pulp, where twice as much AC was detected compared to CC. Clearly, the distribution of AC did not parallel CC distribution on the surface of untreated fibers. The total cellulose (CC and AC) detected at the surface was the lowest for SK pulp, where the fibrillations are almost nonexistent as was observed in Figure 5.1. This leads to a decrease in high surface area fibrils or fiber fragments, which are primary targets for CBMs binding to fiber polymers. Despite containing more cellulose than CTM pulps, the kraft pulps returned a weaker binding signal for both CC and AC. Even if the abundance of glucose in the kraft pulp hydrolysates is consistent with higher cellulose content (Figures 5.2 and 5.3), FTCM shows that CTM pulp fiber

surface have a greater number of exposed binding sites for cellulose-specific probes, despite containing less cellulose than kraft pulps overall. One has to consider that the size of probes used here, with diameters of few nanometers, is closer to water than to most fibrous material. Any probe used here has access to all interstices detectable by electronic microscopy.

OC15 probe, which was used to signal the presence of xylan, returned a more intense signal from untreated hardwood pulps than for softwood (Figure 5.5), which is consistent with the previously reported tendency of hardwoods have a greater xylan content than softwoods [17, 78], and with the monosaccharide content of the samples already shown in Figure 5.2. This phenomenon resembles the one observed for CC (Figure 5.4), with higher signal for hardwood pulps than for softwood.

The signal produced by the mannan-specific probe (CC27) does not follow the trend described by the probes that have already been described in this section. Mannans were detected in greater abundance on the surfaces of the CTM pulps, and were nearly absent from the kraft pulps. Mechanical pulping of softwoods has been known to partially dissolve mannans [88], but the dearth of mannan on the probe-accessible surface of kraft pulps suggests that some element of the kraft process removes mannans even more extensively [89], while by contrast the mechanical treatment leaves them available for probe binding. The disparity in mannan detected on SK and HK corresponds to the relative abundance of mannose contained in the samples as determined in Figure 5.2. Comparison of the four pulps signal suggests that mannans are strongly associated with lignin. These observations confirm other studies on the lignin-carbohydrate complex organization and changes according to the pulping process [17, 90–93].

The impact of enzymatic treatments on the amount of each polymer present on the surface of paper discs was characterized using FTCM. In Figure 5.6, the signal intensity from each probe is presented in terms of its change relative to the intensity of the corresponding probe on untreated (Std) pulps shown in Figures 5.4 and 5.5.

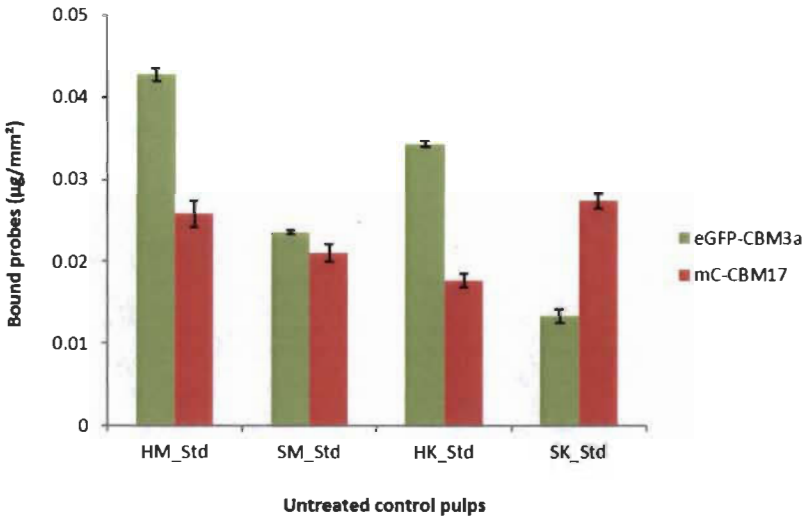


**Figure 5.4.** **CBM binding to the surface of untreated pulps. The quantity of probe bonded to crystalline cellulose (in green) and amorphous (non-crystalline) cellulose (in red)**

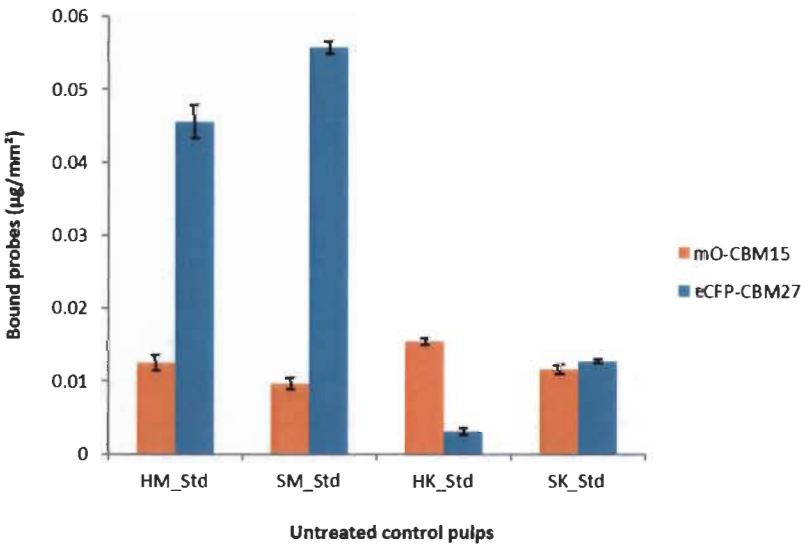


**Figure 5.5.** **CBM binding to the surface of untreated pulps. The quantity of probe attached to xylan and mannan are shown in orange and cyan, respectively**

Generally, enzymatic treatments resulted in a decrease in the number of bound probes, although there were some exceptions. This decrease can be a consequence of the preferred degradation of high specific surface components such as fines, filaments and fibrils by enzymes as discussed above. The overall diminution of probe signal intensity may also indicate that the enzymatic treatment results in an increase in the proportion of substances on the substrate surface which are affected neither by the enzymes nor by the probes (*e.g.* lignin). AC detection invariably decreased after enzymatic treatments, which supports the hypothesis that this component was degraded preferentially by cellulases in both enzymatic cocktails during short time hydrolysis suggested by several studies [17, 56, 94, 95]. In our assay, changes in AC probe binding did not directly correlate to the yield of hydrolysis products of cellulose (cellobiose and glucose, Figure 5.3). Generation of simple sugars such as glucose or cellobiose is a consequence not only of AC but of CC hydrolysis, and the proportions of AC and CC hydrolysis may vary for different pulps and enzyme cocktails.

A general inspection of Figure 5.6 reveals that differences in signal intensity from probes bound to the substrate were due to a combination of the disparity in pulp properties and the character of the enzyme cocktails used for their treatment (which both have cellulase, xylanase and mannanase activity). The results of Figure 5.6 show that removal of surface hemicelluloses appeared to be more substantial with T enzymes treatment. This corroborates chromatographic analyses showing higher liberation of xylose and mannose after T enzyme treatment and may be attributed to a superior cellulase and xylanase activities in T enzyme preparation. Also, it can be seen that CTM softwood pulp (SM) responded differently to enzymatic treatments compared to HM. After enzymatic treatment, more CC was detected on the surface of the SM substrate, but less on the surface of the HM substrate.

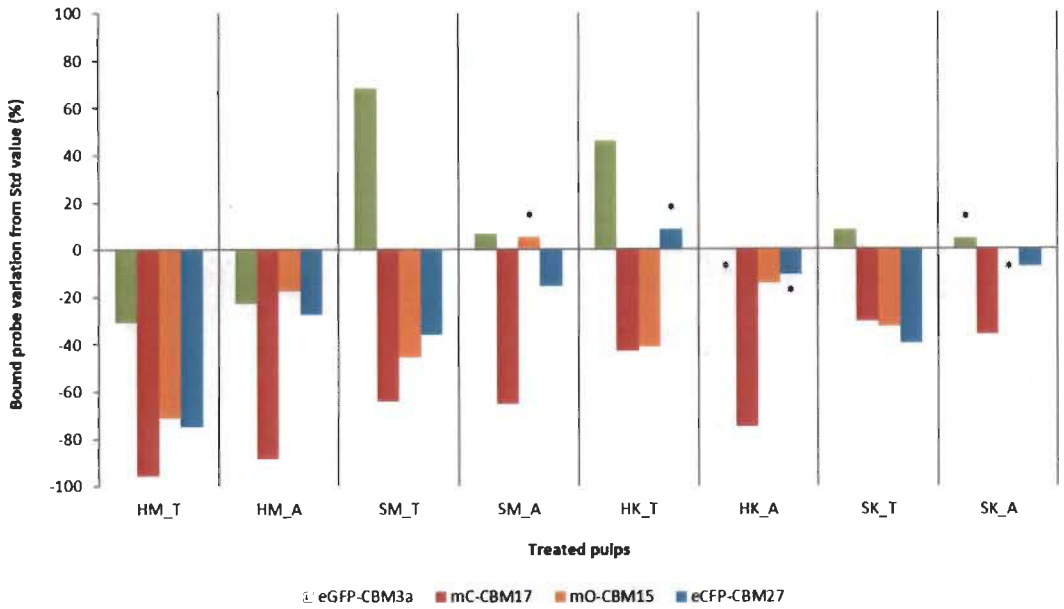


**Figure 5.6. Impact of enzyme (T and A) hydrolysis on the binding of different polymer by probes (crystalline cellulose bound by GC3a, amorphous (non-crystalline) cellulose bound by CC17, xylan bound by OC15 and mannan by CC27), on the surface of fiber discs**

Results that did not deviate significantly from untreated (Std) values (where significance was determined using Dunnet's comparison test) are indicated with an asterisk (*).

The concurrent increase in CC and decrease in AC indicates that the glucose and cellobiose recovered from the hydrolysate (shown in Figure 5.3) are principally the products of AC hydrolysis, as opposed to CC hydrolysis. CC hydrolysis cannot be ruled out however, since FTCM detects CC probe binding sites left after treatment. Hydrolysis of first polymers on the surface (including CC) can lead to exposure of previously buried CC.

When treated by A enzyme, the increase in CC at the surface of SM pulp was not as significant as after treatment with T enzymes. AC was decreased with similar efficacy, but other polymers were removed with different intensity. The signal from xylan-binding

probes was found to be unaffected at the fiber surface after treatment with A enzyme, while that from mannan-binding probes decreased by 15 %. As shown in Figure 5.3, no xylose was detected in the hydrolysate from treatment with enzymes A, while the hydrolysate produced by T enzymes cocktail contained some xylose. The absence of xylose in A hydrolysate is consistent with the hypothesis that xylan was not consumed in this treatment, as shown in FTCM results, although xylanase activity was measured in this enzyme cocktail.

Despite major differences in fiber properties and pulping conditions, the proportion of HK binding sites is modified in a similar way to SM when HK pulp was exposed to enzymatic hydrolysis. More CC was exposed at the surface of HK after T enzyme treatment, despite results on fiber length (Additional file 5.2) and simple sugar analysis (Figure 5.3) that suggest extensive cellulose hydrolysis. Although more CC was exposed on the surface of SM after treatment with T enzymes, this was not accompanied either by fiber length reduction or by substantial hydrolysate sugar yields, which suggests that enzyme treatment was less severe with SM than with HK. The change in CC exposure was limited to 46 % for HK (less CC was left on the surface of HK after T enzyme than on SM). Regarding HK pulp, Figure 5.6 shows that both AC and xylan decreased on the surface of HK paper discs after either enzymatic treatment, but mannan variations were not significant. These results were suggested by chromatographic analyses but were confirmed by FTCM, which also reveals that CC exposure increased after T treatment, information that cannot be obtained by any other method discussed here.

Enzymatic hydrolysis of softwood (SK) and hardwood (HK) kraft pulps occurred in an approximately similar pattern, although both enzymes A and T lead to a smaller change in CC on the fiber surface of SK pulp than on HK pulp. AC decreased after both treatments by about 30 %. Hydrolysis with cocktail T leads to a 33 % decrease in xylan binding in FCTM but treatment with A enzyme left xylan unchanged. This observation is compatible with the detection of free xylose in the hydrolysate. Mannans were consumed to a greater extent in the softwood pulp. Changes in mannan surface coverage observed by FTCM for SK with T enzymes (a decrease of 40 %) were not indicated by hydrolysate

analysis, although a decrease in surface polymers does not necessarily lead to simple sugar release if the enzymes involved are also of endo-type. In this case, a drop in relative abundance of mannan at the fiber surface cannot be revealed by a chromatographic analysis of simple sugars but is easily detected using FTCM.

### 5.4.6 Surface polymer distribution after enzymatic treatments

Here the quantity of each probe bound to surface is expressed as a percent of the total number of probes detected, removing from our assessment any general change in surface binding or availability for binding (such as the decrease in binding due to loss of high surface fragments in kraft pulps or change in sheet density as hypothesized earlier [68]). There might be some cross-reactivity among substrates and CBM15 (*i.e.* OC15 binding mainly to xylan, but having some affinity toward cellulose). We found that the affinity of each probe for its main target surpassed affinity for a similar target by 10-fold or more [67, 68].

The proportions of polymers on the surface of pulps prior to enzymatic treatment are shown in Figure 5.7. As expected, given the nature of kraft pulping, the proportion of AC and CC on the surface of kraft pulps is higher than in CTM pulps, and although the number of cellulose-binding probes detected on the kraft pulps surface is less than what was detected on mechanical pulps, a greater proportion of the probes detected on the kraft pulps were cellulose-binding. Also, softwood exposed proportionally more mannan and hardwood more xylan, although the difference between hardwood and softwood was less pronounced for the mechanical pulps. Such distribution of hemicelluloses on the surface is compatible with bulk composition of fibers, and also compatible with the generally-accepted understanding of softwood and hardwood hemicelluloses composition [17, 78]. In general, CC exposure detection was greater than that of AC regardless of wood or pulping, except for SK pulp, where amorphous (non-crystalline) regions exposure was twice the exposure of CC (the same trend was observed in Figure 5.4).

Treatment with enzyme cocktail T, consistently left a larger proportion of CC on substrate surfaces, at the expense of AC at the fiber surface. An exception was for SK

pulp, where relative amount of AC probe remained stable regardless of enzymatic treatment. SK pulp had the most balanced proportions of probe binding, and this equilibrium between various fractions was barely affected by hydrolysis with T enzyme cocktail. Because analysis of hydrolysates (Figure 5.3) revealed a significant release of simple sugars for SK pulp treated with T enzyme, all of the components must have been degraded equally during hydrolysis. Conversely, the relatively small yield of hydrolysate sugars from SK pulp after A enzyme treatment, correlated with nearly same balanced proportion of probe binding, means that SK pulp was not significantly degraded after A enzyme hydrolysis.

Inspection of proportions and not individual probe binding allows reconciliation of apparent contradictions between the increase in CC in the SM pulp, shown in Figure 5.6, and the low release of sugar after T enzyme treatment (Figure 5.3), because the proportion of CC for SM is lower than in HK and HM pulps.

Treatment with enzyme cocktail T results in decreased hemicellulose binding (in proportion to total binding) for all pulps, while treatment with enzyme cocktail A results probe signal proportions that are in between the control and enzyme T treated substrates. Enzyme A also left larger proportions of hemicelluloses on the surface of fibers at the expense of AC or CC.

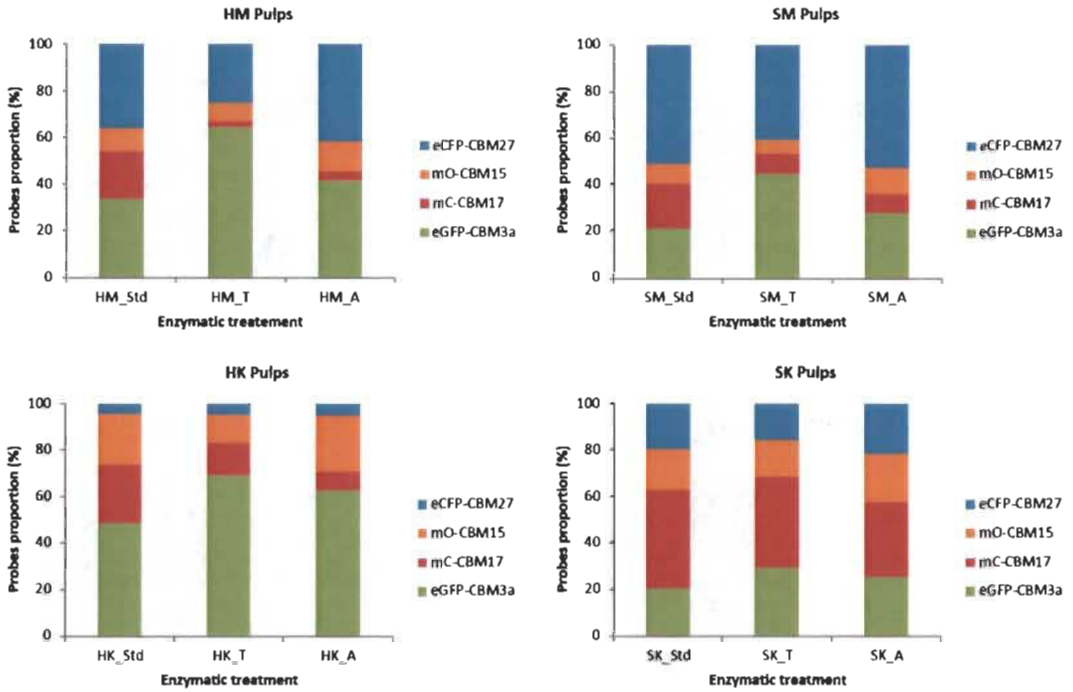


**Figure 5.7. Proportion (in percent) of each probe by treatment on the total probes content for each pulp**

The results presented here can be useful in predicting whether an enzymatic treatment of a given biomass is well suited for a given application of wood biomass. For biofuel production, for example, the hydrolysate analysis suggests that best conditions would involve using the most aggressive enzyme (T) with the most exposed fibers (kraft pulp). Absolute change in probe binding observed by FTCM confirmed the reduction of cellulose at the surface of fibers. FTCM analysis can also be useful for biofuel production, because it can provide precious information about the deconstruction of complex substrates and can monitor the progressive removal of polymers, which permits the optimization of enzymatic treatments. For example, treatment with T enzymes left a higher number of CC binding sites on all pulps tested here. FTCM would be instrumental in determining the operating conditions which allow for total digestion of CC with minimal costs.

FTCM could also provide information for partial hydrolysis of fibers for specific applications. Unlike other methods, such as hydrolysate analysis, chemical analysis, or XPS, FTCM can characterize the surface after treatment. This information can be used to select biomass stock and treatment that will yield the surface properties or composition needed for a given application.

Enzyme T was the most effective for increasing the crystalline cellulose surface proportion and decreasing amorphous (non-crystalline) cellulose and hemicelluloses. A high production of CC was observed for CTM pulps, but kraft hardwood harbored the highest proportion of CC at surface after treatment. Treatment of HK with T enzymes would be more appropriate for production of purified cellulose products, such as nanocellulose. Treatment with enzyme T would promote generating fiber surfaces (nanofibrillated cellulose) that are mechanically stronger, more chemically resistant, and less sensitive to humidity. These characteristics suggest applications like reinforcement in composite materials (in industries like transport, furniture or construction).

Enzyme A is more selective than T. Its use resulted in a significant reduction of the proportion of AC on substrate surfaces while leaving mannan and xylan proportions relatively untouched. This enzyme mixture also hydrolyzed CTM more efficiently than kraft pulp. Enzyme A allowed the relatively reactive xylan and mannan polymers to be preserved, yielding a product which could be used to develop specialty paper products or insulation materials. The enzymatic treatment of kraft softwood pulp appears more relevant for applications where an equilibrated distribution of amorphous (non-crystalline) cellulose and hemicelluloses is preferred. This includes paper products with controlled physical properties, although the strength of these paper products may be decreased by either enzyme.

## 5.5 Conclusion

FTCM can be used as a rapid, affordable and direct method to evaluate the surface composition of lignocellulosic substrates, thereby permitting processes to be understood in terms of compositional changes on the substrate surface which could not otherwise have

been observed. Comparable methods for fiber analysis such as compositional analysis of the substrate after treatment (using FTIR, XPS) or of the hydrolysates (hydrolysis products content, using GC or HPLC), surface imaging (using SEM, TEM and AFM), index of crystallinity (using XRD and NMR) and mass balance calculations [64–66] cannot directly monitor processing by enzymatic action. The FTCM analysis presented here directly provided valuable information about the quantification of exposed amorphous (non-crystalline) and crystalline cellulose, xylan and mannan, which could then be used to determine the effects of pulping and enzymatic hydrolysis on the surface composition of substrates. The variation of these components at surface before and after treatment can guide strategies for preparation of wood fiber derived products.

**List of Abbreviations**

AC: amorphous (non-crystalline) cellulose; AFM: atomic force microscopy; CC: crystalline cellulose; CMCase: carboxymethyl cellulase; CTM: chemical-thermo-mechanical; DNS: 3,5-dinitrosalicylic acid; FQA: fiber quality analyzer; FTCM: fluorescent protein-tagged carbohydrate-binding module method; ft-CBM: fluorescent-tagged recombinant carbohydrate-binding module; FTIR: Fourier transform infrared spectroscopy; GC: gas chromatography; HK: hardwood kraft pulp; HM: hardwood chemical-thermo-mechanical pulp; HPLC: high-performance liquid chromatography; LCB: lignocellulosic biomass; NMR: nuclear magnetic resonance; NREL: national renewable energy laboratory; SEM: scanning electron microscopy; SK: softwood kraft pulp; SM: softwood chemical-thermo-mechanical pulp; TAPPI: technical association of the pulp and paper industry; TEM: transmission electron microscopy; XPS: X-ray photoelectron spectrometry; XRD: X-ray diffraction.

## 5.6 References


1. Naik SN, Goud V V, Rout PK, Dalai AK. Production of first and second generation biofuels: A comprehensive review. Renew Sustain Energy Rev. 2010;14:578–97.
2. Nigam PS, Singh A. Production of liquid biofuels from renewable resources. Prog Energy Combust Sci. 2011;37:52–68. doi:10.1016/j.pecs.2010.01.003.
3. Scheffran J. The Global Demand for Biofuels: Technologies, Markets and Policies. In: Vertès A, Qureshi N, Blaschek H, Yukawa H, editors. Biomass to Biofuels: Strategies for Global Industries. Wiley and Sons; 2010. p. 27–54.
4. Agbor VB, Cicek N, Sparling R, Berlin A, Levin DB. Biomass pretreatment: Fundamentals toward application. Biotechnol Adv. 2011;29:675–85. doi:http://doi.org/10.1016/j.biotechadv.2011.05.005.
5. Zhu H, Luo W, Ciesielski PN, Fang Z, Zhu JY, Henriksson G, et al. Wood-Derived Materials for Green Electronics, Biological Devices, and Energy Applications. Chem Rev. 2016;116:9305–74. doi:10.1021/acs.chemrev.6b00225.
6. Wegner TH, Ireland S, Jones JPE. Cellulosic Nanomaterials: Sustainable Materials of Choice for the 21st Century. In: Postek M, Moon R, Rudie A, Bilodeau M, editors. Production and Applications of Cellulose Nanomaterials. TAPPI Press; 2013. p. 3–8.
7. Dufresne A. Nanocellulose: From nature to high performance tailored materials. Berlin: de Gruyter; 2012.
8. Christopher L. Integrated forest biorefineries: current state and development potential. In: Christopher L, editor. Integrated Forest Biorefineries: challenges and opportunities. Cambridge: The Royal Society of Chemistry; 2013. p. 1–66.
9. Zhu J, Zhang X, Pan X. Sustainable Production of Fuels, Chemicals, and Fibers from Forest Biomass. American Chemical Society; 2011.
10. Fargione J, Hill J, Tilman D, Polasky S, Hawthorne P. Land Clearing and the Biofuel Carbon Debt. Science (80- ). 2008;319:1235 LP-1238.
11. Runge CF, Senauer B. How Biofuels Could Starve the Poor. Foreign Aff. 2007;86:41–53.

12. Eisentraut A. Sustainable Production of Second-Generation Biofuels: Potential and perspectives in major economies and developing countries. 2010. doi:10.1787/20792581.
13. Mohr A, Raman S. Lessons from first generation biofuels and implications for the sustainability appraisal of second generation biofuels. Energy Policy. 2013;63:114–22. doi:10.1016/j.enpol.2013.08.033.
14. Hendriks ATWM, Zeeman G. Pretreatments to enhance the digestibility of lignocellulosic biomass. Bioresour Technol. 2009;100:10–8.
15. Goldsworthy G, Chandrakant S, Opuku-Ware K. Adipokinetic hormone enhances nodule formation and phenoloxidase activation in adult locusts injected with bacterial lipopolysaccharide. J Insect Physiol. 2003;49:795–803. doi:10.1016/S0022-1910(03)00118-5.
16. Fengel D, Wegener G. Wood: Chemistry, Ultrastructure, Reactions. Berlin: de Gruyter; 1984.
17. Stevanovic T, Perrin D. Chimie du bois. Lausanne: PPUR; 2009.
18. Himmel ME, Ding S-Y, Johnson DK, Adney WS, Nimlos MR, Brady JW, et al. Biomass Recalcitrance: Engineering Plants and Enzymes for Biofuels Production. Science (80- ). 2007;315:804 LP-807.
19. Sun Y, Cheng J. Hydrolysis of lignocellulosic materials for ethanol production : a review. Bioresour Technol. 2002;83:1–11. doi:10.1016/S0960-8524(01)00212-7.
20. Kumar P, Barrett D, Delwiche M, Stroeve P. Methods for pretreatment of lignocellulosic biomass for efficient hydrolysis and biofuel production. Ind Eng Chem Res. 2009;48:3713 – 3729.
21. Chaturvedi V, Verma P. An overview of key pretreatment processes employed for bioconversion of lignocellulosic biomass into biofuels and value added products. 3 Biotech. 2013;3:415–31. doi:10.1007/s13205-013-0167-8.
22. Limayem A, Ricke SC. Lignocellulosic biomass for bioethanol production: Current perspectives, potential issues and future prospects. Prog Energy Combust Sci. 2012;38:449–67. doi:http://doi.org/10.1016/j.pecs.2012.03.002.

23. Zhang X, Tu M, Paice MG. Routes to Potential Bioproducts from Lignocellulosic Biomass Lignin and Hemicelluloses. BioEnergy Res. 2011;4:246–57. doi:10.1007/s12155-011-9147-1.
24. FitzPatrick M, Champagne P, Cunningham MF, Whitney RA. A biorefinery processing perspective: Treatment of lignocellulosic materials for the production of value-added products. Bioresour Technol. 2010;101:8915–22. doi:https://doi.org/10.1016/j.biortech.2010.06.125.
25. Huang H-J, Ramaswamy S, Tschirner UW, Ramarao B V. A review of separation technologies in current and future biorefineries. Sep Purif Technol. 2008;62:1–21. doi:http://dx.doi.org/10.1016/j.seppur.2007.12.011.
26. Gupta VK, Potumarthi R, O'Donovan A, Kubicek C, Sharma G, Tuohy M. Bioenergy research: an overview on technological developments and bioresources. In: Gupta V, Tuohy M, Kubicek C, Saddler J, Xu F, editors. Bioenergy Research: Advances and Applications. Amsterdam: Elsevier Ltd; 2014. p. 23–47.
27. Sims REH, Mabee W, Saddler JN, Taylor M. An overview of second generation biofuel technologies. Bioresour Technol. 2010;101:1570–80. doi:http://dx.doi.org/10.1016/j.biortech.2009.11.046.
28. Budarin VL, Shuttleworth PS, Dodson JR, Hunt AJ, Lanigan B, Marriott R, et al. Use of green chemical technologies in an integrated biorefinery. Energy Environ Sci. 2011;4:471–9. doi:10.1039/C0EE00184H.
29. Clark JH, Budarin V, Deswarte FEI, Hardy JJE, Kerton FM, Hunt AJ, et al. Green chemistry and the biorefinery: a partnership for a sustainable future. Green Chem. 2006;8:853–60. doi:10.1039/B604483M.
30. Sheldon RA. Green and sustainable manufacture of chemicals from biomass: state of the art. Green Chem. 2014;16:950–63. doi:10.1039/C3GC41935E.
31. Alvira P, Tomás-Pejó E, Ballesteros M, Negro MJ. Pretreatment technologies for an efficient bioethanol production process based on enzymatic hydrolysis: A review. Bioresour Technol. 2010;101:4851–61. doi:10.1016/j.biortech.2009.11.093.

32. Ragauskas AJ, Williams CK, Davison BH, Britovsek G, Cairney J, Eckert CA, et al. The Path Forward for Biofuels and Biomaterials. Science (80- ). 2006;311:484 LP-489.
33. Yang S-T, Yu M. Integrated Biorefinery for Sustainable Production of Fuels, Chemicals, and Polymers. In: Yang S-T, El-Enshasy HA, Thongchul N, editors. Bioprocessing Technologies in Biorefinery for Sustainable Production of Fuels, Chemicals and Polymers. First. Hoboken, NJ, USA: John Wiley & Sons, Inc.; 2013. p. 1–26. doi:10.1002/9781118642047.
34. Mohanty AK, Misra M, Hinrichsen G. Biofibres, biodegradable polymers and biocomposites: An overview. Macromol Mater Eng. 2000;276–277:1–24. doi:10.1002/(SICI)1439-2054(20000301)276:1<1::AID-MAME1>3.0.CO;2-W.
35. Mohanty AK, Misra M, Drzal LT. Sustainable Bio-Composites from Renewable Resources: Opportunities and Challenges in the Green Materials World. J Polym Environ. 2002;10:19–26. doi:10.1023/A:1021013921916.
36. John MJ, Thomas S. Biofibres and biocomposites. Carbohydr Polym. 2008;71:343–64. doi:https://doi.org/10.1016/j.carbpol.2007.05.040.
37. Xu Y, Rowell R. Biofibers. In: Zhu J, Zhang X, Pan X, editors. Sustainable Production of Fuels, Chemicals, and Fibers from Forest Biomass. American Chemistry Society; 2011. p. 323–66.
38. Jiang L, Tsai M-H, Anderson S, Wolcott M, Zhang J. Development of Biodegradable Polymer Composites. In: Zhu J, Zhang X, Pan X, editors. Sustainable Production of Fuels, Chemicals, and Fibers from Forest Biomass. American Chemistry Society; 2011. p. 367–91.
39. Orts WJ, Shey J, Imam SH, Glenn GM, Guttman ME, Revol J-F. Application of Cellulose Microfibrils in Polymer Nanocomposites. J Polym Environ. 2005;13:301–6. doi:10.1007/s10924-005-5514-3.
40. Oksanen T, Pere J, Buchert J, Viikari L. The effect of Trichoderma reesei cellulases and hemicellulases on the paper technical properties of never-dried bleached kraft pulp. Cellulose. 1997;4:329–39. doi:10.1023/A:1018456411031.

41. Bajpai P. Application of enzymes in the pulp and paper industry. Biotechnol Prog. 1999;15:147–57. doi:10.1021/bp990013k.
42. Cui L, Meddeb-Mouelhi F, Laframboise F, Beauregard M. Effect of commercial cellulases and refining on kraft pulp properties: Correlations between treatment impacts and enzymatic activity components. Carbohydr Polym. 2015;115:193–9.
43. Sabo R, Zhu J. Integrated Production of Cellulose Nanofibrils and Cellulosic Biofuels by Enzymatic Hydrolysis of Wood Fibers. In: Postek M, Moon R, Rudie A, Bilodeau M, editors. Production and Applications of Cellulose Nanomaterials. TAPPI Press; 2013. p. 191–4.
44. Duran N, Lemes A, Duran M, Freer J, Baeza J. A minireview of cellulose nanocrystals and its potential integration as co-product in bioethanol production. J Chil Chem Soc. 2011;56:672–7.
45. Pääkkö M, Ankerfors M, Kosonen H, Nykänen A, Ahola S, Österberg M, et al. Enzymatic Hydrolysis Combined with Mechanical Shearing and High-Pressure Homogenization for Nanoscale Cellulose Fibrils and Strong Gels. Biomacromolecules. 2007;8:1934–41. doi:10.1021/bm061215p.
46. Siqueira G, Tapin-Lingua S, Bras J, da Silva Perez D, Dufresne A. Morphological investigation of nanoparticles obtained from combined mechanical shearing, and enzymatic and acid hydrolysis of sisal fibers. Cellulose. 2010;17:1147–58. doi:10.1007/s10570-010-9449-z.
47. Gehmayr V, Schild G, Sixta H. A precise study on the feasibility of enzyme treatments of a kraft pulp for viscose application. Cellulose. 2011;18:479–91. doi:10.1007/s10570-010-9483-x.
48. Qing Y, Sabo R, Zhu JY, Agarwal U, Cai Z, Wu Y. A comparative study of cellulose nanofibrils disintegrated via multiple processing approaches. Carbohydr Polym. 2013;97:226–34. doi:http://doi.org/10.1016/j.carbpol.2013.04.086.
49. de Campos A, Correa AC, Cannella D, de M Teixeira E, Marconcini JM, Dufresne A, et al. Obtaining nanofibers from curauá and sugarcane bagasse fibers using enzymatic hydrolysis followed by sonication. Cellulose. 2013;20:1491–500. doi:10.1007/s10570-013-9909-3.

50. Torres CE, Negro C, Fuente E, Blanco A. Enzymatic approaches in paper industry for pulp refining and biofilm control. Appl Microbiol Biotechnol. 2012;96:327–44. doi:10.1007/s00253-012-4345-0.
51. Yarbrough JM, Zhang R, Mittal A, Vander Wall T, Bomble YJ, Decker SR, et al. Multifunctional Cellulolytic Enzymes Outperform Processive Fungal Cellulases for Coproduction of Nanocellulose and Biofuels. ACS Nano. 2017;11:3101–9. doi:10.1021/acsnano.7b00086.
52. Mansfield SD, Mooney C, Saddler JN. Substrate and enzyme characteristics that limit cellulose hydrolysis. Biotechnol Prog. 1999;15:804–16.
53. Ho DP, Ngo HH, Guo W. A mini review on renewable sources for biofuel. Bioresour Technol. 2014;169:742–9. doi:10.1016/j.biortech.2014.07.022.
54. Larsson S, Palmqvist E, Hahn-Hägerdal B, Tengborg C, Stenberg K, Zacchi G, et al. The generation of fermentation inhibitors during dilute acid hydrolysis of softwood. Enzyme Microb Technol. 1999;24:151–9. doi:http://dx.doi.org/10.1016/S0141-0229(98)00101-X.
55. Palmqvist E, Hahn-Hägerdal B. Fermentation of lignocellulosic hydrolysates. II: inhibitors and mechanisms of inhibition. Bioresour Technol. 2000;74:25–33. doi:http://dx.doi.org/10.1016/S0960-8524(99)00161-3.
56. Hall M, Bansal P, Lee JH, Realff MJ, Bommarius AS. Cellulose crystallinity - A key predictor of the enzymatic hydrolysis rate. FEBS J. 2010;277:1571–82.
57. Hu J, Arantes V, Saddler JN. The enhancement of enzymatic hydrolysis of lignocellulosic substrates by the addition of accessory enzymes such as xylanase: is it an additive or synergistic effect? Biotechnol Biofuels. 2011;4:36. doi:10.1186/1754-6834-4-36.
58. Várnai A, Huikko L, Pere J, Siika-aho M, Viikari L. Synergistic action of xylanase and mannanase improves the total hydrolysis of softwood. Bioresour Technol. 2011;102:9096–104.
59. Merino ST, Cherry J. Progress and challenges in enzyme development for Biomass utilization. Biofuels. 2007;108. doi:10.1007/10_2007_066.

60. Penttilä PA, Várnai A, Pere J, Tammelin T, Salmén L, Siika-aho M, et al. Xylan as limiting factor in enzymatic hydrolysis of nanocellulose. Bioresour Technol. 2013;129:135–41.
61. Lee RA, Lavoie J-M. From first- to third-generation biofuels: Challenges of producing a commodity from a biomass of increasing complexity. Anim Front. 2013;3:6–11. doi:10.2527/af.2013-0010.
62. Lennartsson PR, Erlandsson P, Taherzadeh MJ. Integration of the first and second generation bioethanol processes and the importance of by-products. Bioresour Technol. 2014;165:3–8. doi:http://dx.doi.org/10.1016/j.biortech.2014.01.127.
63. Klein-Marcuschamer D, Oleskowicz-Popiel P, Simmons BA, Blanch HW. The challenge of enzyme cost in the production of lignocellulosic biofuels. Biotechnol Bioeng. 2012;109:1083–7. doi:10.1002/bit.24370.
64. Miller GL. Use of Dinitrosalicylic Acid Reagent for Determination of Reducing Sugar. Anal Chem. 1959;31:426–8. doi:10.1021/ac60147a030.
65. Berezin I V, Rabinovich ML, Sinitsyn AP. Applicability of quantitative kinetic spectrophotometric method for glucose determination. Biokhimiia. 1977;42:1631—1636.
66. Berlin A, Maximenko V, Bura R, Kang K-Y, Gilkes N, Saddler J. A rapid microassay to evaluate enzymatic hydrolysis of lignocellulosic substrates. Biotechnol Bioeng. 2006;93:880–6. doi:10.1002/bit.20783.
67. Khatri V, Hébert-Ouellet Y, Meddeb-Mouelhi F, Beauregard M. Specific tracking of xylan using fluorescent-tagged carbohydrate-binding module 15 as molecular probe. Biotechnol Biofuels. 2016;9:74. doi:10.1186/s13068-016-0486-1.
68. Hebert-Ouellet Y, Meddeb-Mouelhi F, Khatri V, Cui L, Janse B, MacDonald K, et al. Tracking and predicting wood fibers processing with fluorescent carbohydrate binding modules. Green Chem. 2017. doi:10.1039/C6GC03581G.
69. Sluiter A, Crocker D, Hames B, Ruiz R, Scarlata C, Sluiter J, et al. Determination of Structural Carbohydrates and Lignin in Biomass. Lab Anal Proced. 2008.
70. Gourlay K, Hu J, Arantes V, Penttilä M, Saddler JN. The use of carbohydrate binding modules (CBMs) to monitor changes in fragmentation and cellulose fiber

surface morphology during cellulase- And swollenin-induced deconstruction of lignocellulosic substrates. J Biol Chem. 2015;290:2938–45.

71. Bradford MM. A rapid and sensitive method for the quantitation of microgram quantities of protein utilizing the principle of protein-dye binding. Anal Biochem. 1976;72:248–54. doi:10.1016/0003-2697(76)90527-3.
72. Vanderghem C, Boquel P, Blecker C, Paquot M. A Multistage Process to Enhance Cellobiose Production from Cellulosic Materials. Appl Biochem Biotechnol. 2010;160:2300–7. doi:10.1007/s12010-009-8724-7.
73. Vanderghem C, Jacquet N, Danthine S, Blecker C, Paquot M. Effect of Physico-chemical Characteristics of Cellulosic Substrates on Enzymatic Hydrolysis by Means of a Multi-Stage Process for Cellobiose Production. Appl Biochem Biotechnol. 2012;166:1423–32. doi:10.1007/s12010-011-9535-1.
74. Mooney CA, Mansfield SD, Beatson RP, Saddler JN. The effect of fiber characteristics on hydrolysis and cellulase accessibility to softwood substrates. Enzyme Microb Technol. 1999;25:644–50.
75. Biermann CJ. 3 - Pulping Fundamentals. In: Biermann CJ, editor. Handbook of Pulping and Papermaking (Second Edition). Second Edi. San Diego: Academic Press; 1996. p. 55–100. doi:https://doi.org/10.1016/B978-012097362-0/50007-8.
76. Petit-Conil M. Procédés papetiers - Fabrication des pâtes. Tech l'Ingénieur, les Sélections. 1999;j6900.
77. Rahikainen J, Mikander S, Marjamaa K, Tamminen T, Lappas A, Viikari L, et al. Inhibition of enzymatic hydrolysis by residual lignins from softwood-study of enzyme binding and inactivation on lignin-rich surface. Biotechnol Bioeng. 2011;108:2823–34. doi:10.1002/bit.23242.
78. Timell TE. Recent progress in the chemistry of wood hemicelluloses. Wood Sci Technol. 1967;1:45–70. doi:10.1007/BF00592255.
79. Ek M, Gellerstedt G, Henriksson G. Wood Chemistry and Biotechnology. Walter de Gruyter; 2009.

80. Öhgren K, Bura R, Saddler J, Zacchi G. Effect of hemicellulose and lignin removal on enzymatic hydrolysis of steam pretreated corn stover. Bioresour Technol. 2007;98:2503–10.
81. Mooney CA, Mansfield SD, Touhy MG, Saddler JN. The effect of initial pore volume and lignin content on the enzymatic hydrolysis of softwoods. Bioresour Technol. 1998;64:113–9. doi:http://dx.doi.org/10.1016/S0960-8524(97)00181-8.
82. Studer MH, DeMartini JD, Davis MF, Sykes RW, Davison B, Keller M, et al. Lignin content in natural Populus variants affects sugar release. Proc Natl Acad Sci . 2011;108:6300–5. doi:10.1073/pnas.1009252108.
83. Yu Z, Jameel H, Chang H, Park S. The effect of delignification of forest biomass on enzymatic hydrolysis. Bioresour Technol. 2011;102:9083–9. doi:http://dx.doi.org/10.1016/j.biortech.2011.07.001.
84. Zhang J, Tang M, Viikari L. Xylans inhibit enzymatic hydrolysis of lignocellulosic materials by cellulases. Bioresour Technol. 2012;121:8–12. doi:10.1016/j.biortech.2012.07.010.
85. Zhu L, O'Dwyer JP, Chang VS, Granda CB, Holtzapple MT. Structural features affecting biomass enzymatic digestibility. Bioresour Technol. 2008;99:3817–28.
86. Yamada R, Yoshie T, Sakai S, Wakai S, Asai-Nakashima N, Okazaki F, et al. Effective saccharification of kraft pulp by using a cellulase cocktail prepared from genetically engineered Aspergillus oryzae. Biosci Biotechnol Biochem. 2015;79:1034–7. doi:10.1080/09168451.2015.1006568.
87. Mittal A, Katahira R, Himmel ME, Johnson DK. Effects of alkaline or liquid-ammonia treatment on crystalline cellulose: changes in crystalline structure and effects on enzymatic digestibility. Biotechnol Biofuels. 2011;4:41. doi:10.1186/1754-6834-4-41.
88. Thornton J, Ekman R, Holmbom B, Örså F. Polysaccharides Dissolved from Norway Spruce in Thermomechanical Pulping and Peroxide Bleaching. J Wood Chem Technol. 1994;14:159–75. doi:10.1080/02773819408003092.

89. Ragauskas AJ, Nagy M, Kim DH, Eckert CA, Hallett JP, Liotta CL. From wood to fuels: Integrating biofuels and pulp production. Ind Biotechnol. 2006;2:55–65. doi:10.1089/ind.2006.2.55.

90. Lawoko M, Henriksson G, Gellerstedt G. New Method for Quantitative Preparation of Lignin- Carbohydrate Complex from Unbleached Softwood kraft Pulp: Lignin-Polysaccharide Networks I. Holzforschung. 2003;57:69. doi:10.1515/HF.2003.011.

91. Lawoko M, Rickard B, Fredrik B, Gunnar H, Göran G. Changes in the lignin-carbohydrate complex in softwood kraft pulp during kraft and oxygen delignification. Holzforschung. 2004;58:603. doi:10.1515/HF.2004.114.

92. Lawoko M, Henriksson G, Gellerstedt G. Structural differences between the lignin-carbohydrate complexes present in wood and in chemical pulps. Biomacromolecules. 2005;6:3467–73.

93. Choi JW, Choi D-H, Faix O. Characterization of lignin-carbohydrate linkages in the residual lignins isolated from chemical pulps of spruce (Picea abies) and beech wood (Fagus sylvatica). J Wood Sci. 2007;53:309–13. doi:10.1007/s10086-006-0860-x.

94. Pu Y, Ziemer C, Ragauskas AJ. CP/MAS 13C NMR analysis of cellulase treated bleached softwood kraft pulp. Carbohydr Res. 2006;341:591–7.

95. Lynd LR, Weimer PJ, van Zyl WH, Pretorius IS. Microbial Cellulose Utilization: Fundamentals and Biotechnology. Microbiol Mol Biol Rev . 2002;66:506–77. doi:10.1128/MMBR.66.3.506-577.2002.

## 5.7 Additional Files

**Additional file 5.1** **Protein content and activities of the two commercial enzymes mixtures**

Enzyme cocktail T refers to CelluClast 1.5L from *Trichoderma reesei* and enzyme cocktail A refers to Carezyme 1000L from *Aspergillus* sp.

| Characteristic | Enzymes T | Enzymes A |
|---|---|---|
| Protein content ($mg.ml^{-1}$) | 55,42 | 10,85 |
| CMCase activity ($IU.mg^{-1}$) | 24,70 | 17,87 |
| Xylanase activity ($IU.mg^{-1}$) | 18,95 | 13,76 |
| Mannanase activity ($IU.mg^{-1}$) | 3,94 | 4,17 |

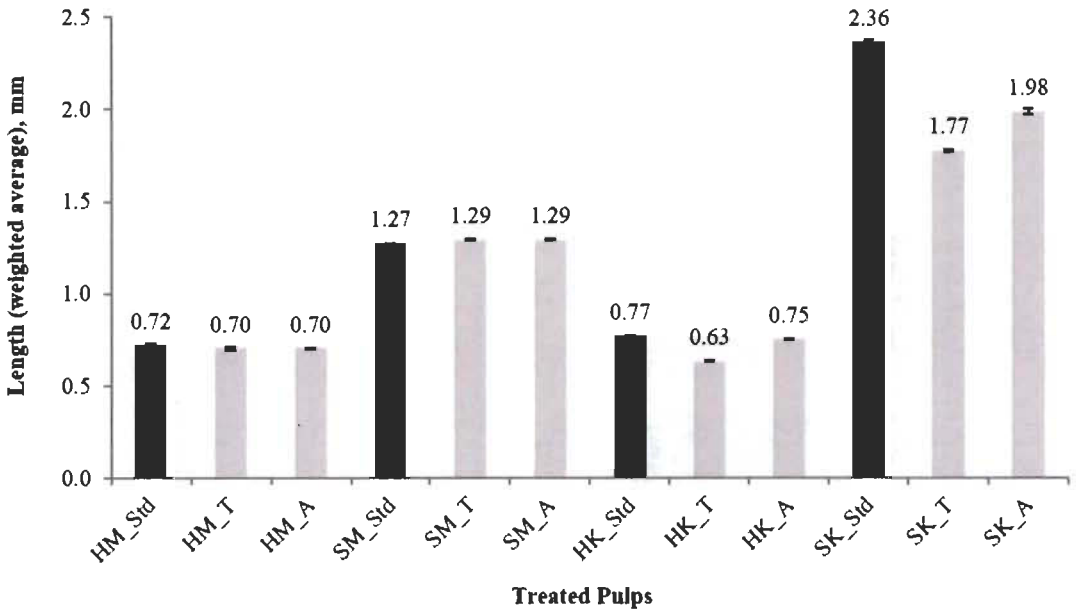


**Additional file 5.2** **Weighted average values of fiber lengths (mm) and standard deviations for control Std, T and A enzymes treated pulps of different grades**

(HM) hardwood CTM pulp; (SM) softwood CTM pulp; (HK) hardwood kraft pulp and (SK) softwood kraft pulp.

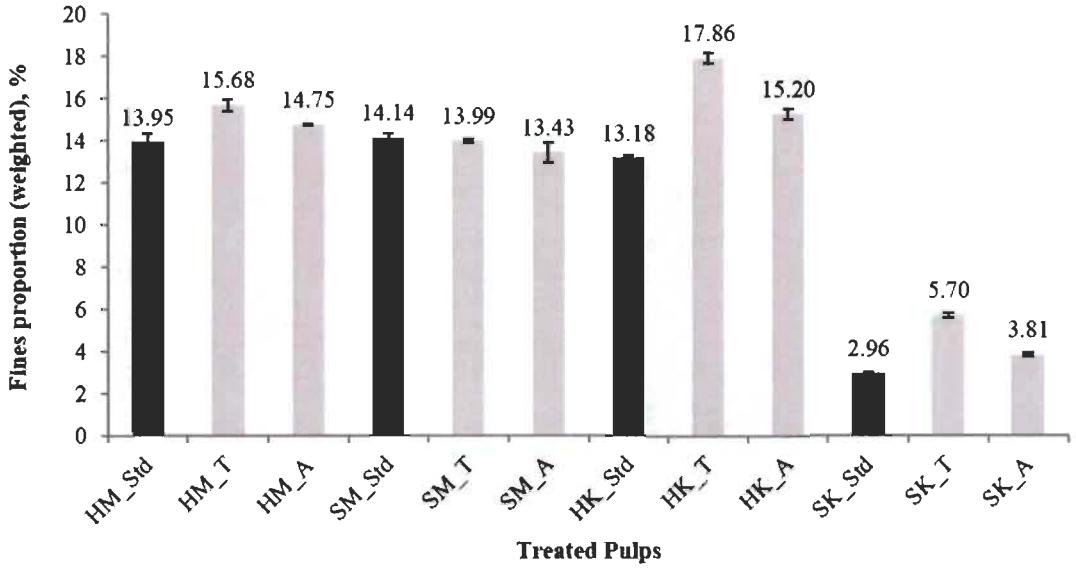


**Additional file 5.3** **Weighted proportion (%) and standard deviations of fines (fiber with length <0.2 mm) for control Std, T and A enzymes treated pulps of different grades**

(HM) hardwood CTM pulp; (SM) softwood CTM pulp; (HK) hardwood kraft pulp and (SK) softwood kraft pulp.

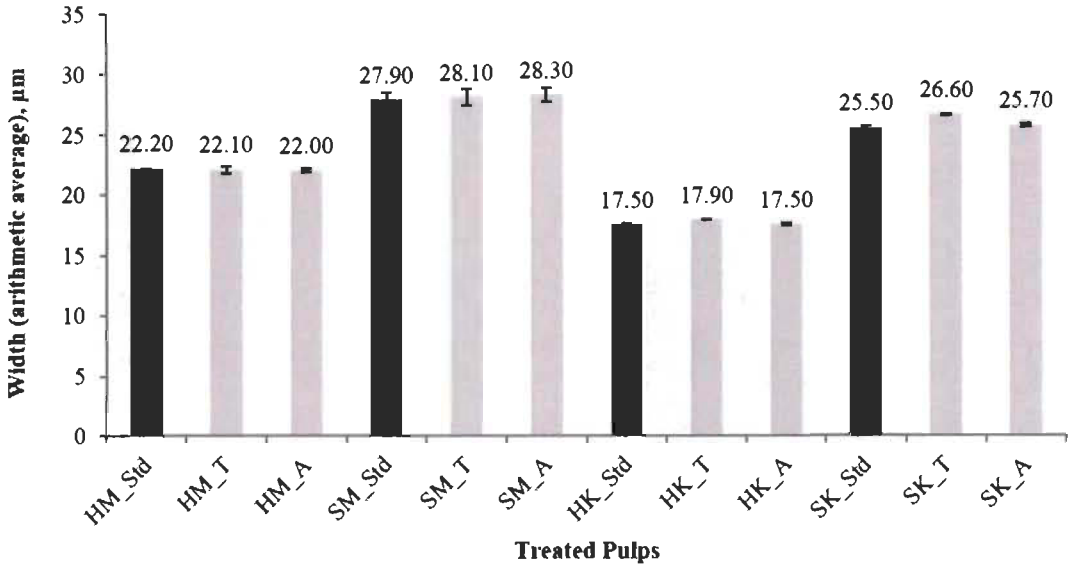


**Additional file 5.4** **Arithmetic average values (µm) and standard deviations of fiber widths for control Std, T and A enzymes treated pulps of different grades**

(HM) hardwood CTM pulp; (SM) softwood CTM pulp; (HK) hardwood kraft pulp and (SK) softwood kraft pulp.

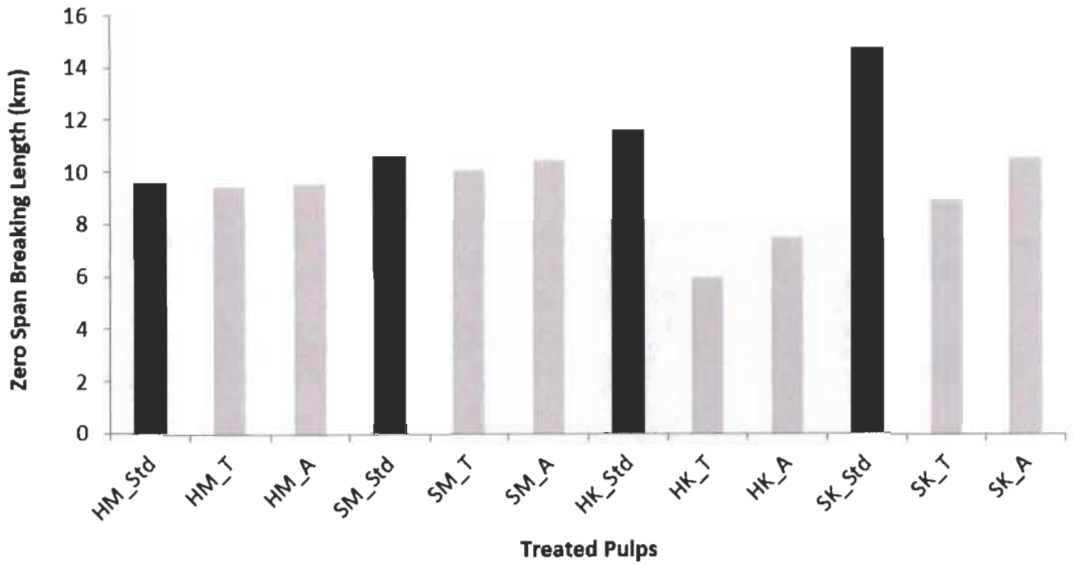


**Additional file 5.5** **Zero span breaking length (km) for control Std, T and A enzymes treated pulps of different grades**

(HM) hardwood CTM pulp; (SM) softwood CTM pulp; (HK) hardwood kraft pulp and (SK) softwood kraft pulp.

# Chapter 6 - Scientific Article V

**Determination of optimal biomass pretreatment strategies for biofuel production: Exclusive correlation between surface-exposed cellulose and enzymatic conversion of polysaccharides**

Vinay Khatri[1, 2] Fatma Meddeb-Mouelhi[1, 2], Kokou Adjalle[1], Simon Barnabé[1], and Marc Beauregard[1, 2*]

[1] Centre de recherche sur les matériaux lignocellulosiques, Université du Québec à Trois-Rivières, Trois-Rivières (Québec) G9A 5H7, Canada.

[2] PROTEO, Université Laval, Québec (Québec) G1V 4G2, Canada.

*Corresponding author: Centre de recherche sur les matériaux lignocellulosiques, Université du Québec à Trois-Rivières, C.P. 500, Trois-Rivières (Québec), G9A 5H7 Canada, Tel: (819) 376-5011 # 3354, Fax: (819) 376-5084, E-mail: marc.beauregard@uqtr.ca

## Authors' contributions

VK carried out all the experiments and drafted the manuscript. KA performed pretreatments and contributed to analysis of biomass samples. FMM, SB and MB helped to draft and revise the manuscript. All authors read and approved the final manuscript.

## Acknowledgments

This research was supported in part by PROTEO and the Industrial Research Chair on Environment and Biotechnology of University of Quebec at Trois-Rivières (Quebec, Canada). We would like to thank Dr. Roberto Chica (University of Ottawa) for the donation of fluorescent protein and Dr. Nicolas Doucet (INRS-Institut Armand-Frappier) for his expert assistance while performing isothermal titration calorimetry (ITC) measurements. We would also like to thank Dr. Alisdair Boraston (University of Victoria) for his valuable editorial contributions.

## Competing interests

VK, FMM, KA, SB and MB declare that they have no competing interests.

## 6.1 Abstract

Pretreatment of LCB is a key step for its efficient bioconversion into ethanol. Determining the best pretreatment and its parameters requires monitoring its impacts at the surface of the biomass material because, for biochemical conversion, it is believed that pretreatment efficiency is linked to the surface exposure of cellulose (also known as cellulose accessibility). Here we used fluorescent protein-tagged carbohydrate-binding modules (method known as FTCM) to study the correlation between surface-exposed polysaccharides and enzymatic hydrolysis of LCB. FTCM was originally optimized for pulp and paper investigations. Hence, we adapted this approach to a FTCM-depletion assay for LCB suspension analysis and monitored the impact of three different pretreatments on alfalfa stover, corn crop residues, cattail stems and flax shives. Our results indicated that alkali-extrusion pretreatment led to the highest hydrolysis rates for alfalfa stover, cattail stems and flax shives, despite its lower lignin removal efficiency compared to alkali pretreatment. Corn crop residues were more sensitive to alkali pretreatments, leading to higher hydrolysis rates. A clear correlation was consistently observed between total surface cellulose detected by the FTCM-depletion assay and biomass enzymatic hydrolysis. Changes in surface hemicelluloses did not reflect the hydrolysis yield, despite the presence of hemicellulases in the enzyme preparation used for this study. Comparison of bioconversion yield and total composition analysis of LCB prior to or after pretreatments did not show any close correlation. Lignin removal efficiency and total cellulose content led to an unreliable prediction of enzymatic polysaccharide hydrolysis. When considering surface crystalline cellulose and non-crystalline (amorphous) cellulose separately, we observed that increased exposure of non-crystalline cellulose lead to a faster, short term hydrolysis rate, while after 24 hours, the correlation with total surface cellulose (crystalline cellulose plus non-crystalline cellulose) was always prevailing, regardless of biomass or pretreatment. FTCM-depletion assay provided direct evidence that cellulose exposure is the key determinant of hydrolysis yield. The clear and robust correlations that were observed between the cellulose accessibility by FTCM probes and enzymatic hydrolysis rates could

be evolved into a powerful prediction tool for the easy and efficient determination of optimal biomass pretreatment strategies for biofuel production.

## 6.2 Introduction

Global production of biofuels from LCB is increasing steadily because such products are greener alternatives to fossil fuels.[1,2] For the production of biofuels from LCB, such as bioethanol, the principal goal is the complete hydrolysis of the polysaccharide components (mainly cellulose) in the raw material into monomers for subsequent fermentation.[3] Although LCB is a promising, abundant and renewable resource, the complete hydrolysis of its polysaccharides remains difficult. Indeed, it is difficult to treat plant biomass due to its complex structure, which consists of cellulose fibrils wrapped in a network of lignin and hemicelluloses. This network, collectively referred to as the lignin-carbohydrate complex, is highly recalcitrant and difficult to modify.[3,4] Consequently, several steps including pretreatments are needed to improve access to polysaccharides, mainly cellulose, before it can be used in value-added applications.[5]

The main objective of pretreatments for subsequent biochemical conversion is to increase access to cellulose (also known as cellulose accessibility), which can later be hydrolyzed by enzymatic hydrolysis processes.[5] However, pretreatments vary greatly in the way they help to expose cellulose. Physical pretreatments help reduce particles size and fiber crystallinity;[6,7] alkali (and acid) pretreatments remove lignin and hemicelluloses, and can lead to loss of cellulose;[8-10] solvent fractionation leads to disruption of biomass components with lesser impact on lignin,[11-13] while liquid hot water mainly removes hemicelluloses.[14-16] Because of the variety of lignocellulosic composition found among feedstocks, not all feedstocks require the same pretreatment.[16,17]

An in-depth understanding of the impact of pretreatment on a particular biomass is believed to be a key issue for reducing costs associated with biofuel production.[18,19] Indeed, pretreatment is the most important and costly step in biofuel production.[20] Accordingly, optimizing pretreatment is part of on-going development efforts that will help the competitiveness of LCB-derived ethanol. Furthermore, any variation in such impact

(due to variation in feedstock properties, chemicals efficiency, mechanical wearing, changes in temperature and humidity) should be monitored on a continuous basis, or "on line" when feasible, in order to maintain optimal process operations.

The effectiveness and impact of pretreatment on a biomass substrate can be monitored using physical and chemical methods. Among them, the most commonly used are: compositional analysis (e.g., by NREL/TP-510-42618), scanning electron microscopy (SEM), transmission electron microscopy (TEM), atomic force microscopy (AFM), X-ray diffraction (XRD), Fourier transform spectroscopy (FTIR), nuclear magnetic resonance (NMR), X-ray photoelectron spectroscopy (XPS), nitrogen adsorption, water swelling capacity etc.[21-26] However, unfortunately, these methods are laborious (tedious sample preparation and long analysis time), expensive and low throughput.[25-27]

One of the major difficulties in studying pretreatments and process parameters is the lack of rapid, high throughput and reliable tools for monitoring and/or tracking lignocellulosic polymers at the surface of biomass.[28] A promising avenue involves the use of molecules that bind specifically to a target individual polymer, such as monoclonal antibodies or carbohydrate-binding modules (CBMs). CBMs are more powerful and advantageous as detection probes compared to others (such as chemical dyes, monoclonal antibodies etc.) due to their high specificity towards the polysaccharide components of lignocellulosic polymers.[29-31] They are non-catalytic protein modules that are typically attached to glycoside hydrolases via a linker and whose function is to act as substrate-recognition devices thereby enhancing the catalytic efficiency of these enzymes.[29-35] They have been successfully employed for the characterization of fiber surfaces composed of simple and complex carbohydrates.[29,36,37] Advances in applying CBMs as bioprobes were achieved by using CBMs fused to a fluorescence protein, such as the green fluorescent protein (GFP or any of its variants).[27,33,38] CBMs coupled with fluorescence protein have been used for mapping the chemistry and structure of various carbohydrate-containing substrates (LCB).[27,38-41] Using fluorescent-tagged CBMs, Gao *et al.* (2014) and Hong *et al.* (2007) successfully quantified the change in crystalline and non-crystalline (amorphous) celluloses accessibilities during enzymatic hydrolysis.[33,39]

Considering that the ability to directly and rapidly monitor changes to the surface of LCB fibers after a pretreatment is essential, we developed a rapid and low-cost method to directly monitor the surface of wood fibers using selected CBMs. Named "Fluorescent protein-Tagged Carbohydrate-binding module Method", or FTCM, this method relies on the use of four specific ready-to-use probes made of recombinant CBMs genetically linked to a designated fluorescent protein of the Green Fluorescent Protein (GFP) family.[27,38,40,41] In these probes, the recombinant CBM part binds to a specific component of the substrate surface. The fluorescence emitted by the GFP (or a selected derivative of GFP with different spectroscopic properties) permits rapid and specific quantification of the probes bound to the surface. The fluorescence can be measured by using an ordinary fluorescence plate reader. We developed four fluorescent protein-tagged fusion proteins for FTCM: Probe GC3a, specific to crystalline cellulose (made of the fluorescent protein eGFP and CBM3a); Probe CC17, specific to non-crystalline cellulose (fluorescent protein mC linked to CBM17); Probe OC15, specific to xylan (composed of mOrange2 and CBM15); and Probe CC27, specific to mannan (a chimera made of eCFP and CBM27). Probes production and characterization (spectroscopic maxima, affinity to related substrate, and discrimination among substrates) were described in our earlier reports.[27,38,40]

We successfully used FTCM for monitoring mechanical, chemical and enzymatic treatment on many wood biomass samples.[27,38,40,41] This allowed us to detect layers of polysaccharides as they were exposed by treatments (mechanical, chemical and enzymatic),[27] confirming existing models of the location of mannan and xylan in relationship to cellulose and lignin. [38] An investigation of pulp treatments and papers produced from such pulps allowed us to correlate FTCM probes binding with paper properties.[40] Recently, the potential of FTCM as a powerful surface analysis method was demonstrated using pulps treated with different enzymes. It promoted prediction of biomass compatibility and enzymatic treatments with related target bioproducts, such as nanocellulose production, composites or new paper products.[41] Throughout these studies, FTCM was shown

to be more informative than X-ray photoelectron spectroscopy (XPS) and total composition analysis (using NREL/TP-510-42618),[27,40] because it specifically detects surface cellulose and hemicelluloses separately.

In this study, we explored the applicability and adaptability of FCTM to the study of LCB pretreatments in a biofuel production perspective. To this end, four LCB residues with varying lignin and cellulose contents (alfalfa stover, corn crop residues, cattail stems and flax shives) and three well established pretreatments (liquid hot water, alkali and alkali-extrusion) were selected. To characterize suspensions of biomass fibers (untreated (hereafter named raw) and after various pretreatments), we used an adaptation of FTCM (named FTCM-depletion assay) and investigated the correlations between FTCM probes binding and enzymatic production of reducing sugars.

## 6.3 Materials and methods

### 6.3.1 Chemicals, microbial strains and LCB

Unless otherwise noted, all chemicals were reagent grade and purchased from Sigma-Aldrich and/or Fisher Scientific. *Escherichia coli* XL10 cells (Agilent Technologies) were used for all DNA manipulations while *E. coli* BL21-Gold(DE3)pLysS competent cells (Agilent Technologies) were used for recombinant protein expression. Samples: α-cellulose (C8002; Sigma-Aldrich) and Avicel PH-105 microcrystalline cellulose (FMC corporation) were used as positive controls, whereas lignin (370959; Sigma-Aldrich) was used as a negative control for this study. Regenerated amorphous cellulose (RAC) was prepared from Avicel PH-105 microcrystalline cellulose as described by Zhang *et al.*, 2006.[42] Four different LCB were used in this study to quantify and compare the lignocellulosic composition and their enzymatic hydrolysis. These LCB were derived from alfalfa (*Medicago sativa*) stover provided by TH-Alfalfa Inc (Quebec, Canada), corn (*Zea mays*) crop residues provided by Ferme Olivier and Sébastien Lépine of Agrosphère Co. (Quebec, Canada), cattail (*Typha*) stems provided by International Institute for Sustainable De-

velopment (IISD) (Manitoba, Canada) and flax (*Linum*) shives provided by SWM international (Manitoba, Canada). Accellerase® DUET (Dupont Industrial Biosciences, USA) was used in this study to hydrolyse LCB. Carboxymethyl cellulose sodium salt (CMC; C5678; Sigma), 4-nitrophenyl-β-D-glucopyranoside (*p*NPG; Sigma) and arabinoxylan (ABX; Megazyme) were used for enzymatic activity measurements using the 3,5-dinitrosalicylic acid (DNS) method.[43] The activities of Accellerase® DUET enzyme determined using commercial substrates are presented in Additional file 6.1. Carboxymethyl cellulose sodium salt (C5678; Sigma), xylan from beechwood (X4252; Sigma) and galactomannan (P-GALML; Megazyme) were used for affinity gel electrophoresis (AGE). Xylohexaose (O-XHE; Megazyme), mannohexaose (O-MHE; Megazyme) and cellohexaose (O-CHE; Megazyme) were used for determination of the probes affinity using isothermal titration calorimetry (ITC).

### 6.3.2 Construction, expression and purification of fluorescent-tagged carbohydrate-binding module probes

Four different fluorescent protein-tagged carbohydrate-binding modules were used in this study. The fluorescent protein genes (eGFP, mOrange2, mCherry and eCFP) and CBM genes (CBM3a, CBM17, CBM15 and CBM27) were cloned into the pET11a expression vectors. All gene fusions were sequenced to ascertain the integrity and fidelity of the probes. The resulting probes eGFP-CBM3a (GC3a), mCherry-CBM17 (CC17), mOrange2-CBM15 (OC15) and eCFP-CBM27 (CC27) were used to detect crystalline cellulose, non-crystalline cellulose, xylan and mannan, respectively. The detailed information about these recombinant probes is described in Additional file 6.2. Expression systems, production and purification of all the four probes used in this study are described in our previous studies.[27,40] Probe purity was assessed by SDS-PAGE (Additional file 6.3). The amount of proteins was quantified by the Bradford method.[44]

### 6.3.3 Determination of probes affinities and specificities

CBM probe affinities and specificities towards soluble and insoluble polysaccharides, and soluble hexasaccharides, were determined using affinity gel electrophoresis (AGE), solid state depletion assay (SSDA) and isothermal titration calorimetry (ITC), respectively (Additional files 6.4 and 6.5). SSDA was used to measure the binding affinities of GC3a and CC17 probes using the insoluble polysaccharides Avicel and RAC. Experimental conditions for AGE, ITC and SSDA are described in Khatri *et al.*, 2016 and 2018 and Hébert-Ouellet *et al.*, 2017.[27,38,40] Experiments were performed in triplicate.

### 6.3.4 LCB preparation and pretreatments

The LCB residues underwent various pretreatment processes to either partially or completely remove hemicelluloses and/or lignin. All four raw LCB named: alfalfa stover (AR), corn crop residues (CoR), cattail stems (CaR) and flax shives (FR) were subjected to three different treatments: 1) liquid hot water 2) alkali and 3) alkali-extrusion. The pretreatment conditions were as followed: 1) For liquid hot water pretreatment, 10% (w/v) of LCB were mixed with water and held at 121°C and 15 Psi for 60 minutes using a laboratory scale autoclave. This pretreatment essentially removes the hemicelluloses. 2) For alkali pretreatment, 10% (w/v) of LCB were mixed with 5% NaOH and held at 121°C and 15 Psi for 60 minutes using an autoclave. This pretreatment removes a significant portion of both lignin and hemicelluloses. 3) For alkali-extrusion pretreatment, LCB were subjected to reactive extrusion fractionation using an E-max 27 mm twin-screw extruder (Entek Extruder, OR, US) using 5% NaOH a speed of 200 rpm at 180°C. This pretreatment substantially helps to break the fiber walls, causing them to release their main components (cellulose, hemicelluloses and extractives), which are bound together by lignin. This process also removes (partially) the lignin and hemicelluloses.[45] After each pretreatment, all the samples were washed 8-10 times with distilled water at room temperature until the filtrate becomes clear. These pretreated sample residues were dried at 50°C for 48 hours to ensure a moisture content of <2%. They were then ground and passed through a 2-mm-mesh sieve.

### 6.3.5 Determination of cellulose, hemicellulose and lignin content

The National Renewable Energy Laboratory (NREL/TP-510-42618) standard method described by Sluiter *et al.*, 2008[21] was used to determine the quantitative composition of cellulose, hemicellulose and acid insoluble lignin content in α-cellulose, Avicel and in the different raw and pretreated LCB. The hydrolyzed monosaccharides contents of α-cellulose, Avicel and LCB (raw and pretreated) were determined by ion-exchange chromatography (ICS-5000, Dionex) and detection was performed using an electrochemical detection cell (combined pH-Ag/AgCl reference electrode). Each experiment was conducted at 40°C with 1 mL/min isocratic elution of NaOH (1 mM) on a Dionex CarboPac SA10 (250 × 4 mm) column coupled with a Dionex CarboPac PA100 (50 × 4 mm) guard column. Data analysis was performed using Dionex Chromeleon 7 software. Experiments were performed in triplicate.

### 6.3.6 Enzymatic treatment of LCB

The enzymatic hydrolysis of substrates (α-cellulose, Avicel and LCB all set at 5% w/v) were carried out using Accellerase® DUET enzyme (0.25 mL/g) in 0.05 M of citric acid buffer at pH 4.4. Each enzymatic hydrolysis was performed over 144-hour (6 days) period at 55°C with continuous agitation at 200 rpm. An aliquot (1 mL) of the enzymatic reactions were collected every 24$^{th}$ hour. All the aliquots were centrifuged at 4000 rpm for 1 minute and the supernatant was then transferred to a clean tube before storing them at -20°C until the analysis of total reducing sugar. The release of the total reducing sugars was measured using the 3,5-dinitrosalicylic acid method (DNS) as described by Miller, 1959.[43] All absorption readings (at 540 nm) were typically performed in triplicates for a statistical significance.

### 6.3.7 Quantification of the variations of the carbohydrates on the surface of LCB using FTCM-depletion assay

The FTCM-depletion assay is a modified version of the FTCM methodology described by Khatri *et al.*, 2016 and 2018[27,38] and Hebert-Ouellet *et al.*, 2017,[40] which is

adapted from a SSDA.[46,47] SSDA has been defined as a method for qualitative and quantitative assessment of the interaction between CBMs and insoluble polysaccharides.[46,48] Insoluble polysaccharide substrates (α-cellulose or Avicel or LCB) were prepared by weighing 25 mg of dry powder and suspending it in Eppendorf tubes. To keep polysaccharides suspended, the reactions were performed under constant tumbling in a 20 Tris-HCl pH 7.5 buffer containing 20 mM NaCl, 5 mM $CaCl_2$ and 3% (w/v) bovine serum albumin (BSA). Reaction series were set up with identical substrates amounts (2.5% w/v) and identical CBM probe concentrations (0.5μg/μL) of either GC3a, CC17, OC15 and CC27 (for the detection of crystalline cellulose, non-crystalline cellulose, xylan and mannan, respectively). Following an hour incubation under constant tumbling at room temperature, all the reactions were centrifuged (20,000 × g for 5 minutes) to separate solid and liquid phase. The supernatant was then removed and quantitatively analyzed by fluorescence spectroscopy. A volume of 200 μL of each reaction supernatant samples were transferred into a 96-wells, black microplate (Costar, Corning Life Sciences). Later, fluorescence measurement of supernatants, containing unbound probes or free probes ($F_{Free}$), were acquired using a Synergy Mx microplate reader (BioTek) with the end point feature active and the filters bandwidth set at 9 mm. Fluorescence intensities (total ($F_{Total}$) and background ($F_{Background}$)) were measured using the reaction set containing CBM probes without polysaccharides and polysaccharides in buffer (without CBM probes), respectively. The excitation and emission wavelengths for measuring fluorescence intensities of fluorescent-tagged CBM probes were set at 488 and 510 nm, 587 and 610, 549 and 568 nm and 434 and 477 nm for GC3a, CC17, OC15 and CC27, respectively. The fluorescence intensities of bound probes ($F_{Bound}$) to the α-cellulose, Avicel, raw and pretreated LCB were calculated using the following equation:

$$F_{Bound} = F_{Total} - (F_{Free} - F_{Background})$$

These fluorescence values were then converted into μmol/g of substrate using the appropriate fluorescence standard curves for each probe (Additional file 6.6). Control experiments using FTCM probes without substrates, and substrates without FTCM probes, were

carried out in order to evaluate and eliminate non-specific fluorescence emission contributions to final FTCM signals. All reactions were performed in triplicate.

### 6.3.8 X-ray diffraction (XRD)

X-ray diffraction patterns of α-cellulose and Avicel samples were recorded with an X'Pert PRO X-ray diffractometer (PANanalytical) at room temperature from 10 to 60°C, using Cu/Kα irradiation (1.542 Å) at 45 kV and 40 mA. The scan speed was 0.021425° $s^{-1}$ with a step size of 0.0167°. Crystallinity index (CrI) was calculated using the peak intensity method[49]:

$$CrI = (I_{002} - I_{am})/I_{002} \times 100$$

Where $I_{002}$ is the intensity of the peak at $2\theta = 22.5°$ and $I_{am}$ is the minimum intensity, corresponding to the non-crystalline content, at $2\theta = 18°$.

## 6.4 Results and Discussion

### 6.4.1 Adaptation of FTCM to a depletion assay for investigation of biomass suspensions

As described earlier, FTCM method was designed to perform monitoring surface composition of pulp and paper samples.[27,38,40,41] The original method relies on the formation of a fiber sheet to which probes are allowed to bind. Then, fluorescence measurements of bound probes on drained sheets are recorded and converted into number of probes bound per surface area (typically square mm). Here we adapted the method to biomass suspension analysis, and recorded unbound probe fluorescence in what is hereafter referred to as a "FTCM-depletion assay". This adaptation of FTCM to suspension measurements was tested by simple control experiments with well characterized cellulose preparation. To this end, we used two different commercialized cellulose having different crystallinity index (CrI): α-cellulose (CrI = 62%) and Avicel (CrI = 81%). Avicel has a higher crystallinity index as a consequence of a lower content of non-crystalline cellulose than α-cellulose.[50,51] The binding of all four probes to these purified cellulose preparations are

represented in Figure 6.1A. The surface analysis by the FTCM-depletion assay clearly shows the domination of crystalline cellulose at surface of both α-cellulose and Avicel samples. The non-crystalline cellulose specifically recognized by CC17 probe was found in smaller amount, but it was higher in α-cellulose when compared to Avicel, which is compatible with their crystallinity index. Binding of CC17 was more important for α-cellulose compared to binding to Avicel, indicating that adaptation of the FTCM probes to a solid-state depletion assay performed adequately.

No binding of probes OC15 and CC27 were detected for Avicel while very low binding of OC15 (xylan specific probe) was detected in α-cellulose. This is fully compatible with the high purity of such cellulose preparations and the sensitivity of FTCM-depletion assay. We then added the binding of GC3a and CC17 to represent total cellulose surface exposure or cellulose accessibility to probes; likewise, OC15 and CC27 binding were added to obtain total hemicelluloses accessibility at surface.

Total cellulose surface exposure was found to be higher in α-cellulose compared to Avicel (Figure 6.1B). The total composition analysis (NREL/TP-510-42618) of such cellulose preparations also confirmed that both were mainly composed of cellulose in the bulk, without information on their exposure at surface (Figure 6.1C). After demonstrating that adaptation of FTCM probes to FTCM-depletion assay worked well with such simple cellulose preparations (positive controls), we then applied it to purified lignin (negative control). Non-specific binding of CBMs to lignin was reported earlier[52-54] and such a phenomenon would affect FTCM-depletion assay reliability. No binding was observed between FTCM probes and lignin under our assay conditions (data not shown), possibly a consequence of our blocking strategy that specifically minimizes non-specific probe binding or adsorption.[13,38,40,53,55] It has been reported that cellulose crystallinity plays a key role to determining the enzymatic hydrolysis rate of a biomass: crystalline cellulose was shown to be more resistant to the enzymatic hydrolysis compared to non-crystalline cellulose.[51,56-60]

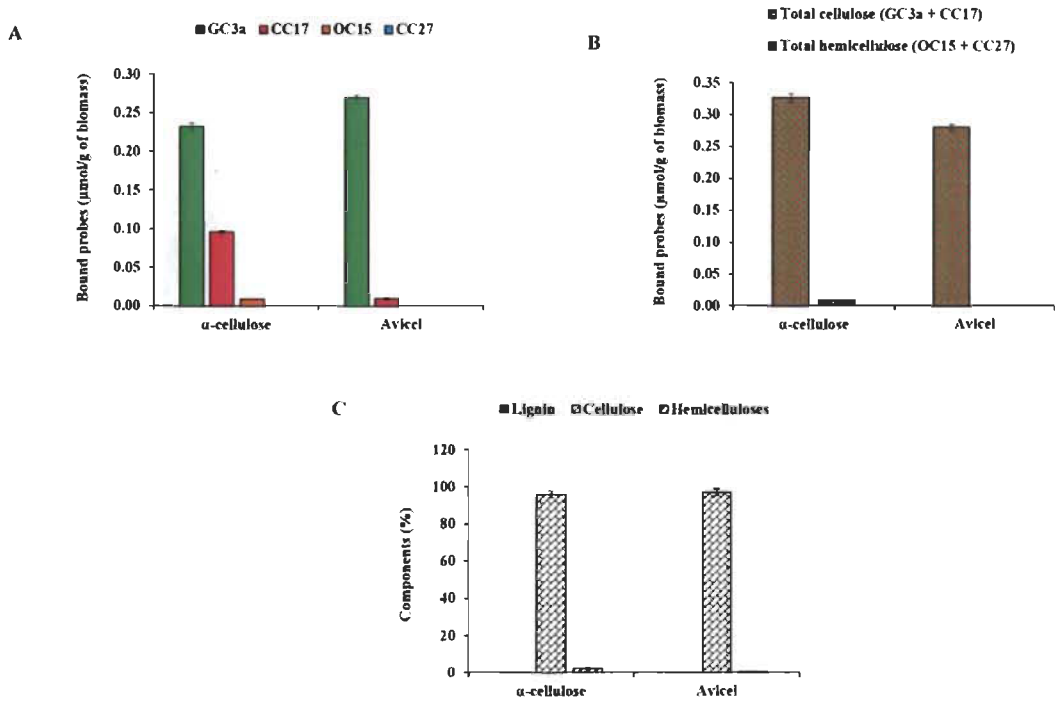


**Figure 6.1 Tracking surface accessibility of lignocellulosic components in α-cellulose and Avicel using FTCM-depletion assay (A, B) and total composition analysis using NREL/TP-510-42618 method (C)**

**A)** α-cellulose and Avicel were incubated with the GC3a probe (0.5 µg/µL; for crystalline cellulose detection), CC17 probe (0.5 µg/µL; for non-crystalline cellulose detection, OC15 probe (0.5 µg/µL; for xylan detection) and the CC27 probe (0.5 µg/µL; for mannan detection) for 1h at room temperature under tumbling agitation. The fluorescence values were converted to bound probes (µmol/g of biomass) by using the standard curves (Additional file 6.6). Green, cherry, orange and cyan color represents the GC3a, CC17, OC15 and CC27 probes detection, respectively. **B)** The addition of the binding of GC3a and CC17, from Figure 6.1A, represents the total cellulose (GC3a + CC17) and the addition of the binding of OC15 and CC27, from Figure 6.1A, represents the total hemicelluloses (OC15 + CC27). **C)** Total composition analysis of α-cellulose and Avicel using standard NREL/TP-510-42618 method.

Therefore, in order to detect possible correlations between the binding of FTCM-depletion assay probes and carbohydrate conversion (reducing sugars released by enzy-

matic hydrolysis), we studied the enzymatic hydrolysis of both commercial cellulose preparations using Accellerase® DUET enzyme. α-cellulose showed a higher rate of carbohydrate conversion than Avicel (Figure 6.2A). The results also show a robust correlation with the total surface cellulose detected by FTCM-depletion assay and carbohydrate conversion (Figure 6.2B) which is in full agreement with their crystallinity index.

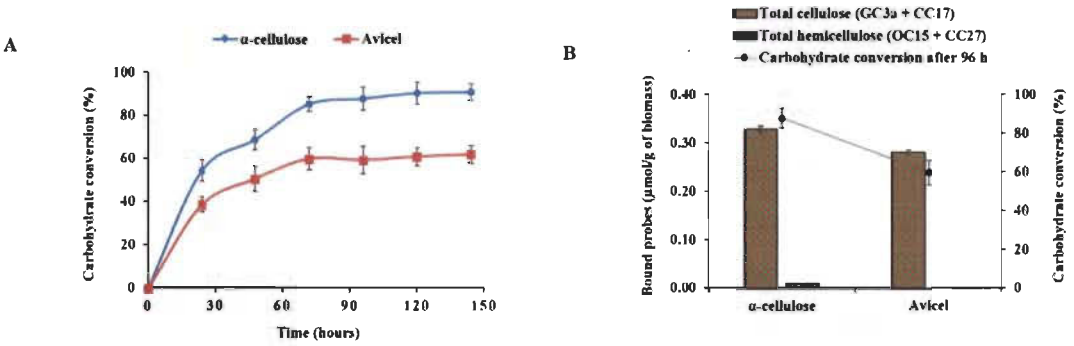


**Figure 6.2 Comparison of hydrolysis and surface polysaccharide detected by FTCM-depletion assay**

**A)** Enzymatic hydrolysis of α-cellulose and Avicel. **B)** Surface polymer detection by FTCM-depletion assay and its correlation with the percent carbohydrate conversion after 96 hours of enzymatic hydrolysis of α-cellulose and Avicel.

### 6.4.2 Tracking surface accessibility of lignocellulosic components in LCB

Four types of biomass were used in this study: alfalfa stover, corn crop residues, cattail stems and flax shives. Prior to performing any pretreatments, these biomasses were investigated to determine differences in the lignocellulosic polymer content and their exposure at the fiber surface via FTCM-depletion assay. The binding of all four probes are represented in the Figure 6.3A. We added the binding of GC3a and CC17 to represent total cellulose (GC3a + CC17) and added OC15 to CC27 signals in order to represent total hemicelluloses (OC15 + CC27) (Figure 6.3B). The surface analysis by the FTCM-depletion assay indicates the dominance of hemicelluloses in all the raw biomass studied here,

except for corn crop residues (CoR). Further, the total cellulose surface exposure was found to be higher in both corn crop residues (CoR) and cattail stems (CaR) compared to other biomasses.

The total composition analysis of biomass was also conducted using standard NREL method (NREL/TP-510-42618) for comparison. The total composition analysis of biomass indicates the dominance of cellulose (Figure 6.3C) and confirms the earlier observations that cellulose dominates hemicelluloses by nearly two-fold, and that the lignin content is similar to hemicelluloses, in these LCB residues.[61-64] The picture at the fiber surface is different: probe binding indicates that hemicelluloses dominate at surface of such biomass preparations (probably in the form of lignin-hemicelluloses complexes) which is compatible with the typical organization of plant cell wall ultrastructure.[65]

The accessibility of lignocellulosic polymers is an important substrate characteristic that influences the enzymatic hydrolysis rates.[39,66-68] Based on a previous study of CBM adsorption to cellulose, it has been shown that enzyme access to cellulose was determinant for saccharification yield.[39] Here, by using multiple CBM probes on diverse biomasses we address surface exposure of various polysaccharides, not only cellulose, which might reflect on enzymatic efficiency of multi-enzyme commercial cellulase formulations.

In this context, we studied the enzymatic hydrolysis of the raw biomass in order to establish a correlation between the binding of FTCM-depletion assay probes to biomass and the hydrolysis of polysaccharide into soluble reducing sugars. Without any pretreatment, the raw LCB residues were exposed to Accellerase® DUET cellulase preparation and then the release of reducing sugars was measured over time (Figure 6.4A).

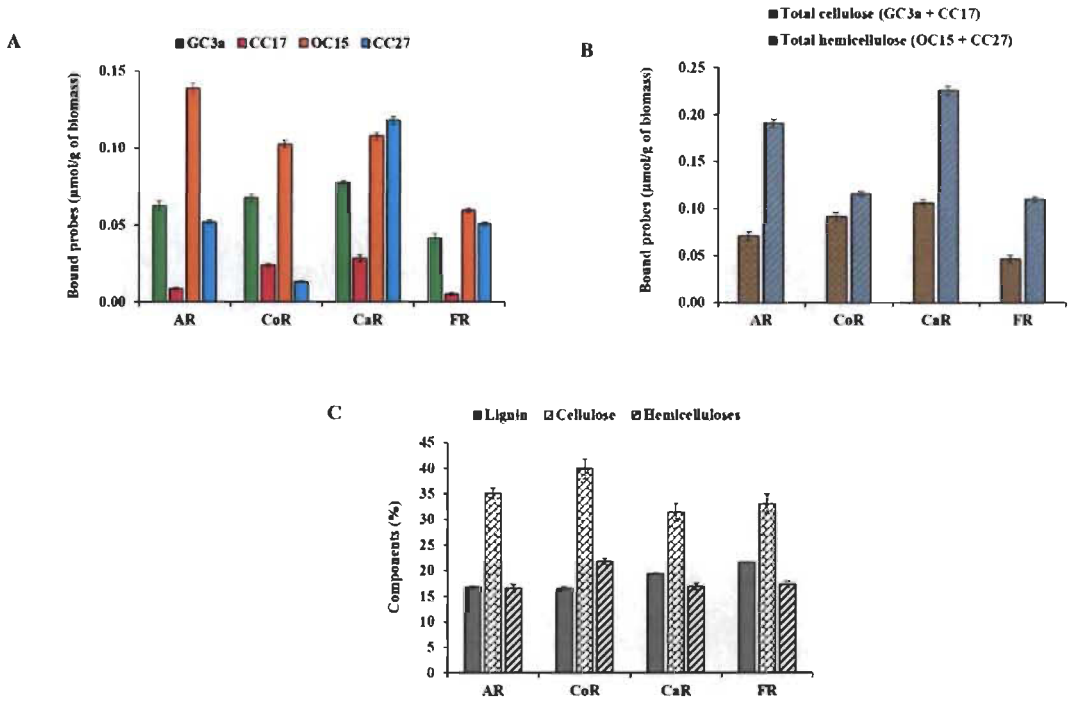


**Figure 6.3 Tracking surface accessibility of lignocellulosic components in raw LCB**

**A)** Individual probe binding to LCB (GC3a, CC17, OC15 and CC27). **B)** The addition of the binding of GC3a and CC17, from Figure 6.3A, representing the total cellulose (GC3a + CC17) and the addition of the binding of OC15 and CC27, from Figure 6.3A, representing the total hemicelluloses (OC15 + CC27). **C)** Total composition analysis of raw LCB using NREL/TP-510-42618 method.

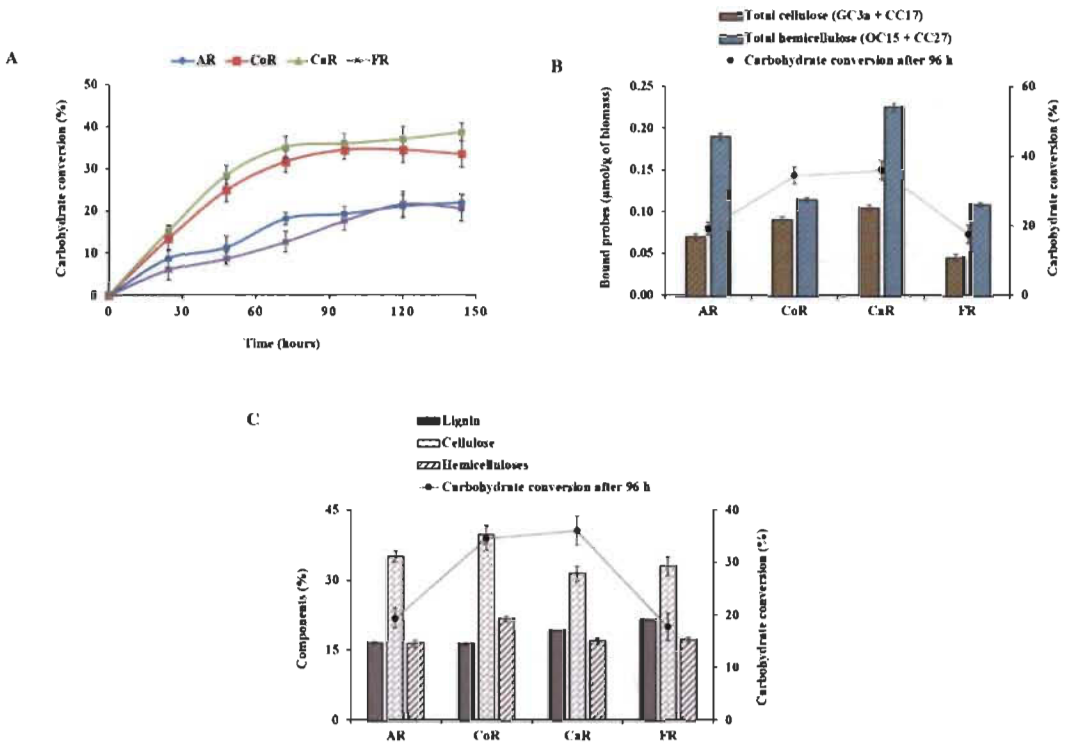


**Figure 6.4 Comparison of hydrolysis and polysaccharides detected by FTCM-depletion assay and total composition analysis**

**A)** Enzymatic hydrolysis of AR, CoR, CaR and FR LCB. **B)** Surface polymer detection by FTCM-depletion assay and its correlation with the percent carbohydrate conversion after 96 hours of enzymatic hydrolysis of AR, CoR, CaR and FR LCB. **C)** Total composition analysis using NREL/TP-510-42618 method and their correlation with the percent carbohydrate conversion after 96 hours of enzymatic hydrolysis of AR, CoR, CaR and FR LCB.

The result showed that highest rates of carbohydrate conversion were detected with corn crop residues (CoR) and cattail stems (CaR) biomass (Figure 6.4A). Comparing the binding of FTCM-depletion assay probes with the percent carbohydrate conversion reveals that the total cellulose content at the surface (as revealed by FTCM-depletion assay) was correlated with reducing sugar production (Figure 6.4B). No correlation was observed between the total hemicelluloses (as revealed by FTCM-depletion assay) and the percent carbohydrate conversion. Also, there was no clear trend in total composition analysis,

which would explain the high rates of hydrolysis measured for corn crop residues (CoR) and cattail stems (CaR) biomass (Figure 6.4C). The results suggest that the lignocellulosic polymers accessibility monitored by FTCM probes can be used to predict the efficiency of enzymatic hydrolysis for such crop and herbaceous residues.

### 6.4.3 Tracking surface accessibility of lignocellulosic components in pre-treated LCB

Subsequently, we also investigated the impacts of various pretreatments on biomass. All four types of LCB were exposed to three different pretreatments: liquid hot water, alkali and alkali-extrusion. Biomass (raw and pretreated) were first analyzed for their total polymer contents (using NREL/TP-510-42618 method) as shown in Additional file 6.7. When comparing to raw biomass, all pretreatments lead to a decrease in hemicelluloses, while lignin was only removed from fibers treated with alkali and alkali-extrusion treatments. These results are consistent with earlier observations on the general impact of liquid hot water, alkali and alkali-extrusion on plant fibers.[45,69-73] The goal of a pretreatment is to make cellulose more accessible to the enzymatic hydrolysis, which leads to improved yield and decreased processing costs.[5] From total composition analysis, one can reasonably infer that more cellulose will become available at the fiber surface when lignin and/or hemicelluloses are removed from biomass. But such an interpretation of pretreatment impact is indirect: total composition analysis does not interrogate fiber surface properties (such as cellulose accessibility).

The impact of pretreatments on the surface exposure of lignocellulosic polymers was studied using FTCM-depletion assay probes. When compared with raw biomasses, alkali pretreated biomass led to the highest loss in surface hemicelluloses, followed by the alkali-extrusion pretreated samples (Figure 6.5).

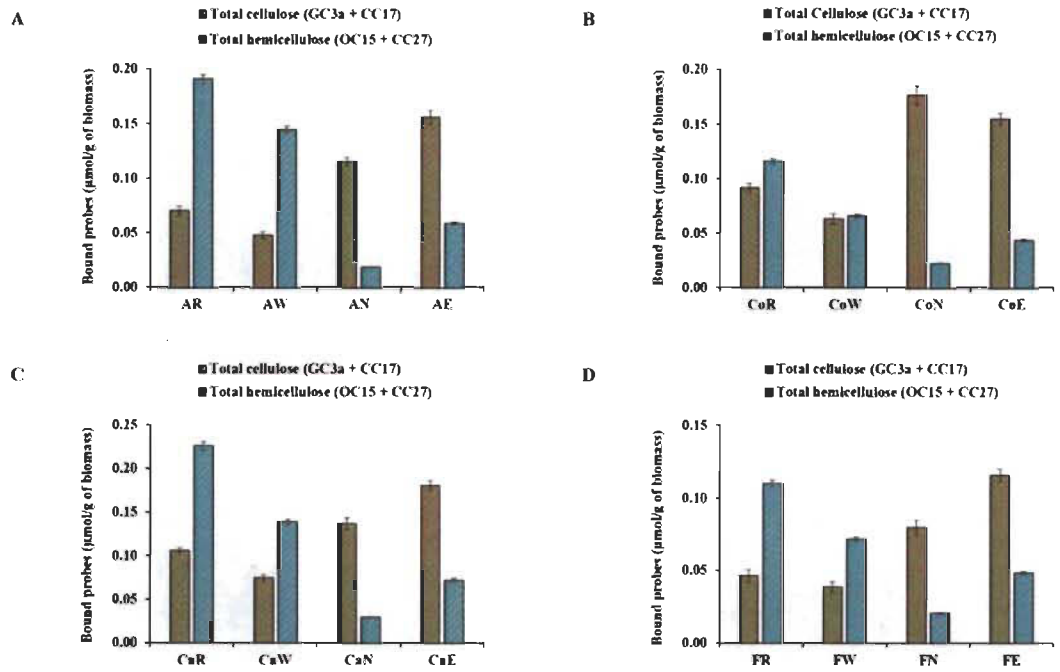


**Figure 6.5 Tracking surface accessibility of lignocellulosic components of un-treated (raw) and pretreated LCB using FTCM-depletion assay**
**A)** alfalfa stover **B)** corn crop residues **C)** cattail stems and **D)** flax shives.

The impact of alkali pretreatment led to significant (5-fold or more) removal of hemicelluloses at the surface of alfalfa stover, corn crop residues, cattail stems and flax shives. The hemicelluloses removal was accompanied by a moderate increase (less than 2-fold) in the accessibility of cellulose at the surface of all LCBs (Figure 6.5). Regarding alkali-extrusion pretreatment, the hemicelluloses detection was reduced by a lesser extent than with alkali and cellulose was increased by about 2-fold for all LCBs (Figure 6.5). The individual binding of all the four probes to LCB are represented in Additional file 6.8. The results from FTCM-depletion assays provide strong support for the contention that cellulose accessibility at surface has been increased after both alkali and alkali-extrusion pretreatments. Possible correlations between the biomass pretreatments and the hydrolysis efficiency were also explored. Polysaccharide hydrolysis is presented in Figure 6.6 for all the raw and pretreated biomasses.

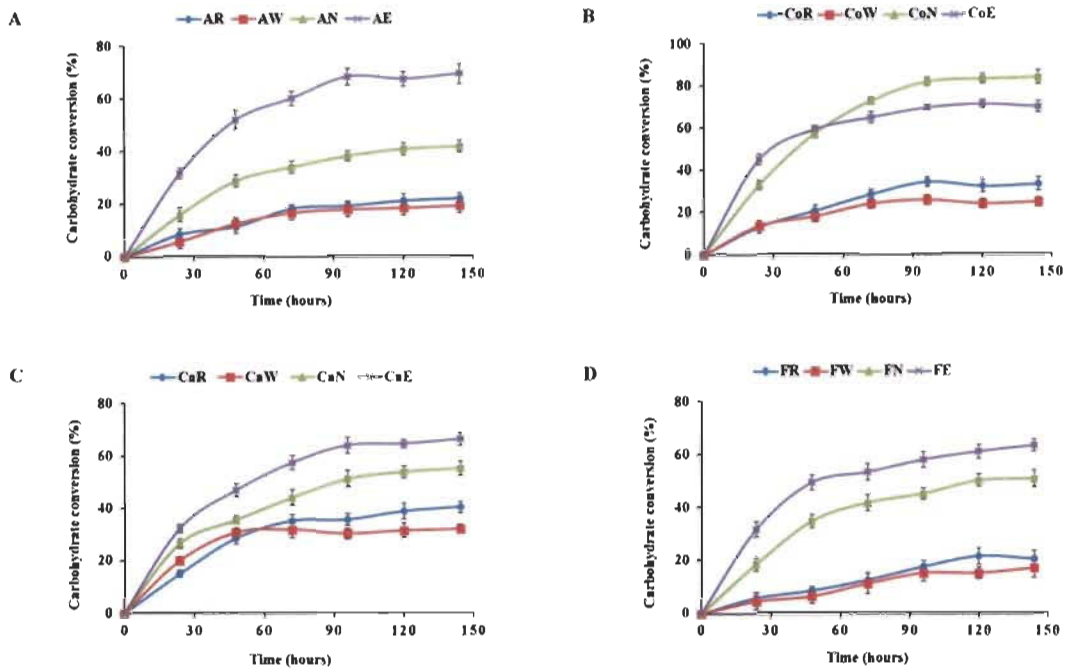


**Figure 6.6 Enzymatic hydrolysis of the untreated (raw) and pretreated LCB** **A)** alfalfa stover **B)** corn crop residues **C)** cattail stems and **D)** flax shives.

For alfalfa stover, maximal carbohydrate conversion was detected for alkali-extrusion pretreated biomass (AE), followed by alkali pretreated biomass (AN) (Figure 6.6A). Similar trends were observed for both cattail stems and flax shives biomasses, where maximal carbohydrate conversion was observed for alkali-extrusion pretreated (CaE and FE) biomass (Figure 6.6 C and D). In the case of corn biomass, alkali pretreatment (CoN) led to the highest conversion into reducing sugars, followed by alkali-extrusion (CoE) pretreatment of corn crop residues (Figure 6.6B).

Figure 6.7 provides a direct comparison of probe binding and production of reducing sugars after 96 hours. Conversion to reducing sugars by enzymes is clearly correlated with total cellulose at the fiber surface (GC3a + CC17) observed by FTCM-depletion assay, for all biomasses and all pretreatments. However, there is no such correlation between reducing sugar production and any polymer content variation shown by total composition analysis (using NREL/TP-510-42618 method) (Additional file 6.9).

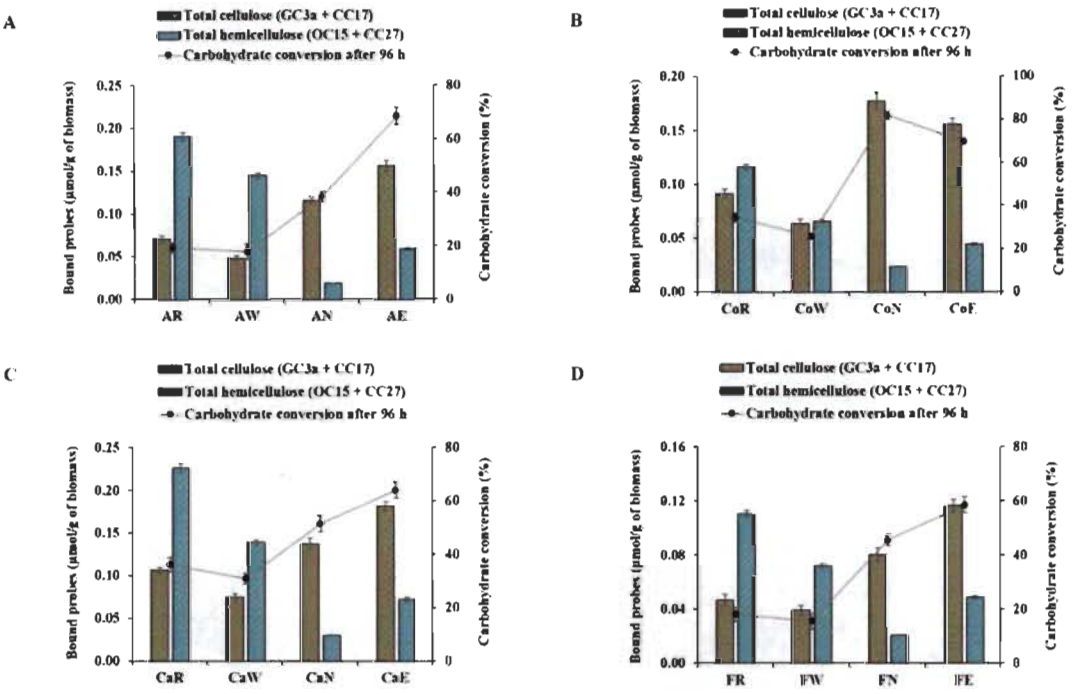


**Figure 6.7 Correlation between carbohydrate conversion at 96h and total surface cellulose detected by FTCM-depletion assay**

**A)** alfalfa stover, **B)** corn crop residues, **C)** cattail stems and **D)** flax shives.

The correlation between exposed total cellulose and conversion into reducing sugars after 96 hours did not prevail for all hydrolysis periods. Detailed examination of Figure 6.6B revealed that alkali-extrusion pretreated corn crop residues (CoE) has a higher carbohydrate conversion rate in the first 24 hours of incubation compared to the alkali pretreated sample (CoN). Carbohydrate conversion at 24 hours did not correlate well with the total cellulose content (GC3a + CC17) observed by FTCM-depletion assay, as shown in Additional file 6.10, while it was clearly correlated after 96 hours (Figure 6.7). The initial phase of carbohydrate release over 24 hours did, however, correlate with the exposure of the non-crystalline cellulose at surface (detected using CC17), which was maximal for alkali-extrusion pretreated biomass (Figure 6.8).

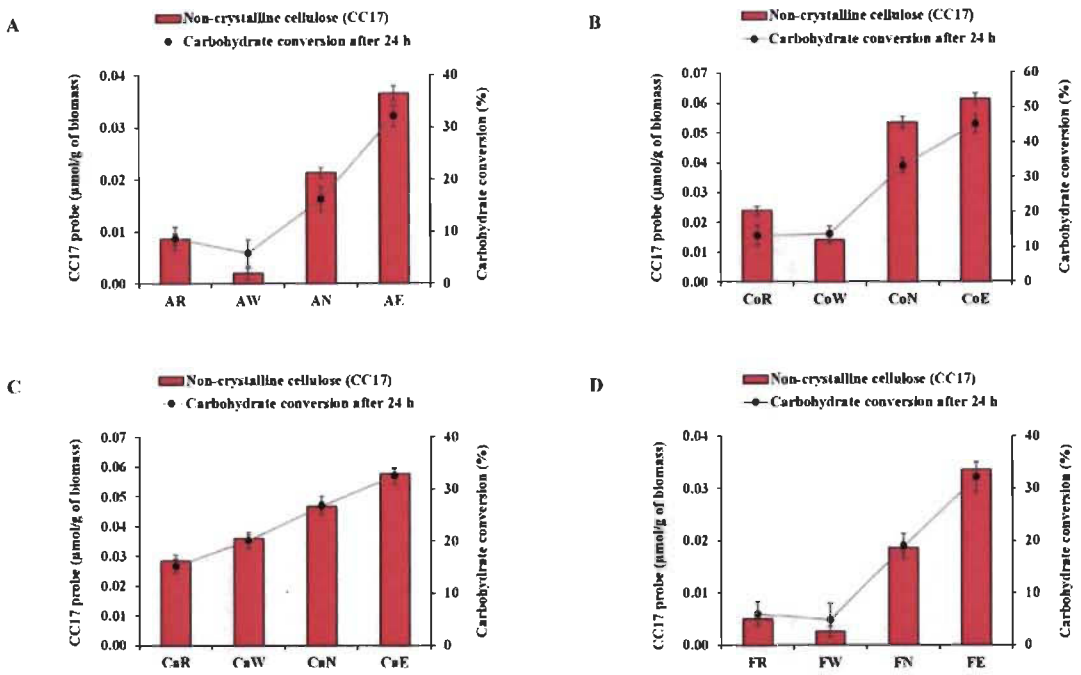


**Figure 6.8 Correlation between carbohydrate conversion at 24h and non-crystalline cellulose detected by FTCM-depletion assay**

**A)** alfalfa stover, **B)** corn crop residues, **C)** cattail stems and **D)** flax shives.

We also observed the same correlation between surface-exposed non-crystalline cellulose and early digestion of polymers for raw cattail stems (CaR) and liquid hot water pretreated cattail stems (CaW) biomass (Figure 6.6C and Figure 6.8).

Comparison of the biomass hydrolysis results indicates that FTCM-depletion assay corroborates the preferential digestion of non-crystalline cellulose in early phase of hydrolysis, and that past this first phase, the yield becomes dependent on total cellulose exposure. To our knowledge, there are no other methods available for biomass fiber tracking and characterization that can directly and unambiguously demonstrate the sequential removal of various forms of cellulose as hydrolysis progresses.

As described earlier, current analytical methods to study the pretreatment efficiency are cumbersome and cannot unambiguously predict their impact on bioconversion

yield. In contrast, our results suggest that FTCM-depletion assay, which is rapid and affordable, provides an unambiguous approach for direct assessment of surface-exposed cellulose, which correlates very well with the enzymatic hydrolysis of all biomass-pretreatment combinations studied here. Regarding the total composition analysis (NREL/TP-510-42618), a decrease in total lignin content and an increased cellulose content (*i.e.* alkali and alkali-extrusion pretreatment) generally lead to increased hydrolysis efficiency. But the correlation did not apply to all biomass-pretreatment combinations, and would be less reliable when optimizing or predicting pretreatment efficiency.

Thus far, several studies have addressed the possible association of lignin content, crystallinity, degree of polymerization, porosity, enzyme adsorption and cellulose accessibility to enzyme with bioethanol production yield. In some of these studies, cellulose accessibility to cellulase has been shown to be an important factor for achieving a high scarification yield.[13,19,39] However, these studies neither look for both non-crystalline cellulose and hemicelluloses, nor introduced a possible correlation between cellulose accessibility and sugar yield as a prediction indicator for pretreatment selection. In this study, by using multiple CBM probes we can monitor surface exposure of various polysaccharides, not only crystalline cellulose, which might reflect on enzymatic efficiency of multi-enzyme commercial cellulases and on a LCB with higher hemicellulose content. Even though Accellerase® DUET contains hemicellulases activities, FTCM-depletion assay did not show any strong correlation between surface hemicelluloses and hydrolysis yield. However, binding of FTCM probes allowed to directly monitor hemicellulose removal at surface, in support of the expected impact of pretreatments used here.

## 6.5 Conclusion

Adaptation of FTCM method to a FTCM-depletion assay allowed analyzing surface exposure of polysaccharides of various LCB samples. The results suggest that surface cellulose (total and non-crystalline) were strongly correlated with production of reducing sugars by hydrolysis, in a much better way than with total lignin and/or total cel-

lulose content (using NREL/TP-510-42618 method) of LCB. The clear and robust correlations that were observed here, between the polysaccharides accessibility by FTCM probes and enzymatic hydrolysis of the biomasses, can be evolved into a powerful prediction tool for the simple, rapid and efficient determination of optimal biomass and pretreatment strategies for bioenergy production (one hundred samples can be analyzed in less than 2 hours with FTCM-depletion assay).

**List of abbreviations**

LCB: Lignocellulosic biomass; R: Raw lignocellulosic biomass; W: Liquid hot water pretreatment; N: Alkali pretreatment; E: Alkali-extrusion pretreatment; AR: Raw alfalfa stover; CoR: Raw corn crop residues; CaR: Raw cattail stems; FR: Raw flax shives; AW: Alfalfa stover pretreated by liquid hot water; AN: Alfalfa stover pretreated by alkali; AE: Alfalfa stover pretreated by alkali-extrusion; CoW: Corn crop residues pretreated by liquid hot water; CoN: Corn crop residues pretreated by alkali; CoE: Corn crop residues pretreated by alkali-extrusion; CaW: Cattail stems pretreated by liquid hot water; CaN: Cattail stems pretreated by alkali; CaE: Cattail stems pretreated by alkali-extrusion; FW: Flax shives pretreated by liquid hot water; FN: Flax shives pretreated by alkali; FE: Flax shives pretreated by alkali-extrusion; AGE: Affinity gel electrophoresis; BSA: Bovine serum albumin; CBM: Carbohydrate-binding module; CBM3a: Family 3a carbohydrate-binding module; CBM17: Family 17 carbohydrate-binding module; CBM15: Family 15 carbohydrate-binding module; CBM27: Family 27 carbohydrate-binding module; CMC: Carboxymethyl cellulose; eGFP: Enhanced green fluorescent protein; mOrange2: Monomeric orange2; mCherry: Monomeric cherry; CFP: Cyan fluorescent protein; GC3a: Green fluorescent protein linked to a family 3a carbohydrate-binding module; CC17: mCherry fluorescent protein linked to a family 17 carbohydrate-binding module; OC15: mOrange2 fluorescent protein linked to a family 15 carbohydrate-binding module; CC27: Cyan fluorescent protein linked to a family 27 carbohydrate-binding module; NREL: National Renewable Energy Laboratory; DNS: 3,5-dinitrosalicylic acid; ITC: Isothermal titration calorimetry; SDS-PAGE: Sodium dodecyl sulfate-polyacrylamide gel electropho-

resis; SSDA: Solid state depletion assay; FTCM: Fluorescent protein-tagged carbohydrate-binding module method; RAC: Regenerated amorphous cellulose; *p*NPG: 4-nitrophenyl-β-D-glucopyranoside; ABX: Arabino-xylan.

## 6.6 References


1. C. E. Wyman, *Trends. Biotechnol.*, 2007, **25**(4), 153-157.
2. L. R. Lynd, M. S. Laser, D. Bransby, B. E. Dale, B. Davison, R. Hamilton, M. Himmel, M. Keller, J. D. McMillan, J. Sheehan, C. E. Wyman, *Nat. Biotechnol.*, 2008, **26**(2), 169-172.
3. M. E. Himmel, S. Y. Ding, D. K. Johnson, W. S. Adney, M. R. Nimlos, J. W. Brady, T. D. Foust, *Science,* 2007, **315**, 804-807.
4. L. R. Lynd, C. E. Wyman, T. U. Gerngross, *Biotechnol. Prog.,* 1999, **15**(5), 777-793.
5. C. E. Wyman, B. E. Dale, V. Balan, R. T. Elander, M. T. Holtzapple, R. S. Ramirez, M. R. Ladisch, N. S. Mosier, Y. Y. Lee, R. Gupta, S. R. Thomas, B. R. Hames, R. Warner, R. Kumar, *Aqueous Pretreatment of Plant Biomass for Biological and Chemical Conversion to Fuels and Chemicals, John Wiley and Sons, Ltd,* 2013, 239-259.
6. M. A. Millet, A. J. Baker, L. D. Scatter, *Biotech. Bioeng. Symp.,* 1976, **6**, 125-153.
7. L. Cadoche, G. D. Lopez, *Biol. Wastes,* 1989, **30**, 153-157.
8. H. E. Grethlein, A. O. Converse, *Bioresour. Technol.,* 1991, **36**(1), 77-82.
9. B. Yang, C. E. Wyman, *Methods Mol. Biol.,* 2009, **581**, 103-114.
10. G. Bali, X. Meng, J. I. Deneff, Q. Sun, A. J. Ragauskas, *ChemSusChem,* 2015, **8** (2), 275-279.
11. N. Sathitsuksanoh, Z. Zhu, N. Templeton, J. Rollin, S. Harvey, Y. H. P. Zhang, *Ind. Eng. Chem. Res.*, 2009, **48**, 6441-6447.
12. Y. H. P. Zhang, S. Y. Ding, J. R. Mielenz, R. Elander, M. Laser, M. Himmel, J. D. McMillan, L. R. Lynd, *Biotechnol. Bioeng.,* 2007, **97**(2), 214-223.
13. Z. Zhu, N. Sathitsuksanoh, T. Vinzant, D. J. Schell, J. D. McMillan, Y. H. P. Zhang, *Biotechnol. Bioeng.*, 2009, **103**, 715-724.
14. O. Bobleter, R. Niesner, M. Röhr, *J. Appl. Polym. Sci.,* 1976, **20**(8), 2083-2093.
15. P. Kumar, D. Barrett, M. Delwiche, P. Stroeve, *Ind. Eng. Chem. Res.*, 2009, **48**, 3713-3729.

16. N. Mosier, C. Wyman, B. Dale, R. Elander, Y. Y. Lee, M. Holtzapple, M. Ladisch, *Bioresour. Technol.,* 2005, **96**(6), 673-686.
17. R. Kumar, C. E. Wyman, *Aqueous Pretreatment of Plant Biomass for Biological and Chemical Conversion to Fuels and Chemicals. John Wiley and Sons, Ltd,* 2013, 281-310.
18. Y. H. P. Zhang, L. R. Lynd, *Biotechnol. Bioeng.*, 2006, **94**, 888-898.
19. J. A. Rollin, Z. Zhu, N. Sathitsuksanoh, Y. H. P. Zhang, *Biotechnol. Bioeng.*, 2011, **108**(1), 22-30.
20. B. Yang, C. E. Wyman, *Biofuels, Bioprod. Biorefin.*, 2008, **2**(1), 26-40.
21. A. Sluiter, D. Crocker, B. Hames, R. Ruiz, C. Scarlata, J. Sluiter, D. Templeton, *Laboratory Analytical Procedure (LAP)*, 2008, NREL/TP-510-42618.
22. J. B. Sluiter, R. O. Ruiz, C. J. Scarlata, A. D. Sluiter, D. W. Templeton, *J. Agric. Food. Chem.*, 2010, **58**, 9043-9053.
23. T. P. Schultz, M. C. Templeton, G. D. McGinnis, *Anal. Chem.*, 1985, **57**, 2867-2869.
24. S. Burkhardt, L. Kumar, R. Chandra, J. Saddler, *Biotechnol. Biofuels,* 2013, **6**, 1754-6834.
25. K. Karimi, M. J. Taherzadeh, *Bioresour. Technol.*, 2016a, **200**, 1008-1018.
26. K. Karimi, M. J. Taherzadeh, *Bioresour. Technol.*, 2016b, **203**, 348-356.
27. V. Khatri, Y. Hebert-Ouellet, F. Meddeb-Mouelhi and M. Beauregard, *Biotechnol. Biofuels,* 2016, **9**, 74.
28. J. D. DeMartini, S. Pattathil, J. S. Miller, H. Li, M. G. Hahn, C. E. Wyman, *Energy Environ. Sci.*, 2013, **6**(3), 898-909.
29. J. P. Knox, *Cellulases,* 2012, **510**, 233-245.
30. J. P. Knox, *Curr. Opin. Plant Biol.,* 2008, **11**(3), 308-313.
31. C. Oliveira, V. Carvalho, L. Domingues, F. M. Gama, *Biotechnol. Adv.,* 2015, **33**(3), 358-369.
32. A. B. Boraston, D. Bolam, H. Gilbert, G. J. Davies, *Biochem. J.,* 2004, **382**, 769-781.

33. S. Gao, C. You, S. Renneckar, J. Bao, Y. H. P. Zhang, *Biotechnol. Biofuels,* 2014, **7**(1), 1-11.
34. H. J. Gilbert, J. P. Knox, A. B. Boraston, *Curr. Opin. Struct. Biol.,* 2013, **23**(5), 669-677.
35. C. Hervé, S. E. Marcus, J. P. Knox, *The Plant Cell Wall,* 2011, **715**, 103-113.
36. K. Gourlay, J. Hu, V. Arantes, M. Penttilä and J. N. Saddler, *J. Biol. Chem.*, 2015, **290**, 2938.
37. T. Kawakubo, S. Karita, Y. Araki, S. Watanabe, M. Oyadomari, R. Takada, F. Tanaka, K. Abe, T. Watanabe, Y. Honda, T. Watanabe, *Biotechnol. Bioeng.,* 2010, **105**, 499.
38. V. Khatri, F. Meddeb-Mouelhi, M. Beauregard, *Sustainable Energy Fuels*, 2018, DOI: 10.1039/C7SE00427C.
39. J. Hong, X. Ye, Y. H. P. Zhang, *Langmuir*, 2007, **23**(25), 12535-12540.
40. Y. Hébert-Ouellet, F. Meddeb-Mouelhi, V. Khatri, L. Cui, B. Janse, K. MacDonald, M. Beauregard, *Green Chem.*, 2017, **19**, 2603-2611.
41. P. L. Bombeck, V. Khatri, F. Meddeb-Mouelhi, D. Montplaisir, A. Richel, M. Beauregard, *Biotechnol. Biofuels*, 2017, **10**(1), 293.
42. Y. H. P. Zhang, J. Cui, L. R. Lynd, L. R. Kuang, *Biomacromolecules*, 2006, **7**(2), 644-648.
43. G. L. Miller, *Anal. Chem.,* 1959, **31,** 426-428.
44. M. M. Bradford, *Anal. Biochem.,* 1976, **72**(1), 248-254.
45. K. Adjalle, L. V. Larose, J. Bley, S. Barnabé, *Cellulose*, 2017, **24**(3), 1395-1406.
46. D. W. Abbott, A. B. Boraston, *Methods Enzymol.*, 2012, **510**, 211-231.
47. A. B. Boraston, M. Healey, J. Klassen, E. Ficko-Blean, A. L. van Bueren, V. Law, *J. Biol. Chem.*, 2006, **281**(1), 587-598.
48. N. R. Gilkes, E. Jervis, B. Henrissat, B. Tekant, R. C. Miller, R. A. Warren, D. G. Kilburn, *J. Biol. Chem.*, 1992, **267**(10), 6743-6749.
49. L. G. J. M. A. Segal, J. J. Creely, A. E. Martin Jr, C. M. Conrad, *Text. Res. J.*, 1959, **29**(10), 786-794.
50. R. Gupta, Y. Y. Lee, *Biotechnol. Bioeng.*, 2009, **102**(6), 1570-1581.

51. M. Hall, P. Bansal, J. H. Lee, M. J. Realff, A. S. Bommarius, *FEBS J.*, 2010, **277**(6), 1571-1582.
52. H. Palonen, F. Tjerneld, G. Zacchi, M. Tenkanen, *J. Biotechnol.*, 2004, **107**(1), 65-72.
53. B. Yang, C. E. Wyman, *Biotechnol. Bioeng.*, 2006, **94**(4), 611-617.
54. J. L. Rahikainen, R. Martin-Sampedro, H. Heikkinen, S. Rovio, K. Marjamaa, T. Tamminen, O. J. Rojas, K. Kruus, *Bioresour. Technol.*, 2013, **133**, 270-278.
55. T. Eriksson, J. Börjesson, F. Tjerneld, *Enzyme Microb. Technol.*, 2002, **31**(3), 353-364.
56. L. T. Fan, Y. Lee, D. H. Beardmore, *Biotechnol. Bioeng.*, 1980, **22**, 177-199.
57. A. Goshadrou, K. Karimi, M. J. Taherzadeh, *Ind. Crops Prod.*, 2011, **34** (1), 1219-1225.
58. A. Jeihanipour, K. Karimi, M. J. Taherzadeh, *Biotechnol. Bioeng.*, 2010, **105**, 469-476.
59. S. Ostovareh, K. Karimi, A. Zamani, *Ind. Crops Prod.*, 2015, **66**, 170-177.
60. P. Salehian, K. Karimi, *Ind. Eng. Chem. Res.*, 2013, **52**, 972-978.
61. C. Girometta, A. Zeffiro, M. Malagodi, E. Savino, E. Doria, E. Nielsen, A. Buttafava, D. Dondi, *Cellulose*, 2017, **24**(9), 3803-3813.
62. D. W. Templeton, A. D. Sluiter, T. K. Hayward, B. R. Hames, S. R. Thomas, *Cellulose*, 2009, **16**(4), 621-639.
63. D. Rebaque, R. Martínez-Rubio, S. Fornalé, P. García-Angulo, A. Alonso-Simón, J. M. Álvarez, D. Caparros-Ruiz, J. L. Acebes, A. Encina, *Carbohydr. Polym.*, 2017, **175**, 679-688.
64. A. U. Buranov, G. Mazza, *Ind. Crops Prod.*, 2012, **35**(1), 77-87.
65. G. M. Gübitz, D. W. Stebbing, C. I. Johansson, J. N. Saddler, *App. Microbiol. Biotechnol.*, 1998, **50**(3), 390-395.
66. Y. H. P. Zhang, L. R. Lynd, *Biotechnol. Bioeng.*, 2004, **88**(7), 797-824.
67. S. D. Mansfield, C. Mooney, J. N. Saddler, *Biotechnol. Progr.*, 1999, **15**(5), 804-816.
68. V. Arantes, J. N. Saddler, *Biotechnol. Biofuels*, 2010, **3**(1), 4.

69. N. Mosier, R. Hendrickson, N. Ho, M. Sedlak, M. R. Ladisch, *Bioresour. Technol.*, 2005, **96**(18), 1986-1993.
70. A. Limayem, S. C. Ricke, *Prog. Energy Combust. Sci.*, 2012, **38**(4), 449-467.
71. C. Liu, E. van der Heide, H. S. Wang, B. Li, G. Yu, X. D. Mu, *Biotechnol. Biofuels,* 2013, **6**(1), 97.
72. J. S. Kim, Y. Y. Lee, T. H. Kim, *Bioresour. Technol.*, 2016, **199**, 42-48.
73. J. Zheng, L. Rehmann, *Int. J. Mol. Sci.*, 2014, **15**(10), 18967-18984.
74. J. Lehtiö, J. Sugiyama, M. Gustavsson, L. Fransson, M. Linder, T. T. Teeri, *PNAS*, 2003, **100**(2), 484-489.
75. O. Yaniv, G. Fichman, I. Borovok, Y. Shoham, E. A. Bayer, R. Lamed, L. J. Shimon, F. Frolow, *Acta Crystallogr., Sect. D: Biol. Crystallogr.*, 2014, **70**(2), 522-534.
76. J. Tormo, R. Lamed, A. J. Chirino, E. Morag, E. A. Bayer, Y. Shoham, T. A. Steitz, *EMBO J.*, 1996, **15**(21), 5739.
77. V. Notenboom, A. B. Boraston, P. Chiu, A. C. Freelove, D. G. Kilburn, D. R. Rose, *J. Mol. Biol.*, 2001, **314**(4), 797-806.
78. A. B. Boraston, P. Chiu, R. A. J. Warren, D. G. Kilburn, *Biochemistry*, 2000, **39**(36), 11129-11136.
79. A. B. Boraston, E. Kwan, P. Chiu, R. A. J. Warren, D. G. Kilburn, *J. Biol. Chem.*, 2003, **278**(8), 6120-6127.
80. L. Szabó, S. Jamal, H. Xie, S. J. Charnock, D. N. Bolam, H. J. Gilbert, G. J. Davies, *J. Biol. Chem.*, 2001, **276**(52), 49061-49065.
81. A. B. Boraston, T. J. Revett, C. M. Boraston, D. Nurizzo, G. J. Davies, *Structure*, 2003, **11**(6), 665-675.
82. K.N. Parker, S. R. Chhabra, D. Lam, W. Callen, G. D. Duffaud, M. A. Snead, J. M. Short, E. J. Mathur, R. M. Kelly, *Biotechnol. Bioeng.*, 2001, **75**(3), 322-333.

## 6.7 Additional Files

**Additional file 6.1 Specific activities of Accellerase® Duet enzyme**

| | Specific activities (U/g) |
|---|---|
| Endoglucanase (CMC) | 2400-3000 |
| β-Glucosidase (*p*NPG) | > 400 |
| Xylanase (ABX) | > 3600 |

**Additional file 6.2 Information related to the construction of recombinant FTCM-depletion assay probes**

| Probes (abbreviations) | CBM family | CBM gene accession number | Protein | Fold/PDB_ID | Organism | Target | References |
|---|---|---|---|---|---|---|---|
| eGFP-CBM3a (GC3a) | 3a | CP000568 | Endo-β-1,4-glucanase I (CelI; Cthe_0040) **(Cel9I) CBM3 1 CBM3a/CipA** | β-Sandwich / 4B9F (M) | *Clostridium Thermocellum* ATCC 27405 | Crystalline cellulose | Lehtiö *et al.*,2003;[74] Yaniv *et al.*, 2013;[75] Tormo *et al.*, 1996[76] |
| mC-CBM17 (CC17) | 17 | U37056 | Endo-β-1,4-glucanase EngF **(Cel5A)** | β-Sandwich / 1J83 (M) | *Clostridium Cellulovorans* ATCC 484 | Non-crystalline cellulose | Notenboom *et al.*,2001;[77] Boraston *et al.*,2000 and 2003[78,79] |
| mOrange2-CBM15 (OC15) | 15 | Z48928 | Xylanase F (Xyn10C) | β-Sandwich / 1GNY (M) | *Cellvibrio japonicas* | Xylan | Szabó *et al.*, 2001[80] |
| eCFP-CBM27 (CC27) | 27 | Y17980 | β -mannanase **(Man5)** | β-Sandwich / 1OF4 (M) | *Thermotoga Maritima* MSB8 | Mannan | Boraston *et al.*, 2003;[81] Parker *et al.*, 2001[82] |

eGFP: enhanced green fluorescent protein; mC: mono-cherry; mOrange2: Mono-orange2 and eCFP: enhanced cyan fluorescent protein; M: Metal binding

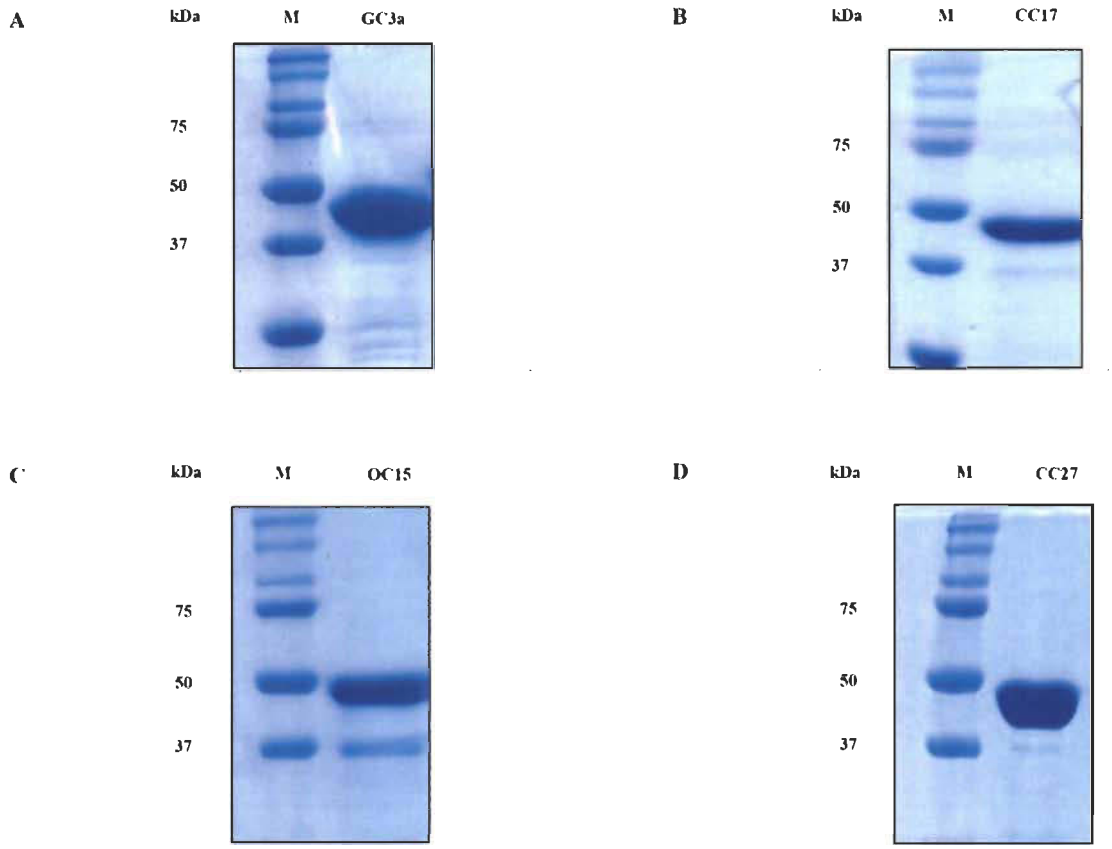


**Additional file 6.3 SDS-PAGE analysis of the probes after purification**

**A)** GC3a, **B)** CC17, **C)** OC15 and **D)** CC27 probes. The expected molecular weight of the GC3a, CC17, OC15 and CC27 fusion proteins are 46.26, 50.56, 44.68 and 48.06 kDa, respectively. A 12% polyacrylamide gel was used for SDS-PAGE analysis. Well M: Precision plus protein standards (5 µg); Well GC3a, CC17, OC15 and CC27: Purified probes (10 µg).

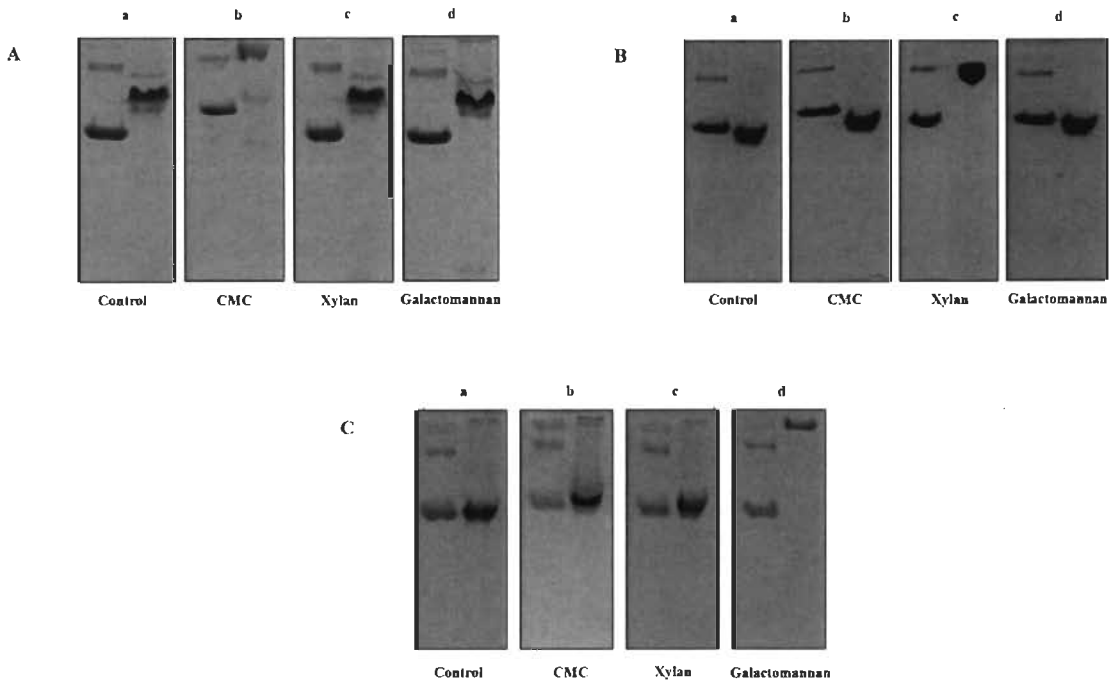


**Additional file 6.4** **Affinity gel electrophoresis (AGE) of the probes**

**A)** CC17, **B)** OC15 and **C)** CC27 probes. Panel a: control (no polysaccharide); Panel b: CMC; Panel c: xylan; Panel d: galactomannan. In each panel the first well contained BSA as a negative control (10 μg) and the second well was loaded with an appropriate probe (10 μg). All soluble polysaccharides were used at final concentration of 0.5% (w/v) and a 12% polyacrylamide gel was used for affinity analysis.

**Additional file 6.5** **Adsorption parameters and affinities of the binding of probes to various substrates**

Interaction with Avicel, regenerated amorphous cellulose (RAC) and various hexaoses was determined by SSDA and ITC in 20 Tris-HCl pH 7.5 containing 20 mM NaCl and 5 mM $CaCl_2$.

| Probes | Ligand | $K_a$ x $10^5$ ($M^{-1}$) | n |
|---|---|---|---|
| GC3a | Avicel | 91.41[a] (± 2.5) | 0.76[b] (± 0.9) |
| | Cellohexaose | - | - |
| | Xylohexaose | - | - |
| | Mannohexaose | - | - |
| CC17 | RAC | 23.67[a] (± 3.9) | 6.88[b] (± 0.7) |
| | Cellohexaose | 3.34 (± 0.8) | 1.1[c] (± 0.1) |
| | Xylohexaose | - | - |
| | Mannohexaose | - | - |
| OC15 | Cellohexaose | 0.02 (± 0.01) | 0.9[c] (± 0.3) |
| | Xylohexaose | 0.82 (± 0.1) | 1.0[c] (± 0.1) |
| | Mannohexaose | - | - |
| CC27 | Cellohexaose | - | - |
| | Xylohexaose | - | - |
| | Mannohexaose | 6.93 (± 0.5) | 1.1[c] (± 0.3) |

[a]: Values were determined by SSDA
[b]: Density of binding sites per gram of substrate (µmol/g);
[c]: Number of ligand binding sites on the protein
-: No binding detected

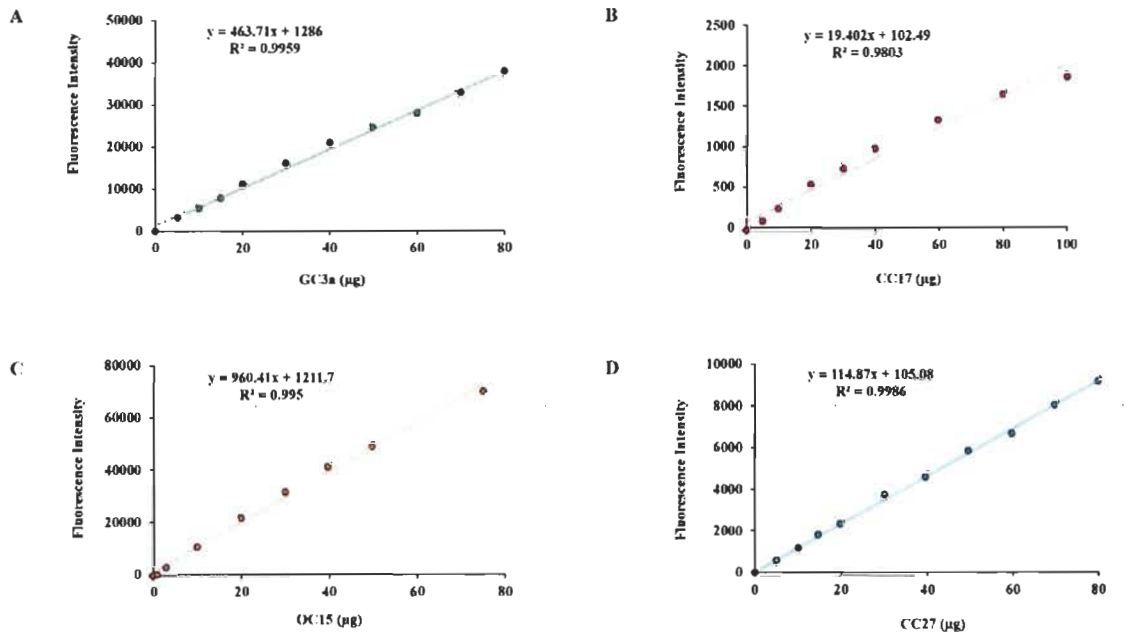


**Additional file 6.6 Standard curves for the conversion of fluorescence intensities into µg of probes**

**A)** GC3a, **B)** CC17, **C)** OC15 and **D)** CC27 probes.

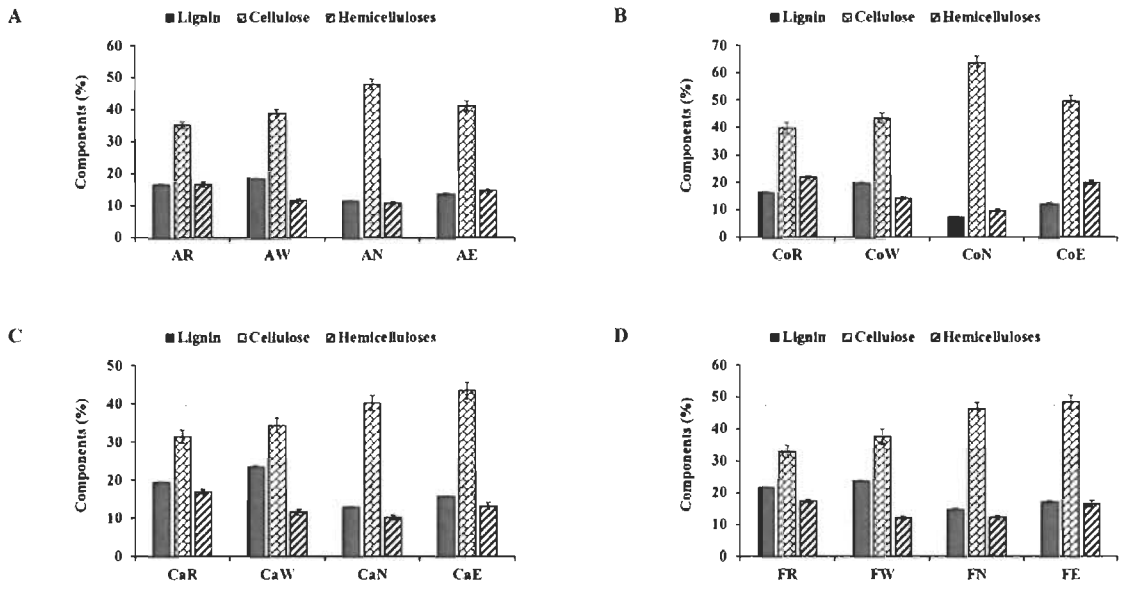


**Additional file 6.7 Total composition analysis (NREL/TP-510-42618) of untreated (raw) and pretreated LCB**

**A)** alfalfa stover, **B)** corn crop residues, **C)** cattail stems and **D)** flax shives.

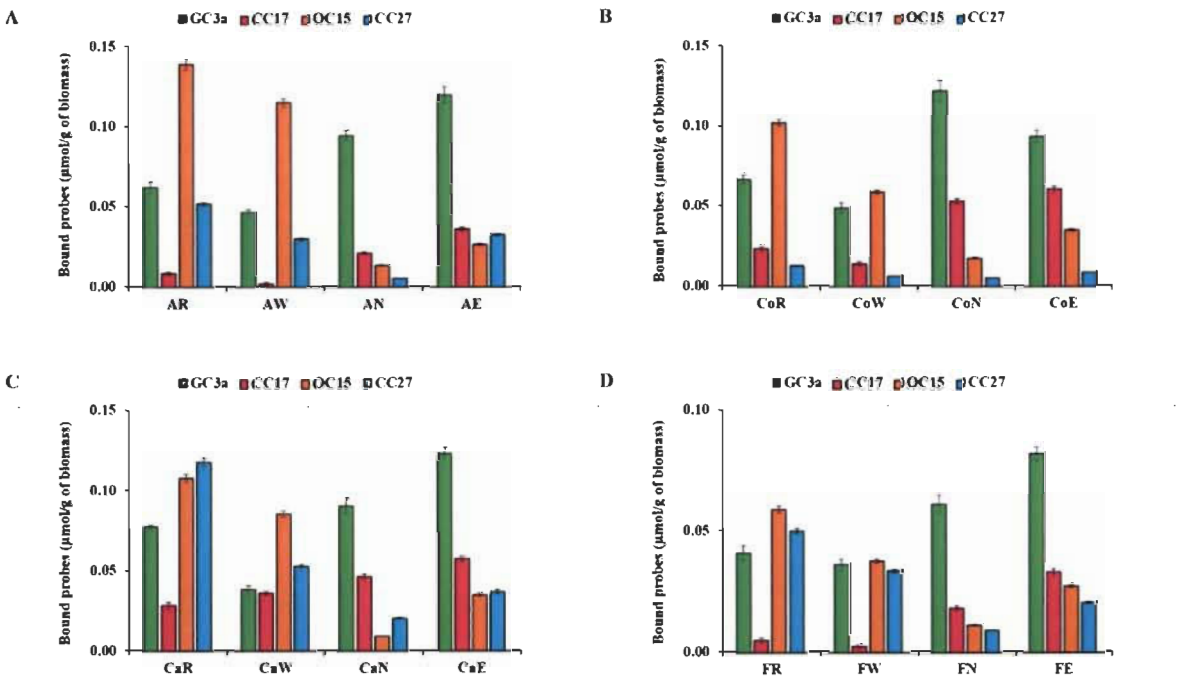


**Additional file 6.8** **Tracking surface accessibility of polysaccharides in untreated (raw) and pretreated LCB using FTCM-depletion assay**

**A)** alfalfa stover, **B)** corn crop residues, **C)** cattail stems and **D)** flax shives.

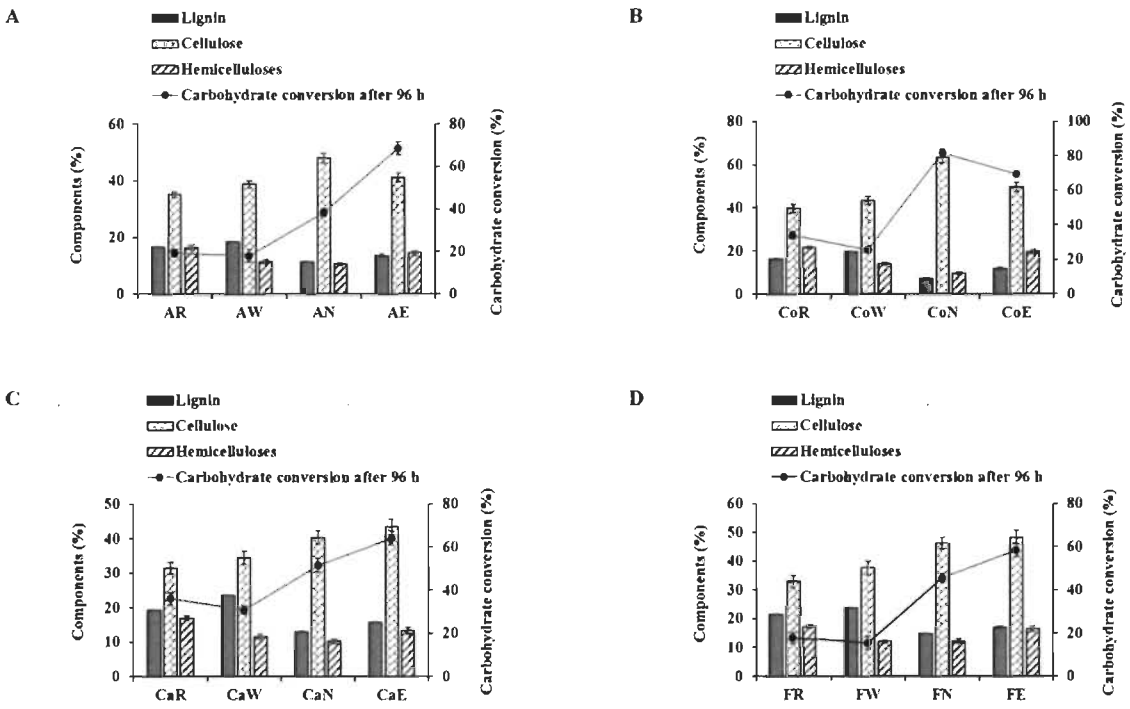


**Additional file 6.9** **Correlation between carbohydrate conversion after 96 h and total composition analysis of untreated (raw) and pretreated LCB**

**A)** alfalfa stover, **B)** corn crop residues, **C)** cattail stems and **D)** flax shives.

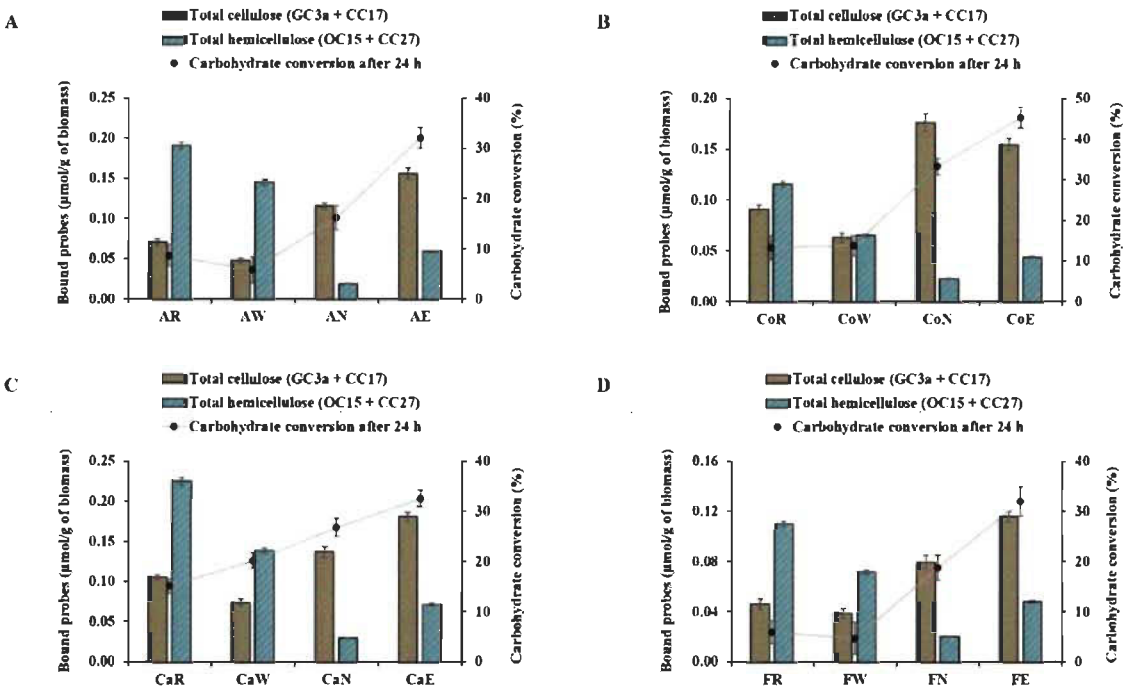


**Additional file 6.10 Correlation between carbohydrate conversion after 24 h and total cellulose and total hemicelluloses detected by FTCM-depletion assay**

**A)** alfalfa stover, **B)** corn crop residues, **C)** cattail stems and **D)** flax shives.

# Chapter 7 - Conclusions

Monitoring the impact of mechanical, chemical and enzymatic modifications of biopolymers found in LCB is a complex endeavor. The currently available methods for chemical composition analysis of biopolymers, such as total chemical composition analysis (using NREL/TP-510-42618), are limited to analysis of bulk composition and give no information on biopolymers specifically found at the surface of fibers. On the other hand, XPS, while being highly sensitive for surface polymers, cannot unambiguously monitor changes in surface polysaccharides since cellulose and hemicellulose share similar C 1s carbon functionalities (leading to identical XPS signatures). These standard methods are poorly adapted to important problematics associated with biofuels and pulp and paper industries. To address those issues, in this Ph.D. work, we developed a novel LCB detection approach that is sensitive, specific, reproducible, rapid (hundreds of samples analyzed in less than 4 hours), high throughput, cost-effective and that requires minimal specialized equipment. This approach, named FTCM, involves solely the utilization of four two-domain probes, each of them harnesses the specific polysaccharide recognition power of CBM and the high sensitivity of GFP's (or any of its variants) fluorescence emission. FTCM is believed to be robust and insensitive to a number of artefacts, considering that for an impurity to contribute to FTCM signal, a perfect match of spectrosopice features between a given impurity and any of the probes designed here is required.

Throughout this Ph.D. study, the capabilities of FTCM were explored, with appropriate modifications when needed. We showed that it can specifically track mechanical, chemical and enzymatic-induced variations of polysaccharides on the surface of different wood fibers in a rapid and high throughput format. The first objective established the potential of a fluorescent-tagged fusion protein OC15 for monitoring xylan at the surface of paper samples. The results demonstrated that OC15 probe enables the specific tracking of chemical and enzymatic-induced variations of xylan on the surface of kraft pulps. In addition, the study also demonstrated that such probes could form the basis of a rapid,

easy to use, unambiguous and affordable diagnostic approach, helping optimizing treatment strategy and reducing the cost of processes, which rely on controlled xylan removal.

The second objective investigated the potential of FTCM for bolstering our understanding of hemicelluloses hydrolysis and factors that have impact on such hydrolysis. The results demonstrated that the optimum hydrolysis parameters for both xylanase and mannanase enzymes, for all the studied pulps, were 0.1 U of enzyme/paper disc at 50°C for a treatment duration of 1h. FTCM identified the major factor limiting hydrolysis efficiency as enzyme inactivation (by any mechanism). By directly detecting polymers remaining after various enzymatic treatments, using CBM probes revealed additive and/or synergistic interactions between Celluclast 1.5L, xylanase and mannanase enzymes. The ability of FTCM to directly map layers of cellulose and hemicelluloses fractions as they were attacked by enzymes provided support for an embedded population of mannan, protected by xylan, probably associated to cellulose-hemicellulose complexes.

The third objective examined the potential of FTCM specifically for pulp and paper industries. We demonstrated a strong correlation between the FTCM probes binding and the paper strength properties (*i.e.* fiber mean length, tear index, tensile index and internal bond strength). This study enables the rapid determination of these properties and allow one to predict, in a high throughput yet low volume, the optimal conditions with which to treat a given biomass.

The fourth objective exploited the FTCM approach to predict the most appropriate wood biomass for selected industrial applications. This study demonstrated that treatment with enzymes from *Trichoderma* is appropriate for generating crystalline cellulose at fiber surface. Applications such as nanocellulose or composites requiring chemical resistance would benefit from this enzymatic treatment. The milder enzyme mixture from *Aspergillus* allowed for removal of non-crystalline (amorphous) cellulose while preserving hemicelluloses at fiber surface, which makes this treatment appropriate for new paper products where surface chemical responsiveness is required.

The fifth objective of this study demonstrated the use and adaptation of FTCM to study the potential correlation between surface-exposed polysaccharides and enzymatic hydrolysis of LCB. FTCM was originally optimized for pulp and paper investigations. Hence, we adapted this approach to a FTCM-depletion assay for LCB suspension analysis and monitored the impact of three different pretreatments on alfalfa stover, corn crop residues, cattail stems and flax shives. The results suggest that surface cellulose (total and non-crystalline) were strongly correlated with production of reducing sugars by hydrolysis, in a much better way than with total lignin and/or total cellulose content (using NREL/TP-510-42618 method) of LCB. The clear and robust correlations that were observed here, between the polysaccharides accessibility by FTCM probes and enzymatic hydrolysis of the biomasses, can be evolved into a powerful prediction tool for the simple, rapid and efficient determination of optimal biomass and pretreatment strategies for bioenergy production.

Throughout these studies, FTCM proved to be instrumental for our understanding of LCB processing, and exhibited both process optimizing and outcome predicting potential. Once adapted to to industrial constraints, we believe that FTCM could perform various functions, such as 1) help fine-tuning the conditions surrounding the mechanical and enzymatic removal of polysaccharides; 2) allow for decreasing costs associated with LCB processes; 3) expanding our understanding of biofuels and papermaking productions; 4) correlating surface polysaccharides with performances of the relevant lignocellulosic products; and 5) allow for improving the productivity of large-scale operations. This Ph.D. study testifies to the incredible versatility of CBMs as spearhead of innovations, which can successfully tackle biotechnological challenges. We anticipate that such advances would support engineers for increasing yields and mitigate production costs associated with LCB based industries.

# Bibliography


1. Lynd, L.R., Laser, M.S., Bransby, D., Dale, B.E., Davison, B., Hamilton, R., Himmel, M., Keller, M., McMillan, J.D., Sheehan, J., & Wyman, C.E. (2008). How biotech can transform biofuels. *Nature Biotechnology*, *26*(2), 169.
2. Wyman, C. E. (2007). What is (and is not) vital to advancing cellulosic ethanol. *TRENDS in Biotechnology*, *25*(4), 153-157.
3. Zhu, H., Luo, W., Ciesielski, P.N., Fang, Z., Zhu, J.Y., Henriksson, G., Himmel, M.E., & Hu, L. (2016). Wood-derived materials for green electronics, biological devices, and energy applications. *Chemical Reviews*, *116*(16), 9305-9374.
4. Wegner, T.H., Ireland, S., & Jones, J.P.E. (2013). *Cellulosic Nanomaterials: Sustainable Materials of Choice for the 21st Century*. In: Postek, M., Moon, R., Rudie, A., & Bilodeau, M., editors. Production and Applications of Cellulose Nanomaterials. TAPPI Press. p. 3–8.
5. Christopher, L. P. (2013). *Integrated forest biorefineries: current state and development potential*. In: Christopher, L. P., editor. Integrated Forest Biorefineries: challenges and opportunities. The Royal Society of Chemistry, Cambridge. p. 1–66.
6. Fargione, J., Hill, J., Tilman, D., Polasky, S., & Hawthorne, P. (2008). Land clearing and the biofuel carbon debt. *Science*, *319*(5867), 1235-1238.
7. Runge, C. F., & Senauer, B. (2007). How biofuels could starve the poor. *Foreign Affairs*, 41-53.
8. Mohr, A., & Raman, S. (2013). Lessons from first generation biofuels and implications for the sustainability appraisal of second generation biofuels. *Energy Policy*, *63*, 114-122.
9. Limayem, A., & Ricke, S. C. (2012). Lignocellulosic biomass for bioethanol production: current perspectives, potential issues and future prospects. *Progress in Energy and Combustion Science*, *38*(4), 449-467.

10. Hu, G., Heitmann, J. A., & Rojas, O. J. (2008). Feedstock pretreatment strategies for producing ethanol from wood, bark, and forest residues. *BioResources*, *3*(1), 270-294.
11. Cardona, C. A., Quintero, J. A., & Paz, I. C. (2010). Production of bioethanol from sugarcane bagasse: status and perspectives. *Bioresource Technology*, *101*(13), 4754-4766.
12. Hoadley, R. B. (2000). *Understanding wood: a craftsman's guide to wood technology*. Taunton press.
13. Markwardt, L. J., & Wilson, T. R. C. (1935). *Strength and related properties of woods grown in the United States* (No. 479). US Government Printing Office.
14. Zhu, J. Y., & Pan, X. J. (2010). Woody biomass pretreatment for cellulosic ethanol production: technology and energy consumption evaluation. *Bioresource Technology*, *101*(13), 4992-5002.
15. Knauf, M., & Moniruzzaman, M. (2004). Lignocellulosic biomass processing: A perspective. *International Sugar Journal*, *106*(1263), 147-150.
16. Rodolfi, L., Chini Zittelli, G., Bassi, N., Padovani, G., Biondi, N., Bonini, G., & Tredici, M. R. (2009). Microalgae for oil: Strain selection, induction of lipid synthesis and outdoor mass cultivation in a low-cost photobioreactor. *Biotechnology and Bioengineering*, *102*(1), 100-112.
17. Ferrell, J., & Sarisky-Reed, V. (2010). *National algal biofuels technology roadmap* (No. DOE/EE--0332). EERE Publication and Product Library.
18. Demirbas, A. (2010). Use of algae as biofuel sources. *Energy Conversion and Management*, *51*(12), 2738-2749.
19. Hendriks, A. T. W. M., & Zeeman, G. (2009). Pretreatments to enhance the digestibility of lignocellulosic biomass. *Bioresource Technology*, *100*(1), 10-18.
20. Subramaniyan, S., & Prema, P. (2002). Biotechnology of microbial xylanases: enzymology, molecular biology, and application. *Critical Reviews in Biotechnology*, *22*(1), 33-64.

21. Pérez, J., Munoz-Dorado, J., de la Rubia, T. D. L. R., & Martinez, J. (2002). Biodegradation and biological treatments of cellulose, hemicellulose and lignin: an overview. *International Microbiology*, *5*(2), 53-63.

22. Hall, M., Bansal, P., Lee, J. H., Realff, M. J., & Bommarius, A. S. (2010). Cellulose crystallinity–a key predictor of the enzymatic hydrolysis rate. *The FEBS Journal*, *277*(6), 1571-1582.

23. Demirbaş, A. (2005). Bioethanol from cellulosic materials: a renewable motor fuel from biomass. *Energy Sources*, *27*(4), 327-337.

24. Saha, B. C. (2003). Hemicellulose bioconversion. *Journal of Industrial Microbiology and Biotechnology*, *30*(5), 279-291.

25. Gírio, F. M., Fonseca, C., Carvalheiro, F., Duarte, L. C., Marques, S., & Bogel-Łukasik, R. (2010). Hemicelluloses for fuel ethanol: a review. *Bioresource Technology*, *101*(13), 4775-4800.

26. Timell, T. E. (1967). Recent progress in the chemistry of wood hemicelluloses. *Wood Science and Technology*, *1*(1), 45-70.

27. Jordan, D.B., Bowman, M.J., Braker, J.D., Dien, B.S., Hector, R.E., Lee, C.C., Mertens, J.A., & Wagschal, K. (2012). Plant cell walls to ethanol. *Biochemical Journal*, *442*(2), 241-252.

28. Penttilä, P.A., Várnai, A., Pere, J., Tammelin, T., Salmén, L., Siika-aho, M., Viikari, L., & Serimaa, R. (2013). Xylan as limiting factor in enzymatic hydrolysis of nanocellulose. *Bioresource Technology*, *129*, 135-141.

29. Kumar, P., Barrett, D. M., Delwiche, M. J., & Stroeve, P. (2009). Methods for pretreatment of lignocellulosic biomass for efficient hydrolysis and biofuel production. *Industrial & Engineering Chemistry Research*, *48*(8), 3713-3729.

30. Tolbert, A., Akinosho, H., Khunsupat, R., Naskar, A. K., & Ragauskas, A. J. (2014). Characterization and analysis of the molecular weight of lignin for biorefining studies. *Biofuels, Bioproducts and Biorefining*, *8*(6), 836-856.

31. Mielenz, J. R. (2001). Ethanol production from biomass: technology and commercialization status. *Current Opinion in Microbiology*, *4*(3), 324-329.

32. Li, C., Zheng, M., Wang, A., & Zhang, T. (2012). One-pot catalytic hydrocracking of raw woody biomass into chemicals over supported carbide catalysts: simultaneous conversion of cellulose, hemicellulose and lignin. *Energy & Environmental Science*, *5*(4), 6383-6390.

33. Ladisch, M. R., Mosier, N. S., Kim, Y., Ximenes, E., & Hogsett, D. (2010). Converting cellulose to biofuels. *Chemical Engineering Progress*, *106*(3), 56-63.

34. Himmel, M. E., Ding, S. Y., Johnson, D. K., Adney, W. S., Nimlos, M. R., Brady, J. W., & Foust, T. D. (2007). Biomass recalcitrance: engineering plants and enzymes for biofuels production. *Science*, *315*(5813), 804-807.

35. Jørgensen, H., Kristensen, J. B., & Felby, C. (2007). Enzymatic conversion of lignocellulose into fermentable sugars: challenges and opportunities. *Biofuels, Bioproducts and Biorefining*, *1*(2), 119-134.

36. Li, M., Tu, M., Cao, D., Bass, P., & Adhikari, S. (2013). Distinct roles of residual xylan and lignin in limiting enzymatic hydrolysis of organosolv pretreated loblolly pine and sweetgum. *Journal of Agricultural and Food Chemistry*, *61*(3), 646-654.

37. Lynd, L. R., Wyman, C. E., & Gerngross, T. U. (1999). Biocommodity engineering. *Biotechnology Progress*, *15*(5), 777-793.

38. Waldron, K. W. (Ed.). (2010). *Bioalcohol production: biochemical conversion of lignocellulosic biomass*. Elsevier. Pp. 73–121.

39. Wyman, C. E. (Ed.). (2013). *Aqueous pretreatment of plant biomass for biological and chemical conversion to fuels and chemicals*. John Wiley & Sons. pp. 281–310.

40. Studer, M.H., DeMartini, J.D., Davis, M.F., Sykes, R.W., Davison, B., Keller, M., Tuskan, G.A., & Wyman, C. E. (2011). Lignin content in natural Populus variants affects sugar release. *Proceedings of the National Academy of Sciences*, *108*(15), 6300-6305.

41. Ding, S. Y., Liu, Y. S., Zeng, Y., Himmel, M. E., Baker, J. O., & Bayer, E. A. (2012). How does plant cell wall nanoscale architecture correlate with enzymatic digestibility?. *Science*, *338*(6110), 1055-1060.

42. Kumar, R., Tabatabaei, M., Karimi, K., & Sárvári Horváth, I. (2016). Recent updates on lignocellulosic biomass derived ethanol-A review. *Biofuel Research Journal*, *3*(1), 347-356.

43. Wyman, C.E., Dale, B.E., Balan, V., Elander, R.T., Holtzapple, M.T., Ramirez, R.S., Ladisch, M.R., Mosier, N.S., Lee, Y.Y., Gupta, R., & Thomas, S. R. (2013). Comparative performance of leading pretreatment technologies for biological conversion of corn stover, poplar wood, and switchgrass to sugars. *Aqueous Pretreatment of Plant Biomass for Biological and Chemical Conversion to Fuels and Chemicals*, 239-259.

44. Millett, M. A., Baker, A. J., & Satter, L. D. (1976). *Pretreatments to enhance chemical, enzymatic, and microbiological attack of cellulosic materials*. US Department of Agriculture, Forest Service, Forest Products Laboratory.

45. Cadoche, L., & López, G. D. (1989). Assessment of size reduction as a preliminary step in the production of ethanol from lignocellulosic wastes. *Biological Wastes*, *30*(2), 153-157.

46. Grethlein, H. E., & Converse, A. O. (1991). Common aspects of acid prehydrolysis and steam explosion for pretreating wood. *Bioresource Technology*, *36*(1), 77-82.

47. Yang, B., & Wyman, C. E. (2009). Dilute acid and autohydrolysis pretreatment. In *Biofuels* (pp. 103-114). Humana Press, Totowa, NJ.

48. Bali, G., Meng, X., Deneff, J. I., Sun, Q., & Ragauskas, A. J. (2015). The effect of alkaline pretreatment methods on cellulose structure and accessibility. *ChemSusChem*, *8*(2), 275-279.

49. Sathitsuksanoh, N., Zhu, Z., Templeton, N., Rollin, J. A., Harvey, S. P., & Zhang, Y. P. (2009). Saccharification of a potential bioenergy crop, Phrag-

mites australis (common reed), by lignocellulose fractionation followed by enzymatic hydrolysis at decreased cellulase loadings. *Industrial & Engineering Chemistry Research*, *48*(13), 6441-6447.

50. Zhang, Y.H.P., Ding, S.Y., Mielenz, J.R., Cui, J.B., Elander, R.T., Laser, M., Himmel, M.E., McMillan, J.R., & Lynd, L. R. (2007). Fractionating recalcitrant lignocellulose at modest reaction conditions. *Biotechnology and Bioengineering*, *97*(2), 214-223.

51. Zhu, Z., Sathitsuksanoh, N., Vinzant, T., Schell, D. J., McMillan, J. D., & Zhang, Y. H. P. (2009). Comparative study of corn stover pretreated by dilute acid and cellulose solvent-based lignocellulose fractionation: Enzymatic hydrolysis, supramolecular structure, and substrate accessibility. *Biotechnology and Bioengineering*, *103*(4), 715-724.

52. Bobleter, O., Niesner, R., & Röhr, M. (1976). The hydrothermal degradation of cellulosic matter to sugars and their fermentative conversion to protein. *Journal of Applied Polymer Science*, *20*(8), 2083-2093.

53. Mosier, N., Wyman, C., Dale, B., Elander, R., Lee, Y. Y., Holtzapple, M., & Ladisch, M. (2005). Features of promising technologies for pretreatment of lignocellulosic biomass. *Bioresource Technology*, *96*(6), 673-686.

54. Zhang, Y. H. P., & Lynd, L. R. (2006). A functionally based model for hydrolysis of cellulose by fungal cellulase. *Biotechnology and Bioengineering*, *94*(5), 888-898.

55. Rollin, J. A., Zhu, Z., Sathitsuksanoh, N., & Zhang, Y. H. P. (2011). Increasing cellulose accessibility is more important than removing lignin: A comparison of cellulose solvent-based lignocellulose fractionation and soaking in aqueous ammonia. *Biotechnology and Bioengineering*, *108*(1), 22-30.

56. Yang, B., & Wyman, C. E. (2008). Pretreatment: the key to unlocking low-cost cellulosic ethanol. *Biofuels, Bioproducts and Biorefining*, *2*(1), 26-40.

57. Igarashi, K., Uchihashi, T., Koivula, A., Wada, M., Kimura, S., Okamoto, T., Penttilä, M., Ando, T., & Samejima, M. (2011). Traffic jams reduce hydrolytic efficiency of cellulase on cellulose surface. *Science*, *333*(6047), 1279-1282.

58. Zhu, L., O'Dwyer, J. P., Chang, V. S., Granda, C. B., & Holtzapple, M. T. (2008). Structural features affecting biomass enzymatic digestibility. *Bioresource Technology*, *99*(9), 3817-3828.

59. Mansfield, S. D., Mooney, C., & Saddler, J. N. (1999). Substrate and enzyme characteristics that limit cellulose hydrolysis. *Biotechnology Progress*, *15*(5), 804-816.

60. Chundawat, S.P., Donohoe, B.S., da Costa Sousa, L., Elder, T., Agarwal, U.P., Lu, F., Ralph, J., Himmel, M.E., Balan, V., & Dale, B. E. (2011). Multi-scale visualization and characterization of lignocellulosic plant cell wall deconstruction during thermochemical pretreatment. *Energy & Environmental Science*, *4*(3), 973-984.

61. DeMartini, J. D., Pattathil, S., Miller, J. S., Li, H., Hahn, M. G., & Wyman, C. E. (2013). Investigating plant cell wall components that affect biomass recalcitrance in poplar and switchgrass. *Energy & Environmental Science*, *6*(3), 898-909.

62. Hu, J., Arantes, V., & Saddler, J. N. (2011). The enhancement of enzymatic hydrolysis of lignocellulosic substrates by the addition of accessory enzymes such as xylanase: is it an additive or synergistic effect?. *Biotechnology for Biofuels*, *4*(1), 36.

63. Selig, M. J., Vinzant, T. B., Himmel, M. E., & Decker, S. R. (2009). The effect of lignin removal by alkaline peroxide pretreatment on the susceptibility of corn stover to purified cellulolytic and xylanolytic enzymes. *Applied Biochemistry and Biotechnology*, *155*(1-3), 94-103.

64. Bura, R., Chandra, R., & Saddler, J. (2009). Influence of xylan on the enzymatic hydrolysis of steam-pretreated corn stover and hybrid poplar. *Biotechnology Progress*, *25*(2), 315-322.

65. Frommhagen, M., Sforza, S., Westphal, A.H., Visser, J., Hinz, S.W., Koetsier, M.J., van Berkel, W.J., Gruppen, H., & Kabel, M. A. (2015). Discovery of the combined oxidative cleavage of plant xylan and cellulose by a new fungal polysaccharide monooxygenase. *Biotechnology for Biofuels*, *8*(1), 101.

66. Suurnäkki, A., Li, T. Q., Buchert, J., Tenkanen, M., Viikari, L., Vuorinen, T., & Ödberg, L. (1997). Effects of enzymatic removal of xylan and glucomannan on the pore size distribution of kraft fibres. *Holzforschung-International Journal of the Biology, Chemistry, Physics and Technology of Wood*, *51*(1), 27-33.

67. Vincken, J. P., de Keizer, A., Beldman, G., & Voragen, A. G. J. (1995). Fractionation of xyloglucan fragments and their interaction with cellulose. *Plant Physiology*, *108*(4), 1579-1585.

68. Oksanen, T., Buchert, J., & Viikari, L. (1997). The role of hemicelluloses in the hornification of bleached kraft pulps. *Holzforschung-International Journal of the Biology, Chemistry, Physics and Technology of Wood*, *51*(4), 355-360.

69. Köhnke, T., Lund, K., Brelid, H., & Westman, G. (2010). Kraft pulp hornification: A closer look at the preventive effect gained by glucuronoxylan adsorption. *Carbohydrate Polymers*, *81*(2), 226-233.

70. Zhang, J., Siika-aho, M., Tenkanen, M., & Viikari, L. (2011). The role of acetyl xylan esterase in the solubilization of xylan and enzymatic hydrolysis of wheat straw and giant reed. *Biotechnology for Biofuels*, *4*(1), 60.

71. Berlin, A., Maximenko, V., Gilkes, N., & Saddler, J. (2007). Optimization of enzyme complexes for lignocellulose hydrolysis. *Biotechnology and Bioengineering*, *97*(2), 287-296.

72. Öhgren, K., Bura, R., Saddler, J., & Zacchi, G. (2007). Effect of hemicellulose and lignin removal on enzymatic hydrolysis of steam pretreated corn stover. *Bioresource Technology*, *98*(13), 2503-2510.

73. Gübitz, G. M., Stebbing, D. W., Johansson, C. I., & Saddler, J. N. (1998). Lignin-hemicellulose complexes restrict enzymatic solubilization of mannan and xylan from dissolving pulp. *Applied Microbiology and Biotechnology*, *50*(3), 390-395.

74. García-Aparicio, M. P., Ballesteros, M., Manzanares, P., Ballesteros, I., González, A., & Negro, M. J. (2007). Xylanase contribution to the efficiency of cellulose enzymatic hydrolysis of barley straw. In *Applied Biochemistry and Biotecnology* (pp. 353-365). Humana Press.

75. Kumar, R., & Wyman, C. E. (2009). Effects of cellulase and xylanase enzymes on the deconstruction of solids from pretreatment of poplar by leading technologies. *Biotechnology Progress*, *25*(2), 302-314.

76. Kumar, R., & Wyman, C. E. (2014). Strong cellulase inhibition by Mannan polysaccharides in cellulose conversion to sugars. *Biotechnology and Bioengineering*, *111*(7), 1341-1353.

77. Qing, Q., & Wyman, C. E. (2011). Supplementation with xylanase and β-xylosidase to reduce xylo-oligomer and xylan inhibition of enzymatic hydrolysis of cellulose and pretreated corn stover. *Biotechnology for Biofuels*, *4*(1), 18.

78. Várnai, A., Huikko, L., Pere, J., Siika-Aho, M., & Viikari, L. (2011). Synergistic action of xylanase and mannanase improves the total hydrolysis of softwood. *Bioresource Technology*, *102*(19), 9096-9104.

79. Klein-Marcuschamer, D., Oleskowicz-Popiel, P., Simmons, B. A., & Blanch, H. W. (2012). The challenge of enzyme cost in the production of lignocellulosic biofuels. *Biotechnology and Bioengineering*, *109*(4), 1083-1087.

80. Ximenes, E., Kim, Y., Mosier, N., Dien, B., & Ladisch, M. (2010). Inhibition of cellulases by phenols. *Enzyme and Microbial Technology*, *46*(3-4), 170-176.

81. Kim, Y., Ximenes, E., Mosier, N. S., & Ladisch, M. R. (2011). Soluble inhibitors/deactivators of cellulase enzymes from lignocellulosic biomass. *Enzyme and Microbial Technology*, *48*(4-5), 408-415.

82. Mandels, M., & Reese, E. T. (1965). Inhibition of cellulases. *Annual Review of Phytopathology*, *3*(1), 85-102.

83. Reese, E. T., & Mandels, M. (1980). Stability of the cellulase of Trichoderma reesei under use conditions. *Biotechnology and Bioengineering*, *22*(2), 323-335.

84. Halliwell, G., & Griffin, M. (1973). The nature and mode of action of the cellulolytic component C1 of Trichoderma koningii on native cellulose. *Biochemical Journal*, *135*(4), 587.

85. Kumar, R., & Wyman, C. E. (2008). An improved method to directly estimate cellulase adsorption on biomass solids. *Enzyme and Microbial Technology*, *42*(5), 426-433.

86. Kumar, R., & Wyman, C. E. (2009). Effect of enzyme supplementation at moderate cellulase loadings on initial glucose and xylose release from corn stover solids pretreated by leading technologies. *Biotechnology and Bioengineering*, *102*(2), 457-467.

87. Qing, Q., Yang, B., & Wyman, C. E. (2010). Xylooligomers are strong inhibitors of cellulose hydrolysis by enzymes. *Bioresource Technology*, *101*(24), 9624-9630.

88. Holtzapple, M., Cognata, M., Shu, Y., & Hendrickson, C. (1990). Inhibition of Trichoderma reesei cellulase by sugars and solvents. *Biotechnology and Bioengineering*, *36*(3), 275-287.

89. Andrić, P., Meyer, A. S., Jensen, P. A., & Dam-Johansen, K. (2010). Reactor design for minimizing product inhibition during enzymatic lignocellulose hydrolysis: I. Significance and mechanism of cellobiose and glucose inhibition on cellulolytic enzymes. *Biotechnology Advances*, *28*(3), 308-324.

90. Culbertson, A., Jin, M., da Costa Sousa, L., Dale, B. E., & Balan, V. (2013). In-house cellulase production from AFEX™ pretreated corn stover using Trichoderma reesei RUT C-30. *RSC Advances*, *3*(48), 25960-25969.

91. Hong, Y., Nizami, A. S., Pour Bafrani, M., Saville, B. A., & MacLean, H. L. (2013). Impact of cellulase production on environmental and financial metrics for lignocellulosic ethanol. *Biofuels, Bioproducts and Biorefining*, *7*(3), 303-313.

92. Stephen, J. D., Mabee, W. E., & Saddler, J. N. (2012). Will second-generation ethanol be able to compete with first-generation ethanol? Opportunities for cost reduction. *Biofuels, Bioproducts and Biorefining*, *6*(2), 159-176.

93. Zhang, Y. H. P., Himmel, M. E., & Mielenz, J. R. (2006). Outlook for cellulase improvement: screening and selection strategies. *Biotechnology Advances*, *24*(5), 452-481.

94. Zhang, Z., Donaldson, A. A., & Ma, X. (2012). Advancements and future directions in enzyme technology for biomass conversion. *Biotechnology Advances*, *30*(4), 913-919.

95. Kumar, R., & Wyman, C. E. (2009). Effect of additives on the digestibility of corn stover solids following pretreatment by leading technologies. *Biotechnology and Bioengineering*, *102*(6), 1544-1557.

96. Kumar, R., & Wyman, C. E. (2009). Effects of cellulase and xylanase enzymes on the deconstruction of solids from pretreatment of poplar by leading technologies. *Biotechnology Progress*, *25*(2), 302-314.

97. Yang, B., & Wyman, C. E. (2006). BSA treatment to enhance enzymatic hydrolysis of cellulose in lignin containing substrates. *Biotechnology and Bioengineering*, *94*(4), 611-617.

98. Nguyen, T. Y., Cai, C. M., Osman, O., Kumar, R., & Wyman, C. E. (2016). CELF pretreatment of corn stover boosts ethanol titers and yields from high solids SSF with low enzyme loadings. *Green Chemistry*, *18*(6), 1581-1589.

99. Nguyen, T. Y., Cai, C. M., Kumar, R., & Wyman, C. E. (2015). Co-solvent pretreatment reduces costly enzyme requirements for high sugar and ethanol yields from lignocellulosic biomass. *ChemSusChem*, *8*(10), 1716-1725.

100. Merino, S. T., & Cherry, J. (2007). Progress and challenges in enzyme development for biomass utilization. In *Biofuels* (pp. 95-120). Springer, Berlin, Heidelberg.

101. Ogeda, T. L., & Petri, D. F. (2010). Biomass enzymatic hydrolysis. *Quimica Nova*, *33*(7), 1549-1558.

102. Pribowo, A. Y., Hu, J., Arantes, V., & Saddler, J. N. (2013). The development and use of an ELISA-based method to follow the distribution of cellulase monocomponents during the hydrolysis of pretreated corn stover. *Biotechnology for Biofuels*, *6*(1), 80.

103. Di Risio, S., Hu, C. S., Saville, B. A., Liao, D., & Lortie, J. (2011). Large-scale, high-solids enzymatic hydrolysis of steam-exploded poplar. *Biofuels, Bioproducts and Biorefining*, *5*(6), 609-620.

104. Bajpai, P. (1999). Application of enzymes in the pulp and paper industry. *Biotechnology Progress*, *15*(2), 147-157.

105. Roncero, M. B., Torres, A. L., Colom, J. F., & Vidal, T. (2005). The effect of xylanase on lignocellulosic components during the bleaching of wood pulps. *Bioresource Technology*, *96*(1), 21-30.

106. Viikari, L., Kantelinen, A., Sundquist, J., & Linko, M. (1994). Xylanases in bleaching: from an idea to the industry. *FEMS Microbiology Reviews*, *13*(2-3), 335-350.

107. Roberts, J. C., McCarthy, A. J., Flynn, N. J., & Broda, P. (1990). Modification of paper properties by the pretreatment of pulp with Saccharomonospora viridis xylanase. *Enzyme and Microbial Technology*, *12*(3), 210-213.

108. Savitha, S., Sadhasivam, S., & Swaminathan, K. (2009). Modification of paper properties by the pretreatment of wastepaper pulp with Graphium putredinis, Trichoderma harzianum and fusant xylanases. *Bioresource Technology*, *100*(2), 883-889.

109. Johansson, L. S. (2002). Monitoring fibre surfaces with XPS in papermaking processes. *Microchimica Acta*, *138*(3-4), 217-223.

110. Fardim, P., & Durán, N. (2003). Modification of fibre surfaces during pulping and refining as analysed by SEM, XPS and ToF-SIMS. *Colloids and Surfaces A: Physicochemical and Engineering Aspects*, *223*(1-3), 263-276.

111. Fardim, P., Gustafsson, J., von Schoultz, S., Peltonen, J., & Holmbom, B. (2005). Extractives on fiber surfaces investigated by XPS, ToF-SIMS and AFM. *Colloids and Surfaces A: Physicochemical and Engineering Aspects*, *255*(1-3), 91-103.

112. Belgacem, M. N., Czeremuszkin, G., Sapieha, S., & Gandini, A. (1995). Surface characterization of cellulose fibres by XPS and inverse gas chromatography. *Cellulose*, *2*(3), 145-157.

113. Matuana, L. M., Balatinecz, J. J., Sodhi, R. N. S., & Park, C. B. (2001). Surface characterization of esterified cellulosic fibers by XPS and FTIR spectroscopy. *Wood Science and Technology*, *35*(3), 191-201.

114. Li, J., Kisara, K., Danielsson, S., Lindström, M. E., & Gellerstedt, G. (2007). An improved methodology for the quantification of uronic acid units in xylans and other polysaccharides. *Carbohydrate Research*, *342*(11), 1442-1449.

115. Sluiter, A., Hames, B., Ruiz, R., Scarlata, C., Sluiter, J., Templeton, D., & Crocker, D. (2008). Determination of structural carbohydrates and lignin in biomass. *Laboratory Analytical Procedure*, *1617*, 1-16.

116. Lupoi, J. S., Singh, S., Simmons, B. A., & Henry, R. J. (2014). Assessment of lignocellulosic biomass using analytical spectroscopy: an evolution to high-throughput techniques. *BioEnergy Research*, *7*(1), 1-23.

117. Andrade, J. D. (1985). X-ray photoelectron spectroscopy (XPS). In *Surface and Interfacial Aspects of Biomedical Polymers* (pp. 105-195). Springer, Boston, MA.

118. Knox, J. P. (2012). In situ detection of cellulose with carbohydrate-binding modules. In *Methods in Enzymology* (Vol. 510, pp. 233-245). Academic Press.

119. Knox, J. P. (2008). Revealing the structural and functional diversity of plant cell walls. *Current Opinion in Plant Biology*, *11*(3), 308-313.

120. Hervé, C., Marcus, S. E., & Knox, J. P. (2011). Monoclonal antibodies, carbohydrate-binding modules, and the detection of polysaccharides in plant cell walls. In *The Plant Cell Wall* (pp. 103-113). Humana Press, Totowa, NJ.

121. Oliveira, C., Carvalho, V., Domingues, L., & Gama, F. M. (2015). Recombinant CBM-fusion technology—applications overview. *Biotechnology Advances*, *33*(3-4), 358-369.

122. Arantes, V., & Saddler, J. N. (2010). Access to cellulose limits the efficiency of enzymatic hydrolysis: the role of amorphogenesis. *Biotechnology for Biofuels*, *3*(1), 4.

123. Gilkes, N. R., Henrissat, B., Kilburn, D. G., Miller, R. C., & Warren, R. (1991). Domains in microbial beta-1, 4-glycanases: sequence conservation, function, and enzyme families. *Microbiological Reviews*, *55*(2), 303-315.

124. Boraston, A. B., Bolam, D. N., Gilbert, H. J., & Davies, G. J. (2004). Carbohydrate-binding modules: fine-tuning polysaccharide recognition. *Biochemical Journal*, *382*(3), 769-781.

125. Gao, S., You, C., Renneckar, S., Bao, J., & Zhang, Y. H. P. (2014). New insights into enzymatic hydrolysis of heterogeneous cellulose by using carbohydrate-binding module 3 containing GFP and carbohydrate-binding module 17 containing CFP. *Biotechnology for Biofuels*, *7*(1), 24.

126. Nagy, T., Simpson, P., Williamson, M. P., Hazlewood, G. P., Gilbert, H. J., & Orosz, L. (1998). All three surface tryptophans in Type IIa cellulose binding domains play a pivotal role in binding both soluble and insoluble ligands. *FEBS Letters*, *429*(3), 312-316.

127. Tormo, J., Lamed, R., Chirino, A. J., Morag, E., Bayer, E. A., Shoham, Y., & Steitz, T. A. (1996). Crystal structure of a bacterial family-III cellulose-binding domain: a general mechanism for attachment to cellulose. *The EMBO Journal*, *15*(21), 5739-5751.

128. McLean, B. W., Bray, M. R., Boraston, A. B., Gilkes, N. R., Haynes, C. A., & Kilburn, D. G. (2000). Analysis of binding of the family 2a carbohydrate-binding module from Cellulomonas fimi xylanase 10A to cellulose: specificity and identification of functionally important amino acid residues. *Protein Engineering*, *13*(11), 801-809.

129. Gilbert, H. J., Knox, J. P., & Boraston, A. B. (2013). Advances in understanding the molecular basis of plant cell wall polysaccharide recognition by carbohydrate-binding modules. *Current Opinion in Structural Biology*, *23*(5), 669-677.

130. Lynd, L. R., Weimer, P. J., Van Zyl, W. H., & Pretorius, I. S. (2002). Microbial cellulose utilization: fundamentals and biotechnology. *Microbiology and Molecular Biology Reviews*, *66*(3), 506-577.

131. Raghothama, S., Simpson, P. J., Szabó, L., Nagy, T., Gilbert, H. J., & Williamson, M. P. (2000). Solution structure of the CBM10 cellulose binding module from Pseudomonas xylanase A. *Biochemistry*, *39*(5), 978-984.

132. Irwin, D. C., Spezio, M., Walker, L. P., & Wilson, D. B. (1993). Activity studies of eight purified cellulases: specificity, synergism, and binding domain effects. *Biotechnology and Bioengineering*, *42*(8), 1002-1013.

133. Wang, L., Zhang, Y., & Gao, P. (2008). A novel function for the cellulose binding module of cellobiohydrolase I. *Science in China Series C: Life Sciences*, *51*(7), 620-629.

134. Gao, P. J., Chen, G. J., Wang, T. H., Zhang, Y. S., & Liu, J. (2001). Non-hydrolytic Disruption of Crystalline Structure of Cellulose by Cellulose Binding Domain and Linker Sequence of Cellobiohydrolase I from Penicillium janthinellum. *Sheng wu hua xue yu sheng wu wu li xue bao Acta Biochimica et Biophysica Sinica*, *33*(1), 13-18.

135. Pinto, R., Moreira, S., Mota, M., & Gama, M. (2004). Studies on the cellulose-binding domains adsorption to cellulose. *Langmuir*, *20*(4), 1409-1413.

136. Southall, S. M., Simpson, P. J., Gilbert, H. J., Williamson, G., & Williamson, M. P. (1999). The starch-binding domain from glucoamylase disrupts the structure of starch. *FEBS Letters*, *447*(1), 58-60.

137. Sorimachi, K., Le Gal-Coëffet, M. F., Williamson, G., Archer, D. B., & Williamson, M. P. (1997). Solution structure of the granular starch binding domain of Aspergillus niger glucoamylase bound to β-cyclodextrin. *Structure*, *5*(5), 647-661.

138. Klyosov, A. A. (1990). Trends in biochemistry and enzymology of cellulose degradation. *Biochemistry*, *29*(47), 10577-10585.

139. Klyosov, A. A., & Rabinowitch, M. L. (1980). *Enzymatic conversion of cellulose to glucose: present state of the art and potential.* In *Enzyme Engineering* (pp. 83-165). Springer, Boston, MA.

140. Esteghlalian, A. R., Srivastava, V., Gilkes, N., Gregg, D. J., & Saddler, J. N. (2001). *An overview of factors influencing the enzymatic hydrolysis of lignocellulosic feedstocks*. In: Himmel, M.E., Baker, W., Saddler, J.N. (Eds.), Glycosyl Hydrolases for Biomass Conversion. ACS, pp. 100–111.

141. Levy, I., & Shoseyov, O. (2002). Cellulose-binding domains: biotechnological applications. *Biotechnology Advances*, *20*(3-4), 191-213.

142. Shoseyov, O., Shani, Z., & Levy, I. (2006). Carbohydrate binding modules: biochemical properties and novel applications. *Microbiology and Molecular Biology Reviews*, *70*(2), 283-295.

143. Berdichevsky, Y., Lamed, R., Frenkel, D., Gophna, U., Bayer, E.A., Yaron, S., Shoham, Y., & Benhar, I. (1999). Matrix-assisted refolding of single-chain Fv–cellulose binding domain fusion proteins. *Protein Expression and Purification*, *17*(2), 249-259.

144. Berdichevsky, Y., Ben-Zeev, E., Lamed, R., & Benhar, I. (1999). Phage display of a cellulose binding domain from Clostridium thermocellum and its application as a tool for antibody engineering. *Journal of Immunological Methods*, *228*(1-2), 151-162.

145. Cavaco-Paulo, A. (1998). Mechanism of cellulase action in textile processes. *Carbohydrate Polymers*, *37*(3), 273-277.

146. Berry, M. J., Davis, P. J., & Gidley, M. J. (2001). *U.S. Patent No. 6,225,462*. Washington, DC: U.S. Patent and Trademark Office.

147. Hsu, S. H., Whu, S. W., Hsieh, S. C., Tsai, C. L., Chen, D. C., & Tan, T. S. (2004). Evaluation of chitosan-alginate-hyaluronate complexes modified by an RGD-containing protein as tissue-engineering scaffolds for cartilage regeneration. *Artificial Organs*, *28*(8), 693-703.

148. Hsu, S. H., Chu, W. P., Lin, Y. S., Chiang, Y. L., Chen, D. C., & Tsai, C. L. (2004). The effect of an RGD-containing fusion protein CBD-RGD in promoting cellular adhesion. *Journal of Biotechnology*, *111*(2), 143-154.

149. Xu, Z., Bae, W., Mulchandani, A., Mehra, R. K., & Chen, W. (2002). Heavy metal removal by novel CBD-EC20 sorbents immobilized on cellulose. *Biomacromolecules*, *3*(3), 462-465.

150. Kauffmann, C., Shoseyov, O., Shpigel, E., Bayer, E. A., Lamed, R., Shoham, Y., & Mandelbaum, R. T. (2000). Novel methodology for enzymatic removal

of atrazine from water by CBD-fusion protein immobilized on cellulose. *Environmental Science & Technology*, *34*(7), 1292-1296.

151. Levy, I., Ward, G., Hadar, Y., Shoseyov, O., & Dosoretz, C. G. (2003). Oxidation of 4-bromophenol by the recombinant fused protein cellulose-binding domain-horseradish peroxidase immobilized on cellulose. *Biotechnology and Bioengineering*, *82*(2), 223-231.

152. McCartney, L., Gilbert, H. J., Bolam, D. N., Boraston, A. B., & Knox, J. P. (2004). Glycoside hydrolase carbohydrate-binding modules as molecular probes for the analysis of plant cell wall polymers. *Analytical Biochemistry*, *326*(1), 49-54.

153. Jamal-Talabani, S., Boraston, A. B., Turkenburg, J. P., Tarbouriech, N., Ducros, V. M. A., & Davies, G. J. (2004). Ab initio structure determination and functional characterization of CBM36: a new family of calcium-dependent carbohydrate binding modules. *Structure*, *12*(7), 1177-1187.

154. Phelps, M. R., Hobbs, J. B., Kilburn, D. G., & Turner, R. F. (1994). Technology for regenerable biosensor probes based on enzyme-cellulose binding domain conjugates. *Biotechnology Progress*, *10*(4), 433-440.

155. Shoseyov, O., Shpiegl, I., Goldstein, M. A., & Doi, R. H. (1999). *U.S. Patent No. 5,856,201*. Washington, DC: U.S. Patent and Trademark Office.

156. Ofir, K., Berdichevsky, Y., Benhar, I., Azriel-Rosenfeld, R., Lamed, R., Barak, Y., Bayer, E.A., & Morag, E. (2005). Versatile protein microarray based on carbohydrate-binding modules. *Proteomics*, *5*(7), 1806-1814.

157. Cavaco–Paulo, A., Morgado, J., Andreaus, J., & Kilburn, D. (1999). Interactions of cotton with CBD peptides. *Enzyme and Microbial Technology*, *25*(8-9), 639-643.

158. Pala, H., Lemos, M. A., Mota, M., & Gama, F. M. (2001). Enzymatic upgrade of old paperboard containers. *Enzyme and Microbial Technology*, *29*(4-5), 274-279.

159. Ramos, R., Pinto, R., Mota, M., Sampaio, L., & Gama, F. M. (2007). Textile depilling: Superior finishing using cellulose-binding domains with residual enzymatic activity. *Biocatalysis and Biotransformation*, *25*(1), 35-42.

160. Machado, J., Araújo, A., Pinto, R., & Gama, F. M. (2009). Studies on the interaction of the carbohydrate binding module 3 from the Clostridium thermocellum CipA scaffolding protein with cellulose and paper fibres. *Cellulose*, *16*(5), 817-824.

161. Shi, X., Zheng, F., Pan, R., Wang, J., & Ding, S. (2014). Engineering and comparative characteristics of double carbohydrate binding modules as a strength additive for papermaking applications. *Bioresources*, *9*(2), 3117-3131.

162. Degani, O., Gepstein, S., & Dosoretz, C. G. (2004). A new method for measuring scouring efficiency of natural fibers based on the cellulose-binding domain-β-glucuronidase fused protein. *Journal of Biotechnology*, *107*(3), 265-273.

163. Lakowicz JR. Principles of fluorescence spectroscopy. Springer Science & Business Media; 2013.

164. Ding, S., Xu, Q., Ali, M.K., Baker, J.O., Bayer, E.A., Barak, Y., Lamed, R., Sugiyama, J., Rumbles, G., & Himmel, M. E. (2006). Versatile derivatives of carbohydrate-binding modules for imaging of complex carbohydrates approaching the molecular level of resolution. *Biotechniques*, *41*(4), 435.

165. Kawakubo, T., Karita, S., Araki, Y., Watanabe, S., Oyadomari, M., Takada, R., Tanaka, F., Abe, K., Watanabe, T., Honda, Y., & Watanabe, T. (2010). Analysis of exposed cellulose surfaces in pretreated wood biomass using carbohydrate-binding module (CBM)–cyan fluorescent protein (CFP). *Biotechnology and Bioengineering*, *105*(3), 499-508.

166. Shimomura, O., Johnson, F. H., & Saiga, Y. (1962). Extraction, purification and properties of aequorin, a bioluminescent protein from the luminous hydromedusan, Aequorea. *Journal of Cellular Physiology*, *59*(3), 223-239.

167. Tsien, R. Y. (1998). The green fluorescent protein. 509-544.

168. Shaner, N. C., Steinbach, P. A., & Tsien, R. Y. (2005). A guide to choosing fluorescent proteins. *Nature Methods*, *2*(12), 905.

169. Tsien, R. Y. (2005). Building and breeding molecules to spy on cells and tumors. *FEBS Letters*, *579*(4), 927-932.

170. Zimmer, M. (2002). Green fluorescent protein (GFP): applications, structure, and related photophysical behavior. *Chemical Reviews*, *102*(3), 759-782.

171. Hong, J., Ye, X., & Zhang, Y. H. P. (2007). Quantitative determination of cellulose accessibility to cellulase based on adsorption of a nonhydrolytic fusion protein containing CBM and GFP with its applications. *Langmuir*, *23*(25), 12535-12540.

172. Notenboom, V., Boraston, A. B., Chiu, P., Freelove, A. C., Kilburn, D. G., & Rose, D. R. (2001). Recognition of cello-oligosaccharides by a family 17 carbohydrate-binding module: an X-ray crystallographic, thermodynamic and mutagenic study1. *Journal of Molecular Biology*, *314*(4), 797-806.

173. Szabó, L., Jamal, S., Xie, H., Charnock, S. J., Bolam, D. N., Gilbert, H. J., & Davies, G. J. (2001). Structure of a family 15 carbohydrate-binding module in complex with xylopentaose evidence that xylan binds in an approximate 3-fold helical conformation. *Journal of Biological Chemistry*, *276*(52), 49061-49065.

174. Boraston, A. B., Revett, T. J., Boraston, C. M., Nurizzo, D., & Davies, G. J. (2003). Structural and thermodynamic dissection of specific mannan recognition by a carbohydrate binding module, TmCBM27. *Structure*, *11*(6), 665-675.

# Appendix A

Khatri et al. Biotechnol Biofuels (2016) 9:74
DOI 10.1186/s13068-016-0486-1

Biotechnology for Biofuels

RESEARCH Open Access

# Specific tracking of xylan using fluorescent-tagged carbohydrate-binding module 15 as molecular probe

Vinay Khatri[1,2], Yannick Hébert-Ouellet[1,2], Fatma Meddeb-Mouelhi[1,2,3] and Marc Beauregard[1,2*]

**Abstract**

**Background:** Xylan has been identified as a physical barrier which limits cellulose accessibility by covering the outer surface of fibers and interfibrillar space. Therefore, tracking xylan is a prerequisite for understanding and optimizing lignocellulosic biomass processes.

**Results:** In this study, we developed a novel xylan tracking approach using a two-domain probe called OC15 which consists of a fusion of *Cellvibrio japonicus* carbohydrate-binding domain 15 with the fluorescent protein mOrange2. The new probe specifically binds to xylan with an affinity similar to that of CBM15. The sensitivity of the OC15-xylan detection approach was compared to that of standard methods such as X-ray photoelectron spectroscopy (XPS) and chemical composition analysis (NREL/TP-510-42618). All three approaches were used to analyze the variations of xylan content of kraft pulp fibers. XPS, which allows for surface analysis of fibers, did not clearly indicate changes in xylan content. Chemical composition analysis responded to the changes in xylan content, but did not give any specific information related to the fibers surface. Interestingly, only the OC15 probe enabled the highly sensitive detection of xylan variations at the surface of kraft pulp fibers. At variance with the other methods, the OC15 probe can be used in a high throughput format.

**Conclusions:** We developed a rapid and high throughput approach for the detection of changes in xylan exposure at the surface of paper fibers. The introduction of this method into the lignocellulosic biomass-based industries should revolutionize the understanding and optimization of most wood biomass processes.

**Keywords:** Carbohydrate-binding module, Fluorescent protein, Kraft pulp, X-ray photoelectron spectroscopy, Xylan, Xylanase

## Background

Lignocellulosic biomass is a major source of sugars for the production of biofuel [1, 2]; however, its production has always been hindered by several economical and technical obstacles [3, 4]. One of these obstacles is the complex structure of the lignocellulosic substrate. As a consequence, the enzymatic hydrolysis of lignocellulosic components to fermentable sugars is considered as one of the major rate-limiting and costly steps [3, 5–8]. One way to better understand and control hydrolysis of lignocellulosic biomass is to monitor the complex polymers composition of fibers at every stage of processing.

Lignocellulosic biomass is a complex structure consisting of cellulose (β-1,4-linked glucose polymer), hemicellulose (polysaccharide of varying compositions), and lignin [9]. Cellulose is the most abundant polysaccharide in nature and constitutes about 35–50 % of the total lignocellulosic biomass [10]. Hemicelluloses, which represent about 20–30 % of the total biomass, are the second most common polysaccharides [10, 11]. Unlike cellulose, hemicelluloses are heterogeneous polymers of pentoses (xylose, arabinose), hexoses (mannose, glucose, galactose), and/or uronic acids (glucuronic acid, galacturonic acid) [9, 12]. Hemicellulose in softwood (from

*Correspondence: marc.beauregard@uqtr.ca
[1] Centre de recherche sur les matériaux lignocellulosiques, Université du Québec à Trois-Rivières, C.P. 500, Trois-Rivières, QC G9A 5H7, Canada
Full list of author information is available at the end of the article

gymnosperms) contains mostly glucomannans whereas in hardwood (from angiosperms) mostly consists of xylan [13]. The hemicelluloses distribution on the surface of wood fibers/cellulose fibrils is of utmost importance for the complex structure of lignocellulosic biomass, since hemicelluloses have been proposed to act as a physical barrier which increases the stiffness of the cellulose fiber network by coating the rigid cellulose crystallites and forming links between the fibrils [3, 14].

Among hemicelluloses, xylans are the most abundant and complex hemicelluloses comprising a backbone of β-1,4-linked xylopyranosyl residues [10, 11, 13]. Xylan has been shown to limit the accessibility of cellulase enzymes to cellulose [15–20]. As a consequence, biomass bioconversion requires the presence of accessory enzymes such as xylanase, which allows for controlling the significant effect of residual xylan on cellulose accessibility during bioconversion [4]. The cost associated to enzyme utilization is an important aspect of bioenergy production. [15, 21–23]. Enzymes cost can be minimized by tighter control of process parameters (such as dosage and incubation time). To this end, one needs to track lignocellulosic polymers, including xylan, at various stages of processing.

Pulp and paper production is another lignocellulosic biomass-based industry which has to deal with the complexities described above. In addition, this industry faces immense pressure from the society and/or governments to move toward green chemistry. Biocatalysts are recognized as a key element of green chemistry and are being progressively introduced in a number of processes with extremely positive consequences for the environment [24, 25]. An increasing number of enzymatic strategies are used by paper makers, including the application of xylanase enzymes in the pre-bleaching or bio-bleaching of kraft pulp. The presence of xylan, and its redeposition on the surface of cellulose fiber during the kraft pulping of hardwood, inhibits the bleaching process. Xylanase enzymes have been found to be most effective for limiting this problem and are now in use at several mills worldwide for bio-bleaching [13, 15, 24–26]. Further, xylan is also known to contribute to fiber strength and its removal is known to influence pulp fiber properties [15, 27, 28]. Xylan is believed to contribute to physical properties of the paper by enhancing the inter-fiber bonding [27]. Here again, the close monitoring of xylan would help optimize the enzymatic treatment, better control of paper properties, and minimize its cost.

In order to make these lignocellulosic biomass-based processes highly productive and cost-effective while improving quality of end-products, one should correlate the process parameters (such as enzyme loading, temperature, or treatment time) to the substrate availability in a given biomass sample, or to a given percent removal target (*i.e.*, × % decrease in xylan at the surface of cellulose fibers). Unfortunately, current methods for tracking xylan are not compatible with industrial constraints. To date, tools such as X-ray photoelectron spectroscopy (XPS or ESCA) [29, 30], atomic force microscopy (AFM) [31], scanning electron microscopy (SEM) [30], time-of-flight secondary ion mass spectrometry (ToF–SIMS) [30], gas chromatography (GC) [32], Fourier transform infrared spectroscopy (FTIR) [33], and chemical methods [34, 35] have been used to study the surface and bulk chemistry of wood fibers. However, use of these methods for lignocellulosic biomass analysis is laborious, requires specialized equipment, tedious sample preparation, and long analysis time (typically hours for each sample) [36, 37]. As a result, it is highly challenging to tightly modulate the amount of xylanase used for complete or selective xylan removal for process optimization.

Over the past decade, other techniques have been developed for the direct and rapid detection of lignocellulosic biomass polymers. The use of chemical dyes to stain lignocellulosic biopolymers was one of the initial approaches for the detection of cellulose within various materials. Unfortunately, these dyes are rarely specific to cellulose [38]. In recent years, several in situ detection techniques have been developed, not only for cellulose but also for other cell wall components, including hemicellulose and pectic polysaccharides detection [39]. Among these techniques, monoclonal antibodies (mAbs) have been used successfully for developmental studies of vegetal materials. However, antibodies targeting complex polysaccharides, made of crystalline and insoluble structures, are difficult to generate [38, 40]. Like antibodies, carbohydrate-binding modules (CBMs) are highly specific toward their substrate polysaccharides. They have been shown to discriminate crystalline cellulose from amorphous cellulose [38, 40].

CBMs are the non-catalytic polysaccharide-recognizing module of enzymes such as glycoside hydrolases [41–43]. CBMs play a central role in the optimization of the catalytic activity of plant cell wall hydrolases by their specific binding to plant polysaccharides. These CBMs are grouped into 71 different families, based on amino acid sequence homology, in the Carbohydrate Active enZymes (CAZy) database (http://www.cazy.org/) [41]. CBMs are further classified into three types A, B, and C, on the basis of three-dimensional structure and functional similarity. Type A CBMs recognize the surface of crystalline cellulose, type B and type C CBMs are identified as CBMs that recognize internal glycan chain (*endo*-type) and terminal (*exo*-type) glycans, respectively [43, 44]. Among type B CBMs, the family 15 CBM (CBM15) includes the non-catalytic xylan-recognizing module of

a xylanase (Xyn10C from *Cellvibrio japonicus)* which has been demonstrated to bind xylan, including substituted xylan and xylooligosaccharides [45]. The high specificity of CBMs toward lignocellulosic polymers makes them more interesting as probes compared to mAbs [38, 40, 41]. CBMs have been used for several applications related to biomedicine, environment, molecular biology, microarrays, paper, textile, food, and biofuel industries [41]. Considering the importance of xylan detection for industrial processing of lignocellulosic biomass, we propose to use nature's own recognition molecules (CBMs) as the spearhead of an efficient xylan detection method.

Fluorescence is a very sensitive and specific spectroscopy where absorption and emission wavelengths determine what molecules contribute to the detected signals [43, 46]. Further, plate readers allow increasing measurement throughput, a valuable criterion in the development of any novel assay. Hence, detection of CBM probes that would emit fluorescence would be advantageous. Fluorescence detection can be achieved directly or indirectly depending on the methods used [38]. The indirect methods involve the use of a secondary or tertiary reagent such as anti-His-IgG coupled to a fluorophore to detect the His-tag of a CBM, which may also allow amplification of signal intensities. This method provides great flexibility in CBM use but has a potential disadvantage related to multi-step incubations which decrease analysis speed and are less compatible with a high throughput strategy [38]. On the other hand, in direct methods, coupled CBMs would require a straightforward, single-step incubation, affording the possibility of rapid, high throughput protocols. In the first direct method reported, a CBM was chemically coupled with a fluorophore (such as FITC/Alexa Fluor) [38]. Unfortunately these molecules react non-specifically with various moieties at the surface of CBMs, deleteriously impacting specificity, affinity, and detection reproducibility. Another direct detection method uses CBMs as fusion with a fluorescence protein such as the green fluorescent protein (or any of its variants) [38]. This method allows maintenance of the original CBM behavior, avoiding the limitations described for the first direct method discussed. Hence, CBMs coupled with fluorescence protein have been used for mapping the chemistry and structure of various carbohydrate-containing substrates (lignocellulosic biomass) [47, 48]. More recently, two different recombinant fluorescent CBM probes have been used for quantitative study of the change of accessibilities of amorphous cellulose and crystalline cellulose regions during the enzymatic hydrolysis of Avicel [43].

In this study, we demonstrate the potential of a fluorescent-tagged fusion protein mOrange2-CBM15 probe (hereafter named OC15) for monitoring xylan at the surface of paper samples. To evaluate the potential of our novel method, we decided to use two different grades of kraft pulps (unbleached and bleached), and we analyzed xylanase-treated pulp in order to study the sensitivity of the developed method. Our results suggest that such probes can form the basis of a rapid, easy to use, unambiguous and affordable diagnostic approach, helping optimizing treatment strategy, and reducing the cost of processes which rely on controlled xylan removal.

## Results and discussion

### OC15 expression and purification

A two-domain recombinant probe named OC15 was designed for specific tracking of variations of xylan on the surface of lignocellulosic material (Fig. 1). *Cellvibrio japonicus* CBM15 composed the xylan recognition domain (C-terminal) while monomeric fluorescent protein Orange2 constituted the probe detection domain (N-terminal). OC15 was expressed in *E. coli* BL21-Gold(DE3)pLysS cells which contained the pET11a-mOrange2-CBM15 plasmid (Fig. 1a, b). The expected molecular weight of OC15 is 44.68 kDa. Following affinity and size exclusion chromatography steps, the probe purity was verified using SDS-PAGE (Additional file 1). Interestingly, the gel analysis of OC15 revealed two bands: one intense band, corresponding to OC15 expected size (44.68 kDa), and another, less intense band (less than 1 % on the basis of staining intensity) of a smaller size. A similar result has been observed for the purified mCherry-CBM17 probe designed by Gao et al. [43]. These authors showed that the smaller hand was the result of an incomplete denaturation of the probe under standard SDS-PAGE conditions. We investigated this possibility and found that increasing the SDS concentration in the gel, sample, and running buffers decreased the intensity of the smaller band (data not shown). Therefore, we concluded that, like the probes of Gao et al., the OC15 probe is incompletely denatured under standard SDS-PAGE conditions.

### Determination of OC15 ligand specificity using affinity gel electrophoresis (AGE)

Affinity gel electrophoresis (AGE) was used to qualitatively evaluate the specificity of the OC15 probe toward soluble polysaccharides [49]. Interaction between the studied protein and the gel-embedded polysaccharide is revealed by a reduced mobility compared to the mobility of the protein in absence of saccharide. BSA, which has no affinity toward carbohydrates, was used as negative control [49]. Figure 2 shows that OC15 interacts only with beechwood xylan (Fig. 2b). Similarly to BSA, no binding was detected between OC15 and carboxymethyl cellulose (Fig. 2c) or galactomannan (Fig. 2d). These

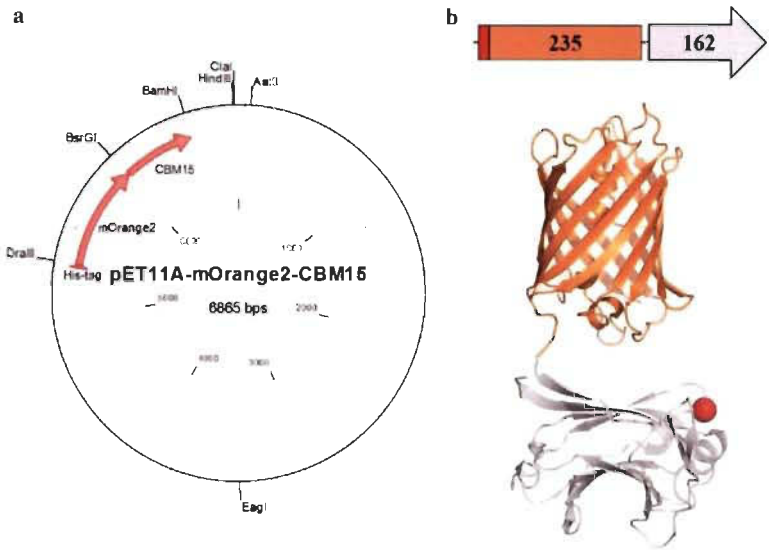


**Fig. 1** Plasmid map (**a**), construction *scheme* and *pictorial* representation (**b**) of the OC15 probe. mOrange2 C-terminal end is linked to the N-terminal end of CBM15 (*Cellvibrio japonicus*). The *red rectangle* represents N-terminal six histidines tag. The *red sphere* represent the metal ion in CBM15. The *structural model* shown was constructed using PDB files 1GNY and 2H5O (obtained for the closely related mOrange fluorescent protein). The sequence linking the fluorescent protein to the CBM is composed of a glycine residue

results confirm that the well-known specific binding to xylan of CBM15 is unaltered by its fusion with mOrange2 in the OC15 probe. However, the affinity of the recognition module of the OC15 must still be determined in order to ascertain its ability to sensitively detect xylan on the surface of paper.

#### Determination of OC15 ligand affinity using isothermal titration calorimetry (ITC)

The affinity of OC15 toward hexaoses was also investigated by ITC (Table 1; Additional file 2). Analysis of the binding isotherms showed that the recognition module of the OC15 probe bound to both cellohexaose and xylohexaose, albeit with different affinities, but not to mannohexaose (Table 1). As expected, OC15 interacted 16 times more strongly with xylohexaose ($34 \times 10^4\ M^{-1}$) than with cellohexaose ($2.1 \times 10^3\ M^{-1}$). These affinity values are similar to those previously reported for CBM15 and confirm that the binding site of the recognition module of the OC15 probe is unaltered by the fusion with mOrange2 [45]. However, a small 1.7-fold increase is observed in the affinity constant of OC15 toward xylohexaose compared to CBM15 [45]. We attributed this increase to difference in experimental conditions in our study compared to those used previously. For instance, the sodium and calcium salt added to the binding buffer in our study may account for the observed difference. Such ions have also been observed in the crystallographic structure of CBM15 [45], although no biological relevance to their presence was given. We hypothesize that such a metallic ion may be important for the affinity and specificity of OC15 toward xylohexaose. We also found that OC15 bound weakly to cellohexaose but not to CMC (Fig. 2c). This result was unexpected, since the concentration of gel-embedded cellulose was 2.9 times higher than the $K_d$ for cellohexaose (Table 1). This suggests that the bulkier carboxymethyl substitutions found in CMC may interfere with the affinity of the binding module of OC15 for cellulose. On the other hand, the presence of xylose moieties and/or xylan in a cellohexaose sample of high but imperfect purity (90 %) would also explain such an apparent contradiction.

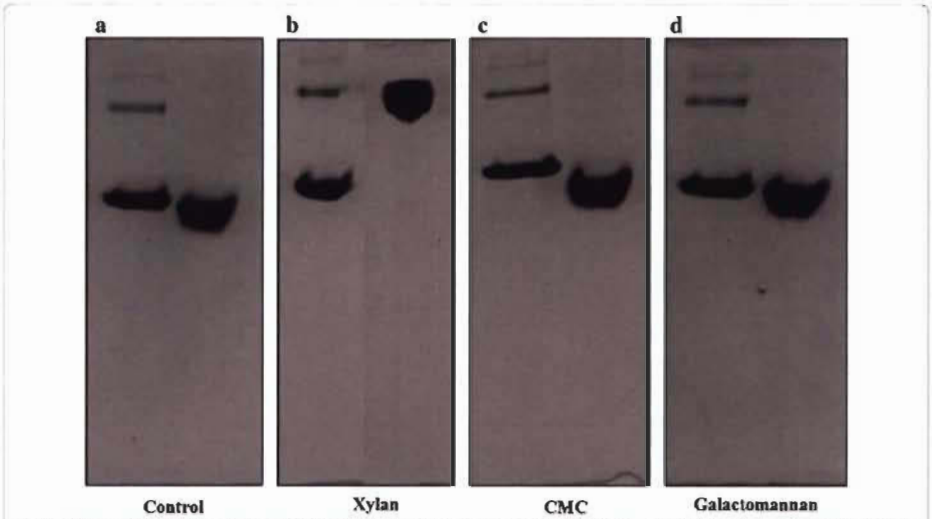


**Fig. 2** Affinity gel electrophoresis (AGE) of OC15 probe. **a** Control (no polysaccharide), **b** xylan, **c** CMC, **d** galactomannan. In *each panel* the first well contained BSA (10 µg) and the second well was loaded with OC15 probe (10 µg). All soluble polysaccharides were used at final concentration of 0.5 % (w/v) and a 12 % polyacrylamide gel was used for affinity analysis

**Table 1 Affinity of the OC15 probe for various hexaoses as determined by ITC**

| Ligand | $K_a \times 10^3 (M^{-1})$ | $K_d$ (M) | n[a] |
|---|---|---|---|
| Xylohexaose | 34 ± 0.2 | $2.938 \times 10^{-3} \pm 0.8$ | 0.922 ± 0.1 |
| Mannohexaose | NB[b] | – | – |
| Cellohexaose | 2.1 ± 0.3 | $4.795 \times 10^{-4} \pm 0.1$ | 1 ± 0.7 |

[a] Number of ligand binding sites

[b] No binding detected

### Comparing XPS, NREL/TP-510-42618, and OC15 methodologies for the detection of xylan

Pulps composed of a mixture of softwood and hardwood from an Eastern Canadian paper mill were used as lignocellulosic biomass for the formation of handsheets utilized in this study. Handsheets prepared from two grades of kraft pulp, UBKP and BKP, were investigated to determine differences in biopolymers content and their exposure at fiber surfaces. Kraft pulping and bleaching processes degrade and/or dissolve lignin. The removal of lignin through pulping increased access to xylan. In addition, removed xylan may redeposit onto the surface of cellulose fibers during pulping [26, 50–53]. The standard methods usually used for the detection of xylan are NREL/TP-510-42618 and XPS [35, 54–56]. These two approaches will be used and compared to our OC15 probe method.

The chemical composition of UBKP and BKP was determined by NREL/TP-510-42618 (Additional file 3) [35]. As expected, the pulp bleaching process decreased lignin by 2.3-fold without affecting the other biopolymers. Unfortunately, due to the nature of this technique, NREL/TP-510-42618 can only provide an overall bulk estimation of biopolymers content. It cannot detect small biopolymers changes nor measure variations of biopolymers exposition on the surface of fibers.

In contrast XPS has been extensively used for surface analysis of simple lignocellulosic biomasses to detect changes in surface coverage by cellulose, lignin, and extractives [54–56]. Elementary identification and bonding state discrimination are advantages associated to XPS analysis [37]. The C 1s band associated with lignocellulosic biomass which is monitored by XPS carries the most relevant information on surface polymers. C 1s spectrum has been suggested to result from the contribution of four different carbon functionalities: C1 (C–C, C–H, C=C), C2 (C–O or C–O–C), C3 (C=O or O–C–O), and C4 (O–C=O), which account for the chemical heterogeneity of paper fibers [54]. In cellulose, each glucose monomer harbors five C2 carbon atoms and one C3 carbon. Hemicelluloses are heterogeneous in their composition.

Its monomers typically comprise fewer than five C2 carbon atoms, less than one C4 carbon atom and one C3 carbon atom. In contrast, lignin is more complex, having all four types of carbons with a greater contribution from C1 and C2 atoms [57–59]. In a typical fiber XPS analysis, C1 component mainly arises from lignin and extractives, while C2 signal is primarily associated to cellulose and hemicelluloses. C3 component is not easily assigned to a given polymer, as it is related to either carbonyl groups of lignin and extractives, or to carbon atoms bonded to two oxygen atoms in cellulose and hemicellulose [57–60]. C1 to C4 peaks were inferred from the deconvolution of the C 1s band for UBKP and BKP (Additional file 4). These deconvolutions were calculated using spectra as shown in Additional files 5 and 6. The bleaching process led to a 2.2-fold decrease in C1 functionality at the surface of the paper. This difference may be attributed to the removal of lignin from the surface as a normal consequence of bleaching. The decrease in lignin associated to C1 functionality is in line with the corresponding decrease in lignin measured by NREL/TP-510-42618 (Additional file 3). Interestingly, the bleaching process increased the C2 functionality by 1.1-fold, suggesting that cellulose and/or hemicellulose are slightly more exposed on the surface of BKP. The exposure of cellulose and hemicelluloses also increased C3 carbon detection by 1.2-fold. Due to the low concentration of carboxylic groups on the surface of kraft pulp, the C4 carbon functionality was minor and rather similar for either pulps. Like NREL/TP-510-42618, XPS analysis revealed the impact of the bleaching process on lignin. Moreover, XPS analyses suggested that lignin loss resulted in the increased exposure of cellulose and hemicellulose on the surface of BKP. Unfortunately, the C 1s spectra cannot distinguish cellulose from hemicellulose since both biopolymers possess similar carbon types. Moreover, XPS is not always reproducible due to the problems resulting from X-ray contamination and samples degradation [54, 61].

Using OC15, we attempted to monitor the difference in xylan on the surface of UBKP and BKP papers resulting from the bleaching process. Complex lignocellulosic biomass fluoresces naturally when excited at the same wavelength as that for fluorescent protein mOrange2 *i.e.*, 549 nm (data not shown). This auto-fluorescence is mainly attributed to the lignin biopolymer found in kraft paper [62]. Thus, in order to minimize paper auto-fluorescence, we added a milk blocking step that also acted as a non-specific binding deterrent. Figure 3 describes the quantification of OC15 bound to the surface of UBKP and BKP papers. The bleached paper bound twice the amount of OC15 compared to the unbleached one, indicating that xylan exposure on the surface of kraft paper has increased after bleaching. This increase is fully compatible with the 2.3-fold decrease in lignin observed by chemical analysis, which was shielding xylan from surface detection before bleaching. This result confirms the loss of lignin that we measured using NREL/TP-510-42618 and XPS, demonstrating that our approach can efficiently detect the impact of the bleaching process on xylan. Therefore, introducing this xylan tracking approach as a quality control measurement would assuredly bolster the effectiveness of the lignocellulosic biomass process for selective as well as complete xylan removal.

#### Monitoring xylan hydrolysis using NREL/TP-510-42618, XPS, and the OC15 probe

The effectiveness of xylan removal by xylanase hydrolysis of UBKP was investigated using NREL/TP-510-42618, XPS, and the OC15 probe. Chemical composition of untreated and xylanase-treated UBKP was analyzed (Additional file 7). As expected, xylanase treatment of pulp decreased xylose content by 1.7-fold without affecting lignin. The extractive content increased from 0.1 to 3.2 after xylanase treatment. This unexpected result is a consequence of the NREL lipids extraction methodology which consists into weighting the pulp before and after acetone solubilization of lipids [63]. Since the added xylanase accounts for 24.3 % of the pulp initial weight, its acetone removal from the pulp induces an apparent but false increase in lipids extractives.

We then studied the surface of untreated and xylanase-treated UBKP papers using XPS (deconvolution results described in Additional file 8). Overall, xylanase treatment of UBKP induced rather small variations in the carbon functionalities (C1 to C4). As such, the curve fitting component ascribed to C1 atoms slightly decreased (1.1-fold), indicating that the lignin biopolymer was marginally affected by xylose removal. Surprisingly, the C2 functionality associated to cellulose and hemicellulose was not altered by xylan hydrolysis. This result may be attributed to the exposure of cellulose on the fibers surface as a consequence of xylan removal by hydrolysis. The exposure of cellulose also increased C3 carbon functionality by 1.2-fold. The C4 carbon signal was minor and rather similar for either pulps. This study reveals that the impact of xylan digestion [which was clearly detected by NREL/TP-510-42618 (Additional file 7)] cannot be monitored unambiguously or directly by XPS.

The impact of xylanase on xylan at the surface of UBKP paper discs was investigated using OC15 probe. A decrease in xylan was clearly indicated by the 7.7-fold decrease in OC15 binding after xylanase treatment (Fig. 4). The use of OC15 probe confirmed the loss of xylan suggested by chemical analysis (NREL/TP-510-42618) with the distinction that OC15 specifically probes fiber surface. We also studied the binding of OC15 to

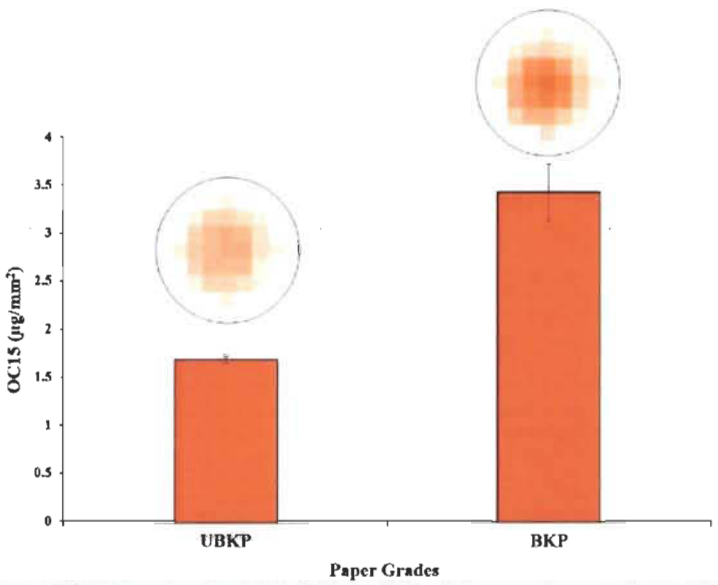


**Fig. 3** Quantification of OC15 binding to the surface of UBKP and BKP papers. UBKP and BKP paper punches were incubated with OC15 probe (0.5 µg/µL) for 1 h at room temperature under agitation. Three percent (w/v) milk (20 mM Tris–HCl, pH 7.5 with 20 mM NaCl and 5 mM $CaCl_2$) was used to minimize paper auto-fluorescence and the non-specific binding of the OC15 probe. The *fluorescence* values were converted to OC15 (µg/mm²) using a standard curve (Additional file 9). The *inset* above each histogram columns represents the fluorescence intensity acquired by area scanning of the surface of each paper disc

xylanase-treated UBKP paper discs as a function of time and enzyme dosages (0.4 vs 0.1 U). The xylanase digestions were performed on paper discs glued in 96-wells microtiter plates over an 18 h incubation period at room temperature. Figure 5 reveals that after 1 h a significant removal of surface xylan was detected. Xylan was reduced 8.2-fold by 0.1 xylanase units and 17-fold when 0.4 units were used. The complete removal of xylan was detected after 18 h of incubation (0.4 unit dosage). OC15 binding responded proportionally to enzyme load and allowed monitoring xylanase treatment kinetics. This high throughput method enables the screening for optimal xylanase hydrolysis conditions, necessary for removal of xylan from kraft paper. We predict that OC15 usefulness is not limited to kraft paper analysis, but should include optimization of any biomass process for which surface xylan is determinant.

## Conclusion

Monitoring the impact of mechanical, chemical, and enzymatic modifications of biopolymers found in lignocellulosic biomasses is a complex endeavor. The currently available methods for chemical composition analysis of biopolymers in pulp, such as NREL/TP-510-42618, are able to only quantify bulk xylan but give no information on biopolymers surface exposition. On the other hand, XPS, while being highly sensitive, cannot unambiguously monitor changes in surface xylan since cellulose and hemicellulose share similar C 1s carbon functionalities. These standard methods are poorly adapted to important problematics associated with biofuels and pulp and paper industries. To address those issues, we developed a novel xylan detection approach that is sensitive, specific, reproducible, rapid (hundreds of samples analyzed in less than 4 h), high throughput, cost-effective, and that requires minimal specialized equipment. This approach involves solely the utilization of a two-domain probe, OC15, which harnesses the specific xylan recognition power of CBM15 and the high sensitivity of mOrange2 fluorescence emission.

Our results demonstrate that OC15 enables the specific tracking of chemical and enzymatic-induced variations of

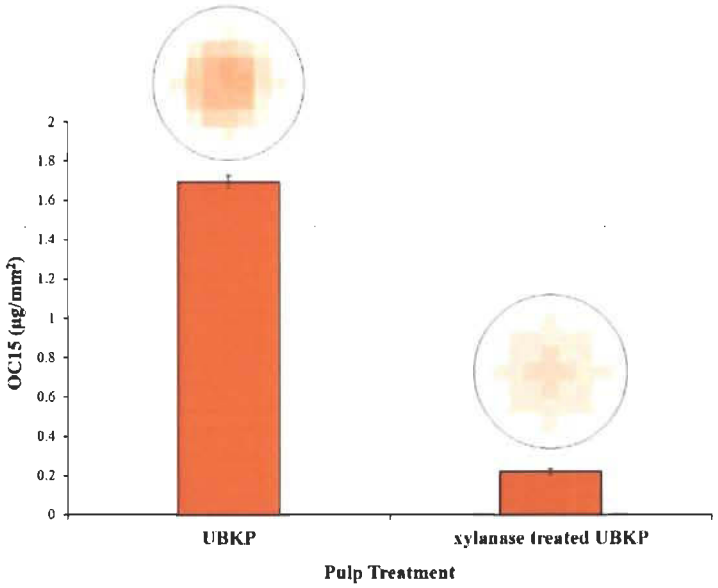


**Fig. 4** Quantification of OC15 binding to the surface of untreated and xylanase-treated UBKP papers. Pulps were incubated with or without the xylanase (500 U/g of pulp) for 1 h (pH 6) at room temperature under continuous agitation (150 rpm). Untreated UBKP and xylanase-treated UBKP paper discs were incubated with OC15 probe (0.5 µg/µL) for 1 h at room temperature under agitation. Three percent (w/v) milk (20 mM Tris-HCl, pH 7.5 with 20 mM NaCl and 5 mM $CaCl_2$) was used to minimize paper auto-fluorescence and the non-specific binding of the OC15 probe. The *fluorescence* values were converted to OC15 (µg/mm²) using a standard curve (Additional file 9). The *inset* above each histogram columns represents the fluorescence intensity acquired by area scanning of the surface of each paper disc

xylan on the surface of kraft pulps. In addition, we demonstrated here that our approach can be readily adapted to a high throughput format (tests were performed in multiwell plates and analyzed with a plate reader). We believe that this tracking approach could perform various functions, such as (1) fine-tuning the conditions surrounding the mechanical and enzymatic removal of xylan; (2) decreasing costs associated with lignocellulosic biomass processes; (3) expanding our understanding of biofuels and papermaking productions; (4) correlating surface xylan with performances of the relevant lignocellulosic products; and (5) improving the productivity of large-scale operations. This study testifies to the incredible versatility of CBMs as spearheads of innovations which can successfully tackle biotechnological challenges.

## Methods

### Chemicals and strains

Unless otherwise noted, all chemicals were reagent grade and purchased from Sigma-Aldrich or Fisher Scientific. *Escherichia coli* XL10 cells (Agilent Technologies) were used for all DNA manipulations while *E. coli* BL21-Gold(DE3)pLysS competent cells (Agilent Technologies) were used for recombinant protein expression. *Trichoderma viride* xylanase from glycoside hydrolase (GH) family 11 (cat no. 95595; Sigma-Aldrich) was used for the digestion of lignocellulosic biomasses. Xylanase activity was 16.57 U/g.

### Construction of pET11a-mOrange2-CBM15 expression vector

The CBM15 gene (xylan binding domain) was cloned into the C-terminal end of the mOrange2 gene (detection domain) in a pET11a vector. Briefly, *Cellvibrio japonicus* CBM15 (GenBank Accession Z48928) was synthetized by GenScript and provided as part of the pUC57-CBM15 vector. In order to insert the *Bsr*GI and *Bam*HI restriction sites (underlined) at each end of CBM15, we amplified the gene using forward (5′-*TGTA CA*AGGGTGTCGCTGCCAGC-3′) and reverse primers

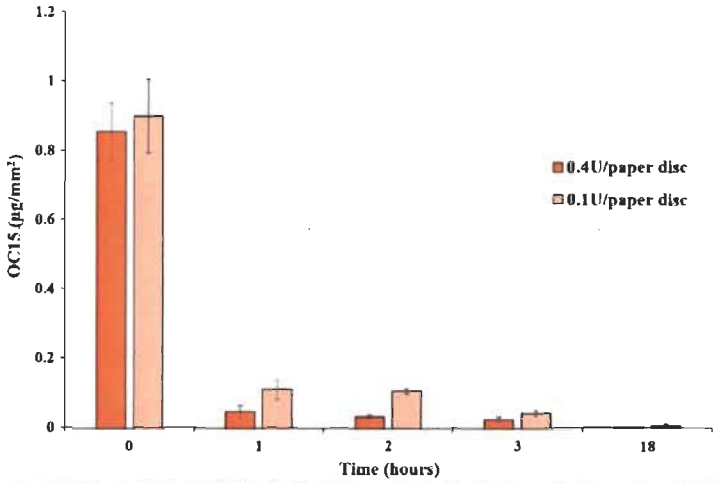


**Fig. 5** Tracking xylanase hydrolysis of UBKP using OC15 probe. Paper discs were incubated with xylanase (0.4 U/paper disc and 0.1 U/paper disc) for up to 18 h (pH 6) at room temperature under continuous agitation (150 rpm). Untreated UBKP and xylanase-treated UBKP paper discs were incubated with OC15 probe (0.06 µg/µL) for 1 h at room temperature under agitation. Three percent (w/v) milk (20 mM Tris–HCl, pH 7.5 with 20 mM NaCl and 5 mM $CaCl_2$) was used to minimize paper auto-fluorescence and non-specific binding of the OC15 probe. The *fluorescence* values were converted to OC15 (µg/mm²) using a standard curve (Additional file 9)

(5′-*GGATCC*TTAATTGGCTGAATAGGCTTCC-3′). The resulting PCR product was then purified using Qiagen MinElute PCR purification kit. In addition, the mOrange2 gene was excised from the pmOrange2 vector (Clontech) using a *Dra*III and *Bam*HI double digestion and inserted into the corresponding sites of pET11a vector. Finally, the double *Bsr*GI and *Bam*HI digestion of CBM15 was purified and inserted into the corresponding site of the pET11a-mOrange2 vector, resulting into the pET11a-mOrange2-CBM15 expression vector. At each step, the constructs were sequenced to ascertain the integrity and fidelity of the products DNA sequence.

#### Expression and purification of OC15 probe

*Escherichia coli* BL21-Gold(DE3)pLysS cells (Agilent Technologies) bearing the OC15 expression plasmid were grown at 37 °C and 200 rpm in Luria-Bertani broth containing 100 µg/mL of ampicillin. Induction of recombinant protein expression was performed by the addition of 500 µM IPTG (Thermo Fisher Scientific) to mid-log-phase cells ($O.D._{600nm}$ of 0.6–0.8) and subsequent incubation for 18 h at 25 °C. Cells were then harvested and kept at −80 °C. Thawed cell pellets were resuspended in 50 mM sodium phosphate pH 8 containing 300 mM NaCl, 2 mM imidazole, 1 mM PMSF, and then lysed by sonication using six cycles of 60 s (Branson Ultrasonics Corporation) at 200 W. Clarification of lysate was achieved by centrifuging at 10,000*g* for 30 min at 4 °C. The protein of interest was purified by affinity chromatography over a HisPrep FF 16/10 column (GE Healthcare Life Sciences) equilibrated in 50 mM sodium phosphate buffer pH 8.0 containing 300 mM NaCl and 10 mM imidazole. After washing with ten column volumes of buffer, the desired protein was eluted using a gradient of imidazole (10–250 mM) in 50 mM sodium phosphate pH 8.0 buffer containing 300 mM NaCl. A final purification step was performed using a Superdex 200 HR 16/50 column (GE Healthcare Life Sciences) in 50 mM Tris–HCl pH 7.5 buffer containing 300 mM NaCl to insure its homogenous purity. The purified probe was then dialyzed in a 20 Tris–HCl pH 7.5 buffer containing 20 mM NaCl and 5 mM $CaCl_2$ at 4 °C and concentrated using a 10K Macrosep Advance centrifugal device (Pall Corporation). Concentrated protein solutions were stored at −80 °C using flash freezing. Protein purity (expected mass 44.68 kDa) was verified by SDS-PAGE. The amount of protein was quantified by the Bradford method [64].

#### Affinity gel electrophoresis (AGE)

AGE was used for qualitative assessment of OC15 (10 μg) specificity toward selected ligands. The experiment was performed as described elsewhere [49, 65], by adding 0.5 % (w/v) of beechwood xylan (Sigma-Aldrich), carboxymethyl cellulose (CMC) (Sigma-Aldrich), and galactomannan (Megazyme) to a native, 12 % polyacrylamide gel. Bovine serum albumin (BSA) (10 μg/well) was used as negative control since it has no affinity toward carbohydrates [49].

#### Isothermal titration calorimetry (ITC)

ITC was employed to measure the affinity of the OC15 probe toward selected hexaoses (Megazyme). Cellohexaose, xylohexaose, and mannohexaose were reconstituted in a 20-mM Tris–HCl pH 7.5 buffer which contained 20 mM NaCl and 5 mM $CaCl_2$. The purified OC15 probe was also dialyzed into that same buffer. All experiments were performed with a Nano ITC microcalorimeter (TA Instruments) operated at 25 °C with a stirring rate set of 250 rpm. Pre-equilibrated solutions of probe (200 μM) and hexaoses (5 mM) were used for each assay. The control experiments were based on titrations of hexaoses into the buffer and buffer into the OC15 probe. Each experiment consisted of 25 injections of 2 μL hexaose into the probe solution, with an interval of 130 s between injections. All experiments were performed in triplicates. Data were analyzed and fitted using the NanoAnalyze software v2.3.6 (TA Instruments).

#### Pulp characterization

The kraft pulps used for this study were provided by an Eastern Canadian pulp and paper company. The kraft pulping was performed using a mixture of softwood and hardwood. Two different grades of pulps, unbleached kraft pulp (UBKP) and bleached kraft pulp (BKP), were used. The cellulose, hemicellulose, and lignin contents of these pulps were analyzed according to NREL/TP-510-42618 protocol [35]. The hydrolyzed monosaccharides contents of the pulps (10 μL injection) were determined by ion chromatography (ICS-5000, Dionex) and detection was performed using an electrochemical detection cell (combined pH-Ag/AgCl reference electrode). Each experiment was conducted at 40 °C with 1 mL/min isocratic elution of NaOH (1 mM) on a Dionex CarboPac SA10 (250 × 4 mm) column coupled with a Dionex CarboPac PA100 (50 × 4 mm) guard column. Data analysis was performed using Dionex Chromeleon 7 software.

#### Handsheets preparation

UBKP and BKP were used as lignocellulosic substrates for the preparation of handsheets and paper discs. Handsheets (basis weight of 60 ± 2 g/m$^2$) were prepared from pulp according to TAPPI standard method T 205 sp-02. Prior to testing, the handsheets were conditioned for 24 h at room temperature and 50 % of relative humidity according to TAPPI method T 402 sp-03 [66]. These handsheets were then used for the preparation of the paper punches. The paper punches are defined as paper discs having diameter of 3 mm.

#### Xylanase digestion of unbleached kraft pulp

Xylanase digestion of UBKP was done according to Li et al. [66]. Briefly, the presoaked, disintegrated pulp at 2 % consistency was incubated 1 h at pH 6 and room temperature under continuous agitation (150 rpm), with or without xylanase (500 U/g of pulp). The reactions were stopped by a 15-min incubation on ice. The pulp was then used for chemical composition analysis (NREL/TP-510-42618) and handsheets formation.

#### X-ray photoelectron spectroscopy (XPS)

The 300 Watts monochromatic Al K-α radiation source originating from an AXIS-ULTRA apparatus (KRATOS ANALYTICAL) was used to study xylan. The analyser was set in the constant pass energy mode, the lens set to the hybrid configuration (both magnetic and electrostatic lenses), and the electrostatic lens aperture in the slot position. This configuration provided the highest sensitivity for scanning 700 × 300 μm area. Three different spots were analyzed to obtain an average. The pressure of the system was set at $10^{-8}$ Torr. Elemental analysis of the surface area was performed by recording survey spectra at 160 eV with energy increment of 1 eV per channel. High resolution spectra were recorded at 20 eV with energy increment of 0.05 eV. This setup gave an overall instrumental resolution of 0.6 eV as measured on $Ag3d_{5/2}$. Analyses of the peak decompositions were performed using the CasaXPS software.

#### Xylan tracking on the surface of papers using the OC15 probe

All fluorescence readings were acquired at room temperature with a Synergy Mx microplate reader (BioTek) using the area scanning feature (3 × 3) with the top detection height set at 4.5 mm and the filters bandwidth at 9 mm. The excitation and emission wavelengths were set at 549 and 568 nm for the OC15 probe. Each experiment was done in triplicates. Two different grades of kraft pulps, unbleached (UBKP) and bleached (BKP), were investigated regarding their xylan content. The following method is a modified high throughput version of the methodology described by Knox [38]. Hence, it was performed into 96-well black microtiter plates (Corning), where each well contained a 3 mm diameter paper disc obtained from 60 g/m$^2$ handsheet. The discs were glued to the bottom of each well and first incubated for 1 h at room temperature with agitation in 3 % (w/v) milk (20 mM Tris–HCl, pH 7.5 with

20 mM NaCl, and 5 mM $CaCl_2$) to minimize paper autofluorescence and the non-specific binding of the OC15 probe. Milk excess was then removed with 3 × 5 washing steps using the assay buffer. At this stage, the fluorescence intensity of the paper discs was measured and referred as to blank fluorescence. The specific binding of the OC15 probe to the surface of the paper discs was initiated by adding 0.5 µg/µL of the OC15 probe in assay buffer to each well. After a 1 h incubation at room temperature under agitation, the excess and/or non-specifically bound probe were removed by 3 × 5 min washes with buffer that also contained 0.05 % (v/v) of Tween 20. The residual fluorescence intensity associated with the specific detection of xylan was then recorded. Quantification of the bound OC15 probe was achieved by subtracting the value of the mean blank fluorescence from the mean residual fluorescence obtained for each well. These fluorescence values were then converted into µg/mm² using the appropriate standard curves (Additional file 9) and the surface area of paper discs.

## Additional files

**Additional file 1: Figure S1.** SDS-PAGE analysis of the OC15 probe purified by affinity chromatography. The expected molecular weight of the OC15 fusion protein is 44.68 kDa. A 12 % polyacrylamide gel was used for SDS-PAGE analysis. Well M: Precision plus protein standards (5 µg). Well OC15: Purified OC15 probe (10 µg).

**Additional file 2: Figure S2.** Isothermal calorimetric titration of the OC15 probe with xylohexaose. Top panel: Typical ITC experiment carried out by adding 25 injections of 2 µL xylohexaose (5 µM) into the OC15 probe (200 nM) solution, with an interval of 130 s between each injection. Bottom panel: Heat release per mole of xylohexaose as a function of xylohexaose/OC15 molar ratio. The titration was performed at 25 °C in a 20 mM Tris-HCl pH 7.5 buffer which contained 20 mM NaCl and 5 mM $CaCl_2$. Injectant: xylohexaose.

**Additional file 3: Table S1.** Chemical composition of UBKP and BKP determined by NREL/TP-510-42618. UBKP: Unbleached kraft pulp. BKP: Bleached kraft pulp.

**Additional file 4: Table S2.** XPS analysis of UBKP and BKP. Results include O/C ratios and contributions (%) from each carbon type (C1–C4) to curve fitting of the C 1s peak measured by low- and high-resolution XPS. UBKP: Unbleached kraft pulp. BKP: Bleached kraft pulp.

**Additional file 5: Figure S3.** Low resolution XPS spectrum of UBKP surface. UBKP: unbleached kraft pulp. Unextracted pulp samples were analysed.

**Additional file 6: Figure S4.** Deconvolution of high-resolution XPS spectrum of UBKP. UBKP: unbleached kraft pulp. Unextracted pulp samples were analysed.

**Additional file 7: Table S3.** Chemical composition of untreated and xylanase-treated UBKP determined by NREL/TP-510-42618. UBKP: Unbleached kraft pulp.

**Additional file 8: Table S4.** XPS analysis of UBKP and xylanase-treated UBKP. Results include O/C ratios and contributions (%) from each carbon type (C1–C4) to curve fitting of the C 1s peak measured by low- and high-resolution XPS. UBKP: Unbleached kraft pulp.

**Additional file 9: Figure S5.** Standard curve for the conversion of fluorescence intensity into µg of OC15 probes. The excitation and emission wavelengths were set at 549 and 568 nm respectively.

### Abbreviations

AGE: affinity gel electrophoresis; BSA: bovine serum albumin; BKP: bleached kraft pulp; CAZy: carbohydrate active enzymes; CBMs: carbohydrate-binding modules; CBM15: family 15 carbohydrate-binding module; CMC: carboxymethyl cellulose; GH: glycoside hydrolase; IPTG: isopropyl-β-D-thiogalactopyranoside; ITC: isothermal titration calorimetry; LB: Luria–Bertani; mAbs: monoclonal antibodies; mOrange2: mono-orange2; NREL: national renewable energy laboratory; OC15: mono-orange2 fluorescent protein linked to a family 15 carbohydrate-binding module; PCR: polymerase chain reaction; SDS-PAGE: sodium dodecyl sulfate polyacrylamide gel electrophoresis; UBKP: unbleached kraft pulp; XPS: X-ray photoelectron spectroscopy.

### Authors' contributions

VK carried out all the experiments and drafted the manuscript. YHO contributed to experiments related to the construction of plasmid for OC15 expression, design of high throughput assay, and drafted the manuscript. FMM and MB participated in its design and coordination, and helped to draft and revise the manuscript. All authors read and approved the final manuscript.

### Author details

[1] Centre de recherche sur les matériaux lignocellulosiques, Université du Québec à Trois-Rivières, C.P. 500, Trois-Rivières, QC G9A 5H7, Canada. [2] PROTEO, Université Laval, Quebec, QC G1V 4G2, Canada. [3] Buckman North America, Vaudreuil-Dorion, QC J7V 5V5, Canada.

### Acknowledgements

This research was supported in part by Buckman Laboratories of Canada and funded by grants from CRIBIQ and NSERC (CRDPJ445143-12). We would like to thank Dr. Roberto Chica (University of Ottawa) for the donation of fluorescent protein and Dr. Nicolas Doucet (INRS-Institut Armand-Frappier) for his expert assistance while performing isothermal titration calorimetry (ITC) measurements. The skillful technical assistance of Nikolas Beauchesne, Vincent Bolduc, Daniel Agudelo, Rene Diene, and Guillaume L. Lemieux is acknowledged. We would like to thank Mary A. Hefford for her valuable editorial contributions.

### Competing interests

VK, YHO, and MB declare that they have no competing interests. FMM was an employee of Buckman North America which financially supported parts of this work. The project results are included in a provisional patent (assignee Buckman International, Memphis, TN, USA).

Received: 2 December 2015 Accepted: 14 March 2016
Published online: 25 March 2016

### References

1. Himmel ME, Ding SY, Johnson DK, Adney WS, Nimlos MR, Brady JW, Foust TD. Biomass recalcitrance: engineering plants and enzymes for biofuels production. Science. 2007;315:804–7.
2. Jørgensen H, Kristensen JB, Felby C. Enzymatic conversion of lignocellulose into fermentable sugars: challenges and opportunities. Biofuels, Bioprod Biorefin. 2007;1:119–34.
3. Penttilä PA, Várnai A, Pere J, Tammelin T, Salmén L, Siika-aho M, Viikari L, Serimaa R. Xylan as limiting factor to enzymatic hydrolysis of nanocellulose. Bioresour Technol. 2013;129:135–41.
4. Li M, Tu M, Cao D, Bass P, Adhikari S. Distinct roles of residual xylan and lignin in limiting enzymatic hydrolysis of organosolv pretreated loblolly pine and sweetgum. J Agric Food Chem. 2013;61(3):646–54.
5. Igarashi K, Uchihashi T, Koivula A, Wada M, Kimura S, Okamoto T, Penttilä M, Ando T, Samejima M. Traffic jams reduce hydrolytic efficiency of cellulase on cellulose surface. Science. 2011;333:1279–82.
6. Zhu L, O'Dwyer JP, Chang VS, Granda CB, Holtzapple MT. Structural features affecting biomass enzymatic digestibility. Bioresour Technol. 2008;99:3817–28.
7. Mansfield SD, Mooney C, Saddler JN. Substrate and enzyme characteristics that limit cellulose hydrolysis. Biotechnol Prog. 1999;15:804–16.
8. Hall M, Bansal P, Lee JH, Realff MJ, Bommarius AS. Cellulose crystallinity-a key predictor of the enzymatic hydrolysis rate. FEBS J. 2010;277(6):1571–82.

9. Hendriks ATWM, Zeeman G. Pretreatments to enhance the digestibility of lignocellulosic biomass. Bioresour Technol. 2009;100(1):10–8.
10. Subramaniyan S, Prema P. Biotechnology of microbial xylanases: enzymology, molecular biology, and application. Crit Rev Biotechnol. 2002;22(1):33–64.
11. Saha BC. Hemicellulose bioconversion. J Ind Microbiol Biotechnol. 2003;30(5):279–91.
12. Girio FM, Fonseca C, Carvalheiro F, Duarte LC, Marques S, Bogel-Lukasik R. Hemicelluloses for fuel ethanol: a review. Bioresour Technol. 2010;101(13):4775–800.
13. Timell TE. Recent progress in the chemistry of wood hemicelluloses. Wood Sci Technol. 1967;1(1):45–70.
14. Kumar P, Barrett DM, Delwiche MJ, Stroeve P. Methods for pretreatment of lignocellulosic biomass for efficient hydrolysis and biofuel production. Ind Eng Chem Res. 2009;48(8):3713–29.
15. Hu J, Arantes V, Saddler JN. The enhancement of enzymatic hydrolysis of lignocellulosic substrates by the addition of accessory enzymes such as xylanase: is it an additive or synergistic effect? Biotechnol Biofuels. 2011;4(1):1–14.
16. Selig MJ, Vinzant TB, Himmel ME, Decker SR. The effect of lignin removal by alkaline peroxide pretreatment on the susceptibility of corn stover to purified cellulolytic and xylanolytic enzymes. Appl Biochem Biotechnol. 2009;155(1–3):397–406.
17. Bura R, Chandra R, Saddler J. Influence of xylan on the enzymatic hydrolysis of steam-pretreated corn stover and hybrid poplar. Biotechnol Prog. 2009;25(2):315–22.
18. Frommhagen M, Sforza S, Westphal AH, Visser J, Hinz SW, Koetsier MJ, van Berkel WJ, Gruppen H, Kabel MA. Discovery of the combined oxidative cleavage of plant xylan and cellulose by a new fungal polysaccharide monooxygenase. Biotechnol Biofuels. 2015;8(1):1–12.
19. Suurnakki A, Li TQ, Buchert J, Tenkanen M, Viikari L, Vuorinen T, Odberg L. Effects of enzymatic removal of xylan and glucomannan on the pore size distribution of kraft fibres. Holzforschung. 1997;51(1):27–33.
20. Zhang J, Siika-aho M, Tenkanen M, Viikari L. The role of acetyl xylan esterase in the solubilization of xylan and enzymatic hydrolysis of wheat straw and giant reed. Biotechnol Biofuels. 2011;4(1):1–10.
21. Merino ST, Cherry J. Progress and challenges in enzyme development for Biomass utilization. Biofuels. 2007;108:95–120.
22. Ogeda TL, Petri DFS. Biomass Enzymatic Hydrolysis. Quim Nova. 2010;33(7):1549–58.
23. Pribowo AY, Hu J, Arantes V, Saddler JN. The development and use of an ELISA-based method to follow the distribution of cellulase monocomponents during the hydrolysis of pretreated corn stover. Biotechnol Biofuels. 2013;6(1):1–15.
24. Bajpai P. Application of enzymes in the pulp and paper industry. Biotechnol Prog. 1999;15(2):147–57.
25. Roncero MB, Torres AL, Colom JF, Vidal T. The effect of xylanase on lignocellulosic components during the bleaching of wood pulps. Bioresour Technol. 2005;96(1):21–30.
26. Viikari L, Kantelinen A, Sundquist J, Linko M. Xylanases in bleaching: from an idea to the industry. FEMS Microbiol Rev. 1994;13(2–3):335–50.
27. Roberts JC, McCarthy AJ, Flynn NJ, Broda P. Modification of paper properties by the pretreatment of pulp with *Saccharomonospora viridis* xylanase. Enzyme Microb Technol. 1990;12(3):210–3.
28. Savitha S, Sadhasivam S, Swaminathan K. Modification of paper properties by the pretreatment of wastepaper pulp with *Graphium putredinis*, *Trichoderma harzianum* and fusant xylanases. Bioresour Technol. 2009;100(2):883–9.
29. Johansson LS. Monitoring fibre surfaces with XPS in papermaking processes. Microchim Acta. 2002;138(3–4):217–23.
30. Fardim P, Durán N. Modification of fibre surfaces during pulping and refining as analysed by SEM, XPS and ToF-SIMS. Colloids Surf A. 2003;223(1):263–76.
31. Fardim P, Gustafsson J, von Schoultz S, Peltonen J, Holmbom B. Extractives on fiber surfaces investigated by XPS, ToF-SIMS and AFM. Colloids Surf A. 2005;255(1):91–103.
32. Belgacem MN, Czeremuszkin G, Sapieha S, Gandini A. Surface characterization of cellulose fibres by XPS and inverse gas chromatography. Cellulose. 1995;2(3):145–57.
33. Matuana LM, Balatinecz JJ, Sodhi RNS, Park CB. Surface characterization of esterified cellulosic fibers by XPS and FTIR spectroscopy. Wood Sci Technol. 2001;35(3):191–201.
34. Li J, Kisara K, Danielsson S, Lindström ME, Gellerstedt G. An improved methodology for the quantification of uronic acid units in xylans and other polysaccharides. Carbohydr Res. 2007;342(11):1442–9.
35. Sluiter A, Crocker D, Hames B, Ruiz R, Scarlata C, Sluiter J, Templeton D. Determination of Structural Carbohydrates and Lignin in Biomass. Laboratory Analytical Procedure (LAP). 2008;NREL/TP-510-42618.
36. Lupoi JS, Singh S, Simmons BA, Henry RJ. Assessment of lignocellulosic biomass using analytical spectroscopy: an evolution to high-throughput techniques. BioEnergy Res. 2014;7(1):1–23.
37. Andrade JD. X-ray photoelectron spectroscopy (XPS). In: Surface and interfacial aspects of biomedical polymers. Springer; 1985. p. 105–95.
38. Knox JP. In Situ Detection of Cellulose with Carbohydrate-Binding Modules. Cellulases. 2012;510:233–45.
39. Knox JP. Revealing the structural and functional diversity of plant cell walls. Curr Opin Plant Biol. 2008;11(3):308–13.
40. Hervé C, Marcus SE, Knox JP. Monoclonal antibodies, carbohydrate-binding modules, and the detection of polysaccharides in plant cell walls. Methods Mol Biol. 2011;715:103–13.
41. Oliveira C, Carvalho V, Domingues L, Gama FM. Recombinant CBM-fusion technology-Applications overview. Biotechnol Adv. 2015;33(3):358–69.
42. Boraston AB, Bolam D, Gilbert H, Davies GJ. Carbohydrate-binding modules: fine-tuning polysaccharide recognition. Biochem J. 2004;382:769–81.
43. Gao S, You C, Renneckar S, Bao J, Zhang YHP. New insights into enzymatic hydrolysis of heterogeneous cellulose by using carbohydrate-binding module 3 containing GFP and carbohydrate-binding module 17 containing CFP. Biotechnol Biofuels. 2014;7(1):1–11.
44. Gilbert HJ, Knox JP, Boraston AB. Advances in understanding the molecular basis of plant cell wall polysaccharide recognition by carbohydrate-binding modules. Curr Opin Struct Biol. 2013;23(5):669–77.
45. Szabó L, Jamal S, Xie H, Charnock SJ, Bolam DN, Gilbert HJ, Davies GJ. Structure of a family 15 carbohydrate-binding module in complex with xylopentaose evidence that xylan binds in an approximate 3-fold helical conformation. J Biol Chem. 2001;276(52):49061–5.
46. Lakowicz JR. Principles of fluorescence spectroscopy. Berlin: Springer Science & Business Media; 2013.
47. Ding S, Xu Q, Ali MK, Baker JO, Bayer EA, Barak Y, Lamed R, Sugiyama J, Rumbles G, Himmel ME. Versatile derivatives of carbohydrate-binding modules for imaging of complex carbohydrates approaching the molecular level of resolution. Biotechniques. 2006;41(4):435.
48. Kawakubo T, Karita S, Araki Y, Watanabe S, Oyadomari M, Takada R, Tanaka F, Abe K, Watanabe T, Honda Y, Watanabe T. Analysis of exposed cellulose surfaces in pretreated wood biomass using carbohydrate-binding module (CBM)-cyan fluorescent protein (CFP). Biotechnol Bioeng. 2010;105(3):499–508.
49. Abbott DW, Boraston AB. Quantitative approaches to the analysis of carbohydrate-binding module function. Methods Enzymol. 2012;510:211–31.
50. Tavast D, Mansoor ZA, Brännvall E. Xylan from agro waste as a strength enhancing chemical in kraft pulping of softwood. Ind Eng Chem Res. 2014;53(23):9738–42.
51. Linder Å, Bergman R, Bodin A, Gatenholm P. Mechanism of assembly of xylan onto cellulose surfaces. Langmuir. 2003;19(12):5072–7.
52. Gierer J. Chemical aspects of kraft pulping. Wood Sci Technol. 1980;14(4):241–66.
53. Bajpai P. Pulp bleaching and bleaching effluents. In: Bleach plant effluents from the pulp and paper industry. Springer International Publishing; 2013. p. 13–9.
54. Fardim P, Hultén AH, Bolsvert JP, Johansson LS, Ernstsson M, Campbell JM, Lejeune A, Holmbom B, Laine J, Gray D. Critical comparison of methods for surface coverage by extractives and lignin in pulps by X-ray photoelectron spectroscopy (XPS). Holzforschung. 2006;60(2):149–55.
55. Inari GN, Petrissans M, Dumarcay S, Lambert J, Ehrhardt JJ, Šernek M, Gérardin P. Limitation of XPS for analysis of wood species containing high amounts of lipophilic extractives. Wood Sci Technol. 2011;45(2):369–82.

56 Istone WK. X-ray photoelectron spectroscopy (XPS). Boca Raton: CRC Press; 1995. p. 235–68.
57 Inari GN, Petrissans M, Lambert J, Ehrhardt JJ, Gérardin P. XPS characterization of wood chemical composition after heat-treatment. Surf Interface Anal. 2006;38(10):1336–42.
58 Nzokou P, Kamdem DP. X-ray photoelectron spectroscopy study of red oak (*Quercus rubra*), black cherry (*Prunus serotina*) and red pine (*Pinus resinosa*) extracted wood surfaces. Surf Interface Anal. 2005;37(8):689–94.
59 Sernek M. Comparative analysis of inactivated wood surfaces. Doctoral dissertation. Virginia Polytechnic Institute and State University; 2002.
60 Awada H, Elchinger PH, Faugeras PA, Zerrouki C, Montplaisir D, Brouillette F, Zerrouki R. Chemical modification of kraft cellulose fibres: influence of pretreatment on paper properties. BioResources. 2015;10(2):2044–56.
61 Johansson LS, Campbell JM, Fardim P, Huitén AH, Boisvert JP, Ernstsson M. An XPS round robin investigation on analysis of wood pulp fibres and filter paper. Surf Sci. 2005;584(1):126–32.
62 Radotić K, Kalauzi A, Djikanović D, Jeremić M, Leblanc RM, Cerovć ZG. Component analysis of the fluorescence spectra of a lignin model compound. J Photoch Photobio B. 2006;83(1):1–10.
63 Sluiter A, Ruiz R, Scarlata C, Sluiter J, Templeton D. Determination of extractives in biomass. Laboratory Analytical Procedure (LAP). 2005. p. 1617.
64 Bradford MM. A rapid and sensitive method for the quantitation of microgram quantities of protein utilizing the principle of protein-dye binding. Anal Biochem. 1976;72(1):248–54.
65 Tomme P, Boraston A, Kormos JM, Warren RAJ, Kilburn DG. Affinity electrophoresis for the identification and characterization of soluble sugar binding by carbohydrate-binding modules. Enzyme Microb Technol. 2000;27(7):453–8.
66 Cui L, Meddeb-Mouelhi F, Laframboise F, Beauregard M. Effect of commercial cellulases and refining on kraft pulp properties: correlations between treatment impacts and enzymatic activity components. Carbohyd Polym. 2015;115:193–9.

# Appendix B

Sustainable Energy & Fuels

PAPER

View Article Online
View Journal | View Issue

Check for updates

Cite this: Sustainable Energy Fuels, 2018, 2, 479

# New insights into the enzymatic hydrolysis of lignocellulosic polymers by using fluorescent tagged carbohydrate-binding modules†

Vinay Khatri,[ab] Fatma Meddeb-Mouelhi[ab] and Marc Beauregard *[ab]

The development of a bio-based economy requires the utilization of lignocellulosic biomass in a cost-effective way. The economic viability of lignocellulosic biomass-based industries is hindered by our imperfect understanding of biomass structure and suboptimal industrial processes. To achieve such goals requires direct and rapid monitoring of lignocellulosic polymers as they are physically, chemically, and/or enzymatically treated. In this study, the recently reported fluorescent protein tagged carbohydrate binding modules method (FTCM) was used to specifically track mechanical, chemical and enzymatic-induced variations of hemicelluloses at the surface of different wood fibers. Our results showed that susceptibility to hydrolysis in kraft pulp was higher for xylan, while mannan was more vulnerable in mechanical pulps. Furthermore, FTCM rapidly and efficiently detected enzymatic inactivation and the apparent complementarity (additive and/or synergistic effect) between cellulase and other enzymes (xylanase and mannanase), significantly bolstering cellulose and hemicelluloses hydrolysis. Subsequent addition of xylanase and mannanase enzymes directly proved that xylan was acting as a physical shield which was covering mannan in bleached kraft pulp. This study suggests that mannan was closely associated with cellulose or was deeply embedded in the cell wall organization of such fibers. FTCM provided direct support for previous models on fiber structure that were based on time-consuming and complicated approaches (*i.e.* chromatography, spectroscopy and microscopy). FTCM allowed for the monitoring of layers of polymers as they were exposed after treatments, providing key information regarding hydrolysis optimization and the specific susceptibility of xylan and mannan to biomass treatments. We believe that by applying this simple and rapid method on site, biomass industries could substantially improve cost-effectiveness of production of biofuels and other lignocellulosic biomass-based products.

Received 4th September 2017
Accepted 15th December 2017

DOI: 10.1039/c7se00427c

rsc.li/sustainable-energy



## Introduction

Lignocellulosic biomass is the most abundant, renewable and sustainable feedstock allowing our ever-increasing energy demand to be satiated while fossil fuels progressively disappear.[1–5] In addition, the greenhouse gas mitigation and near carbon neutrality afforded by the conversion of biomass to bio energy (biofuel) and chemicals are important advantages over conventional fossil fuels.[4,6–8] The development of a bio-based economy, however promising, is faced with challenges related to the cost-effective utilization of the lignocellulosic biomass. Improving biomass processes would increase cost effectiveness and competitiveness for large scale applications.[4,9,10] The main obstacle for biofuel and chemicals production is associated with the inherent recalcitrant nature of lignocellulosic biomass.[3,11–14] Due to the structural complexity of lignocellulosic biomass, the bioconversion of biomass to biofuel is a multiple stage process.[8,15] The enzymatic hydrolysis of the lignocellulosic component to fermentable sugars is a crucial step in this bioconversion. It is considered as one of the major rate limiting and costly step.[16–21]

The complex recalcitrance nature of biomass is partly attributed to hemicelluloses. They constitute about 20–30% of the total biomass, and are the second most common polysaccharides[22–24] in nature, after cellulose. Unlike cellulose, hemicelluloses are heterogeneous polymers of pentoses (xylose, arabinose), hexoses (mannose, glucose, galactose) and/or uronic acids (glucuronic acid, galacturonic acid).[22,25] Hemicelluloses in hardwood (from angiosperms) mostly consist of xylan, whereas softwood (from gymnosperms) typically contains glucomannans.[26] The hemicelluloses have frequently been recognized to act as a physical barrier, that cover the outer

*Centre de recherche sur les matériaux lignocellulosiques, Université du Québec à Trois-Rivières, C.P. 500, Trois-Rivières, Québec G9A 5H7, Canada. E-mail: vinay.khatri@uqtr.ca; fatma.meddeb@uqtr.ca, marc.beauregard@uqtr.ca; Fax: +1-819-376-5084; Tel: +1-819-376-5011 ext. 3354

[b]PROTEO, Université Laval, Québec G1V 4G2, Canada

† Electronic supplementary information (ESI) available. See DOI: 10.1039/c7se00427c

surface of cellulose fibers and interfibrillar space, limiting the accessibility of cellulase enzymes to cellulose.[47,51] The hemicellulose-degrading activities in most commercially available cellulase enzymes are too low to achieve sufficient hydrolysis of the hemicelluloses.[36,37] Therefore, addition of enzyme extracts or additives with higher level of hemicellulases are important for eliminating the significant hindering effect of residual hemicelluloses (mostly xylan and mannan) on the enzymatic hydrolysis of cellulose.[27,29,37,38,41] In order to increase the efficiency of wood fiber utilization, it is important to utilize all wood fiber constituents (including hemicelluloses and lignin) in an economically feasible way (providing other valuable wood-derived materials beside biofuel). However, this requires a better understanding of the ultrastructure of the cell wall and its organization, which are not yet fully understood.[20] Different chromatography, spectroscopy and microscopy techniques have been used to study lignin–carbohydrate complexes,[38] polymers interactions[44] and plant cell wall deconstruction.[20] For instance, an FT-IR study of softwood fiber (kraft pulp) dedicated to investigate the interactions between wood polymers revealed that glucomannan was closely associated to cellulose while there existed no mechanical interactions between xylan and cellulose.[44] Current models suggest that hemicelluloses play a major role in biomass recalcitrance and are closely associated with both lignin and cellulose, forming lignin–hemicellulose complexes and cellulose–hemicellulose complexes.[38] These techniques revealed important information on hemicellulose's location and their influence on the recalcitrance nature of fibers, and enhanced our understanding of the structural arrangement of fibers. They are however invasive, time-consuming, complex and are dependent on specialized equipment and expertise.

The inherent recalcitrance nature of plants directly or indirectly impacts enzyme accessibility,[12,13,38,41] inactivation,[45] inhibition[40,41,46–53] and, as a consequence, cost of use.[9,10,37] The recent improvement in enzymes stabilization, activity, cost-effectiveness[41,43,54–61] and development of new promising pretreatment conditions[62–64] improved production yields. However, the high dose requirements of these enzymes often jeopardize commercial viability.[37,43,45,61,65] Therefore, investigating biomass recalcitrance of typical wood biomass substrates, and correlating process parameters such as enzyme dosage, temperature, incubation time, inactivation and inhibition, with polymers hydrolysis efficiency is important. We anticipate that such advances would support engineers for increasing yields and mitigate production costs associated with lignocellulosic biomass based industries.

One of the major difficulties in studying biomass recalcitrance and process parameters is the lack of rapid, high throughput and reliable tools[21] for monitoring and/or tracking hemicelluloses at the surface of wood fibers. Over the past decade, several techniques have been developed for direct and rapid detection of biomass polymers.[66–71] Among these techniques, carbohydrate-binding modules (CBMs) are more powerful and advantageous as detection probes compared to others (such as chemical dyes, monoclonal antibodies *etc.*) due to their high specificity towards lignocellulosic polymers.[70,71] CBMs are the non-catalytic polysaccharide-recognizing modules of glycoside hydrolases enzymes.[70,72] Until now, CBMs have been implemented for various fundamental research on plant cell chemistry and their structure,[27,73] cellulose accessibility and surface morphology,[74–79,80] as well as for several industrial applications.[72,81–83]

Considering the importance of lignocellulosic biomass tracking, we have recently established a novel, rapid, high-throughput, easy-to-use, unambiguous and affordable approach to track lignocellulosic polymers at the surface of mechanically, chemically and enzymatically treated pulps.[82,83] This approach is based on the use of four highly specific probes made of fluorescent-tagged carbohydrate binding modules. The CBM part of these genetically modified probes recognizes and binds to biopolymers (*i.e.* mannan, xylan, crystalline and amorphous cellulose) while the fluorescent protein part makes it possible to quickly detect and measure binding of probes to their intended targets. This approach, called fluorescent tagged CBM method (FTCM), proved to be instrumental for our understanding of lignocellulosic biomass processing, and exhibited both process optimizing and outcome predicting potential.[82,83]

Here we investigated the potential of FTCM for bolstering our understanding of hemicelluloses hydrolysis and factors that have an impact on such hydrolysis. To this end, we used two fluorescent-tagged fusion proteins of FTCM: mOrange2-CBM15 (OC15) and eCFP-CBM27 (CC27). The family 15 CBM (CBM15) is a xylan recognizing module of a xylanase (Xyn10C) from *Cellvibrio japonicus*[84] and family 27 CBM (CBM27) consists of the mannan recognizing module of mannanase (Man5) from *Thermotoga maritima*.[85] Both CBM15 and CBM27 are classified as type B CBMs and have been demonstrated to bind specifically to xylooligosaccharides and mannooligosaccharides, respectively.[84,85] Mono-orange2 (mOrange2) and cyan fluorescent protein (CFP) were used as fluorescent proteins (detector molecules), and can be quantitatively measured with very high sensitivity and specificity, due to their independent fluorescent signals (each probe has its specific pair of emission and absorption maxima). For this study, we used four different pulp samples (unbleached mechanical pulp, bleached mechanical pulp, unbleached kraft pulp and bleached kraft pulp) to investigate and track variations in hemicelluloses after various treatments. Our results showed that FTCM can monitor the impact of mechanical and chemical treatment on the surface distribution of hemicelluloses, and helped understand and optimize enzymatic-induced hydrolysis of lignocellulosic polymers. We anticipate that FTCM can be developed into a monitoring tool for optimization of treatments and process strategies leading to a cost effective hydrolysis of hemicelluloses.

## Experimental

### Materials and methods

**Chemicals and microbial strains.** Unless otherwise noted, all chemicals were reagent grade and purchased from Sigma-Aldrich and/or Fisher Scientific. *Escherichia coli* XL10 cells (Agilent Technologies) were used for all DNA manipulations

while *E. coli* BL21-Gold(DE3)pLysS competent cells (Agilent Technologies) were used for recombinant proteins expression. *Trichoderma viride* xylanase (*endo*-1,4-β-xylanase) from glycoside hydrolase (GH) family 11 (E-XYTRI; Megazyme), *Cellvibrio japonicus* mannanase (*endo*-1,4-β-mannanase) from glycoside hydrolase (GH) family 26 (E-BMACJ; Megazyme) and *Trichoderma reesei* Celluclast 1.5L (C2730; Sigma-Aldrich) were used for the hydrolysis of lignocellulosic biomass. Carboxymethyl cellulose sodium salt (C5678; Sigma), xylan from beechwood (X4252; Sigma) and galactomannan (P-GALML; Megazyme) were used for affinity gel electrophoresis (AGE) and for enzymatic assays using the 3,5-dinitrosalicylic acid (DNS) method.

**Construction, production and purification of CBM recombinant probes.** Probes were produced and purified from recombinant *E. coli* BL21-Gold(DE3)pLysS cells as described by Khatri *et al.* (2016)[82] and Hébert-Ouellet *et al.* (2017)[83] (note that in this study, probe eGFP-CBM3a was named GC3a; probe mOrange2-CBM15 was named OC15 and probe eCFP-CBM27 was named CC27, for the sake of simplicity). Following affinity and size exclusion chromatography steps, the probes purities were verified using SDS-PAGE (additional files 1 and 8). The amount of protein was quantified using the Bradford method.[86] Concentrated protein solutions were stored at −80 °C following flash freezing.

**Affinity gel electrophoresis (AGE).** AGE was used as described by Khatri *et al.* (2016)[82] for qualitative assessment of the CC27 (10 μg) specificity toward selected ligands.

**Isothermal titration calorimetry (ITC).** ITC was employed as described by Khatri *et al.* (2016)[82] to measure the affinity of the CC27 probe towards selected hexaoses (xylohexaose (O-XHE; Megazyme), mannohexaose (O-MHE; Megazyme), cellohexaose (O-CHE; Megazyme)). All experiments were performed in triplicates. Data were analyzed and fitted using the NanoAnalyze software v2.3.6 (TA Instruments).

**Pulp characterization.** The mechanical and kraft pulps used for this study were provided by an Eastern Canadian pulp and paper company. Both mechanical and kraft pulping were performed using a mixture of softwood (80–85%) and hardwood (20–15%). Four different grades of pulps: unbleached mechanical pulp (UBMP), bleached mechanical pulp (BMP), unbleached kraft pulp (UBKP) and bleached kraft pulp (BKP), were used. The cellulose, hemicellulose, and lignin contents of these pulps were analyzed in triplicates using NREL/TP-510-42618 protocol[87] as described in Khatri *et al.* (2016).[82]

**Handsheets preparation.** UBMP, BMP, UBKP and BKP were used as lignocellulosic substrates for the preparation of handsheets and paper discs. Handsheets (basis weight of 60 ± 2 g $m^{-2}$) were prepared from pulps according to the Tappi standard method T 205 sp-02 as described in Khatri *et al.* (2016).[82] These handsheets were then used for the preparation of the paper punches. These punches were defined as paper discs having a diameter of 3 mm.

**Enzymatic digestion of paper discs.** The enzymatic digestions of paper discs were performed in triplicates using *Trichoderma viride* xylanase, *Cellvibrio japonicus* mannanase and *Trichoderma reesei* Celluclast 1.5L enzyme(s). Celluclast 1.5L is a mixture of fungal hydrolytic enzymes containing mostly two cellobiohydrolases, two endoglucanases and various accessory enzymes such as hemicellulases.[47,88] We used the 3,5-dinitrosalicylic acid (DNS) method[97] to monitor the accessory enzymes activities (such as xylanase and mannanase) in the Celluclast 1.5L (additional file 12). Xylanase and mannanase treatment concentrations ranged from 0.1 to 0.4 U per paper discs. Celluclast 1.5L enzyme was used at 0.1 U per paper discs. Cocktail CX was prepared by mixing Celluclast 1.5L (0.1 U per paper disc) with *Trichoderma viride* xylanase (0.1 U per paper disc). Cocktail CM was prepared by mixing Celluclast 1.5L (0.1 U per paper disc) with *Cellvibrio japonicus* mannanase (0.1 U per paper disc) and cocktail CXM was prepared by mixing Celluclast 1.5L (0.1 U per paper disc) with *Trichoderma viride* xylanase (0.1 U per paper disc) and *Cellvibrio japonicus* mannanase (0.1 U per paper disc). Units used here were as specified by respective enzyme suppliers. All experiments were performed with paper discs placed/glued at the bottom of 96-well black microtiter plate (Corning). All reactions were performed at room temperature or 50 °C, in sodium phosphate buffer (100 mM), pH 7.0 supplemented with 0.5 mg $mL^{-1}$ BSA under continuous agitation (150 rpm) in order to reduce enzyme adsorption. Unless otherwise noted, after each enzymatic digestion, the reactions were removed and paper discs were washed (3 × 5 minutes) with buffer (20 mM Tris–HCl, pH 7.5 with 20 mM NaCl and 5 mM $CaCl_2$) and later washed (3 × 5 minutes) with 0.05% (v/v) Tween 20. This buffer was shown to remove most proteins from paper discs in a previous report.[82] Following Tween 20 washing, paper discs were washed again with buffer (without Tween) before analyzing the variations in biopolymers levels, or digested again with refreshing enzymes solution every hour to reach maximum possible hydrolysis when specified.

**Lignocellulosic polymers tracking on the surface of paper discs using the OC15, CC27 and GC3a probes.** The FTCM tracking assay was performed as described by Khatri *et al.* (2016).[82] All fluorescence readings were acquired at room temperature with a Synergy Mx microplate reader (BioTek). These fluorescence values were then converted into μg $mm^{-2}$ using the appropriate standard curves (additional files 6, 7 and 9) and the surface area of the paper discs.

## Results and discussion

### Determination of the CC27 probe specificity using affinity gel electrophoresis (AGE)

In this study we have used three FTCM probes (GC3a, OC15 and CC27). GC3a and OC15 were previously characterized and shown to be specific to their intended target.[82,83] Affinity gel electrophoresis (AGE) was used to qualitatively evaluate the specificity of the CC27 probe (mannan specific) towards soluble polysaccharides.[82] In AGE, interactions between the studied protein and the gel-embedded polysaccharide are typically revealed by a reduced mobility compared to the mobility of the protein in absence of saccharide. Fig. 1 shows that CC27 interacts only with galactomannan (Fig. 1B). Similar to BSA, no binding was detected between CC27 and beechwood xylan (Fig. 1C) or carboxymethyl cellulose (CMC) (Fig. 1D). These results confirm that the well-known specific binding of CBM27

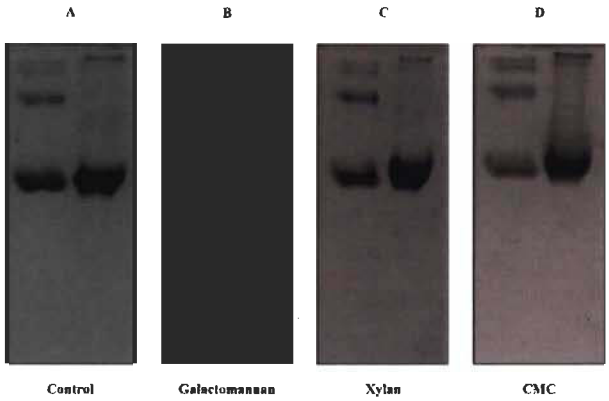


Fig. 1 Affinity gel electrophoresis (AGE) of the CC27 probe (Panel A) control (no polysaccharide), (panel B) galactomannan, (panel C) xylan, (panel D) CMC. In each panel the first well contained BSA (10 μg) and the second well was loaded with the CC27 probe (10 μg). All soluble polysacchandes were used at final concentration of 0.5% (w/v) and a 12% polyacrylamide gel was used for affinity analysis.

to mannan is unaltered by its fusion with CFP in the CC27 probe. BSA, which has no affinity towards carbohydrates, was used as negative control.[87]

### Determination of CC27 probe affinity using isothermal titration calorimetry (ITC)

The affinity of the recognition module of CC27 was investigated to quantify its sensitivity for a representative derivative of mannan. To this end, the affinity of CC27 toward various hexaoses was investigated by ITC (Table 1 and additional file 2). Analysis of the binding isotherms showed that the recognition module of CC27 probe bound tightly to mannohexaose ($K_a$ = 692.6 × $10^3$ $M^{-1}$), but not to cellohexaose or xylohexaose (Table 1). The affinity value is similar to the one previously reported for CBM27 ($K_a$ (×$10^4$ $M^{-1}$) = 136.5 ± 17.68) confirming that the binding site of the recognition module of the CC27 probe is unaltered by its fusion with CFP.[83]

### Tracking hemicelluloses at the surface of wood biomass

Pulps composed of a mixture of softwood (80–85%) and hardwood (20–15%) from an Eastern Canadian paper mill were used as lignocellulosic biomass samples. Four different types of pulps were used in this study, allowing for the comparison of mechanically and chemically treated wood biomass: unbleached mechanical pulp (UBMP), bleached mechanical pulp (BMP), unbleached kraft pulp (UBKP) and bleached kraft pulp (BKP). These pulps were first investigated to determine differences in the hemicelluloses polymer content and their exposure at fiber surface.

Table 1 Affinity of the CC27 probe for various hexaoses as determined by ITC[a]

| Ligand | $K_a$ × $10^{-4}$ ($M^{-1}$) | $K_d$ (M) | $n$ |
|---|---|---|---|
| Xylohexaose | NB | — | — |
| Mannohexaose | 692.6 ± 0.5 | 4.413 × $10^{-6}$ ± 0.2 | 1.1 ± 0.3 |
| Cellohexaose | NB | — | — |

[a] $n$: number of ligand binding sites. NB: no binding detected. –: binding not detected.

Comparison of CC27 with OC15 binding to pulps (Fig. 2) revealed that mannan exposure is 2.3-fold higher than xylan exposure in both mechanical pulps (UBMP and BMP). Only minute differences were observed between exposures of both hemicelluloses studied here in kraft pulps: mannan exposure was 1.13-fold higher than xylan exposure in UBKP and only 1.08-fold higher in BKP (Fig. 2). The dominance of mannan for all pulps is compatible with the high softwood content of the four different pulps studied here.[26] Our results also indicate that mannan was the dominant hemicellulose at the surface of mechanical pulps in agreement with an earlier study on lignin–hemicellulose complexes.[88] Even though the pulp was primarily composed of softwood fibers, kraft processing led to the exposure of similar amounts of xylan and mannan on the surface of both kraft pulps (Fig. 2, UBKP and BKP). Note that the trends observed in FTCM signals, which responds to surface polymers, were in accordance with the bulk measurements of simple sugars by chemical composition analysis (NREL/TP-510-42618) of these pulps (additional file 3).

Bleaching of mechanical pulp resulted in no significant difference between the exposure of xylan and mannan (Fig. 2). These results can be attributed to the pulping methodology involved. Mechanical pulping is a high yield process which tends to retain most wood constituents when producing UBMP and during the transformation of UBMP to BMP.[89] FTCM indicates that the distribution of hemicelluloses at the surface of mechanically treated fibers were comparable to fiber bulk composition (revealed by NREL/TP-510-42618) (additional file 3).

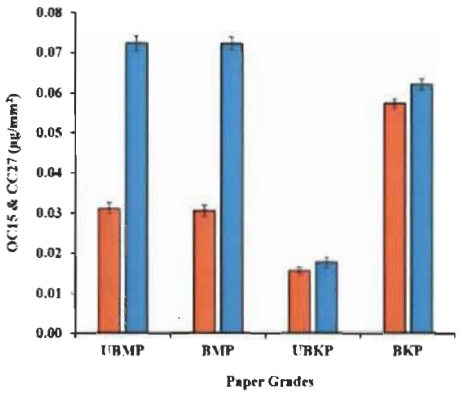


Fig. 2 Tracking hemicelluloses on the surface of UBMP, BMP, UBKP and BKP papers using OC15 and CC27 probes. UBMP, BMP, UBKP and BKP paper discs were incubated with the OC15 probe (0.5 µg µL$^{-1}$) (for xylan detection) and the CC27 probe (0.5 µg µL$^{-1}$) (for mannan detection) for 1 h at room temperature under agitation. Three percent (w/v) milk (20 mM Tris–HCl, pH 7.5 with 20 mM NaCl and 5 mM $CaCl_2$) was used to minimize the auto-fluorescence of paper discs and the non-specific binding of the OC15 and CC27 probes. The fluorescence values were converted to OC15 (µg mm$^{-2}$) and CC27 (µg mm$^{-2}$) by using the standard curves (additional file 6 and 7). Orange color represents the OC15 probe detection and cyan color represents the CC27 probe detection. Error bars represent the standard deviation.

The goal of kraft pulping process is to degrade and/or dissolve lignin with minimum dissolution or degradation of hemicelluloses.[90] UBKP was characterized by the smallest exposure of hemicelluloses, a possible consequence of the dissolution or degradation of lignin–hemicelluloses complexes[91] during kraft pulping. Bleaching of kraft pulp completely changed hemicelluloses exposure. As shown in Fig. 2, BKP binds 3.6-fold the amount of OC15 and 3.5-fold the amount of CC27 in comparison to UBKP, indicating that the surface exposure of xylan and mannan has increased after the bleaching process. Kraft pulping did not remove all lignin (lignin still represents 4.3% according to chemical composition analysis, additional file 3) in UBKP. Bleaching revealed additional hemicelluloses at the surface of BKP, resulting from the removal of this residual lignin. These "deep" hemicelluloses would become accessible after the full removal of lignin. Another explanation for this higher exposure or detection of hemicelluloses would involve mannan and xylan redeposition onto the surface of cellulose fibers during kraft processes.[91–93]

The strength of FTCM lies in its ability to detect changes in hemicelluloses exposure at the surface of fibers. While the trends observed were in general compatible with overall composition analysis (additional file 3), the amplitude of changes at the surface could not be predicted by chemical analysis. For instance, mannan dropped by 71% when comparing both mechanical pulps (UBMP and BMP) with UBKP (Fig. 2). Chemical analysis detected a mere decrease of 30–34% in mannan for the same comparison. In kraft pulps, the impact of bleaching on hemicelluloses exposure (an increase of 67%) (Fig. 2) could not be predicted by chemical composition analysis (showing an increase of only 13–15%, additional file 3). We also confirmed that the fluorescent proteins (alone, without CBM) did not bind to the biomass surface (data not shown), and we found no difference in binding signals, regardless of using the OC15 and CC27 probes together or separately (additional file 4 and 5). This indicates that the probes did not interfere with one another, as expected from the different targets to which they are specific. We also confirmed that there was no unspecific interactions between lignin and probes (data not shown).

We also investigated physical parameters such as roughness and porosity of paper discs made from pulps and their impact on probe binding. For the four pulps and all probes used in this study, we found that porosity had no obvious impact on probe binding (even when porosity was varied over a 40-fold range, see additional files 10 and 11†). Probes are much smaller than pores or crevices that may be of various sizes or numbers in pulps with different porosities. Roughness was found to vary by about 10% when we compared papers made from pulp in our experiments. Increased roughness did result into moderate increase of probe binding, but we did not observe any change in comparative binding of probes due to roughness (*i.e.* relative binding of a probe *vs.* binding of other probes is unchanged by roughness, see additional files 10 and 11†).

### Investigation of reaction parameters by FTCM

Fig. 3 and 4 show probe binding to various pulps using increasing concentrations of enzymes. Our results revealed that the maximal impact of xylanase and mannanase enzymes on pulps were detected at the minimal loading used here (0.1 U of enzyme/paper disc). All the pulps (UBMP, BMP, UBKP and BKP) showed no significant loss in the exposure of xylan and mannan as we increased the concentration from 0.1 U to 0.4 U per paper disc. This suggests that a 0.1 U per paper disc concentration of both xylanase and mannanase was sufficient for the maximal digestion of available/exposed xylan and mannan. The impact of temperature was also studied. All the pulps showed maximal hydrolysis or decrease in the exposure of xylan and mannan at 50 °C. This suggests that both xylanase and mannanase enzymes were comparatively more active at 50 °C than at room temperature. At room temperature, an overnight treatment showed relatively higher decrement in the exposure of hemicelluloses than a treatment duration of one hour. In contrast, at 50 °C, both 1 h and overnight treatments led to a maximal and similar decrement for both xylanase and mannanase enzymes treatments. FTCM unambiguously reveals that using 0.1 U of enzyme/paper disc for 1 h at 50 °C was sufficient for maximal reduction in available/exposed xylan and mannan. Production of reducing sugars by enzymatic hydrolysis was also monitored using the DNS method. Conditions chosen for this control experiment were the ones that lead to maximal removal of xylan (Fig. 3D). Using same biomass and same treatments, we found that reducing sugar production correlated with the decrease in xylan as detected by the probes (see additional file 13†).

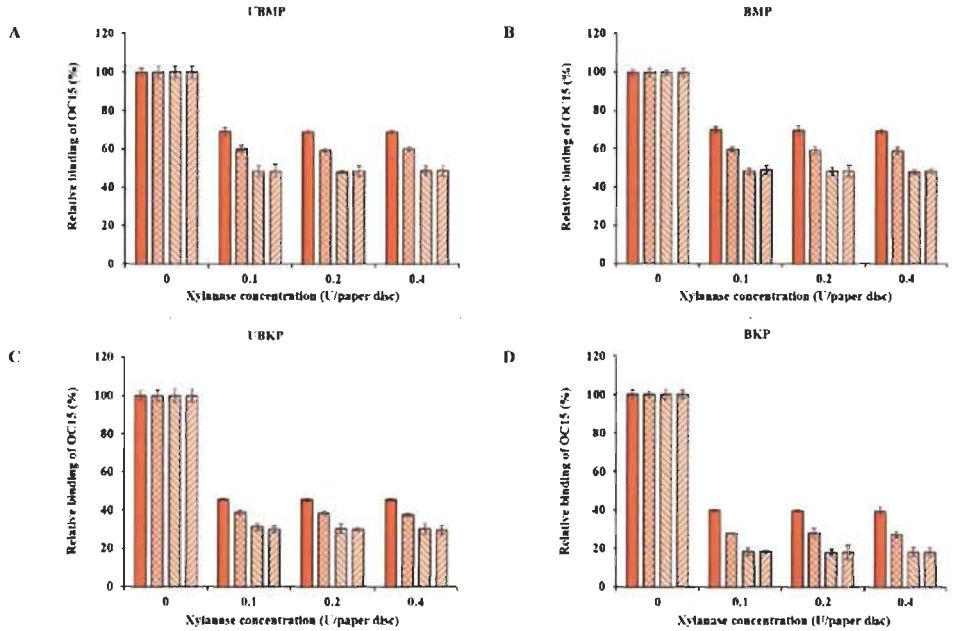


Fig. 3 Tracking xylan for optimizing hydrolysis conditions for xylanase treatments using the OC15 probe. (A) UBMP, (B) BMP, (C) UBKP and (D) BKP paper discs were incubated with xylanase (0.1, 0.2 and 0.4 U per paper disc) at four different opted conditions (1 h, RT, overnight; RT, 1 h; 50 °C and overnight; 50 °C) under continuous agitation (150 rpm). Following this, untreated and treated paper discs were incubated with the OC15 probe (0.5 μg $\mu L^{-1}$) for 1 h at room temperature under agitation to detect xylan exposure. Three percent (w/v) milk (20 mM Tris–HCl, pH 7.5 with 20 mM NaCl and 5 mM $CaCl_2$) was used to minimize the auto-fluorescence of paper discs and the non-specific binding of the OC15 probe. Orange color represents the OC15 probe detection. Error bars represent the standard deviation.

The xylanase enzyme appeared to hydrolyze xylan more efficiently in BKP than all the other pulps (Fig. 3). Xylanase-treated BKP paper discs showed a maximum decrement of 82% in the exposure of xylan. This may be ascribed to the most efficient removal of lignin in BKP compared to all other pulps studied here, as described earlier (Fig. 2 and additional file 3). In contrast, the mannanase enzyme was more efficient on both mechanical pulps (UBMP and BMP) (Fig. 4) due to the very high exposure of mannan in mechanical pulps as described earlier (Fig. 2 and additional file 3). Both UBMP and BMP paper discs showed a maximum decrement of at least 55% in the exposure of mannan after mannanase hydrolysis under our assay conditions. Although hemicelluloses were detectable by our probes, these were not completely hydrolyzed or reachable by the enzyme used. This suggests a possible hindrance or inactivation of enzymes during our assay.

Mannanase hydrolysis showed that the relative amounts of mannan removed from mechanical pulps are higher than the percentage removed from the kraft pulps (Fig. 4). This suggests a higher digestibility of lignin-associated mannan (lignin-hemicelluloses complexes) in mechanical pulp. The hydrolysis of mannan polymers in kraft pulps might be hindered by significant exposure of xylan (mostly associated to cellulose–hemicelluloses complexes), in agreement with an earlier study on lignin–hemicellulose complexes.[38]

In contrast, xylanase hydrolysis showed that xylan was more susceptible to hydrolysis in kraft pulps compared to mannan. In kraft pulps, bleaching increased the exposure of xylan and eventually increased hydrolysis of xylan by a few percentage points. This suggests that after removal of lignin and the so-called lignin–hemicelluloses complexes *via* kraft pulping, xylan is more vulnerable or exposed at the surface of kraft pulps fibers than mannan. The xylanase hydrolysis in mechanical pulps seems to be hindered by the abundance of mannan, which is the main hemicellulose associated with lignin and/or lignin–hemicelluloses complexes, as shown by the lower binding of OC15 to xylan in both mechanical pulps (Fig. 2). This study revealed that FTCM, a rapid and high throughput approach, can improve our knowledge and understanding of biomass hydrolysis as well as the economic feasibility of lignocellulosic biomass based industries.

### Addressing possible impact of enzyme inactivation

Above results suggested that neither of these enzymes were able to completely eliminate all the available hemicelluloses at the

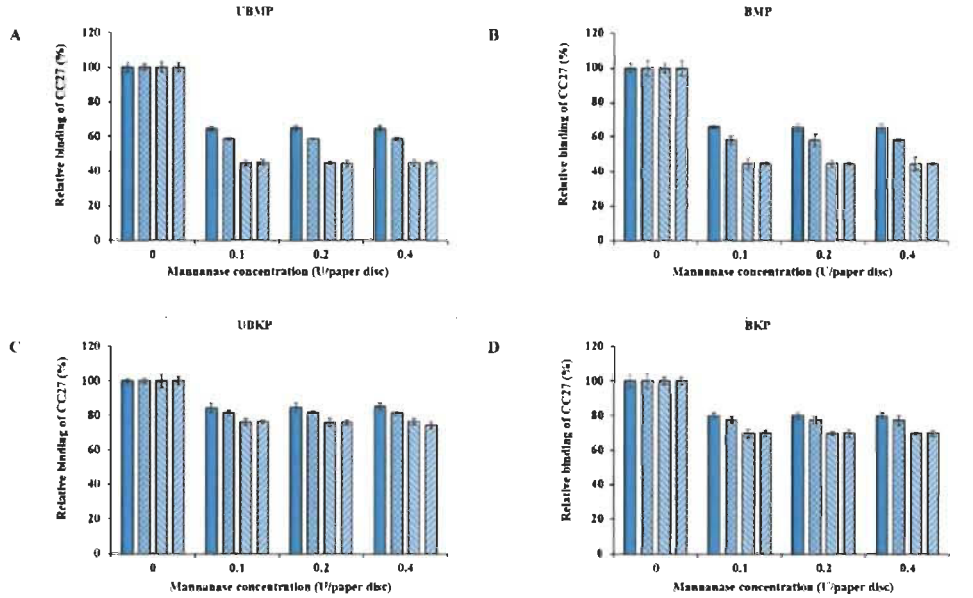


Fig. 4 Tracking mannan for optimizing hydrolysis conditions for mannanase treatments using the CC27 probe. (A) UBMP, (B) BMP, (C) UBKP and (D) BKP paper discs were incubated with mannanase (0.1, 0.2 and 0.4 U per paper disc) at four different opted conditions (1 h; RT ■, overnight; RT ■, 1 h; 50 °C ■ and overnight; 50 °C ■) under continuous agitation (150 rpm). Following this, untreated and treated paper discs were incubated with the CC27 probe (0.5 μg μL$^{-1}$) for 1 h at room temperature under agitation to detect mannan exposure. Three percent (w/v) milk (20 mM Tris–HCl, pH 7.5 with 20 mM NaCl and 5 mM $CaCl_2$) was used to minimize the auto-fluorescence of paper discs and the non-specific binding of the CC27 probe. Cyan color represents the CC27 probe detection. Error bars represent the standard deviation.

surface of fibers under our conditions. This might be explained, in part, by the inactivation of enzymes by reaction products, plant derived inhibitors, adsorption to fibers or denaturation of the enzymes over time.[11] Recent studies have suggested that enzyme inhibition by their own end products and other components, generated during the bioconversion process, can be a key factor which impedes the hydrolysis processes.[40,11,46–55] To further investigate a potential inactivation scenario, we chose BKP paper discs and treated them using optimum hydrolysis conditions (0.1 U of enzyme/paper disc, 50 °C). After a one-hour treatment, the enzymatic reactions were removed and the surfaces of the paper discs were tracked with the OC15 and CC27 probes, individually, for residual hemicelluloses. The tracking of xylan and mannan showed an 80% and 30% decrement, respectively (Fig. 5) (similar to the results described in Fig. 3D and 4D). Prolonging enzymatic reactions longer than one hour (and/or overnight) at 50 °C did not promote any further drop in the exposure of hemicelluloses. Therefore, we washed paper discs to remove the inactivated enzyme which might be inhibiting hydrolysis. To this end, the BKP paper discs, which were already incubated with enzymes for an hour, were washed with buffer and Tween (0.05%) before adding another load of freshly prepared enzymes. After refreshing enzymes (xylanase or mannanase) solution, the reactions were kept again under optimum hydrolysis conditions (0.1 U of enzyme/paper disc, 50 °C) for another hour. Later, the tracking of xylan and mannan showed an additional decrement of 2.3% and 5.3%, respectively, in the exposure of hemicelluloses (Fig. 5). Likewise, the enzymatic reactions were washed again before adding fresh enzymes for an additional one-hour reaction period and then measured by probes, for up to 24 hours. The results exhibited a gradual decrement in the binding of OC15 and CC27 probes. After 24 hours, the maximum decrement in the exposure of xylan was 92% and 50% in the exposure of mannan. The maximal impact was reached after 12 hours (in the case of xylanase hydrolysis) and 5 hours (in the case of mannanase hydrolysis), regardless of washing paper discs and adding freshly prepared enzymes (Fig. 5). This suggests that the xylanase and mannanase enzymes might have reached their maximum possible hydrolysis activity, or that such activity had no more detectable impact on the hemicelluloses. Nevertheless, FTCM indicates that there was an inactivation (and/or inhibition) which was somewhat overcome by washing followed by a fresh load of enzyme (xylanase or mannanase). FTCM reveals that despite an apparent interruption of net hydrolysis, there remains a large amount of mannan at the surface of BKP fibers. Such information cannot be provided by chromatographic analysis of hydrolysis products. Chemical analysis, which

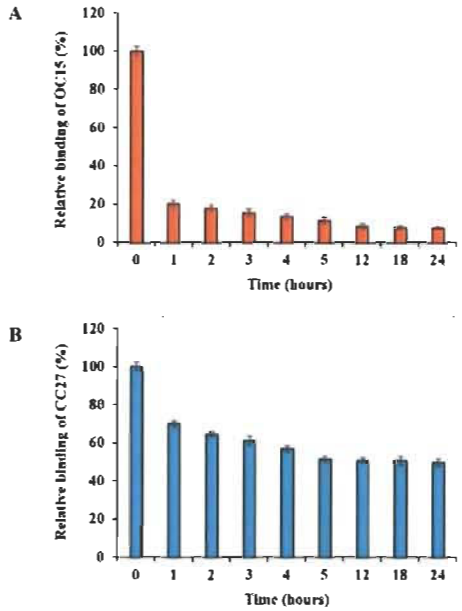


Fig. 5 Tracking (A) xylan and (B) mannan to address the impact of xylanase and mannanase inactivation on BKP paper discs using the OC15 and CC27 probes. (A) Paper discs were incubated with xylanase (0.1 U per paper disc) at 50 °C under continuous agitation (150 rpm) with refreshing enzyme solution every hour up to 24 hours. Following this, untreated and xylanase treated BKP paper discs were incubated with the OC15 probe (0.5 μg $\mu L^{-1}$) for 1 h at room temperature under agitation. (B) Paper discs were incubated with mannanase (0.1 U per paper disc) at 50 °C under continuous agitation (150 rpm) with refreshing enzyme solution every hour up to 24 hours. Following this, untreated and mannanase treated BKP paper discs were incubated with the CC27 probe (0.5 μg $\mu L^{-1}$) for 1 h at room temperature under agitation. For fluorescence measurements, three percent (w/v) milk (in a buffer made of 20 mM Tris–HCl, pH 7.5 with 20 mM NaCl and 5 mM $CaCl_2$) was used to minimize the auto-fluorescence of paper discs and non-specific binding of the probes. Orange color (■) and cyan color (■) represent the OC15 and CC27 probes detection, respectively. Error bars represent the standard deviations.

depends on total hemicellulose content would not be as sensitive as FTCM for detecting changes in hemicellulose hydrolysis at surface and for optimizing enzymatic processes. Note that measurements of reducing sugars production by enzymes were performed allowing to confirm that smaller quantities of sugars were released upon renewing enzymes, but that maximal production of sugars was generated in the first hour with the first exposure to enzyme (additional files 14 and 15†).

### Investigating the impact of cellulose on the hydrolysis of hemicelluloses

Despite finding out the optimum hydrolysis conditions and achieving additional removal of hemicelluloses by spiking enzymes, both xylanase and mannanase enzymes were unable to completely eliminate/hydrolyze all the available hemicelluloses that could be detected by FTCM. To achieve additional hydrolysis of hemicelluloses and simultaneously improve our understanding of fiber deconstruction, we explored the potential impact of cellulase treatments on hemicelluloses availability. The use of enzyme cocktails comprised of cellulase and so-called accessory enzymes (xylanase and/or mannanase) has been previously studied and found to enhance the cellulose hydrolysis.[27,29,33,37,40,42,43] Here we reexamined the apparent complementarity between enzymes using FTCM. To this end, BKP paper discs were hydrolyzed with commercial cellulase enzyme (Celluclast 1.5L) under conditions which were optimal for hemicelluloses hydrolysis (0.1 U per paper disc, 50 °C) for an hour. Celluclast 1.5L possesses some contaminant activity of both xylanase and mannanase (additional file 12). After hydrolysis, an eGFP-CBM3a (named GC3a here) probe was used to track the exposure of crystalline cellulose (as described by Hébert-Ouellet *et al.* 2017).[31] Results in Fig. 6A suggest that Celluclast 1.5L treatment reduced exposure of crystalline cellulose by 63%. Then, supplementation of Celluclast 1.5L with a xylanase accessory enzyme (cocktail CX) and a mannanase accessory enzyme (cocktail CM) was investigated. Addition of hemicellulases led to an additional reduction of exposed cellulose, suggesting that they helped the hydrolysis of cellulose by the Celluclast 1.5L enzyme (Fig. 6A). Finally, the supplementation of Celluclast 1.5L with both xylanase and mannanase enzymes (cocktail CXM) drastically decreased the cellulose exposure (down by 88%, see Fig. 6A). These results confirm that to achieve highest cellulose hydrolysis at surface of BKP fibers, it is vital to supplement cellulase with accessory enzymes such as xylanase and mannanase. These results also suggest that not only one type but both types of hemicelluloses (xylan and mannan) restrict cellulose accessibility or cellulase action.

We then investigated a potential reciprocal additive and/or synergistic action by supplementing xylanase and mannanase enzymes with Celluclast 1.5L and monitoring hemicelluloses removal after treatment. Using the same BKP paper discs treated as explained above, we found that the xylanase enzyme led to 81% decrement in the exposure of xylan (Fig. 6B), which is compatible with the result shown in Fig. 3D. BKP paper discs were also treated with cocktail CX, cocktail CM and cocktail CXM and all led to the nearly complete elimination of xylan at the surface of BKP fibers. Likewise, BKP paper discs hydrolyzed with the mannanase enzyme showed 30% decrement in mannan exposure (Fig. 6C). Subsequently, cocktail CX, cocktail CM and cocktail CXM promoted further hydrolysis of BKP paper, leading to the near complete elimination of mannan from the surface of BKP fibers. These results suggest that cellulose is an important barrier limiting access to hemicelluloses in BKP.

The presence of both hemicellulases (xylanase and mannanase) were required with Celluclast 1.5L for maximal hydrolysis of crystalline cellulose. In contrast, either one of the hemicellulases or both were required with Celluclast 1.5L for maximal hydrolysis of xylan and mannan. This suggests that xylan and mannan were providing protection to cellulose, but that a portion of cellulose remains protected by other fiber

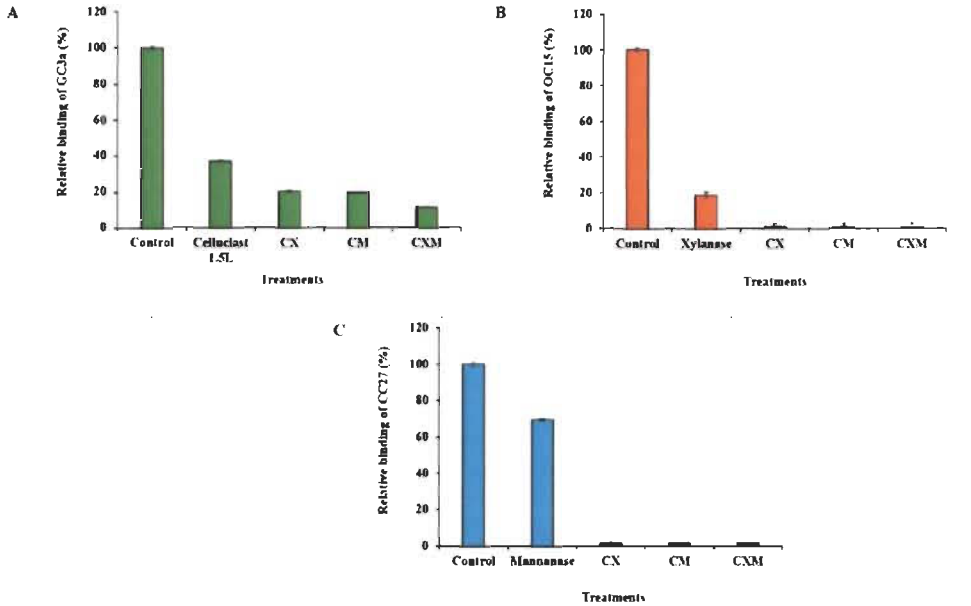


Fig. 6 Impact of Celluclast 1.5L, xylanase, mannanase and their cocktails hydrolysis of BKP on the exposure of (A) crystalline cellulose, (B) xylan and (C) mannan polymers. (A) Paper discs were incubated with Celluclast 1.5L (0.1 U per paper disc), cocktail CX, cocktail CM and cocktail CXM at 50 °C for 1 h under continuous agitation (150 rpm). Following this, untreated and treated BKP paper discs were incubated with the GC3a probe (0.5 μg μL$^{-1}$) for 1 h at room temperature under agitation. (B) Paper discs were incubated with xylanase (0.1 U per paper disc), cocktail CX, cocktail CM and cocktail CXM at 50 °C for 1 h under continuous agitation (150 rpm). Following this, untreated and treated BKP paper discs were incubated with the OC15 probe (0.5 μg μL$^{-1}$) for 1 h at room temperature under agitation. (C) Paper discs were incubated with mannanase (0.1 U per paper disc), cocktail CX, cocktail CM and cocktail CXM at 50 °C for 1 h under continuous agitation (150 rpm). Following this, untreated and treated BKP paper discs were incubated with the CC27 probe (0.5 μg μL$^{-1}$) for 1 h at room temperature under agitation. Green, orange and cyan color were used for GC3a, OC15 and CC27 probes detection, respectively. Error bars represent the standard deviations.

components, or that a portion of exposed cellulose remains stable despite enzymatic attack. Such results are compatible with the existence of deeply embedded hemicelluloses, part of a carbohydrate–hemicellulose complexes, shielding the cellulose fibers. Note that in BKP, the hemicelluloses associated with lignin are expected to be mostly absent. These results suggest that FTCM can also be used to design enzyme cocktails preparations for specific applications. Exposure of fibers to enzymes had a drastic impact on all polysaccharides at surface. The question of "what is left" at surface after such important decrease in probe binding is legitimate but not necessarily relevant. Note that when preparing paper discs prior to FTCM reading, the discs were washed, and any loosen material was removed. Hydrolysis of high surface fragments such as microfibrils and their removal prior to FTCM may explain the important decrease in probe binding observed here.

### Exploring the impact of xylan polymers on the hydrolysis of mannan

The previous section has revealed the proximity of cellulose and "deep" hemicelluloses. Here we focused on the impact of xylan on the hydrolysis of mannan in order to address structural relationships and their potential impact on hydrolysis yield. To this end, BKP paper discs were hydrolyzed with mannanase enzyme as a control reaction. Results showed a decrement of at least 30% in the exposure of mannan for all the enzyme concentrations used (Fig. 7A, solid cyan color bars). The results were as expected and fully compatible with Fig. 4D.

In another reaction, BKP paper discs were digested with the xylanase enzyme. In order to reach the maximum xylan hydrolysis, the reaction was performed as described above (section Addressing possible impact of enzyme inactivation) with refreshing enzyme solution every hour up to 12 hours. By refreshing enzyme solution, this treatment led to a stronger reduction in xylan exposure (an additional 10–13%) as detected with the OC15 probe (Fig. 7B, solid orange color bars). The results were as expected and fully compatible with Fig. 5A. The same xylanase hydrolyzed paper discs were then inspected using the CC27 probe to track mannan exposure. The results revealed that mannan exposure at the surface of xylanase hydrolyzed BKP paper discs increased by 20% when pulp was treated with a 0.4 xylanase U per paper disc (Fig. 7B, cyan color

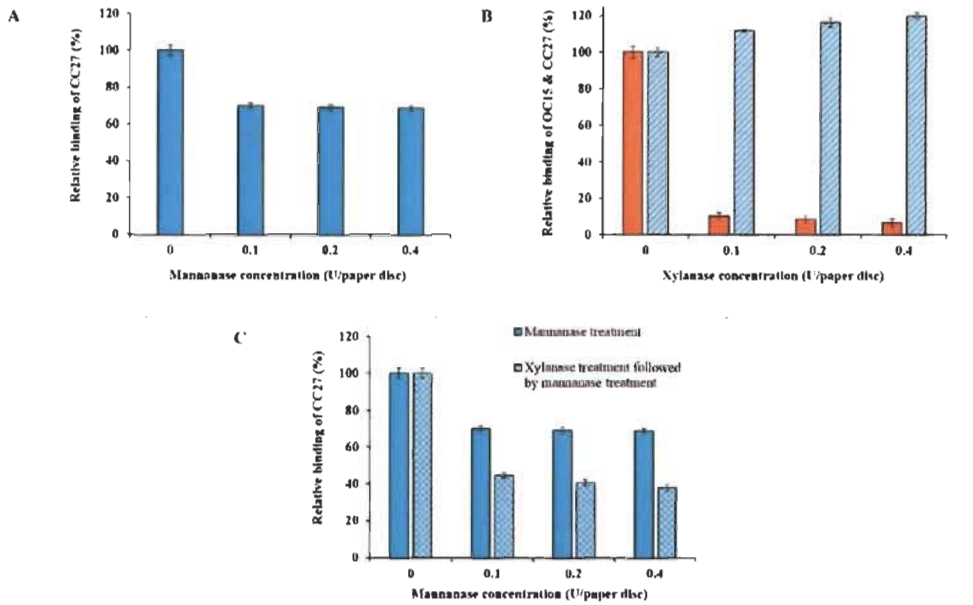


Fig. 7 Impact of mannanase and xylanase hydrolysis of BKP on the exposure of mannan polymers. (A) Untreated and mannanase treated (0.1, 0.2 and 0.4 U per paper disc, at 50 °C for 1 h) BKP paper discs were incubated with the CC27 probe (0.5 μg μL$^{-1}$) for 1 h at room temperature under agitation to detect mannan exposure (■). (B) Untreated and xylanase treated BKP paper discs (0.1, 0.2 and 0.4 U per paper disc, at 50 °C with refreshing enzyme solution every hour up to 12 hours) were incubated with the OC15 probe (0.5 μg μL$^{-1}$) for 1 h at room temperature under agitation (■) for xylan detection. The same xylanase hydrolyzed BKP paper discs were also incubated with the CC27 probe (0.5 μg μL$^{-1}$) to detect mannan exposure (■). (C) Previously xylanase treated BKP paper discs (as described in panel B) were later treated with mannanase enzyme (0.1, 0.2 and 0.4 U per paper disc, at 50 °C for 1 h). Following this, untreated and mannanase treated BKP paper discs were incubated with CC27 probe (0.5 μg μL$^{-1}$) (■). Data of panel A (■) is also shown in panel C for comparison. Orange color (■) represents the OC15 probe detection and cyan color (■) represents the CC27 probe detection. Error bars represent the standard deviations.

bars with upward diagonal stripes). Xylanase hydrolysis for 1 h or overnight, without refreshing enzyme solution (as described above in section Investigation of reaction parameters by FTCM), lead to no significant mannan exposure at the surface of xylanase hydrolyzed BKP paper discs (data not shown).

In another reaction, the xylanase hydrolyzed BKP paper discs were later washed and exposed to the hydrolysis with mannanase enzyme. In this case, mannan exposure decreased by 55% (in case of 0.1 mannanase U per paper disc) which is an additional decrement of 23% compared to when xylanase was not used as a pretreatment (Fig. 7C, cyan color bars with checker board). This study showed that xylan hydrolysis exposed more detectable mannan on the surface of BKP wood fibers, leading to higher enzymatic hydrolysis of mannan. This suggests that xylan was wrapping or covering mannan in the so-called cellulose–hemicellulose complexes. The mannan detected here seems to be deeply embedded in the BKP wood fibers.

Plant cell wall organization directly affects the nature of biomass recalcitrance.[20,21] Therefore, it is important to understand the organization of hemicelluloses and FTCM offers a unique means of addressing this issue. So far, various studies looking for the arrangement of the different wood polymers in delignified samples have revealed that mannan is closely associated with cellulose and xylan is more associated with condensed lignin in the secondary cell wall of the softwood fibers.[44,94] This FTCM study provides direct evidence in support of this suggested model. Using FTCM probes, we detected two different mannan populations in the wood fibers. The first mannan population was associated with lignin–hemicellulose complexes as seen in mechanical pulps. This population was dominant at the outer surface of wood fibers. In contrast, during kraft pulping, lignin and lignin–hemicellulose complexes get dissolved and/or degraded, which exposes deeper hemicelluloses. The second mannan population was found deeper in fiber, probably associated to the earlier proposed cellulose–hemicellulose complexes in kraft pulps. Overall the results suggest that xylan was acting as a physical shield which was covering or wrapping the mannan polymers in BKP fibers. This also indicates that the second population of mannan is hidden beneath the surface of xylan polymers, closely associated to cellulose or deeply embedded in the cell wall organization in BKP fibers. FTCM analysis fully supports the concept of

a complex network of hemicelluloses around the cellulose fibers as reported by Varnai *et al.* (2011)[41] but in addition, FTCM highlighted the presence of deeply embedded hemicelluloses. Working with bleached softwood dissolving pulp, Gübitz *et al.* (1998)[38] proposed that hemicelluloses hydrolysis is stronger when cellulase enzymes are used with hemicellulases and proposed two different fractions of hemicelluloses: one associated with lignin and another one with cellulose. The FTCM results are compatible with the findings of Gübitz *et al.* (1998)[38] which suggested two different mannan populations. This study also provides a rationale for the findings of Kansoh *et al.* (2004)[37] and Clarke *et al.* (2000)[36] which indicated that the use of the mannanase enzyme is not very efficient if xylan is still present in kraft pulps.

Overall, FTCM has been shown to help understanding cell wall ultrastructure and its organization by studying the presence of hemicelluloses in various parts of fibers, as lignin is progressively removed by kraft pulping and bleaching processes. Although most FTCM investigations reported here were compatible with chemical analysis (dependent on overall/bulk composition analysis; NREL/TP-510-42618), they revealed that changes in surface hemicelluloses after various treatments are much more important than indicated by chemical analysis. Monitoring surface modifications is much more informative on biomass recalcitrance than performing analysis of fiber bulk composition.

## Conclusion

FTCM showed that it can specifically track mechanical, chemical and enzymatic-induced variations of hemicelluloses on the surface of different wood fibers in a rapid and high throughput format. Optimum hydrolysis parameters for both xylanase and mannanase enzymes, for all the studied pulps, were 0.1 U of enzyme/paper disc at 50 °C for a treatment duration of 1 h. FTCM identified the major factor limiting hydrolysis efficiency as enzyme inactivation (by any mechanism). By directly detecting polymers remaining after various enzymatic treatments, using CBM probes revealed additive and/or synergistic interactions between Celluclast 1.5L, xylanase and mannanase enzymes. The ability of FTCM to directly map layers of cellulose and hemicelluloses fractions as they were attacked by enzymes provided support for an embedded population of mannan, protected by xylan, probably associated to cellulose–hemicellulose complexes.[38] We believe that this method can enhance our understanding of lignocellulosic polymers response to various treatments, therefore bolstering development of cost-effective processes for production of biofuels and other lignocellulosic biomass-based products.

## List of abbreviations

| | |
|---|---|
| AGE | Affinity gel electrophoresis |
| BSA | Bovine serum albumin |
| BKP | Bleached kraft pulp |
| BMP | Bleached mechanical pulp |
| CAZy | Carbohydrate active enzymes |
| CBMs | Carbohydrate binding modules |
| CBM15 | Family 15 carbohydrate binding module |
| CMC | Carboxymethyl cellulose |
| CFP | Cyan fluorescent protein |
| DNS | 3,5-Dinitrosalicylic acid |
| GFP | Green fluorescent protein |
| GH | Glycoside hydrolase |
| IPTG | Isopropyl-β-D-thiogalactopyranoside |
| ITC | Isothermal titration calorimetry |
| LB | Luria–Bertani |
| mOrange2 | Mono-orange2 |
| NREL | National renewable energy laboratory |
| CC27 | Cyan fluorescent protein linked to a family 27 carbohydrate binding module |
| GC3a | Green fluorescent protein linked to a family 3a carbohydrate binding module |
| OC15 | Mono-orange2 fluorescent protein linked to a family 15 carbohydrate binding module |
| SDS-PAGE | Sodium dodecyl sulfate - polyacrylamide gel electrophoresis |
| UBKP | Unbleached kraft pulp |
| UBMP | Unbleached mechanical pulp. |

## Authors' contributions

VK carried out all the experiments and drafted the manuscript. FMM and MB helped to draft and revise the manuscript. All authors read and approved the final manuscript.

## Conflicts of interest

VK and MB declare that they have no competing interests. FMM was an employee of Buckman North America which financially supported parts of this work.

## Acknowledgements

This research was supported in part by Buckman Laboratories of Canada and funded by grants from CRIBIQ and NSERC (CRDPJ445143-12). We would like to thank Dr Roberto Chica (University of Ottawa) for the donation of fluorescent protein and Dr Nicolas Doucet (INRS-Institut Armand-Frappier) for his expert assistance while performing isothermal titration calorimetry (ITC) measurements. The skillful technical assistance of Nikolas Beauchesne, Vincent Bolduc, and Guillaume L. Lemieux is acknowledged. We would like to thank Ojas Bhatia for his valuable editorial contributions.

## Notes and references

1 M. E. Himmel, S. Y. Ding, D. K. Johnson, W. S. Adney, M. R. Nimlos, J. W. Brady and T. D. Foust, *Science*, 2007, **315**, 804–807.
2 C. E. Wyman, *Trends Biotechnol.*, 2007, 25(4), 153–157.
3 L. R. Lynd, M. S. Laser, D. Branshy, B. E. Dale, B. Davison, R. Hamilton, M. Himmel, M. Keller, J. D. McMillan,

J. Sheehan and C. E. Wyman, *Nat. Biotechnol.*, 2008, **26**(2), 169–172.
4 L. R. Lynd, J. H. Cushman, R. J. Nichols and C. E. Wyman, *Science*, 1991, **251**(4999), 1318–1323.
5 H. Jørgensen, J. B. Kristensen and C. Felby, *Biofuels, Bioprod. Biorefin.*, 2007, 1, 119–134.
6 C. E. Wyman, *Bioresour. Technol.*, 1994, **50**(1), 3–16.
7 A. E. Farrell, R. J. Plevin, B. T. Turner, A. D. Jones, M. O'hare and D. M. Kammen, *Science*, 2006, **311**(5760), 506–508.
8 R. Kumar, M. Tabatabaei, K. Karimi and I. Sárvári Horváth, *Biofuel Res. J.*, 2016, 3(1), 347–356.
9 A. Culbertson, M. Jin, L. da Costa Sousa, B. E. Dale and V. Balan, *RSC Adv.*, 2013, 3(48), 25960–25969.
10 Y. Hong, A. S. Nizami, M. Pour bafrani, B. A. Saville and H. L. MacLean, *Biofuels, Bioprod. Biorefin.*, 2013, 7(3), 303–313.
11 L. R. Lynd, C. E. Wyman and T. U. Gerngross, *Biotechnol. Prog.*, 1999, **15**(5), 777–793.
12 R. Kumar and C. E. Wyman, *Bioalcohol production: Biochemical conversion of lignocellulosic biomass*, ed. K. Waldon, Woodhead publishing limited, Oxford, 2010, pp. 73–121.
13 R. Kumar and C. E. Wyman, *Aqueous Pretreatment of Plant Biomass for Biological and Chemical Conversion to Fuels and Chemicals*, ed. C. E. Wyman, John Wiley and Sons, Ltd, 2013, pp. 281–310.
14 P. A. Penttilä, A. Várnai, J. Pere, T. Tammelin, L. Salmén, M. Siika-aho, L. Viikari and R. Serimaa, *Bioresour. Technol.*, 2013, **129**, 135–141.
15 M. Li, M. Tu, D. Cao, P. Bass and S. Adhikari, *J. Agric. Food Chem.*, 2013, **61**(3), 646–654.
16 K. Igarashi, T. Uchihashi, A. Koivula, M. Wada, S. Kimura, T. Okamoto, M. Penttilä, T. Ando and M. Samejima, *Science*, 2011, **333**, 1279–1282.
17 L. Zhu, J. P. O'Dwyer, V. S. Chang, C. B. Granda and M. T. Holtzapple, *Bioresour. Technol.*, 2008, **99**, 3817–3828.
18 S. D. Mansfield, C. Mooney and J. N. Saddler, *Biotechnol. Prog.*, 1999, **15**, 804–816.
19 M. Hall, P. Bansal, J. H. Lee, M. J. Realff and A. S. Bommarius, *FEBS J.*, 2010, 277(6), 1571–1582.
20 S. P. Chundawat, B. S. Donohoe, L. da Costa Sousa, T. Elder, U. P. Agarwal, F. Lu, J. Ralph, M. E. Himmel, V. Balan and B. E. Dale, *Energy Environ. Sci.*, 2011, **4**(3), 973–984.
21 J. D. DeMartini, S. Pattathil, J. S. Miller, H. Li, M. G. Hahn and C. E. Wyman, *Energy Environ. Sci.*, 2013, **6**(3), 898–909.
22 A. T. W. M. Hendriks and G. Zeeman, *Bioresour. Technol.*, 2009, **100**(1), 10–18.
23 S. Subramaniyan and P. Prema, *Crit. Rev. Biotechnol.*, 2002, **22**(1), 33–64.
24 B. C. Saha, *J. Ind. Microbiol. Biotechnol.*, 2003, **30**(5), 279–291.
25 F. M. Girio, C. Fonseca, F. Carvalheiro, L. C. Duarte, S. Marques and R. Bogel-Lukasik, *Bioresour. Technol.*, 2010, **101**(13), 4775–4800.
26 T. E. Timell, *Wood Sci. Technol.*, 1967, **1**(1), 45–70.
27 J. Hu, V. Arantes and J. N. Saddler, *Biotechnol. Biofuels*, 2011, **4**(1), 1–14.
28 M. J. Selig, T. B. Vinzant, M. E. Himmel and S. R. Decker, *Appl. Biochem. Biotechnol.*, 2009, **155**(1–3), 397–406.
29 R. Bura, R. Chandra and J. Saddler, *Biotechnol. Prog.*, 2009, **25**(2), 315–322.
30 M. Frommhagen, S. Sforza, A. H. Westphal, J. Visser, S. W. Hinz, M. J. Koetsier, W. J. van Berkel, H. Gruppen and M. A. Kabel, *Biotechnol. Biofuels*, 2015, **8**(1), 1–12.
31 A. Suurnakki, T. Q. Li, J. Buchert, M. Tenkanen, L. Viikari, T. Vuorinen and L. Odberg, *Holzforschung*, 1997, **51**(1), 27–33.
32 J. P. Vincken, A. de Keizer, G. Beldman and A. G. J. Voragen, *Plant Physiol.*, 1995, **108**(4), 1579–1585.
33 T. Oksanen, J. Buchert and L. Viikari, *Holzforschung*, 1997, **51**(4), 355–360.
34 T. Kohnke, K. Lund, H. Brelid and G. Westman, *Carbohydr. Polym.*, 2010, **81**(2), 226–233.
35 J. Zhang, M. Siika-aho, M. Tenkanen and L. Viikari, *Biotechnol. Biofuels*, 2011, **4**(1), 1–10.
36 A. Berlin, V. Maximenko, N. Gilkes and J. Saddler, *Biotechnol. Bioeng.*, 2007, **97**(2), 287–296.
37 K. Ohgren, R. Bura, J. Saddler and G. Zacchi, *Bioresour. Technol.*, 2007, **98**(13), 2503–2510.
38 G. M. Gübitz, D. W. Stebbing, C. I. Johansson and J. N. Saddler, *Appl. Microbiol. Biotechnol.*, 1998, **50**(3), 390–395.
39 M. P. Garcia-Aparicio, M. Ballesteros, P. Manzanares, I. Ballesteros, A. Gonzalez and M. J. Negro, *Appl. Biochem. Biotechnol.*, 2007, **137**, 353–365.
40 R. Kumar and C. E. Wyman, *Biotechnol. Prog.*, 2009a, 25(2), 302–314.
41 R. Kumar and C. E. Wyman, *Biotechnol. Bioeng.*, 2014, **111**(7), 1341–1353.
42 Q. Qing and C. E. Wyman, *Biotechnol. Biofuels*, 2011, **4**(1), 18.
43 A. Varnai, L. Huikko, J. Père, M. Siika-aho and L. Viikari, *Bioresour. Technol.*, 2011, **102**(19), 9096–9104.
44 M. Åkerholm and L. Salmén, *Polymer*, 2001, **42**(3), 963–969.
45 D. Klein-Marcuschamer, P. Oleskowicz-Popiel, B. A. Simmons and H. W. Blanch, *Biotechnol. Bioeng.*, 2012, **109**(4), 1083–1087.
46 E. Ximenes, Y. Kim, N. Mosier, B. Dien and M. Ladisch, *Enzyme Microb. Technol.*, 2010, **46**, 170–176.
47 Y. Kim, E. Ximenes, N. S. Mosier and M. R. Ladisch, *Enzyme Microb. Technol.*, 2011, **48**(4–5), 408–415.
48 M. Mandels and E. T. Reese, *Annu. Rev. Phytopathol.*, 1965, 3, 85–102.
49 E. T. Reese and M. Mandels, *Biotechnol. Bioeng.*, 1980, 22(2), 323–335.
50 G. Halliwell and M. Griffin, *Biochemistry*, 1973, **135**(4), 587–594.
51 R. Kumar and C. E. Wyman, *Enzyme Microb. Technol.*, 2008, **42**(5), 426–433.
52 R. Kumar and C. E. Wyman, *Biotechnol. Bioeng.*, 2009b, **102**(2), 457–467.
53 Q. Qing, B. Yang and C. E. Wyman, *Bioresour. Technol.*, 2010, **101**(24), 9624–9630.
54 M. Holtzapple, M. Cognata, Y. Shu and C. Hendrickson, *Biotechnol. Bioeng.*, 1990, **36**(3), 275–287.

55 P. Andric, A. S. Meyer, P. A. Jensen and K. Dam-Johansen, *Biotechnol. Adv.*, 2010, **28**(3), 308–324.
56 J. D. Stephen, W. E. Mabee and J. N. Saddler, *Biofuels, Bioprod. Biorefin.*, 2012, **6**(2), 159–176.
57 Y. H. P. Zhang, M. E. Himmel and J. R. Mielenz, *Biotechnol. Adv.*, 2006, **24**(5), 452–481.
58 Z. Zhang, A. A. Donaldson and X. Ma, *Biotechnol. Adv.*, 2012, **30**(4), 913–919.
59 R. Kumar and C. E. Wyman, *Biotechnol. Bioeng.*, 2009c, **102**(6), 1544–1557.
60 R. Kumar and C. E. Wyman, *Biotechnol. Prog.*, 2009d, **25**(2), 302–314.
61 B. Yang and C. E. Wyman, *Biotechnol. Bioeng.*, 2006, **94**(4), 611–617.
62 T. Y. Nguyen, C. M. Cai, O. Osman, R. Kumar and C. E. Wyman, *Green Chem.*, 2015a, **18**(6), 1581–1589.
63 T. Y. Nguyen, C. M. Cai, R. Kumar and C. E. Wyman, *ChemSusChem*, 2015b, **8**(10), 1716–1725.
64 H. P. Zhang, S. Y. Ding, J. R. Mielenz, J. B. Cui, R. T. Elander, M. Laser, M. E. Himmel, J. R. Mcmillan and L. R. Lynd, *Biotechnol. Bioeng.*, 2007, **97**(2), 214–223.
65 S. T. Merino and J. Cherry, *Biofuels*, 2007, **108**, 95–120.
66 T. L. Ogeda and D. F. S. Petri, *Quim. Nova*, 2010, **33**(7), 1549–1558.
67 A. Y. Pribowo, J. Hu, V. Arantes and J. N. Saddler, *Biotechnol. Biofuels*, 2013, **6**(1), 1–15.
68 S. D. Risio, C. S. Hu, B. A. Saville, D. Liao and J. Lortie, *Biofuels, Bioprod. Biorefin.*, 2011, **5**(6), 609–620.
69 J. D. DeMartini, S. Pattathil, U. Avci, K. Szekalski, K. Mazumder, M. G. Hahn and C. E. Wyman, *Energy Environ. Sci.*, 2011, **4**(10), 4332–4339.
70 J. P. Knox, *Cellulases*, 2012, **510**, 233–245.
71 J. P. Knox, *Curr. Opin. Plant Biol.*, 2008, **11**(3), 308–313.
72 C. Oliveira, V. Carvalho, L. Domingues and F. M. Gama, *Biotechnol. Adv.*, 2015, **33**(3), 358–369.
73 A. B. Boraston, D. Bolam, H. Gilbert and G. J. Davies, *Biochem. J.*, 2004, **382**, 769–781.
74 S. Gao, C. You, S. Renneckar, J. Bao and Y. H. P. Zhang, *Biotechnol. Biofuels*, 2014, **7**(1), 1–11.
75 H. J. Gilbert, J. P. Knox and A. B. Boraston, *Curr. Opin. Struct. Biol.*, 2013, **23**(5), 669–677.
76 C. Hervé, S. E. Marcus and J. P. Knox, *The Plant Cell Wall*, 2011, vol. 715, pp. 103–113.
77 S. Ding, Q. Xu, M. K. Ali, J. O. Baker, E. A. Bayer, Y. Barak, R. Lamed, J. Sugiyama, G. Rumbles and M. E. Himmel, *BioTechniques*, 2006, **41**(4), 435.
78 T. Kawakubo, S. Karita, Y. Araki, S. Watanabe, M. Oyadomari, R. Takada, F. Tanaka, K. Abe, T. Watanabe, Y. Honda and T. Watanabe, *Biotechnol. Bioeng.*, 2010, **105**(3), 499–508.
79 K. Gourlay, V. Arantes and J. N. Saddler, *Biotechnol. Biofuels*, 2012, **5**(1), 51.
80 J. Hong, X. Ye and Y. H. P. Zhang, *Langmuir*, 2007, **23**(25), 12535–12540.
81 J. M. Fox, P. Jess, R. B. Jambusaria, G. M. Moo, J. Liphardt, D. S. Clark and H. W. Blanch, *Nat. Chem. Biol.*, 2013, **9**(6), 356–361.
82 V. Khatri, Y. Hebert-Ouellet, F. Meddeb-Mouelhi and M. Beauregard, *Biotechnol. Biofuels*, 2016, **9**, 74.
83 Y. Hébert-Ouellet, F. Meddeb-Mouelhi, V. Khatri, L. Cui, B. Janse, K. MacDonald and M. Beauregard, *Green Chem.*, 2017, **19**, 2603–2611.
84 L. Szabó, S. Jamal, H. Xie, S. J. Charnock, D. N. Bolam, H. J. Gilbert and G. J. Davies, *J. Biol. Chem.*, 2001, **276**(52), 49061–49065.
85 A. B. Boraston, T. J. Revett, C. M. Boraston, D. Nurizzo and G. J. Davies, *Structure*, 2003, **11**(6), 665–675.
86 M. M. Bradford, *Anal. Biochem.*, 1976, **72**(1), 248–254.
87 A. Sluiter, D. Crocker, B. Hames, R. Ruiz, C. Scarlata, J. Sluiter and D. Templeton, *Laboratory Analytical Procedure (LAP)*, 2008, NREL/TP-510-42618.
88 K. Gourlay, J. Hu, V. Arantes, M. Penttilä and J. N. Saddler, *J. Biol. Chem.*, 2015, **290**, 2938–2945.
89 D. W. Abbott and A. B. Boraston, *Methods Enzymol.*, 2012, **510**, 211–231.
90 G. A. Smook, *Handbook for pulp & paper technologists*, Tappi, 1992.
91 L. Viikari, A. Kantelinen, J. Sundquist and M. Linko, *FEMS Microbiol. Rev.*, 1994, **13**(2–3), 335–350.
92 D. Tavast, Z. A. Mansoor and E. Brännvall, *Ind. Eng. Chem. Res.*, 2014, **53**(23), 9738–9742.
93 Å. Linder, R. Bergman, A. Bodin and P. Gatenholm, *Langmuir*, 2003, **19**(12), 5072–5077.
94 M. Åkerholm, B. Hinterstoisser and L. Salmén, *Carbohydr. Res.*, 2004, **339**(3), 569–578.
95 A. L. Kansoh and Z. A. Nagieb, *Antonie van Leeuwenhoek*, 2004, **85**(2), 103–114.
96 J. H. Clarke, K. Davidson, J. E. Rixon, J. R. Halstead, M. P. Fransen, H. J. Gilbert and G. P. Hazlewood, *Appl. Microbiol. Biotechnol.*, 2000, **53**(6), 661–667.
97 G. L. Miller, *Anal. Chem.*, 1959, **31**, 426–428.

# Appendix C

Green Chemistry

PAPER

View Article Online
View Journal | View Issue





Cite this: Green Chem., 2017, 19, 2603

## Tracking and predicting wood fibers processing with fluorescent carbohydrate binding modules†

Yannick Hébert-Ouellet,[a,b,c] Fatma Meddeb-Mouelhi,[a,b,d] Vinay Khatri,[a,b,c] Li Cui,[a,b,c] Bernard Janse,[d] Kevin MacDonald[d] and Marc Beauregard *[a,b,c]

Received 27th December 2016,
Accepted 24th April 2017

DOI: 10.1039/c6gc03581g

rsc.li/greenchem

Wood fiber is a source of raw materials for established wood-based industries and for the nascent biofuel sector. Efficient processing of wood fiber polymers such as cellulose and hemicellulose requires close monitoring with methods such as FTIR, XPS or chemical analysis. Such methods are time-consuming and require the availability of specialized equipment and expertise. Recently, the carbohydrate recognition domains of glycohydrolases, known as carbohydrate binding modules, were used for studying the development and the biochemistry of plant cell walls. In this study, we engineered a series of color-coded fluorescent carbohydrate binding modules with specificities for four major carbohydrate fiber polymers. This approach allowed for quick, high-throughput analysis of fiber surface carbohydrates signatures and is herein used for monitoring and predicting the impact of various treatments on the strength properties of paper produced from such processed fibers. We believe that the simplicity of this environment-friendly approach could change the way industry optimizes wood fibers processing and deconstruction.

## Introduction

Wood fiber is a major source of raw, renewable material for both the paper and biofuel industries. However, its complex organization involves a network of tightly ordered cellulose chains intertwined with other biopolymers, making it recalcitrant to modifications.[1] Accordingly, lignocellulosic biomass conversion into paper and/or its deconstruction for biofuel production are costly, energy avid processes.[2–4] Key advances in biochemistry have the potential to change this situation. One promising way of dealing with plant biomass recalcitrance involves the manipulation of plant genes that are associated with cell wall architecture, leading to easier access to cellulose.[5] In wood-degrading fungi, such recalcitrance is dealt with by an array of enzymes, which are sometimes associated in cellulosomes.[6] Such organised enzymatic machinery is highly informative when considering how we can make biofuel from wood materials more efficiently.[7]

Currently, our ability to track the effect of any industrial processing, including enzymatic processing, is limited as most methods are not suitable for quantifying changes in individual lignocellulosic biopolymers. Such methods include the following: compositional analysis (FTIR, XPS and NREL), surface imaging (SEM, TEM and AFM), index of crystallinity (XRD and NMR) and measurements of the degree of polymerization. They are low-throughput, time-consuming and require access to specialized equipment and expertise.[8–10] Among these methods, XPS can be used to monitor lignin and the combination of celluloses (crystalline and amorphous) and hemicellulose at the surface of fibers but without any distinction between these polymers. Also, it is sensitive to X-ray contamination and sample degradation which may prevent XPS analysis reproductibility.[11,12] Currently, there is no available method which rapidly provides specific information on each major class of polymers at the surface of fibers. Unfortunately, this greatly impairs monitoring fiber surface composition, which essentially limits technological developments and governs the economic viability of several lignocellulosic biomasses processes (biofuels production) and/or of its end products (papers manufacturing). The development of a diagnostic approach, which would afford rapid, easy and, if possible, on-site monitoring of fiber structure and composition, would change the way biomass industries achieve optimization of their processes. To this end, carbohydrate-binding modules (CBMs) have tremendous potential. CBMs are defined as

[a]Département de Chimie-Biochimie et Physique, Université du Québec à Trois-Rivières, Trois-Rivières, Québec, G9A 5H7, Canada.
E-mail: Marc.Beauregard@uqtr.ca
[b]Centre de recherche sur les matériaux lignocellulosiques, Université du Québec à Trois-Rivières, Trois-Rivières, Québec, G9A 5H7, Canada
[c]Proteo, Université Laval, Québec, Québec, G1V 4G2, Canada
[d]Buckman, Tennessee, 38108-1241, USA

†Electronic supplementary information (ESI) available. See DOI: 10.1039/c6gc03581g

small, non-catalytic proteins (which are often attached to glycoside hydrolases *via* a linker) whose function is to act as substrate-recognition devices thereby enhancing the catalytic efficiency of these enzymes.[13,14] They have been successfully employed for the characterization of fiber surfaces composed of simple and complex carbohydrates.[15–17] Specific advances were achieved using CBMs as fusion with a fluorescence protein such as the green fluorescent protein (or any of its variants).[18] CBMs coupled with fluorescence protein have been used for mapping the chemistry and structure of various carbohydrate-containing substrates (lignocellulosic biomass).[15,19] Gao *et al.*, using fluorescent CBM3 and CBM17, successfully quantified the change of accessibilities to crystalline and amorphous celluloses during enzymatic hydrolysis.[20] Recently, using fluorescent CBM15, we developed a rapid assay that specifically track surface variations of xylan which enable a better understanding and facilitate the optimization of the lignocellulosic biomasses processes.[21]

In this study, we exploited the specificity of CBMs CBM3, CBM15, CBM17 and CBM27 and constructed four fluorescent CBM probes (Fig. S1†), each of which tracks a particular lignocellulosic carbohydrate polymer, *i.e.* crystalline cellulose, amorphous cellulose, xylan and mannan, respectively. Mixing the probes with wood fiber and measuring fluorescence (after removing CBMs that are not specifically bound) allows for quick monitoring of the distribution of the targeted polymers on the fiber, as depicted in Fig. 1. Here we demonstrate that these probes can monitor processing impact, and help fine-tune wood fiber refining and deconstruction. Applying this approach in an industrial setting will lead to improving the cost efficiency and energy efficiency of fiber treatments.

## Results and discussion

Wood pulping is a well-known treatment that promotes exposure of carbohydrate polymers such as cellulose and hemicellulose.[22–24] Depending on the treatment, changes in polymers are expected. For example, the lignin covering kraft pulp fibers is substantially lower than for high yield kraft pulp (HYK) fiber. Typically, total chemical analyses (NREL/TP-510-42618) are used to determine the chemical composition of pulps.[25] As expected, these analyses revealed that HYK has a higher lignin content (1.4-fold) than kraft pulp (Table S2†). Unfortunately, this approach can only provide an overall bulk estimation of polymers content. It cannot detect nor than measure variations of polymers specifically located at the surface of fibers. Another classical method for fiber analysis is X-ray photoelectron spectroscopy (XPS). XPS analysis consists in acquiring and deconvoluting the C 1s band of high-resolution spectra in order to expose the C1 to C4 peaks (Fig. S3 and Table S3†). The C1 component of the C 1s band mainly arises from lignin and extractives, while C2 is primarily associated to cellulose and hemicelluloses. The C3 component is not easily assigned to a given polymer, as it is related to either carbonyl groups of lignin and/or extractives, or to carbon atoms bonded to two oxygen atoms in cellulose and hemicellulose.[26–28] Consequently, XPS has been used extensively for surface analysis of simple lignocellulosic biomasses for detection of changes in surface coverage by cellulose, lignin, and extractives.[11,29,30] When comparing HYK paper to kraft paper, we found a 1.4-fold increase in C1 spectral component intensity at HYK surface (Table S3†). Again, this result suggests that HYK has a higher lignin content. The C2 functionality in HYK paper is 1.1-fold lower than for kraft paper, suggesting that

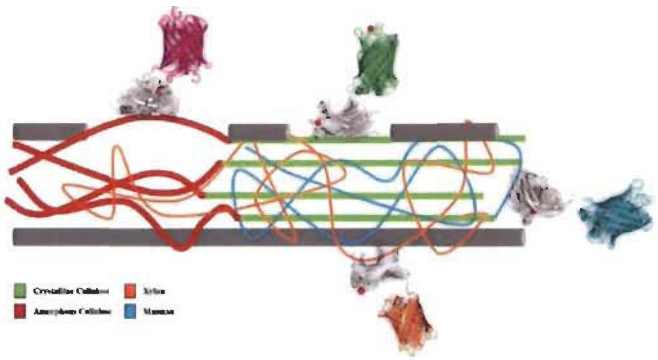


Fig. 1 Schematic representation of probe binding to wood fiber. The left side of the fiber depicts a partially lignin-free fiber where amorphous cellulose dominates (red strings). On the right side, the straight green bars represent crystalline cellulose. Hemicelluloses such as xylan (orange) and mannan (cyan) are shown as polymers that help keep the fiber together. The grey cylinders represent the lignin coating. The probes designed in this study were shown to attach specifically to their respective target polymer, as indicated in this figure by the matching color of their fluorescent module. The affinity of the four probes toward their specified target polymer was confirmed (see Table S1 and Fig. S2†).

cellulose and/or hemicellulose are slightly less present on its surface. The values of the C3 and C4 functionalities were relatively low and similar for either paper. XPS analysis did reveal the impact of the different pulping processes on the exposure of major polymer classes. Unfortunately, the C 1s spectra cannot distinguish cellulose (be it amorphous or crystalline) from hemicellulose since these polymers (or polymer forms) possess similar carbon types.

Using CBM-probes, we endeavored to avoid such limitations associated with chemical and XPS analyses. We attempted to monitor the difference in the exposure of carbohydrate polymers on the surface of fibers from the same pulps as described above (HYK and kraft). The binding of CBM probes to fiber discs made of two pulp grades is shown in Fig. 2. The calibrated fluorescence signals indicate that the most abundant carbohydrate polymer at the surface of the fiber discs was crystalline cellulose, followed by amorphous cellulose, and then by hemicelluloses. This distribution of individual fiber polymers is compatible with the measured chemical compositions of these pulps (Table S2†). The access of CBM-probes to surface carbohydrates appears to be hindered in high yield kraft pulp (HYK). This pulp contains 1.4 fold the amount of fiber-coating lignin found in the other kraft pulp (Table S2†). Clearly, the probes allow to quickly distinguish between two pulping grades. In addition, the analysis of fiber surface with CBM probes indicates that mannan, and not xylan, is the primary hemicellulose carbohydrates detected in kraft pulp, confirming that both fiber discs were manufactured principally from softwood. These results suggest that introducing this tracking approach as a quality control measurement would bolster the effectiveness of the lignocellulosic biomass processes.

Mechanical refining is essential for modifying the characteristics of wood fibers.[31,34] One important consequence of refining is the external fibrillation of the wood fiber S2 layer which promotes the formation of hydrogen bonds between fibers. On the molecular level, refining translates into the partial conversion of crystalline into amorphous cellulose (made of hydrated cellulose fibrils), a phenomenon known as amorphogenesis.[32,33] In addition to being the primary source of hydrogen bonds strengthening the fiber matrices in paper, amorphous cellulose is also more sensitive to enzymatic hydrolysis into fermentable sugars.[3,17,32,33] Monitoring amorphous cellulose formation during refining would help detect the minimal amount of mechanical energy required to promote efficient amorphogenesis which is critical for both wood based biofuel and papermaking industries. Optimizing energy input would also reduce possible mechanical sheer and help maintain fiber integrity.

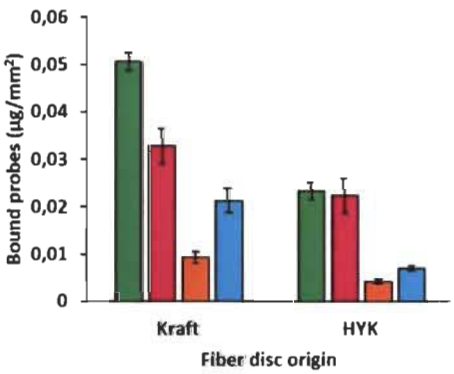


Fig. 2 CBM binding to the surface of unrefined kraft and high yield kraft (HYK) fiber discs. The probes attached to crystalline and amorphous celluloses are shown in green and cherry, while hemicelluloses xylan and mannan probes are shown in orange and cyan, respectively.

Fig. 3 shows the evolution of the carbohydrates surface signatures as a function of increasing refining intensities as revealed by the CBM probes. This experiment revealed that the amorphous cellulose to crystalline cellulose ratio (AC/CC) is maximal at 2000 PFI revolutions, suggesting that amorphogenesis would be optimal using the corresponding mechanical energy (Fig. 3A). Interestingly, the mannan to crystalline cellulose ratio (Man/CC) also peaked at 2000 (Fig. 3B) meaning that exposure of the cellulose-sheathing mannan layer is maximal at such refining intensity. In contrast, the xylan to crystalline cellulose ratio (Xyl/CC) initially increased but then remained constant after reaching 1500 revolutions. Overall, the application of mechanical energy to wood fibers lowered the surface detection of all carbohydrates. This result is consistent with the lowering of probe accessibility that results from the production of a tighter fiber network in the paper discs after refining.[19,31,34]

A critical issue in the wood biomass industry is the cost of process optimization. The ability to not only rapidly monitor, but also predict the impact of a treatment on a small scale would be of great benefit to the industry. In this context, we measured the physical properties of paper hand sheets after various refining intensities in order to establish correlations between the carbohydrate to crystalline cellulose ratios (revealed by the probes) and the paper strength properties. Fig. 4 reveals that the optimal values of a number of important paper strength properties (such as internal bond strength and tear and tensile indices) were effectively correlated with optimal AC/CC ratio at 2000 revolutions. Note that all these parameters are a function of fiber mean length, since shorter and deformed fibers lower the paper's strength properties.[35,36] However, taking only fiber length into account would have been misleading since this parameter peaked at 1500 revolutions. We show here that the carbohydrate surface signatures closely correlated with the paper strength properties. Consequently, we believe that the correlations between the developed probe surface signatures and paper strength properties can be evolved into a powerful prediction tool for the quick and efficient determination of optimal refining conditions.

Enzymes have been used for many years to improve papermaking as well as for the deconstruction processes of ligno-

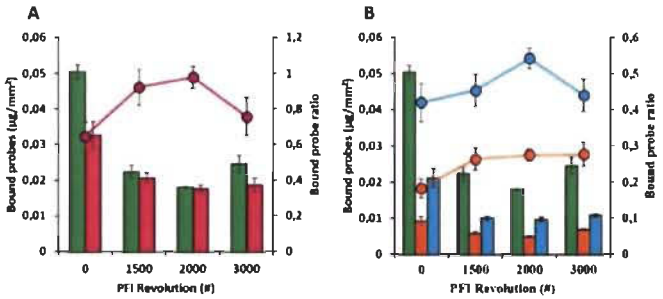


Fig. 3 Impact of refining intensity on the binding of CBM-probes to kraft fiber discs. (A) Variations of crystalline (green bars) and amorphous (cherry bars) cellulose as a function of refining intensity. The cherry circles correspond to the evolution of the amorphous cellulose to crystalline cellulose ratio (AC/CC). (B) Variations of xylan (orange bars), mannan (cyan bars) and crystalline cellulose as a function of refining intensity. The orange and cyan circles correspond to the variations of the xylan to crystalline cellulose ratio (Xyl/CC) and mannan to crystalline cellulose (Man/CC), respectively.

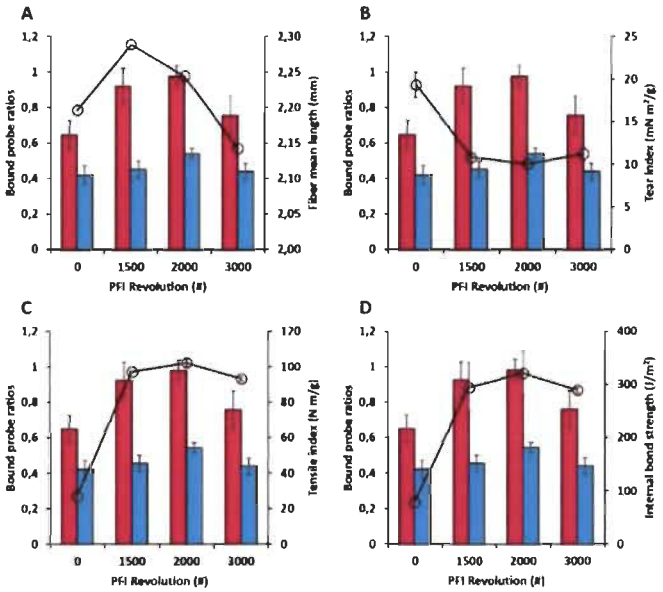


Fig. 4 Impact of refining intensity on the relationship between the bound probe AC/CC, Man/CC ratios and paper physical properties. (A) Fiber mean length (mm). (B) Tear index (mN $m^2$ $g^{-1}$). (C) Tensile index (N m $g^{-1}$). (D) Internal bound strength (J $m^{-2}$). The variations in physical properties values are shown by black lines and circles, while the AC/CC and Man/CC ratios are shown with bars in cherry and in cyan, respectively.

cellulosic biomasses in order to reduce energy consumption and increase productivity.[17–19] One such enzyme, mannanase, was found to be particularly effective when used on kraft pulp and in relieving mannan inhibition of cellulases.[16,42] Unfortunately, mannanase usage is frequently restricted to certain biomasses and conditions, and this mixed success has limited its usage on the industrial scale. As a result, efficient prediction of the impacts of mannanase activity on biomass properties is imperative. Therefore, we developed a small scale paper discs digestion assay and applied our CBM technology

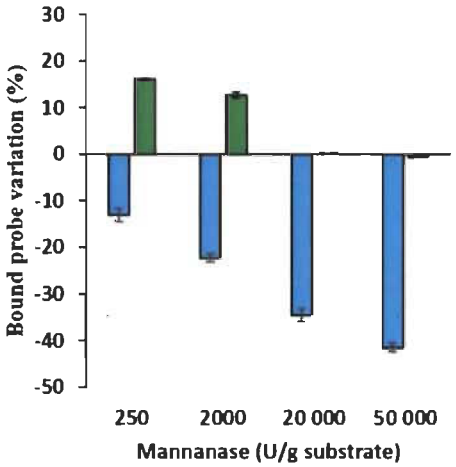


Fig. 5 Impact of mannanase hydrolysis (250–50 000 U g$^{-1}$ substrate) on the binding of mannan (cyan) and crystalline cellulose (green) probes on the surface of unrefined kraft fiber discs

to detect the optimal condition required for mannanase to promote the efficient uncovering of crystalline cellulose and thereby improve the reactiveness of fibers towards mechanical refining without negatively affecting paper properties. Fig. 5 shows the impact of mannanase hydrolysis on the removal of mannan and on the exposure of crystalline cellulose at the surface of unrefined kraft fiber discs. The negative percentage values indicate that mannan removal was commensurate with enzyme concentration (12.9% for 250 U g$^{-1}$ substrate up to 41.3% for 50 000 U g$^{-1}$ substrate). This result shows that our experimental conditions were adequate for hydrolyzing mannan in a complex lignocellulosic biomass. Optimal crystalline cellulose exposure was detected using 250 U g$^{-1}$ substrate of mannanase. The probes signals indicated that increasing mannanase concentrations beyond 250 U g$^{-1}$ did not lead to additional detection of cellulose on the fiber surface.

Subsequently we investigated the impact of mannanase pretreatment on the fibers response to mechanical refining and the consequent paper properties. To identify possible correlations between probe binding to surface polymers and paper properties, larger pulp samples were treated with mannanase, then by mechanical refinining and then converted into handsheets for further analysis. Fig. 6A shows the changes in polymer detection measured on unrefined fiber discs (0 revolution) and on refined fibers. All samples were pre-treated with mannanase. Without refining, mannan and crystalline cellulose detection was similar to results previously recorded on smaller samples (Fig. 5). Before any mechanical energy was applied (0 revolution) cellulose (both crystalline and amorphous) and xylan detection was increased by mannanase treatment. Applying mechanical refining on enzyme treated pulp samples resulted in increased binding of probes, suggesting that refining generated increased fibrillation, as observed earlier for a similar treatment sequence (refining applied onto enzyme-treated pulp, see ref. 34). The impact of refining on mannanase treated pulp lead to a complete reversal in

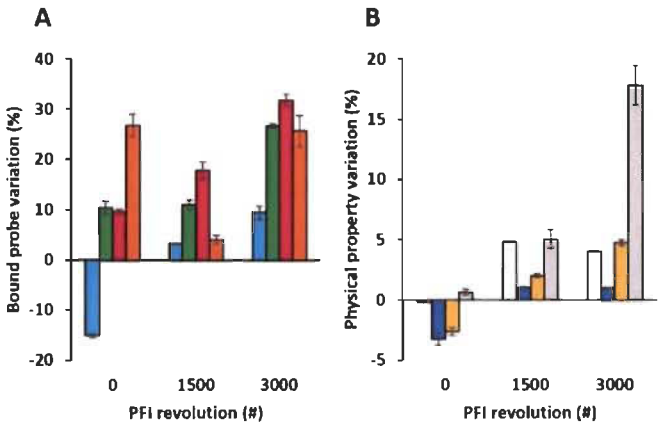


Fig. 6 Impact (%) of mannanase hydrolysis (250 U g$^{-1}$ substrate) and mechanical refining of kraft pulp on (A) the variations of the carbohydrate signatures on the surface of paper discs and on (B) the variations of the strength properties of the resulting paper sheets. Variations of mannan, xylan, crystalline and amorphous celluloses are colored blue, orange, green and cherry while those for fiber mean length, tear index, tensile index and internal bound strength are colored white, dark blue, yellow and grey, respectively.

mannan exposure (−15% without refining, +3.5% after 1500 revolutions, +10% after 3000 revolutions). It appears that refining exposed new mannan polymers compensating for surface mannan that was hydrolysed before refining. Crystalline cellulose detection was not stimulated by moderate refining intensity (1500 revolutions) but after 3000 revolutions on a PFI refiner, exposure of crystalline cellulose was increased by 26%. Amorphous cellulose steadily increased with refining intensity, in agreement with the well-known impact of refining on amorphogenesis, while xylan detection did not correlate with refining intensity. Xylan was severely reduced at moderate refining (from 27% down to 3% variation *vs.* control), and then made available again for detection after 3000 revolutions.

Fig. 6B reveals the impact of mannanase hydrolysis and mechanical refining of kraft pulp on the strength properties of the paper sheets from which paper discs were sampled and exposed to probes (Fig. 6A). Overall these results indicate that exposure of hemicelluloses and cellulose (crystalline or amorphous) correlated with important paper strength properties (maximal exposure and best properties were observed after treatment with 3000 revolutions on the PFI). Specific correlations were observed for each probe. Mannan detection was correlated with tear index and internal bond, showing negative variations after mannan hydrolysis but positive values after refining of mananase treated fibers. Amorphous cellulose variations were correlated with tensile and internal bond in its response to refining. For xylan and crystalline cellulose, detection was maximal after 3000 revolutions where optimal paper properties were observed too. But it did not correlate with paper properties trends observed at 0 or 1500 revolutions. The fiber length peaked at 1500 revolutions where sub-optimal paper properties were observed. These results attest to the close relationship that exists between the carbohydrates signatures (especially mannan and amorphous cellulose) on the surface of wood fibers on the one hand, and the properties of paper derived from such fibers on the other hand. We suggest that these correlations form the basis of a novel approach for predicting the impact of mechanical and enzymatic processes in wood biomass industries.

## Experimental

### Materials and methods

**Reagents and pulps.** Unless otherwise noted, all reagents were supplied by Sigma-Aldrich. Softwood (resinous) paper sheets were used here to quantify the variations of the carbohydrates-recognition probes on their surface. These paper sheets were derived from two different kraft pulps, albeit HYKP (Jack pine) and KP (Black spruce). *Cellvibrio japonicus* mannanase (*endo*-1,4-β-mannanase) purchased from Megazyme was utilized to digest pulp and paper discs.

**Pulps characterization.** Quantification of the pulps cellulose, hemicellulose, lignin as well as monosaccharides contents were determined using NREL/TP-510-42618 methodologies.[23,25] Determination of the surface exposed polymers of the papers was achieved using X-ray photoelectron spectroscopy.[11,21,29,30]

**Pulps refining and paper sheets formation.** A PFI laboratory refiner was used to reproduce the industrial refining process.[34] Refining of pulps (from 0 to 3000 revolutions) was performed according to the standard Tappi method T248 sp-00. Afterward, paper sheets of 60 ± 2 g m$^{-2}$ in density were prepared as per the Tappi T205 sp-02 methodology.

**Enzymatic digestions of pulps and paper discs.** The enzymatic digestions of pulp and paper discs were performed in duplicates using *Cellvibrio japonicus* mannanase enzyme. All reactions were performed over a 1 h period at room temperature with agitation in 0.1 M phosphare buffer pH 7 supplemented with 0.5 mg ml$^{-1}$ BSA. Mannanase concentrations ranged from 250 to 50 000 U g$^{-1}$ substrate for paper discs (3 mm) digestions while pulp trials were done at 250 U g$^{-1}$ substrate.

**Fiber quality analysis and paper physical properties determination.** The impact of the mechanical and mannanase treatments of pulps on fiber properties was determined using a HiRes LDA02-090 Fibre Quality Analyzer (Optest Equipment Inc.). Paper sheets physical strength properties such as tear, burst, tensile and internal bond strength were determined according to Tappi standard methods T414 om-98, T403 om-02, T494 om-01 and T569 pm-00, respectively.

**Construction of the recombinant probe expression systems.** All carbohydrate-recognition probes genes were inserted into pET11a expression vectors. CBM 3a (*Clostridium thermocellum* CipA, NZYTech), CBM15 (*Cellvibrio japonicas*, Z48928), CBM17 (*Clostridium cellulovorans*, U37056) and CBM27 (*Thermotoga maritima*, NC 000853) genes were synthetized by GenScript. The fluorescent protein genes (eGFP, mOrange2, mCherry and eCFP) were cloned into the *Dra*III and *Bam*HI sites while the CBM genes were introduced into the *Bsr*GI and *Bam*HI sites. All encoding genes were sequenced to ascertain the integrity and fidelity of the probes. The resulting probes eGFP-CBM3a, mOrange2-CBM15, mCherry-CBM17 and eCFP-CBM27 (Fig. S1†) were used to detect crystalline cellulose, xylan, amorphous cellulose and mannan, respectively.

**Expression and purification of recombinant probes.** *E. coli* BL21(DE3) Gold pLysS cells (AgilentTechnologies) bearing the selected pET11a expression plasmids were grown at 37 °C in Luria-Bertani broth. Induction of recombinant protein expression was performed by the addition of 0.5 M IPTG (ThermoFisher Scientific) to mid-log-phase cells ($O.D._{600\ nm}$ of 0.6–0.8) and their subsequent incubation for 18 hours at 25 °C. Cells were afterward harvested and kept at −80 °C. Thawed cell pellets were resuspended in 50 mM sodium phosphate pH 8 containing 300 mM NaCl, 2 mM imidazole, 1 mM PMSF and then lysed using six cycles (60 s) of sonication (Branson Ultrasonics Corporation) at 200 W. Clarification of the lysate was achieved by centrifugation at 10 000*g* for 30 minutes at 4 °C. The protein of interest was then purified by affinity chromatography over a HisPrep FF 16/10 column (GE Healthcare Life Sciences) equilibrated in 50 mM sodium phosphate pH 8.0 buffer containing 300 mM NaCl and 10 mM

 

imidazole. Following washes with ten column volumes of buffer, the desired protein was eluted using a gradient (ten column volumes) of imidazole (10 to 100 mM) in 50 mM sodium phosphate pH 8.0 buffer containing 300 mM NaCl. A final purification step was performed using a Superdex 200 HR 16/50 column (GE Healthcare Life Sciences) and 50 mM Tris-HCl pH 7.5 buffer containing 300 mM NaCl to insure purity. The purified probes were then dialyzed against a 20 Tris-HCl pH 7.5 buffer containing 20 mM NaCl and 5 mM $CaCl_2$ at 4 °C and concentrated using a 10k Macrosep Advance centrifugal device (Pall Corporation). Concentrated protein solutions were stored at −80 °C after flash freezing. Protein purity was verified by SDS-PAGE. The amount of protein was quantified by the Bradford method.

**Quantification of the variations of the carbohydrates signatures on the surface of fiber discs.** All fluorescence readings were acquired at room temperature on a Synergy Mx microplate reader using the 3 × 3 area scanning feature with the top detection height set at 4.5 mm and the filter bandwidth at 9 nm. The excitation and emission wavelengths were set at 488 and 510 nm for eGFP-CBM3a, 587 and 610 nm for mCherry-CBM17, 549 and 568 nm for mOrange2-CBM15 and 434 and 477 nm for eCFP-CBM27. Fluorescence measurements were recorded after each step of the assay. Each experiment was done in triplicates. Preparation of the microplate was carried out by gluing 3 mm diameter paper discs on the bottom of 96-wells, black microplate (Costar, Corning Life Sciences) using a transparent nail polish. The carbohydrates quantification assay started by incubating the paper discs 1 h, at room temperature with agitation in a 20 mM Tris-HCl pH 7.5 buffer containing 20 mM NaCl, 5 mM CaCl2 and 3% milk (binding buffer). Unbound milk constituents were removed by washing three times with the 20 mM Tris-HCl pH 7.5 buffer containing 20 mM NaCl, 5 mM CaCl2 (washing buffer). Afterward, the blocked paper discs were incubated with agitation for 1 h, at room temperature into the binding buffer containing 0.5 μg $\mu l^{-1}$ of the appropriate probe. Non-specifically bound probe was removed with three buffer washes (washing buffer) followed by three 0.05% Tween 20 washes. Treatment of the resulting data involved subtraction of the mean blocked fluorescence values from the mean residual ones. Then these corrected mean residual fluorescence values were converted into μg and μg $g^{-1}$ of cellulose using the appropriate standard curves and weight of cellulose in each fiber discs.

**Determination of the probes affinity for Avicel and fiber discs.** Solid state depletion assays[43] were used to measure the affinity of all probes using heterogeneous substrates such as Whatman, HYKP and KP fiber discs, and substrate Avicel PH105 (crystalline cellulose) for eGFP-CBM3a probe. Determination of the affinity of eGFP-CBM3a regarding Avicel was performed under the following procedure. The assay started with a 1 h incubation at room temperature of 10 mg of the presoaked Avicel with increasing concentrations of eGFP-CBM3a in a 20 mM Tris-HCl pH 7.5 buffer containing 20 mM NaCl, 5 mM CaCl2 and 3% milk. Following equilibration, the solid phase was separated from the liquid phase by centrifugation at 20 000g for 5 min. Fluorescence measurements of the supernatant (containing free protein ($P_{free}$)) were acquired using a Synergy Mx microplate reader (BioTek) with the end point feature active and the filters bandwidth set at 9 nm. The excitation and emission wavelengths for eGFP-CBM3a were set at 488 and 510 nm, respectively. Protein concentrations were determined using the appropriate standard curves. All binding isotherms were calculated using the OriginLab software and fitted to a one binding site equation follows:

$$[P_{bound}] = N_0 K_a [P_{free}] / (1 + K_a [P_{free}])$$

where ($K_a$) represent binding affinity and ($N_0$) represent the capacity of CBM probe (Table S1†).

The determination of the probes affinity for fibers discs was achieved using the acquisition settings as described in the previous paragraph for the quantification. Fluorescence measurements were again recorded after each step of the assay. Briefly, the glued fiber discs were incubated for 1 h at room temperature with agitation in the binding buffer. Unbound milk constituents were removed by washing three times with the washing buffer. Afterward, the blocked paper discs were incubated 1 h at room temperature with binding buffer which contained increasing concentrations of the appropriate probe. Non-specifically bound probe was then removed with three washing steps. Treatment of the resulting data involved subtraction of the mean blocked fluorescence values from the mean residual ones. These corrected mean residual fluorescence values were converted into μg and μg $g^{-1}$ of substrate using the appropriate standard curves and weight of cellulose in each paper disc. All binding isotherms fitted to a one binding site equation.

## Conclusions

We developed a simple yet powerful approach that allows for the surface characterization of fiber surfaces. The CBM probes were successfully employed to characterize the impacts of pulping, mechanical and enzymatic modifications on the carbohydrates distribution on lignocellulosic biomass surfaces. Correlations with paper strength properties would enable the rapid determination of these properties and allow one to predict in a high throughput yet low volume the optimal conditions with which to treat a given biomass. Such probes provide a new and novel approach for monitoring process development and scale-up of processes that affect fiber properties - in either the manufacture of paper or the deconstruction of cellulose into sugars for biofuel production.

## Acknowledgements

This work was supported by Buckman International, the Natural Sciences and Engineering Council of Canada (NSERC grant CRDPJ 445143 - 2012), the Consortium de recherche et innovations en bioprocédés industriels au Québec (CRIBIQ)

and by MITACS *via* partial stipends to YHO, LC, and VK (Accelerate program). We would like to thank Dr Roberto Chica (University of Ottawa) for the donation of mCherry plasmid. The skillful technical assistance of Daniel Steven Agudelo, Rene Diene and Nikolas Beauchesne is acknowledged. We would like to thank Mary A. Hefford for her valuable editorial contributions as well as Dr N. Voyer and Dr J. Bowie for insightful discussions.

## Notes and references

1 M. E. Himmel, S. Y. Ding, D. K. Johnson, W. S. Adney, M. R. Nimlos, J. W. Brady and T. D. Foust, *Science*, 2007, **315**, 804–807.
2 V. Arantes and J. N. Saddler, *Biotechnol. Biofuels*, 2010, **3**, 4.
3 M. Sabourin, paper presented at the 2003 Fall Technical Conference, Chicago, IL, 2003.
4 L. P. Walker and D. B. Wilson, *Bioresour. Technol.*, 1991, **36**, 3–14.
5 B. Vanholme, T. Desmet, F. Ronsse, K. Rabaey, F. Van Breusegem, M. De Mey, W. Soetaert and W. Boerjan, *Front. Plant Sci.*, 2013, **4**, 174.
6 Q. Xu, M. G. Resch, K. Podkaminer, S. Yang, J. O. Baker, B. S. Donohoe, C. Wilson, D. M. Klingeman, D. G. Olson, S. R. Decker, R. J. Giannone, R. L. Hettich, S. D. Brown, L. R. Lynd, E. A. Bayer, M. E. Himmel and Y. J. Bomble, *Sci. Adv.*, 2016, **2**, e1501254.
7 R. A. Dixon, *Nature*, 2013, **493**, 36–37.
8 T. P. Schultz, M. C. Templeton and G. D. McGinnis, *Anal. Chem.*, 1985, **57**, 2867–2869.
9 S. Burkhardt, L. Kumar, R. Chandra and J. Saddler, *Biotechnol. Biofuels*, 2013, **6**, 90.
10 K. Karimi and M. J. Taherzadeh, *Bioresour. Technol.*, 2016, **200**, 1008–1018.
11 P. Fardim, H. Hultén Anette, J.-P. Boisvert, L.-S. Johansson, M. Ernstsson, M. Campbell Joseph, A. Lejeune, B. Holmbom, J. Laine and D. Gray, *Holzforschung*, 2006, **60**, 149.
12 L.-S. Johansson, J. M. Campbell, P. Fardim, A. H. Hultén, J.-P. Boisvert and M. Ernstsson, *Surf. Sci.*, 2005, **584**, 126–132.
13 A. B. Boraston, V. Notenboom, R. A. J. Warren, D. G. Kilburn, D. R. Rose and G. Davies, *J. Mol. Biol.*, 2003, **327**, 659–669.
14 O. Shoseyov, Z. Shani and I. Levy, *Microbiol. Mol. Biol. Rev.*, 2006, **70**, 283–295.
15 S. Y. Ding, Q. Xu, M. K. Ali, J. O. Baker, E. A. Bayer, Y. Barak, R. Lamed, J. Sugiyama, G. Rumbles and M. E. Himmel, *Biotechniques*, 2006, **41**, 435.
16 M. C. Hernandez-Gomez, M. G. Rydahl, A. Rogowski, C. Morland, A. Cartmell, L. Crouch, A. Labourel, C. M. G. A. Fontes, W. G. T. Willats, H. J. Gilbert and J. P. Knox, *FEBS Lett.*, 2015, **589**, 2297–2303.
17 K. Gourlay, J. Hu, V. Arantes, M. Penttilä and J. N. Saddler, *J. Biol. Chem.*, 2015, **290**, 2938.
18 J. P. Knox, *Cellulases*, 2012, **510**, 233–245.
19 T. Kawakubo, S. Karita, Y. Araki, S. Watanabe, M. Oyadomari, R. Takada, F. Tanaka, K. Abe, T. Watanabe, Y. Honda and T. Watanabe, *Biotechnol. Bioeng.*, 2010, **105**, 499.
20 S. Gao, C. You, S. Renneckar, J. Bao and Y. H. P. Zhang, *Biotechnol. Biofuels*, 2014, **7**, 1.
21 V. Khatri, Y. Hebert-Ouellet, F. Meddeb-Mouelhi and M. Beauregard, *Biotechnol. Biofuels*, 2016, **9**, 74.
22 G. Smook, *Handbook for pulp and paper technologists*, Angus Wilde Publications Inc., Vancouver, 2003.
23 C. J. Biermann, *Handbook of pulping and papermaking*, Academic Press, San Diego, 1996.
24 P. Bajpai, in *Biotechnology for pulp and paper processing*, ed. P. Bajpai, Springer, New York, 1st edn, 2012, ch. 2, pp. 7–14.
25 A. Sluiter, B. Hames, R. Ruiz, C. Scarlata, J. Sluiter, D. Templeton and D. Crocker, *Laboratory Analytical Procedure*, 2008, NREL/TP-510-42618.
26 G. N. Inari, M. Pétrissans, J. Lambert, J. J. Ehrhardt and P. Gérardin, *Surf. Interface Anal.*, 2006, **38**, 1336–1342.
27 P. Nzokou and D. Pascal Kamdem, *Surf. Interface Anal.*, 2005, **37**, 689–694.
28 H. Awada, P. H. Elchinger, P. A. Faugeras, C. Zerrouki, D. Montplaisir, F. Brouillette and R. Zerrouki, *BioResources*, 2015, **10**(2), 2044–2056.
29 G. N. Inari, M. Pétrissans, S. Dumarcay, J. Lambert, J. J. Ehrhardt, M. Sernek and P. Gérardin, *Wood Sci. Technol.*, 2011, **45**(2), 369.
30 W. K. Istone, *X-ray photoelectron spectroscopy (XPS)*, CRC Press, Boca Raton, 1995.
31 S. Gharehkhani, E. Sadeghinezhad, S. N. Kazi, H. Yarmand, A. Badarudin, M. R. Safaei and M. N. M. Zubir, *Carbohydr. Polym.*, 2015, **115**, 785.
32 J. O. Baker, M. R. King, W. S. Adney, S. R. Decker, T. B. Vinzant, S. E. Lantz, R. E. Nieves, S. R. Thomas, L.-C. Li, D. J. Cosgrove and M. E. Himmel, *Appl. Biochem. Biotechnol.*, 2000, **84**, 217.
33 M. P. Coughlan, *Biotechnol. Genet. Eng. Rev.*, 1985, **3**, 39.
34 L. Cui, F. Meddeb-Mouelhi and M. Beauregard, *Nord. Pulp Pap. Res. J.*, 2015, **31**, 315.
35 R. E. Mark, in *Handbook of Physical Testing of Paper*, ed. R. E. Mark, C. C. Habeger Jr, J. Borch and M. B. Lyne, Marcel Dekker Inc., New York, 2nd edn, 2002, ch. 14, pp. 727–872.
36 M. A. Hubbe, R. A. Venditti and O. J. Rojas, *BioResources*, 2007, **2**, 739.
37 T. Oksanen, J. Pere, L. Paavilainen, J. Buchert and L. Viikari, *J. Biotechnol.*, 2000, **78**, 39.
38 S. D. Mansfield, K. K. Y. Wong, E. D. De Jong and J. N. Saddler, *Tappi J.*, 1996, **79**, 125–132.
39 A. Suurnäkki, M. Tenkanen, J. Buchert and L. Viikari, in *Biotechnology in the Pulp and Paper Industry*, ed. K. E. L. Eriksson, W. Babel, H. W. Blanch, C. L. Cooney, S. O. Enfors, K. E. L. Eriksson, A. Fiechter, A. M. Klibanov, B. Mattiasson, S. B. Primrose, H. J. Rehm, P. L. Rogers, H.

 

Sahm, K. Schügerl, G. T. Tsao, K. Venkat, J. Villadsen, U. von Stockar and C. Wandrey, Springer, Berlin, Heidelberg, 1997, pp. 261–287.

40 R. Kumar and C. E. Wyman, *Biotechnol. Bioeng.*, 2014, **111**, 1341–1353.

41 G. Strey, J. Wesley-Smith and F. Wolfaardt, *Holzforschung*, 2009, **63**, 521–527.

42 E. J. Taylor, A. Goyal, C. I. P. D. Guerreiro, J. A. M. Prates, V. A. Money, N. Ferry, C. Morland, A. Planas, J. A. Macdonald, R. V. Stick, H. J. Gilbert, C. M. G. A. Fontes and G. J. Davies, *J. Biol. Chem.*, 2005, **280**, 32761.

43 D. W. Abbott and A. B. Boraston, *Methods Enzymol.*, 2012, **510**, 211.

# Appendix D

Bombeck et al. Biotechnol Biofuels (2017) 10:293
https://doi.org/10.1186/s13068-017-0980-0

Biotechnology for Biofuels

RESEARCH Open Access

# Predicting the most appropriate wood biomass for selected industrial applications: comparison of wood, pulping, and enzymatic treatments using fluorescent-tagged carbohydrate-binding modules

Pierre-Louis Bombeck[1], Vinay Khatri[2,3†], Fatma Meddeb-Mouelhi[2,3†], Daniel Montplaisir[4], Aurore Richel[1] and Marc Beauregard[2,3*]

**Abstract**

**Background:** Lignocellulosic biomass will progressively become the main source of carbon for a number of products as the Earth's oil reservoirs disappear. Technology for conversion of wood fiber into bioproducts (wood biorefining) continues to flourish, and access to reliable methods for monitoring modification of such fibers is becoming an important issue. Recently, we developed a simple, rapid approach for detecting four different types of polymer on the surface of wood fibers. Named fluorescent-tagged carbohydrate-binding module (FTCM), this method is based on the fluorescence signal from carbohydrate-binding modules-based probes designed to recognize specific polymers such as crystalline cellulose, amorphous cellulose, xylan, and mannan.

**Results:** Here we used FTCM to characterize pulps made from softwood and hardwood that were prepared using Kraft or chemical-thermo-mechanical pulping. Comparison of chemical analysis (NREL protocol) and FTCM revealed that FTCM results were consistent with chemical analysis of the hemicellulose composition of both hardwood and softwood samples. Kraft pulping increased the difference between softwood and hardwood surface mannans, and increased xylan exposure. This suggests that Kraft pulping leads to exposure of xylan after removal of both lignin and mannan. Impact of enzyme cocktails from *Trichoderma reesei* (Celluclast 1.5L) and from *Aspergillus* sp. (Carezyme 1000L) was investigated by analysis of hydrolyzed sugars and by FTCM. Both enzymes preparations released cellobiose and glucose from pulps, with the cocktail from *Trichoderma* being the most efficient. Enzymatic treatments were not as effective at converting chemical-thermomechanical pulps to simple sugars, regardless of wood type. FTCM revealed that amorphous cellulose was the primary target of either enzyme preparation, which resulted in a higher proportion of crystalline cellulose on the surface after enzymatic treatment. FTCM confirmed that enzymes from *Aspergillus* had little impact on exposed hemicelluloses, but that enzymes from the more aggressive *Trichoderma* cocktail reduced hemicelluloses at the surface.

**Conclusions:** Overall, this study indicates that treatment with enzymes from *Trichoderma* is appropriate for generating crystalline cellulose at fiber surface. Applications such as nanocellulose or composites requiring chemical

*Correspondence: marc.beauregard@uqtr.ca
†Vinay Khatri and Fatma Meddeb-Mouelhi contributed equally to this work
[2] Université du Québec à Trois-Rivières, Centre de Recherche sur les Matériaux Lignocellulosiques, C.P. 500, Trois-Rivières, QC G9A 5H7, Canada
Full list of author information is available at the end of the article

resistance would benefit from this enzymatic treatment. The milder enzyme mixture from *Aspergillus* allowed for removal of amorphous cellulose while preserving hemicelluloses at fiber surface, which makes this treatment appropriate for new paper products where surface chemical responsiveness is required.

**Keywords:** FTCM, Carbohydrate-binding module, Fluorescent protein, LCB (lignocellulosic biomass), Cellulose, Hemicellulose, Enzymes

## Background

Global production of biofuels and bioproducts is increasing steadily because such products are greener alternatives to fossil fuels and their derivatives [1–3]. Concomitantly, numerous new products and technologies based on the conversion of biomass have been developed over the last decade [4–9]. Securing sufficient biomass as raw materials is a prerequisite to moving from a petro-chemical to a bio-chemical economy. Using feedstocks to support first-generation biofuel and bioproducts has shown its limits and produces certain undesirable socio-economic and environmental outcomes [10, 11]. The use of lignocellulosic biomass (LCB, including dedicated lignocellulosic crops, agricultural and forestry residues and municipal and industrial wastes) to produce second-generation biofuel and bioproducts would avoid the negative impacts associated with first-generation feedstocks use [12, 13].

Although LCB is a promising, abundant and renewable resource, it is difficult to treat due to its complex structure consisting of cellulose fibrils wrapped in a network of lignin and hemicelluloses. This network, collectively referred to as the lignin-carbohydrate complex, is highly recalcitrant and difficult to modify [8, 14–18]. Consequently, several steps of pretreatments are needed to isolate each of the components before they can be used in value-added applications.

For the production of biofuels based on carbohydrates from LCB, such as bioethanol, the principal goal is the complete hydrolysis of polysaccharide components (mainly cellulose) of the raw material into monomers for subsequent fermentation [18–22]. Utilization of all other lignocellulosic components is not as well developed but is the focus of intensive research efforts [8, 9, 23, 24]. This "integrated biorefinery" concept involves a succession of steps for transforming the entire lignocellulosic biomass into biofuels and bioproducts. This concept has been demonstrated using a variety of physical, chemical and biological treatments [25–27] in a range of configurations [28–31]. Total utilization of LCB will permit commercial exploitation of the entire lignocellulosic biomass in a wide spectrum of bioproducts and bioenergy [5, 32, 33]. In this context, new bioproducts (e.g. biomaterials, biocomposites, biomembranes and biofilms) from previously unused components of LCB are receiving growing interest because they are also biodegradable, produced from a renewable carbon source and can have a wide variety of applications [5, 7, 34–36]. Unlike bioethanol, specific bioproducts based on lignocellulosic fibers do not require complete separation or deconstruction of the raw lignocellulosic polymers. Removal of some specific components or alteration of structural features of fibers leading to modulation of their physical and chemical properties is often sufficient [5, 7, 32, 37–39].

A largely used green process for the removal or alteration of specific structural features of the biomass is the enzymatic hydrolysis or biocatalysis. Enzymes have been used for improving papermaking processes (for fiber cutting action, peeling, delamination, weakening effect, bleaching, refining) [40–42] and also for the deconstruction of lignocellulosic biopolymers [7, 43–51]. Actually, cellulases from *Trichoderma reesei* are subject to many studies and have been used to efficiently hydrolyze cellulose for decades [40, 52]. Enzymes have high selectivity and turnover frequency, permitting processes with high selectivity and increased productivity on a variety of substrates [53]. For example, enzymatic hydrolysis avoids or drastically decreases the production of degradation products that are generated by classical acid hydrolysis (e.g. 5-hydroxymethylfurfural, 2-furfural) [54, 55]. Many types of enzyme can catalyze LCB hydrolysis: endo- and exoglucanase, cellobiase, xylanase, mannanase and many others. Synergy between several enzymes in a mixture of their lignocellulosic substrates has also been demonstrated, but are not yet completely known [52, 56–58]. In addition to this, enzymes are costly, and accordingly, real-time dosage control is an important parameter in most industrial processes [57, 59–63].

The effectiveness and impact of enzymatic processes on a substrate can be quantified using physical and chemical methods. Among them, the most commonly used are: compositional analysis of the substrate after treatment (using FTIR, XPS) or of the hydrolysates (hydrolysis products content, using GC or HPLC), surface imaging (using SEM, TEM and AFM), index of crystallinity (using XRD and NMR) and mass balance calculations [64–66]. However, current methods of analysis cannot directly monitor enzymatic action. It is not possible to determine the precise order in which components of the substrate were hydrolyzed as the enzymes penetrate the materials

and what components are left exposed on fibers after treatment. While direct chemical characterization of the surface is possible with XPS, it remains that this method is expensive and does not distinguish between different polysaccharides because they harbor similar functional groups [67].

The ability to directly monitor changes to the surface of LCB fibers during enzymatic treatment is essential for controlling and optimizing processes according to the final bioproducts targeted. To this end, a rapid and low-cost method to directly monitor the deconstruction of heterogeneous LCB during enzymatic hydrolysis has been developed [67, 68]. Called fluorescent-tagged carbohydrate-binding module method, or FTCM, this method is based on the use of four specific ready-to-use probes made of fluorescent-tagged recombinant carbohydrate-binding modules (named ft-CBM or probes throughout the text). In these probes, the recombinant CBM part binds to a specific component of the substrate surface. The fluorescence of the probe permits rapid quantification of the probes bound to the surface. The fluorescence can be measured by using an ordinary fluorescence plate reader. This new approach allows for specific surface changes to be tracked and for changes to biopolymers, in this case mannan, xylan, crystalline and amorphous cellulose, to be monitored. FTCM can detect these polymers at the surface of the substrate before and after any given treatment, be it mechanical, chemical or enzymatic [67, 68].

In this study, we use FTCM to characterize how the surfaces of a variety of lignocellulosic biomass are modified by two different commercial enzyme cocktails. The substrates include two chemical-thermo-mechanical pulps, referred to as CTM pulps, and two Kraft wood pulps. This investigation provides information on which combination of enzyme treatment and biomass substrate is best suited for industrial applications in which various levels of fiber deconstruction and precise control of fiber surface composition are desirable, such as the production of nanocellulose, fiber-reinforce composites, or paper.

## Methods

### Lignocellulosic biomass

Four wood pulps were selected to evaluate the effect of woody biomass composition and pretreatment on the experiment. Hardwood mix Kraft pulp (here referenced as HK) was kindly provided by Burgo Ardennes S.A. (Virton, Belgium). Softwood from spruce chemical-thermo-mechanical pulp (referenced as SM) and hardwood from poplar chemical-thermo-mechanical pulp (referenced as HM) were kindly provided by SAPPI Lanaken N.V. (Lanaken, Belgium). Softwood mix Kraft pulp (referenced as SK) was kindly provided by Kruger Wayagamac Inc. (Trois-Rivières, Canada). All pulps used in this study were unbleached. The chemical composition of the of the pulps was determined according to the NREL-TP-510-42618 standard method [69]. The length, width, fine percentage and zero span breaking length of wood pulp fibers were analyzed with a fiber quality analyzer (FQA) (LDA02-090 HiRes, OpTest Equipment Inc, Hawkesbury Canada) following the TAPPI T271 om-12 and T231 standard methods.

### Enzyme solutions

Two different commercial enzyme mixtures were used in this study, CelluClast 1.5L (Cat No #C2730) and Carezyme 1000L (Cat No #C2605), which were purchased from Sigma-Aldrich. CelluClast 1.5L (named "T" in this study) is a mixture of fungal hydrolytic enzymes from *T. reesei* and principally consists of two cellobiohydrolases and two endoglucanases, as well as small amounts of other cellulases and also various accessory enzymes which function as hemicellulases [40, 57, 70]. Carezyme 1000L (named "A" in this study) consists of a mixture of several hydrolytic enzymes mixture from *Aspergillus* sp.

Both enzyme mixtures are widely employed for hydrolysis and deconstruction of lignocellulosic biomass. Both enzymes mixtures contain cellulase (CMCase), xylanase, and mannanase enzymes, whose activities were tested using carboxymethyl cellulose, xylan from birch wood, and galactomannan as substrates, respectively. The activities of cellulase, mannanase, and xylanase were assayed quantitatively using the 3,5-dinitrosalicylic acid (DNS) method which measures the reducing sugars generated by enzymatic hydrolysis from their absorption at 540 nm) as described by Miller [64]. Protein content was quantified using the assay developed by Bradford [71].

### Enzymatic treatments of pulp

Three samples of each pulp were prepared in suspension for three different treatments: one without enzyme addition (control sample, called "Std"), a second to which CelluClast 1.5L was added (called "T"), and third to which Carezyme 1000L was added (called "A"). Prior to enzyme addition, each sample was disintegrated in citrate buffer (having a concentration of 0.05 M and pH 4.8) at 1.2% consistency (24 grams of pulp on an oven dry matter basis in 2 L of buffer) with a standard pulp disintegrator and transferred into a 4-L Erlenmeyer flask. Suspensions were pre-heated until 50 °C using a controlled-environment incubator-shaker (New Brunswick Scientific Inc.). Enzyme solutions were then added to a final loading of 1275 mg of enzyme per gram of oven dry pulp. Hydrolysis was carried out in the incubator at 50 °C for 4 h

under continuous orbital agitation (150 rpm). Enzymatic hydrolysis was stopped by incubating the pulp on ice for 15 min. Each sample was filtered and filtrate was boiled in a 95 °C water bath for 10 min and kept frozen at − 20 °C until sugars analysis. Filtration of untreated and enzymes treated pulps produced paper sheets, of 60 ± 2 g $m^{-2}$ in basis weight, as per the TAPPI T205 sp-02 standard methodology. The pH was measured before and after enzymatic treatment.

Optimization of hydrolysis conditions, such as duration and enzymes loading, was done on a small scale at high throughput using 96-wells microtiter plates with 3 mm diameter paper discs. After enzymatic digestion of the discs, FTCM test was applied to detect the optimal condition required for enzymes to promote the efficient degradation in cellulose and hemicellulose.

#### Handsheet and paper disc preparation

Four different pulps were used for the preparation of handsheets and paper discs. Handsheets of 60 ± 2 g $m^{-2}$ basis weight were prepared as per the TAPPI T205 sp-02 standard. 3-mm paper discs were punched from handsheet [67].

#### Construction of recombinant probe expression systems

All carbohydrate-recognition probe genes were inserted into pET11a expression vectors. CBM 372 3a (*Clostridium thermocellum* CipA, NZYTech), CBM15 (*Cellvibrio japonicas*, Z48928), CBM17 (*Clostridium cellulovorans*, U37056), and CBM27 (*Thermotoga maritima*, NP_229032) genes were synthetized by GenScript. The fluorescent protein genes (eGFP, mOrange2, mCherry, and eCFP) were cloned into the *Dra*III and *Bam*HI sites while the CBM genes were introduced into the *Bsr*GI and *Bam*HI sites. All encoding genes were sequenced to ascertain the integrity and fidelity of the probes. The resulting probes GC3a, OC15, CC17, and CC27 [67, 68] were used to detect crystalline cellulose, xylan, amorphous cellulose, and mannan, respectively.

#### Expression and purification of probes

All probes were produced in *E. coli* BL21(DE3) Gold pLysS cells and purified as described by Hébert-Ouellet et al. [68].

#### Quantification of the carbohydrates on the surface of fiber paper discs using FTCM

Tracking of the variation of carbohydrate on the surface of paper discs using the four different probes was done as described by Khatri et al. and Hébert-Ouellet et al. [67, 68]. Note that lignin fluorescence was subtracted from total fluorescence and that affinity of all probes used here for their respective substrates was previously characterized, as detailed in [67, 68].

#### Sugar analysis

After enzymatic hydrolysis, a filtered hydrolysate was analyzed for cellobiose, glucose, xylose, and mannose concentrations using a HPAEC-PAD (Dionex ICS-5000+) and a GC-FID (Agilent Technologies 7890B) following methods from the work of Vanderghem et al. [72, 73]. Results were processed using Chromeleon 7® and OpenLAB CDS ChemStation software.

#### Scanning electron microscope (SEM) images

Scanning electron microscope (SEM) images were used to analyze surface morphology and to characterize the effect of the pulping process on paper fibers. Samples of dried handsheets having a basis weight of 60 g ± 2 g $m^{-2}$ were coated with gold in a Quorum SC-7620 sputter-coater. Images were produced of several different locations on the surface of SM and SK pulp samples with a scanning electron microscope (JEOL, JSM-5500).

#### Statistical analysis

Minitab 17© and Microsoft Excel 2010© software were used for statistical analysis of data.

## Results and discussion

#### Enzyme characterization

Two commercial enzyme mixtures produced by *T. reesei* and by *Aspergillus* sp. were used for this study. Under our specific assay conditions, both commercial preparations contained cellulase (CMCase), xylanase, and moderate mannanase activities. Enzyme mixture T was characterized by higher cellulase and xylanase activities, although its low mannanase activity was roughly equal to mixture A (Additional file 1).

#### Pulp fiber characterization

Pulp fiber characteristics prior to treatments are presented in Table 1, which show how the pulp grades used in this experiment differed from one another. As expected, softwood fibers were longer and wider than

**Table 1 Pulp fibers properties before enzymatic treatments**

| Fibers characteristics (average values) | HM | SM | HK | SK |
|---|---|---|---|---|
| Length (mm) | 0.71 | 1.31 | 0.76 | 2.35 |
| Fines (0–0.2 mm) (%) | 15.31 | 13.25 | 13.64 | 3.01 |
| Width (μm) | 22.6 | 27.4 | 17.7 | 26.0 |

*HM* hardwood CTM pulp, *SM* softwood CTM pulp, *HK* hardwood Kraft pulp, and *SK* softwood Kraft pulp

hardwood fibers [17]. All of the grades contained similar quantities of fine fibers except for the softwood Kraft pulp. These fine fibers could impair hydrolysis yield on full fibers because finer fibers have a greater susceptibility for hydrolysis, so hydrolysis yield is altered by the quantity of fine fiber in a sample during our 4-h hydrolysis [74]. Hardwood pulp was only slightly affected by Kraft pulping, while for softwood pulp, the Kraft treatment had an obvious impact on length and fines, but none on width. SEM images showed that softwood Kraft pulp has lower fibrillation and greater homogeneity than softwood CTM (Fig. 1) as observed earlier [75, 76] and which is fully compatible with a decreased content in fines.

Mechanically treated pulps contained more lignin than the Kraft pulps (Fig. 2). The Kraft process dissolves lignin from wood raw material to liberate fibers, while by contrast mechanical separation of wood fibers does not involve the extraction of lignin [76]. Lignin protects the other components of the biomass against degradation, so the absence of lignin in Kraft pulp permits enzymatic hydrolysis to occur more effectively [77]. As expected, softwood hemicelluloses were glucomannan-rich, while hardwood hemicelluloses were xylose-rich [17, 78, 79]. HK and SK pulps yield the greatest quantity of glucose, making them the most promising of the samples as a potential biofuel substrate.

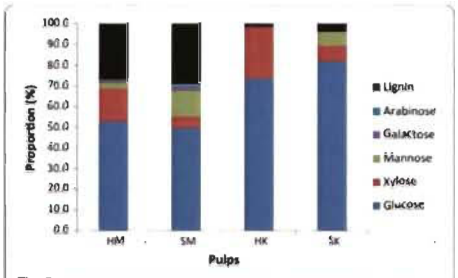


**Fig. 2** Lignin and carbohydrate monomer content of pulps. *HM* hardwood CTM pulp, *SM* softwood CTM pulp, *HK* hardwood Kraft pulp, and *SK* softwood Kraft pulp

### Hydrolysate analysis

Hydrolysate sugar content of the control samples (i.e. without enzyme addition) was negligible (data not shown). This demonstrates that hydrolysis did not occur

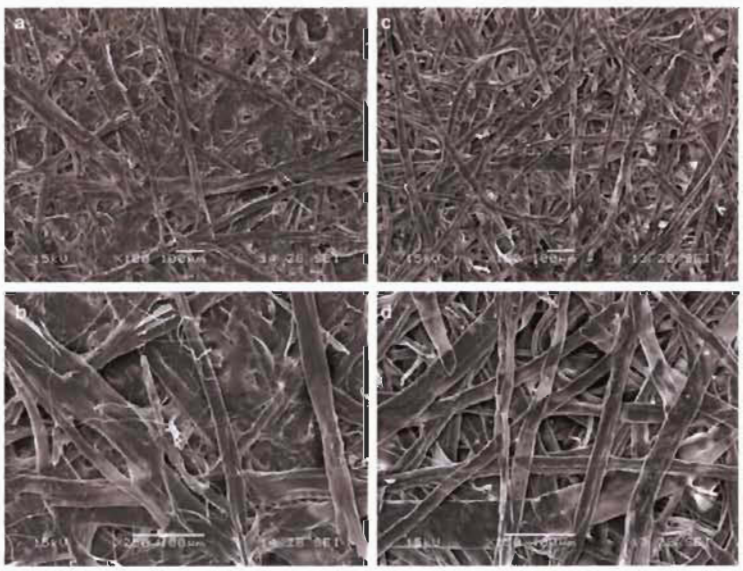


**Fig. 1** SEM micrographs obtained from (SM) untreated softwood CTM pulp (**a**, **b**), and from (SK) untreated softwood Kraft pulp (**c**, **d**) at two levels of resolution

in the absence of enzymes. Figure 3 shows cellobiose, glucose, xylose, and mannose concentration of hydrolysate solutions recovered after treating pulps with T and A enzyme cocktails.

Figure 3 presents the amounts of selected mono- and disaccharides which were liberated by enzymatic hydrolysis of pulp fibers. The quantity of sugar detected in the hydrolysate was better related to pulp grade than to the enzyme cocktail used. Kraft pulps released more of each sugar, indicating they are more susceptible to enzymatic hydrolysis in the relevant conditions. This can be explained by the difference in lignin content, since the presence of lignin protects polysaccharides from enzymatic hydrolysis [60, 80–84]. As discussed earlier and in the literature, pretreatments which remove lignin and hemicellulose expose a greater proportion of the cellulose in the substrate and increase pore volume and surface area, which results in increased hydrolysis rate [85]. The high glucose content of the Kraft pulps presented in Fig. 2 suggests that these pulps are composed primarily of cellulose, an inference that is consistent with the composition of the hydrolysate produced from their enzymatic hydrolysis. Hydrolysate sugar content also demonstrated that enzyme "A" was less effective than "T" under same hydrolysis conditions. More xylose was released from hardwood pulp in the presence of T enzyme cocktail, which again corresponds with the abundance of xylose monomers in the substrate, as shown in Fig. 2. The cellobiose yield from hydrolysis of SK was greater than that from hydrolysis of HK, although HK hydrolysis produced more glucose when catalyzed by T treatment. Finally, hydrolysate composition suggests that the mannanase activity of both enzyme cocktails is low. Such results may indicate that mannans are not as accessible as other polymers, or that mannanase activity is too low (consistent with activity measurements for both enzyme preparations; see Additional file 1). The sugar content of the hydrolysates is a good indicator of enzyme activity with respect to specific carbohydrates, but does not provide any information on the surface chemistry of the treated fiber.

#### Effect of enzymatic treatment on pulp fibers

Biofuel production from LCB depends on polymer accessibility during enzymatic treatment, but many other applications require specific surface functionality linked to distribution of polymers left after treatment at the surface of fibers. One way to obtain information about the outcome of an enzymatic treatment on LCB is by investigating properties of its fibers and of paper formed using these fibers. Enzyme hydrolysis used here only affected the length of Kraft pulp grade. Treatment of hardwood Kraft pulp with T enzymes decreased length by 20%. Enzymes, A and T, decreased softwood Kraft fiber length by 15 and 25%, respectively (Additional file 2: Figure S1). These results suggest a fiber cutting action, ascribed to endoglucanase activity in enzyme cocktails [57, 70]. While Kraft pulp fiber length decreased as a consequence of treatment, fines increased (Additional file 2: Figure S2). This phenomenon has been suggested as a consequence of the combination of cutting, peeling, delaminating, and weakening effects on the surface of the fibers by enzymatic hydrolysis [40–42]. Although the enzymatic hydrolysis reduced the length of some fibers, it did not affect the average width of any samples, regardless of pulping or enzymes used (Additional file 2: Figure S3). Concerning zero span breaking length, a measure of the average strength of individual fibers (Additional file 2:

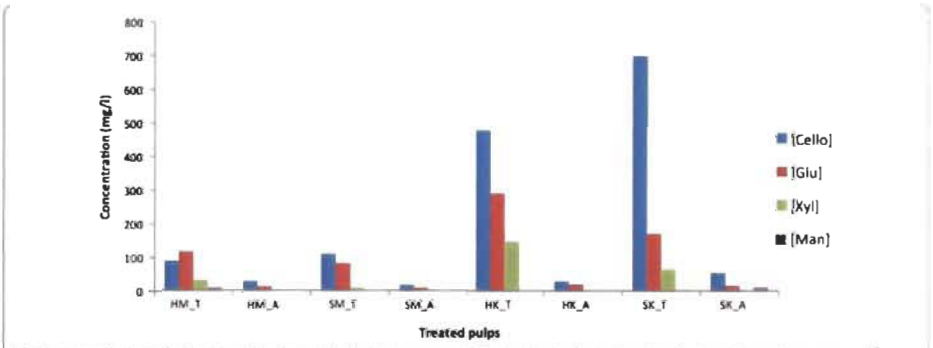


**Fig. 3** Concentrations of selected carbohydrates in hydrolysate recovered after hydrolysis of pulp. T and A refer to mixtures of enzymes used for hydrolysis

Figure S4), treatment had no effect on mechanical CTM pulps but both enzymes degraded chemical Kraft pulp strength. The higher lignin content of the mechanical pulps may explain why their mechanical strength was not affected by the treatment. Analysis of these paper properties corroborates previous studies of simple sugars release by hydrolysis of paper pulp and confirms that Kraft pulps are more susceptible to enzymatic treatments [47, 50, 86, 87]. For applications where strength properties are very important, such combination pulp-enzymatic treatments (Kraft pulps treated with cellulase mixtures) would be deleterious.

#### Detection of pulp fiber polymers using FTCM analysis before and after enzymatic treatments

Fluorescent-tagged carbohydrate-binding module method probes provide a rapid and cost-effective method to map the surface of LCB samples in terms of composition. Running 96 experiments requires a simple plate reader, is currently performed in less than 3 h, and would cost a few dollars when scaled up. Here this analysis was performed using the four probes in order to characterize pulp fibers prior to enzymatic treatments (Figs. 4 and 5). A probe (GC3a) which indicates the presence of crystalline cellulose regions (referred to here as CC) indicated greater CC exposure on hardwood surfaces than on softwood. CC made up a greater proportion of CTM pulps surface than of Kraft pulps surface, despite the higher lignin content of CTM pulps. This result is counterintuitive, since lignin is thought to act as protective barrier around cellulose, but the higher proportion of fibrils and fines in CTM pulps may explain the result since fine fibers tend to have greater specific area and, therefore, offer the most accessible polymers for the probes [68]. Fibrils and fines are partially removed by Kraft pulping, which may explain such results.

Figure 4 also shows the FTCM performed using the amorphous cellulose (referred to as AC) specific probe (named CC17). Mechanical pulps had the strongest AC-binding signal, also in accordance with the explanation of its higher content in high specific surface areas such as fibrils. Although three of the four pulps exposed much less AC than CC, the opposite was observed for SK pulp, where twice as much AC was detected compared to CC. Clearly, the distribution of AC did not parallel CC distribution on the surface of untreated fibers. The total cellulose (CC and AC) detected at the surface was the lowest for SK pulp, where the fibrillations are almost nonexistent as was observed in Fig. 1. This leads to a decrease in high surface area fibrils or fiber fragments, which are primary targets for CBMs binding to fiber polymers. Despite containing more cellulose than CTM pulps, the Kraft pulps returned a weaker binding signal for both CC and AC. Even if the abundance of glucose in the Kraft pulp hydrolysates is consistent with higher cellulose content (Figs. 2 and 3), FTCM shows that CTM pulp fiber surface has a greater number of exposed binding sites for cellulose-specific probes, despite containing less cellulose than Kraft pulps overall. One has to consider that the size of probes used here, with diameters of few nanometers, is closer to water than to most fibrous material. Any probe used here has access to all interstices detectable by electronic microscopy.

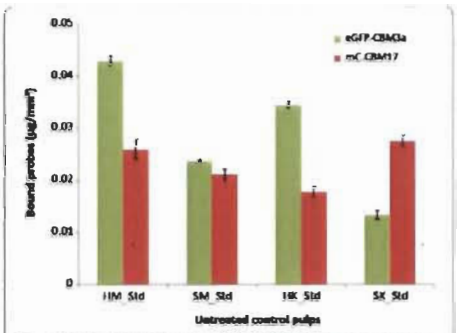


**Fig. 4** CBM binding to the surface of untreated pulps. The quantity of probe bonded to crystalline cellulose (in green) and amorphous cellulose (in red)

OC15 probe, which was used to signal the presence of xylan, returned a more intense signal from untreated hardwood pulps than for softwood (Fig. 5), which is consistent with the previously reported tendency of hardwoods to have a greater xylan content than softwoods [17, 78], and with the monosaccharide content of the samples already shown in Fig. 2. This phenomenon resembles the one observed for CC (Fig. 4), with higher signal for hardwood pulps than for softwood.

The signal produced by the mannan-specific probe (CC27) does not follow the trend described by the probes that have already been described in this section. Mannans were detected in greater abundance on the surfaces of the CTM pulps and were nearly absent from the Kraft pulps. Mechanical pulping of softwoods has been known to partially dissolve mannans [88], but the dearth of mannan on the probe-accessible surface of Kraft pulps suggests that some element of the Kraft process removes mannans even more extensively [89], while by contrast the mechanical treatment leaves them available for probe binding. The disparity in mannan detected on SK and HK corresponds to the relative abundance of mannose contained in the samples as determined in Fig. 2. Comparison of the four pulps' signals suggests that mannans are

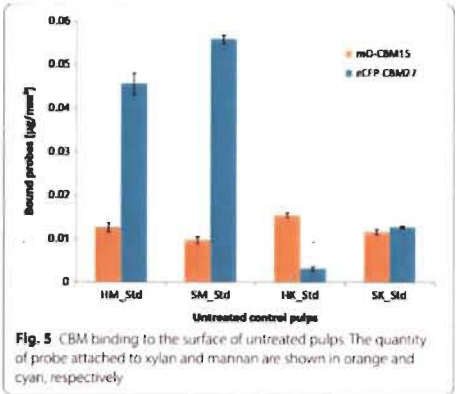


**Fig. 5** CBM binding to the surface of untreated pulps. The quantity of probe attached to xylan and mannan are shown in orange and cyan, respectively

strongly associated with lignin. These observations confirm other studies on the lignin–carbohydrate complex organization and changes according to the pulping process [17, 90–93].

The impact of enzymatic treatments on the amount of each polymer present on the surface of paper discs was characterized using FTCM. In Fig. 6, the signal intensity from each probe is presented in terms of its change relative to the intensity of the corresponding probe on untreated (Std) pulps shown in Figs. 4 and 5. Generally, enzymatic treatments resulted in a decrease in the number of bound probes, although there were some exceptions. This decrease can be a consequence of the preferred degradation of high specific surface components such as fines, filaments and fibrils by enzymes as discussed above. The overall diminution of probe signal intensity may also indicate that the enzymatic treatment results in an increase in the proportion of substances on the substrate surface which are affected neither by the enzymes nor by the probes (e.g. lignin). AC detection invariably decreased after enzymatic treatments, which supports the hypothesis that this component was degraded preferentially by cellulases in both enzymatic cocktails during short-time hydrolysis suggested by several studies [17, 56, 94, 95]. In our assay, changes in AC probe binding did not directly correlate to the yield of hydrolysis products of cellulose (cellobiose and glucose, Fig. 3). Generation of simple sugars such as glucose or cellobiose is a consequence not only of AC but of CC hydrolysis, and the proportions of AC and CC hydrolysis may vary for different pulps and enzyme cocktails.

A general inspection of Fig. 6 reveals that differences in signal intensity from probes bound to the substrate were due to a combination of the disparity in pulp properties and the character of the enzyme cocktails used for their treatment (which both have cellulase, xylanase, and mannanase activity). The results of Fig. 6 show that removal of surface hemicelluloses appeared to be more substantial with T enzymes treatment. This corroborates chromatographic analyses showing higher liberation of xylose and mannose after T enzyme treatment and may be attributed to a superior cellulase and xylanase activities in T enzyme preparation. Also, it can be seen that CTM softwood pulp (SM) responded differently to enzymatic treatments compared to HM. After enzymatic treatment, more CC was detected on the surface of the SM substrate, but less on the surface of the HM substrate. The

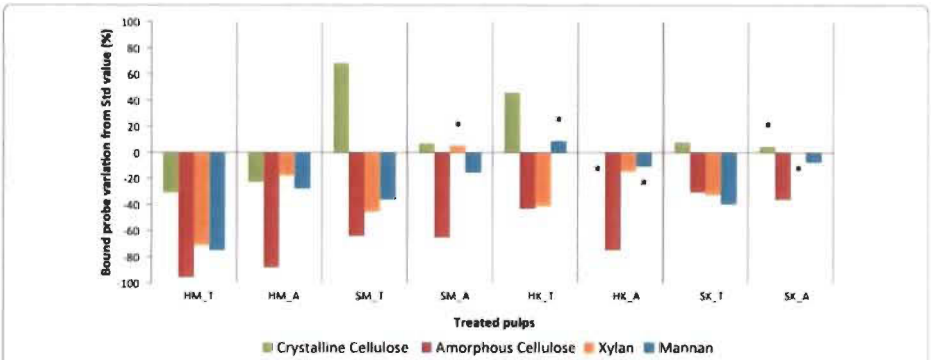


**Fig. 6** Impact of enzyme (T and A) hydrolysis on the binding of different polymer by probes (crystalline cellulose bound by GC3a, amorphous cellulose bound by CC17, xylan bound by OC15 and mannan by CC27), on the surface of fiber discs. Results that did not deviate significantly from untreated (Std) values (where significance was determined using Dunnet's comparison test) are indicated with an asterisk (*)

concurrent increase in CC and decrease in AC indicate that the glucose and cellobiose recovered from the hydrolysate (shown in Fig. 3) are principally the products of AC hydrolysis, as opposed to CC hydrolysis. CC hydrolysis cannot be ruled out, however, since FTCM detects CC probe-binding sites left after treatment. Hydrolysis of first polymers on the surface (including CC) can lead to exposure of previously buried CC.

When treated by A enzymes, the increase in CC at the surface of SM pulp was not as significant as after treatment with T enzymes. AC was decreased with similar efficacy, but other polymers were removed with different intensity. The signal from xylan-binding probes was found to be unaffected at the fiber surface after treatment with A enzymes, while that from mannan-binding probes decreased by 15%. As shown in Fig. 3, no xylose was detected in the hydrolysate from treatment with enzymes A, while the hydrolysate produced by T enzymes cocktail contained some xylose. The absence of xylose in A hydrolysate is consistent with the hypothesis that xylan was not consumed in this treatment, as shown in FTCM results, although xylanase activity was measured in this enzyme cocktail.

Despite major differences in fiber properties and pulping conditions, the proportion of HK-binding sites is modified in a similar way to SM when HK pulp was exposed to enzymatic hydrolysis. More CC was exposed at the surface of HK after T enzyme treatment, despite results on fiber length (Additional file 2) and simple sugar analysis (Fig. 3) that suggest extensive cellulose hydrolysis. Although more CC was exposed on the surface of SM after treatment with T enzymes, this was not accompanied either by fiber length reduction or by substantial hydrolysate sugar yields, which suggests that enzyme treatment was less severe with SM than with HK. The change in CC exposure was limited to 46% for HK (less CC was left on the surface of HK after T enzyme than on SM). Regarding HK pulp, Fig. 6 shows that both AC and xylan decreased on the surface of HK paper discs after either enzymatic treatment, but mannan variations were not significant. These results were suggested by chromatographic analyses but were confirmed by FTCM, which also reveals that CC exposure increased after T treatment, information that cannot be obtained by any other method discussed here.

Enzymatic hydrolysis of SK and HK Kraft pulps occurred in an approximately similar pattern, although both enzymes A and T lead to a smaller change in CC on the fiber surface of SK pulp than on HK pulp. AC decreased after both treatments by about 30%. Hydrolysis with cocktail T leads to a 33% decrease in xylan binding in FCTM but treatment with A enzyme left xylan unchanged. This observation is compatible with the detection of free xylose in the hydrolysate. Mannans were consumed to a greater extent in the softwood pulp. Changes in mannan surface coverage observed by FTCM for SK with T enzymes (a decrease of 40%) were not indicated by hydrolysate analysis, although a decrease in surface polymers does not necessarily lead to simple sugar release if the enzymes involved are also of endo- type. In this case, a drop in relative abundance of mannan at the fiber surface cannot be revealed by a chromatographic analysis of simple sugars but is easily detected using FTCM.

#### Surface polymer distribution after enzymatic treatments

Here the quantity of each probe bound to surface is expressed as a percent of the total number of probes detected, removing from our assessment any general change in surface binding or availability for binding (such as the decrease in binding due to loss of high surface fragments in Kraft pulps or change in sheet density as hypothesized earlier [68]). There might be some cross-reactivity among substrates and CBM15 (i.e. OC15 binding mainly to xylan, but having some affinity toward cellulose). We found that the affinity of each probe for its main target surpassed affinity for a similar target by tenfold or more [67, 68].

The proportions of polymers on the surface of pulps prior to enzymatic treatment are shown in Fig. 7. As expected, given the nature of Kraft pulping, the proportion of AC and CC on the surface of Kraft pulps is higher than in CTM pulps, and although the number of cellulose-binding probes detected on the Kraft pulps surface is less than what was detected on mechanical pulps, a greater proportion of the probes detected on the Kraft pulps were cellulose binding. Also, softwood exposed proportionally more mannan and hardwood more xylan, although the difference between hardwood and softwood was less pronounced for the mechanical pulps. Such distribution of hemicelluloses on the surface is compatible with bulk composition of fibers, and also compatible with the generally accepted understanding of softwood and hardwood hemicellulose composition [17, 78]. In general, CC exposure detection was greater than that of AC regardless of wood or pulping, except for SK pulp, where amorphous regions' exposure was twice the exposure of CC (the same trend was observed in Fig. 4).

Treatment with enzyme cocktail T consistently left a larger proportion of CC on substrate surfaces, at the expense of AC at the fiber surface. An exception was for SK pulp, where relative amount of AC probe remained stable regardless of enzymatic treatment. SK pulp had the most balanced proportions of probe binding, and this equilibrium between various fractions was barely affected

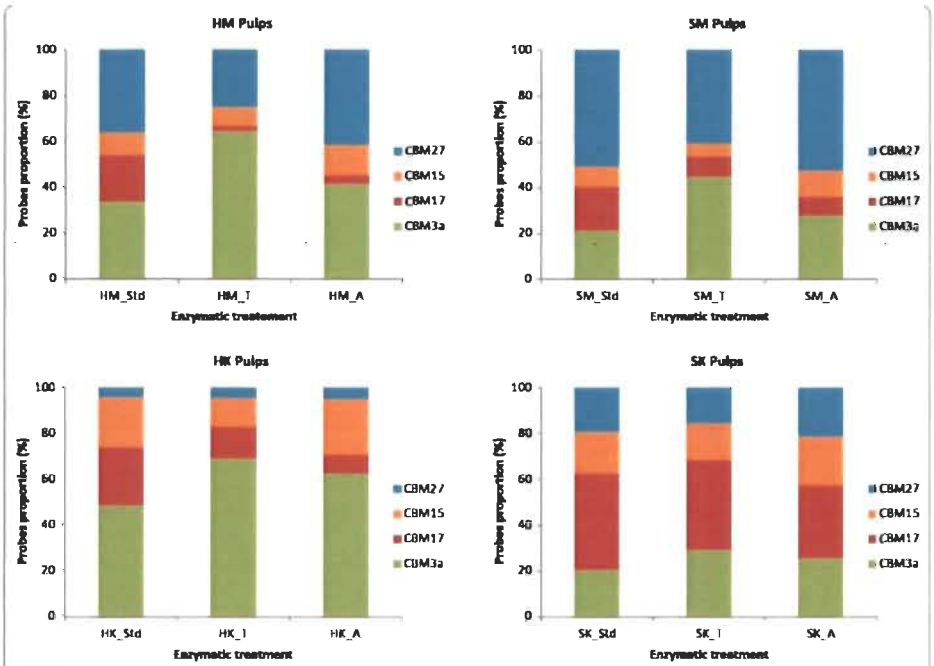


**Fig. 7** Proportion (in percent) of each probe by treatment on the total probes content for each pulp

by hydrolysis with T enzyme cocktail. Because analysis of hydrolysates (Fig. 3) revealed a significant release of simple sugars for SK pulp treated with T enzyme, all of the components must have been degraded equally during hydrolysis. Conversely, the relatively small yield of hydrolysate sugars from SK pulp after A enzyme treatment, correlated with nearly same balanced proportion of probe binding, means that SK pulp was not significantly degraded after A enzyme hydrolysis.

Inspection of proportions, and not individual probe binding, allows reconciliation of apparent contradictions between the increase in CC in the SM pulp, shown in Fig. 6, and the low release of sugar after T enzyme treatment (Fig. 3), because the proportion of CC for SM is lower than in HK and HM pulps.

Treatment with enzyme cocktail T results in decreased hemicellulose binding (in proportion to total binding) for all pulps, while treatment with enzyme cocktail A results in probe signal proportions that are in between the control and enzyme T treated substrates. Enzyme A also left larger proportions of hemicelluloses on the surface of fibers at the expense of AC or CC.

The results presented here can be useful in predicting whether an enzymatic treatment of a given biomass is well suited for a given application of wood biomass. For biofuel production, for example, the hydrolysate analysis suggests that best conditions would involve using the most aggressive enzyme (T) with the most exposed fibers (Kraft pulp). Absolute change in probe binding observed by FTCM confirmed the reduction of cellulose at the surface of fibers. FTCM analysis can also be useful for biofuel production, because it can provide precious information about the deconstruction of complex substrates and can monitor the progressive removal of polymers, which permits the optimization of enzymatic treatments. For example, treatment with T enzymes left a higher number of CC-binding sites on all pulps tested here. FTCM would be instrumental in determining the operating conditions which allow for total digestion of CC with minimal costs.

Fluorescent-tagged carbohydrate-binding module method could also provide information for partial hydrolysis of fibers for specific applications. Unlike other methods, such as hydrolysate analysis, chemical analysis, or XPS, FTCM can characterize the surface after treatment. This information can be used to select biomass stock and treatment that will yield the surface properties or composition needed for a given application.

Enzyme T was the most effective for increasing the crystalline cellulose surface proportion and decreasing amorphous cellulose and hemicelluloses. A high production of CC was observed for CTM pulps but Kraft hardwood harbored the highest proportion of CC at surface after treatment. Treatment of HK with T enzymes would be more appropriate for production of purified cellulose products, such as nanocellulose. Treatment with enzyme T would promote generating fiber surfaces that are mechanically stronger, more chemically resistant, and less sensitive to humidity. These characteristics suggest applications like reinforcement in composite materials (in industries like transport, furniture or construction).

Enzyme A is more selective than T. Its use resulted in a significant reduction of the proportion of AC on substrate surfaces while leaving mannan and xylan proportions relatively untouched. This enzyme mixture also hydrolyzed CTM more efficiently than Kraft pulp. Enzyme A allowed the relatively reactive xylan and mannan polymers to be preserved, yielding a product which could be used to develop specialty paper products or insulation materials. The enzymatic treatment of Kraft softwood pulp appears more relevant for applications where an equilibrated distribution of amorphous cellulose and hemicelluloses is preferred. This includes paper products with controlled physical properties, although the strength of these paper products may be decreased by either enzyme.

## Conclusions

Fluorescent-tagged carbohydrate-binding module method can be used as a rapid, affordable, and direct method to evaluate the surface composition of lignocellulosic substrates, thereby permitting processes to be understood in terms of compositional changes on the substrate surface which could not otherwise have been observed. Comparable methods for fiber analysis such as compositional analysis of the substrate after treatment (using FTIR, XPS) or of the hydrolysates (hydrolysis products content, using GC or HPLC), surface imaging (using SEM, TEM, and AFM), index of crystallinity (using XRD and NMR) and mass balance calculations [64–66] cannot directly monitor processing by enzymatic action. The FTCM analysis presented here directly provided valuable information about the quantification of exposed amorphous and crystalline cellulose, xylan, and mannan, which could then be used to determine the effects of pulping and enzymatic hydrolysis on the surface composition of substrates. The variation of these components at surface before and after treatment can guide strategies for preparation of wood fiber derived products.

## Additional files

**Additional file 1: Table S1.** Protein content and activities of the two commercial enzyme mixtures. Enzyme cocktail T refers to Cellu Clast 1.5L from *Trichoderma reesei* and enzyme cocktail A refers to Carezyme 1000L from *Aspergillus* sp.

**Additional file 2: Figure S1.** Weighted average values of fiber lengths (mm) and standard deviations for control Std, T, and A enzymes treated pulps of different grades. (HM) hardwood CTM pulp; (SM) softwood CTM pulp; (HK) hardwood Kraft pulp; and (SK) softwood Kraft pulp. **Figure S2.** Weighted proportion (%) and standard deviations of fines (fiber with length <0.2 mm) for control Std, T, and A enzymes treated pulps of different grades. (HM) hardwood CTM pulp; (SM) softwood CTM pulp; (HK) hardwood Kraft pulp and (SK) softwood Kraft pulp. **Figure S3.** Arithmetic average values (μm) and standard deviations of fiber widths for control Std, T, and A enzymes treated pulps of different grades. (HM) hardwood CTM pulp; (SM) softwood CTM pulp; (HK) hardwood Kraft pulp, and (SK) softwood Kraft pulp. **Figure S4.** Zero span breaking length (km) for control Std, T, and A enzymes treated pulps of different grades. (HM) hardwood CTM pulp; (SM) softwood CTM pulp; (HK) hardwood Kraft pulp, and (SK) softwood Kraft pulp.

### Abbreviations

AC: amorphous cellulose; AFM: atomic force microscopy; CC: crystalline cellulose; CMCase: carboxymethyl cellulase; CTM: chemical-thermo-mechanical; DNS: 3,5-dinitrosalicylic acid; FQA: fiber quality analyzer; FTCM: fluorescent tagged carbohydrate-binding module method; ft-CBM: fluorescent-tagged recombinant carbohydrate-binding module; FTIR: Fourier transform infrared spectroscopy; GC: gas chromatography; HK: hardwood Kraft pulp; HM: hardwood chemical thermo mechanical pulp; HPLC: high performance liquid chromatography; LCB: lignocellulosic biomass; NMR: nuclear magnetic resonance; NREL: national renewable energy laboratory; SEM: scanning electron microscopy; SK: softwood Kraft pulp; SM: softwood chemical-thermo mechanical pulp; TAPPI: technical association of the pulp and paper industry; TEM: transmission electron microscopy; XPS: X-ray photoelectron spectrometry; XRD: X-ray diffraction.

### Authors' contributions

PLB carried out all the experiments and drafted the manuscript. VK contributed to experiments related to the construction of ft-CBM probes and drafted the manuscript. FMM drafted the manuscript. VK and FMM have contributed equally to this work. DM, AR, FMM and MB participated in its design and coordination, and helped to draft and revise the manuscript. All authors read and approved the final manuscript.

### Author details

[1] AgroBioChem Department, Laboratory of Biomass and Green Technologies, University of Liège, Gembloux Agro-Bio Tech, 5030 Gembloux, Belgium. [2] Université du Québec à Trois-Rivières, Centre de Recherche sur les Matériaux Lignocellulosiques, C.P. 500, Trois-Rivières, QC G9A 5H7, Canada. [3] PROTEO, Université Laval, Québec, QC G1V 0A6, Canada. [4] Département de Chimie, Biochimie et Physique, Université du Québec à Trois-Rivières, C.P. 500, Trois-Rivières, QC G9A 5H7, Canada.

### Acknowledgements

This work was supported by Wallonie-Bruxelles International through the WBI World program and by grants awarded by the Consortium de recherche et innovations en bioprocédés industriels au Québec (CRIBIQ) and Kruger inc.

The skillful technical assistance of Nikolas Beauchesne and Virginie Bytteber is acknowledged. The authors would like to thank Glenn Bousfield (University of Liège) for his valuable support and editorial contributions.

**Competing interests**
FTCM is patent pending (Buckman International, USA). The authors declare that they have no competing interests.

**Availability of data and materials**
The datasets used and/or analyzed during the current study are available from the corresponding author on reasonable request.

**Consent for publication**
Not applicable.

**Ethic approval and consent to participate**
Not applicable.

**Funding**
This work was supported by Wallonie-Bruxelles International through the WBI World program and by grants awarded by the Consortium de recherche et innovations en bioprocédés industriels au Québec (CRIBIQ) and Kruger Inc.

## Publisher's Note



**Received: 29 August 2017 Accepted: 26 November 2017**
**Published online: 06 December 2017**

**References**

1. Naik SN, Goud VV, Rout PK, Dalai AK. Production of first and second generation biofuels: a comprehensive review. Renew Sustain Energy Rev. 2010;14:578–97.
2. Nigam PS, Singh A. Production of liquid biofuels from renewable resources. Prog Energy Combust Sci. 2011;37:52–68. https://doi.org/10.1016/j.pecs.2010.01.003.
3. Scheftran J. The global demand for biofuels: technologies, markets and policies. In: Vertès A, Qureshi N, Blaschek H, Yukawa H, editors. Biomass to biofuels: strategies for global industries. Hoboken: Wiley; 2010. p. 27–54.
4. Agbor VB, Cicek N, Sparling R, Berlin A, Levin DB. Biomass pretreatment: fundamentals toward application. Biotechnol Adv. 2011;29:675–85. https://doi.org/10.1016/j.biotechadv.2011.05.005.
5. Zhu H, Luo W, Ciesielski PN, Fang Z, Zhu JY, Henriksson G, et al. Wood-derived materials for green electronics, biological devices, and energy applications. Chem Rev. 2016;116:9305–74. https://doi.org/10.1021/acs.chemrev.6b00225.
6. Wegner TH, Ireland S, Jones JPE. Cellulosic nanomaterials: sustainable materials of choice for the 21st century. In: Postek M, Moon R, Rudie A, Bilodeau M, editors. Production and applications of cellulose nanomaterials. Peachtree Corners: TAPPI Press; 2013. p. 3–8.
7. Dufresne A. Nanocellulose: from nature to high performance tailored materials. Berlin: de Gruyter; 2012.
8. Christopher L. Integrated forest biorefineries: current state and development potential. In: Christopher L, editor. Integrated forest biorefineries: challenges and opportunities. Cambridge: The Royal Society of Chemistry; 2013. p. 1–66.
9. Zhang X, Paice MG, Deng J. Modify existing pulp and paper mills for biorefinery operations. In: Zhu J, Zhang X, Pan X, editors. Sustainable production of fuels, chemicals, and fibers from forest biomass. American Chemical Society; 2011. p. 395–408.
10. Fargione J, Hill J, Tilman D, Polasky S, Hawthorne P. Land clearing and the biofuel carbon debt. Science. 2008;319:1235–8.
11. Runge CF, Senauer B. How biofuels could starve the poor. Foreign Aff. 2007;86:41–53.
12. Eisentraut A. Sustainable production of second-generation biofuels: potential and perspectives in major economies and developing countries. Paris: OECD; 2010. https://doi.org/10.1787/20792581.
13. Mohr A, Raman S. Lessons from first generation biofuels and implications for the sustainability appraisal of second generation biofuels. Energy Policy. 2013;63:114–22. https://doi.org/10.1016/j.enpol.2013.08.033.
14. Hendriks ATWM, Zeeman G. Pretreatments to enhance the digestibility of lignocellulosic biomass. Bioresour Technol. 2009;100:10–8.
15. Goldsworthy G, Chandrakant S, Opuku-Ware K. Adipokinetic hormone enhances nodule formation and phenoloxidase activation in adult locusts injected with bacterial lipopolysaccharide. J Insect Physiol. 2003;49:795–803. https://doi.org/10.1016/S0022-1910(03)00118-5.
16. Fengel D, Wegener G. Wood: chemistry, ultrastructure, reactions. Berlin: de Gruyter; 1984.
17. Stevanovic T, Perrin D. Chimie du bois. Lausanne: PPUR; 2009.
18. Himmel ME, Ding S-Y, Johnson DK, Adney WS, Nimlos MR, Brady JW, et al. Biomass recalcitrance: engineering plants and enzymes for biofuels production. Science. 2007;315:804–7.
19. Sun Y, Cheng J. Hydrolysis of lignocellulosic materials for ethanol production: a review. Bioresour Technol. 2002;83:1–11. https://doi.org/10.1016/S0960-8524(01)00212-7.
20. Kumar P, Barrett D, Delwiche M, Stroeve P. Methods for pretreatment of lignocellulosic biomass for efficient hydrolysis and biofuel production. Ind Eng Chem Res. 2009;48:3713–29.
21. Chaturvedi V, Verma P. An overview of key pretreatment processes employed for bioconversion of lignocellulosic biomass into biofuels and value added products. 3 Biotech. 2013;3:415–31. https://doi.org/10.1007/s13205-013-0167-8.
22. Limayem A, Ricke SC. Lignocellulosic biomass for bioethanol production: current perspectives, potential issues and future prospects. Prog Energy Combust Sci. 2012;38:449–67. https://doi.org/10.1016/j.pecs.2012.03.002.
23. Zhang X, Tu M, Paice MG. Routes to potential bioproducts from lignocellulosic biomass lignin and hemicelluloses. BioEnergy Res. 2011;4:246–57. https://doi.org/10.1007/s12155-011-9147-1.
24. FitzPatrick M, Champagne P, Cunningham MF, Whitney RA. A biorefinery processing perspective: treatment of lignocellulosic materials for the production of value-added products. Bioresour Technol. 2010;101:8915–22. https://doi.org/10.1016/j.biortech.2010.06.125.
25. Huang H-J, Ramaswamy S, Tschirner UW, Ramarao BV. A review of separation technologies in current and future biorefineries. Sep Purif Technol. 2008;62:1–21. https://doi.org/10.1016/j.seppur.2007.12.011.
26. Gupta VK, Potumarthi R, O'Donovan A, Kubicek C, Sharma G, Tuohy M. Bioenergy research: an overview on technological developments and bioresources. In: Gupta V, Tuohy M, Kubicek C, Saddler J, Xu F, editors. Bioenergy research: advances and applications. Amsterdam: Elsevier Ltd; 2014. p. 23–47.
27. Sims REH, Mabee W, Saddler JN, Taylor M. An overview of second generation biofuel technologies. Bioresour Technol. 2010;101:1570–80. https://doi.org/10.1016/j.biortech.2009.11.046.
28. Budarin VL, Shuttleworth PS, Dodson JR, Hunt AJ, Lanigan B, Marriott R, et al. Use of green chemical technologies in an integrated biorefinery. Energy Environ Sci. 2011;4:471–9. https://doi.org/10.1039/C0EE00184H.
29. Clark JH, Budarin V, Deswarte FEI, Hardy JJE, Kerton FM, Hunt AJ, et al. Green chemistry and the biorefinery: a partnership for a sustainable future. Green Chem. 2006;8:853–60. https://doi.org/10.1039/B604483M.
30. Sheldon RA. Green and sustainable manufacture of chemicals from biomass: state of the art. Green Chem. 2014;16:950–63. https://doi.org/10.1039/C3GC41935E.
31. Alvira P, Tomás-Pejó E, Ballesteros M, Negro MJ. Pretreatment technologies for an efficient bioethanol production process based on enzymatic hydrolysis: a review. Bioresour Technol. 2010;101:4851–61. https://doi.org/10.1016/j.biortech.2009.11.093.
32. Ragauskas AJ, Williams CK, Davison BH, Britovsek G, Cairney J, Eckert CA, et al. The path forward for biofuels and biomaterials. Science. 2006;311:484–9.
33. Yang ST, Yu M. Integrated biorefinery for sustainable production of fuels, chemicals, and polymers. In: Yang ST, El-Enshasy HA, Thongchul N, editors. Bioprocessing technologies in biorefinery for sustainable production of fuels, chemicals and polymers. First. Hoboken: Wiley; 2013. p. 1–26. https://doi.org/10.1002/9781118642047.

34 Mohanty AK, Misra M, Hinrichsen G. Biofibres, biodegradable polymers and biocomposites: an overview. Macromol Mater Eng. 2000;276–277:1–24. https://doi.org/10.1002/(SICI)1439-2054(20000301)276:1<1:AID-MAME1>3.0.CO;2-W.

35 Mohanty AK, Misra M, Drzal LT. Sustainable bio-composites from renewable resources: opportunities and challenges in the green materials world. J Polym Environ. 2002;10:19–26. https://doi.org/10.1023/A:1021013921916.

36 John MJ, Thomas S. Biofibres and biocomposites. Carbohydr Polym. 2008;71:343–64. https://doi.org/10.1016/j.carbpol.2007.05.040.

37 Xu Y, Rowell R. Biofibers. In: Zhu J, Zhang X, Pan X, editors. Sustainable production of fuels, chemicals, and fibers from forest biomass. Washington, DC: American Chemistry Society; 2011. p. 323–66.

38 Jiang L, Tsai M-H, Anderson S, Wolcott M, Zhang J. Development of biodegradable polymer composites. In: Zhu J, Zhang X, Pan X, editors. Sustainable production of fuels, chemicals, and fibers from forest biomass. Washington, DC: American Chemistry Society; 2011. p. 367–91.

39 Orts WJ, Shey J, Imam SH, Glenn GM, Guttman ME, Revol J-F. Application of cellulose microfibrils in polymer nanocomposites. J Polym Environ. 2005;13:301–6. https://doi.org/10.1007/s10924-005-5514-3.

40 Oksanen T, Pere J, Buchert J, Viikari L. The effect of *Trichoderma reesei* cellulases and hemicellulases on the paper technical properties of never-dried bleached kraft pulp. Cellulose. 1997;4:329–39. https://doi.org/10.1023/A:1018456411031.

41 Bajpai P. Application of enzymes in the pulp and paper industry. Biotechnol Prog. 1999;15:147–57. https://doi.org/10.1021/bp990013k.

42 Cui L, Meddeb-Mouelhi F, Laframboise F, Beauregard M. Effect of commercial cellulases and refining on kraft pulp properties: correlations between treatment impacts and enzymatic activity components. Carbohydr Polym. 2015;115:193–9.

43 Sabo R, Zhu J. Integrated production of cellulose nanofibrils and cellulosic biofuels by enzymatic hydrolysis of wood fibers. In: Postek M, Moon R, Rudie A, Bilodeau M, editors. Production and applications of cellulose nanomaterials. Peachtree Corners: TAPPI Press; 2013. p. 191–4.

44 Duran N, Lemes A, Duran M, Freer J, Baeza J. A minireview of cellulose nanocrystals and its potential integration as co-product in bioethanol production. J Chil Chem Soc. 2011;56:672–7.

45 Pääkkö M, Ankerfors M, Kosonen H, Nykänen A, Ahola S, Österberg M, et al. Enzymatic hydrolysis combined with mechanical shearing and high-pressure homogenization for nanoscale cellulose fibrils and strong gels. Biomacromolecules. 2007;8:1934–41. https://doi.org/10.1021/bm061215p.

46 Siqueira G, Tapin-Lingua S, Bras J, da Silva Perez D, Dufresne A. Morphological investigation of nanoparticles obtained from combined mechanical shearing, and enzymatic and acid hydrolysis of sisal fibers. Cellulose. 2010;17:1147–58. https://doi.org/10.1007/s10570-010-9449-z.

47 Gehmayr V, Schild G, Sixta H. A precise study on the feasibility of enzyme treatments of a kraft pulp for viscose application. Cellulose. 2011;18:479–91. https://doi.org/10.1007/s10570-010-9483-x.

48 Qing Y, Sabo R, Zhu JY, Agarwal U, Cai Z, Wu Y. A comparative study of cellulose nanofibrils disintegrated via multiple processing approaches. Carbohydr Polym. 2013;97:226–34. https://doi.org/10.1016/j.carbpol.2013.04.086.

49 de Campos A, Correa AC, Cannella D, de M Teixeira E, Marconcini JM, Dufresne A, et al. Obtaining nanofibers from curauá and sugarcane bagasse fibers using enzymatic hydrolysis followed by sonication. Cellulose. 2013;20:1491–500. https://doi.org/10.1007/s10570-013-9909-3.

50 Torres CE, Negro C, Fuente E, Blanco A. Enzymatic approaches in paper industry for pulp refining and biofilm control. Appl Microbiol Biotechnol. 2012;96:327–44. https://doi.org/10.1007/s00253-012-4345-0.

51 Yarbrough JM, Zhang R, Mittal A, Vander Wall T, Bomble YJ, Decker SR, et al. Multifunctional cellulolytic enzymes outperform processive fungal cellulases for coproduction of nanocellulose and biofuels. ACS Nano. 2017;11:3101–9. https://doi.org/10.1021/acsnano.7b00086.

52 Mansfield SD, Mooney C, Saddler JN. Substrate and enzyme characteristics that limit cellulose hydrolysis. Biotechnol Prog. 1999;15:804–16.

53 Ha DP, Ngo HH, Guo W. A mini review on renewable sources for biofuel. Bioresour Technol. 2014;169:742–9. https://doi.org/10.1016/j.biortech.2014.07.022.

54 Larsson S, Palmqvist E, Hahn-Hägerdal B, Tengborg C, Stenberg K, Zacchi G, et al. The generation of fermentation inhibitors during dilute acid hydrolysis of softwood. Enzyme Microb Technol. 1999;24:151–9. https://doi.org/10.1016/S0141-0229(98)00101-X.

55 Palmqvist E, Hahn-Hägerdal B. Fermentation of lignocellulosic hydrolysates. II: inhibitors and mechanisms of inhibition. Bioresour Technol. 2000;74:25–33. https://doi.org/10.1016/S0960-8524(99)00161-3.

56 Hall M, Bansal P, Lee JH, Realff MJ, Bommarius AS. Cellulose crystallinity—a key predictor of the enzymatic hydrolysis rate. FEBS J. 2010;277:1571–82.

57 Hu J, Arantes V, Saddler JN. The enhancement of enzymatic hydrolysis of lignocellulosic substrates by the addition of accessory enzymes such as xylanase: is it an additive or synergistic effect? Biotechnol Biofuels. 2011;4:36. https://doi.org/10.1186/1754-6834-4-36.

58 Várnai A, Huikko L, Pere J, Siika-aho M, Viikari L. Synergistic action of xylanase and mannanase improves the total hydrolysis of softwood. Bioresour Technol. 2011;102:9096–104.

59 Merino ST, Cherry J. Progress and challenges in enzyme development for biomass utilization. Biofuels. 2007;108:95–120. https://doi.org/10.1007/10_2007_066.

60 Penttilä PA, Várnai A, Pere J, Tammelin T, Salmén L, Siika-aho M, et al. Xylan as limiting factor in enzymatic hydrolysis of nanocellulose. Bioresour Technol. 2013;129:135–41.

61 Lee RA, Lavoie J-M. From first- to third-generation biofuels: challenges of producing a commodity from a biomass of increasing complexity. Anim Front. 2013;3:6–11. https://doi.org/10.2527/af.2013-0010.

62 Lennartsson PR, Erlandsson P, Taherzadeh MJ. Integration of the first and second generation bioethanol processes and the importance of by-products. Bioresour Technol. 2014;165:3–8. https://doi.org/10.1016/j.biortech.2014.01.127.

63 Klein-Marcuschamer D, Oleskowicz-Popiel P, Simmons BA, Blanch HW. The challenge of enzyme cost in the production of lignocellulosic biofuels. Biotechnol Bioeng. 2012;109:1083–7. https://doi.org/10.1002/bit.24370.

64 Miller GL. Use of dinitrosalicylic acid reagent for determination of reducing sugar. Anal Chem. 1959;31:426–8. https://doi.org/10.1021/ac60147a030.

65 Betezin IV, Rabinovich ML, Sinitsyn AP. Applicability of quantitative kinetic spectrophotometric method for glucose determination. Biokhimiia. 1977;42:1631–6.

66 Berlin A, Maximenko V, Bura R, Kang K-Y, Gilkes N, Saddler J. A rapid microassay to evaluate enzymatic hydrolysis of lignocellulosic substrates. Biotechnol Bioeng. 2006;93:880–6. https://doi.org/10.1002/bit.20783.

67 Khatri V, Hébert-Ouellet V, Meddeb-Mouelhi F, Beauregard M. Specific tracking of xylan using fluorescent-tagged carbohydrate-binding module 15 as molecular probe. Biotechnol Biofuels. 2016;9:74. https://doi.org/10.1186/s13068-016-0486-1.

68 Hebert-Ouellet V, Meddeb-Mouelhi F, Khatri V, Cui L, Janse B, MacDonald K, et al. Tracking and predicting wood fibers processing with fluorescent carbohydrate binding modules. Green Chem. 2017; https://doi.org/10.1039/C6GC03581G.

69 Sluiter A, Crocker D, Hames B, Ruiz R, Scarlata C, Sluiter J, et al. Determination of structural carbohydrates and lignin in biomass. Lab Anal Proced. 2008;1617:1–6.

70 Gourlay K, Hu J, Arantes V, Penttilä M, Saddler JN. The use of carbohydrate binding modules (CBMs) to monitor changes in fragmentation and cellulose fiber surface morphology during cellulase- and swollenin-induced deconstruction of lignocellulosic substrates. J Biol Chem. 2015;290:2938–45.

71 Bradford MM. A rapid and sensitive method for the quantitation of microgram quantities of protein utilizing the principle of protein-dye binding. Anal Biochem. 1976;72:248–54. https://doi.org/10.1016/0003-2697(76)90527-3.

72 Vandergheynst C, Boquet P, Blecker C, Paquot M. A multistage process to enhance cellobiose production from cellulosic materials. Appl Biochem Biotechnol. 2010;160:2300–7. https://doi.org/10.1007/s12010-009-8724-7.

73 Vandergheynst C, Jacquet N, Danthine S, Blecker C, Paquot M. Effect of physicochemical characteristics of cellulosic substrates on enzymatic hydrolysis by means of a multi-stage process for cellobiose production. Appl Biochem Biotechnol. 2012;166:1423–32. https://doi.org/10.1007/s12010-011-9535-1.

74 Mooney CA, Mansfield SD, Beatson RP, Saddler JN. The effect of fiber characteristics on hydrolysis and cellulase accessibility to softwood substrates. Enzym Microb Technol. 1999;25:644–50.

75. Biermann CJ. 3 Pulping fundamentals. In: Biermann CJ, editor. Handbook of pulping and papermaking. 2nd ed. San Diego: Academic Press; 1996. p. 55–100. https://doi.org/10.1016/B978-012097362-0/50007-6.
76. Sixta H. Fiber properties. In: Sixta H, editor. Handbook of pulp. Weinheim: Wiley-VCH Verlag GmbH; 2006. p. 1269–80. http://doi.org/10.1002/9783527619887.ch31.
77. Rahikainen JL, Mikander S, Marjamaa K, Tamminen T, Lappas A, Viikari L, et al. Inhibition of enzymatic hydrolysis by residual lignins from soft wood-study of enzyme binding and inactivation on lignin-rich surface. Biotechnol Bioeng. 2011;108:2823–34. https://doi.org/10.1002/bit.23242.
78. Timell TE. Recent progress in the chemistry of wood hemicelluloses. Wood Sci Technol. 1967;1:45–70. https://doi.org/10.1007/BF00592255.
79. Ek M, Gellerstedt G, Henriksson G. Wood chemistry and biotechnology. Berlin: Walter de Gruyter; 2009.
80. Öhgren K, Bura R, Saddler J, Zacchi G. Effect of hemicellulose and lignin removal on enzymatic hydrolysis of steam pretreated corn stover. Bioresour Technol. 2007;98:2503–10.
81. Mooney CA, Mansfield SD, Touhy MG, Saddler JN. The effect of initial pore volume and lignin content on the enzymatic hydrolysis of softwoods. Bioresour Technol. 1998;64:113–9. https://doi.org/10.1016/S0960-8524(97)00181-8.
82. Studer MH, DeMartini JD, Davis MF, Sykes RW, Davison B, Keller M, et al. Lignin content in natural Populus variants affects sugar release. Proc Natl Acad Sci. 2011;108:6300–5. https://doi.org/10.1073/pnas.1009252108.
83. Yu Z, Jameel H, Chang H, Park S. The effect of delignification of forest biomass on enzymatic hydrolysis. Bioresour Technol. 2011;102:9083–9. https://doi.org/10.1016/j.biortech.2011.07.001.
84. Zhang J, Tang M, Viikari L. Xylans inhibit enzymatic hydrolysis of lignocellulosic materials by cellulases. Bioresour Technol. 2012;121:8–12. https://doi.org/10.1016/j.biortech.2012.07.010.
85. Zhu L, O'Dwyer JP, Chang VS, Granda CB, Holtzapple MT. Structural features affecting biomass enzymatic digestibility. Bioresour Technol. 2008;99:3817–28.
86. Yamada R, Yoshie T, Sakai S, Waikai S, Asai-Nakashima N, Okazaki F, et al. Effective saccharification of kraft pulp by using a cellulase cocktail prepared from genetically engineered Aspergillus oryzae. Biosci Biotechnol Biochem. 2015;79:1034–7. https://doi.org/10.1080/09168451.2015.1006568.
87. Mittal A, Katahira R, Himmel ME, Johnson DK. Effects of alkaline or liquid-ammonia treatment on crystalline cellulose: changes in crystalline structure and effects on enzymatic digestibility. Biotechnol Biofuels. 2011;4:41. https://doi.org/10.1186/1754-6834-4-41.
88. Thornton J, Ekman R, Holmbom B, Örså F. Polysaccharides dissolved from norway spruce in thermomechanical pulping and peroxide bleaching. J Wood Chem Technol. 1994;14:159–75. https://doi.org/10.1080/02773819408003092.
89. Ragauskas AJ, Nagy M, Kim DH, Eckert CA, Hallett JP, Liotta CL. From wood to fuels: integrating biofuels and pulp production. Ind Biotechnol. 2006;2:55–65. https://doi.org/10.1089/ind.2006.2.55.
90. Lawoko M, Henriksson G, Gellerstedt G. New method for quantitative preparation of lignin-carbohydrate complex from unbleached softwood kraft pulp: lignin-polysaccharide networks I. Holzforschung. 2003;57:69. https://doi.org/10.1515/HF.2003.011.
91. Lawoko M, Rickard B, Fredrik B, Gunnar H, Göran G. Changes in the lignin carbohydrate complex in softwood kraft pulp during kraft and oxygen delignification. Holzforschung. 2004;58:603. https://doi.org/10.1515/HF.2004.114.
92. Lawoko M, Henriksson G, Gellerstedt G. Structural differences between the lignin-carbohydrate complexes present in wood and in chemical pulps. Biomacromolecules. 2005;6:3467–73.
93. Choi JW, Choi D-H, Faix O. Characterization of lignin-carbohydrate linkages in the residual lignins isolated from chemical pulps of spruce (*Picea abies*) and beech wood (*Fagus sylvatica*). J Wood Sci. 2007;53:309–13. https://doi.org/10.1007/s10086-006-0860-x.
94. Pu Y, Ziemer C, Ragauskas AJ. CP/MAS 13C NMR analysis of cellulase treated bleached softwood kraft pulp. Carbohydr Res. 2006;341:591–7.
95. Lynd LR, Weimer PJ, van Zyl WH, Pretorius IS. Microbial cellulose utilization: fundamentals and biotechnology. Microbiol Mol Biol Rev. 2002;66:506–77. https://doi.org/10.1128/MMBR.66.3.506-577.2002.